Systematics of Miocene angiosperm woods from the Panama Canal, and their palaeoenvironmental implications

Oris Rodríguez Reyes

Royal Holloway, University of London

A thesis submitted for the degree of Doctor of Philosophy

October, 2014

Declaration of authorship

I, Oris Rodríguez Reyes, hereby declare that this thesis

Systematics of Miocene angiosperm woods from the Panama Canal, and their palaeoenvironmental implications

The work presented in it is entirely my own. Where I have consulted the work of others, this is fully cited and referenced, and/or with the appropriate acknowledgment given.

Signature:

Date: 20 October 2014

Miss Oris Rodríguez Reyes

ABSTRACT

Systematics of Miocene woods from the Panama Canal, and their palaeoenvironmental implications

Miocene fossil woods exposed during the recent widening of the Panama Canal are described and their palaeoecological, palaeoclimatic and biogeographic implications are discussed. The woods occur in the Cucaracha Formation (early to mid-Burdigalian, 18 – 20 Ma) and comprise (1) a forest of charred and silicified stumps preserved in growth position by a pyroclastic flow and (2) calcareous permineralised trunks, bored by *Teredolites* and transported within fluvio-estuarine channel deposits. Woods were identified using a searchable authoritative online database (Inside Wood) and through detailed comparison with modern woods, mostly at the Jodrell Laboratory, Kew, UK. The two assemblages differ at genus-level, and to some extent, family-level. The permineralised wood assemblage contains dicots and is dominated by Malvaceae with some Leguminosae, Cannabaceae and Elaeocarpaceae. It includes representatives of several extant genera tolerant of flooding and exposed coastal conditions, consistent with the estuarine setting inferred from the geological evidence. In contrast, the charcoalified wood assemblage contains monocot palms (Arecaceae) but also includes dicots (Leguminosae, Malvaceae, Sapotaceae, ?Melastomataceae, Meliaceae) and dicot indeterminate forms. The extant relatives of this assemblage include a mixture of coastal and forest interior taxa representing a more diverse floodplain forest. Reflectance data from the charred stumps indicate that entombing pyroclastic flows reached minimum temperatures that ranged from 490 – 505ºC. Palaeoclimatic inferences, based on anatomical comparison of fossil woods and present-day woods and floras from Panama, suggest that Miocene forests were somewhat cooler and drier than

modern equivalents. The fossil wood assemblages contain several taxa endemic to South America, despite Panama being part of the North American continent in Miocene times. This implies that the collision of the Americas, which was traditionally thought to have occurred around 3 – 4 million years ago (mid – to late Pliocene) may have begun much earlier, with intercontinental exchange of tree species beginning by 18 – 20 Ma.

ACKNOWLEDGMENTS

I would like to express my deepest thanks to my supervisors: Dr. Howard Falcon-Lang and Dr. Margaret E. Collinson that patiently gave me thoughtful guidance from my very first day in Royal Holloway until the last days of my thesis writing; as well as to Dr. Carlos Jaramillo who inspired this work in the first place and constantly supported me to continue in the field of palaeobotany. Very special thanks go also to Dr. Peter Gasson in the Jodrell Laboratory (Royal Botanic Gardens Kew), who kept my motivation in the study of wood anatomy and gave me invaluable guidance, teaching and support.

I would like to acknowledge the advice from Dr. Gary Nichols, Dr. Elisabeth Wheeler and Dr. Pieter Baas during the first years of the project and to Dr. Pieter Hietz, during my internship in Vienna. They have been of greatest inspiration and helped to greatly improve this research project. Advice from Dr. Emiliano Peralta-Medina was also important during the first years of my thesis.

I am very thankful to Kevin D'Souza, Neil Holloway and Sharon Gibbons that offered excellent aid in the imaging, preparation and analysis of samples, respectively. I would also like to thank to Dr. Sergio Cevallos-Ferriz and Dr. Laura Calvillo-Canadell (UNAM, Mexico) for the preparation of some of the samples included herein.

Thanks to the paleontology/geology team in CTPA (Center for Tropical Palaeoecology and Archaelogy, STRI, Panama), but particularly to Dr. Camilo Montes, who provided with important information about the geology of the field area. Thanks to Aldo Rincón, Catalina Suárez, César Silva, Carlos De Gracia, Maritza Moya, Jorge W. Moreno, Federico Moreno, Enrique Moreno, Felix Rodríguez, Juan David Carrillo, María Camilla Vallejo, Andrés Baresch, Luz Elena Oviedo, María Inés Barreto and Liliana Londoño for all the help during fieldwork. Thanks to Alina Screuer and Sabine

Rosner for all the help with the samples during my internship in the BOKU in Vienna.

Valuable comments from my examiners, Professor Will Chaloner and Dr. Jakub Sakala greatly improved this thesis. I am also grateful for all those valuable suggestions from my colleagues and friends: Vicky Hudspith, Francy Carvajal, Gabriela Doria, Fabiany Herrera, Monica Carvalho, Camilla Crifó, Emilio Estrada-Ruiz, Luis Palazzesi, Silvia D'apolito, LuisDanise and Heather Graham.

Very special thanks to my good friends that gave me all the strength and support in the good and weakest moments: Ivan Hernández, Miguel Andrés Martínez, Celine Tschirhart, Lidia Rodríguez, Gerd Winterleitner, Sila Pla Pueyo, Arnaud Gallois, Sebastian Zimmermann, Silvia Crosetto, Giulia Zazzeri, Damiano Della Lunga, , Jéssica García, Eldert Advokaat, Giovanni Pezzati, Jorge Belenguer, Zsuzsanna Döbröntei, Elena Ros, Denise Gutiérrez, Liliane Mendoza, Eva Baker, Maria Reilly, Irina Calero Bieberach and Elena García Antón. Muchas gracias!

My deepest love and thanks go to my family for their constant and incredible support: my mom, Lilia Reyes de Rodriguez; my father, Alfonso Rodríguez and my siblings, Lily, Edwin and Osiris.

Finally, I take this space to say thanks to you, Mena Schemm-Gregory. Among paleontologists, you were my greatest model to follow because of your perseverance despite all adversities. You would have been so happy and proud watching me submitting this work. Thanks for encouraging me so much during my Phd.!

APPENDICES (CD)

Appendix I: Rodriguez-Reyes, O., Falcon-Lang, H., Gasson, P., Collinson, M., Jaramillo, C.A., 2014. Fossil woods (Malvaceae) from the lower Miocene (early to mid-Burdigalian)

part of the Cucaracha Formation of Panama (Central America) and their biogeographic implications. Review of Palaeobotany and Palynology 209, 11–34.

FIGURES

Chapter 1

Chapter 4

Chapter 5

Chapter 7

Chapter 8

Chapter 9

PLATES

Chapter 4

Chapter 5

TABLES

Chapter 2

Chapter 3

Chapter 4

Chapter 5

Chapter 6

Chapter 7

Chapter 8

CHAPTER 1. INTRODUCTION

1.1. THESIS STRUCTURE

This thesis describes the facies context and systematics of assemblages of fossil woods found in Miocene strata in the Panama Canal, Central America, and considers their implications for palaeoecology, palaeoclimatology, and biogeography. The structure of the thesis is as follows:

Chapter 1 (this chapter) provides a geological introduction to the Miocene Epoch, with special reference to events in Central America and their bearing on global climate.

Chapter 2 describes the geological localities investigated in this study, reviewing previous fossil collections and the new discoveries reported here.

Chapter 3 explains the process by which fossil wood can be identified through detailed anatomical comparison with modern material.

Chapters 4 – 6, then, describe the systematics of the various types of fossil wood reported for the Miocene localities based on new collections and analyses.

Chapter 7 utilises reflectance microscopy to investigate taphonomic aspects of one particular fossil wood assemblage that was entombed by a hot pyroclastic flow.

Chapter 8 explores the palaeoclimatic implications of the fossil wood assemblages studied herein through anatomical comparison with a collection of woods from present day Panama.

Chapter 9, the discussion, draws together the new findings, and places them in their wider geological context. It also provides suggestions for future work.

Chapter 10 summarises conclusions.

1.2. SIGNIFICANCE OF THIS THESIS

This thesis provides new data about Miocene forests in Panama. However, its wider importance is that it sheds light on regional vegetation patterns leading up to the collision of the Americas and the formation of the Panama Isthmus – arguably one of the most important events in the recent history of the planet. Closure of the Panama Isthmus altered global patterns of ocean circulation (Schneider and Schmittner, 2006), possibly contributing to the onset of the termohaline circulation (Nisancioglu et al., 2003; Von der Heydt and Dijkstra, 2006) and also triggered what has been called the Great American Biological Interchange – the migration of animals and plants between North and South America (Marshall et al., 1982; Burnham and Graham, 1999). Traditionally, the collision of the Americas was thought to have occurred around 3 – 4 million years ago (mid – to late Pliocene), coinciding with the sharp rise in the proportion of North American ungulate genera in South America (Webb, 1991). However, more recent work (reviewed below) suggests that the event may have commenced earlier and was more complex than previously thought (Montes et al., 2012). Therefore a study of Miocene woods potentialy contributes a detailed knowledge of this earlier sequence of events, and helps us to better understand the collision of the Americas.

1.3. TIMELINESS OF THIS THESIS

The current study has been made possible by the recent widening of the Panama Canal, commenced in 2007, which has provided once-in-a-century access to Miocene-

Pliocene successions deposited immediately before, and during, the complex convergence of the Americas. Therefore the window of opportunity for this current study has been narrow. Geological outcrops cut only a few years ago are already becoming degraded in the tropical climate of Panama, and once construction work ceases, the opportunity to make further collections will quickly pass.

In the new geological sections, beautifully preserved assemblages of fossil wood have been exposed in the lower Miocene Cucaracha Formation, in particular, and these are the focus of this thesis. Determining the identity of these trees as precisely as possible, and assessing whether their affinities are with present-day North or South American taxa, is especially important because it could shed light on the timing and magnitude of intercontinental exchange of tree species prior to the final closure of the Panama Isthmus – a key biogeographic question.

1.4. INTRODUCTION TO MIOCENE EPOCH

The Miocene is an epoch in the Neogene Period. It spans from 23.0 – 5.33 Ma according to the 2009 IUGS Geologic Time Scale. Its base is defined by the base of magnetic polarity chronozone C6Cn.2n and the FAD (First Appearance Datum) of the planktonic foraminifer *Paragloborotalia kugleri* and the LAD (Last Appearance Datum) of the calcareous nannofossil *Reticulofenestra bisecta* (base Zone NN1). Its top is defined by the top of magnetic polarity chronozone C3r, ~100 kyr at its boundary with the Thvera normal polarity subchronozone (C3n.4n) and the LAD level of the calcareous nannofossil *Triquetrorhabdulus rugosus* (base Zone CN10b) and the FAD of *Ceratolithus acutus* (Gradstein *et al*., 2004).

The Miocene is subdivided into several global ages recognized by the International Commission of Stratigraphy (ICS), from youngest to oldest, as follows:

Upper Miocene: Messinian (7.246 ± 0.005 To 5.333 ± 0.005 Ma)

Tortonian (11.62 ± 0.005 To 7.246 ± 0.005 Ma)

Middle Miocene: Serravalian (13.82 ± 0.05 To 11.62 ± 0.005 Ma)

Langhian (15.97 ± 0.05 To 13.82 ± 0.05 Ma)

Lower Miocene: Burdigalian (20.44 ± 0.05 to 15.97 ± 0.05 Ma)

Aquitanian (23.03 ± 0.05 to 20.44 ± 0.05 Ma);

1.4.1. Major tectonic events

During the Miocene, some globally significant tectonic events took place (Figure 1.1) and are reviewed here. In Africa, the Atlas Mountains in the north uplifted during the Burdigalian, and later the Tunisian Mountains in the south uplifted during the Tortonian (Piqué et al., 2002). One of the most important and influential Miocene events in Africa was the temporary closure of the Strait of Gibraltar, presumably causing the drying out of the Mediterranean Basin in the Messinian (Hsü, 1983; Krijgsman et al., 1999).

Eurasia also experienced significant changes throughout the Miocene. The two most significant events were the development of the Alps between 23 and 11 Ma in the Alpine Orogeny (Frisch et al., 2000) and the accelerated opening of the Red Sea following an initial Late Oligocene opening (Purser and Bosence, 1998).

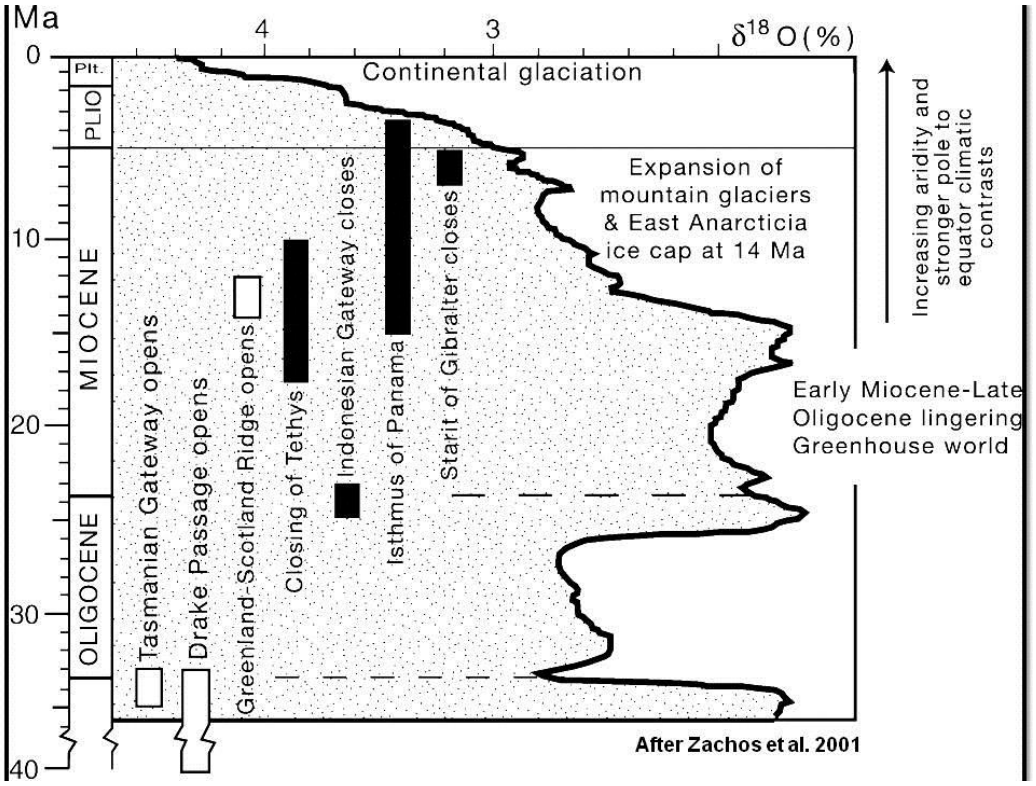

Figure 1.1. Global events during Late Cenozoic and associated atmospheric events in the Middle and Upper Miocene. Taken from Zachos et al. (2001).

In South America, the Andes developed most of their present form in the Middle and Late Miocene. In North America, the northern part of the San Andreas Fault developed throughout the Miocene (Graham et al., 1989). There was widespread basaltic volcanism in British Columbia, Washington, Oregon during the late Burdigalian and the Rocky Mountains began to uplift during the Middle Miocene (Christiansen and Yeats, 1992).

All this global tectonic activity, especially in the Middle and Late Miocene, coincided with increased desertification, alpine glaciation and the growth of the Antarctic ice sheet (Potter and Szatmari, 2009). The linkage between tectonics and climate will be discussed in the next section of this chapter.

1.4.2. Global climate trends

Compared with today, the Miocene climate was considerably warmer (Scotese, 2011); however, there were a number of climate fluctuations during this interval. A warming trend is recognised from the latest Oligocene to the Middle Miocene, as indicated by deep-sea $\delta^{18}O$ values (Miller et al., 1991; Wright et al., 1992; Zachos et al., 2001) (Figure 1.2). This trend kept Antarctica ice masses relatively subdued and bottom water temperatures were slightly higher than present, with the exception of some aberrant brief but deep glaciation periods (24 Ma). Peak warmth occurred in the late Middle Miocene (14-16 Ma), the warmest interval in the entire Neogene (Miller et al., 1991). Thereafter, gradual cooling established, and the Antarctic ice-sheets grew throughout the latest Miocene (Zachos et al., 2001) as indicated by a gentle rise in $\delta^{18}O$ values (Figure 1.2). Increasing ice volume on Antarctica during the Miocene steepened the latitudinal thermal gradients and caused sea-level fluctuations (Cane and Molnar, 2001).

A well agreed major event is recognized as causing the end of the warming trend during the Middle Miocene and initiating a subsequent cooling effect: the closure of the eastern portal of the Tethyan seaway which enhanced the poleward heat transport and strengthened the Southern ocean circumpolar circulation (Kennet et al., 1985). In addition, another important factor was a decline of carbon dioxide concentrations, which has been linked to an intensification of the Asian Monsoon after 15 Ma (Ramstein et al., 1997), the erosion of the Himalayan belt (Goddéris and François, 1996; France-Lanord and Derry, 1997) and the uplift of the Andean Cordillera (Lagabrielle et al., 2009).

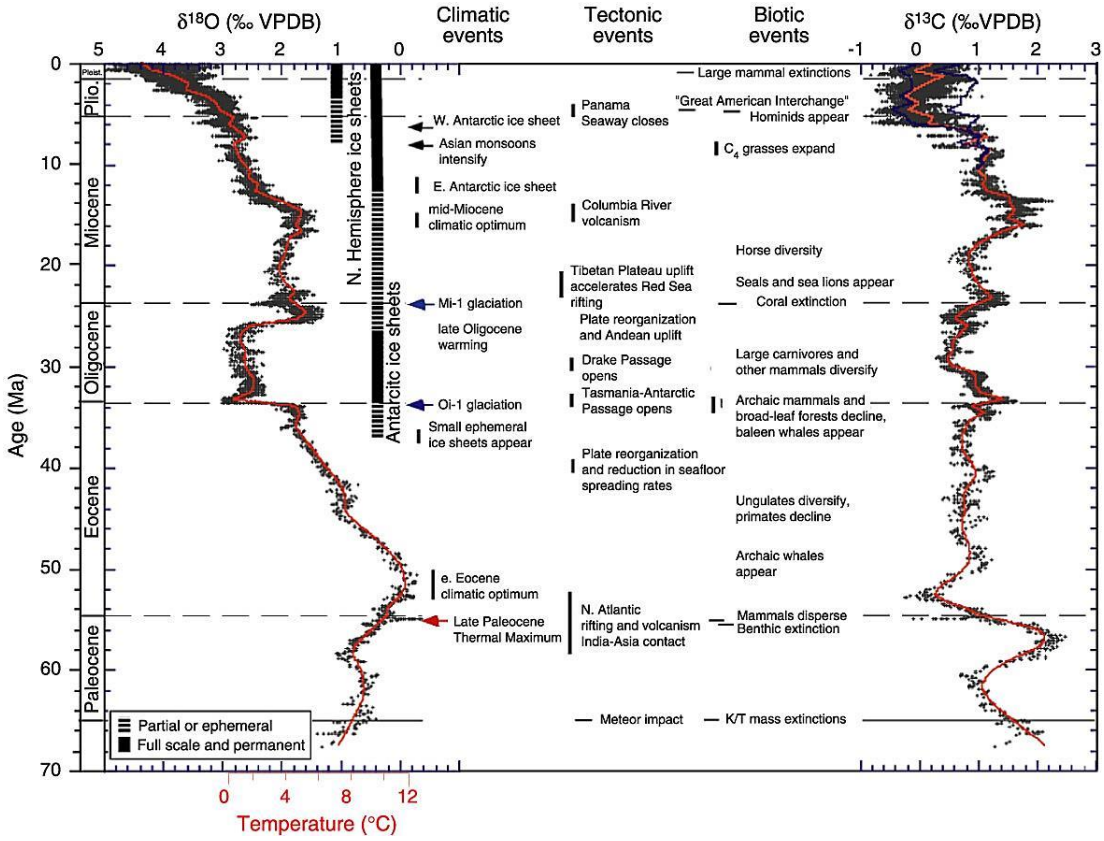

Figure 1.2. Temperature trends, global deep-sea oxygen and carbon isotope records for the past 70 million years. The Miocene shows a gradual decrease in temperatures with the maximum temperatures occurring in the Middle Miocene as indicated by the positive excursion in the delta 18 O data. Taken from Zachos et al. (2001).

The effect of Miocene cooling on terrestrial ecosystems was profound. There was a general expansion of deserts across all the continents at mid-latitudes during the Middle and Late Miocene. For example, in Asia, the combination of the rising of mountains in the Himalayas and the progressive closing of the Tethyan Ocean is synchronous with an increase in aridification and grassland biomes (Ramstein et al., 1997). Overall, the Miocene witnessed some major climatic changes clearly reflected in the floral and faunal composition, migrations and evolution, e.g., wide development of tundra biomes and grasslands (Bliss et al., 1981; Thomasson 1991; Behrensmeyer and Potts, 1992) as described in detail below.

1.4.3. Miocene savannas with special reference to the Americas

The spread of grass savannas and associated fauna is broadly recognized in the Miocene (Janis, 1993). Especially in North America, several studies have pointed to expanded open vegetation (Webb, 1977; Webb, 1984). Therefore, even though grass systems are first reported back as far as the Eocene, or earlier, C4 plants and modern grasslands did not dominate until 7 Ma (Leopold et al., 1992; Janis, 1993; Retallack, 2001). Recent studies in Central America show strong affinities between the taxa found there and those in North American savanna-adapted faunas (Macfadden and Higgins, 2004; MacFadden, 2006; Kirby, 2008; MacFadden, et al, 2010), supporting the interpretations of an expanded area for this ecosystem during the Miocene. A trend can be, also, detected in the transition from the Late Miocene to the Pleistocene in Asia, with faunal changes to more savanna-like conditions (Barry et al., 1985; Barry et al., 1991), coinciding with a shifting from C3 to C4 plants, although C4 plants were still not dominant until the Middle Pleistocene (Cerling et al., 1991).

In Colombia and Western Venezuela, palynological analyses show a strong correlation between diversity fluctuations and global climatic changes from Cretaceous to Pleistocene (Jaramillo et al., 2006). For the epoch of thermal maximum (Eocene) the floras are considerably more diverse than Holocene floras; however when early Miocene and Holocene are compared in terms of floristic diversity, a lower level is clear for the Miocene, although this could be taphonomic bias (Jaramillo et al., 2006).

In contrast, there has been a steady decline in the abundance and diversity of browsing mammals since the early Miocene (Janis and Damuth 1990; MacFadden 2000), including a major faunal turnover in the Late Miocene, the dispersal of hipparonid horses from North America (Bernor et al., 1989), and the diversification of more open-habitat hominoids (Bernor, 1984). However, Janis (1993) states that despite

the recognition of the "*Hipparion* fauna" as a typical savanna community, microwear studies of teeth reveal a mixed browsing-grazing diet different from the fully grazing diet of living equids. Therefore these faunas were more likely adapted to "wooded grasslands" rather than open savannas.

From the Middle to Late Miocene time, as noted above, an extensive desertification occurred, especially in mid-latitudes, as a result of mountain uplift combined with the closure of the Tethyan Ocean (Medeanic, 2002; Maki et al., 2003; Velichko and Spasskaya, 2003; Velichko, 2005). Other remarkable evidences for the global expansion of dry areas are comprised in Retallack's paleosol studies. Calcic horizons in paleosols are closely related to grassland environments (Retallack, 1994; Retallack, 2001). Retallack found these indicators at depths of 40 cm or less for the Lower and Middle Miocene. For the Late Miocene the depths go down to 1 mm, evidencing an expansion of grasslands at about 6-7 Ma into wetter zones (Retallack, 2001).

1.5. PANAMA DURING THE MIOCENE

The Isthmus of Panama is located in Central America between Costa Rica and Colombia with coasts in both the Pacific and the Caribbean seas. It is located between the geographical coordinates, 7º12'07"N and 9º38'46" N and 77º09'24"W and 83º03'07" 7° W. Its total area comprises 75,517 km^2, it is 772 km in length, and is 60-177 km in width. The highest point is the Volcán Barú (formerly known as the Volcán de Chiriquí), which rises to 3,475 m (ATP, 2011) (Figure 1.3).

Figure 1.3. Satellite image of the Isthmus of Panama and its location in America. After Arauz (2004).

1.5.1. Tectonic hypothesis for convergence of Americas

Although still incompletely understood, there is a growing consensus that the Panama Isthmus formed through the uplift of a jumble of small allochthonous terranes caught between the Farallon, Cocos and Nazca plates to the south and the Caribbean Plate to the north, in response to the northward convergence of South America (Case et al., 1984) (Figure 1.4). There are two hypotheses about the nature and evolution of the Panama Isthmus in early Miocene times: (1) the isthmus region comprised a continuous southernmost peninsula of North America and (2) the isthmus region comprised a disconnected archipelago of volcanic islands (an island arc) extending south from North America. The Peninsula Hypothesis (Figure 1.5, Figure 1.6) is supported by the close similarity between Panamanian and North American mammals (Whitmore and Stewart, 1965; Kirby and McFadden, 2005) and also by inferences about body size, which are

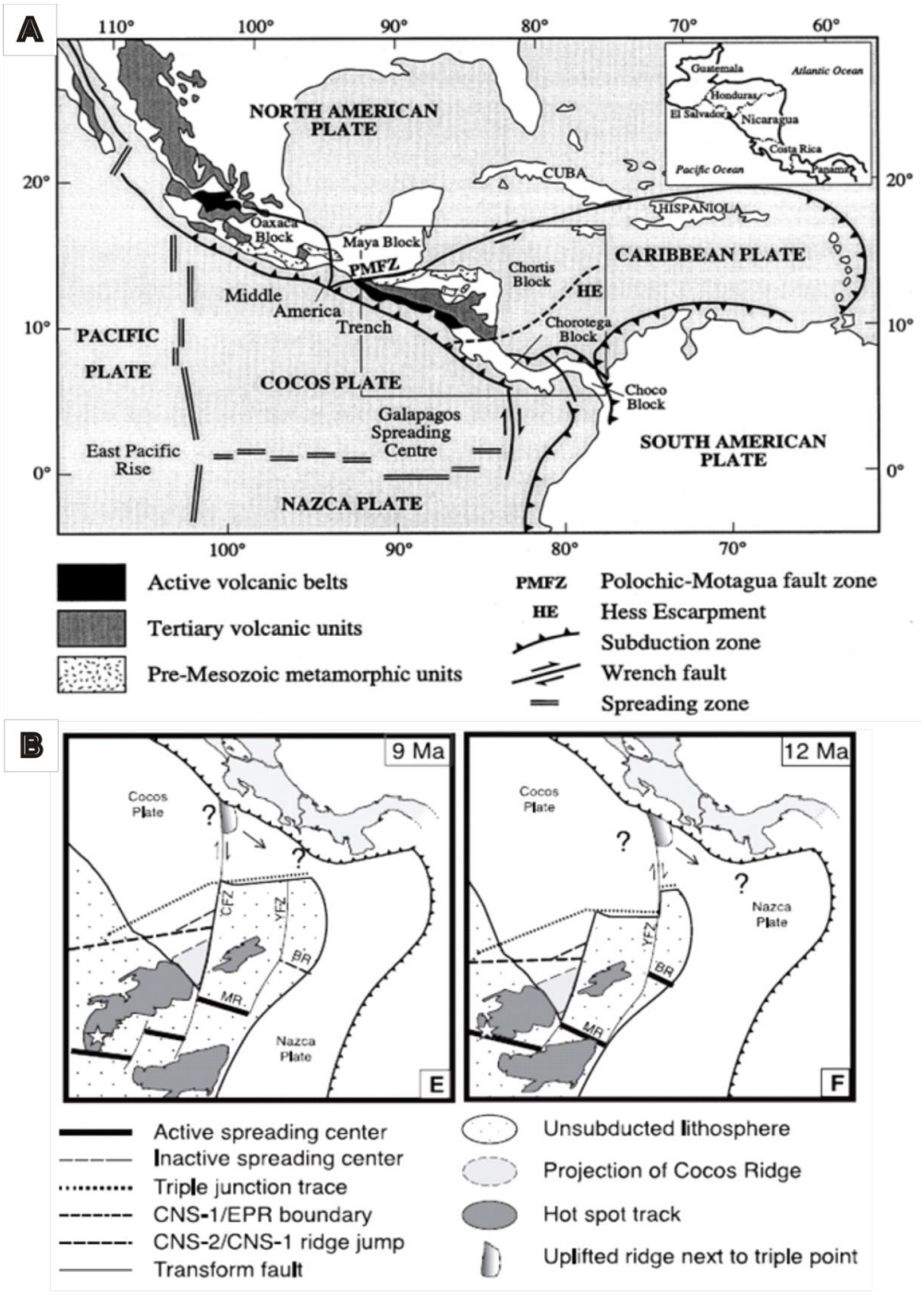

Figure 1.4. A) Major crustal blocks of Central America (from Elming et al., 2001). (B). Plate reconstructions of Central America from Middle to Late Miocene. Taken from MacMillan et al., (2004).

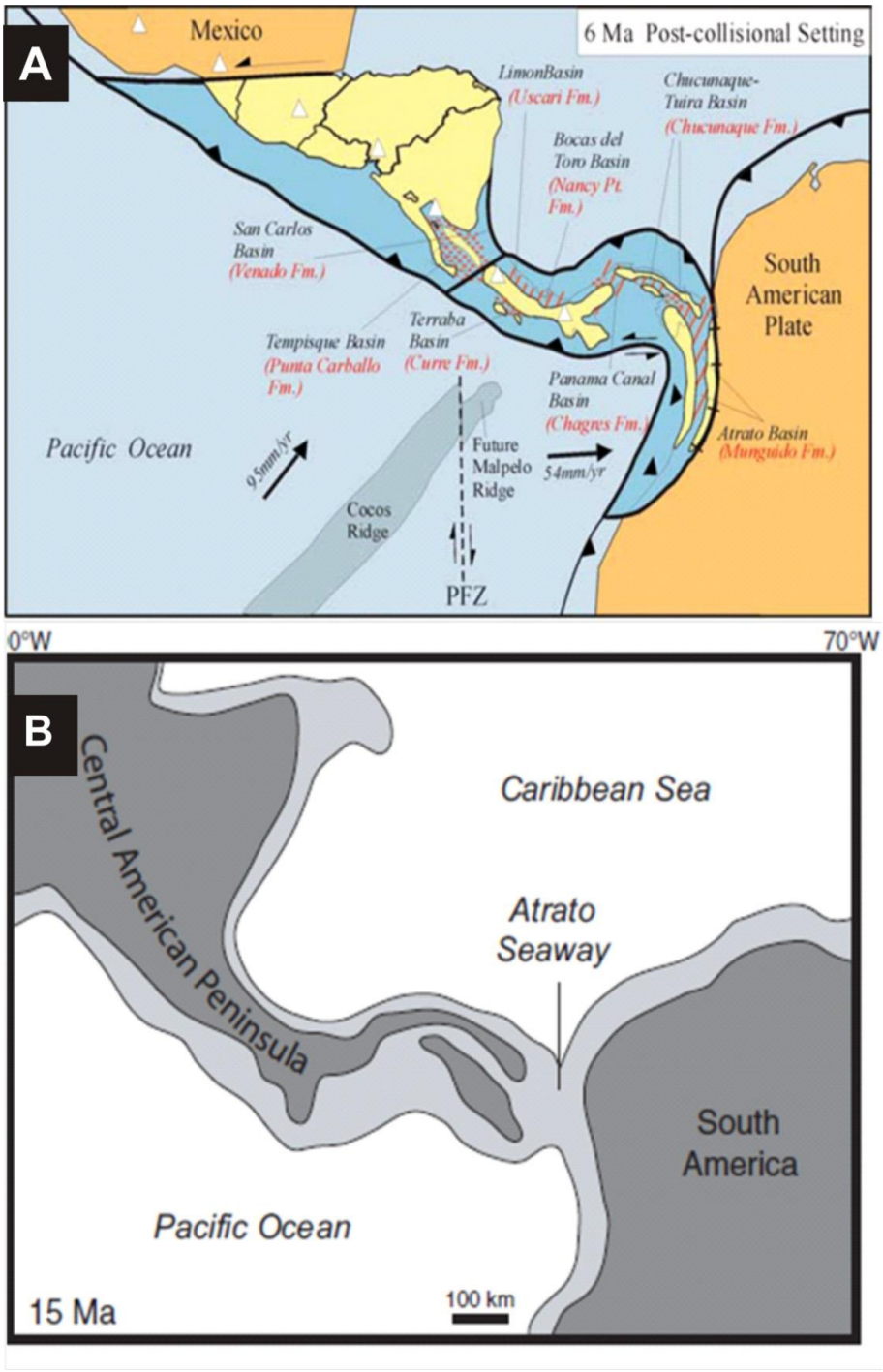

Figure 1.5. Contrasting reconstructions of Panama for the Miocene. (A) Last stage of the interpretation of Panama as an island and an arch of islands (from Coates et al., 2003). (B) Interpretation of Panama as a peninsula attached to North America. Taken from Kirby et al. (2007).

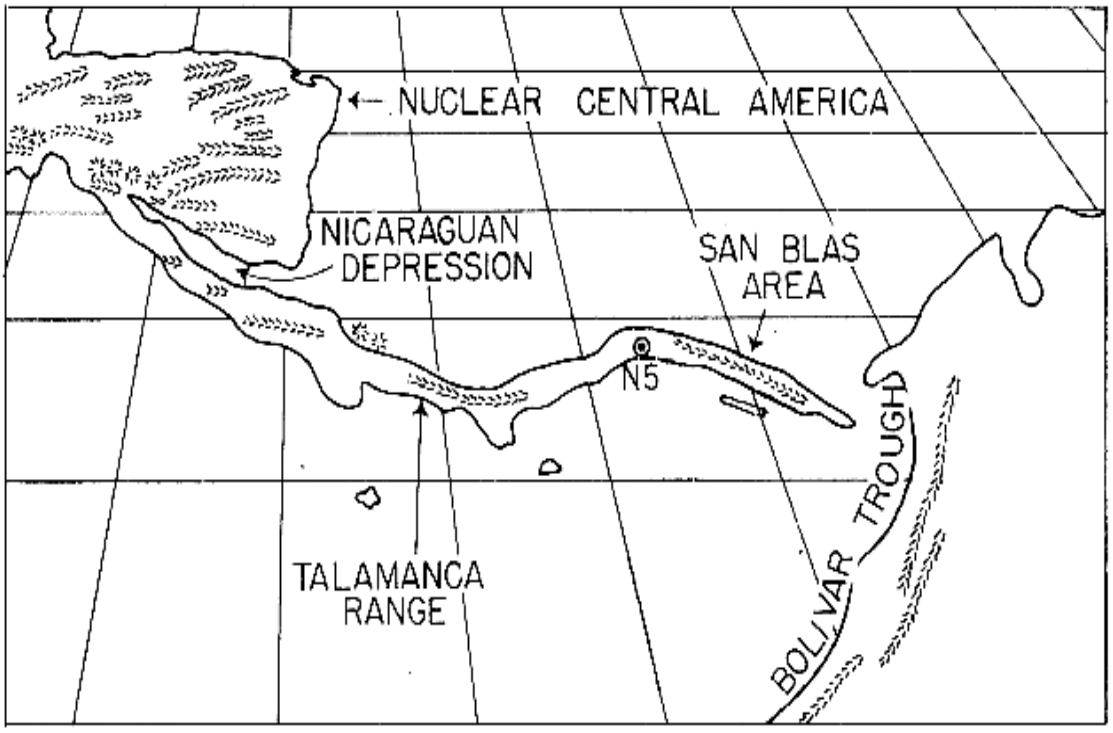

Figure 1.6. Early proposed reconstruction of Panama as a peninsula. Taken from Whitmore and Stewart (1965).

inconsistent with concepts of island biogeography (Kirby and MacFadden, 2005). The Archipelago Hypothesis (Figure 1.5) is supported by geological studies of isolated outcrops, biostratigraphic and radiometric dating, and paleobathymetric data from benthic foraminifera (Coates and Obando, 1996; Coates et al., 2004). Whichever hypothesis is correct, marine units in Panama show that a moderately deep, but narrow, marine seaway, represented by sediments of the Punta Alegre Formation, connected northwestern Panama to the Pacific along a portion of the Central American Seaway in early Miocene times (c. 18.5 – 21.5 Ma; Coates et al., 2003). The seaway shallowed significantly by the Middle Miocene, and by latest Middle Miocene times, the pre-isthmian Bocas del Toro region shallowed even further, so that by ~ 12 Ma there existed

a substantial subaerial volcanic backarc parallel to the main Central Cordilleran arc (Montes et al., 2012). However, the degree to which this feature facilitated intercontinental biotic exchange is currently uncertain.

1.5.2. The Panama Canal Basin, and its stratigraphy

The Panama Canal Basin (Figure 1.7) is a Paleogene structural and depositional basin that straddles the tectonic boundary between the Chorotega and Choco blocks of the Panama microplate (Coates and Obando, 1996; Coates, 1999). It contains a thick sequence of sediments and volcanic rocks (2900 m) of Eocene to Pleistocene age (Stewart et al., 1980; Jones, 1950; Escalante, 1990). The lowermost sedimentary unit is the Eocene Gatuncillo Formation, which contains marine mudstone, siltstone and limestone, and unconformably overlies pre-Paleogene volcanic basement (Woodring, 1957-1982; Escalante, 1990).

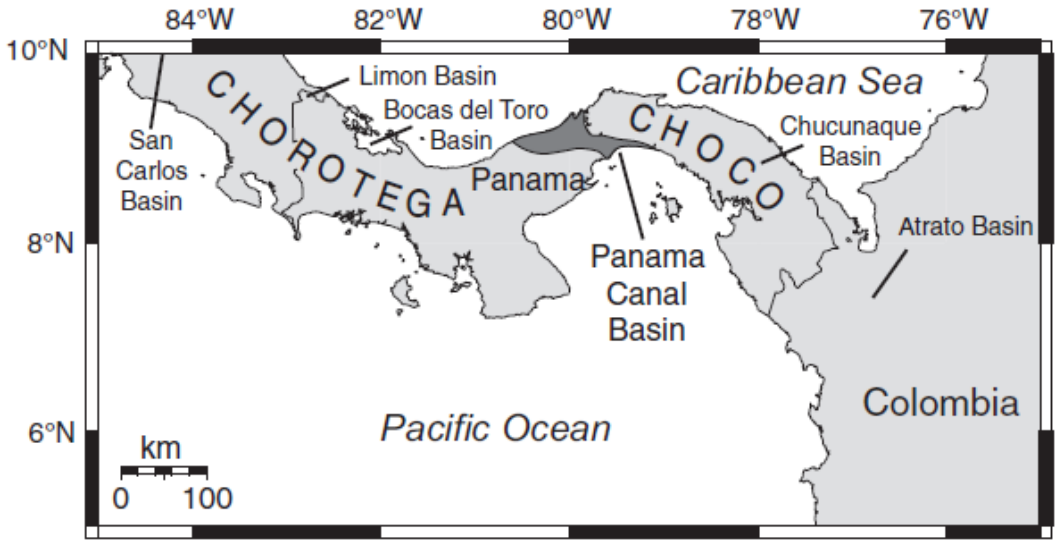

Figure 1.7. Location of the Panama Canal Basin in relation to South America. Taken from Kirby et al. (2008).

A summary of the different proposed stratigraphic distribution of the formations along the Gaillard Cut, a major section of the Panama Canal, is provided in the Figure 1.8.

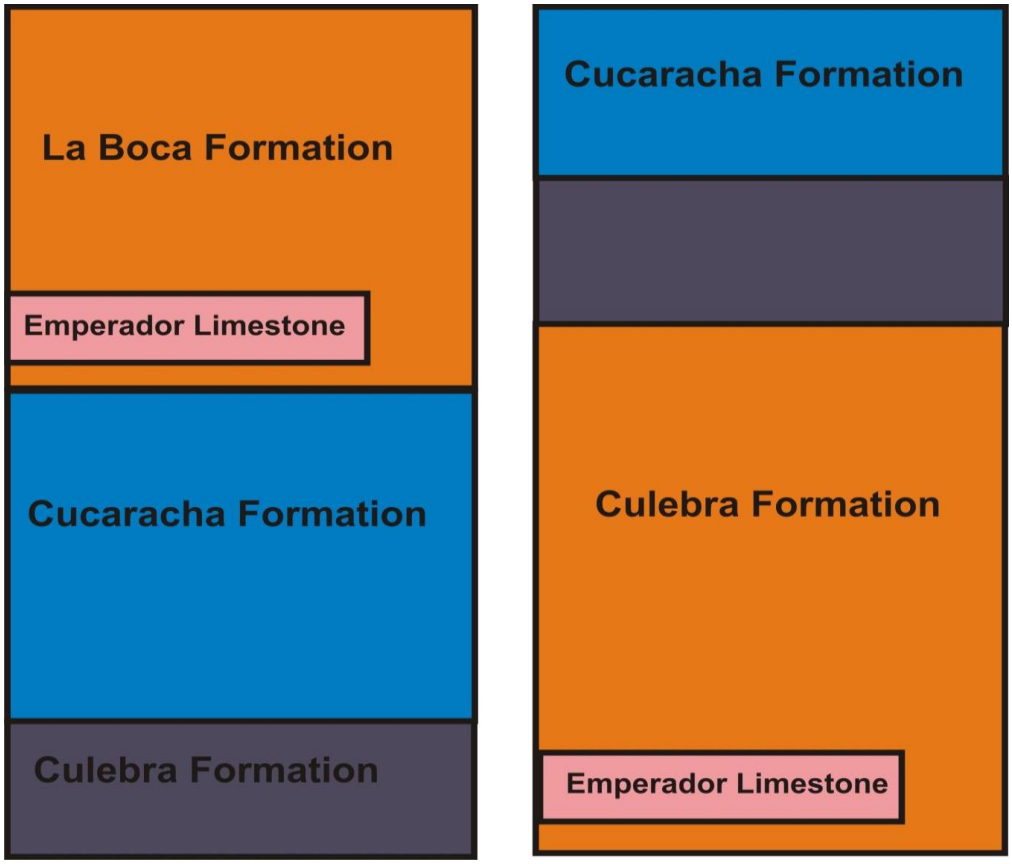

Figure 1.8. Two proposed stratigraphic models for the formations along the Gaillard Cut. A, the Culebra Model (Woodring and Thompson, 1949; Van den Bold, 1972; Escalante, 1990). B, the La Boca Model (Stewart et al., 1980; Woodring, 1964; Graham et al., (1985).

Hill (1898) was the first to formally describe and name formations around the Gaillard Cut, being followed by a series of contributions describing new formations or re-describing the position of them (Woodring and Thompson, 1949; Woodring 1974; Stewart et al., 1980; Van Der Bold, 1972). The two models in Figure 1.8 summarise over 100 years of stratigraphic models in the Gaillard Cut. The Culebra places the Cucaracha Formation underneath the Culebra Formation whereas the La Boca Model places the lower portion of the Culebra Formation into the La Boca Formation above the Cucaracha Formation. In the current understanding of the stratigraphy the Culebra Formation Model is supported and the La Boca Model is rejected based on more recent stratigraphic data (Kirby et al., 2008).

CHAPTER 2. GEOLOGICAL CONTEXT OF STUDY SITES

2.1. INTRODUCTION

This chapter describes the geological context of three new study sites located in the Gaillard Cut of the Panama Canal Zone. All fossil material was obtained from the Cucaracha Formation (Gaillard Group).

2.2. BACKGROUND OF THE CUCARACHA FORMATION

2.2.1. Previous works in the Cucaracha Formation

The construction of the Panama Canal (1904-1914) promoted paleontological studies in the Isthmus for the first time and allowed a better access to the formations in the Canal Basin. The Cucaracha Formation is particularly rich in fossil plants (seeds, woods, leaves) and mammal bones. Berry (1918) mostly described leaves and identified new taxa, e.g., *Ficus culebrensis*, *Myristicophyllum panamense*, *Mespilodaphne culebrensis*, *Melastomites culebrensis*, *Inga oligocaenica*, *Cassia culebrensis.* Other taxa were defined from the study of woods (*Palmoxylon palmacites*, *Taenioxylon multiradiatum*). In 1919, Francis MacDonald, a geologist of the Panama Canal Commission published stratigraphic logs and geological maps of the Panama Canal Zone (Woodring, 1955). Later, geological maps of the Panama Canal Zone and adjoining areas were published by Woodring (1955, 1981).

The first faunal list of fossils from the Cucaracha Formation was provided in Withmore and Stewart (1965). The identified mammal taxa had exclusive affinity with North America and brought controversy to the traditional thinking of the Miocene

Isthmus conformation. Further studies on mammal were undertaken, e.g., Patton and Taylor (1973), Slaughter (1981).

Palynological studies were also undertaken by Graham (1988). Most of the identified pollen grains were related to marsh settings (e.g., *Achrostichum*) and suggested coastal setting. Other identified taxa in pollen grains from the Cucaracha Fm include: *Manicaria* and *Crysophila* (Arecaceae), *Ilex* (Aquifoliaceae), *Alchornea* (Euphorbiaceae), *Alfaroa/Engelhardia* (Juglandaceae), *Crudia* (Fabaceae), *Eugenia/Myrcia* (Myrtaceae), *Rizophora* (Rhizophoraceae) and some grains of Asteraceae (Graham, 1988).

Herrera et al., (2010) retrieved endocarps of *Sacoglottis* (*S. tertiaria*, Humiriaceae), an element of lowland rainforests. Other families have been reported from endocarps collected in the Cucaracha Formation such as Anacardiaceae, Annonaceae, Araceae, Arecaceae, Cannabaceae, Chrysobalanaceae, Euphorbiaceae, Fabaceae, Icacinaceae, Lauraceae, Malpighiaceae, Malvaceae, Meliaceae, Menispermaceae, Salicaceae, Sapotaceae, Vitaceae (Herrera et al., 2010, 2012).

Fossil mammals are also abundant in the formation, thus several studies have been done, including: MacFadden and Higgins (2004), performed Carbon analysis to determine the dominance of C3 plants; Kirby and MacFadden (2005) analysed tooth size as a proxy for body size, which confirmed similarity with North American taxa and with no insular size effect; MacFadden (2006), described *Tomarctus brevirostris*, a Hemingfordian Canidae first reported from Colorado, U.S.A. Other mammals were studied in MacFadden (2009) and MacFadden et al., (2010).

Further studies done in the Cucaracha Formation include: Retallack and Kirby (2007) in which 12 different pedotypes that represent vegetation types, including

mangrove, freshwater swamp, marine-influenced swamp, early successional riparian woodland, colonizing forest, dry tropical forest and woodland were recognised; Head et al., (2012) reported boid snakes; Cadena et al. (2012) described and reported new turtles. Montes et al. (2012), presented a complete geochronological analysis of the Panama Canal Formations. Hastings et al., (2013) studied crocodilians.

2.2.2. Age of formation

The Cucaracha Formation conformably overlies the Culebra Formation, which contains a rich marine fauna in its lower part (Retallack and Kirby, 2007; Hendy, 2011) of Lower Miocene (Aquitanian age) (Figure 2.1), and has yielded Lower Miocene (early Burdigalian) strontium dates of 19.38 – 19.12 Ma in its upper part (Kirby et al., 2008). The Cucaracha Formation conformably underlies basalts and agglomerates in the lower part of Pedro Miguel Formation (Figure 2.2). A radiometric date of 18.4 ± 1.07 Ma was obtained from these volcanic strata in a different area, indicative of a Lower Miocene (mid- to late Burdigalian age; Wegner et al., 2011); however, its exact stratigraphic position in relation to the studied section herein is uncertain (Montes et al., 2012 (Figure 2.2). Detrital zircon populations with maximal ages of 19 – 20 Ma (early Burdigalian) were recovered from the upper part of the Culebra Formation and the lower part of the Cucaracha Formation (Montes et al., 2012).

The charcoalified woods preserved in growth position are directly below a 1-m-thick welded silicic tuff near the top of the Formation, named the "Cucaracha Tuff" which has been recently dated with Pb/U analysis, giving a mean age of 18.81± 0.30 Ma (MacFadden et al., 2014). These absolute dates are in generally good agreement with relative ages for the Cucaracha Formation based on its mammalian assemblage, found in its upper part, which includes seven North American species typical of the

Hemingfordian-early Bastovian regional stages (Lower Miocene, Burdigalian – early Langhian; MacFadden and Higgins, 2004; MacFadden, 2006) as well (Figure 2.1) as magnetostratigraphic inferences (McFadden et al., 2014).

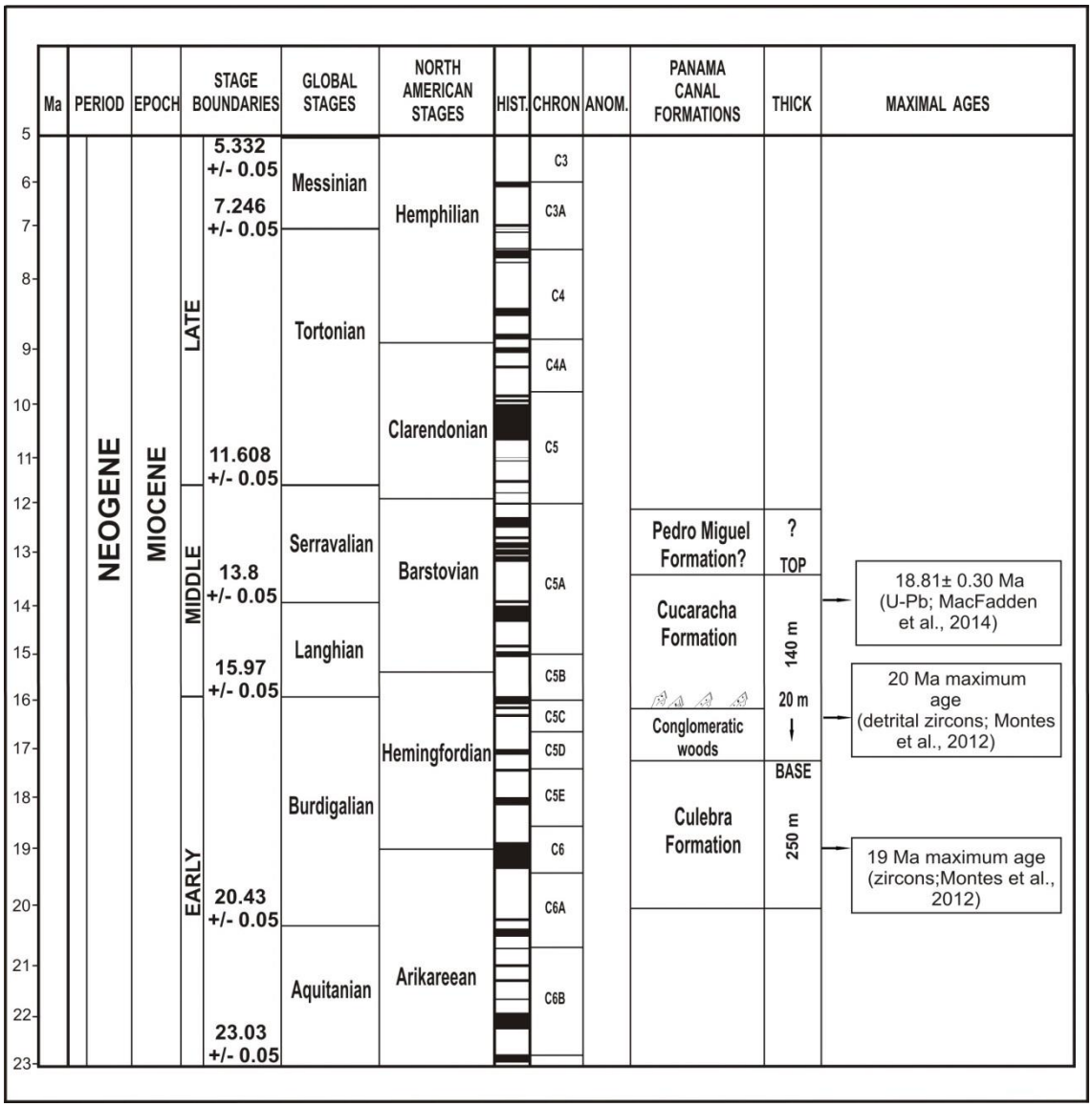

Figure 2.1. Miocene chart showing stratigraphic position of fossil wood assemblages and age data.

The fossil woods described here come from two intervals, the lowermost assemblage – a calcified permineralised assemblage – is positioned ~ 20 m above the base of the Cucaracha Formation, and is therefore, probably, of early to mid-Burdigalian age. The uppermost fossils – a charcoalified assemblages – is positioned 70

m above the base of the formation, directly beneath the welded silicic (Cucaracha) tuff, and is therefore precisely dated (see radiometric data above) and no younger than mid-Burdigalian age (Figure 2.2).

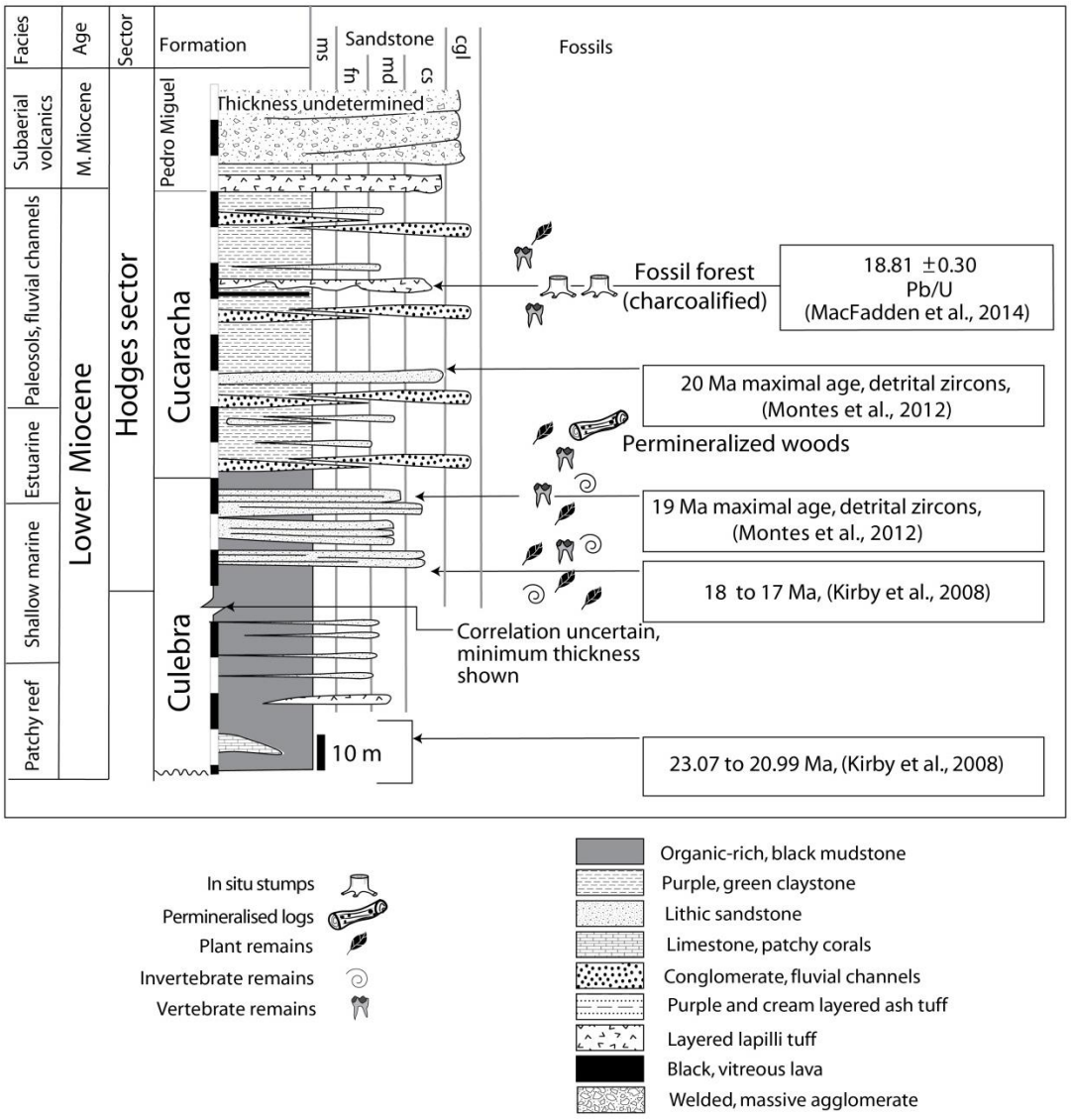

Figure 2.2. Stratigraphic log of the Cucaracha Formation. After Montes et al. (2012).

2.2.3. Stratigraphic succession

The Cucaracha Formation is about 140 m thick and consists mostly of claystone with a minor amount of conglomerate, sandstone, and welded tuff (Figure 2.2). A

distinctive pebble conglomerate bed with volcanic pebble clasts and fragments of oyster and woods marks the base of the Cucaracha Formation and the succession is generally interpreted as a volcanically-influenced fluvial floodplain. Two horizons contain spherical to platy barite nodules (2 cm in diameter) in olive-gray claystone (Kirby et al., 2008). Retallack and Kirby (2007) recognized 12 different pedotypes in the formation (Figure 2.3) that represent the soils of many vegetation types, including mangrove, freshwater swamp, marine-influenced swamp, early successional riparian woodland, colonizing forest, dry tropical forest and woodland (Kirby et. al, 2008). Paleosols indicate periods of stability in between fluvial events of thousands to tens of thousands of years when soils developed on flood-basin or channel deposits (Retallack, 2001).

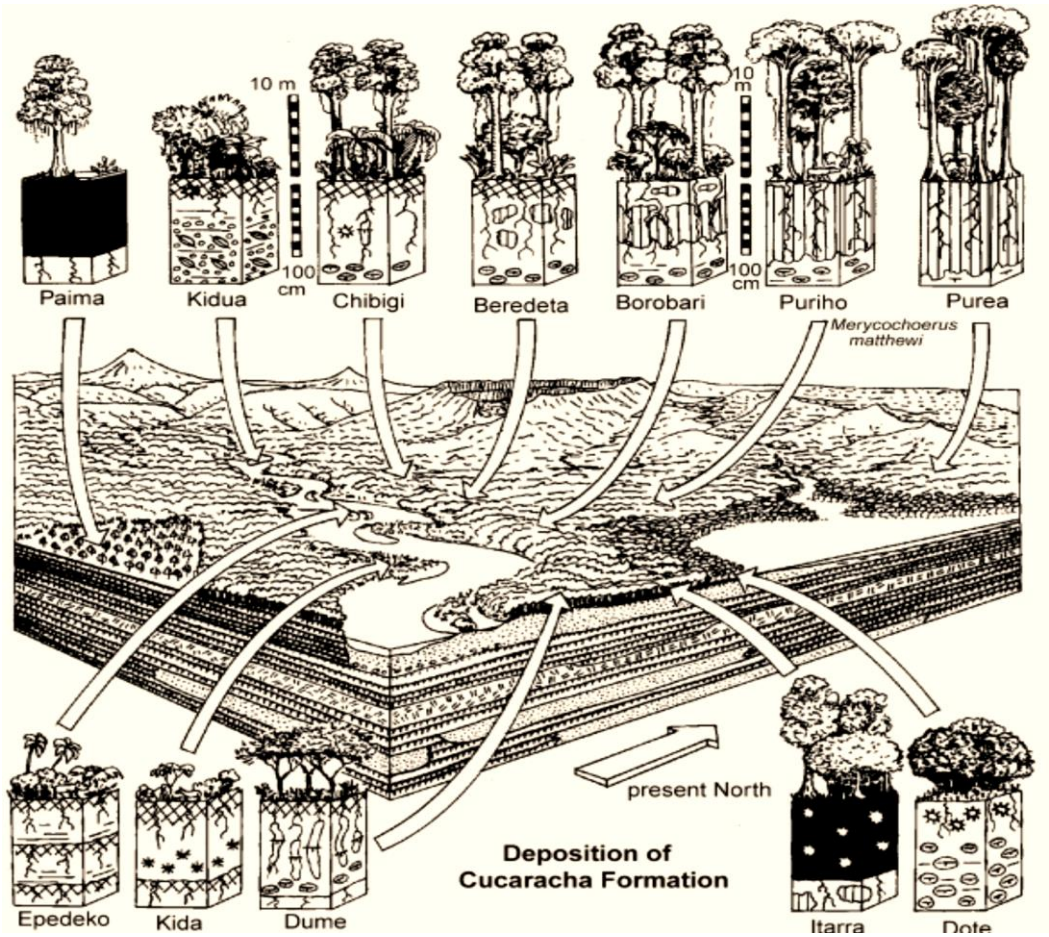

Figure 2.3. Reconstruction of soils and vegetation for the Cucaracha Formation. After Retallack and Kirby, (2007).

2.2.4. Fossil fauna of the Cucaracha Formation

The first extensive paleontological studies were undertaken as a result of the initial construction of the Panama Canal in 1914 (see section 2.2.1). The first faunal lists published by Stewart (1960) were subsequently published in several other works (e.g., Whitmore and Stewart, 1965; Tedford, 1970; Ferrusquía-Villafranca, 1978; Rich and Rich, 1983; Tedford et. al, 1987; Slaughter, 1981).

More recently, mammal taxa found along the Cucaracha Formation include *Paratoceras wardi, Merycochoerus matthewi, Menoceras barbouri* and *Floridaceras whitei,* which are highlighted by MacFadden (2004) and Kirby et al. (2008) as fauna with exclusive North American affinities (Table 2.1). They contrast with South America faunas of the same age found La Venta in Colombia (Whitmore and Stewart, 1965). The mammals found in the Cucaracha Formation were also identified at other localities only a few kilometers from the end of the San Blas area of north Central America. This finding is the key factor supporting the hypothesis that Panama was a peninsula attached to North America during the Miocene (See figure 1.6 for the original model of Whitmore and Stewart, 1965).

A particularly remarkable discovery was the specimens of *"Cynorca" occidentale* reported by the Paleontology team of University of Florida (UF) and CTPA, collected in the lower two-thirds of the Cucaracha Formation. Although such peccaries were biogeographically widespread in the Americas, these fossils provide evidence for the antiquity of the family Tayassuidae and the subfamily Tayassunnae in particular (MacFadden et al., 2010). The abundance of the peccaries in this locality raises questions about which kind of habitats were being exploited by these mammals, since they had a diverse range of habitats today, but particular favour open scrub.

Species	Reference	Common name	Biogeographic affinity
*Protoceratidae	Whitmore and Stewart, 1965	Slenodont artiodactyl	North America
Tomarctus brevirostris	MacFadden and Higgins, 2004	dog	North America
Amphicyonidae-Hemicyonidae MacFadden	MacFadden and Higgins, 2004	extinct bear-dog	North America
Cynorca sp	Kirby and MacFadden, 2005	extinct peccary	North America
Merycochoerus matthewi	MacFadden and Higgins, 2004	piglike oreodont	North America
Paratoceras wardi	MacFadden and Higgins, 2004	small protoceratid cameloid	North America
Anchitherium clarenci	MacFadden and Higgins, 2004	large browsing horse	North America
Archaeohippus sp. indet.	MacFadden and Higgins, 2004	small browsing horse	North America
Menoceras barbouri	MacFadden and Higgins, 2004	small two horn rhinoceros	North America
Floridaceras whitei	MacFadden and Higgins, 2004	large rhinoceros	North America
Texomys stewarti	MacFAdden and Higgins, 2004	pocket gopher	North America
"Cynorca" occidentale	MacFadden et al., 2010	peccary	North America

Table 2.1. Most common fossil mammals from the Cucaracha Formation found by Whitmore and Stewart (1965).

2.2.5. Fossil flora of the Cucaracha Formation

The plant fossil record of the Cucaracha Formation is summarised in Table 2.2. All of Berry's fossil plant records comprised new taxa for America, except for *Hyeronima*, *Palmoxylon* and *Taenoxylum* which are common in other Miocene formations in North and South America (e.g., Felix, 1882-1886; Martinez-Cabrera et al., 2006; Thomas and De Franceschi, 2012). The families that Berry identified included similar taxa to the dominant families of present day in Panama, except for Sterculiaceae, Tiliaceae and Anacardiaceae and some families of monocotyledonous plants, such as Cyperaceae and Poaceae. Berry (1918) concluded that the assemblage represented a typical rain forest community very similar to the present forests in Panama, based on the lack of discoveries of mountainous forests indicators. It is important to note that several of the Berry's identifications have been revised and occasionally there are misidentifications (e.g., Herrera et al., 2014). Hence, these results should be considered cautiously.

The extensive palynological discoveries of Graham (see section 2.2.1) in the Cucaracha Formation (1988), suggested typical estuarine habitats in tectonically unstable regions. The number of palaeocommunities revealed by the pollen in Cucaracha Formation is limited, including tropical wet, moist and sub-montane forests. It is very noticeable that Graham (1988) never found any pollen grains of Poaceae or other taxa associated with savannah habitats or dry vegetation.

The identifications of the more recently retrieved seeds and endocarps from the Cucaracha Formation revealed a mix of elements from North and South America adapted to warm and wet conditions (Herrera et al., 2010, 2012, 2014) (Table 2.2).

Family	Genus/Species	Organ	Reference	Extant distribution of the family
Cyatheaceae	*Cyathea*	pollen and spores	Graham, 1988	moist environments
Pteridaceae	*Achrostichum*	fern pinnules	*Berry, 1918	related to mangrove and coastal biomes
Pteridaceae	*Ceratopteris*	pollen and spores	Graham, 1988	Pantropical
Vittariaceae	*Antrophyum*	pollen and spores	Graham, 1988	Tropical
Anacardiaceae	*Spondias*	endocarp	Herrera et al., 2012	pantropical
Anacardiaceae	*?Pentoperculum*	endocarp	Herrera et al., 2012	pantropical
Arecaceae	*Palmoxylon palmacites*	wood/vascular bundles	*Berry, 1918	tropical
Arecaceae	*Crysophila*	pollen and spores	Graham, 1988	tropical
Arecaceae	*Manicaria*	pollen and spores	Graham, 1988	tropical
Arecaceae		endocarp	Herrera et al., 2012	pantropical
Aquifoliaceae	*Illex*	pollen and spores	Graham, 1988	mostly America and South East Asia-Malasya
Annonaceae	*Guatteria culebrensis*	leaf	*Berry, 1918	tropical
Asteraceae		Pollen and spores	Graham, 1988	worldwide
Cannabaceae		endocarp	Herrera et al., 2012	worldwide
Chrysobalanaceae	Parinari	endocarp	Herrera et al., 2012	pantropical
Euphorbiaceae	*Alchornea*	Pollen and spores	Graham, 1988	pantropical,
Euphorbiaceae		seed	Herrera et al., 2012	pantropical
Fabaceae	*Crudia*	pollen and spores	Graham, 1988	pantropical; dominates dry tropical forests
Fabaceae	*Inga oligocaenica*	leaf	*Berry, 1918	tropical; dominates dry tropical forests
Fabaceae	*Schwartzia*	wood	Whitmore and Stewart, 1965	tropical, dominates dry tropical forests
Fabaceae	*Taenoxylum multiradiatum*	wood	*Berry, 1918	tropical; dominates dry tropical forest
Humiriaceae	*Sacoglottis tertiaria*	endocarp	Herrera et al., 2010	rainforests
Icacinaceae		endocarp	Herrera et al., 2012	North temperate to Argentina
Juglandaceae	*Alfaroa/Englehar-dia*	pollen and spores	Graham, 1988	and Malaysia
Lauraceae	Mespilodaphne culebrensis	leaf	*Berry, 1918	lowland-montane forests
Malpighiaceae	*Banistieria praenuntia*	leaf	*Berry, 1918	tropical
Moraceae	*Ficus*	leaf	*Berry, 1918	mostly tropical warm
Myristicaceae	*Myristicophyllum panamense*	leaf	*Berry, 1918	pantropical
Myristicaceae		seed	Herrera et al., 2012	Mostly tropical to
Myrtaceae	*Eugenia/Myrcia*	pollen and spores	Graham, 1988	warm temperates
Passifloraceae		seed	Herrera et al., 2012	tropical
Rizophoraceae	*Rizophora*	pollen and spores	Graham, 1988	worldwide/Mangrove
Vitaceae	*Cissus*	seed	Herrera et al., 2012	Europe, North America and South America

Table 2.2. Summary of plant fossil record in the Cucaracha Formation. * identifications have been revised

2.3. NEW FIELD INVESTIGATIONS: LOCALITIES AND CORRELATION

Three extensive, but somewhat weathered, slope-forming outcrops were studied in the course of my own research along the southwest side of the Panama Canal, in the narrowest part of the canal called Gaillard Cut, approximately 14 km WNW of Panama City (Figure 2.4). The three sites expose the Cucaracha Formation and are spaced along a 2.8 km NW-SW transects. Here the formation is ~65 m thick. The localities are: Centenario Bridge (09°01'42.65''N; 79°38'04.90''W; Contractors Hill (09°02'21.57''N; 79°38'46.39''W) and Hodges Hill (09°02'51.75''N; 79°39'14.02''W). These localities are correlated by means of a distinctive welded silicic tuff unit (Figure 2.5) (The Cucaracha Tuff; for radiometric dates see McFadden et al., 2014)

Figure 2.4. Google Earth image of the southern part of the Panama Canal, showing the three localities studied in this thesis.

Figure 2.5. Localities correlated by distinct tuff unit. A, Overview of Centenario Bridge (scribble marks the charred wood layer). B, one of the few sections in Centenario Bridge with exposure of the charred layer with stumps (TSL). C, scribble marks charred layer with stumps in Contractors Hill (marked by lines), "T" marks the overlying tuff. D, log engulfed in volcanic material, it shows the transition of “top soil level” (TSL) of stumps and overlying tuff. Centenario Bridge seen from the Hodges Hill locality. F, poorly exposed charred layer in Hodges Hill (highlighted).

2.4. SEDIMENTARY FACIES

Three major facies from oldest to youngest are observed in the new sections as described below:

2.4.1. Description

Facies 1: The most common facies comprises mudstone-dominated units, tens of meters thick, with thin (0.1-0.2 m) sandstone sheets. These were categorized as structureless to slickensided claystone by Kirby et al. (2008), and interpreted as paleosols. Paleosols are commonly developed, and include red mottled units with prominent carbonate rhizoconcretions (Figure 2.6) (caliche), or grey mudstones with a hackly fracture (Figure 2.7.) and some poorly preserved pieces of woods. Very rarely, thin (0.2 m thick) units of dark platy shales with indeterminate plant axes are present.

Figure 2.6. Rhizoconcretions in Facies 1.

Figure 2.7. Units of platy shales with plant fragments, representing swamp environments.

Facies 2: The base of the Cucaracha Formation is marked by a distinctive pebble conglomerate bed that lies unconformably over the Culebra Formation (Kirby et al. 2008). This can be observed in the field as poorly exposed lenses and coarse- to very coarse-grained sandstone, and their first appearance defines the lower lithostratigraphic boundary (base) of the formation. The lenses are typically tens of metres wide, 1-3 m thick, and fine upwards, but may comprise composite sheets up to 10 m thick. Locally, conglomerate lenses shallowly incise into laterally equivalent paleosols (described below). Pebbles are sub-rounded and locally show invertebrate borings while others show a haematitic varnish (indicator for dry environment). Where trough cross-beds are seen, they show herringbone beds (Figure 2.8) and bimodal palaeocurrents (100°- 280° paleoflows). At Hodges and Contractor's Hill, abundant calcified logs containing *Teredolites* borings occur in the conglomerate facies (Figure 2.9).

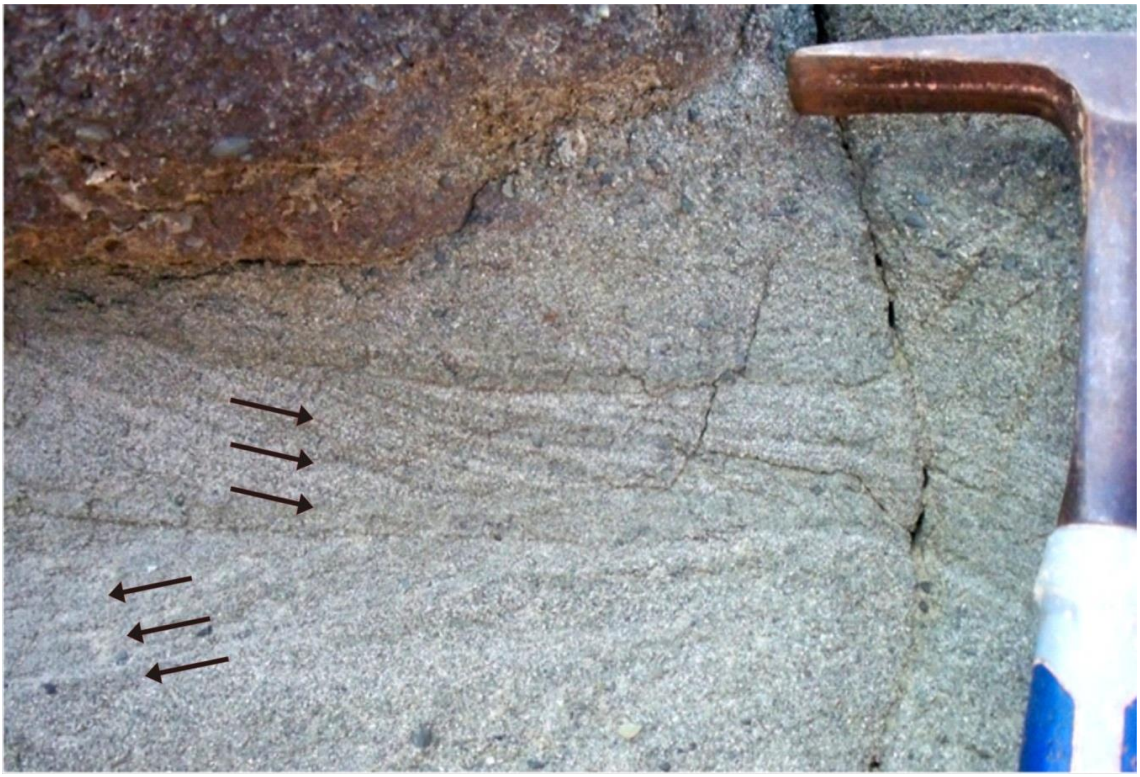

Figure 2.8. Facies 2. Bimodal paleocurrents based on cross-beds (arrows indicate direction of flows).

Figure 2.9. Facies 2. Fossil woods with abundant *Teredolites* borings (arrows).

Facies 3: A single ≤ 3.5 m thick layer in the formation comprises fine to very coarsely crystalline, graded crystal tuffs cut by steep-sided channels, up to 4 m wide and 1.5 m deep, containing welded silicic ignimbrites with strong N-S flow elongation of crystals. These entomb a fossil forest, preserved in a charred state (Figure 2.10).

Figure 2.10. Contractors Hill locality. Trunk (T) entrained in the welded ignimbrite (WI).

2.4.2. Palaeoenvironmental interpretation

The claystones that dominate the lower part of the formation (Facies 1) are interpreted as a succession of cumulative paleosols. These units represent a variety of seasonal dry to more humid soil profiles, with dark platy shales recording intermittent

swamp development. The paleosols in this formation were originally studied by Retallack (2004) and were part of the research of Master's student, Sarah Moron (University of Minnesota); hence, they were not described for this project. Fossils of mammals, turtles, fish, crocodiles and gastropods have been found in these mudstone units, as reported by Kirby et al., (2008).

The pebbly sandstone units (Facies 2) are interpreted as fluvial deposits (Miall, 1977, 1992). Based on (1) the presence of pebbles with invertebrate borings, (2) the occurrence of rare ostreid bivalve clasts, (3) the weak indications of bimodal palaeoflow, (4) the stratigraphic proximity to the shallow marine facies of the underlying Culebra Formation (Hendy, 2011), and (5) the abundant terrestrial vertebrate fossil fauna (MacFadden, 2006; MacFadden et al., 2010), these fluvial channels are interpreted as existing close to the marine coast, and could represent tidally-influenced estuaries (there is no indication of upward coarsening that might suggest a deltaic setting). This interpretation is supported by widespread *Teredolites* borings in the fossil wood, produced by xylophagous bivalves (Lane, 1959; Carlton and Ruckelshaus, 1997; Rowley, 2005) found in a broad range of marine habitats including estuaries (Cohen and Carlton, 1995; Didziulis, 2007), and reported from the Pacific Coast of Panama and Colombia (Cantera, 2010).

The welded tuff layer (Facies 3) is interpreted as hot pyroclastic flow deposit, and associated air fall deposits, which buried a fossil forest; they are described in more detail below.

2.5. FOSSIL WOOD ASSEMBLAGES

There are two fossil wood assemblages in the Cucaracha Formation: a lower permineralised association and an upper charcoalified association

2.5.1. Permineralised woods

The fossil woods are found ~ 20 m above the base of the Cucaracha Formation, and occur as an allochthonous assemblage within the pebbly sandstone beds (Facies 2) (fluvial-estuarine channel). In some parts of the Hodges Hill locality, these woods are abundant and comprise trunks, 0.4 – 3 m long and typically 0.2 – 0.6 m diameter. The fossil wood commonly contains *Teredolites* borings (Figure 2.9). These fossil woods are described in Chapters 4 - 5.

2.5.2. Charcoalified fossil forest

Geological maps of the Canal Zone show isolated volcanic cones approximately 10 km north to the studied localities (Figure 2.11) (Stewart et al, 1982). Additionally, minor volcanism has also been recorded in the Culebra Formation (a tuff at 19 ± 0.4 Ma), and more widespread younger volcanic in the Cucaracha and Pedro Miguel Formations (Woodring, 1957).

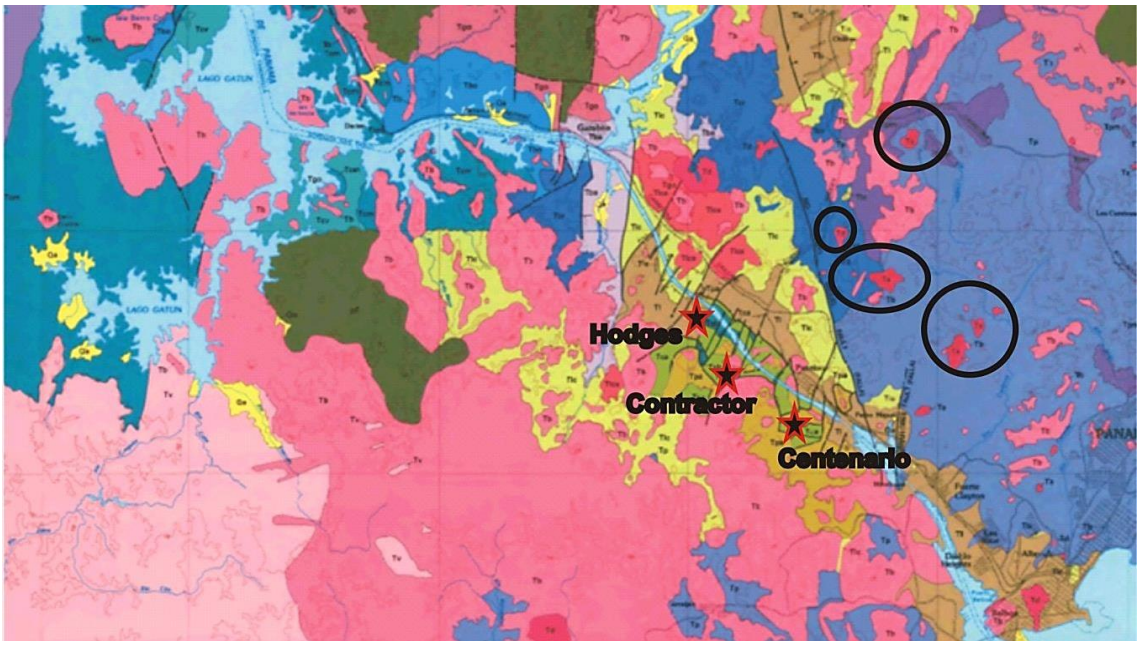

Figure 2.11.Geological Map of the Gaillard area. The circles show the volcanic cones inferred assources of the devastating pyroclastic flow and the stars show the fossil localities. Taken from Stewart et al. (1982).

A fossil forest in growth position is preserved about 20 m from the top of the Cucaracha Formation (Facies 3). A distinctive volcanic tuff (the Cucaracha Tuff), overlies and entombs the trees (Figure 2.12), and allows the forest layer to be correlated within the highly faulted outcrops, and between the three outcrops, over a distance of 2.8 km (Figure 2.11). However, the tuff and associated trees have also been encountered in boreholes, proving the total preserved extent of the fossil forest to be at least 5 km laterally (Kirby et al., 2008).

Figure 2.12. Distinctive volcanic tuff that overlies the charred wood layer. T marks the tuff and the arrow points to a tree log entombed by it. A, dicot stump with its preserved roots. B, monocot stump preserved only as a dense cluster of roots.

Crystalline pyroclastic material frequently coats the fossil wood, confirming this forest being buried by hot ashes. In general, fallen trunks are stripped of leaves and leaf bases (in the case of palms) or branches and bark (in case of dicots). These fossil woods are described in Chapter 6.

2.5.2.1 Forest layer description

The fossil forest comprises stumps in growth position rooted in a paleosol (2.5, 2.10, and 2.12) and buried by coarse (1-2 mm) crystal tuffs and welded ignimbrites, locally channelized. The paleosol is charred to a depth of 0.1–0.24 m with the degree of charring rapidly diminishing downwards. The tree stumps, which are charred to their centre, are preserved to a height of up to 0.15 m above the paleosol surface, but more commonly are truncated at the paleosol surface itself with only the root systems surviving (this is always the case with monocot stumps which are represented only by dense clusters of fine roots) (Figure 2.12). No leaf litter layer is preserved and the paleosol surface shows shallow scours, 50 –70 mm deep, infilled with coarse crystalline tuff, implying that erosion accompanied the deposition of the tuff layer.

2.5.2.2. Tree orientation, inferred blast direction, and probable location of volcanic cone.

Several tree stumps are partly uprooted and tilted towards the SSW (210º), implying that the hot pyroclastic came from the NNE (Figure 2.13) (Table 2.3, Figure 2.13). The overlying tuff also contains abundant horizontal logs, which are always charred to their centre. The orientation of logs that were sufficiently well exposed and sufficiently large (diameter >0.1 m and exposed length >0.5 m) for reliable measurements (see Table 2.3) provide independent support for a volcanic blast coming from the north (See rose diagrams in Figure 2.13).

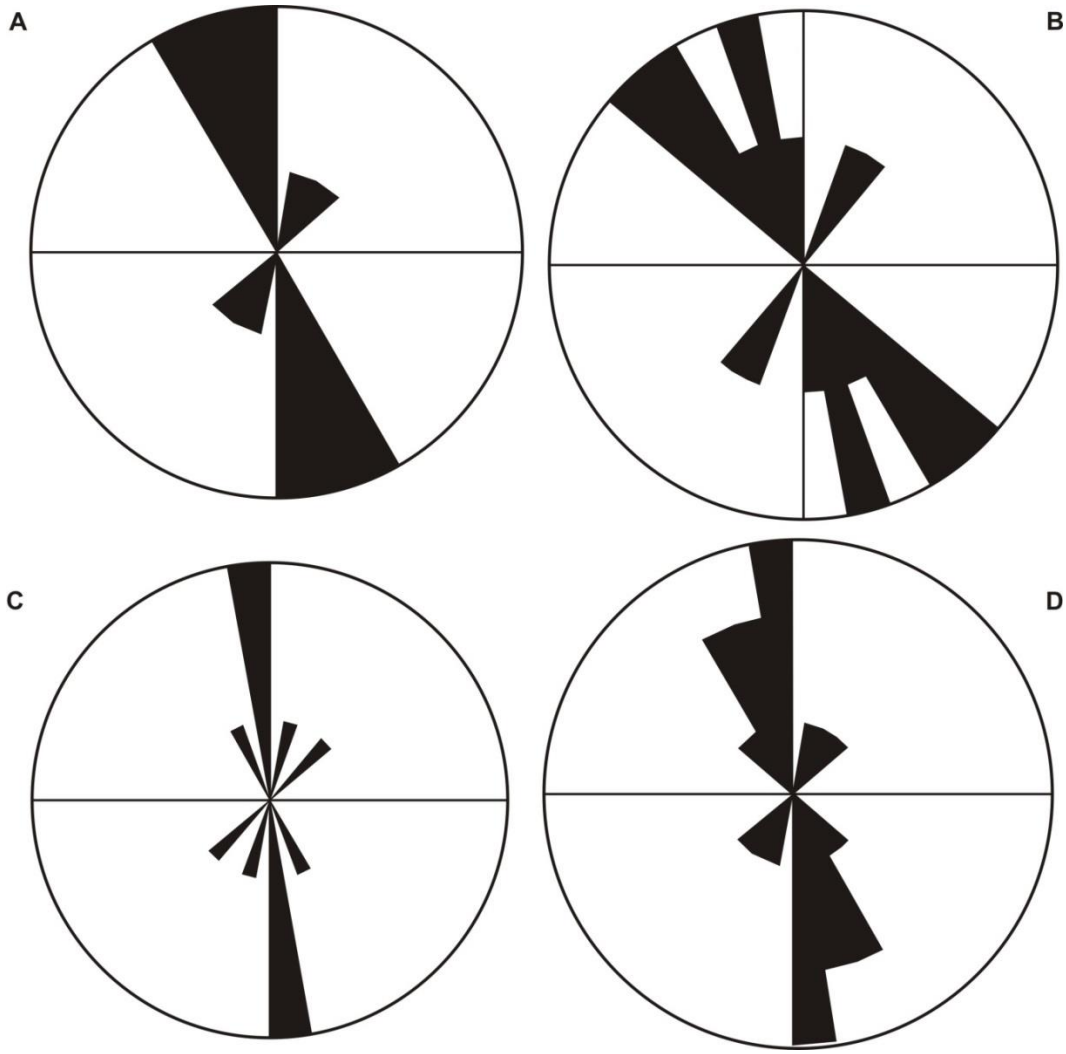

Figure 2.13. Orientation of charcoalified stumps and logs (Facies 3) from the Cucaracha Formation. A, orientations of trees in Centenario Bridge, N= 13; B, orientations of trees in Contractors Hill, N=10; C, orientations of trees in Hodges Hill, N=6; D, orientations of trees from all localities studied in the Cucaracha Formation, N=29.

2.5.2.3 Forest composition

Several of the fossil woods of monocots (probably palms) and of dicots could be distinguished in the field. At the well-exposed Centenario Bridge site, the 120 m long

Centenario Bridge n= 13	Contractor Hill n= 10	Hodges Hill n= 6
020	330	000
050	320	020
030	350	340
350	040	000
350	350	050
340	330	000
340	000	
350	340	
000	320	
040	030	
000		
000		
340		

Table 2.3- Measured orientations of trunks (degrees, 0-360) in the three studied localities (see Figure 2.13).

exposure was divided into five equal-sized parts and the proportion of monocots and dicots was counted based on fifty samples for each part. From SE to NW, monocots comprised 22%, 28%, 10%, 20%, and 19% of the assemblage (mean: 19.8% monocot). At Contractor's Hill, monocots comprised 23% of the assemblage. At Hodges, monocots comprised only 8% of the charcoalified assemblage.

2.5.2.4. Tree size and inferred tree height

The diameters of stumps in growth position and transported logs were measured (see tables 2.4, 2.5 and 2.6 for diameters, means and range of these samples; see histograms in the appendix). An interesting fact is that stumps in growth position (mean 29.9 cm; n=7) (Table 2.4 - 2.7) are usually significantly larger than transported logs

(mean 14.5 cm, n=33) suggesting that what we are seeing is the upper parts of the tree trunk entrained in the assemblage. Some biomechanical equations for "woody and no woody plants" (Niklas, 1994) were applied to stump diameter to infer tree height: $\log_{10}H = 1.81 + 0.70 (\log_{10}D) - 0.13 (\log_{10} D)^2$. These equations were developed under the principle that the height and diameter are correlated within and among species, despite ontogenic or phylogenetic anatomical differences (Whittaker and Woodwell, 1968; Niklas, 1994). Therefore, the allometry of stem height and taper can be used to reconstruct the size and general appearance of plants from their fragmented remains. Results are given in Table 2.7 and indicate trees up to 69 m high.

Centenario (diameter/cm)	**Contractors (diameters/cm)**	**Hodges**
11	21	21
8	12	8
22	12	6
16	19	**N=3**
11	17	
10	11	
14	11	
12	18	
11	15	
9	19	
11	13	
21	16	
11	17	
15	**N= 13**	
14		
38		
N= 16		

Table 2.4. Charcoalified trunk diameter (cm) measured in the different localities.

Centenario	Contractors
37	12
29	42
40	17
32	

Table 2.5. charcoalified stump diameter (cm) measured in the different localities.

Centenario	Logs / N= 16	Stumps/ N= 4
Mean diameter (cm)	14.62	34.5
Minimum diameter (cm)	8	29
Maximum diameter (cm)	38	40
Contractors	**N= 13**	**N=3**
Mean diameter (cm)	15.46	23.67
Minimum diameter (cm)	11	12
Maximum diameter (cm)	21	42
Hodges	**N=3**	**N=0**
Mean diameter (cm)	11.67	No data
Minimum diameter (cm)	6	
Maximum diameter (cm)	21	
TOTAL	**N= 33**	**N=7**

Table 2.6. Means and ranges of the measured diameters of chearcoalified trunks and stumps in the three studied localities.

Centenario	**Logs**	**Stumps**
D=diameter (m) / estimated heights (m)	D=0.11 / 1.21	D= 0.37/ 51.62
	D= 0.08 / 0.30	D=0.29/ 28.13
	D= 0.22 / 13.11	D=0.40/ 61.98
	D= 0.16 /4.82	D=0.32/ 36.20
	D= 0.11 /1.21	
	D= 0.10 / 0.81	
	D= 0.14 /3.03	
	D= 0.12 /1.71	
	D= 0.11/1.21	
	D= 0.09 / 0.51	
	D= 0.11 /1.21	
	D= 0.21/11.42	
	D= 0.11/1.21	
	D= 0.15/ 3.87	
	D= 0.14/3.04	
	D= 0.38 / 55	
	N= 16	**N= 4**
Contractors Hill	**Logs**	**Stumps**
D=diameter (m) / estimated heights (m)	D= 0.21/ 11.42	D=0.12 /1.71
	D=0.12 /1.71	D= 0.42/ 69.30
	D=0.12 /1.71	D= 0.17/ 5.90
	D=0.19/ 8.42	
	D= 0.17/ 5.90	
	D= 0.11/1.21	
	D= 0.11/1.21	
	D= 0.18/ 7.10	
	D= 0.15/ 3.87	
	D= 0.19/8.42	
	D= 0.13/ 2.32	
	D= 0.16 /4.82	
	D= 0.07/ 0.15	
	D= 0.17/ 5.90	
	N=14	**N=3**
Hodges Hill	**Logs**	**Stumps**
D=diameter (m) / estimated heights (m)	D= 0.21/11.42	
	D= 0.08 / 0.30	
	D= 0.06/ 0.11	
	N=3	**N= 0**

Table 2.7. Estimated heights of the trees based on diameter data (charcoalified forest) using the Niklas, 1994 equations.

2.5.2.4. Tree spacing and inferred forest density.

At Centenario, the fossil forest is well exposed, allowing measuring the tree-spacing along the transect as follows (from SSE to NNW): 7, 11, 2, 10, 11, 3, 8, 5, 3, 4, 11, 7, 2, 16, and 3 (of which 13 stumps were dicots and 2 were monocots). Spacing could not be measured at the other two sites due to insufficient exposure. It is possible to convert these spacing data into density approximations by assuming an even stacking pattern. Given the average spacing of trees (6.87 m), density would have been 212 trees per hectare.

2.5.2.5. Associated leaf adpressions

Leaf impressions were found in grey mudstone at Hodges Hill directly (1 m) below the fossil forest layer buried by tuff (Figure 2.14) but are being studied by other scientists at STRI and preliminary data are not yet available.

Figure 2.14. Fossil leaf collected in Hodges Hill, below the charred wood layer.

2.6. INITIAL FOREST INTERPRETATION

The systematics of the two fossil assemblages, and their ecologic and palaeoclimatic implications, will be described in detail in the remainder of this thesis. However, based on field investigations alone, some initial inferences can be made. One permineralised assemblage occurs in fluvio-estuarine deposits. Taphonomic studies (Scheihing and Pfefferkorn, 1984) show that most material in these contexts today represents trees stripped from mangrove gallery vegetation. The systematic sections (Chapters 4 – 6) will be used to test this hypothesis. The other charcoalified assemblage, occurs rooted in paleosols that elsewhere in the section occur lateral to fluvio-estuarine channels. Therefore this assemblage, too, might be expected to represent coastal mangrove vegetation. If correct, an expectation is that the composition of the permineralised and charcoalified material would be similar. Again, this can be tested through a study of systematics. Overall, the latter forest seems to have been a mixed-age stand of palms and dicots, of moderate density and canopy height. It was buried by a hot volcanic ignimbrite, which based on tree orientations, seems to have engulf this area of forest from the north. Reflectance and geological data are marshaled in chapter 7, to explore in greater depth, the mode of preservation of this fossil forest.

CHAPTER 3: METHODS FOR WOOD SYSTEMATICS

3.1. INTRODUCTION

This chapter introduces the reader to wood anatomy principles, preparation techniques and identification of permineralised and partially charcoalified and silicified woods (see Chapter 4, 5, 6) from the Cucaracha Formation. It also details the coding, the use of database and comparative collections to identify each specimen and alternatives such as SEM and morphometric analysis to achieve a more precise identification.

Wood is, in a basic definition, the fibrous tissue mainly composed of cellulose and lignin that is found in stems and roots of trees (Hickey and King, 2001). There does not seem to be a strict botanical definition of the term "wood", but it is commonly referred to as secondary xylem (Evert, 2006; Mauseth, 1988; Esau, 1977). The xylem is a multifunctional complex tissue, which, in association with the phloem, constitutes the two types of transport tissues in vascular plants (Evert, 2006). However, it also offers mechanical support and contributes to metabolism by storing and moving carbohydrates (Wheeler and Baas, 2011). Therefore, wood represents an archive of external signals that modified its traits at different timescales (Wheeler and Baas, 2011), for which it provides with valuable information to a range of different research fields, e.g., dendrochronology, plant physiology, biogeography and systematics.

It has been broadly recognized that wood anatomical features are particularly useful to identify trees and to elucidate phylogenetic relationships among plants (Wheeler and Baas, 2011). In this thesis, wood anatomical traits are applied to provide identifications of fossil trunks and to at least assign generic and familial ranks by using detailed descriptions of each specimen. A key tool to achieve this aim is the Inside

Wood Database (IWD). Inside Wood is a large database available online that contains descriptions for more than 200 plant families and over 35000 images, which combines information from literature and direct observations from numerous wood anatomy experts and contributors (InsideWood, 2004 onwards). The database is searchable by an interactive multiple-entry key.

The methodology for descriptions, use of Inside Wood to identify woods and comparison with modern wood microscope slide collections will be explained in the following sections of this chapter and further detailed in Chapters 4, 5, 6.

3.2. WOOD ANATOMY AND GENERAL TERMINOLOGY

3.2.1. How is wood or secondary xylem formed?

The primary tissues are initially arranged in vascular bundles forming an intermittent cylinder around the pith (Figure 3.1A). Primary xylem and primary phloem arise from the procambium, from which the vascular cambium also originates (Evert, 2006; Larson, 1994) (Evert, 2006; Esau, 1977). The vascular cambium is responsible for the formation of the secondary tissues of the plant and it is conformed by vertically elongated fusiform initials and horizontally elongated initials. Therefore the secondary xylem is composed by two systems: the axial (vertical) and the radial (horizontal) (Evert, 2006). There are two types of cambium: bifacial and unifacial. The bifacial cambium, which is more complex, gives rise to secondary xylem towards the centre and phloem towards the outside. Bifacial cambium is present in most of the modern plants. Other type, the unifacial cambium, only produces secondary xylem (Niklas, 1997). Unifacial parenchyma was recognised in early plants and extinct lineages, e.g., Lepidodendrales (Baas, 2013).

In the cambial zone, fusiform initial cells divide vertically to produce the axial components of the secondary growth, such as tracheary elements (vessels and tracheids) and fibres. Ray initials divide horizontally and originate the ray cells that run radially along the secondary vascular tissue (Plomion et al., 2001; Myburg and Sederoff, 2001). These divisions are co-ordinated with cell divisions in the adjacent interfascicular region to produce a continuous cylinder of vascular cambium (Myburg and Sederoff, 2001) (Figure 3.1B).

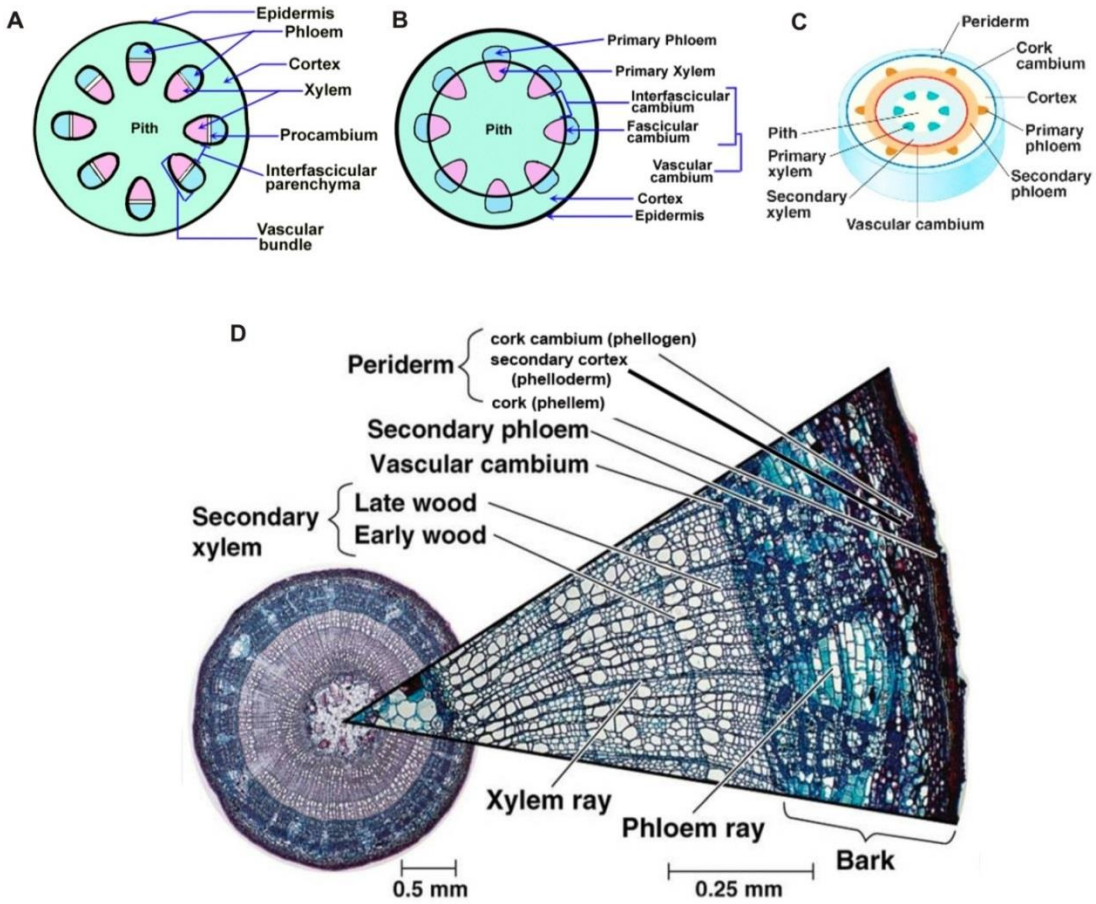

Figure 3.1. Diagram shows different phases of the development of primary and secondary tissues in a typical dicotyledonous plant. A, The vascular bundles arranged in a concentric circle. B, interfascicular cambium is developed. C, primary xylem and phloem develop towards the inner side and secondary xylem and phloem develop to the outside. D, complete development of secondary tissues and periderm. Modified from Rost, 1996 and Azman, 2014.

The differentiation of secondary xylem cells is centripetal (to the inner side). Also, secondary phloem is developed from the vascular cambium, which grows to the outer side (centrifugal).

In the typical type of secondary growth, the vascular cambium becomes a complete cylinder and produces contiguous cylinders of secondary xylem and phloem (Figure 3.1 C). Because the cambium has continuity throughout the tree, the oldest parts are directly connected to the young parts (Evert, 2006; Esau, 1977).

The periderm (Figure 3.1 D) is a protective tissue of secondary origin, replacing the epidermis in stems and roots that increase in thickness by secondary growth. Bark is a generic term that must be separated from the term "periderm". Bark includes all the tissues outside the vascular cambium including the secondary phloem, the peridermis, and the dead tissues outside the peridermis (Figure 3.1 D). The periderm includes the phellogen or cork cambium, the phelloderm and the phellem (commonly called cork) (Figure 3.1 D). The cork cells are normally suberised. The suberin is a fatty substance that usually covers the original primary cellulose wall (Evert, 2006).

3.2.2. Main cells and elements of the secondary xylem

The axial system of the secondary xylem is composed mainly of tracheary elements, fibres and axial parenchyma. The tracheary elements are the most highly specialized cells of the xylem that are concerned with the conduction of water and substances dissolved in water, there are two types: vessels and tracheids. A **vessel** consists of a series of axially arranged cells of which the intervening end walls have been perforated, thus providing a channel for water conduction (Figure 3.2) (Metcalfe and Chalk, 1983). Vessels can have diameters up to 400 µm (IWD, 2014; Metcalfe and Chalk, 1983) and possess secondarily lignified cells that lack living contents at maturity. At the end walls of vessels, cell walls completely or partially break down when the protoplast is lost, leaving an open **perforation plate (Figure 3.2).** Between adjacent vessels there are **intervessel pits** with membranes, through which water must

pass to move from one vessel to the next. **Tracheids** are similar to vessels but with no perforations, although they are pitted. Tracheids can be up to 5 mm in length and 80 µm in width (Metcalfe and Chalk, 1983).Tracheids are present in all softwoods (Figure 3.2), but they can be present in some hardwoods. **Fibres** are generally long pitted cells often lignified and dead at maturity that give mechanical support to the wood (Evert, 2006) (Figure 3.2). **Axial parenchyma** (Figure 3.2) cells have secondary thickenings and may be lignified. These cells remain alive and active for several years (Plomion et al., 2001), and are mainly related to storing of starch grains in the wood, but may also contribute to mechanical support together with the fibres (Wheeler and Baas, 2011).

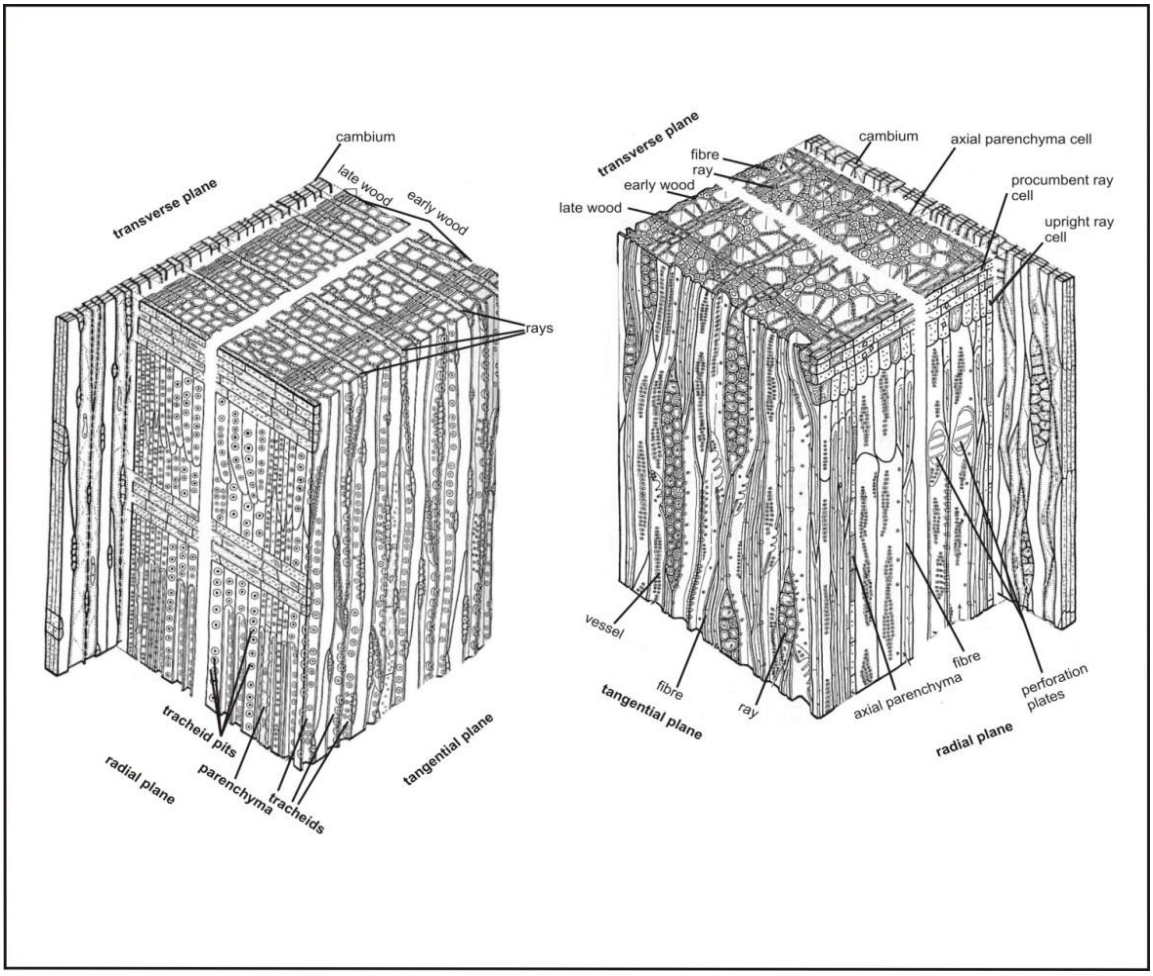

Figure 3.2. Diagram to illustrate features in conifer and angiosperm woods. Block of angiosperm wood showing key tissues of secondary xylem in transverse, tangential and radial planes. Modified from Esau (1977).

The radial system is composed by **rays** (Figure 3.2) that are panels of tissues variable in height and width and that are that are essential to the translocation of nutrients between phloem and xylem (Plomion et al., 2001).

3.2.3. Types of woods

Woods can be divided into two major groups, "softwoods" (conifers) and "hardwoods" (flowering plants) (Table 3.1). Although those terms are broadly used to distinguish woods, they do not express some properties such as specific gravity or hardness (Evert, 2006; Esau, 1977). For instance, some species of *Pinus* possess harder and heavier woods compared to some tropical trees of the genus *Ochroma* (Evert, 2006; Esau, 1977). Softwoods are relatively homogeneous and simple in cell types and arrangement (Figure 3.3A) whereas hardwoods exhibit a great diversity of cell types, forms and patterns (Figure 3.3B).

Cell type/function	Softwoods	Hardwoods
Conduction of water; conduction of solutes	tracheids	vessels
Support	Tracheids, libriform fibres	libriform fibres
Food storage, mobilisation of several substances	tracheids in some conifers, rays, apotracheal parenchyma	parenchyma cells, rays
Defence	Resin ducts in some conifers, traumatic canals	axial parenchyma, traumatic canals

Table 3.1. Summary of the main cell types in secondary xylem and functions. Modified from Esau (2006).

Conifers and ginkgoalean woods are considere softwoods (Evert, 2006). Other gymnosperms such as cycads produce a wood termed "manoxylic" that can be defined as woods with a large amount of parenchyma combined with narrow

rows of tracheids. This contrasts with "pycnoxylic" woods that are mainly composed of tracheids, combined with little parenchyma (e.g., conifer woods) (Mauseth, 2009).

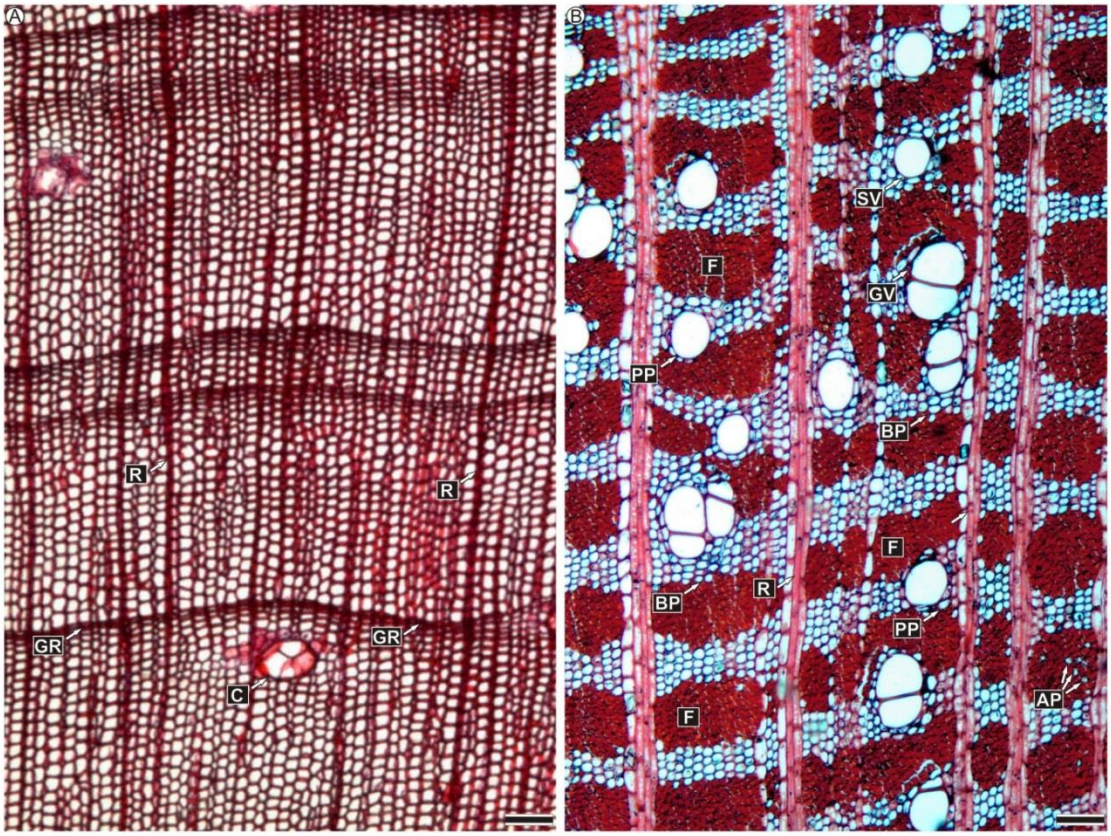

Figure 3.3. Typical transverse sections of conifer and angiosperm woods to contrast a few of the features that help to distinguish them anatomically. A, Cross section of *Pinus* sp (photo modified from VCBIO, 2013) shows the simple arrangement of conifer woods composed of tracheids and rays (R), growth ring boundaries are marked (GR) and an intercellular canal (C) is also shown. B, cross section of *Cola bracteata*, showing a more complex organisation with solitary vessels (SV) and grouped vessels (GV), alternating with fibres (F) and distinct parenchyma, paratracheal parenchyma (PP), apotracheal parenchyma (AP) and banded parenchyma (BP). Scales: A, B = 100 µm.

In a transverse section, conifer woods are relatively homogeneous with rays mainly uniseriate and tracheids with axial resin canals present in some taxa (Figure 3.3 A) (Evert, 2006). In contrast angiosperms exhibit a more complex structure, combining diverse patterns of vessel arrangement, fibres and parenchyma cells and rays in variable width, and occasionally, tracheids are also present (see Table 3.1). This visual difference between conifers and angiosperm woods is also reflected in the different

adaptations for efficient conduction. In conifers, the tracheids have a multitasking role, functioning for transport and support at the same time. Tracheids appeared much earlier than vessels in the fossil record (Sperry, 2003). Because the tracheids reach more limited diameters and length in comparison to the vessels, they are less efficient in conduction. Vessels reduce the number and area of pit membrane barriers in the system and therefore increase water-conducting efficiency (Sperry, 2003). Additionally, hardwoods, have a combination of diverse elements specialized for support (fibres), conduction (vessels, rays) and storage (rays, parenchyma).

Some conifers (e.g., Pinaceae, Cephalotaxaceae) have developed a 'torus', an impermeable, typically lignin-based, thickening at the centre of the pit membrane, surrounded by a 'margo', which is a ring of radial slits or pores that can be much larger than pores in a capillary-sealing membrane. It is understood that the torus protects the membrane from air seeding and potential blockage as refilling cannot occur if bubbles and cavitation develop (Delzon et al., 2010; Tyree and Zimmermann, 2002).

3.2.3.1. Main characters to describe and identify dicotyledonous woods

This section aims to describe the main characters are used to identify dicot woods; specially the characters that are further described and detailed in subsequent chapters (4, 5, 6). The definitions and numbering are according to the IAWA List of Microscopic Features for Hardwood Identification (1989). The list covers the more useful characters to describe the anatomy of fossil woods with the same IAWA number scheme which is used in chapters 4, 5 and 6.

Growth rings: increment of wood during a single growth period (Evert, 2006). In temperate regions rings are clear and mark one year of growth, where it is generally discernable the production of latewood (winter) and early wood

(spring). In the tropics, the growth rings are often incomplete or irregularly developed.

1. **Growth ring boundaries distinct (Figure 3.4 B, C, D, F):** growth rings with an abrupt structural change at the boundaries between them, mainly a change in fibre wall thickness and/or fibre radial diameter. Other structural changes include marked differences in vessel diameter between early wood and late wood, marginal parenchyma, etc.
2. **Growth ring boundaries indistinct (Figure 3.4 A, E):** growth rings are marked by more or less gradual structural changes and their boundaries are poorly defined or not visible.

Vessel porosity: the arrangement of vessels mainly referred to the variation of diameters in early wood and latewood.

3. **Ring-porous wood (Figure 3.4 C, F):** the vessels in the early wood are distinctly larger than those in latewood of the same growth ring.
4. **Semi-ring porous wood (Figure 3.4 D):** the vessels in the early wood are distinctly larger than those in the latewood, but the transition is gradual contrasting with the abrupt change in the ring-porous woods.
5. **Diffuse-porous wood (Figure 3.4 A, B, E):** the most common type present in tropical woods. The vessels are more or less the same diameter throughout the growth ring.

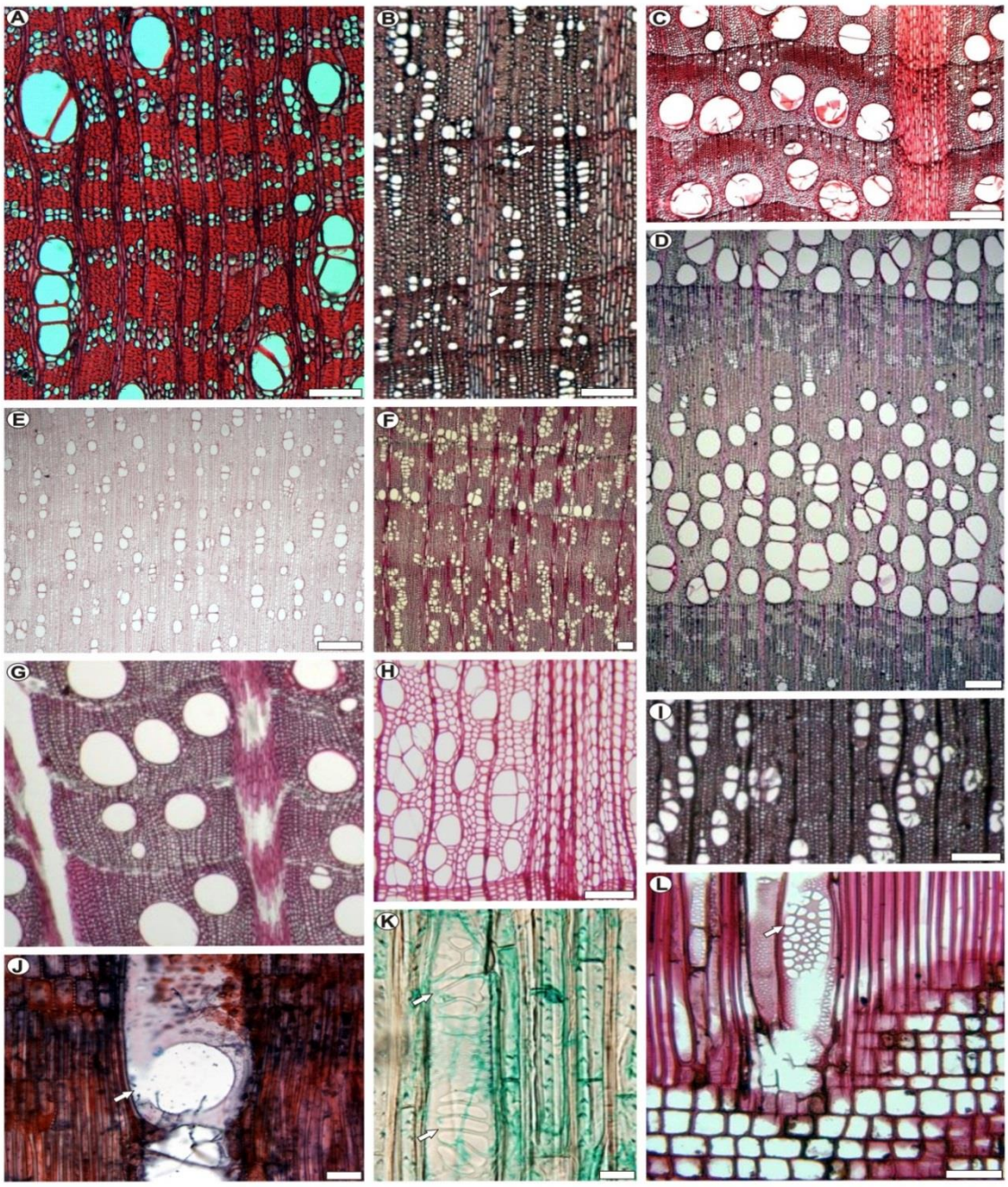

Figure 3.4. Illustrations of characters defined in Section 3.2.2.1 (characters 1-19). A, TS, *Cola acuminata* (Kew Hoyle 1403) shows indistinct growth rings. B, *Ilex aquifolium*, shows distinct rings. C, TS; *Quercus gambeli*, with ring-porous wood. D, TS; Semi-ring porous wood in *Rhus javanica*. E, TS, diffuse porous woods in *Elaeocarpus rugosus* (Kew D 6074). F, TS, Vessels arranged diagonally in *Dendropanax trifidus*. G, TS, Solitary vessels in *Cuervea kappleriana*. H, TS, clusters common in, *Alnus rubra*. I, TS, 4-grouped radial multiples common in *Ecclinusa guianensis*. J, RLS, simple perforation plates in *Elaeocarpus cyaneus*. K, RLS, scalariform perforation plate, *Rinorea* sp. L, RLS, reticulate perforation plate in *Meliosma panamensis*. Scale bars: A, B, D, E, K= 200 µm; C,F, L= 100 µm; J, 40 µm. A, E, images obtained from Jodrell collection. B,C, D, F, G, H, I, J, K, L Images obtained from IWD.

Vessel arrangement: some woods possess vessels arranged in distinct patterns, the most common arrangement types are listed below.

6. **Vessels in tangential bands**: vessels are perpendicular to the rays and form short to long bands that can be straight or wavy
7. **Vessels in diagonal and/ or radial pattern (Figure 3.4 F)**: vessels arranged in oblique lines or intermediate between tangential and radial.
8. **Vessels in dendritic pattern**: vessels are arranged in a branching pattern forming distinct tracts, separated by areas devoid of vessels.

Vessel grouping: the percentage of vessels is grouped in a determined area of minimum 25 vessels in total.

9. **Vessels exclusively solitary (Figure 3.4 G):** 90% or more of the vessels appear not to contact another vessel.

10. **Radial multiples of 4 or more common (Figure 3.4 I):** common occurrence of radial files of 4 or more adjacent vessels.

11. **Clusters common (Figure 3.4 H)**: groups of 3 or more vessels having both radial and tangential contacts.

Solitary vessel outline (Figure 3.4, G, H, I): shape of solitary vessel outline as seen in cross section.

12. **Solitary vessel outline angular (Figure 3.4 H):** shape of solitary vessel outline is angular viewed in cross section

Other types of outline (Figure 3.4 A-G, I): vessels can also be oval or circular as seen in cross section.

Perforation plates: the end wall of a vessel member that is perforated (Metcalfe and Chalk, 1983)

13. **Simple perforation plate (Figure 3.4 J):** a perforation plate with a single circular or elliptical opening.
14. **Scalariform perforation plate (Figure 3.4 K):** a perforation plate with elongated and parallel openings, separated by one to many mainly unbranched bars. The bars are counted and the number can be useful to separate taxa in some cases (charactes 15-18). None of the fossil woods from Panama included here have scalariform perforation plates, thus those characters are not described herein.

19. **Reticulate and other types of perforation plates (Figure 3.4 L)**: other types of perforation plates that are less commonly found are the reticulate and foraminate perforation plates. Reticulate are plates with closely spaced openings separated by wall portions that are much narrower than the spaces between them and foraminate perforations are perforation plates with circular or elliptical openings like a sieve.

Intervessel pitting arrangement, shape and size: the arrangement of the pits (perforations) between adjacent vessel elements.

20. **Scalariform (Figure 3.5 A):** intervessel pits arranged in a ladder-like series.
21. **Opposite (Figure 3.5 B):** intervessel pits arranged in short to long horizontal rows, orientated transversally across the length of the vessel.

22. **Alternate (Figure 3.5 C):** intervessel pits arranged in alternating diagonal rows.
23. **Intervessel pits shape polygonal:** outline of intervessel pits polygonal as seen in surface view (longitudinal sections)
24 – 27. **Size of intervessel pits**: Intervessel pitting size ranges from minute (<4 µm, **24**); small (4 –7 µm, **25**); medium (7–10 µm, **26**); large (>10 µm, **27**).

Vessel–ray pitting: the pits between a ray cell and a vessel element. Those include the next listed types:

30. **Vessel–ray pitting similar to intervessel pits in size and shape throughout the ray cell (Figure 3.5 D).**

31. Vessel–ray pitting rounded or angular (Figure 3.5 E)

32. Vessel–ray pitting horizontal (scalariform-gash-like) to vertical (palisade)

33. Vessel–ray pitting of two distinct sizes in the same ray cell.

34. **Vessel–ray pitting unilaterally composed.**

35. Vessel–ray pitting restricted to marginal row.

Helical thickenings (Figure 3.5 F): ridges on the inner face of the vessel walls**.**

37. Helical thickenings throughout body of vessel elements (Figure 3.5 F)

38. Helical thickenings only in vessel element tails

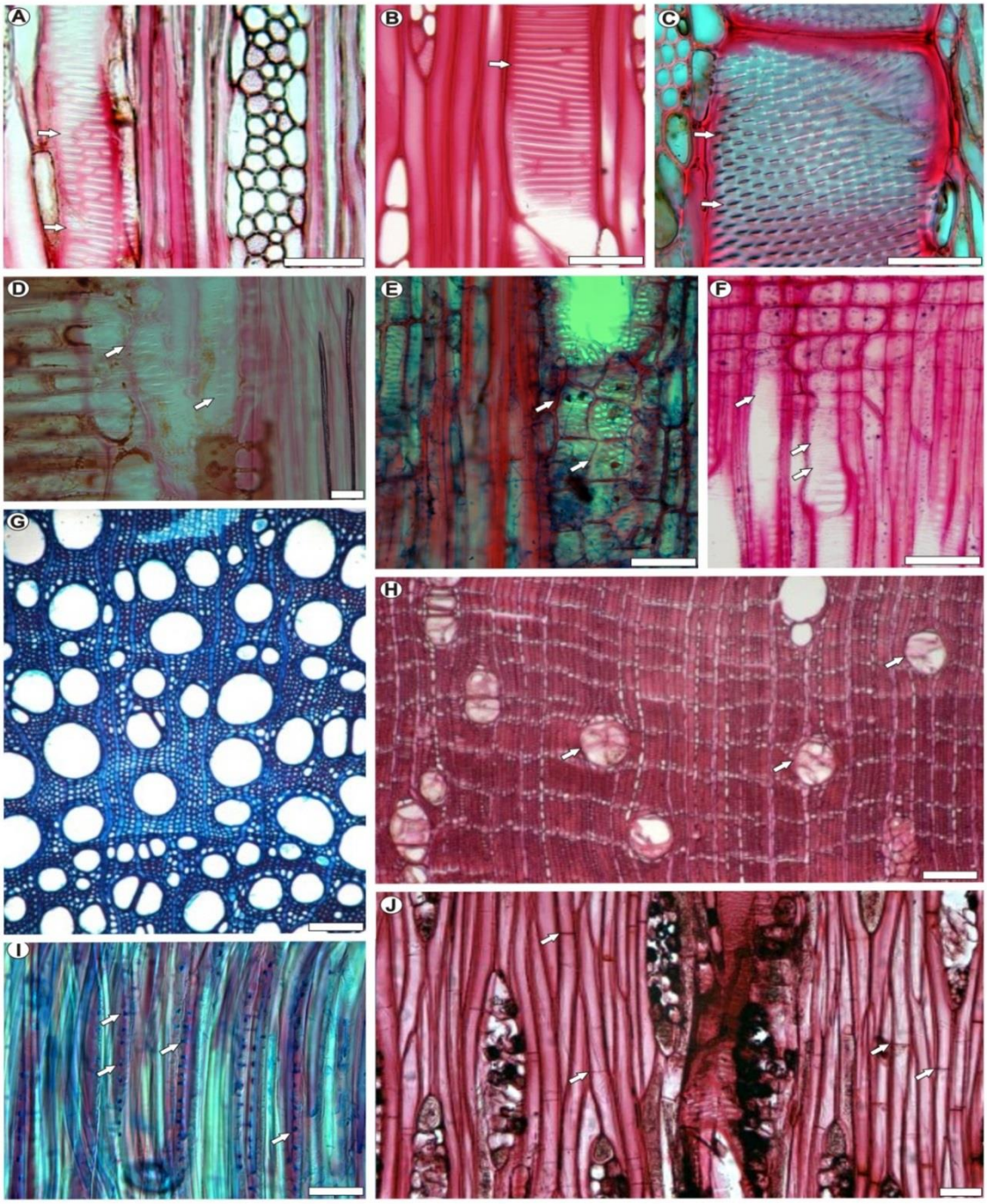

Figure 3.5. Illustrations of characters defined in Section 3.2.2.1 (characters 20 - 65). A, TLS, scalariform intervessel pits in *Oreopanax peltatus*. B, TLS, Opposite intervessel pits (arrow). C, TLS, intervessel pits alternate in *Celtis soyauxii* (FHI 22813). D, RLS, Vessel-ray pits similar to intervessel pitting *in Celtis soyauxii* FHI 22813). E, RLS, Vessel-ray pits with much reduced borders, *Grewia orientalis* (arrows). F, RLS, helical thickenings, *Carrya elliptica*. G, TS, vessels in two diameter classes, *Dolichandra unguis-cati*. H, TS, Tyloses abundant (arrows) *Elaterospermom tapos*. I, RLS, minutely bordered pits, *Pentaplaris doroteae* (KW 20291). J, TLS, Septate fibres, *Canarium schwenfurthii*. Scale bars: A, I= 20 µm; B, C, D,E, F = 50 µm; F, G,H=200 µm. Images obtained from IWD. A,B, G, H, F, J, images obtained from IWD. C, D, E, I, photographed from the Jodrell Collection.

40 – 43. Tangential diameter of vessel lumina: the diameter of vessel lumina, excluding the wall and measured in its widest part in transverse sections. The categories listed in the IWD are: 40, <50 µm; 41, 50 – 100 µm; **42,** 100 – 200 µm; **43**, > 200 µm

45. Vessels of two distinct class diameters (Figure 3.5 G): non- ring porous woods with a bimodal distribution of tangential diameters of vessel lumina.

46 -50. Vessels per square millimeter: the number of vessels in a 1 mm^2 area. It is calculated counting all vessels as individuals, including the grouped ones. The categories listed in IWD are: **46**, < 5 vessels/mm^2; **47,** 5 - 20 vessels/mm^2; **48,** 20 - 40 vessels/$mm^{2;}$ **49,** 40 – 100 vessels/mm^2; **50**, >100 vessels/mm^2

52 - 54. Mean vessel element length: the whole length of each vessel element from one tail to the other. **52, <350 µm**; **53**, 350 – 800 µm; **54,** > 800 µm

Tyloses (Figure 3.5 H): outgrowths from an adjacent ray or axial parenchyma cell though a pit in a vessel wall, partially or completely blocking the vessel lumina, and of common occurrence.

57. Sclerotic tyloses: tyloses with very thick, multilayered, lignified walls

with very thick multilayered lignified walls.

Fibre pits: pits in fibre walls, normally found in radial walls. In a few taxa, pits are common in tangential walls.

61. Minutely bordered pits (Figure 3.5 I): simple pits or with indistinct borders

62. Distinctly bordered pits: pits with borders distinct.

65. **Septate fibres (Figure 3.5 J):** fibres with thin, unpitted, transverse walls or septa. Fibres without septa are called non-septate **(66).**

Fibre wall thickness: the width of the fibre wall in relation to the lumen.

68. **Very thin walled fibre**s **(Figure 3.6 A):** the lumen is 3 or more times wider than the double wall thickness
69. **Thin-to thick-walled fibres (Figure 3.6 B):** the lumen is less than 3 times the double wall thickness
70. **Very thick walled fibres (Figure 3.6 C)**: if the lumen is almost completely closed

Apotracheal parenchyma: Axial parenchyma not associated with the vessels.

76. **Diffuse parenchyma:** single parenchyma strands or pairs of strands distributed irregularly among the fibrous elements

77. **Diffuse in aggregates (Figure 3.6 D)**: parenchyma strands are grouped in short discontinuous lines

Paratracheal parenchyma: the axial parenchyma associated with the vessels or vascular tracheids.

78. **Scanty (Figure 3.6 E):** occasional parenchyma cells associated with the vessel or an incomplete sheath of parenchyma around the vessels.
79. **Vasicentric :** parenchyma cells forming a complete circular to oval sheath around a solitary vessel
80. **Aliform:** parenchyma surrounding or to one side of the vessel and with lateral extensions.
81. **Lozenge-aliform (Figure 3.6 F):** lateral extensions are diamond-shaped.

82. **Winged-aliform (Figure 3.6 F):** lateral extensions (wings) being elongated and narrow.
83. **Confluent (Figure 3.6 G):** coalescing vasicentric or aliform parenchyma surrounding or to one side of two or more vessels, forming irregular bands.
84. **Unilateral (Figure 3.6 H):**: paratracheal parenchyma forming semi-circular hoods or caps only one side of the vessels, and which can extend tangentially or obliquely in an aliform or confluent pattern.

Banded parenchyma: the parenchyma is distributed in bands of diverse numbers of cells in width. It can be associated or not associated with the vessels.

85. **Bands more than 3 cells wide** or **up to 3 cells wide (Figure 3.6 I)**.
86. **Narrow bands or lines up to 3 cells wide**
87. **Reticulate**: the lines are approximately the same width as the rays
88. **Scalariform:** the tangential lines are regularly spaced and are much narrower than the rays.
89. **Marginal:** the bands are at the margins of a growth ring.

91 – 94. Parenchyma strand length (Figure 3.6 J): Number of cells that compose a parenchyma strand in length. The categories of IWD includes: **92**, 3 – 4 cells per parenchyma strand; **93**, 5 – 8 cells per parenchyma strand; **94**, over 8 cells per parenchyma strand

Ray width: the number of cells across the width of rays on TLS**.**

96. **Rays exclusively uniseriate:** most of the rays are composed of 1 cell in width, with occasional biseriate (2 cells) rays.

97. **Rays 1–3-seriate**

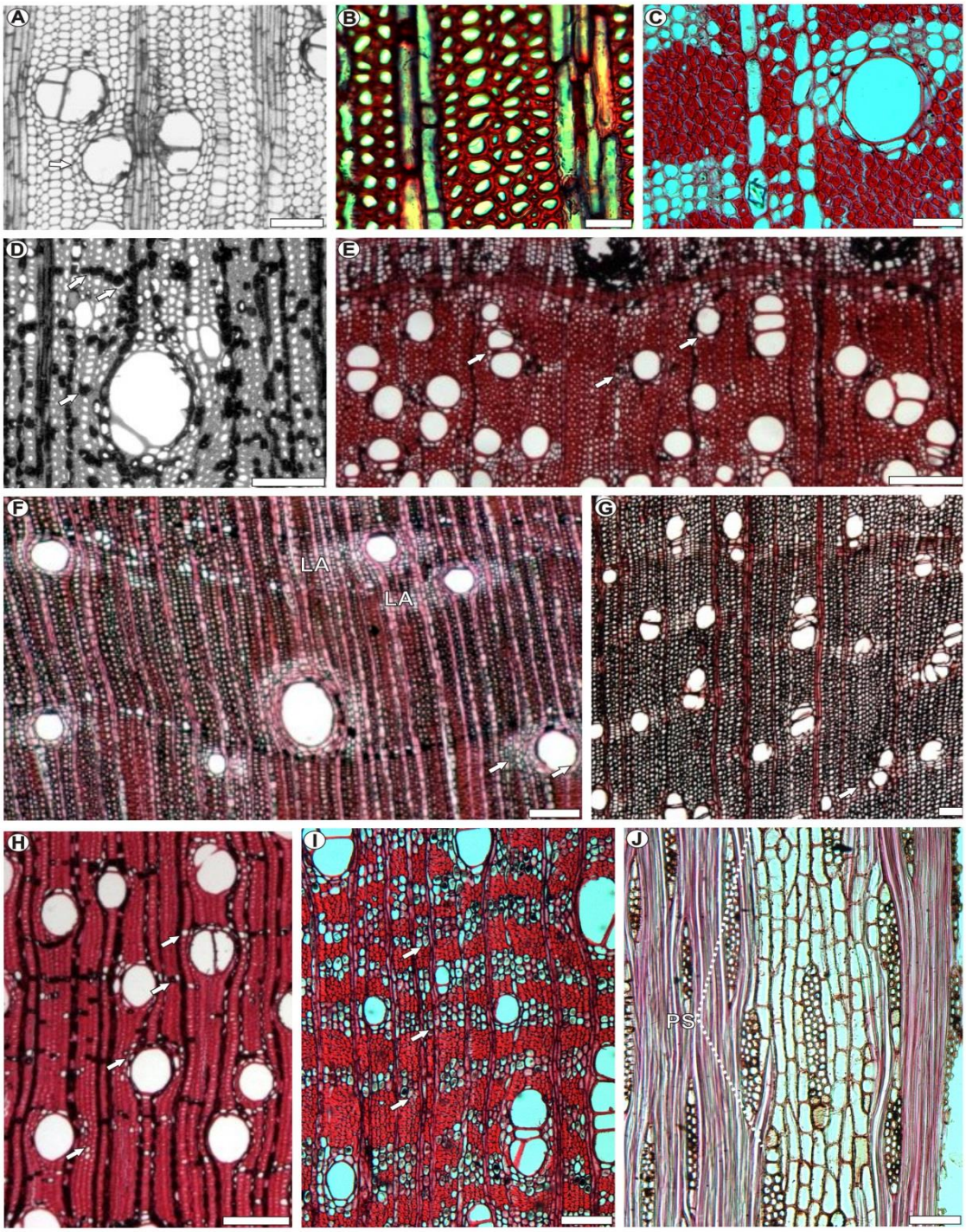

Figure 3.6 . Illustrations of characters defined in Section 3.2.2.1 (characters 66 - 94). A, TS, very thin walled fibres, *Spondias purpurea.* B, TS, thin-to –thick walled fibres *Garcinia dulcis*. C, TS, Very thick walled fibres, *Cola bracteata* (Hoyle 1403). D, TS, diffuse in aggregates (arrow) parenchyma, *Mammea americana*. E, TS, scanty paratracheal parenchyma, *Avicennia germinans*. F, TS, Lozenge aliform parenchyma (LA) and Winged aliform parenchyma (arrow), *Combretum imberbe*. G, TS, confluent parenchyma, *Jacaranda puberula.* H, TS, Unilateral paratracheal parenchyma (arrows), *Sacoglottis gabonensis*. I, TS, Banded parenchyma, *Cola acuminata*. J, TLS, Parenchyma strands, *Celtis soyauxii* (FHI 122813). Scale bars: A, E, F, H= 200 µm; B, 50 µm; C, D, G, I, J= µm. A,D, E, F, G, H, images obtained form IWD. B,C,J, photographed from the Jodrell Collection.

98. Rays 4 – 10-seriate (Figure 3.7 A, H)

99. Rays >10-seriate (Figure 3.7 C)

100. Rays with multiseriate portions as wide as uniseriate portions

101. Aggregate rays (Figure 3.7 B): a number of individual rays so closely associated one another that they appear macroscopically as a single large ray. The individual elements are separated by axial elements.

102. Ray height > 1mm: it is determined in tangential section. Rays > than 1mm are considered tall.

Ray of two distinct sizes (Figure 3.7 C): in tangential sections, rays form two populations by their width and height.

Ray composition (Figure 3.2): the shape of cells that compose the rays in body and marginal zones. Rays can be composed of three different types of cells: procumbent cells, with its longest dimension radial as seen in radial section; square cells are approximately square as seen in radial section; upright cells with longest dimension axial as seen in radial section.

104. All ray cells procumbent (Figure 3.7 D)

105. All rays upright/or square

106. Body ray cells procumbent with one row of upright/square marginal cells.

107. Body ray cell procumbent with 2 – 4 rows of upright/square marginal cell

108. Body ray cell procumbent with over 4 rows of upright/square marginal cells

109. Rays with procumbent, square and upright cells mixed throughout the body (Figure 3.7, E).

110. Sheath cells (Figure 3.7 A, B): ray cells that are located along the sides of broad rays (>3-seriate) and, as seen in tangential section, they are larger than the central ray cells. Sheath cells are further explained and illustrated in Chapter 5

111. Tile cells (Figure 3.7 F): A special type of apparently empty upright (rarely square) ray cells occurring in intermediate horizontal series usually interspersed among the procumbent cells. Tile cells are further explained and illustrated in Chapter 5.

112. Perforated ray cells (Figure 3.7 G): ray cells of the same dimensions or larger than the adjacent cells, but with perforations, which generally are on side walls connecting two vessels on either side of the ray.

Rays per millimeter: the number of rays per linear unit measured from tangential sections. The categories listed in the IWD include: **114**, < 4 rays/mm; **115**, 4-12 rays/mm; **116**, >12 rays/mm.

118 – 122. Storied structures (Figure 3.7 H): rays and/or axial elements arranged in tiers (horizontally) as viewed on tangential sections. It includes categories such as: **118**, all rays storied; **119**, low rays storied, high rays non-storied; **120**, axial parenchyma and/or vessel elements storied; 1**21**, fibres storied.

Intercellular canals: tubular intercellular duct developed by an epithelium, generally containing resins, gums, etc. (IAWA, 1989).

127. Axial canals in long tangential lines (Figure 3.7 I): more than five canals in a tangential line (perpendicular to rays).

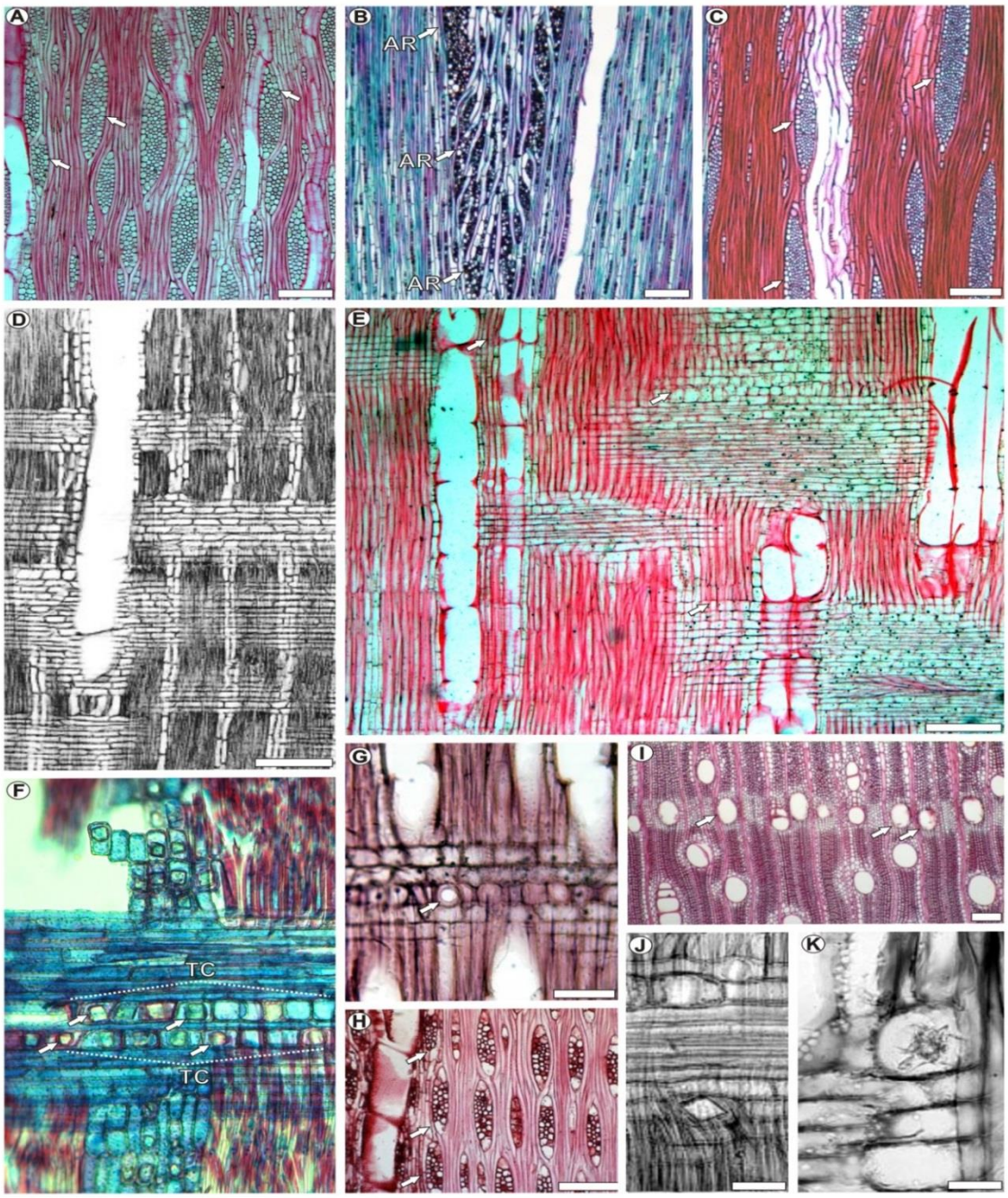

Figure 3.7. Illustrations of characters defined in Section 3.2.2.1 (characters 22-34). A, TLS, wide rays with sheath cells (arrows) in *Hibiscus shizocarpus*. B, TLS, aggregate ray (AR), *Lithocarpus edulis*. C, TLS, bimodal rays, wide and tall rays with sheath cells (arrows), *Celtis sinensis.* D, RLS, rays homocellular, *Eschweleira alata*. E, RLS, heterocellular rays (arrows show marginal square cells), *Hibiscus schizocarpus.* F, RLS, tile cells and abundant prismatic crystals in *Pentaplaris doroteae*. G, RLS, perforated ray cell, *Exostema caribaeum* (arrow). H, storied rays, TLS, *Daniellia oliveri*. I, RLS, intercellular canals (arrows), *Copaifera guyanensis.* J, RLS, solitary rhomboidal crystal in square ray cell, *Pistacia atlantica*. K, RLS, druses in *Hibiscus elatus*. Scale bars, A, C, D, F= 100 µm; B, E, I= 200 µm; G, J= 50 µm. Images obtained from IWD. A, B,C, D, F, G, H, I, J, K images obtained from IWD. E, photographed from Jodrell Collection.

128. Axial canals in short tangential lines: two to five axial canals in a tangential line

129. Axial canals diffuse: solitary canals randomly distributed

130. Radial canals: canals present in rays

131. Traumatic canals: canals formed in response to injury, arranged in tangential bands, generally irregular in outline and closely spaced.

137 – 143. Prismatic crystals (Figure 3.7 F): crystals of rhombohedral shape that can be found in ray cells, parenchyma cells and fibres. Crystals can be present in upright /or square cells **(137) (Figure 3.7 J)**; **138**, in procumbent ray cells; **139**, crystals are aligned in procumbent ray cells; **140**, chambered in upright /square ray cells; **141**, non-chambered in axial parenchyma cells; **142**, chambered in parenchyma cells; **143**; present in fibres.

144. Druses (Figure 3.7 K): a compound crystal, more or less spherical in shape, and with many component crystals protruding from the surface, that gives a star-shaped appearance.

154. **Two distinct sizes of crystals per cell or chamber:** crystals of different sizes in the same cell.

3.2.4. Palm "woods"

Many woody plants are trees, but not all trees are woody plants. Some palms (Arecaceae) attain tall trees with wide diameters, e.g., *Jubaea chilensis* (Molina) Baill can reach stem diameters up to 1m (Tomlinson, 2006). Those dimensions can be realized by thickening the primary xylem together with lignification of fibres and parenchymatous tissues; however palm trees do not develop secondary growth, thus

their tissues are not considered "wood" (Tomlinson, 2006). Therefore, the correct botanical term for a palm tree axis is palm stem.

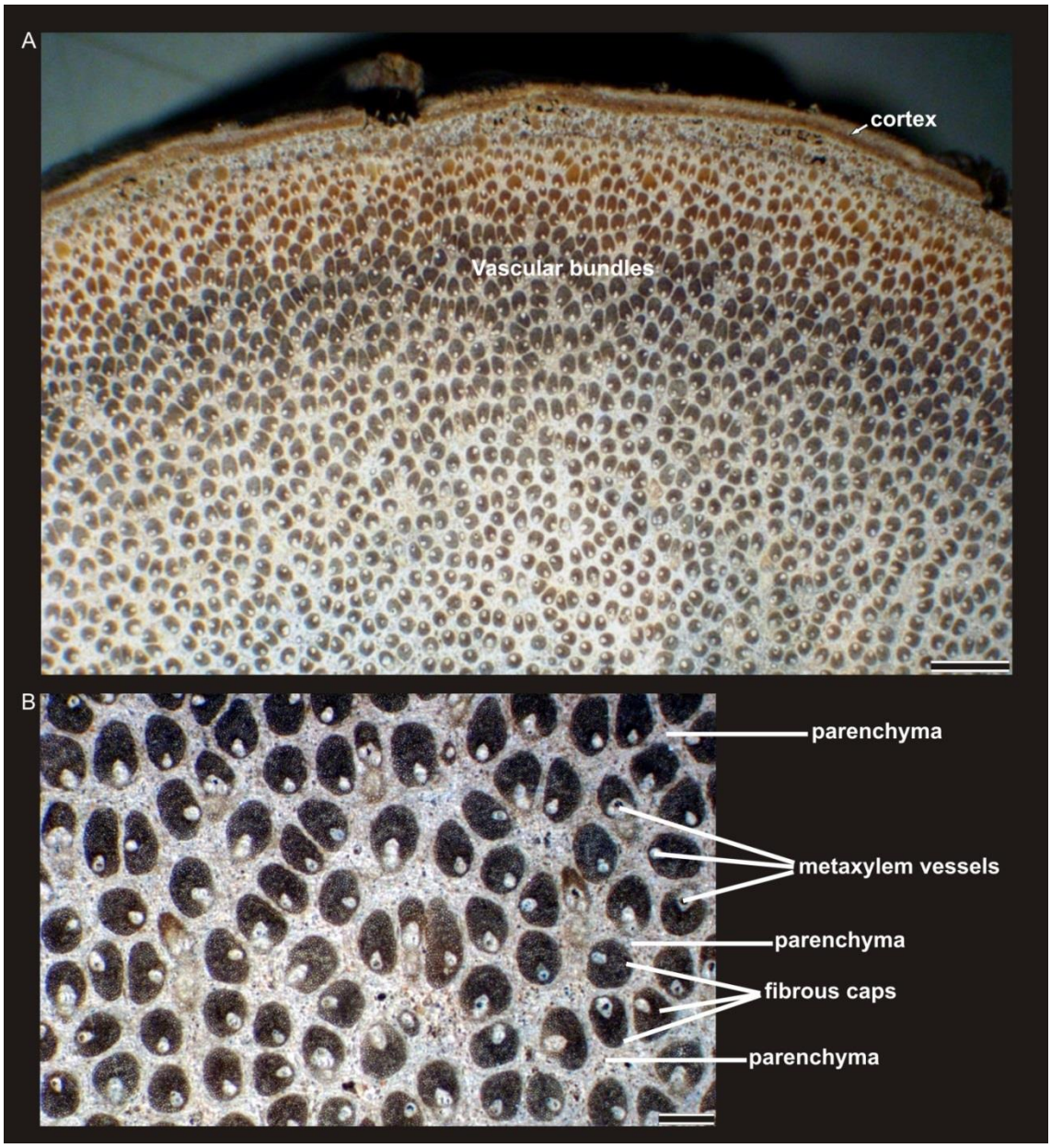

Figure 3.8. Cross section of *Chelyocarpus* sp. A, overview of the typical arrangement in palm stems with a thin cortex and most of the stem composed of fibre-vascular bundles. B, Close-up of a palm stem section showing the vascular bundles with fibrous cap and one metaxylem vessel each and embedded in specialized parenchyma. Photos modified from Thomas, 2013. Scales: A=2 mm, B= 500 µm.

Dicot trees increase diameter by producing bark to the outside and secondary xylem on the inside, palms have a repetitive axis composed by fibre-vascular bundles

from a central cylinder to the outermost parts (Hodel, 2009) (Figure 3.8). Essentially, a cross section of a dicot wood shows vessels interspersed among fibres and rays (arranged perpendicular to the growth ring direction) with diverse parenchyma patterns in some cases. In contrast a palm stem would shows a cortex that is a very narrow band on the outside of the stem composed of thick-walled and lignified cells, and the central cylinder, which occupies most of the palm stem, and it is composed of multiple vascular bundles embedded in a ground tissue of specialized parenchyma (Hodel, 2009) (Figure 3.8). Each vascular bundle is typically composed of a vascular section that contains metaxylem vessels, phloem strands and parenchyma and a fibrous cap that is diverse in form that can help to distinguish groups together with other characteristics (See Thomas and Franceschi, 2013) (Figure 3.8).

3.3. PREPARATION OF SAMPLES FOR SYSTEMATIC ANALYSIS

3.3.1. Thin sectioning

To describe and identify woods at least three different planes need to be studied: a **transverse section (TS)** or a cut perpendicular to the long axis of the trunk; a **tangential longitudinal section (TLS)**, or a cut tangential to the growth rings and a **radial longitudinal section (RLS)** is the vertical plane from the pith at the center of the tree heading out towards the bark or can also be defined as the plane perpendicular to the tangential longitudinal plane (Figure 3.2). These three planes are necessary to study wood anatomy in order to record as many diagnostic features as possible because the radial and tangential walls of cells have different characters. For example, traits such as parenchyma strand length, intervessel pitting and storied structures require a tangential longitudinal section to be observed.

The perforation plates, composition of rays, septate fibres and vessel-ray pitting, can be observed in a radial longitudinal section. Other features can best be seen in transverse section, such as growth rings, ring porous or diffuse porous wood, vessel arrangement, fibre wall thickness. There are other traits that can be seen from a transverse section, but need further confirmation in tangential longitudinal section, for example, the ray width in number of cells. In order to describe the fossil wood specimens as completely as possible, petrographic thin sections orientated in TS, RLS and TLS planes (Figure 3.5) were prepared in three different laboratories (Table 3.2):

1- Department of Earth Sciences, Royal Holloway, University of London, UK
   Neil Holloway
   Types of prepared woods: permineralised, partially charcoalified and silicified
   Sanding thickness: 30 µm
   Size of sections: 7.5 x 2.5 cm, 7.5 x 5.2 cm
   Preparation medium: embedded in Epo Fix resin and mounted with coverslips in Canada balsam.
2- Quality Thin Sections, Tucson, Arizona, U.S.A.
   Type of prepared woods: charcoalified
   Sanding thickness: 30 -35 µm
   Size of sections: 4.5 x 2.5 cm.
   Preparation medium: embedded in Buehler epoxy and mounted with coverslips in Canada balsam.
3- Instituto de Geologia, UNAM, Mexico City, Mexico.
   Type of prepared woods: partially charcoalified and silicified
   Sanding thickness: 30 µm

Size of sections: 7.5 x 2.5 cm.

Preparation medium: embedded in thermoplastic resin and mounted with coverslips and Canada balsam.

Sample	Locality	Description	Preparation	Laboratory
STRI 14151	Hodges Hill	permineralised dicot	petrographic sections	RHUL
STRI 14155	Hodges Hill	permineralised dicot	petrographic sections	RHUL
STRI 14157	Hodges Hill	permineralised dicot	petrographic sections	RHUL
STRI 14159	Hodges Hill	permineralised dicot	petrographic sections	RHUL
STRI 14160	Hodges Hill	permineralised dicot	petrographic sections	RHUL
STRI 14161	Hodges Hill	permineralised dicot	petrographic sections	RHUL
STRI 14164	Hodges Hill	permineralised dicot	petrographic sections	RHUL
STRI 14165	Hodges Hill	permineralised dicot	petrographic sections	RHUL
STRI 15685	Hodges Hill	charcoalified palm	SEM stub	RHUL
STRI 36269	Hodges Hill	permineralised dicot	petrographic sections	RHUL
STRI 36270	Hodges Hill	permineralised dicot	petrographic sections	RHUL
STRI 36272	Hodges Hill	permineralised dicot	petrographic sections	RHUL
STRI 36273	Hodges Hill	permineralised dicot	petrographic sections	RHUL
STRI 36400	Hodges Hill	permineralised dicot	petrographic sections	RHUL
STRI 13625	Contractors Hill	charcoalified dicot	petrographic sections	RHUL
STRI 13691	Contractors Hill	charcoalified dicot	petrographic sections	RHUL
STRI 14193	Contractors Hill	charcoalified dicot	petrographic sections	RHUL
STRI 14193	Contractors Hill	charcoalified dicot	SEM stub	RHUL
STRI 14196	Contractors Hill	charcoalified palm	petrographic sections	RHUL
STRI 14198	Contractors Hill	charcoalified dicot	petrographic sections	RHUL
STRI 14198	Contractors Hill	charcoalified dicot	SEM stub	RHUL
STRI 15364 C	Contractors Hill	charcoalified dicot	SEM stub	RHUL

STRI 15364	Contractors Hill	charcoalified dicot	petrographic sections	Quality Thin
STRI 15367	Contractors Hill	charcoalified dicot	petrographic sections	Quality Thin
STRI 15368	Contractors Hill	charcoalified dicot	petrographic sections	RHUL
STRI 15369	Contractors Hill	charcoalified dicot	petrographic sections	Quality Thin
STRI 15370	Contractors Hill	charcoalified dicot	petrographic sections	Quality Thin
STRI 15406	Contractors Hill	charcoalified dicot	petrographic sections	Quality Thin
STRI 15652	Contractors Hill	charcoalified dicot	SEM stub	RHUL
STRI 21046	Contractors Hill	charcoalified stump	petrographic sections	UNAM
STRI 21047	Contractors Hill	charcoalified stump	petrographic sections	UNAM
STRI 15369 A	Centenario Bridge	charcoalified dicot	SEM stub	RHUL
STRI 15371	Centenario Bridge	charcoalified dicot	petrographic sections	Quality Thin
STRI 15514	Centenario Bridge	charcoalified dicot	petrographic sections	Quality Thin
STRI 15514 A	Centenario Bridge	charcoalified dicot	SEM stub	RHUL
STRI 15515	Centenario Bridge	charcoalified dicot	petrographic sections	Quality Thin
STRI 15516	Centenario Bridge	charcoalified palm	petrographic sections	Quality Thin
STRI 15517	Centenario Bridge	charcoalified palm	petrographic sections	Quality Thin
STRI 15519	Centenario Bridge	charcoalified dicot	petrographic sections	Quality Thin
STRI 15520	Centenario Bridge	charcoalified dicot	petrographic sections	Quality Thin
STRI 15521	Centenario Bridge	charcoalified dicot	SEM stub	RHUL
STRI 15522	Centenario Bridge	charcoalified palm	petrographic sections	Quality Thin
STRI 15523	Centenario Bridge	charcoalified dicot	petrographic sections	Quality Thin

Table 3.2. List of samples used for systematics analysis of the Cucaracha Formation woods.

The woods found at the base of the Cucaracha Formation (See Chapter 2, Chapter 4) are calcified, as shown by high birefringence under polarized transmitted light (Figure 3.9). Calcite is one of the minerals with highest known birefringence

(Amos, 2005; Dana, 1965). The low birefringence colours (indicating quartz) of the partially charcoalified woods suggest that those are also partially silicified.

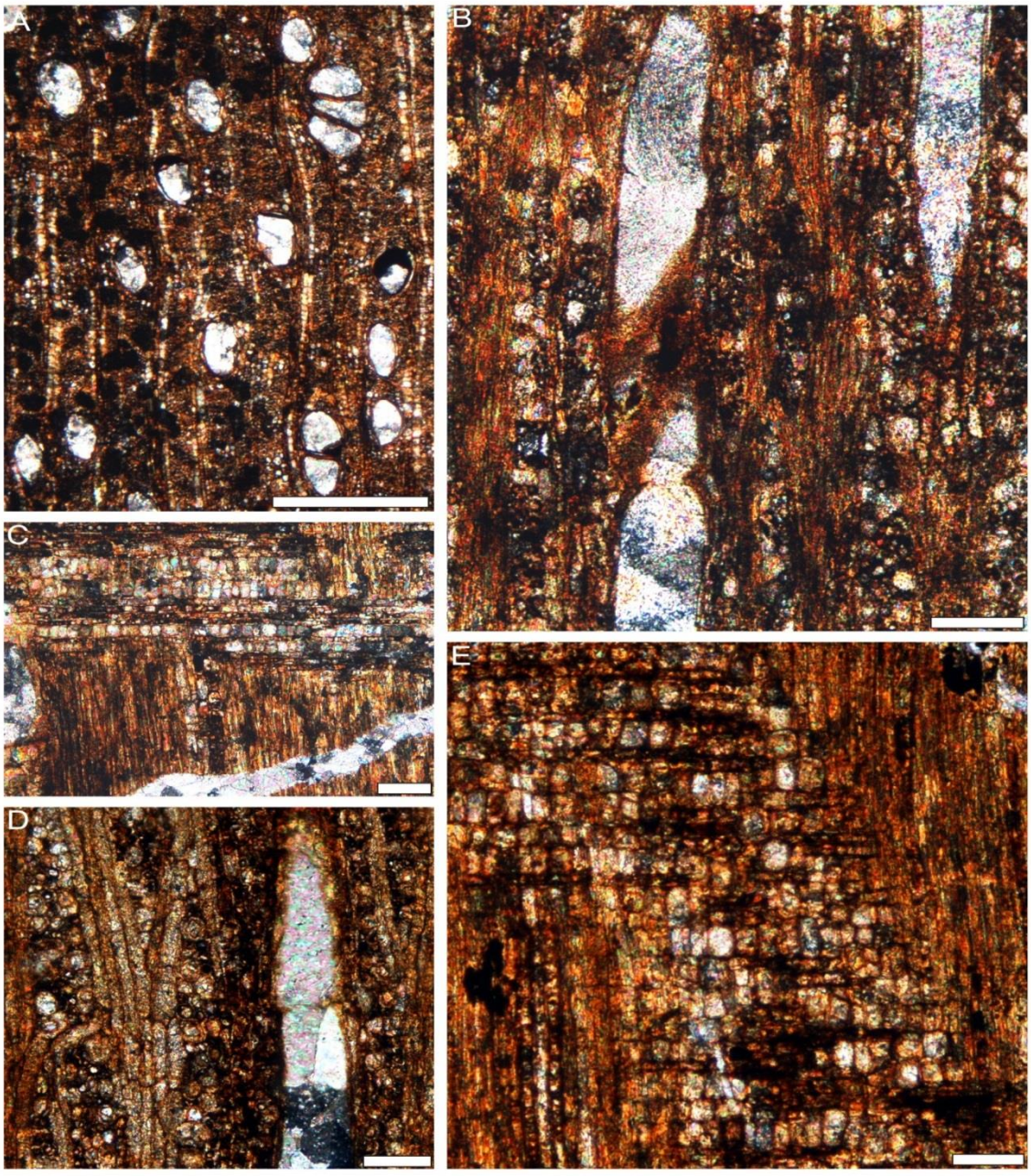

Figure 3.9. Calcified woods from Hodges Hill under polarised light to show calcification of woods based on high birefringence colours. A, Transverse section of STRI 14155. B, Tangential longitudinal section of STRI 14155. C, Radial longitudinal section of STRI 14155. D, Tangential longitudinal section of STRI 14157. F, Radial longitudinal section of STRI 14. Scales: A= 225 µm.; B -E= 100 µm.

The woods were observed, described and imaged using a transmitted light Olympus binocular BH-5 with a Nikon digital camera system and software. Anatomical preservation of these calcareous permineralised woods (Figure 3.9) is generally good allowing for detailed description and comparison with microscope slides of extant woods in reference collections (See Chapter 4, 5, 6)

3.3.2. Acetate peels

A few acetate peels were tested on the permineralised woods during the first stage of this project. Samples were treated with HCL and flooded in acetone before placing the clear acetate sheet over the wood surface (Galtier and Phillips, 1999). The obtained results were not satisfactory and furthermore, the thin sections were a better option due to a better resolution and finer detail of the samples. Therefore, I chose to continue studying samples based on standard petrographic thin sections.

3.3.3. Scanning Electronic Microscopy (SEM) methods for charcoalified woods

Traditionally, charcoal has been studied using fresh splits and observed under a microscope with reflected light (Angeles, 2001; Figueiral, 1999), however fresh splits of charcoal can be very dark and shiny and thus do not allow the observation of certain features as with a clean flat wood surface (Angeles, 2001). Additionally, most of the woods from the Cucaracha Formation are large logs, difficult to break or split in small pieces. Because it was the most accessible option, standard petrographic thin sections were prepared in order to study the charcoalified woods with transmitted light microscopy.

Certain features were challenging to code or observe precisely (e.g., septate/non septate fibres, fibre pits, ray composition) because of the opaque nature of charcoal (Falcon-Lang, 2012; Angeles, 2001) and because the preservation of some samples was

not ideal. The best alternative method to study charcoalified woods is SEM (Scanning Electron Microscopy). Therefore, a few woods were studied with SEM to support the observations done with light microscopy. 8 samples (Table 3.2), included in morphotypes previously analysed with LM (Transmitted Light), and one sample studied under the reflectance microscope (STRI 15652) were prepared for SEM imaging. Each wood was cut into cubes $1cm^2$ to allow the observation of all planes. Specimens were cleaned with HCL (20%) for 30 minutes and then etched with HF, rinsed thoroughly with distilled water and dried to remove quartz contents so that the walls of cells were visible (Collinson, 1999). To avoid charging, all the samples were coated in Au-Pd (Gold-Palladium). After the gold-coating, the samples were attached with silver dag adhesive and mounted on stubs (Gibbons, 2014 pers. com.). All the samples were imaged and the satisfactory images are included in the descriptions in Chapter 6 and a plate in Chapter 7.

3.4. IDENTIFICATION METHODOLOGY FOR DICOTYLEDONOUS WOODS

3.4.1. IAWA coding and feature description

Specimens were described using the IAWA List of Features for Hardwood Identification (IAWA Committee, 1989). In this standard descriptive system, anatomical characters (termed features) are given a numerical code. Most features are qualitative (requiring determination of presence or absence) but others are quantitative (requiring measurement of a population). To obtain quantitative data for vessel and ray density, and the degree of vessel grouping, measurements were made in 10 different fields of $1mm^2$ area. For other quantitative features (e.g., mean vessel diameter, intervessel pit diameter, vessel – ray pit diameter, vessel element length, ray height), a

minimum of 25 measurements was obtained, but where preservation allowed, 50 measurements were obtained. At the start of each of the fossil descriptions, anatomical features are listed as a string of numerical IAWA codes. In this list, features may be qualified by one of two signs as follows: "?" indicates that there is uncertainty as to whether the feature is present and "v" indicates that the feature is variable in occurrence. It is noted that the charcoalified woods followed slightly different description and identification standards due to limitations in the coding of certain features.

3.4.2. Inside Wood Database searches

Following description, I searched in the IWD, using different combinations of features that were considered diagnostic and uncommon. In these searches the strategies recommended by Wheeler (2011) and Falcon-Lang et al. (2012) were followed, and I did not put too much emphasis on variable quantitative features. To follow the aforementioned strategies, only characters where there is certainty of presence absence were used and searches were generally started using less than 10 certain feature. Then, more features were added to constrain the results further. As recommended, I was flexible during the identifications and tried different combinations, including more traits in some cases. Coding "absence" of features is often important in the identification of a wood (wheeler, 2001). For instance, if the mean vessel diameter of the morphotype to search is 100 µm, then I selected on < 50 µm absent (40 a), and > 200 µm absent (43 a), so the menu would exclude the taxa with very small and very big vessels. For the charcoalified woods (see section 3.4.4.), I applied shrinkage correction when numerical data were inserted in the IWD. An exhaustive study of micrographs in the IWD was undertaken, to create a short-list of potentially comparable taxa.

3.4.3. Comparison with wood collections of extant data

The short-list of taxa created from IWD for a specific morphotype/specimen was further supported with direct observations on collections of extant woods. All the identifications and comparisons presented in this thesis are supported on extensive comparisons of the fossils with the microscopic slides available in the Jodrell Laboratory, Royal Botanic Gardens Kew, UK. Images and measurements of modern woods were obtained using a Leica DM LB microscope with Zeiss Axiocam HRc camera attachment and Zeiss Axiovision software. In 2011, the collection of the Nationaal Herbarium Nederland in Leiden was also visited, mainly to analyse the microscopic slides of Malvaceae. Photographs and information from the literature (see subsequent chapters) were also used to refine the identifications.

3.4.4. Dimensional changes and shrinkage during charring of woods

During charring, woods are subject to changes, mainly shrinkage of cells and homogenisation of walls (Slocum et al., 1978; McParland et al., 2007, 2009; Falcon-Lang et al., 2012). The alterations of cells during charring have proven to increase with higher temperatures (McParland, 2007). Just a few studies have explored and quantified the effects of charring on the wood anatomical properties (e.g., Falcon-Lang et al., 2012; Gonçalves et al., 2012; Dias-Leme et al., 2010; February, 1994; Prior and Gasson, 1993; Prior and Alvin, 1986; Prior and Alvin, 1983;Cutter et al., 1980; Slocum et al., 1978). The changes due to charring are not always given as shrinkage, expansion of cells have also been reported as a result of charring >400 ˚C (Gonçalves et al., 2012; February, 1994; Prior and Gasson, 1993). Several factors control the magnitude of shrinkage such as: cell wall thickness, ray width and density and parenchyma abundance, but the most crucial factor is the length of time of charring (Falcon-Lang et

al., 2012; Gonçalves et al., 2012). The estimations provided and considered in Falcon-Lang et al. (2012) were applied here when certain quantitative characters were used in searches or other analysis. The rest of the values were kept unadjusted because corrections for shrinkage are still problematic and somewhat uncertain (Falcon-Lang et al., 2012). The corrected values are: 25 –33% (tangential diameter), 15 –25 % (radial diameter) and 10 –15% (longitudinal) (Falcon-Lang et al., 2012). The corrections were mainly applied in the tangential plane, and a 33 % was used for the mean vessel diameter. For the values of vessel density, the correction was applied in the radial diameter (25%) and tangential diameter (33%), which basically increases with charcoalification. When values were adjusted for charring, this is explained in the discussion of that specific wood type. The use of quantitative features in the searches was generally avoided; therefore, the identifications of charcoalified woods are based almost entirely on qualitative features.

3.4.5. PCA morphometrics methods

To further assess the identity of some of the wood types and to offer a more quantitative test, Principal Component Analysis (PCA) was performed, using features from the IAWA list for the identification of hardwoods (IAWA 1989). PCA is a multivariate analysis that finds hypothetical variables or "components" and where typically the major of variance is accounted for by the first three components (Hammer and Harper, 2006). The aim of this analysis is to project a multivariate dataset into a few dimensions in a coordinate system with axes corresponding to the "principal" or most important components (Hammer and Harper, 2006). If the major percentage of variance is represented in the two first components, the PCA is considered successful, although this varies depending on the number of used variables and the type of characters are used (Hammer and Harper, 2006).

The tests applied herein were mainly focused at familial rank. PCA were applied specifically to compare modern populations to fossil specimens in order to offer a numerical support to the identities (see chapter 4 and 5). In this thesis, the tests were applied to the Malvaceae and Cannabaceae, because a major amount of data was collected from direct observations for the slide collections for these two families. These PCA were applied using qualitative data and coded as present (1) or absent (0). Not all the features were used in the PCA because some of them were not particularly important to that specific family. Also traits that were all absent or all present in the tested species were generally avoided. When the character was variable, it was considered present (1). Therefore the selection of characters depended on the family or the wood characters that were certain and important for that family of plants. In subsequent Chapters 4 and 5, each PCA is discussed and the data matrixes are provided. The data were obtained combining direct observations of the microscopic slide collection in the Royal Botanic Gardens, Kew and the IWD. The features were coded and the results of PCA were obtained using the Palaeontological Statistics (PAST) software package.

CHAPTER 4. TAXONOMY OF PERMINERALISED FOSSIL WOODS (PART 1): CANNABACEAE, FABACEAE AND ELAEOCARPACEAE

4.1. INTRODUCTION

This chapter describes three taxa of permineralised woods (based on four samples), in addition to the dominant Malvaceae-type woods described in Chapter 5. All the samples come from tidally-influenced fluvial channel deposits (described in Chapter 2) from close to the base of the Cucaracha Formation at the Hodges Hill locality, Gaillard Cut, Panama Canal (Figure 4.1). The material constitutes the first reports of the families Cannabaceae, Fabaceae and Elaeocarpaceae in the fossil wood record of the Isthmus of Panama and Central America.

4.2. FOSSIL WOOD TYPE 1

Order: Rosales Bercht. & J.Presl

Family: Cannabaceae Martinov

Celtis aff *zenkeri*

Discussion: The combination of vessels solitary and in radial multiples of 2 – 3; abundant crystals in chambered and non-chambered parenchyma strands, and discontinuous bands of parenchyma, together with more general characters (wood diffuse porous, perforation plates simple, intervessel pitting alternate and long parenchyma strands), indicates an affinity with Cannabaceae, specifically to the genus *Celtis*.

4.1. Permineralised woods in the field. A, abundant logs in Hodges Hill slopes (arrows). B, STRI 14165 in pebbly sandstones. C, STRI 36273. D, close-up of STRI 36273. E, *Teredolites* borings in an internal section of STRI36273.F, STRI 36272 and its context in the field 5m from the main road to access the Hodges Hill slopes. G, close-up of STRI 36272.

Material: STRI 14165, comprising a hand specimen and three sections in TS, TLS and RLS. The preserved diameter of the axis is 0.12 m.

Repository: Center for Tropical Paleoecology and Archaeology, Smithsonian Tropical Research Institute, Panama.

Locality: Hodges Hill (Gaillard Cut of Panama Canal) near Paraiso, Panama City, Panama. Latitude 09°02’51.75’’N; Longitude 79°39’14.02’’W.

Stratigraphic horizon: ~ 20m above the base of the Cucaracha Formation (Gaillard Group); Lower Miocene (19 – 20 Ma).

4.2.1. Description

IAWA feature numbers: 2, 5, 13, 22, 23, 26, 30, 42, 47, 53, 61, 66, 69, 76v, 85, 91v, 92v, 93v, 94, 97, 106v, 108, 137, 141v, 142, 154.

Growth rings indistinct; wood diffuse-porous (Plate 4.1., 1); vessels mostly solitary (74%) and in radial multiples of 2 – 3 (– 5) (Plate 4.1., 2); vessels with oval outline (Plate 4.1., 2); perforation plates, simple (Plate 4.1., 3); intervessel pits alternate, polygonal and medium (mean 7 (SD= 1.1, n = 25; range 4– 8) (Plate 4.1., 4, 5); vessel – ray pitting similar in diameter and shape to intervessel pits (mean 5 (SD= 1.4 μm, n = 25; range 2 – 8) (Plate 4.1., 6, 7); mean tangential vessel diameter 135 (SD= 24.6 μm, n = 50; range 90 – 180 μm); mean vessel density 12 (SD= 4.5 per mm^2, n = 10; range 6 – 18) (Plate 4.1., 1); mean vessel element length 520 (SD= 177.7 μm, n = 25; range 220 – 840 μm); tyloses absent; vascular tracheids not observed.

Fibres thin to thick walled (Plate 4.1., 8), non-septate (Plate 4.1., 9) and with pits difficult to observe, but with seemingly simple to minutely bordered pits and common only in radial walls.

Axial parenchyma mostly in irregularly spaced bands of mostly 3 – 6 cells (Plate 4.1., 10). Axial parenchyma strands with a highly variable number of cells (Plate 4.2., 1, 2, 3), but mostly over 8-celled (Plate 4.2., 1).

Rays heterocellular, 1 – 3-seriate (Plate 4.2., 1, 2, 3, 6, 7) and < 1 mm high (mean height 0.5 (SD= 0.2 mm, n = 50; range: 0. 25 – 0.92 mm); rays commonly with procumbent bodies 4 or > rows of upright and /or square marginal cells (Plate 4.2., 4, 5), with long tails that can also be seen in TLS (Plate 4.2., 4). Mean ray spacing 10 (SD= 2 per mm; n = 15; range 7 – 14).

Solitary rhomboidal prismatic crystals abundantly present in chambered axial parenchyma cells and forming chains (Plate 4.2., 6, 7, 8). Solitary crystals also present in square ray cells but less abundantly (Plate 4.2., 9). More than one crystal of about the same size per cell or chamber (Plate 4. 2., 9).

Plate 4.1. Wood Type 1. *Celtis* aff *zenkeri*

1. Growth rings indistinct, wood diffuse-porous. STRI 14165, TS, scale: 1mm.
2. Vessels solitary and in radial multiples of 2 – 3. STRI 14165, TS, scale: 500 μm
3. Simple perforation plates (SPP). STRI 14165, RLS, scale: 100 μm
4. Intervessel pitting alternate (IVP). STRI14165, TLS, scale: 100 μm.
5. Close-up of intervessel pitting polygonal. STRI 14165, TLS, scale: 25 μm.
6. Vessel – ray pitting similar to intervessel pits (VRP). STRI 14165, RLS, scale: 50 μm.
7. Detail of vessel – ray pitting. STRI 14165, RLS, scale: 100 μm.
8. Thin-to thick-walled fibres. STRI 14165, TLS, scale: 100 μm.
9. Rays 1– 3-seriate and non-septate fibres (NSF). STRI 14165, scale: 100 μm.
10. Irregular parenchyma bands 3 – 6 cells wide (arrows). STRI 14165, TS, scale: 100 μm.

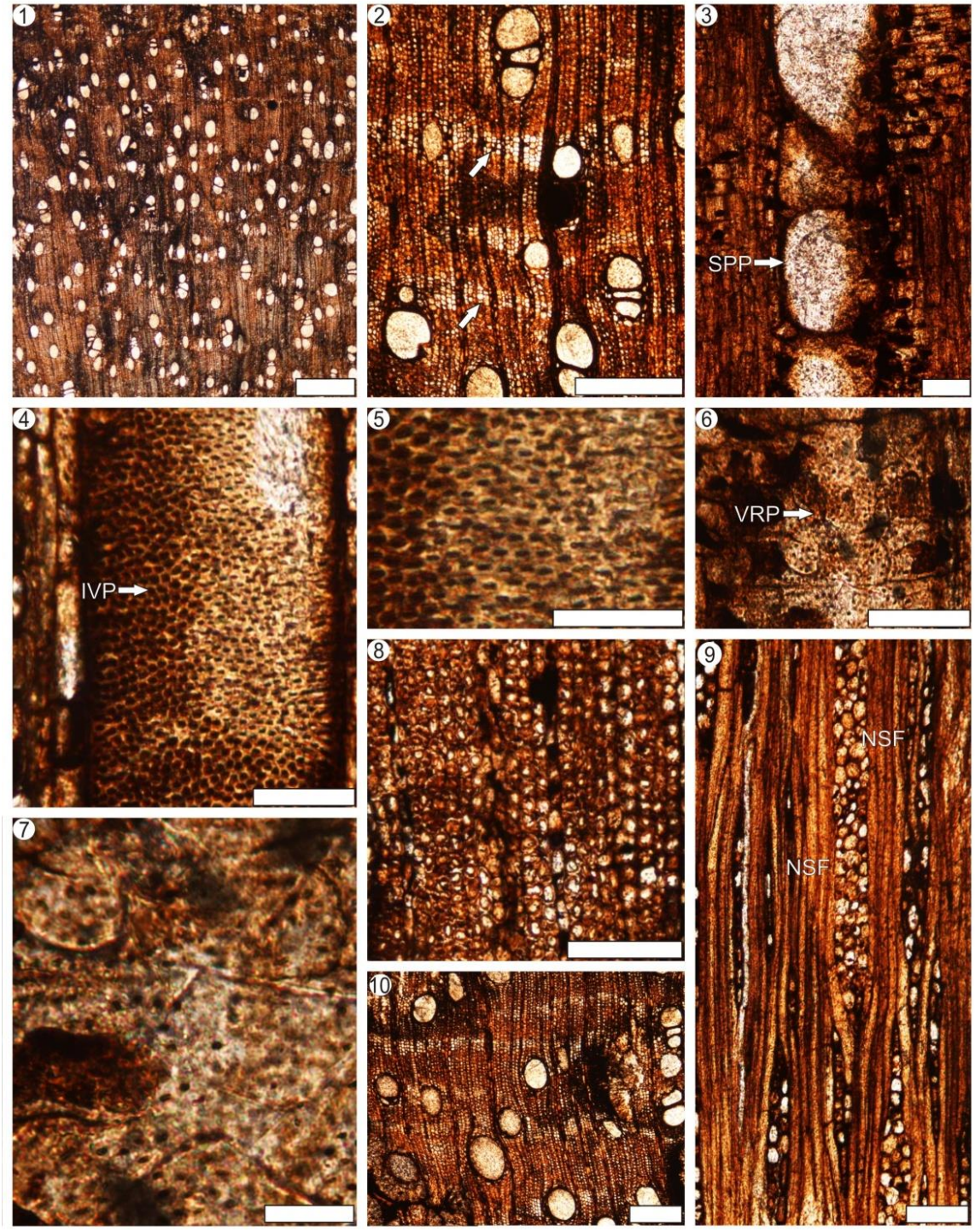

Plate 4.1

Plate 4.2. Wood Type 1. *Celtis* aff *zenkeri*

1. Axial parenchyma strands > 8 cells high (arrows). STRI 14165, TLS, scale: 100 μm.
2. Axial parenchyma strands 4 cells high (arrow). STRI 14165, TLS, scale: 100 μm.
3. Close-up of short axial parenchyma strands. STRI 14165, TLS, scale: 100 μm
4. Ray long tails seen in tangential section (arrows). STRI14165, TLS, scale: 100 μm.
5. Ray composed of procumbent cells (PC) and > 4 marginal rows of square cells. STRI 14165, RLS, scale: 100 μm.
6. Rays 1–3-seriate, rhomboidal crystals in chambered axial parenchyma cells (arrows). STRI 14165, TLS, scale: 100 μm.
7. Close-up of crystals in chambered axial parenchyma cells (arrow). STRI 14165, TLS, scale: 100 μm.
8. Crystals in short axial parenchyma strands (arrows). STRI 14165, TLS, scale: 100 μm.
9. Square ray cells with a few crystals and more than one crystal of about the same size per chamber (arrows). STRI 14165, RLS, scale: 100 μm.

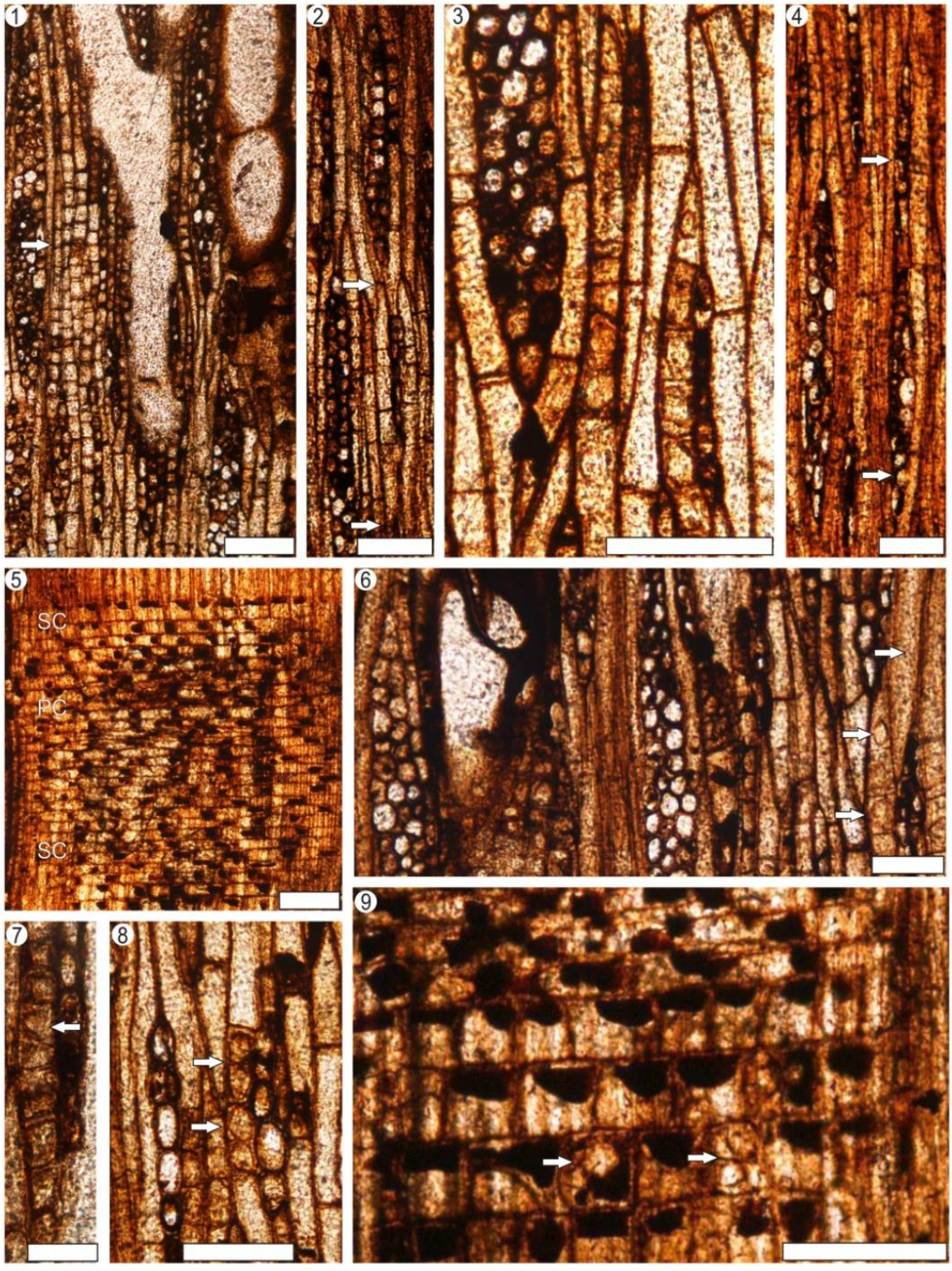

Plate 4.2

4.2.2. Affinities and justification

I used the following suite of features in an initial Inside Wood Database (IWD) search: diffuse porous wood (5p), alternate intervessel pitting (22p), vessel – ray pitting similar to intervessel pitting in size and distribution (30p), non-septate fibres present (66p), parenchyma in bands > 3 cells wide (85p), parenchyma strands > 8 cells high (94p), rays 1 – 3 cells wide (97p) and prismatic crystals present (136p). Allowing no mismatches, there were 23 matches in the IWD comprising 12 families as follows: Cannabaceae, Celastraceae, Combretaceae, Himantandraceae, Irvingiaceae, Ixonanthaceae, Lecythidaceae, Leguminosae, Meliaceae, Myrtaceae, Ochnaceae and Sapotaceae. The anatomical characteristics of these 23 taxa were reviewed using published descriptions (Metcalfe and Chalk, 1950; White and Gasson, 2008; PROTA, 2002; Richter and Dalwitz, 2000), micrographs available in the IWD, and the microscopic slide collection in the Jodrell Laboratory, Kew Gardens. The results of this review are as follows:

Cassine aethiopica Thunb. (Celastraceae) and *Phyllocosmos africanus* (Hook. f.) Klotzsch (Ixonanthaceae) can be excluded from consideration because of their exclusively solitary vessels and very regular and wide bands of parenchyma differ markedly from the fossil. These characters are also common in other species of *Cassine* and other genera of Celastraceae including *Pleurostylia* Wight, *Astrocassine* N. Robson and Arn. and *Salvadoropsis* H. Perrier. *Librevillea klainei* (Harms) Hoyle has distinct tangential axial canals and canals of traumatic origin, as common in some subfamilies of Fabaceae. These traumatic canals are also found in *Chukrasia tabularia* Juss and allow exclusion of these taxa because of their absence of these in the fossil. Several other taxa also show features not seen in the fossil and can be excluded as follows: *Stephonema sericeum* Hook. f. (Combretaceae) possesses exclusively solitary vessels

combined with abundant winged-aliform parenchyma. *Galbulimima baccata* Bailey (Himantandraceae) possesses very abundant parenchyma diffuse-in-aggregates. *Desbordesia insignis* Pierre (Irvingiaceae) shows vessel-ray pits in palisade and with distinct borders combined with winged paratracheal parenchyma and regular apotracheal parenchyma bands. The Lecythidaceae, including *Chydenanthus excelsus* Blume and *Eschweilera tenax* Miers show prominent scalariform parenchyma. Helical thickenings of vessels and vessel clusters are common in most of the *Azadirachta* Juss. (Meliaceae), consequently these are different from the fossil. In other genera of Meliaceae, such as *Chisocheton* Blume, *Eugenia* L. (Myrtaceae) and in some Ochnaceae, such *Lophira* Banks, reticulate parenchyma is common. Finally, *Sideroxylon* L. (Sapotaceae) is quite distinct from the fossil because of the very common vessel clusters arranged in diagonal pattern.

Of the 23 short-listed taxa, only members of the Cannabaceae show close resemblance to the fossils. Consequently, a revision of several genera was undertaken in Kew and in the IWD, of the Cannabaceae, including *Aphananthe* Juss., *Gironniera* Gaudich, *Parasponia* Miquel, *Trema* Loureriro, and *Celtis* L.. Until recently (e.g., Watson and Dalwitz, 1992; Ueda et al., 1997), *Celtis* was placed in the Ulmaceae and so, I also briefly studied some members of this family, such as *Chaetachme* Planchon, *Hemiptelea* Planchon., *Holoptelea* Planchon., and *Ulmus*. The Ulmaceae share characters such as simple perforation plates, alternate intervessel pitting, vessel-ray parenchyma similar in size to intervessel pits, predominantly paratracheal axial parenchyma, non-septate fibres with simple pits, rays mostly compound of procumbent cells and prismatic crystals. These characters are also shared with Cannabaceae except that the Cannabaceae tend to have heterocellular rays (Wheeler and Manchester, 2007. The Ulmaceae, typified by *Ulmus*, possesses a wood with very distinct features, including conspicuous wavy bands of latewood vessel clusters. This peculiar pattern is

known as “ulmiform” vessel distribution (IAWA, 1989). This character is absent in STRI 14165. Other analysed members of Ulmaceae lack this pattern but show only rare crystals. Based on these criteria, this family can been ruled out, and so I focus on the extant Cannabaceae only.

Amongst the Cannabaceae, *Aphananthe* possesses distinct growth rings and helical thickenings. *Trema* usually has very distinct rings, diffuse parenchyma and in a few species, the crystals are absent. There are additionally species of *Trema* (*T. integerrima* Beurl., *T. lamarckiana* Blume) that lack parenchyma and the vessels are exclusively solitary. In species of *Gironniera* the paratracheal parenchyma is the most common pattern. *Parasponia* combines distinct growth rings, abundant tyloses, vessel – ray pits in palisade and marginal parenchyma; all these features absent in the fossil.

To make the comparison more extensive, twigs of the following species were also studied: *Humulus lupulus* L., *Aphananthe aspera* Planch., *Aphananthe phillipensis* Planch., *Gironniera nervosa* Planch., *Gironniera reticulata* Thwaites, *Cannabis sativa* L., *Trema micrantha* L., *Trema orientalis* L., *Trema guinensis* Priemer. All these taxa differ from the fossil based on the following features: semi-ring porous wood and tangential bands of vessels in *Humulus*; rays exclusively uniseriate, vascular tracheids and predominance of short parenchyma strands (3 – 4 cells) in *Aphananthe*; bands of parenchyma very regular in *Gironniera*; vessel-ray pits with much reduced borders and in palisade and rare or absent parenchyma in *Cannabis.* However, the validity of comparing twig wood and mature fossil wood is uncertain due to ontogenetic effects (Falcon-Lang, 2005).

In this comparison, *Celtis* was found to be the most similar genus to the fossil material. Therefore, I focus on this genus for my detailed comparisons as follows:

4.2.3. Comparison with *Celtis*

According to descriptions from Sweitzer, (1971), *Celtis is* diverse in wood anatomy features. One of the main features that distinguish species of *Celtis* is common occurrence of banded parenchyma (Sweitzer, 1971), which contrasts with the irregularly banded parenchyma of the fossil specimen, STRI 14165. The parenchyma is diffuse or scanty in *C. africana* Burm. F. and *C. australis* L. In contrast, it is confluent in *C. bifida* Leroy, *C. biondii* Pamp., *C. bungeana* Blume, *C. sinensis* Willd, and *C. tessmannii* Rendle allowing these taxa to be excluded.

Another important character in the systematics of *Celtis* is vessel grouping. *C. africana, C. australis, C. occidentalis,* and *C. laevigata* Willd commonly have vessels in clusters of more than four vessels, whereas in the fossil, the common solitary vessels are combined with radial multiples of 2 – 3(– 5).

Another important criterion to determine the best match for the fossil wood is the abundance and distribution of the crystals. Most of the observed species of *Celtis* have crystals, but crystals are rarely observed or totally lacking in, at least, two species (e.g., *C. adolphifredrici* Engl., *C. laevigata*). Crystals in *Celti*s, occur abundantly in both ray cells and parenchyma strands, whereas in the fossil, the crystals are clearly more abundant in parenchyma strands. One species with a particular abundance of crystals is *C. timorensis* (formerly *C. cinnamonea)*, in which crystals are not only numerous in the ray cells, but also in the parenchyma strands, including the occurrence of raphides. I did not observe any raphides in the fossil wood, but additionally, *C. timorensis* tends to have wider rays and lacks banded parenchyma.

The best match for the fossil wood is *Celtis zenkeri* Engl (formerly *C. soyauxii*) (Table 4.1) which shares characters such as diffuse porosity (Plate 4.3., 1); a similar percentage of solitary vessels, with a few vessels in groups of 2 – 3 (Plate 4.3., 2); simple perforation plates (Plate 4.3., 3); intervessel pitting alternate (Plate 4.3., 4, 5);

vessel-ray pitting similar than the intervessel pitting (Plate 4.3., 6, 7); non-septate fibres (Plate 4.3., 8) with walls thin to thick (Plate 4.3., 9, 10); banded parenchyma with irregular bands 3 – 6 cells wide (Plate 4.3., 1, 2, 10), rays 1 – 3 cells wide (Plate 4.4., 1, 3, 4); parenchyma strands 8-celled or over (Plate 4.4., 2); rays with long procumbent bodies of 4 or > 4 rows of upright/squared cells (Plate 4.4., 5) and abundant crystals (Plate 4.4., 4, 5, 6). I note that the crystals are distributed differently in *Celtis zenkeri*; in the extant species, crystal abundance is greater in the ray cells, while in the fossil, it is greater in the parenchyma strands.

Species/characters	STRI 14165	*Celtis zenkeri*
Percentage of grouping (%)	26	33
Intervessel pit size (μm)	7 ± 1.1 (4– 8)	7 ± 1.2 (5 – 9)
Vessel-ray pit size	5 ± 1.4 (2 – 7)	6 ± 1.3 (4 – 8)
Mean tangential vessel diameter (μm)	135 ± 25 (90 – 180)	144 ± 33.5 (90– 250)
Vessels/mm^2	12 ± 4.5 (6 – 18)	12 ± 2.8 (7– 16)
Mean vessel element length (μm)	520 ± 178 (220 – 840)	471 ± 83 (343 – 840)
Ray width (n cells)	2 ± 1.1 (1– 4)	3 ± 0.7 (1– 4)
Ray height (mm)	0.5 ± 0.2 (0. 2 – 0.9)	0.3 ± 0.1 (0.2– 0.6)
Rays /mm	10.5 ± 2 (7 – 14)	8 ± 1.2 (6– 11)

Table 4.1. Quantitative comparison of STRI 14165 and *Celtis zenkeri.*

Plate 4.3. *Celtis zenkeri* Engl. Specimen accessioned in Kew as FHI 22813.

1. Growth rings indistinct, wood diffuse-porous; vessels in radial multiples 2 – 5. TS, scale: 500 μm.
2. Vessels in radial multiples of 2 –3. TS, scale: 200 μm.
3. Perforation plates, simple; axial parenchyma strand. RLS, scale: 100 μm
4. Intervessel pitting alternate and small. TLS, scale: 20 μm.
5. Detail of intervessel pitting. TLS, scale: 20 μm.
6. Vessel – ray pitting (VRP) similar to intervessel pits RLS, scale: 10 μm.
7. Close-up of vessel–ray pitting. RLS, scale: 20 μm.
8. Non-septate fibres (NSF). TLS, scale: 50 μm.
9. Thin-to thick-walled fibres and parenchyma cells (PC) interspersing them. TS, scale: 100 μm.
10. Close-up of parenchyma bands 3 – 6 cells wide. TS, scale: 100 μm.

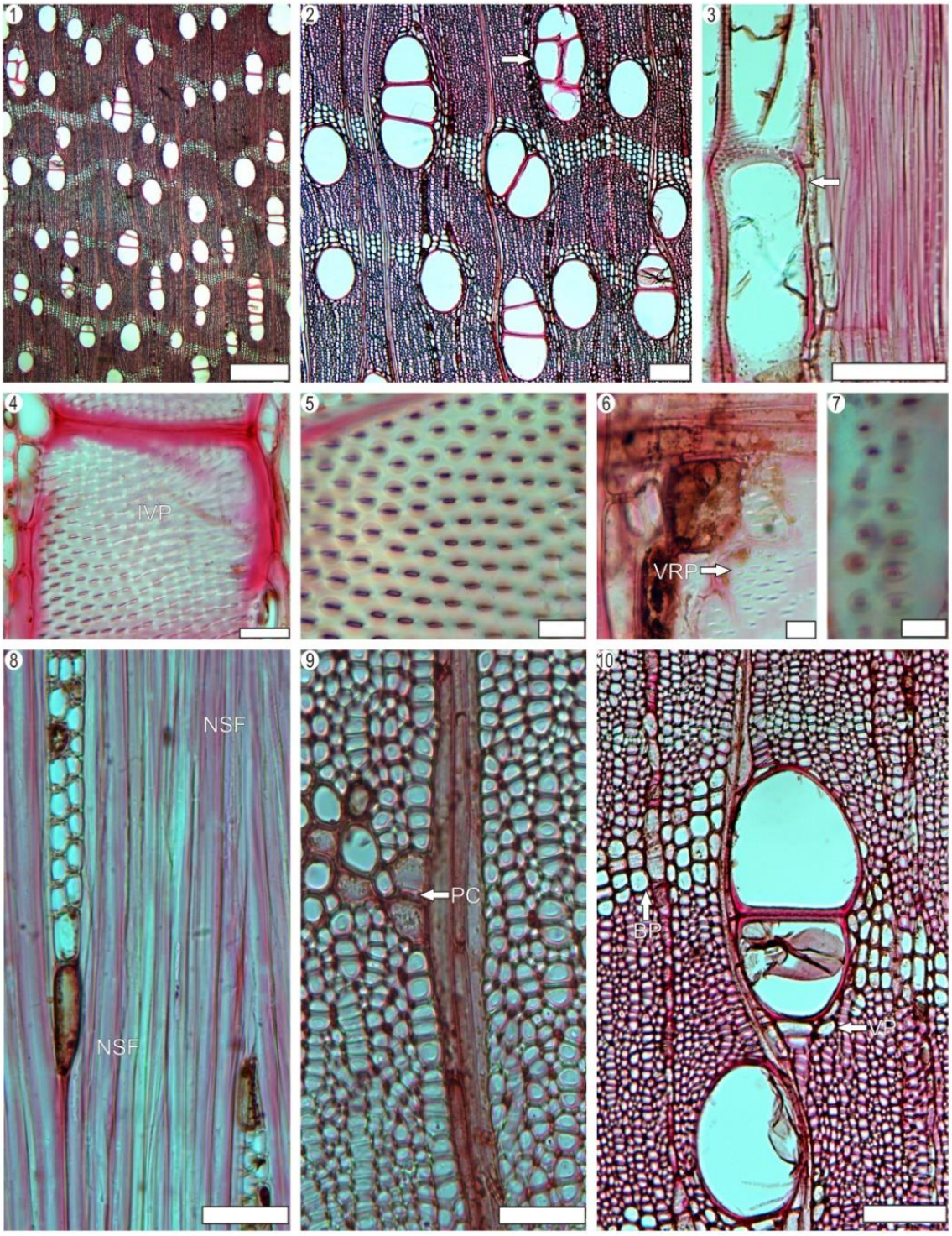

Plate 4.3

Plate 4.4. *Celtis zenkeri* Engl. Specimen accessioned in Kew as FHI 22813.

1. Axial parenchyma strands (PS), 5– 8 cells high and non-septate fibres (NSF). TLS, scale: 100 μm.
2. Detail of a common axial parenchyma strand 8 cells high. TS scale: 10 μm.
3. Rays 1 – 3 cells wide; axial parenchyma strands. TLS, scale: 100 μm.
4. Crystals in axial parenchyma strands. TLS, scale: 50 μm.
5. Rays composed of procumbent cells (PC) and 2 – 6 of upright (UC) and square (SC) cells. RLS, scale: 50 μm.
6. Rhomboidal crystals in axial parenchyma strands and ray cells. TLS, scale: 50 μm.

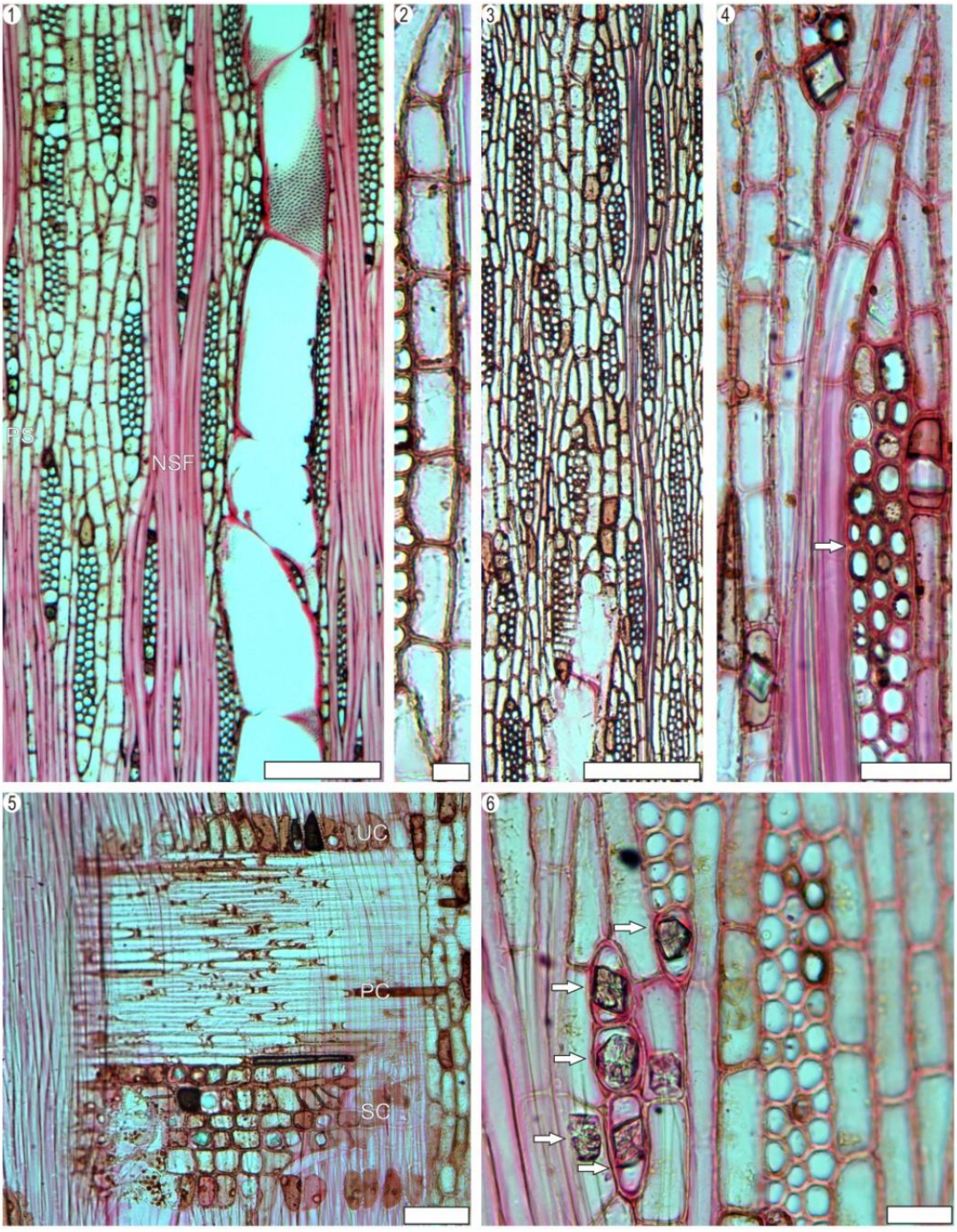

Plate 4.4

Character	Number	Species	Number
Growth rings distinct	**1**	STRI 14165	**1**
Growth rings indistinct	**2**	*Aphananthe philippinensis*	**2**
Ring porous	**3**	*Aphananthe sakalava*	**3**
Semi-ring porous	**4**	*Celtis adolfi -fridereci*	**4**
Diffuse porous	**5**	*Celtis africana*	**5**
Vessels in tangential bands	**6**	*Celtis australis*	**6**
Vessels in diagonal	**7**	*Celtis bifida*	**7**
Vessels exclusively solitary	**8**	*Celtis biondii*	**8**
2-4 groups common	**9**	*Celtis bungeana*	**9**
Clusters common	**10**	*Celtis cinnamomea*	**10**
Vessel outline angular	**11**	*Celtis durandu*	**11**
Simple perforation plates	**12**	*Celtis ehrenbergia*	**12**
Scalarifom perforation plates	**13**	*Celtis glycicarpa*	**13**
Intervessel pits alernate	**14**	*Celtis iguananea*	**14**
Intervessel pits polygonal	**15**	*Celtis jessoensis*	**15**
Vessel-ray pits similar to IV pits	**16**	*Celtis integrifolia*	**16**
Vessel-ray pits with much reduced borders	**17**	*Celtis koraiensis*	**17**
Vessel-ray pits gash like or palisade	**18**	*Celtis laevigata*	**18**
Vessel ray pits of two distinct sizes	**19**	*Celtis latifolia*	**19**
Vessel-ray pits restricted to margins	**20**	*Celtis luzonica*	**20**
Helical thickenings	**21**	*Celtis milbraedii*	**21**
Tyloses common	**22**	*Celtis occidentalis*	**22**
Gums and deposits	**23**	*Celtis occidentalis (RW16se)*	**23**
Vascular tracheids	**24**	*Celtis pacifica*	**24**
Fibre pits minutely bordered	**25**	*Celtis paniculata*	**25**
Fibre pits common in tangential walls	**26**	*Celtis phillipensis*	**26**
Non septate fibres	**27**	*Celtis schippi*	**27**
Fibres very thin walled	**28**	*Celtis sellenia*	**28**
Fibres thin to thick walled	**29**	*Celtis sinensis*	**29**
Fibres very thick walled	**30**	*Celtis vandervoetica*	**30**
Axial parenchyma diffuse	**31**	*Celtis zenkeri*	**31**
Axial parenchyma diffuse in aggregates	**32**	*Humulus lupulus*	**32**
Axial parenchyma scanty paratracheal	**33**	*Pteroceltis tatarinowi*	**33**
Parenchyma vasicentric	**34**	*Trema angustifolia*	**34**
Paratracheal parenchyma lozenge/winged aliform	**35**	*Trema cannabina*	**35**
Parenchyma confluent	**36**	*Trema guinnensis*	**36**
Parenchyma unilateral	**37**	*Trema micrantha*	**37**
Parenchyma bands > 3 cells wide	**38**	*Trema orientalis*	**38**
Parenchyma bands 1-3 cells wide	**39**	*Aphananthe phillipensis* (twig)	**39**

4.2.4. PCA morphometrics

To offer a more quantitative test for this identification, a total of 70 features from the IAWA list for the identification of hardwoods (IAWA 1989) were coded as present (1) or absent (0) for 40 species of Cannabaceae (Table 4.2; Appendix 4.2.4;) using the IWD and direct observations of the microscopic slide collection in the Royal Botanic Gardens, Kew (Appendix 4.2.4). These data were analysed using PCA (see Chapter 3). The loadings of the analysis highlight apotracheal parenchyma types as the characters with the largest influence and potentially explain the grouping of the species seen in the scatter (Figure 4.2). Because of the variation of the types of parenchyma of *Celtis*, this genus does not group together in the PCA plot.

In the PCA (Figure 4.2) the fossil does not seem to group together with any particular genus. The two taxa closest to the fossil are *Celtis iguanaea* and *Trema angustifolia*. *C. iguanaea* was previously discussed as one of the species of *Celtis* with a close resemblance to STRI 14165, whereas the species of *Trema* were not considered. *Celtis* has a variable wood anatomy but the species with ring-porosity seem to be distinct from the ones with diffuse porosity (Wheeler et al., 1989; Jansen et al., 2007). Therefore it would be expected that such species would be separated in the PCA. The closeness of *Trema* to the fossil in this PCA could be explained by the common diffuse –porosity of these species. I note that, with a few exceptions, all the species of *Celtis* of the New World (e.g., *C. iguananea*, *C. sellenia*, *C. occidentalis*, *C. pacifica*, *C. schippi*) are in the same quadrant with STRI 14165, thus separated from the species of *Celtis* in the opposite quadrant, that are almost entirely distributed in the Old World (e.g., *C. sinensis*, *C. Africana*, *C. jessoensis*, *C. bungeana*).

Parenchyma reticulate	**40**	*Cannabis sativa*	**40**
Parenchyma marginal	**41**		
Parenchyma scarce/absent	**42**		
2 cells / strand	**43**		
3-4 cells / strand	**44**		
5-8 cells / strand	**45**		
Over 8 cells / strand	**46**		
Rays exclusively uniseriate	**47**		
Rays 1-3 cells wide	**48**		
Rays 4-10 cells wide	**49**		
Rays > 10 cells wide	**50**		
Rays 2 sizes	**51**		
All ray cells procumbent	**52**		
All ray cells square/upright	**53**		
1 row of upright/square cells	**54**		
2-4 rows of marginal cells	**55**		
> 4 rows of marginal cells	**56**		
Rays with mixed cells	**57**		
Sheath cells	**58**		
Perforated ray cells	**59**		
All rays storied	**60**		
Parenchyma/vessel elements storied	**61**		
Fibres storied	**62**		
Elements irregularly storied	**63**		
Crystals in upright/square ray cells	**64**		
Crystals in procumbent ray cells	**65**		
Crystals aligned in tangential rows in ray cells	**66**		
Crystals in chambered ray cells	**67**		
Crystals in non-chambered parenchyma cells	**68**		
Crystals in chambered parenchyma cells	**69**		
Druses present	**70**		

Table 4.2. Key table for PCA plot of Cannabaceae.

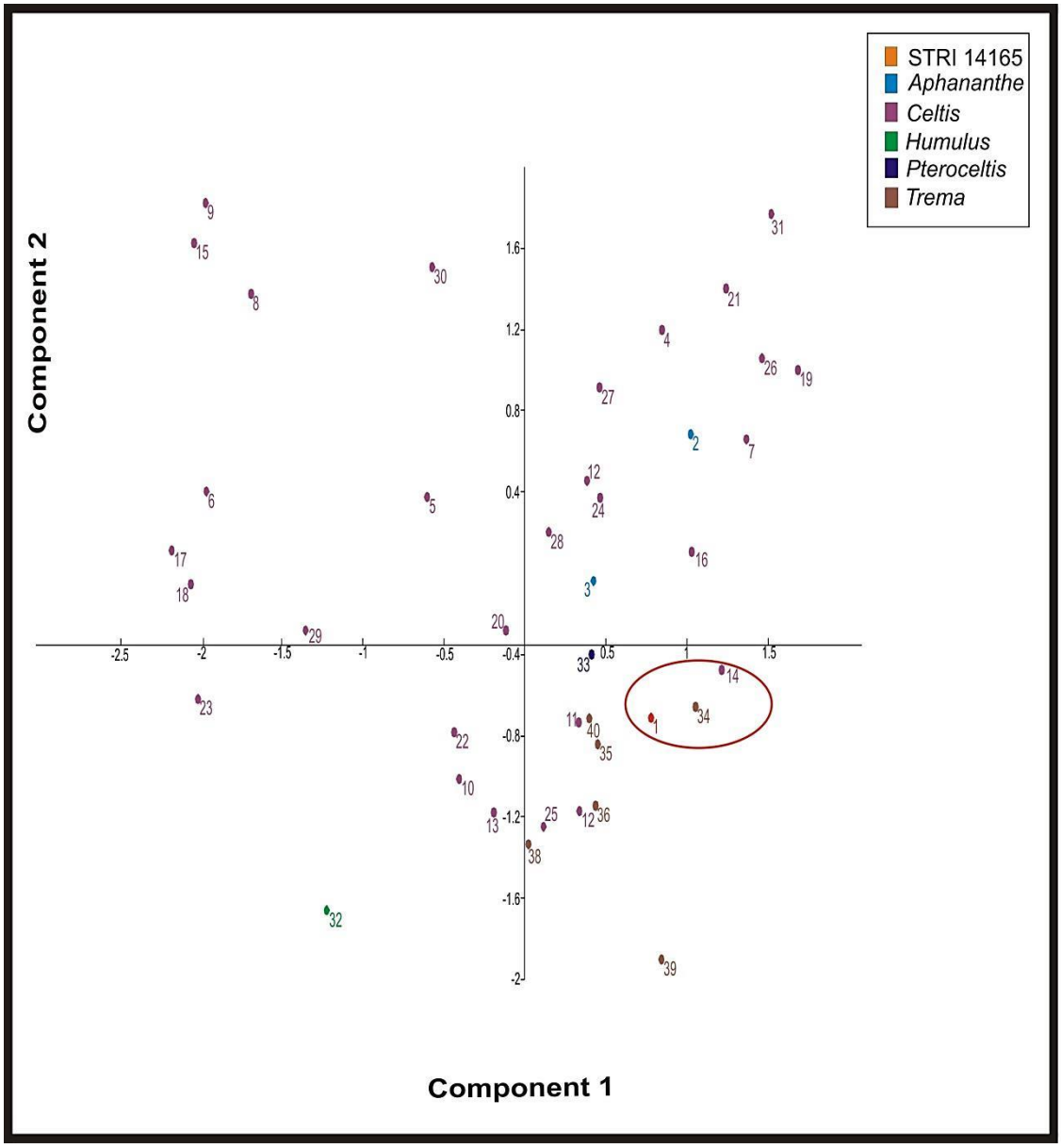

Figure 4.2. PCA plot of modern species of Cannabaceae.

I still consider there is numerical support for the identification of STRI 14165 as similar to species of *Celtis.*

4.2.5. Systematics and ecology of *Celtis*

Celtis is included in an extended Cannabaceae family, according with the Angiosperm Phylogeny Group (2014). Traditionally, Cannabaceae comprised only two

the occurrence of Celtis in Cretaceous times is unproven (Manchester, 2002). For the Paleogene the fossil record of *Celtis* is more assured. A global distribution during the Paleogene for this genus is indicated fruit remains (Chesters, 1957; Manchester, 1989, 1994, 1999, 2002), leaves (Hickey, 1980; Wing et al., 1995) and woods (Hofman, 1928b; Edwards, 1931; Greguss, 1943; Wurzinger, 1953; Selmeier, 1957; Horváth, 1954; Petrescu, 1978; Gottwald, 2004).

Most of the fossil woods related to *Celtis* are from the Miocene. These woods include reports of *Aphananthe wuhanensis* (Yang et al., 1987). Like the modern wood *Aphananthe*, it has very distinct rings and abundant paratracheal parenchyma combined with marginal bands of parenchyma. There are also several reports of *Celtixylon*: *C. campestre* (Greguss, 1969), *C. cristalliferum* (Selmeier, 1989; Selmeier, 2001), *C. dadicum* (Petrescu, 1978), *C. occidentalis* (Horvath, 1954), and *C. palaeohungaricum* (Greguss, 1943). The woods of *Celtixylon* have distinct rings, ring and semi-ring porous wood, vessel clusters common and rays 4 – 10-seriate, all of these features are absent in the Panamanian wood.

The distribution of *Celtis* today is extensive, ranging from tropical to temperate latitudes and is found on all the continents (Manchester, 2002; Angiosperm phylogeny Website, 2012). As a consequence of the rich fossil reports from both hemispheres for the Miocene and the unconfirmed record for the Cretaceous, it is difficult to infer the geographic origin of *Celtis* (Manchester, 2002). Birds are understood as the main dispersers even back to the Paleogene (Manchester, 1989).

4.2.7. The new report of *Celtis* in the Isthmus of Panama

The fossil wood represents the first fossil record of *Celtis* found in Panama. The only previous report confirming the presence of Cannabaceae in the Panamanian Isthmus has

genera, *Cannabis* L. and *Humulus* L. (Takhtajan, 1980; Punt and Malotaux, 1984). The rest of the currently recognized members of the family, namely, *Aphananthe* Planchon, *Celtis* L., *Gironniera* Gaudich., *Lozanella* Greenman, *Parasponia* Miquel, *Pteroceltis* Maxim and *Trema* Loureriro were, as noted above, originally part of the Ulmaceae family (Ueda et al., 1997. In the old classification Ulmaceae was composed by two main subfamilies, the Ulmoideae and Celtidoideae distinguished by differences in fruit type, embryology and leaf venation (Hutchinson, 1967). A few molecular studies have been performed to solve the phylogeny of these groups, and in most of them Celtidoideae is recognized as a paraphyletic to a monophyletic group that comprises Ulmaceae (Zavada and Kim, 1996; Wiegrefe et al., 1998), and closely allied to the Cananabaceae. The current expanded Cannabaceae concept, incorporating the former Celtidoideae, is characterized by serrate leaves with ascending veins not ending straight to the teeth and the fruits are a rounded drupe (Angiosperm Phylogeny Website).

Celtis is a genus with about 100 species (Angiosperm Phylogeny Group, 2012). The species of this genus are commonly known as hackberries and are generally tree habit, except by rare cases of shrubs e.g., *C. tenuifolia* Nutt. (Dwarf Hackberry). *Celtis* is distributed in tropical and temperate regions (eFloras, 2008; Demir et al., 2002) worldwide and are winter food providers for birds and mammals (eFloras, 2008).

4.2.6. Fossil record of *Celtis*

The first putative appearance of *Celtis* in the fossil record comprises pollen of *Triorites minutipori* from Cretaceous (Turonian) to Eocene sediments of Sarawak (Muller, 1968, 1981); however, this report is uncertain because this pollen type is difficult to distinguish from several other genera of Cannabaceae, such as *Aphananthe*, *Celtis*, *Chaetacme*, *Gironniera*, *Lozanella*, *Parasponia*, *Pteroceltis* and *Trema*. Thus

been of seeds recovered from the Cucaracha Formation (Herrera et al., 2012). In the W3 Tropicos Checklist of the Missouri Botanical Garden (2012), approximately 4 species of *Celtis* are listed to occur in Panama. The checklist shows 20 different names but some of them are synonyms of *Trema micrantha* and *Celtis iguananea.* Three images available in the IWD for *C. iguananea* were studied. This wood shows similar patterns in the parenchyma and rays to the STRI 14165, but unfortunately, no microscopic slides of these species are available for a direct comparison.

In Panama, herbarium specimens of *Celtis* have been collected in coastlines and also along rivers (Smithsonian Tropical Research Institute Herbarium, 2012). Although I consider this new report of *Celtis* should not be seen as a definite indicator of any particular environment we remark on the probable adaptation of this plant to riparian niches and/or coastlines, a suggestion also supported by the coexistence with other plants adapted to those environments (as will be detailed further in this thesis). The species of *Celtis* inhabiting the Isthmus of Panama today are, more broadly, part of the lowland rainforest biome.

4.3. FOSSIL WOOD TYPE 2

Order: Fabales Bromhead

Family: Fabaceae Lindley

Prioria aff *copaifera*

Discussion: The specimens possess abundant paratracheal parenchyma combined with narrow bands of marginal parenchyma; axial canals distributed diffusely and in short lines, and some other features typical of the Leguminosae (Wheeler and Baas, 1992; Herendeen, 2000; Gasson et al., 2003), specifically in the tribe Detarieae

(subfamily Caesalpinioideae), for which reason, we assign this wood to the genus, *Prioria.*

Material: STRI 36273 and STRI 36400, designated here, comprising two hand specimens and six sections in TS, TLS and RLS. The original trunk in the field had a length of 2 m and the preserved diameter of the axis is 0.8 m diameter.

Repository: Center for Tropical Paleoecology and Archaeology, Smithsonian Tropical Research Institute, Panama.

Locality: Hodges Hill (Gaillard Cut of Panama Canal) near Paraiso, Panama City, Panama. Latitude 09° 02 ’51.75’’N; Longitude 79° 39’14.02’’W.

Stratigraphic horizon: ~ 20m above the base of the Cucaracha Formation (Gaillard Group); Lower Miocene (19 – 20 Ma).

4.3.1. Description

IAWA features numbers: 2, 5, 13, 22, 24v, 25, 30, 42, 47, 52, 56v, 61, 66, 69, 79, 80, 82, 89, 92v, 93, 94v, 97, 98v, 104v, 106, 107, 115, 127v, 128, 129v, 137, 141v, 142.

Growth rings indistinct; wood diffuse-porous (Plate 4.5., 1); vessels solitary (57 %) or in radial multiples of 2 – 5 (–7) (Plate V, 2); vessels with oval outline; perforation plates, simple (Plate 4.5., 3); intervessel pits alternate (Plate, 4.5., 4, 5) and minute to small (mean 5; SD 0.99 μm; n = 25; range 3 – 7 μm) (Plate 4.5., 5); vessel – ray pitting similar in diameter and shape to intervessel pits (mean 4; SD1.5 μm, n = 25; range 2 – 7 μm) (Plate 4.5., 6); mean tangential vessel diameter 137 (SD 23 μm; n = 50; range 90 – 190 μm); mean vessel density 8 per mm^2; SD 3.1 per mm^2 ; n = 15; range 6 – 18 per mm^2); mean vessel element length 308 μm (SD 72 μm; n = 25; range 210 – 540 μm); tyloses common and sclerotic (Plate 4.5., 7, 8); vascular tracheids not observed.

Fibres non-septate (Plate VI, 1) with minutely bordered pits common in radial walls and occasional in tangential walls (Plate 4.6., 2). Fibres thin to thick-walled (Plate 4.6., 3).

Axial parenchyma mostly paratracheal vasicentric to short winged-aliform (Plate 4.6., 3; apotracheal parenchyma in occasional marginal bands 1 – 4 cells wide that mark ring boundaries (Plate 4.6., 4); axial parenchyma strands 3 – 8 cells high, but mostly 8-celled (Plate 4.6., 5).

Rays heterocellular, 1 – 3 (– 4)-seriate (mean 2.8 ± 0.7, n = 50) (Plate 4.6., 6) and commonly < 1 mm (mean 0.8 ; SD 0.2 mm; n = 50; range 0.4 – 1.5 mm) (Plate 4.6., 6); rays composed of procumbent bodies and 1 or 2 rows of upright and/or square marginal cells (Plate 4.6., 7), also occasionally composed exclusively of procumbent cells. Mean ray spacing 9.1 (SD 2.5 per mm; n = 15; range 5 – 13).

Solitary rhomboidal crystals found in square ray cells (Plate 4.6., 8), but more abundant in chambered parenchyma strands (Plate 4.6., 5). There are also rhomboidal crystals in non-chambered parenchyma strands, but less abundantly. Intercellular axial canals diffuse (Plate 4.6., 9) and commonly forming short lines (Plate 4.6., 10) that alternate with the marginal parenchyma bands. Some long tangential lines of axial canals are also observed, but they are rarely occurring.

alternate with the marginal parenchyma bands. Some long tangential lines of axial canals are also observed, but they are rarely occurring.

Plate 4.5. Wood Type 2. *Prioria* aff *copaifera*

1- Growth rings indistinct, marked by narrow bands of marginal parenchyma (arrows) and wood diffuse- porous. TS scale: 1mm.

2- Vessels in radial multiples of commonly 2 –5. TS scale 250 µm.

3- Perforation plates simple (arrow). RLS, scale: 100 µm.

4- Intervessel pitting alternate. TLS, scale: 100 µm.

5- Close-up of intervessel pitting minute to small. TLS, scale: 50 µm.

6- Vessel – ray pitting (circle) similar to intervessel pits in size and shape. RLS, scale: 100 µm.

7- Tyloses abundant (arrow). TS, scale: 100 µm.

8- Tangential view of tyloses (arrow). TLS, scale: 100 µm.

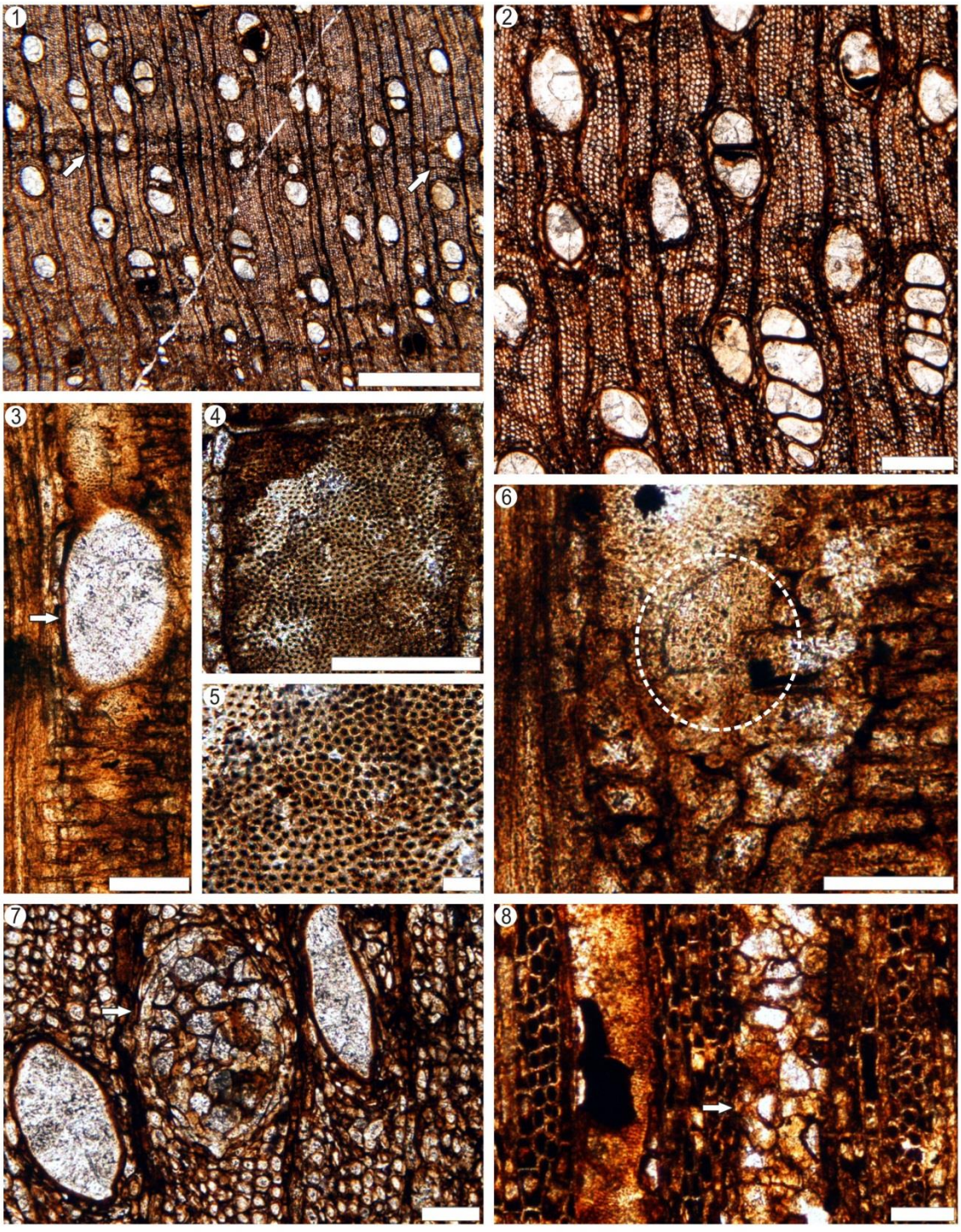

Plate 4.5

Plate 4.6. Wood Type 2. *Prioria* aff *copaifera*

1- Non-septate fibres (NSF). TLS, scale: 100 µm.

2- Minutely bordered fibre pits (arrows) common in radial walls. RLS, scale: 100 µm.

3- Fibres thin to thick walled and vessels with vasicentric winged–aliform parenchyma (arrows). TS, scale: 100 µm.

4- Marginal band of parenchyma 1–4 cells wide (arrows). TS, scale: 100 µm.

5- Parenchyma strands 6 cells high and abundant crystals present in chambered cells. TLS, scale: 50 µm.

6- Rays 3-seriate in average and fibres pitted in tangential walls (arrows). TLS, scale: 100 µm.

7- Ray body composed of procumbent cells (PC) and 1 row of square cells (SC). RLS, scale: 100 µm.

8- Solitary rhomboidal crystal in square ray cell (arrow). RLS, scale: 100 µm.

9- Diffuse axial canals (arrows). TS, scale: 50 µm.

10- Short line of axial canals (arrow). TS, scale: 100 µm.

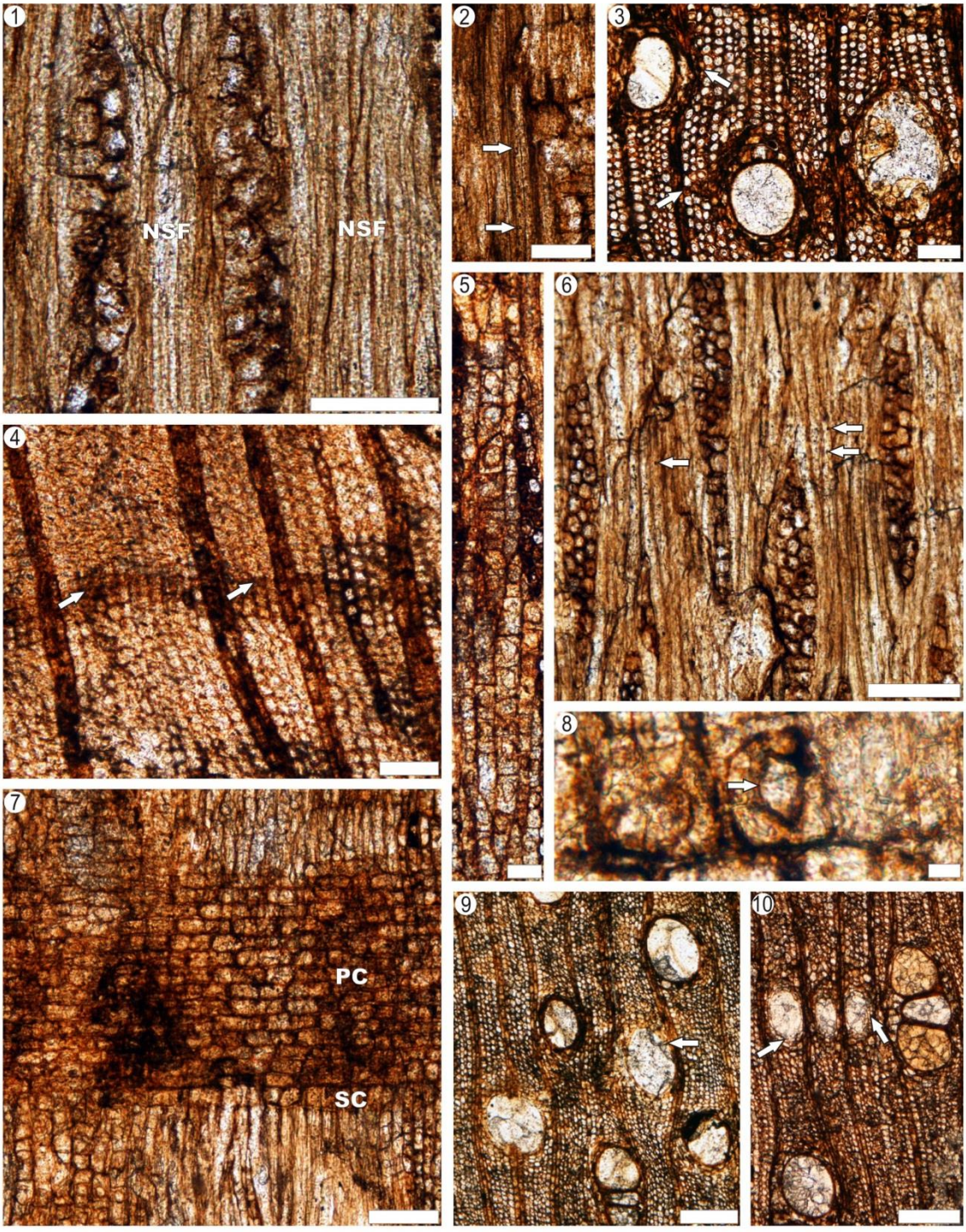

Plate 4.6

4.3.2. Affinities and justification

The following characters present in the specimens STRI 36273 and 36400 were used in IWD searches: wood diffuse-porous (5 p), perforation plates simple (13 p), alternate intervessel pitting (22 p), vessel – ray pitting similar to intervessel pitting in size and shape (30 p), non-septate fibres present (66 p), paratracheal parenchyma vasicentric (79 p) to winged-aliform (82 p), apotracheal parenchyma in marginal bands (89 p), rays 1– 3 cells wide (97 p), axial canals in short tangential lines (128 p) and solitary prismatic crystals in chambered axial parenchyma strands (142 p). The searches only produced results suggesting affinities with the Leguminosae (Fabaceae). Additionally, these features are repeatedly listed in the literature as diagnostic to the family (Metcalfe and Chalk, 1950; Wheeler and Baas, 1992; Gasson, 1994; Gasson et al., 2003; Wheeler and Manchester, 2002; Brandes and Barros, 2007; Pujana et al., 2011).

Leguminosae (Fabaceae s.l.) is the third largest family of flowering plants after the orchids (Orchidaceae) and daisies (Compositae) with ca. 730 genera and ca. 19,400 species. This family is of cosmopolitan distribution (MacKinder et al., 2006) and constitutes a major component of most of the world´s vegetation types (Sprent, 2001). The high variation of legume wood anatomical types and similarity in characters in more than one extant genus, tribe or even subfamily, makes the identification of isolated wood types very problematic (Wheeler and Manchester, 2002). There are legume genera that have very distinct woods (e.g., *Robinia* L., *Dalbergia* L.; Wheeler and Baas, 1992), as there are some others with a lot of similarities in their wood (e.g., *Lonchocarpus* and *Millettia*; Baretta-Kuipers, 1981).

In a survey of the IWD and key literature (Wheeler and Baas, 1992; Herendeen, 2000; Gasson et al., 2003), I found common occurrence of the key characters in the fossil woods and members of the subfamily Caesalpinioideae (e.g., aliform parenchyma combined with marginal narrow bands, thin to thick walled fibres, non-storied and narrow rays, prismatic crystals abundant in chambered parenchyma cells), hence I focused the comparison on this subfamily.

4.3.3. Affinities with Caesalpinioideae

The subfamily Caesalpinioideae is divided into 4 tribes: Caesalpinieae, Cassieae, Cercideae and Detariae. They are mainly trees, shrubs or lianas with a largely tropical distribution with some extension into temperate regions (Klitgaard and Lewis, 2010). The Caesalpinioideae are generally considered the most taxonomically problematic subfamily in the Fabaceae, although recent efforts have been made to improve this situation (Bruneau et al., 2001; Banks and Gasson, 2000; Herendeen, 2000). The 'caesalpinioids' have a lot of variation in their wood anatomy (for an extensive and detailed study of this subfamily see Gasson et al., 2003) but it is common to find winged-aliform, confluent and marginally banded parenchyma, medium to thick walled fibres, non-storied biseriate rays (homocellular or with a row of square or upright cells), vestured pits, and chains of crystals in chambered parenchyma.

Alternate intervessel pitting is characteristic of all of the Fabaceae and it has been remarked that it is a feature of diagnostic potential; pit size is especially useful to distinguish between some Caesalpinioideae groups (e.g., large intervessel pits are found in *Caesalpinia*, *Cassinae* and *Amhertisia*). The presence of vestured pits also proves to be of diagnostic character for this subfamily in different surveys (e.g., Herendeen et al.,

, 2003; Gasson et al., 2003); however, this is a highly problematic and uncertain feature in some cases. The specimens studied here have minute to small intervessel pits, which make it more difficult to assign a IAWA feature number, with certainty, especially in fossil woods where mineral deposits can resemble vestures (Wheeler and Baas, 1992).

A key feature observed in the fossils is the occurrence of normal axial canals distributed diffusely and in short lines. Gasson et al. (2003) and Baretta-Kuipers (1994) state that only members of the tribe Detarieae possess axial canals in variable distribution patterns. Therefore, these groups are proposed as the best match for the fossil specimens discussed here.

4.3.4. Affinities with the Detarieae

The Detarieae comprise 82 genera and are pantropical in distribution (Lewis et al., 2005). This tribe has been informally divided in the following nine groups: 'Cynometra', 'Hymenostegia', 'Hymenaea', 'Crudia', 'Detarium', 'Berlinia', 'Macrolobium', 'Amherstia', and 'Brachystegia' named after their emblematic genera. To discriminate genera and find the best possible match for this wood, the following comparison focuses on four features of the fossil: (1) parenchyma, mainly paratracheal, ranging from vasicentric to winged-aliform combined with narrow bands of marginal parenchyma; (2) the absence of storied structures, especially the absence of storied rays; (3) the occurrence of diffuse normal axial canals and in short lines; and (4) the presence of rhomboidal crystals in ray cells and in parenchyma strands, with prevalence in chambered axial parenchyma cells.

The parenchyma is dominantly paratracheal in most legumes (Gasson et al., 2003; Pujana et al., 2011), and this is also true for the Caesalpinioideae and the tribe

Detarieae. In all of the groups in Detarieae, the parenchyma tends to be a mix of vasicentric and winged-aliform types, but usually combined with abundant wide (in the *'*Cynometra*'*, *'*Detarium*'* and *'*Hymeanea*'* groups) and narrow bands of parenchyma (in the *'*Hymenostegia*'*, *'*Amherstia*'* and *'*Berlinia*'* Group).

The occurrence of storied rays and parenchyma or fibres is highly varied in the Leguminosae. This feature is rarely present in the Detarieae, but there are some genera where all the rays are storied as in *Daniellia.* Normal axial canals are a feature present only in this tribe and these may show diverse distribution patterns: *Daniellia* Benn. (diffuse and in short lines); *Oxystigma* Harms (diffuse); *Kingiodendron* Harms (diffuse); *Gossweilerodendron* Harms (diffuse); *Prioria* Griseb (diffuse and in short lines); *Sindora* Miq. (in long tangential lines); *Copaifera* L. (in long tangential lines); *Pseudosindora* Symington (in long tangential lines); *Detarium* Juss.(in short and long tangential lines) and *Eperua* Aubl. (in long tangential bands).

The prismatic crystals are dominant in apotracheal parenchyma cells in most of the members of the Detarieae. There are some exceptions, for example, crystals are rarely observed in *Loesenera Harms*, *Copaifera* and *Ecuadendron* Ball. (Gasson et al., 2003) or they are observed mainly in the ray cells (*Plagiosiphon* J. Leonard, *Neochevalierodendron* J. Leonard).

Following this comparison, the fossil woods are identified as members of the *'*Crudia*'* Group (*Gossweilerodendron, Kingiodendron, Oxystigma* and *Prioria*). Amongst this group, the genus *Prioria* Griseb is the one with the closest resemblance (Table 4.4.). The fossil cf *Prioria* and *P. copaifera* share the following features: growth rings indistinct, marked by marginal parenchyma; wood diffuse porous (Plate 4.7, 1); vessels in radial multiples of 2 – 3 (–6) (Plate 4.7., 2); perforation plates simple

Species/characters	STRI 36273	*Prioria copaifera*
Percentage of grouping (%)	43	39
Intervessel pit size (μm)	5 ± 0.9 (3– 7.0)	6 ± 1.9 (3 – 8)
Vessel-ray pit size	4 ± 1.5 (2 – 7)	4 ± (3 – 9)
Mean tangential vessel diameter (μm)	137 ± 23 (90 – 190)	162 ± 22.2 (120 – 189)
Vessels/mm^2	10 ± 3.1 (6 – 18)	4 ± 2.0 (2 – 10)
Mean vessel element length (μm)	308 ± 72 (210 – 540)	429 ± 92.6 (244 – 645)
Ray width (number of cells)	3 ± 0.7 (1– 4)	2 ± 0.8 (1 – 4)
Ray height (mm)	0.8 ± 0.2 (0. 4 – 1.5)	0.5 ± 0.3 (0.3– 1.3)
Rays /mm	9.1 ± 2.5(5 – 13)	5.9 ± 1.0 (4– 7)

Table 4.3. Quantitative comparison of STRI 36273 and *Prioria copaifera.*

(Plate 4.7., 3); intervessel pitting alternate (Plate 4.7., 4); vessel – ray pitting similar to intervessel pits in size and shape (Plate 4.7., 5); fibres non-septate commonly pitted in tangential (Plate 4.7., 6) and radial walls (Plate 4.7., 7) and thin to thick walled (Plate 4.8., 1); axial parenchyma mostly paratracheal, ranging from vasicentric to winged-aliform (Plate 4.8., 1); rays heterocellular 1–3-seriate (Plate 4.8., 2) and composed of 1 or 2 rows of square cells in some specimens (Plate 4.8., 3); rhomboidal crystals occasional in ray cells (Plate 4.8., 4) and abundant in axial parenchyma chambered cells (Plate 4.8., 5); normal axial canals diffuse (Plate 4.8., 6) and in short lines (Plate 4.8., 7).

Plate 4.7. *Prioria copaifera*. Specimens accessioned in Kew as IFI 3412, W-16558

1. Growth rings marked by marginal parenchyma bands (arrows). IFI 3412s, scale: 100 µm.
2. Vessels in radial multiples of commonly 2 – 6. IFI 3412, scale: 100 µm.
3. Perforation plate simple (arrow). W-16558, scale: 100 µm.
4. Intervessel pitting alternate. IFI 3412, scale: 20 µm.
5. Vessel– ray pitting similar to intervessel pits. IFI 3412, scale: 40 µm.
6. Non-septate fibres. Arrows mark fibre pits in tangential walls, scale: 100 µm.
7. Fibres minutely bordered common in radial walls. W-16558, scale: 100 µm.

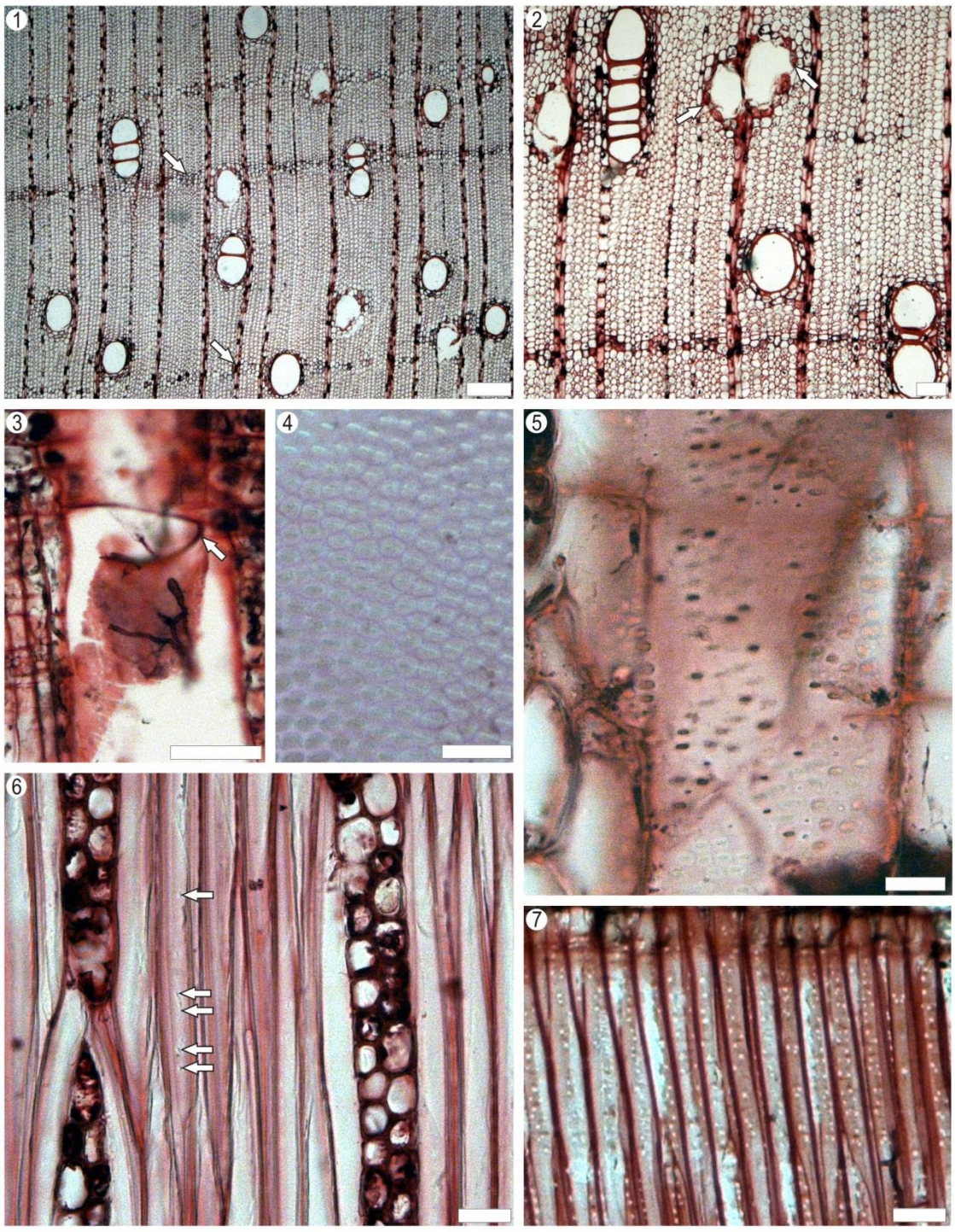

Plate 4.7

Plate 4.8. *Prioria copaifera*. Specimens accessioned in Kew as IFI 3412, W-16558.

1. Axial parenchyma ranging from vasicentric to winged-aliform (arrows). IFI 3412, scale: 100 µm.
2. Rays 1–3-seriate. IFI 3412, scale: 100 µm.
3. Rays composed of procumbent cells (PC) and 1 row of marginal square cells (SC). W-16558, scale: 100 µm.
4. Solitary rhomboidal crystals occasional in square ray cells. IFI 3412, scale: 100 µm.
5. Rhomboidal crystals abundant in parenchyma chambered cells. IFI 3412, scale: 50 µm.
6. Diffuse axial normal canals. IFI 3412, scale: 100 µm.
7. Short line (2) of axial canals. IFI 3412, scale: 50 µm.

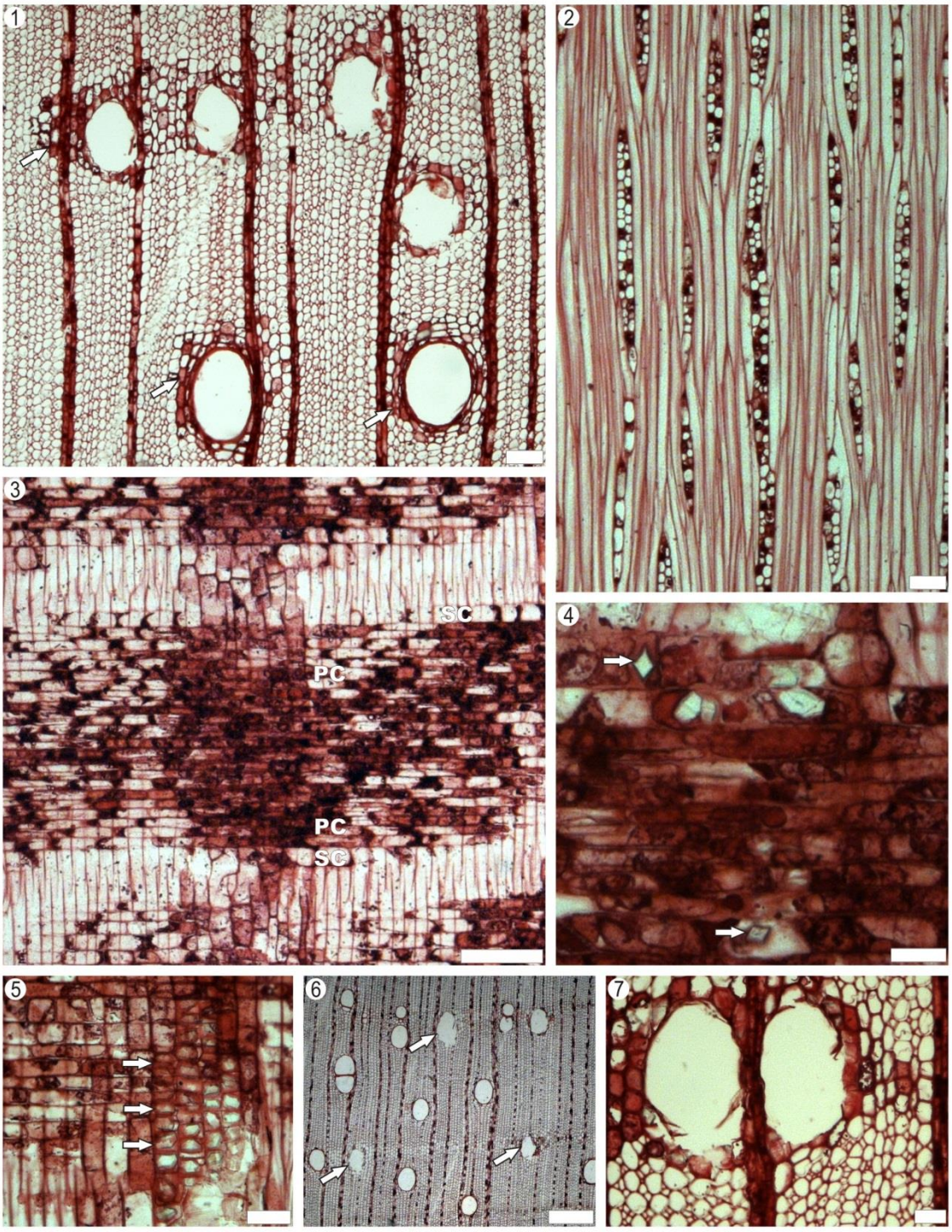

Plate 4.8

I note some differences between the compared modern woods and the fossils as follows: (1) the more common confluent axial parenchyma and marginal upright cells composing the rays in the modern wood contrasting the rarely present confluent parenchyma and square marginal cells in the rays. (2) in some species of *Prioria* (e.g., *P. copaifera*) the diffuse canals are considerably wider than the vessel, which does not occur in the fossils. However, quantitative features in fossil woods should be taken cautiously, so we still consider these wood specimens can certainly be assigned to the genus *Prioria*.

4.3.5. Fossil record of Fabaceae

There is not any other 'dicot' family with a fossil wood record as extensive as Fabaceae. One should be cautious when using the fossil record of this family, due to a considerable number of woods named as *Leguminoxylon* that are not certainly assignable to any particular group in Fabaceae. The most important reference of wood anatomy of fossil Fabaceae is Müller-Stoll and Mädel (1967), but also see Taylor (1985), Crepet and Herendeen (1992), Wheeler and Baas (1992), and Herendeen (2000). for a more comprehensive and extensive survey of the fossil record of Fabaceae. In this section, I highlight the main features to state differences between the woods discussed here and those previously assigned to the subfamily Caesalpinioideae, more specifically to the tribe Detarieae. The fossil woods are reviewed here at generic level and organised by age of occurrence.

The oldest wood acknowledged as member of this subfamily is ?*Caesalpinioxylon moragjonesiae* (Paleocene; Crawley, 1988). It has diffuse porous wood, vestured pits, vessel – ray parenchyma pitting similar to the intervessel pits in size and shape, predominantly vasicentric parenchyma, marginal parenchyma, rays 1– 4-seriate and

homocellular to slightly heterocellular rays, traumatic axial canals and septate fibres (Wheeler and Baas, 1992). C. *moragjonesiae* has canals of traumatic origin; feature absent in the panamanian wood. Numerous other woods have been named under this same generic name (*Caesalpinioxylon*); many of them are related to the other subfamilies or, in some cases, to other families (e.g., *C.owenii,* synonym of *Terminalioxylon primigenium*; *C. palembangense,* synonym of *Shoreoxylon palembangense*). The *Caesalpinioxylon* that could be related to the Caesalpinioideae, tend to have storied rays or lack axial canals. *Aulacoxylon* (Eocene of France; De Francheschi and De Ploeg, 2003) possesses normal canals, but all the rays are storied. Oligocene reports include: *Erythrophloeoxylon* (Boureau, 1957; Müller-Stoll and Mädel, 1967); *Cynometroxylum* (Delteil-Desneux, 1981, *Afzelioxylon* (Louvet, 1966); *Copaiferoxylon* (Fessler-Vrolant, 1977); *Detarioxylon* (Boureau and Louvet, 1970). All these woods, except *Detarioxylon*, lack normal axial canals. *Detarioxylon* has normal canals, but combined with distinct confluent parenchyma and rays 4 – 10-seriate. *Copaiferoxylon* also has normal axial canals, but these are mostly distributed in long tangential lines, additionally it has a remarked winged-aliform parenchyma pattern.

For the Miocene, the reports of Fabaceae fossil woods are rather numerous (Wheeler and Baas, 1992). Fossil Caesalpinioideae reports include: *Acrocarpus* (Yadav, 1989), *Acrocarpoxylon* (Gottwald, 1994), *Afzelioxylon* (Lemoigne, Beuchamp and Samuel, 1974; Lemoigne, 1978), *Brachystegioxylon* (Lakhanpal and Prakash, 1970), *Gleditsia* (Prakash, Barghoorn and Scott, 1962; Watari, 1952); *Peltophoroxylon* (Lemoigne, 1978; Ramanujam, 1954, 1960), *Koompassioxylon* (Bande and Prakash, 1980; Yadav, 1989; Awasthi and Mehrotra, 1990). Some Miocene woods related to Detarieae include: *Crudioxylon* (Pons, 1980), *Cynometroxylon* (Chowdhury and Ghosh, 1946; Navale, 1959; Prakash and Awasthi, 1971; Trivedi and Ahuja, 1978; Prakash,

1978; Bande and Prakash, 1980; Vozenin-Serra et al., 1989; Delteil-Denseux, 1980; Sayadi, 1973); *Kingiodendron* (Awasthi and Prakash, 1987); *Pahudioxylon* (Chowdhury et al., 1960; Navale, 1963; Prakash and Awasthi, 1971; Prakash and Tripathi, 1975; Louvet, 1975; Lorch and Fahn, 1959; Muller-Stoll and Madel, 1967), *Sindoroxylon* (Lemoigne et al., 1974). Most of the previously listed woods lack normal axial canals or at least these are not mentioned in the literature, consequently, these are out of consideration. *Sindoroxylon* possesses normal canals, but it tends to have more abundant confluent parenchyma, frequently forming bands > 3 cells wide. Several reports for the Miocene list woods related to *Bauhinia*: *B. deomalica* (Awasthi and Prakash, 1986; Agarwal, 1991b; Awasthi, 1992), *B. tertiaria* (Awasthi and Mehrotra, 1989); *B. indicum* (Kramer, 1974a), *B. miocenicum* (Trivedi and Panjwani, 1986). All these woods also lack axial canals and most of them tend to have storied rays and axial parenchyma strands.

In the Pliocene, all woods are more equivalent to extant woods. A few legumes have been reported from temperate zones (e.g., *Gleditsia*, *Robinia*, *Cytinus*) and these show features such as ring porosity and vessel clusters abundant that are linked to markedly seasonal climates (Wheeler and Baas, 1994). *Caesalpinioxylon* (Koeniguer, 1973, 1974) has a different combination of features compared to the fossils studied here, having septate fibres, banded parenchyma (> 3 cells wide) and all rays exclusively uniseriate and storied. There are reports of *Saracoxylon* (Du, 1988) and a few other reports of *Cynometroxylon* (India, Lakhanpal et al., 1984 and Guleria, 1984; Thailand, Vozenin-Serra and Privé-Gill, 1989). *Saracoxylon* lacks normal axial canals.

Taenioxylon is a palaeotaxon established and reported from several localities in Central America, Asia and Europe by Felix (1882, 1883, 1886, and 1887). This genus is mostly a synonym of *Pahudioxylon*. Berry (1918) collected large trunks from the

Cucaracha Formation and the upper part of the Culebra Formation during the construction of the Panama Canal. He identified a few of them as *Taenioxylon multiradiatum*. I studied the illustrations from his publication, but the low resolution images, do not allow an appropriate coding of certain features. Still, I note there are no axial canals, nor are abundant crystals in these specimens, as they are not mentioned in the description. Berry (1918) mentions the poor preservation of most of the specimens and the limitations in the prepared sections. There is no obvious similarity between these woods and the ones now recovered from Hodges Hill.

Therefore it is concluded that the new specimens are not likely related to other previously reported Leguminosae woods.

4.3.6. Biogeographical and environmental implications

In this comparison, the modern species most closely related to the Fossil Wood Type 2 is *P. copaifera* Griseb. This species is found in coastal areas of Nicaragua, Costa Rica, Panama and South of Colombia. Trees are often in nearly pure stands, coastal swamp forests, along river estuaries and in seasonally inundated areas (Lewis et al., 2005). Also, this species is found in extensive monospecific forests in Panama, coloquially named “cativales” (Biota Panama, 2013). The typical distribution of this species is consistent with the geological context of this section of Hodges Hill, interpreted as an estuarine environment. Other woods reported herein further support this environmental setting.

4.4. FOSSIL WOOD TYPE 3

Order: Oxalidales Heintze.

Family: Elaeocarpaceae Juss.

cf *Elaeocarpus*

Discussion: The common occurrence of 2 – 3 (– 4) radial multiples, the absent parenchyma, the medium alternate intervessel pits and the very heterocellular rays with long uniseriate tails and abundant crystals are features commonly occurring in a few species of *Elaeocarpus* (Elaeocarpaceae).

Holotype: STRI 36272, designated here comprising one hand specimen, and three thin sections in TS, TLS, RLS. The preserved diameter of the axis is 0.25 m.

Repository: Center for Tropical Paleoecology and Archaeology, Smithsonian Tropical Research Institute, Panama.

Locality: Hodges Hill (Gaillard Cut of Panama Canal) near Paraiso, Panama City, Panama. Latitude 09°02’51.75’’N; Longitude 79°39’14.02’’W.

Stratigraphic horizon: ~ 20m above the base of the Cucaracha Formation (Gaillard Group); Lower Miocene (19 – 20 Ma).

4.4.1. Description

IAWA features numbers: 2, 5, 13, 22, 25v, 26, 30, 31v, 42 48, 53, 56, 57, 61, 63, 66, 70, 75, 97, 98v, 107v, 108, 115, 137, 140, 155.

Growth rings indistinct; wood diffuse-porous (Plate 4.9., 1); vessels mostly in short radial multiples (69 %) of 2 – 3(– 4) (Plate 4.9., 2) combined with a few solitaries (Plate 4.9., 1); vessel with oval outline (Plate 4.9., 1, 2); perforation plates, simple (Plate 4.9., 3); intervessel pits alternate (Plate 4.9., 4) and small to medium (mean 7, SD 2.1 μm, n = 25; range 5 – 12 μm) (Plate 4.9., 5); vessel – ray pitting similar to intervessel pits in diameter and distribution (mean 6, SD1.6 μm, n = 25; range 4 – 10 μm) (Plate 4.9., 6), with much reduced borders or rounded pits occasionally present (Plate 4.9., 7); mean tangential vessel diameter 112 (n = 25; range 60 – 160 μm); mean vessel density, 21 per mm^2 (n= 15; range 15 – 27 per mm^2 ; mean vessel element length, 435.4 (n = 25; range 200 – 850 μm); sclerotic tyloses abundant (Plate 4.9., 8, 9); vascular tracheids not observed.

Fibres very thick walled (Plate 4.9., 8), with minutely bordered pits only common in radial walls (Plate 4.9., 10) and non-septate (Plate 4.9., 11).

Axial paratracheal and apotracheal parenchyma extremely rare or absent (Plate 4.10., 1).

Rays highly heterocellular (Plate 4.9., 11; 4.10., 3), 1 – 3 (– 4)-seriate (mean 3.0 ± 0.8, n = 50) (Plate 4.10., 2, 3) and occasionally >1 mm (mean 0.7 ± 0.3 mm, n = 50; range 0.22 – 1.3) (Plate 4.10., 2). Mean ray spacing 11.3 per linear mm (n = 15; range 9 – 15) with long uniseriate tails (Plate 4.10., 3), composed of procumbent bodies and > 4 rows of marginal square cells (Plate 4.10., 4).

Solitary rhomboidal crystals abundant in non-chambered (Plate 4.10., 5) and chambered (Plate 4.10., 6) square and upright ray cells; Crystals also present in distinct sizes per ray cell chamber (Plate 4.10., 5).

4.4.2. Affinities and justification

A search with of the following characters was made in the IWD: growth rings indistinct or absent (2 p), wood diffuse porous (5 p); perforation plates simple (13 p); alternate intervessel pitting (22 p); vessel– ray pitting similar to intervessel pits in size and distribution (30 p); vessel – ray pitting with much reduced borders or rounded pits (31 p); tyloses common (56 p), axial parenchyma absent or extremely rare (75 p), rays 1–3 cells wide (97 p) and 4–10-seriate (98 p), prismatic crystals present in upright and square cells (137 p). This search produced results for two taxa, *Elaeocarpus clementis* Merr. (Elaeocarpaceae) and *Bridelia micrantha* (Hochst.) Baill. (Phyllanthaceae).

Plate 4.9. Wood Type 3. cf. *Elaeocarpus*

1. Indistinct growth rings and wood diffuse porous. STRI 36272, TS, scale: 500 μm.
2. Short radial multiples of 2 – 3 (4) (arrows) combined with few solitaries. STRI 36272, TS, 100 μm.
3. Perforation plates simple (arrow). STRI 36272, RLS, scale: 100 μm
4. Intervessel pitting alternate. STRI 36272, TLS, scale: 50 μm.
5. Close-up of intervessel pitting. STRI36272, TLS, scale: 50 μm.
6. Vessel – ray pitting similar to intervessel pits (arrow). STRI 36272, RLS, scale: 50 μm.
7. Vessel – ray pitting much bordered or rounded (RP). STRI 36272, RLS, scale: 50 μm.
8. Tyloses abundant (arrows), very thick-walled fibres and parenchyma absent. STRI 36272, TS, scale: 100 μm.
9. Sclerotic tyloses. STRI 36272, TLS, scale: 100 μm.
10. Fibres with minutely bordered pits in radial walls. STRI 36272, RLS, scale: 100 μm.
11. Non-septate fibres and rays highly heterocellular. STRI 36272, TLS, scale 100 μm.

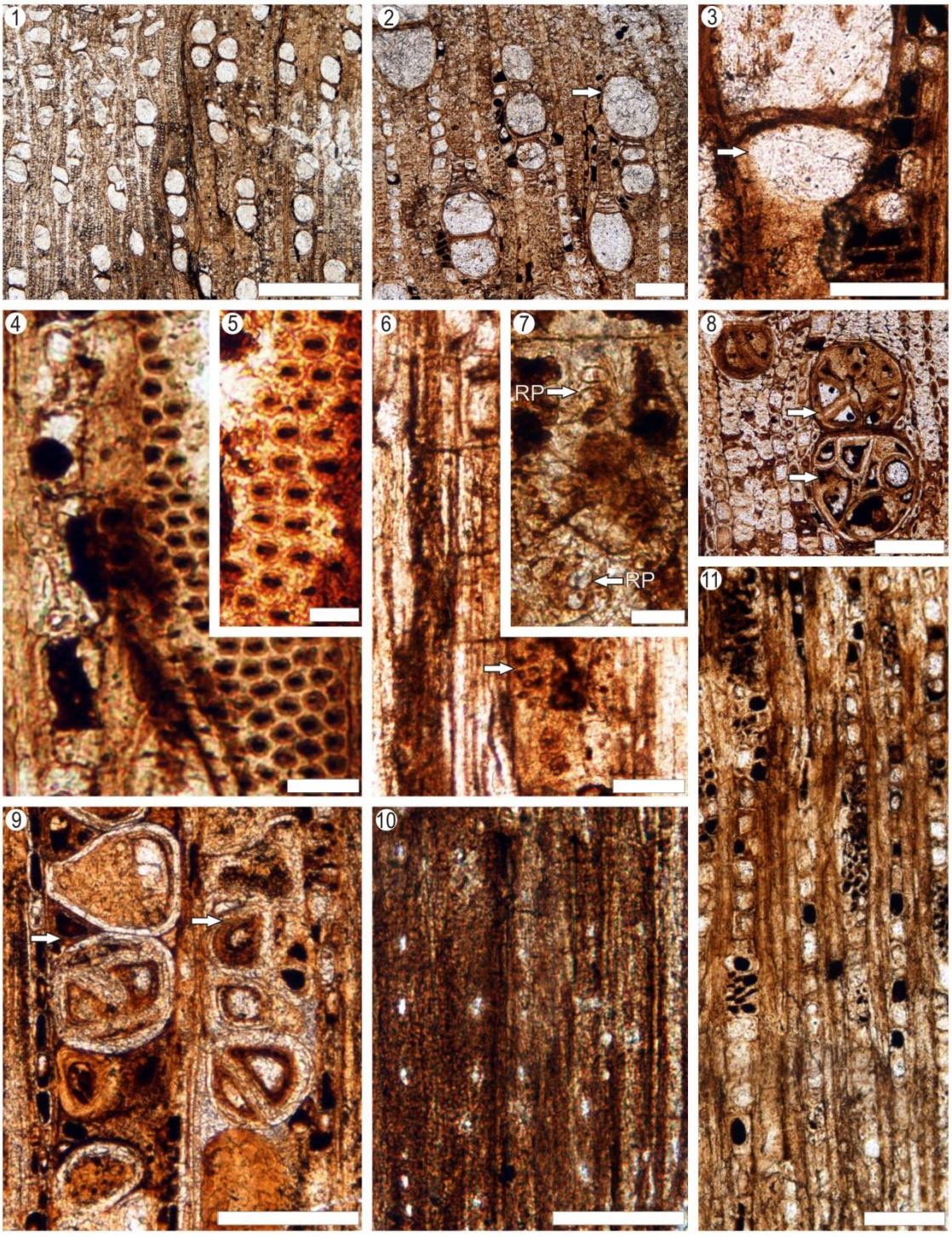

Plate 4.9

Plate 4.10. Wood Type 3. cf. *Elaeocarpus*

1. Parenchyma extremely rare or absent. STRI 36272, TS, scale: 100 μm.
2. Rays highly heterocellular, 1 – 3 (– 4)-seriate. STRI 36272, TLS, scale: 500 μm.
3. Close-up of rays 1 – 3 (– 4)-seriate with long uniseriate tails (arrows). STRI 36272, TLS, scale: 100 μm.
4. Rays with bodies composed of procumbent cells (PC) and >4 rows of marginal square (SC) and upright cells (UC). STRI 36272, TLS, scale: 500 μm.
5. Solitary rhomboidal crystals (arrows) abundant in non-chambered ray cells (arrows) and crystals in distinct sizes per ray cell chamber (DS). STRI 36272, RLS, scale: 100 μm.
6. Abundant crystals in chambered ray cells. STRI 36272, RLS, scale: 100 μm.

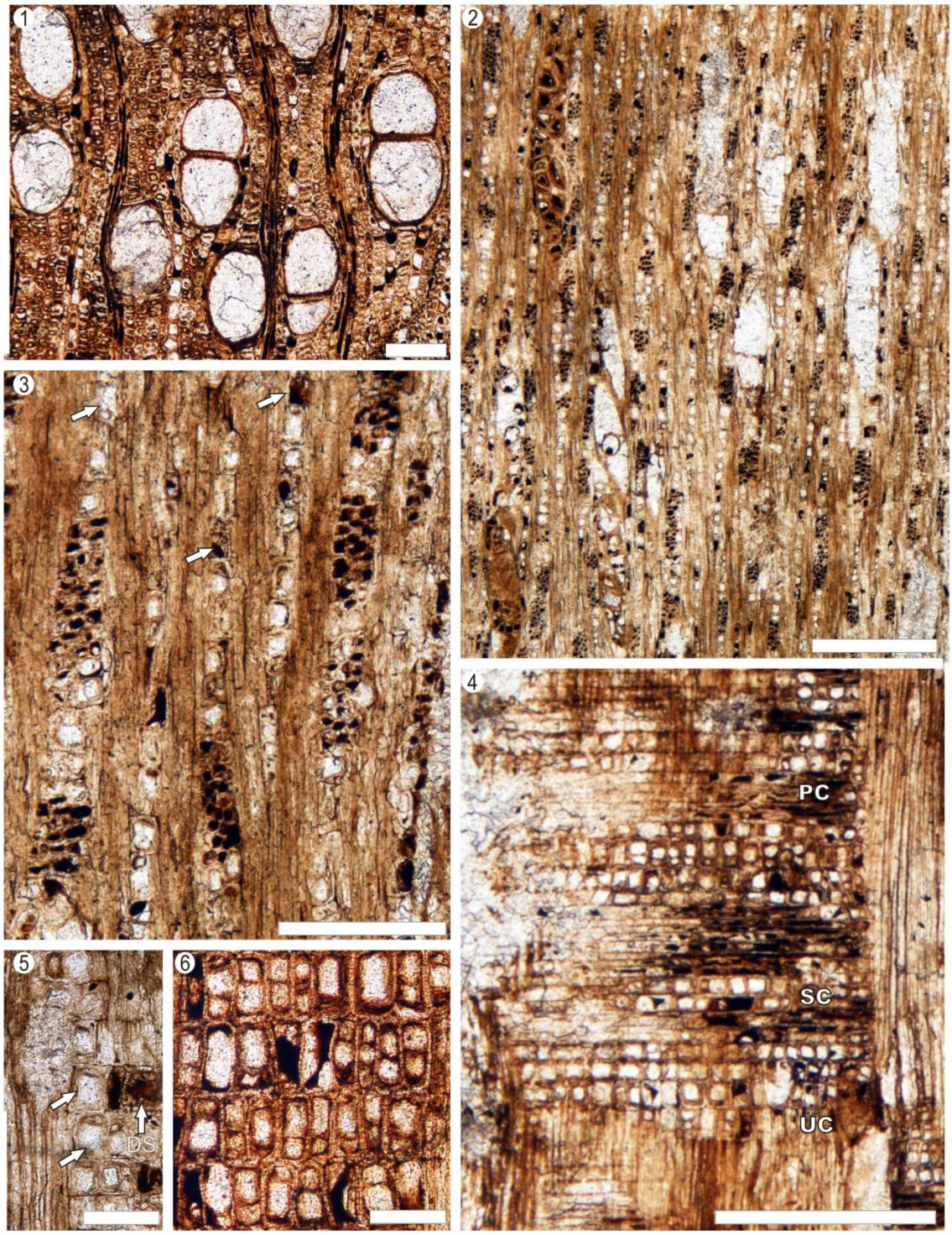

Plate 4.10

Phyllanthaceae is a family of 59 genera and includes most of the taxa formerly in Euphorbiaceae-Phyllanthoideae except for *Drypteres* and relatives (Angiosperm phylogeny Website, 2013). Several differences can be spotted between *B. micrantha* and the fossil, STRI 36272, but the main ones are: the presence of scalarifom, reticulate and foraminate plates; the diffuse apotracheal parenchyma and the scanty and vasicentric paratracheal parenchyma. To do a more precise identification, other species of *Bridelia* available in IWD and the Jodrell Laboratory collection in Kew Gardens were reviewed. Similarly as in *B. micrantha*, other *Bridelia* possess diffuse parenchyma and conspicuous parenchyma strands with abundant crystals. Several species of the genus *Phyllanthus* L. were also observed. Only one of these species, *Phyllanthus discoideus,* has some resemblance with the fossil; however, it has very long radial multiples (up to 9 vessels) that seem to mark seasonal boundaries and some diffuse parenchyma and vessel-ray pits in palisade also present. To extend this examination of the Phyllantaceae, I additionally reviewed the work of Mennega (1987), where 12 tribes of Phyllanthoideae (under the context of the old Euphorbiaceae) are described and photographed in detail. The diffuse apotracheal parenchyma seems to be present in most of the taxa, although the author recognizes a few exceptions. The presence of combined scalariform and simple perforation plates is also a commonly occurrence in the former Phyllanthoideae.

Gasson (1994) summarised the wood anatomy of the Elaeocarpaceae based on specimens from the microscopic slides collection of the Royal Botanical Gardens, Kew. He listed the following characters as the most common occurring in Elaeocarpaceae: distinct rings, vessels in radial multiples of mainly 2, alternate intervessel pitting and vessel –ray pitting similar in size to the intervessel pits, but circular and much opened, perforation plates simple, axial parenchyma rare, rays 1–7-seriate, strongly

heterocellular and with abundant crystals in its cells. At first glance this family could be ruled out, but one of the genera, *Elaeocarpus* L., shares a lot of characters with the specimen studied here (Table 4.5.). The resemblances with this genus are discussed further in the next section.

4.4.3. Comparison with *Elaeocarpus*

Two species of *Elaeocarpus* are very good matches for the fossil: *E. reticulatus* (synom. *E. cyaneus*) and *E. rugosus* (a quantitative comparison is given in Table 4.5). These two species and the fossil share the following characters: wood diffuse porous (Plate 4.11., 1), perforation plates simple (Plate 4.11., 2), intervessel pitting alternate and medium to large in size (Plate 4.11., 3), sclerotic tyloses present (Plate 4.11., 4), non-septate fibres present (although combined with septate fibres) (Plate 4.11., 5), fibres thin to thick walled (Plate 4.11., 6), parenchyma absent or extremely rare (Plate 4.11., 6) with occasional bands of parenchyma, rays highly heterocellular and 1–5-seriate (Plate 4.11., 5), crystals very abundant in non-chambered (Plate 4.11., 7) and chambered ray cells (Plate 4.11., 8) and occasionally with different sizes of crystals per chamber (Plate 4.11., 9). Some qualitative differences that can be listed include: distinct rings, vessel–ray pitting circular and much more opened than intervessel pits and septate fibres present. The characters of the fibres and vessel–ray pitting are of limited observation in the fossils. Some fibres seem to be septate from the radial longitudinal section, but there is some uncertainty on the precise coding of these features; even so, taking these differences in account, it is proposed to identify this fossil wood as an ancient member of *Elaeocarpus* under the new generic name, *Elaeocarpusoxylon. Elaeocarpus* is currently not occurring in the Americas, except by one species reported for Hawaii (E. *bifidus*; NPH, 2009). This is a genus distributed in the tropical and sub-tropical zones of South East Asia, Africa and Australia (Mabberley, 2004), and has been reported from

coastal zones in Australia (Wrigley and Fagg, 1996). *E. reticulatus*, the species with major resemblance to this fossil is mostly known as a very tall (up to 30 m) tree in rainforest environments in, mainly, Queensland, Australia (Wrigley and Fagg, 1996). In New South Wales, it has been reported from very moist areas and surrounding watercourses (Plant Net, 2013 onwards). This environmental context is consistent with the Panama Canal native flora and the geological interpretations from the observations of the study area.

Specimens/characters	STRI 36272	*Elaeocarpus cyaneus*	*Elaeocarpus rugosus*
Percentage of grouping (%)	69	52	72
Intervessel pit size (μm)	7 ± 2.1 (5 – 12)	10 ± 1.5 (9 – 12)	12 ± 2.3 (7 – 17)
Vessel-ray pit size	6 ± 1.6 (4 – 10)	15 ± 5 (9 – 24)	12 ± 2.8 (8 – 18)
Mean tangential vessel diameter (μm)	112 ± 21 (60 – 160)	82 ± 13.4 (50 – 110)	133 ± 31(79 – 174)
Vessels/mm^2	21± 4.0(15 – 27)	18.8 ± 2.8 (12 – 23)	9.7 ± 1.6 (7 – 12)
Mean vessel element length (μm)	435.4 ± 158.4 (200 – 850)	504.8 ± 146.2 (173.2 – 740.5)	439.4 ± 270.9 (150 – 950)
Ray width (n cells)	3 ± 0.8 (1 – 5)	2 ± 1.1 (1 – 3)	2 ± 0.6 (1 – 3)
Ray height (mm)	0.7 ± 0.3 (0.2 – 1.3)	0.5 ± 1.7(0.3 – 1.1)	0.7 ± 0.3 (0.2 – 1.3)
Rays /mm	11.1 ± 1.9 (9 – 15)	15.8 ± 2.9 (12 – 20)	16.4 ± 2.4 (12 – 20)

Table 4.4. Quantitative comparison of STRI 36272 and *Elaeocarpus cyaneus* and *Elaeocarpus rugosus.*

Plate 4.11. *Elaeocarpus cyaneus* and *Elaeocarpus rugosus*, Jodrell Laboratory, Royal Botanic Gardens, Kew, specimen number: D6074 Burma.

1. Wood diffuse porous. *E. cyaneus*, TS, scale: 100 μm.
2. Perforation plates simple (arrows). *E. cyaneus*, RLS, scale: 100 μm.
3. Intervessel pitting alternate. *E. rugosus*, TLS, scale: 50 μm.
4. Sclerotic tyloses. *E. rugosus*, TLS, scale: 100 μm.
5. Non-septate fibres combined with septate fibres and 1–5-seriate rays highly heterocellular. *E. cyaneus*, TLS, scale: 100 μm.
6. Parenchyma absent or extremely rare. *E. cyaneus*, TS, scale: 50 μm.
7. Crystals very abundant in non-chambered ray cells. *E. rugosus*, RLS, scale: 50 μm.
8. Crystals in chambered ray cells. *E. cyaneus*, RLS, scale: 100 μm.
9. Crystals in distinct sizes per ray cell chamber (DS). *E. rugosus*, RLS, scale: 50 μm.

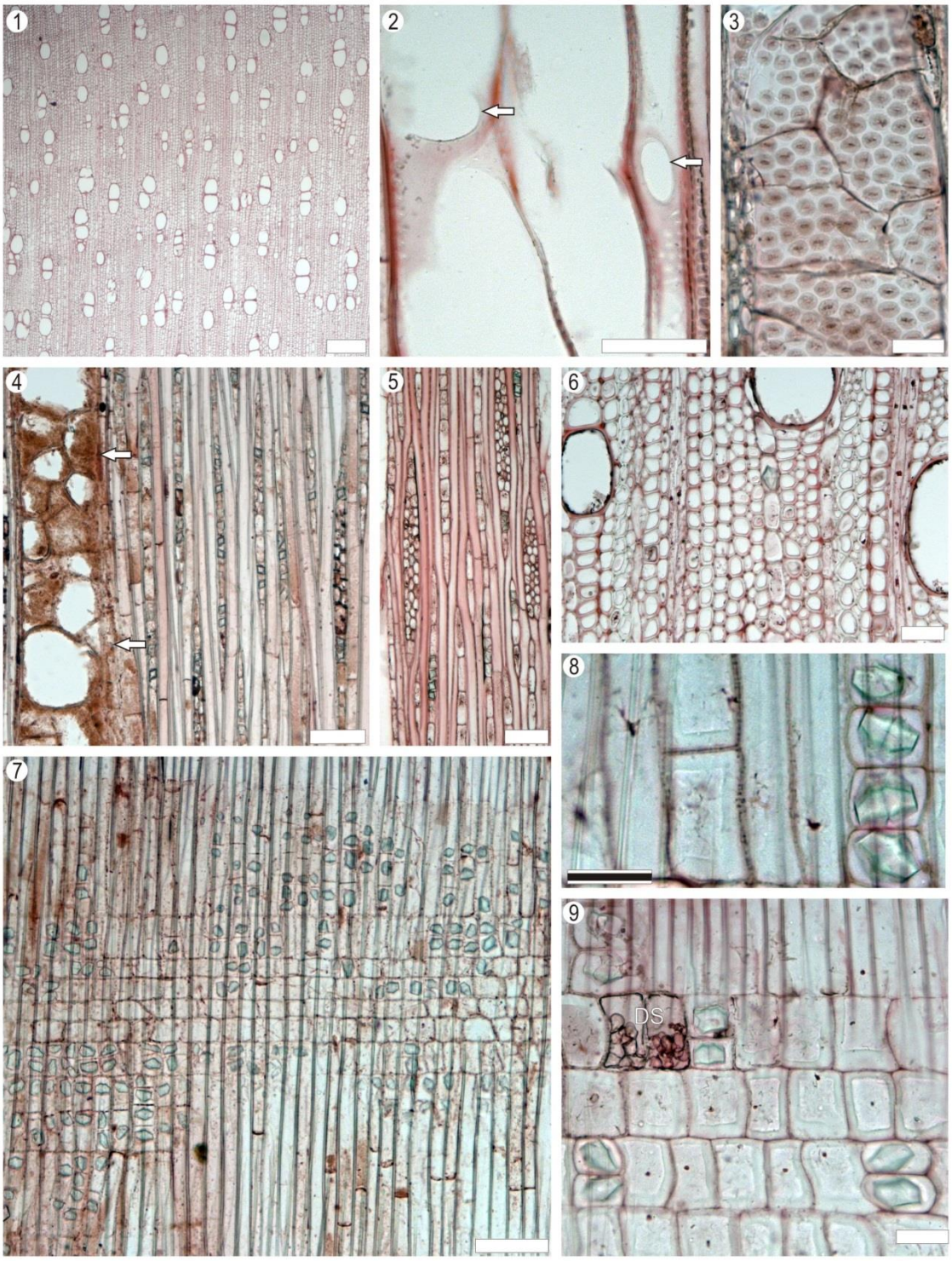

Plate 4.11

4.4.4. Fossil woods of Elaeocarpaceae

Elaeocarpaceae is a small family with c. 12 genera and 605 species. Consequently, the fossil record of this family is also small. The genus *Elaeocarpus* contains more than 50% of the species of the Elaeocarpaceae and most of the Elaeocarpaceae-like fossil woods have been described under modern generic names or under *Elaeocarpoxylon*. The genus *Elaeocarpoxylon* was first established in 1963 by Prakash and Dayal (Cretaceous from Central South Asia) and it was named *Elaeocarpoxylon antiquum*. The main features described from this wood include: growth rings indistinct, wood diffuse porous, septate fibres, axial parenchyma scanty paratracheal, rays 1–3 cells wide and rays heterocellular and numerous. Some reports from India include: *E. elaeocarpoides*, *E. ghughuensis*, *E. hailakandiense*. All these woods have some diffuse parenchyma and all septate fibres. There are some other reports from the Deccan Intertrappean Beds (*E. chitaleyi*, *E. mohgaoense*), also with all septate fibres and some diffuse in aggregates parenchyma. A species of *Paraphyllanthoxylon* (*P. illinoisense*) described by Wheeler et al., (1987) from the Cretaceous of Illinois, USA, is listed by Gregory et al., (2009) among the Elaeocarpaceae. High resolution photographs of this fossil species are available in the IWD, from which considerable similarity can be noticed with STRI 36272; however the rays are of two distinct sizes and the multiseriate rays are much wider in the North American wood (4–7 cells wide), contrasting with the fossil. The only other report of *Eleaocarpus* fossil woods of the Americas is from the Patagonia, *Elaeocarpoxylon sloanoides* (Palaeocene; Petriella, 1972). This wood also possesses septate fibres and diffuses parenchyma, so it is distinct from the Fossil Wood Type 3. The occurrence of a Miocene relative of *Elaeocarpus* in Central America is somewhat

difficult to explain considering that in the Americas, it has been only reported from the East Hawaii, which is the youngest part of the Hawaiian archipielago (300,000 years aprox; USGS, 2006), and possibly an introduced taxon, and all the other species of *Elaeocarpus* are represented in Asia, Australia, part of Africa and New Zealand. Petriella (1972) addressed this problem obliquely, with reference to the presence of *Elaeocarpoxylon* in the Paleocene of Patagonia. She argued that orogenic events had led to new migratory routes that enabled the migration of this taxon.

4.4.5. The new report of *Elaeocarpus* in the Isthmus of Panama

Elaeocarpus mostly comprises rainforest trees and has large fruits, consumed by a range of frugivorous bats and birds, which are the main disperser (Rossetto et al., 2008). Rossetto et al (2008) discuss the narrow distribution and small populations of several species of *Elaeocarpus* in Australia, suggesting that this lineage was probably much more widespread in the past. The current fragmented distribution of the genus and the almost complete absence of reports in similar environments in America make biogeographical inferences rather complicated and uncertain, and I do not intend to explain this here. Probably Rossetto et al.´s inferences about a more widespread distribution in the past are reasonable explanations for these scattered reports (*E. sloanoides* and *cf. Elaeocarpus* in the Isthmus and South America. The finding of this new fossil taxon represents the third (if *P. illinoisense* is taken in consideration) fossil wood record of *Elaeocarpus*-like wood reported for the Americas and the first one for Central America.

CHAPTER 5: TAXONOMY OF THE PANAMA CANAL PERMINERALISED WOODS: MALVACEAE

5.1. INTRODUCTION

This chapter describes two types of malvalean permineralised woods found abundantly in Hodges Hill (Figure 5.1.). These types are based in nine different specimens, STRI 14151, 36270, 14155, 14157, 14159, 14160, 14161, 14164 and 36269. New fossil taxa are erected for this material because the combination of characters observed is very unusual, not only amongst previously described fossil woods but also in extant trees.

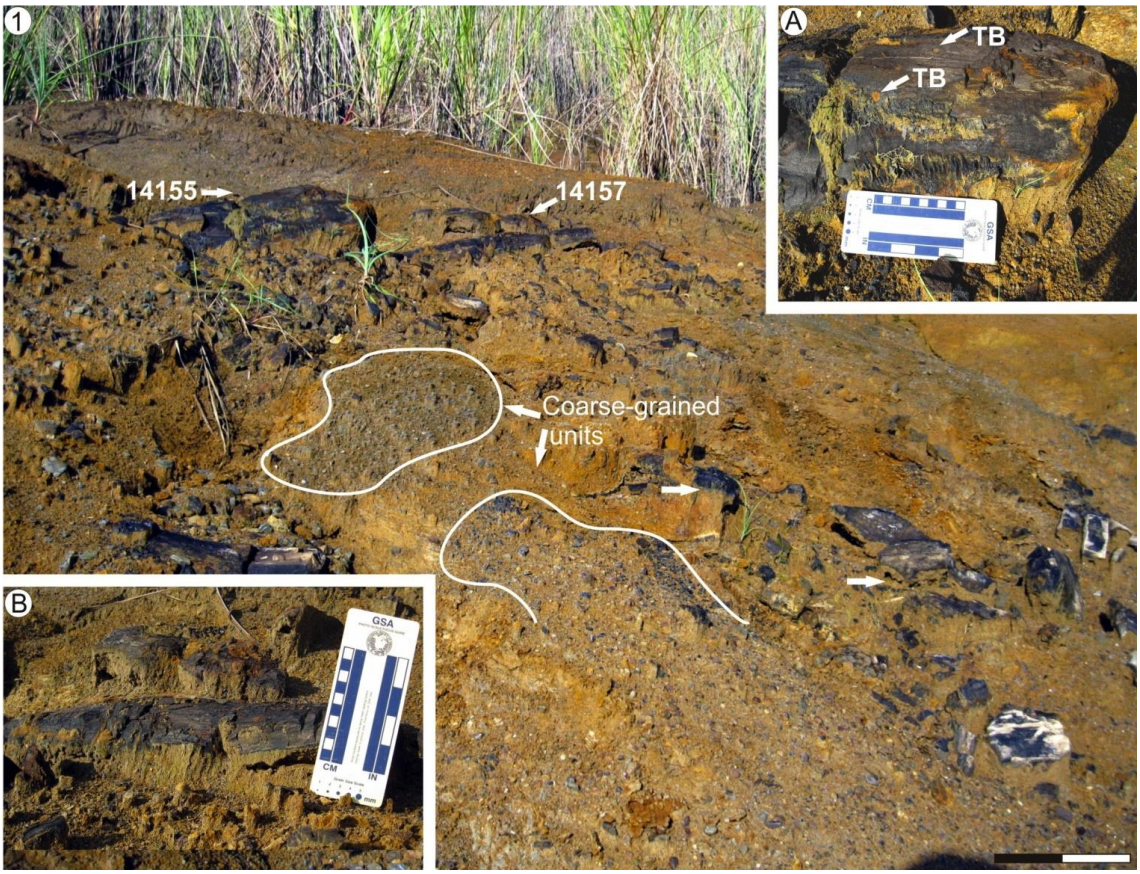

Figure 5.1. . Field context of fossils in coarse-grained sandstone facies, preserved in weathered tropical slopes, and highlighting (A, B) some of the fossil specimens. Abbreviation: TB, *Teredolites* borings.

5.2. FOSSIL WOOD TYPE 4

Order: Malvales Juss.

Family: Malvaceae Juss.

Genus: *Guazumaoxylon* Rodríguez-Reyes, Falcon-Lang, Gasson, Collinson, Jaramillo, *gen. nov.*

Type species*: Guazumaoxylon miocenica* Rodríguez-Reyes, Falcon-Lang, Gasson, Collinson, Jaramillo, *sp. nov.*

Generic diagnosis: Wood diffuse-porous; perforation plates simple; intervessel pitting alternate; rays mostly 1 – 2 (– 4)-seriate; apotracheal axial parenchyma dominantly paratracheal; fibres non-septate alternating with a few septate fibres; sheath cells and *Guazuma* intermediate-type tile cells present. Solitary crystals in square or upright cells.

Specific diagnosis: Wood diffuse-porous; vessels solitary or in radial multiples of 2 – 5 (– 6); perforation plates simple; intervessel pitting alternate and minute; rays are mostly 1 – 2 (– 4)-seriate and > 1 mm high; apotracheal axial parenchyma diffuse and paratracheal broad sheath to winged-aliform; fibres non-septate alternating with a few septate fibres; sheath cells and *Guazuma* intermediate-type tile cells present. Solitary crystals in square or upright cells.

Etymology: in reference to its similarity with extant *Guazuma*.

Discussion: This material shows intermediate-type tile cells, and other features, characteristic of the extant genus *Guazuma*. However, because of the antiquity of the wood a new genus is erected for the fossil to reflect its close inferred similarities to the extant plant. In doing so, I am aware of a number of fossil wood genera (e.g.,

Grewioxylon) with similar, though not completely overlapping features, and recommend a general revision of such malvalean fossil woods, which is well beyond the scope of this thesis.

Holotype: STRI 14151, designated here, comprising hand specimen, in two pieces, and three thin sections in TS, RLS, and TLS orientation. Axis has a preserved diameter of 0.12 m.

Other material: STRI 36270

Repository: Center for Tropical Paleoecology and Archaeology, Smithsonian Tropical Research Institute, Panama.

Type locality: Hodges Hill (Gaillard Cut of Panama Canal) near Paraiso, Panama City, Panama (Latitude 09°02'51.75''N; Longitude 79°39'14.02''W).

Stratigraphic horizon: ~ 20 m above the base of the Cucaracha Formation (Gaillard Group); Lower Miocene, (19 – 20 Ma).

Etymology: specific epithet *miocenica* refers to the age of the wood.

IAWA features numbers: 2, 5, 13, 22, 23, 24, 30, 41v, 42, 47, 53,?61, 65v, 66, 69, 77v, 80, 82, ?92, ?93, 97, ?102, 109, 110, 111, 115, 136, 137.

5.2.1. Description:

Growth rings indistinct; wood diffuse-porous (Plate 5.1, 1); vessels commonly solitary (65 – 67%) or in radial multiples of 2 – 5 (– 6) (Plate 5.1, 1, 2); vessel outline oval (Plate 5.1, 2); perforation plates simple (Plate 5.1., 3); intervessel pits alternate and minute (mean pit diameters 2.7 – 3.4; total range 1.7 – 5.2 μm) (Plate 5.1., 4); vessel – ray pits with distinct borders, similar in diameter (mean pit diameters 2.2 – 2.8; total

range 1.2 – 4.8 μm) and shape to intervessel pits (Plate 5.1., 5); mean tangential vessel diameter with means in the range of 105 – 139.4 μm (total range 70 – 180 μm); mean vessel density with means in the range of 16 per mm^2 (total range 6 – 23 per mm^2); mean vessel element length with means in the range of 376 – 468 μm (total range 250 – 710 μm); tyloses absent; vascular tracheids not observed.

Fibres mostly non-septate, interspersed with a few septate fibres (Plate I, 6), and mostly thin- to thick-walled (Plate 5.1., 7). Fibre pits difficult to observe due to preservation, but probably minutely bordered and on radial walls only.

Axial parenchyma paratracheal with broad vasicentric sheath to winged-aliform (Plate, 5.2, 2); apotracheal axial parenchyma scarce, and diffuse-in-aggregates (Plate 5.2., 1, 2); axial parenchyma strands poorly preserved, but probably 6 – > 8 cells high (Plate 5.2., 3).

Rays heterocellular, 1 – 3 (– 4)-seriate (mean 2.2 ± 0.8, n = 50) (Plate 5.2., 4, 5) and commonly > 1 mm, with means in the range of 0.9 – 1.0 mm (total range 0.6 – 3.0 mm) (Plate 5.2., 4); rays composed of procumbent, square and upright cells mixed throughout the body (Plate 5.2., 6); sheath cells (Plate 5.2., 4, 5) and *Guazuma* intermediate-type tile cells present (Plate 5.2., 6); mean ray spacing ranges 8 – 12.8 per mm (total range 6 – 15 per mm).

Solitary rhomboidal crystals present in square or upright cells (Plate 5.2., 7).

Plate 5.1. Wood Type 4. *Guazumaoxylon miocenica* gen. et sp. nov., Rodríguez-Reyes, Falcon-Lang, Gasson, Collinson, Jaramillo

1. Growth rings indistinct; wood diffuse-porous. STRI 14151, TS, scale: 1 mm.
2. Vessels solitary with oval outline and in radial multiples of 2 – 5. STRI 14151, TS, scale: 250 µm.
3. Perforation plate simple (arrow). STRI 14151, RLS, scale: 100 µm.
4. Intervessel pitting (IVP) alternate and minute. STRI 14151, TLS, scale: 50 µm.
5. Vessel – ray pits (VRP) with distinct borders, similar in size and shape to the intervessel pits. STRI 14151, RLS, scale: 50 µm.
6. A few septate fibres (arrows) interspersed with non-septate fibres. STRI 14151, TLS, scale: 100 µm.
7. Thin- to thick-walled fibres. STRI 14151, TS, scale: 100 µm.

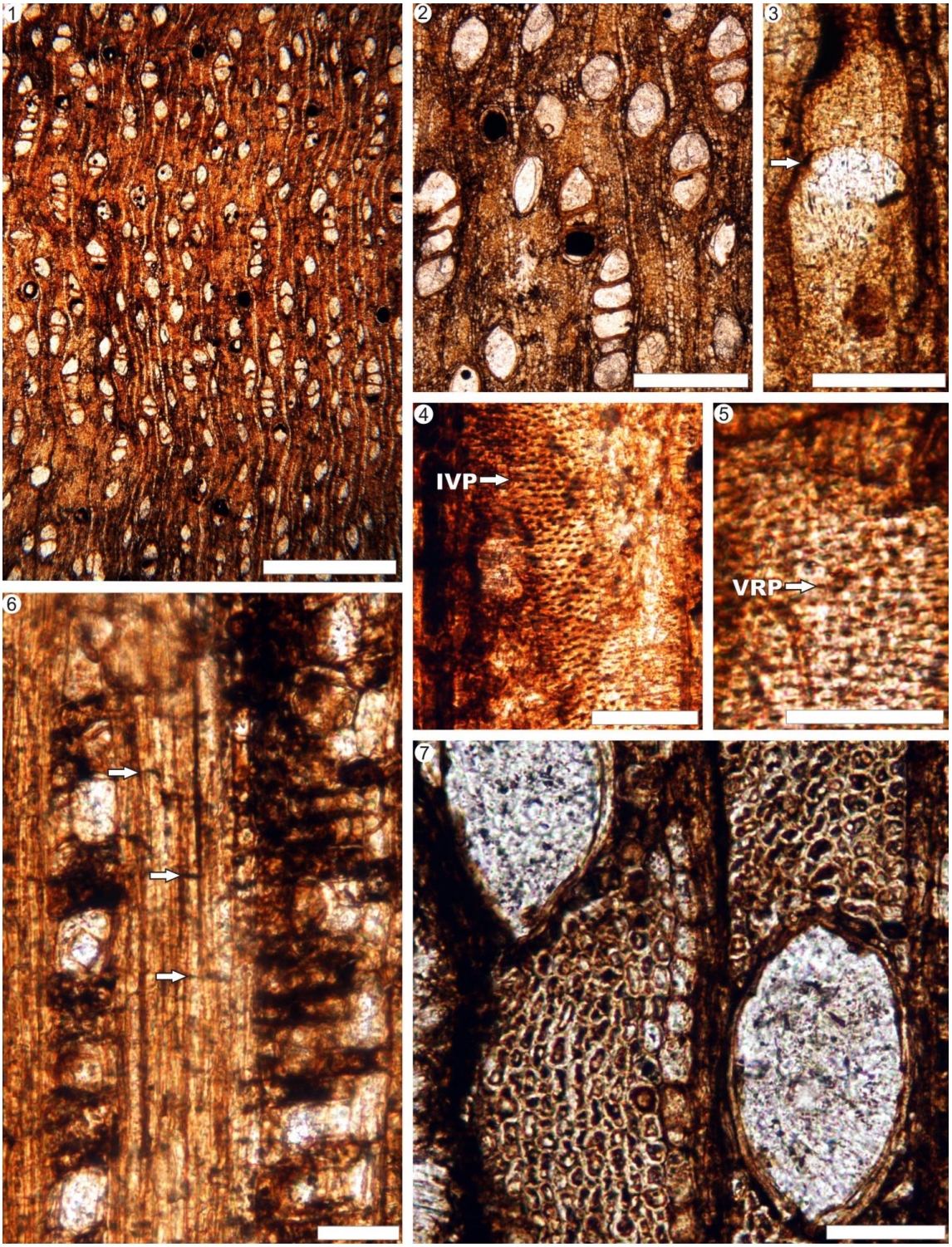

Plate 5.1

Plate 5.2. Wood Type 4. *Guazumaoxylon miocenica* gen. et sp. nov., Rodríguez-Reyes, Falcon-Lang, Gasson, Collinson, Jaramillo

1. Paratracheal parenchyma in broad vasicentric sheath to winged-aliform (arrows mark the wing tips) and scarce diffuse parenchyma (DP). STRI 14151, TS, scale: 250 µm.
2. Paratracheal parenchyma in broad vasicentric sheath to winged-aliform parenchyma (arrows) and scarce diffuse parenchyma (DP). STRI 14151, TS, scale: 100 µm.
3. Parenchyma strands incomplete due to poor preservation (arrows mark some of the cells). STRI 14151, TLS, scale: 50 µm.
4. Rays 1 – 3-seriate and > 1 mm with sheath cells. STRI 14151, TLS, scale: 250 µm.
5. Rays 1 – 3-seriate with sheath cells (arrows). STRI 14151, TLS, scale: 100 µm.
6. Rays composed of procumbent, square and upright cells throughout the body and showing prominent tile cells (TC). STRI 14151, RLS, scale: 100 µm.
7. Crystals in square ray cells (arrows). STRI 14151, RLS, scale: 100 µm.

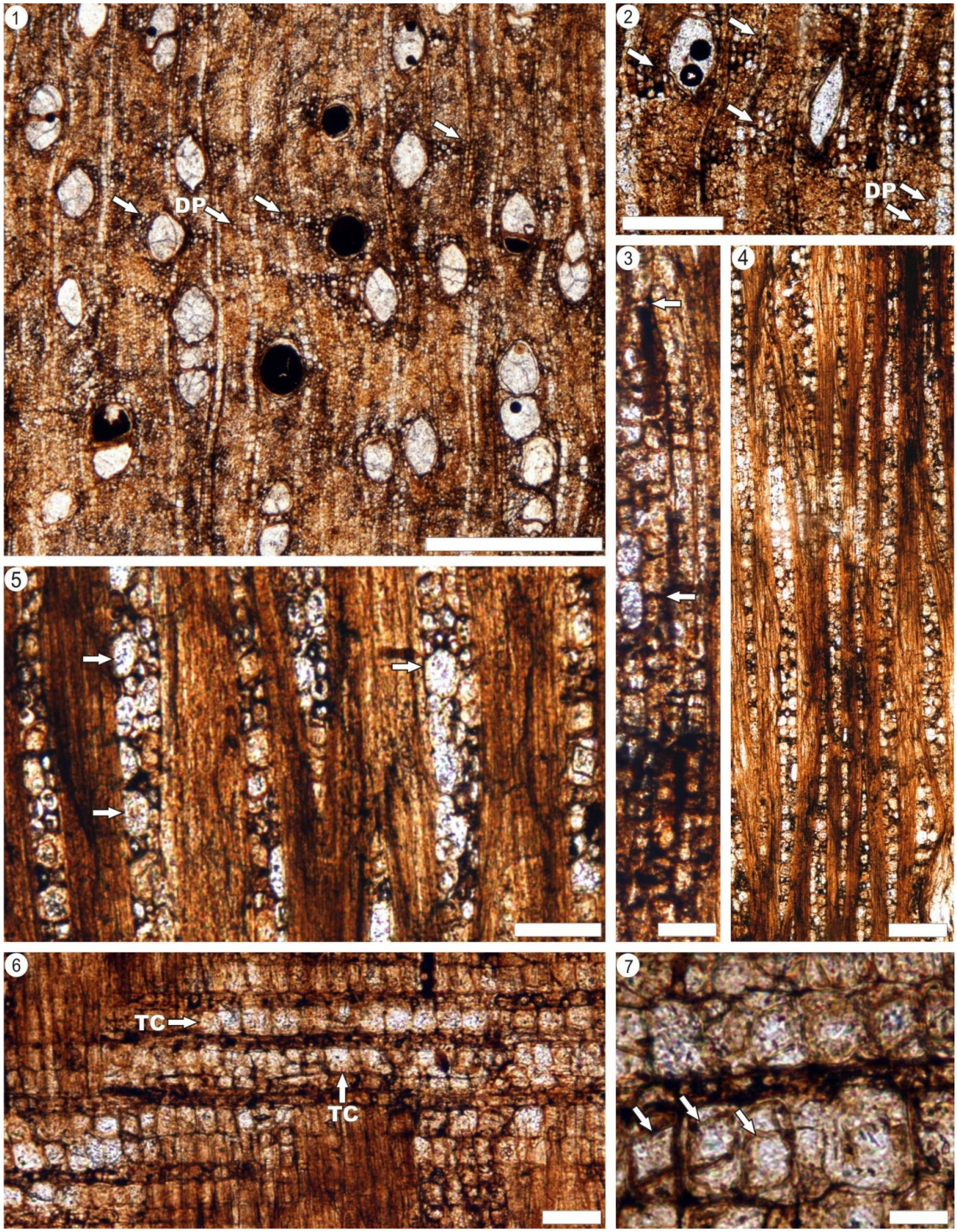

Plate 5.2

5.3. FOSSIL WOOD TYPE 5

Order: Malvales Juss.

Family: Malvaceae Juss.

Genus: *Periplanetoxylon* Rodríguez-Reyes, Falcon-Lang, Gasson, Collinson, Jaramillo, gen. nov.

Type species*: Periplanetoxylon panamense* Rodríguez-Reyes, Falcon-Lang, Gasson, Collinson, Jaramillo, sp. nov.

Generic diagnosis: Wood diffuse-porous; perforation plates simple; intervessel pitting alternate and polygonal; axial parenchyma in regular to irregular bands, 3 – 8 cells wide; rays 1 – 7 cells wide and < 1 mm high; sheath cells and *Pterospermum*-type tile cells prominent; solitary crystals in square or upright ray cells and in parenchyma cells.

Specific diagnosis: Wood diffuse-porous; vessels solitary or in radial multiples of 2 – 4; perforation plates simple; intervessel pitting alternate, polygonal and minute to small; axial parenchyma in regular to irregular bands, 3 – 8 cells wide; rays 1 – 7 cells wide and < 1 mm high; sheath cells and *Pterospermum*-type tile cells prominent; solitary crystals in square or upright ray cells and in parenchyma cells.

Etymology: From the Latin *Periplaneta*, the generic epithet of common "cockroaches", to refer to the Spanish name of the formation containing these woods.

Discussion: Erection of a new genus is warranted because the occurrence of axial parenchyma in bands of > 3 cells wide (85p) and tile cells (111p) is a highly unusual character combination in extant woods (based on searches of the IWD and the wood reference collections) and has never before been described in fossil woods.

Holotype: STRI 14155, designated here, comprising hand specimen, in two pieces, and three thin sections in TS, RLS, and TLS orientation. Axis has a preserved diameter of 0.23 m

Other material: STRI 14157, 14159, 14160, 14161, 14164, and 36269 comprising 6 hand specimens with preserved diameters ranging from 0.11 – 0.23 (mean 0.17 m) and preserved lengths exceeding 2 m. STRI 14157 and 14161 contain lateral branches embedded in a trunk, and may include some juvenile material, and are described separately. I also note that STRI 14155 and 14157 occur closely adjacent to one another at Hodges Hill (about 1 m apart) and are disposed at a similar angle; although organic connection cannot be proven in outcrop, it is possible they represent separate parts of the same trunk (Figure 5.1.).

Repository: Center for Tropical Paleoecology and Archaeology, Smithsonian Tropical Research Institute, Panama. Note that part of the hand specimen of STRI 14161 is also accessioned in the Museum of Biodiversity, Panama.

Type locality: Hodges Hill (Gaillard Cut of Panama Canal) near Paraiso, Panama City, Panama (Latitude 09°02’51.75’’N; Longitude 79°39’14.02’’W).

Stratigraphic horizon: ~ 20 m above the base of the Cucaracha Formation (Gaillard Group); Lower Miocene, (19 – 20 Ma).

Etymology: *panamense*, to reflect the origin of the fossil from Panama.

IAWA features numbers: 2, 5, 13, 22, 23v, 24v, 25v, 30, 41v, 42, 47, 53, 61, 66, 68v, 69, 77v, 85, 93, 94, 97, 98v, 102v, 109, 110, 111, 112, 115, 120v, 137, 141v, 142v (juvenile material additionally shows: ?92, 99v, 101v).

5.3.1. Description of inferred mature specimens:

Growth rings indistinct; wood diffuse-porous (Plate 5.3., 1); vessels commonly solitary (54 – 83 %) or in radial multiples of 2 – 4 (Plate 5.3., 2); vessel outline oval to circular (Plate 5.3., 2); perforation plates simple (Plate 5.3., 3); intervessel pits alternate, minute to small (mean diameters 2.7 – 5.7 μm; total range 1.1 – 9.0 μm) and polygonal (Plate 5.3., 4); vessel – ray pitting distinctly bordered, similar in diameter (means 2.6 – 5.0 μm; ranges 1.2 – 7.5 μm) and shape to intervessel pits (Plate 5.3., 5); mean tangential vessel diameter with means in the range 86 – 139.4 μm (total range 50 – 150 μm); vessel density with means in the range of 14 – 18 per mm^2 (total range 4 – 28 per mm^2); vessel element length with means in the range of 332 – 376 μm (total range 157 – 790 μm); tyloses and vascular tracheids not observed.

Fibres non-septate (Plate 5.3., 6), and mostly thin- to thick-walled (Plate 5.3., 7), although one specimen (14160) trends to have thinner walled fibres (Plate 5.3., 8). The differences are probably due to taphonomic factors; fibre pitting simple to minutely bordered on radial walls only, but preservation only sufficient for observation in STRI 14160 (Plate 5.4., 1).

Axial parenchyma prominent in regular to irregular bands, typically 3 – 8 (– 12) cells wide (Plate 5.4., 2); bands spaced 170 – 210 μm apart (total range 130 – 310 μm); axial parenchyma strands 3 – 12 cells high, with strands 8 or > 8 cells high most common (Plate 5.4., 3, 4, 5).

Rays heterocellular, (1 –) 2– 5 (– 7)-seriate (mean ray width 3.0 – 5.0-seriate) (Plate 5.4., 6); ray height < 1 mm, with means in the range of 0.5 – 1.0 mm (total range 0.2 – 3.0 mm); composed by procumbent, square and upright cells mixed throughout the body (Plate 5.4., 7); sheath cells generally conspicuous (Plate 5.4., 6), but weakly

developed in STRI 14160 (Plate 5.4., 3); *Pterospermum*-type tile cells prominent (Plate 5.4., 7); ray spacing with means of 8.0 – 11.3 per mm (total range 6 – 13 per mm); perforated ray cells present (Plate 5.4., 8).

Solitary rhomboidal crystals present in square or upright ray cells (Plate 5.4., 9, 10) and occasional in non-chambered parenchyma strands.

5.3.2. Description of inferred juvenile specimens (Plate 5.5):

The two specimens containing branches (STRI 14157 and 14161) differ from the mature Wood Type 2 specimens in a few significant features: they may show regular bands of axial parenchyma that are exceptionally broad (up to 20 cells wide) (Plate 5.5, 1) and zones of exceptionally wide rays, which locally comprise aggregate rays (Plate 5.5, 2, 3). In addition, STRI 14157 possibly shows localized storied parenchyma strands and fibres (Plate 5.5., 4) and a particular abundance of rhomboidal crystals, not only in ray cells (Plate 5.5., 5), but also in non-chambered (Plate 5.5, 7) and chambered (Plate 5.5., 6, 8) parenchyma cells.

Plate 5.3. Wood Type 5 (inferred mature material). *Periplanetoxylon panamense* Rodríguez-Reyes, Falcon-Lang, Gasson, Collinson, Jaramillo, sp. nov.

1. Growth rings indistinct; wood diffuse-porous; prominent, regular bands of axial parenchyma. STRI 14155, TS, scale: 1 mm.
2. Vessels in radial multiples of 2 – 4. STRI 14155. TS, scale: 50 µm.
3. Perforation plates simple (arrow). STRI 14155, TLS, scale: 100 µm.
4. Intervessel pits alternate. STRI 14155, TLS, scale: 50 µm.
5. Vessel – ray pits (VRP) bordered, similar in size and shape to the intervessel pits. STRI 14155, RLS, scale: 50 µm.
6. Non-septate fibres (NSF). STRI 14155, TLS, scale: 100 µm.
7. Thin-to thick-walled fibres (F) and diffuse parenchyma (P). STRI 14155, TS, scale: 100 µm.
8. Very thin-walled fibres. STRI 14160, TS, scale: 100 µm.

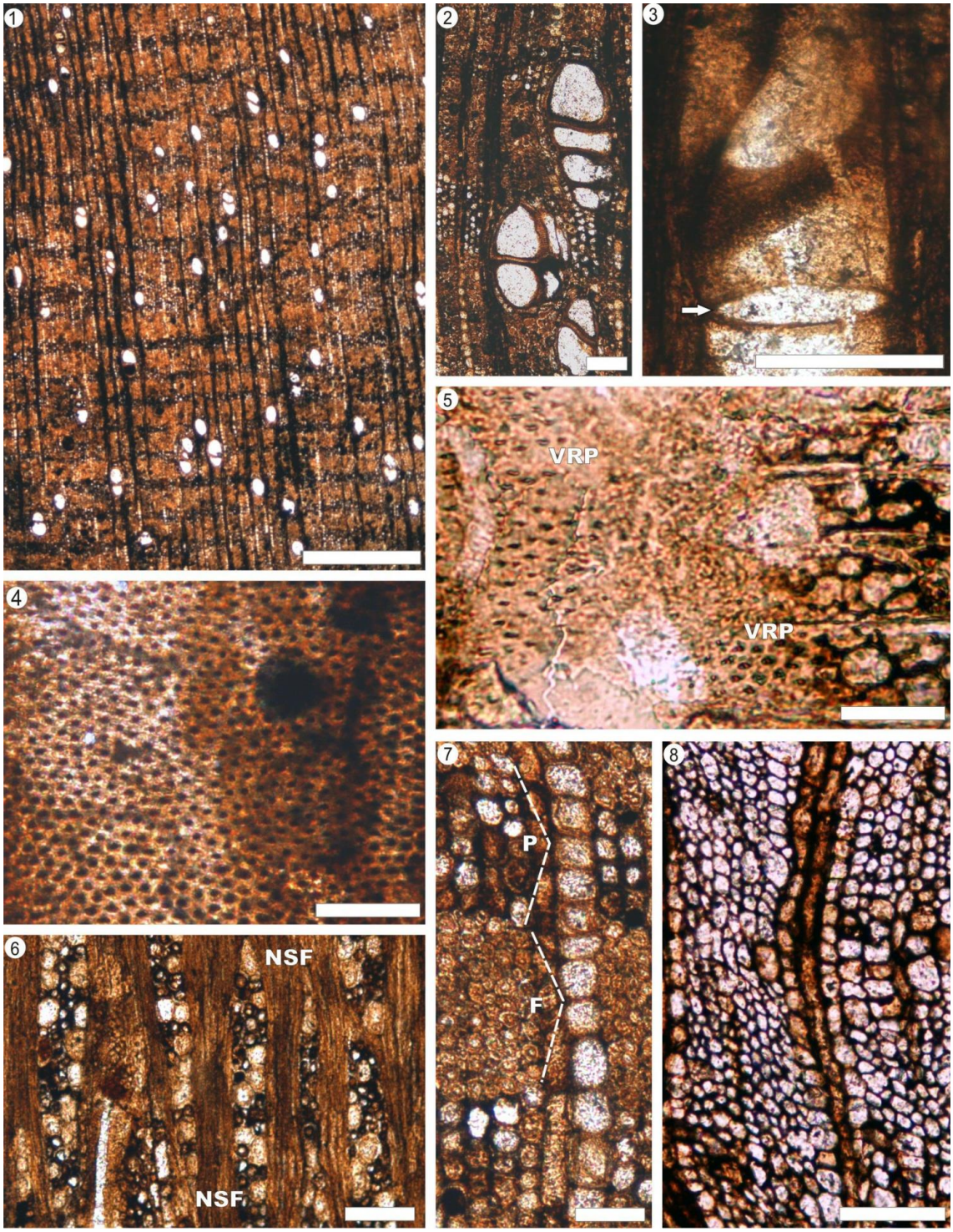

Plate 5.3

Plate 5.4. Wood Type 5 (inferred mature material). *Periplanetoxylon panamense* Rodríguez-Reyes, Falcon-Lang, Gasson, Collinson, Jaramillo, sp. nov.

1. Fibres with minutely bordered pits on radial walls only (arrows). STRI 14160, RLS, scale: 50 µm.
2. Axial parenchyma in regular bands, 3 – 8 cells wide. STRI 14155, TS, scale: 100 µm.
3. Axial parenchyma strands > 8 cells high and sheath cells weakly developed (SC). STRI 14160, TLS, scale: 100 µm.
4. Axial parenchyma strands 5 cells high. STRI 14155, TLS, scale: 25 µm.
5. Axial parenchyma strands 7 – 8 cells high. STRI 14155, TLS, scale: 25 µm.
6. Rays 2 – 5-seriate with sheath cells (arrows) STRI 14155, TLS, scale: 100 µm.
7. Rays composed of procumbent, square and upright cells throughout the body. Prominent *Pterospermum*-type tile cells (TC). STRI 14155, RLS, scale: 100 µm.
8. Perforated ray cell. STRI 14155, RLS, scale: 100 µm.
9. Rhomboidal crystals in square ray cells (arrows). STRI 14155, RLS, scale: 100 µm.
10. Rhomboidal crystals in square ray cells (arrow). STRI 14160, RLS, scale: 50 µm.

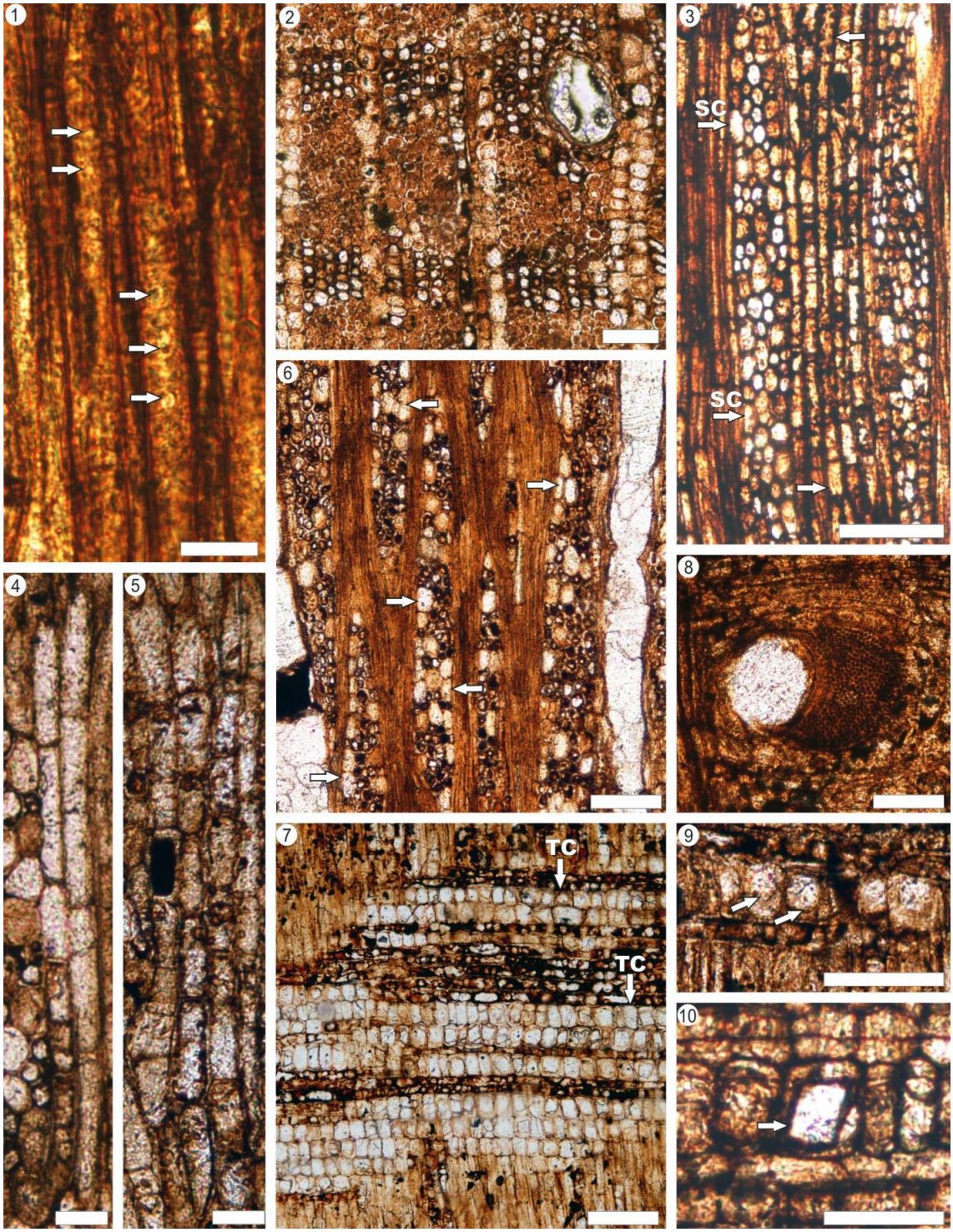

Plate 5.4

Plate 5.5. Wood Type 5 (inferred juvenile material). *Periplanetoxylon panamense* Rodríguez-Reyes, Falcon-Lang, Gasson, Collinson, Jaramillo, sp. nov.

1. Axial parenchyma bands (PB) exceptionally broad (up to 20 cells wide) alternating zones with fibres (F). STRI 14157, TS, scale: 100 µm.
2. Zones of exceptionally wide rays, locally comprising aggregate rays (AR). STRI 14157, TLS, scale: 500 µm.
3. Aggregate rays. STRI 14157, TLS, scale: 100 µm.
4. Localized storied parenchyma strands and fibres (arrows). STRI 14157, TLS, scale: 100 µm.
5. Abundant rhomboidal crystals in ray cells (arrows). STRI 14160, RLS, scale: 100 µm
6. Abundant rhomboidal crystals in chambered parenchyma cells (arrow). STRI 14157, RLS, scale: 100 µm.
7. Rhomboidal crystal in non-chambered parenchyma cells (arrow). STRI 14157, RLS, scale: 50 µm.
8. Rhomboidal crystals in chambered parenchyma cells (arrow). STRI 14157, RLS, scale: 50 µm.

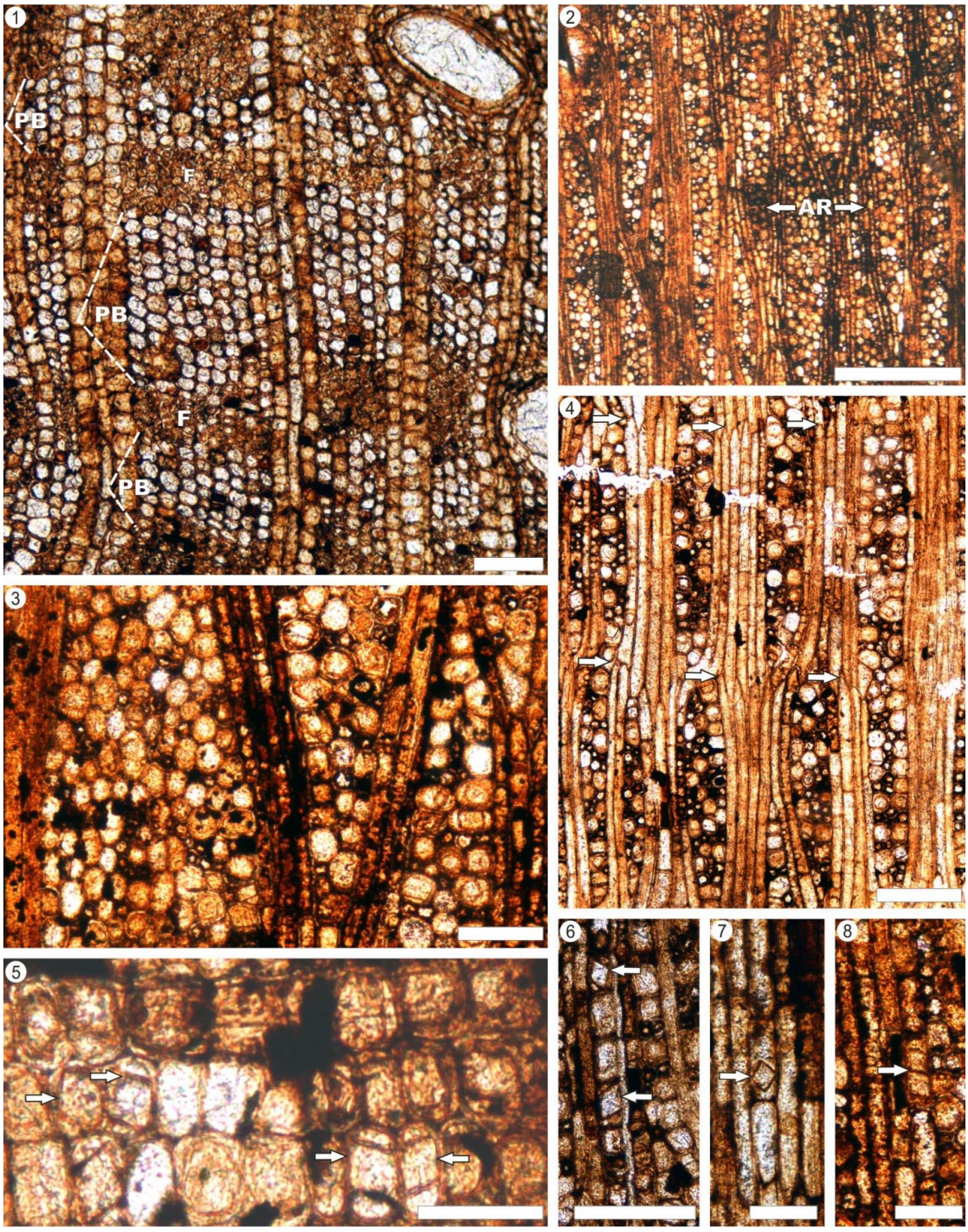

Plate 5.5

5.4. JUSTIFICATION FOR ATTRIBUTION TO MALVACEAE

A key diagnostic feature seen in all five specimens (Fossil Wood Types 1 and 2) is the presence of tile cells (111p). The formal definition of this feature is as follows: "a special type of apparently empty upright (rarely square) ray cells occurring in intermediate horizontal series usually interspersed among the procumbent cells of multiseriate rays" (IAWA, 1989). Two end-member types of tile cells are generally recognised: (1) the *Pterospermum*-type, which is the most common, comprises tile cells that are substantially higher than the procumbent cells, while (2) the *Durio*-type, which is somewhat rare, comprises tile cells that are approximately the same height as the procumbent cells (IAWA, 1964, 1989). However, Chattaway (1933) proposed a broader definition, recognising intermediate types, comprising tile cells that are slightly bigger than the procumbent ray cells, as typified by *Guazuma* Mill. and *Reevesia* Lindl. (Figure 5.2; Manchester and Miller, 1978). As Manchester et al. (2006) point out, there is a somewhat artificial distinction between tile cells and sheath cells (similar features viewed in RLS and TLS, respectively); however because the definition of the former feature precludes its occurrence in 1 – 2-seriate rays, tile cells have a much narrower distribution than sheath cells, and therefore it is very useful to make this distinction.

5.5. OCCURRENCE OF TILE CELLS WITHIN THE MALVALES

Tile cells are restricted to the Order Malvales (IAWA, 1989). Based on searches of the Insidewood Database (IWD), wood anatomical publications (e.g., Chattaway, 1937; Metcalfe and Chalk, 1950; Manchester and Miller, 1978; Carlquist, 2001; Wheeler and Manchester, 2002; Manchester et al., 2006) and observations in the wood reference collections, tile cells are found in at least six families of the Malvales as

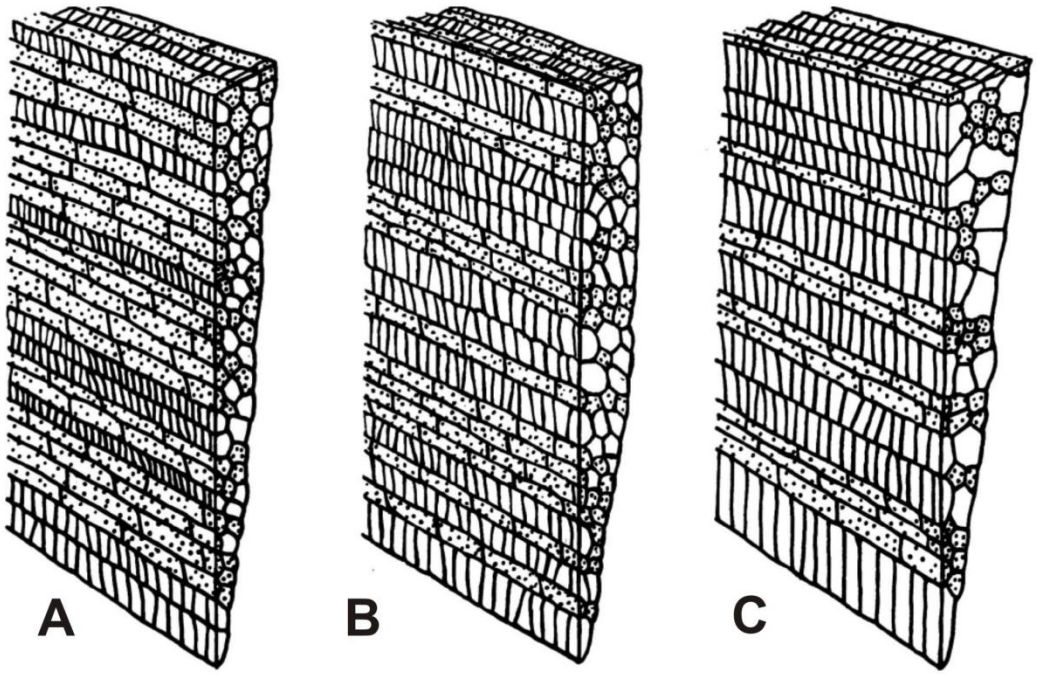

Figure 5.2. Diagram to illustrate the different types of tile cells seen especially in Malvaceae *sensu* APG III (reproduced from Manchester and Miller, 1978). A, *Pterospermum*-type tile cells; B, *Guazuma* intermediate-type tile cells; C., *Durio*-type tile cells. Tile cells are shown from both tangential and radial views and drawn without stipples, while the stippled cells are procumbent ray cells.

follows: Bixaceae, Dipterocarpaceae, Neuradaceae, Sphaerosepalaceae, Thymelaceae, and especially in the Malvaceae *sensu* APG III (comprising the former Bombacaceae, Malvaceae *sensu stricto*, Sterculiaceae, and Tiliaceae).

Several of these families can be immediately excluded from consideration. The Bixaceae show regularly storied rays and fibres, features absent in these fossil specimens (Inside Wood, 2013). The Dipterocarpaceae shows common tile cells only in the sub-family Dipterocarpoideae, especially in *Hopea* Roxb. (Chattaway, 1933; Manchester and Miller, 1978; Cronquist, 1981; IAWA, 1989; IWD accessed 17 June 2013); however, an affinity with the Dipterocarpoideae is unlikely because the fossil and extant record of this group is restricted to Indo-China, and the fossils lack axial

canals, a character found in most dipterocarps (Stevens, 2001). The Neuradaceae, a Saharo-Indian family, is another unlikely match because it exclusively comprises herbs and sub-shrubs (Schweingruber et al., 2013), whereas our fossils come from large trees based on preserved diameter. Also excluded from consideration is the wood of the Thymelaeaceae, which characteristically shows exclusively uniseriate rays, and some species additionally show included phloem (e.g., *Aquilaria*, *Gyrinops*; Van Vliet and Baas, 1984; Gasson, et al., 2011), whereas these fossil woods lack exclusively uniseriate rays (generally in range of 1 – 6-seriate) and included phloem. In the Sphaerosepalaceae, rays are mostly > 10-seriate and > 1 mm high (Carlquist, 2001), much larger than in either of the fossil types. However, there are very good matches between the fossil specimens and several representatives of the Malvaceae *sensu* APG III. Therefore, through this process of elimination, subsequent comparative studies are confined to the Malvaceae *sensu* APG III as described more fully below.

5.6. OCCURRENCE OF TILE CELLS WITHIN THE MALVACEAE SENSU APG III

The distribution of *Guazuma* intermediate-type tile cells (seen in the Fossil Wood Type 1 specimen) and *Pterospermum*-type tile cells (seen in the Fossil Wood Type 2 specimens) was studied in two major data repositories: the Insidewood Database (IWD) and the wood reference collections. Through examination of these online resources and slide collections, I was able to directly or indirectly observe 128 of the c. 243 genera of Malvaceae *sensu* APG III,

Unfortunately, the IWD does not distinguish between the various types of tile cells, so it is not possible to maximize the use of this character for search purposes.

Nonetheless, many IWD records do have micrographs associated with them, allowing searches to be refined. I searched the IWD for Malvaceae species showing tile cells (111p), and manually discarded records with *Durio*-type tile cells based on micrograph images. Excluding synonyms, 34 genera distributed across the 9 subfamilies that show *Pterospermum* and *Guazuma/Reevesia* intermediate-type tile cells were identified as follows: Bombacoideae (*Adansonia* L., *Bombax* L., *Cavanillesia* Ruiz and Pavon, *Ceiba* Mill., *Ochroma* Sw., *Commersonia* J. R. Forster &G. Forster, *Pachira* Aublet, *Quararibea* Aublet), Brownlowioideae (*Berrya* DC), Byttnerioideae (*Abroma* Jacq., *Guazuma* Mill., *Melochia* L., *Scaphopetalum* Mast, *Theobroma* L.), Dombeyoideae (*Dombeya* Cavanilles, *Pterospermum* Schreb.), Grewioideae (*Duboscia* Bocq., *Grewia* L., *Triumfetta* L., *Trichospermum* Blume, *Vasivaea* Baillon), Helicteroideae (*Reevesia* Lind., *Triplochiton* K. Schum.), Malvoideae (*Abutilon* Mill., *Hibiscus* L., *Lagunaria* (DC) Reichenbach, *Lavatera* L., *Thespesia* Sol. ex Correa), Sterculioideae (*Cola* Schott and Endl, *Firmiana* Marsili, *Heritiera* Aiton., *Pterygota* Schott & Endl., *Sterculia* L.) and Tilioideae (*Apeiba* Aubl., *Craigia* W.W. Sm.).

The study of the distribution of *Pterospermum* and *Guazuma/Reevesia* intermediate-type tile cells in Malvaceae *sensu* APG III in the wood reference collections covered herein reveals that a further 9 genera in 5 of the 9 subfamilies show these types of tile cells as follows: Bombacoideae (*Pseudobombax* Dugand), Dombeyoideae (*Melhania* Forssk), Helicteroideae (*Helicteres* L.), Malvoideae (*Azanza* Alef., *Gossypium* L., *Malvaviscus* Fabr., *Pavonia* Cavanilles, *Pentaplaris* L.O. Williams and Standl) and Sterculioideae (*Octolobus* Welw).

In total, 44 genera were identified (out of 128 genera observed) distributed across the 9 subfamilies that show *Pterospermum*-type tile cells and intermediate-type

tile cells (Table 5.1.). This short-list constituted a basis for identification of the two fossil wood types.

Genus	Subfamily	Data source	AP aliform	AP bands	Tile cell type
Abutilon	Malvoideae	IWD/Kew	1	1	P
Adansonia	Bombacoideae	Kew/IWD	0	0	P
Abroma	Byttnerioideae	Leiden/IWD	0	0	P
Apeiba	Tilioideae	Kew/IWD	0	0	P
Ayenia	Byttnerioideae	Kew	0	1	D
Azanza	Malvoideae	Kew	0	1	P
Berrya	Brownlowioideae	Utrecht/Kew/IWD	0	1	P
Bombax	Bombacoideae	Kew/IWD	0	1	P
Boschia	Helicteroideae	Kew/IWD	0	1	D
Cavanillesia	Bombacoideae	Utrecht/Kew/IWD	0	0	P
Ceiba	Bombacoideae	Kew/IWD	0	1	P
Coelostegia	Helicteroideae	IWD	0	1	D
Colona	Grewioideae	IWD	0	1	D
Cola	Sterculioideae	Kew/IWD	1	1	P
Cullenia	Helicteroideae	Kew/IWD	0	1	D
Commersonia	Bombacoideae	Kew/IWD	0	0	P
Craigia	Tilioideae	IWD	0	1	P
Desplatzia	Brownlowioideae	IWD	0	1	D
Dombeya	Dombeyoideae	Kew/IWD	1	1	P
Duboscia	Grewioideae	IWD/Kew	0	1	P
Durio	Helicteroideae	IWD/Kew	0	1	D
Firmiana	Sterculioideae	Kew/Leiden/IWD	1	1	P
Fremontodendron	Bombacoideae	IWD	0	1	D
Gossypium	Malvoideae	Kew	0	0	P

Grewia	Grewioideae	Kew/Utrecht/IWD	1	1	P
Guazuma	Byttnerioidea	IWD/Kew	0	1	I
Hampea	Malvoideae	IWD	0	0	D
Helicteres	Helicteroideae	Kew	0	0	P
Heliocarpus	Grewioideae	Kew/IWD	1	1	D
Heritiera	Sterculioideae	Leiden/Kew/IWD	0	1	P
Hibiscus	Malvoideae	Kew/Utrecht/IWD	1	1	P
Kleinhovia	Byttnerioideae	IWD	0	1	D
Kostermansia	Helicteroideae	Kew/IWD	0	1	D
Kydia	Malvoideae	Kew/IWD	0	1	D
Lagunaria	Malvoideae	Kew/IWD	0	1	P
Lavatera	Malvoideae	Kew/IWD	0	1	P
Leptonychia	Byttnerioideae	IWD	0	0	D
Luehea	Bombacoideae	Kew/IWD	0	1	D
Lueheopsis	Grewioideae	IWD/Kew	0	1	D
Malvaviscus	Malvoideae	Kew	0	0	P
Melhania	Dombeyoideae	Kew	0	0	P
Melochia	Byttnerioideae	Kew/IWD	0	0	P
Microcos	Grewioideae	IWD/Kew	0	1	D
Mollia	Grewioideae	IWD	1	0	D
Mortoniodendron	Tilioideae	Literature	0	0	D
Neesia	Helicteroideae	IWD	0	0	D
Ochroma	Bombacoideae	Kew/IWD	0	1	P
Octolobus	Sterculioideae	Kew	0	1	P
Pachira	Bombacoideae	Kew/IWD	0	1	P
Pavonia	Malvoideae	Kew	0	1	P
Pentaplaris	Malvoideae	Kew	0	1	P
Pseudobombax	Bombacoideae	Kew	0	1	P

Pterospermum	Dombeyoideae	Leiden/IWD	0	1	P
Pterygota	Sterculioideae	Leiden/IWD	0	1	P
Quararibea	Bombacoidae	Kew/IWD	0	1	P
Reevesia	Helicteroideae	Kew/IWD	0	1	I
Scaphopetalum	Byttnerioideae	IWD	0	1	P
Sterculia	Sterculioideae	Kew/Leiden/IWD	1	1	P
Theobroma	Byttnerioideae	Kew/IWD	0	1	P
Thespesia	Malvoideae	Leiden/IWD	0	1	P
Trichospermum	Grewioideae	IWD/Kew	0	0	P
Triplochiton	Helicteroideae	Kew/IWD	0	1	P
Triumfetta	Grewioideae	IWD/Kew	0	0	P
Vasivaea	Grewioideae	IWD	0	1	P

Table 5.1. List of genera of Malvaceae *sensu* APG III showing tile cells in the collections of Kew, Utrecht, and Leiden and those listed in the Inside Wood Database (IWD). Abbreviations: AP, axial parenchyma; P, Pterospermum-type; D, Durio-type; I, intermediate-type; 0, absent; 1, present**.**

5.7. IDENTIFICATION OF THE MALVALEAN WOOD TYPES

5.7.1. Identification of Fossil Wood Type 4 specimen

An initial IWD search, with no mismatches allowed, was made using the following suite of very general features seen in the Fossil Wood Type 4 specimen: Wood diffuse-porous (5p); simple perforation plates (13p); alternate intervessel pitting (22p); axial parenchyma winged-aliform (82p); and tile cells present (111p). This search gave the following limited results: *Hopea* (Dipterocarpaceae), *Grewia* (Malvaceae) and *Mollia* (Malvaceae); however, as noted above, *Hopea* can be excluded from further consideration. Subsequent analysis revealed that it is, specifically, the combination of

axial parenchyma winged-aliform (82p) and tile cells present (111p), which is especially rare in the IWD. Although a broader search for this combination of features in the wood reference collections revealed that this combination has a somewhat wider occurrence (present in certain species of the following nine genera: *Abutilon*, *Cola*, *Dombeya*, *Firmiana*, *Grewia*, *Heliocarpus*, *Hibiscus*, *Hopea*, *Mollia* and *Sterculia*), all these taxa typically also show wide banded parenchyma (85p), with coalescent bands in some cases (e.g., *Cola*, *Abutilon*) and very abundant diffuse in aggregates parenchyma (77p) (e.g., *Grewia*, *Dombeya*), which is not seen in our fossils. The only exceptions we found are *Grewia orientalis* L. and *Mollia lepidota* Spruce ex Benth (both in the subfamily Grewioideae). I therefore made a detailed comparison with these two genera.

Grewia L. (subfamily Grewioideae) is a very large genus, mostly distributed in tropical and sub-tropical parts of Africa, Asia, and Australia. However, after studying all micrographs in the IWD, slides in the wood reference collections, and some published literature (Bancroft, 1935; Agarwal, 1991; Selmeier, 2000; Chung and Lim, 2005) for this genus (*G. asiatica* L., *G. bicolor* Juss., *G. barombiensis* K. Schum, *G. crenata* Schinz & Guillaumin, *G. eriocarpa* Juss., *G. excelsa* Vahl., *G. flavescens* Juss., *G. globulifera* Mast., *G. glyphaeiodes* Baill., *G. latifolia* F. Muell. Ex Benth., *G. microcos* L., *G. miqueliana* Kurz., *G. oppositifolia* Roxb., *G. orientalis* L., *G. paniculata* DC, *G. populnifolia* Vahl., *G. polygama* Roxb., *G. rolfei* Merr., *G. tenax* Fiori, *G. tiliifolia* Vahl., *G. umbellata* Roxb., *G. villosa* Willd.) it is excluded as a probable match for the fossils. In general terms, the genus typically shows distinct growth rings (1p), rays of two distinct sizes (103p), and dominantly diffuse parenchyma, features absent in the fossils. Although *G. orientalis* is somewhat more similar to the fossils when viewed in TS, there are also some important differences such

as vessel – ray pits showing much reduced and rounded borders (31p), rays of two very distinct sizes (103p), and an absence of crystals (136a).

Mollia Mart. (subfamily Grewioideae) is a medium-sized genus distributed especially in tropical Central and South America. Unfortunately, only one species, *M. lepidota*, is reported in IWD, the genus is not represented in the wood reference collections at all, and there are few published micrographs (Kukachka and Rees, 1943; Welle and Detienne, 1995). Acknowledging these very limited data, it is suggested this genus is unlikely a match because it shows distinctly *Durio*-type tile cells and laticifers, features that are both absent in the fossils. In making this assessment, I note that tile cells in the fossil specimens, which are of the rare intermediate-type (Chattaway, 1933), are rather closer to *Pterospermum*-type than to the *Durio*-type (though we recognise that this is a qualitative assessment). Obviously, I cannot be as confident as I would like in excluding *Mollia* from consideration due to lack of comparative material available for study.

With no further taxa on the IWD short-list to investigate, I then reflected on the taxonomic significance of the intermediate-type tile cells, which is restricted to two extant genera, *Guazuma* Mill. and *Reevesia* Lind. After the study of the available images of *Reevesia* in the IWD and the microscopic slides in Kew, it is ruled out, because it shows vessels in clusters of six or more (11p), helical thickenings (36p), parenchyma diffuse in aggregates (77p) and scalariform apotracheal parenchyma, all of which are absent in the fossils. However, an initial assessment of *Guazuma* revealed many promising similarities with the fossils. In this regard, it is also noted that the intermediate-type tile cells seen in the fossils are more similar to the ones in *Guazuma* than those in *Reevesia*.

A detailed study of *Guazuma* (subfamily Byttnerioideae), a genus that is widely distributed in the tropics of Central and South America, was undertaken. It is noted that this taxon is relatively closely related to other comparative taxa, *Grewia* and *Mollia*, within the Byttneriina-clade. Of the four extant species of *Guazuma*, two were available for study in the wood reference collections: *G. crinita* Mart. and G. *ulmifolia* Lam., both present at Kew. These species share the following features with the Fossil Wood Type 1 specimen (Table 5.2.): wood diffuse porous (Plate 5.6., 1); vessels in radial multiples of 2 – 3 (– 6) (Plate 5.6., 1, 2); perforation plates simple (Plate 5.6., 3); intervessel pitting alternate (Plate 5.6., 4); vessel – ray pitting similar to intervessel pitting in size and shape (Plate 5.6., 5); some septate fibres interspersed with non-septate fibres (Plate 5.6., 6); thin- to thick-walled fibres (Plate 5.6., 8); apotracheal axial parenchyma scarce diffuse (the amount of this feature is variable in different observed specimens: Plate 5.6., 7, 8; Plate 5.7., 1, 2, 3, 4); axial parenchyma strands mostly 4 – 5 (– 6) cells high (Plate 5.7., 5); sheath cells present (Plate 5.7., 6); and intermediate-type tile cells present (Plate 5.7., 7, 8).

Taxon	Fossil Wood Type 1 *Guazumaoxylon miocenica*		*Guazuma ulmifolia*	Fossil Wood Type 2 *Periplanetoxylon panamense*							*Pentaplaris doroteae*
Ontogeny	Mature		Mature	Mature					Juvenile		Mature
Specimen number	STRI 14151	STRI 36270	Kew	STRI 14155	STRI 14159	STRI 14160	STRI 14164	STRI 36269	STRI 14157	STRI 14161	Kew
Growth rings	indistinct	indistinct	distinct	indistinct	indistinct	indistinct	indistinct	indistinct	indistinct	indistinct	indistinct
Porosity	diffuse-porous	diffuse-porous	diffuse-porous	diffuse-porous	diffuse-porous	diffuse-porous	diffuse-porous	diffuse-porous	diffuse-porous	diffuse-porous	diffuse-porous
Vessel multiples	2 – 5 (– 6); 67 % sol	2 – 4; 65 % sol	2 – 3 (– 6); 34 % sol	2 – 4; 72 % sol	2 – 3 (– 6); 70 % sol	2 – 3 (– 4); 54 % sol	2 – 3; 78 % sol	2 – 3; 83 % sol	2 – 5; 50 % sol	2 – 4; 53 % sol	2 – 3 (– 4); 41 % sol
Perforation plates	simple	simple	simple	simple	simple	simple	simple	simple	simple	simple	simple
Intervessel pitting	alt	alt	alt	alt, poly	alt	alt, poly	alt, poly	alt, poly	alt	alt	alt, poly
IVP diameter (µm); mean (range); type	3 ± 1 (2 – 5); minute	3 ± 1 (2 – 5); minute	5 ± 1 (3 – 7); small	6 ± 2 (3 – 9); small	3 ± 1 (1 – 6); minute	3 ± 1 (2 – 5); minute	4 ± 1 (2 – 6); minute	4 ± 2 (2 – 8); minute	5 ± 1 (3 – 8); small	3 ± 1 (2 – 7); minute	2 ± 0.4 (2 – 4); minute
Vessel – ray pit diameter (µm); mean (range); type	2 ± 0.8 (1 – 4); similar to IVP	3 ± 1 (2 – 5); similar to IVP	4 ± 1 (2 – 8); similar to IVP	4 ± 1 (2 – 7); similar to IVP	3 ± 1 (2 – 5); similar to IVP	3 ± 1 (2 – 4); similar to IVP	3 ± 1 (1 – 5); similar to IVP	5 ± 1 (3 – 8); similar to IVP	4 ± 1 (2 – 4); similar to IVP	3 ± 1 (2 – 5); similar to IVP	3 ± 0.4 (2 – 4); similar to IVP
Mean tangential vessel diameter (µm); mean (range)	105 ± 14 (70 – 140)	139 ± 23 (100 – 180)	115 ± 24 (60 – 150)	99 ± 16 (57 – 130)	112 ± 30 (75 – 200)	113 ± 22 (80 – 150)	86 ± 16 (70 – 120)	89 ± 22 (50 – 130)	127 ± 21 (94 – 172)	83 ± 15 (50 – 110)	104 ± 30 (65 – 160)
Vessels/ mm^2; mean (range)	16 ± 4.6 (9 – 23)	16 ± 4.4 (6 – 22)	16 ± 5 (8 – 25)	15 ± 4.6 (4 – 18)	18 ± 6.8 (10 – 28)	14 ± 4.3 (8 – 20)	14 ± 5.3 (6 – 22)	7 ± 2.0 (5 – 12)	14 ± 2.6 (10 – 18)	14 ± 2.8 (10 – 17)	8 ± 2.5 (5– 12)
Mean vessel element length (µm); mean (range)	468 ± 135 (340 – 710)	376 ± 133 (250 – 680)	317 ± 69 (220 – 480)	350 ± 11 (157 – 680)	332 ± 105 (160 – 600)	374 ± 106 (230 – 710)	335 ± 60 (230 – 460)	413 ± 158 (210 – 790)	412 ± 131 (260 – 730)	299 ± 74 (200 – 420)	308 ± 58 (250 – 400)
Fibre pits	minutely bordered?	minutely bordered?	minutely bordered	?	minutely bordered	minutely bordered	minutely bordered	minutely bordered	?	?	minutely bordered
Septate fibres	few	few	few	absent	absent	absent	absent	absent	absent	absent	absent
Fibre wall thicknes	thin to thick	thin to thick	thin to thick	thin to thick	thin to thick	very thin or thin to	very thin or thin to	very thin or	thin to thick	thin to thick	very thick

s						thick	thick	thin to thick			
Apotracheal axial parenchyma	locally d-i-a	locally d-i-a	d-i-a	absent	absent	absent	absent	absent	d-i-a	absent	absent
Paratracheal axial parenchyma	broad sheath to winged-aliform	broad sheath to winged-aliform	broad sheath to small winged-aliform	scarce vasicentric	scarce vasicentric; broad-sheathed	absent	winged-aliform occasional	winged-aliform	vasicentric	absent	vasicentric
Banded axial parenchyma (ap)	absent	absent	?few	regular bands, 3 – 8 cells wide	regular bands, 3 – 10 cells wide	regular bands, 3 – >5? cells wide	regular bands, 4 – 9 cells wide	regular bands, 3 – 7 (–12) cells wide	regular bands, 3 – 15 cells wide	regular bands, 3 – 16 (20) cells wide	regular bands, 3 – 5 cells wide
Band (ap) spacing (µm)	n/a	n/a	n/a	210 ± 50; 150 – 310	217 ± 94; 70 – 400	170 ± 30; 130 – 200	172 ± 30; 100 – 450	294 ± 124; 85 – 500	160 ± 30; 120 – 200	210 ± 70; 100 – 400	249 ± 53.3; 195– 475
Axial parenchyma strand length (cells high)	6 – >8*	4*	4 – 5 (locally 6)	> 8 (locally 5 – 8)	> 8 (locally 5 – 12)	6 – 8 (locally 9 – 12)	4 – 6 (locally 4 – 12)	3 – 5 (locally 3 – 9)	3 – 6 (locally 7 – 12)	3 – 8 (locally 9 – 12)	5 – 8 (locally 9)
Ray width (cells); mean (range)	2.2 ± 0.8 (1 – 4)	3 ± 0.7 (1 – 4)	3.8 ± 1.5 (1 – 8)	3.9 ± 1.6 (1 – 7)	4.0 ± 0.9 (2 – 5)	3.7 ± 0.8 (2 – 5)	4 ± 1.1 (1 – 6)	5 ± 1.0 (3 – 6)	3.1 ± 1.3 (1 – 8)	4.4 ± 2.1 (2 – 10)	4.06 ± 1.3 (2 – 7)
Ray height (mm); mean (range)	1.0 ± 0.4 (0.6 – 2.0)	0.9 ± 0.4 (0.3 – 3.0)	0.4 ± 0.1 (0.2 – 1.3)	0.5 ± 0.3 (0.2 – 1.4)	0.5 ± 0.4 (0.2 – 1.2)	0.7 ± 0.3 (0.3 – 1.5)	0.6 ± 0.2 (0.2 – 1.2)	0.8 ± 0.2 (0.2 – 2.6)	0.7 ± 0.4 (0.3 – 2.2)	0.6 ± 0.2 (0.2 – 1.2)	0.3 ± 0.2 (0.1 – 0.6)
Abnormal ray width (cells high); mean (range)	n/a	n/a	n/a	n/a	n/a	n/a	n/a	n/a	8.3 ± 2.7 (4 – 13)	7.2 ± 1.7 (5 – 11)	n/a
Abnormal ray height (mm); mean (range)	n/a	n/a	n/a	n/a	n/a	n/a	n/a	n/a	1.5 ± 0.7 (0.6 – 3.1)	0.7 ± 0.3 (0.3 – 1.4)	n/a
Ray cellular composition	mixed	mixed	1 – 2 rows of marginal up/sq cells	mixed	mixed	mixed	mixed	mixed	mixed	mixed	mixed

Sheath cells	present	present	present	present	present	weakly developed	present	present	present	present	present
Tile cells	present	present	present	present	present	present	present	present	present	present	present
Perforated ray cells	absent	absent	absent	present	absent	present	absent	absent	absent	absent	absent
Rays per linear mm; mean (range)	12.8 ± 1.2 (11 – 15)	8.0 ± 1.3 (6 – 10)	9 ± 1.4 (7 – 12)	11.3 ± 1.4 (9 – 12)	9.0 ± 0.9 (7 – 10)	9.6 ± 1.8 (7 – 12)	8.0 ± 1.3 (6 – 10)	9.0 ± 1.6 (7 – 13)	7.8 ± 1.3 (7 – 10)	11.4 ± 1.7 (9 – 14)	6.9 ± 2.9 (4 – 13)
Storied parenchyma /fibres	absent	absent	few	absent	absent	absent	absent	absent	few	absent	absent
Crystals in non-chambered upr/sq ray cells	present	present	few	present	present	present	present	absent	present	present	present
Crystals in chambered axial parenchyma cells	absent	absent	present	absent	absent	absent	absent	absent	few	absent	absent
Crystals in non chambered axial parenchyma cells	absent	absent	present	absent	absent	absent	absent	present	present	present	present

Table 5.2. Summary of IAWA features of the five fossil wood specimens reported here, and of the extant comparative taxa. Abbreviations: sol, solitary; alt, alternate; poly, polygonal; d-i-a, diffuse in aggregates; upr/sq, upright/square; n/a, feature not present; n/d, no data.

Plate 5.6. *Guazuma ulmifolia* Lam., Jodrell Laboratory, Royal Botanic Gardens, Kew, specimen number: Dominica 166.

1. Wood diffuse-porous; vessels in radial multiples 2 –3. TS, scale: 100 µm.
2. Close-up of vessels in radial multiples of 2 – 3 and a cluster of 6. TS scale: 100 µm.
3. Perforation plates simple (arrows). TS, scale: 100 µm.
4. Intervessel pitting alternate. TLS, scale: 50 µm.
5. Vessel – ray pitting similar to intervessel pits (arrows). RLS, scale: 20 µm.
6. Some septate fibres (SF) combined with non-septate fibres. TLS, scale: 50 µm.
7. Vessels with paratracheal axial parenchyma as broad vasicentric sheaths to small winged-aliform forms (arrows) and scarce diffuse parenchyma. TS scale: 100 µm.
8. Close-up of paratracheal axial parenchyma as broad vasicentric sheaths (arrows). Also observe thin to thick walled fibres. TS, scale: 100 µm.

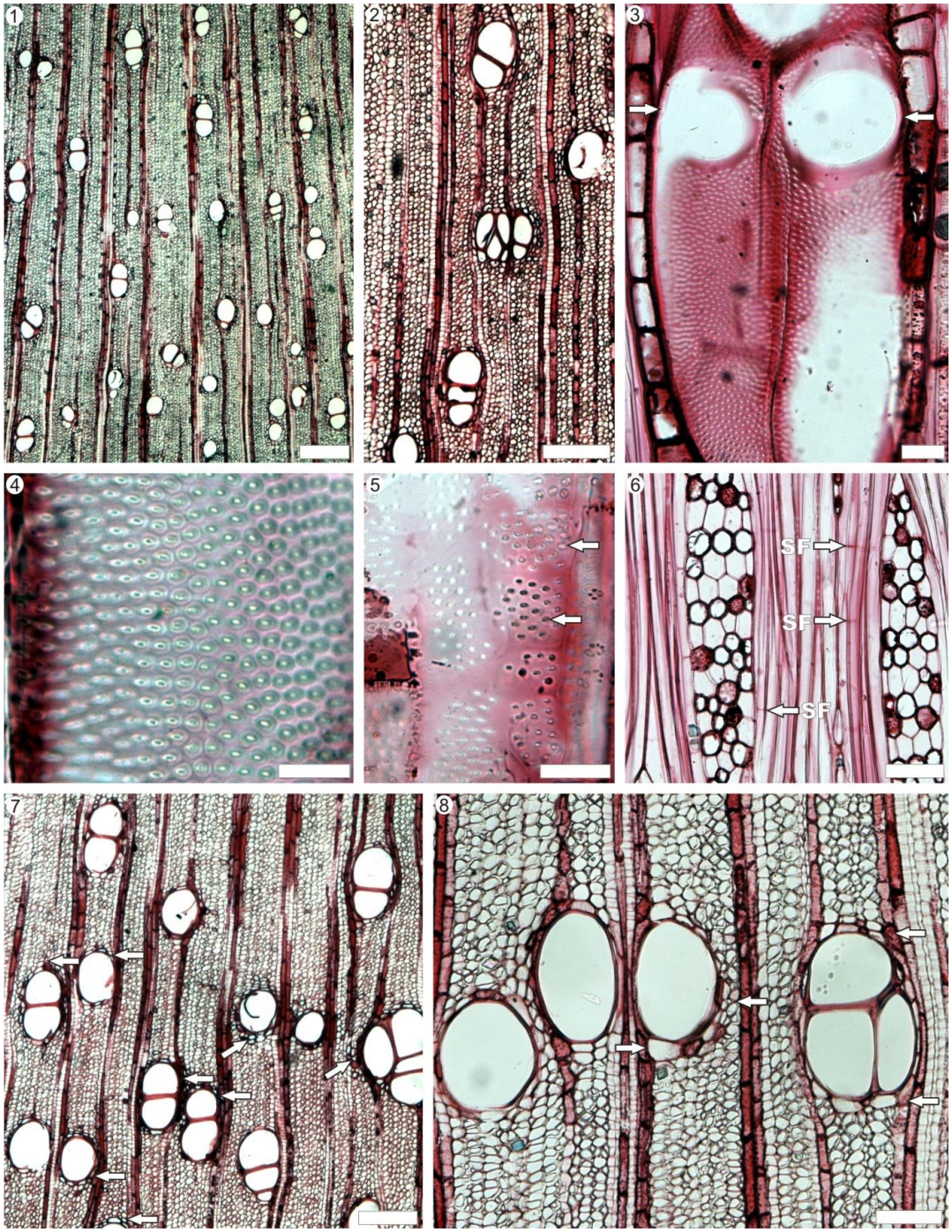

Plate 5.6

Initially it was thought that a significant difference of *Guazuma* would be seen in its axial parenchyma because the IWD does not code this taxon for axial parenchyma of winged-aliform type. However, the fossil material is not classically winged-aliform showing a mixture of broad-sheaths and small wings. Whilst most species of *Guazuma* do, indeed, differ from our fossil specimen in showing mostly diffuse scalariform parenchyma (Plate 5.7, 2, 4), one of the Kew samples (Dominica 166) of *G. ulmifolia* closely resembles the fossils in showing parenchyma with broad vasicentric sheath to small winged-aliform (Plate 5.6., 7, 8) with scarcer diffuse parenchyma (Plate 5.7., 1, 3), compared to other specimens of *G. ulmifolia* (Plate 5.7, 2, 4). Additionally, this species shows solitary rhomboidal crystals present in ray and parenchyma cells (Plate 5.7., 7, 8) as in the fossil. The main differences from the fossil wood include distinct rings, shorter and wider rays on average and diffuse, scalariform parenchyma. However, I do not consider these features of great taxonomic significance and consider *G. ulmifolia* the most credible match for the Fossil Wood Type 1.

5.7.2. Identification of Fossil Wood Type 5 specimens

An initial IWD search, with no mismatches allowed, was undertaken using the following general suite of characters common to all four specimens of Fossil Wood Type 5 specimens: wood diffuse-porous (5p); intervessel pitting alternate (22p); vessel – ray pitting similar to intervessel pitting (30p); non-septate fibres present (66p); axial parenchyma in bands > 3 cells wide (85p); and sheath and tile cells present (110p, 111p). This search produced no matches, and further investigation revealed that the combination of axial parenchyma in bands > 3 cells wide *and* tile cells (85p, 111p) is unknown, not only the Malvaceae *sensu* APG III, but in the entire IWD.

Plate 5.7. *Guazuma ulmifolia* Lam., Jodrell Laboratory, Royal Botanic Gardens, Kew, specimen numbers: Dominica 166, W-16271.

1. Scarce diffuse axial apotracheal parenchyma in Dominica 166 specimen. TS, scale: 100 µm.
2. Abundant scalariform parenchyma (arrows). W-16271. TS scale: 100 µm.
3. Rays 3 – 5-seriate with sheath cells and scarce apotracheal parenchyma strands (arrows). Dominica 166. TLS, scale: 100 µm.
4. Rays 1 – 6-seriate with sheath cells and abundant apotracheal parenchyma strand (arrows). W-16271. TLS, scale: 100 µm.
5. Parenchyma strands 4– 5 cells high Dominica 166. TLS, scale: 25 µm.
6. Sheath cells (arrows). Dominica 166. TLS, scale: 50 µm.
7. *Guazuma* intermediate-type tile cells with abundant crystals (arrows). Dominica 166. RLS, scale: 100 µm.
8. Close-up of tile cells (TC) with crystals. Dominica 166. RLS, scale: 50 µm.

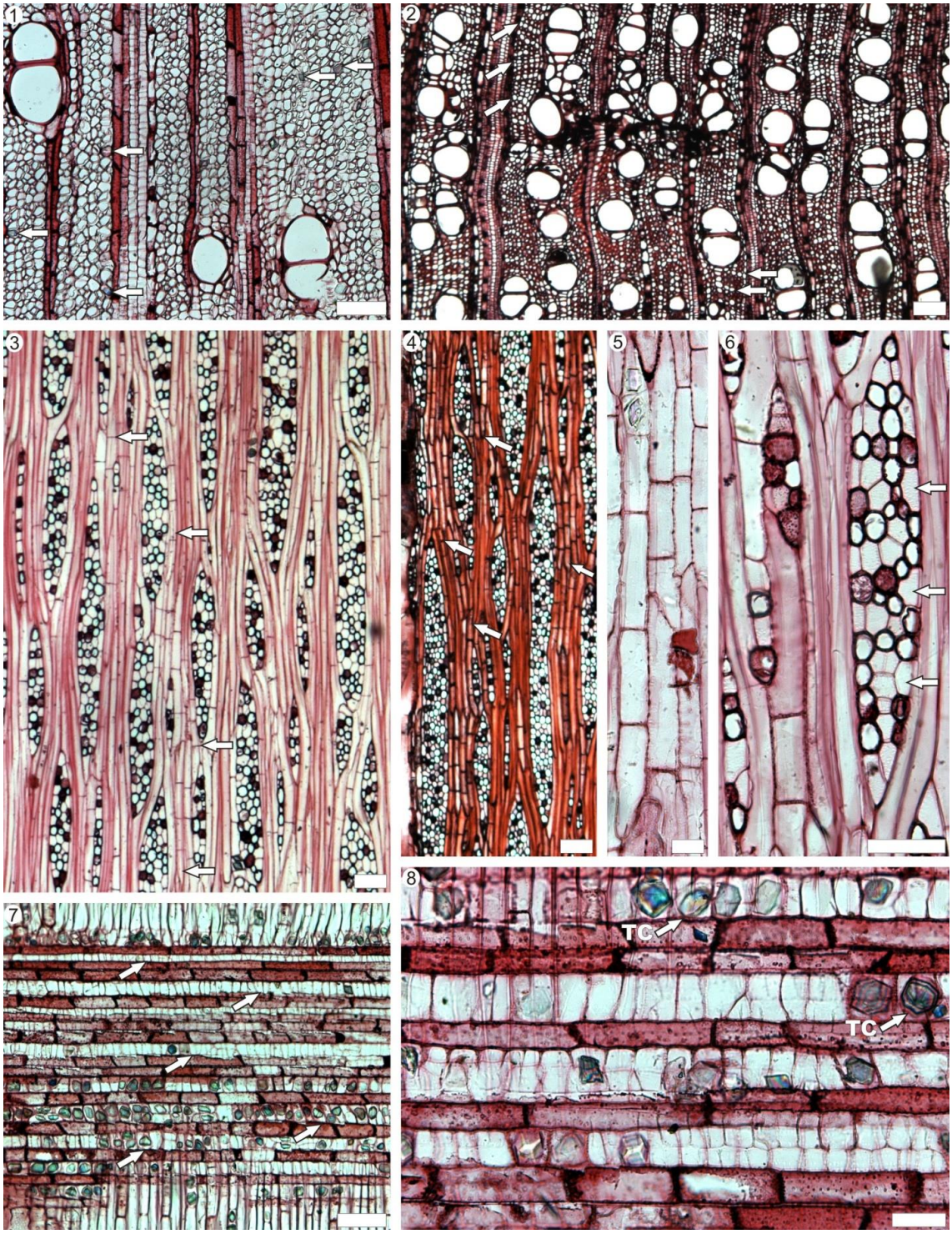

Plate 5.7

A further study of the wood reference collections confirmed that this combination is generally uncharacteristic of the Malvaceae *sensu* APG III. Nonetheless, sixteen genera with tile cells, some of them not coded in IWD at all, show this combination as follows: *Abutilon, Berrya, Cola, Firmiana, Grewia, Herietera, Hibiscus, Lavatera, Ochroma, Octolobus, Pavonia, Pentaplaris, Pseudobombax, Pterygota, Scaphopetalum,* and *Sterculia.* Therefore, a subsequent comparison of the fossil specimens was restricted to these genera. In restricting the search, I am aware that I observed only about half of the genera of Malvaceae *sensu* APG III, and note that it is possible that there may be additional genera showing both of the key features of the Type 5 fossil woods.

Of these comparative taxa, several can be immediately eliminated because they show features not seen in the fossils. *Grewia*, *Hibiscus*, *Ochroma*, *Pseudobombax* and *Sterculia* show parenchyma that is dominantly diffuse or diffuse-in-aggregates. Additionally *Grewia* and *Firmiana* have two distinct sizes of rays. *Abutilon*, *Cola* and one species of *Berrya* (*B. cordifolia)* have very regular festooned bands of parenchyma, although the other two *Berrya* species show very scarce or absent parenchyma. The parenchyma is scalariform in *Heritiera* and some species of *Sterculia.* In *Lavatera*, vessels are grouped in clusters of mainly 5. *Pterygota* has very broad bands of parenchyma, > 8 cells wide, and also contains helical thickenings of vessels.

Close matches with the Fossil Wood Type 5 specimens are only found in *Pentaplaris*, a small archaic genus of the subfamily Malvoideae (Baum et al., 2004), which is found in tropical South America and comprises three species: *P. doroteae* is endemic to Costa Rica, *P. davidsmithii* is found in Bolivia and Peru, and *P. huaoranica* is restricted to Ecuador. Only one specimen (Kw 20291) of one species, *Pentaplaris doroteae* L.O. Williams and Standley, was available in the wood reference collections at

Kew, so those observations may not have captured the full of variability of the genus. Nonetheless, this specimen shows remarkable similarity with the fossil woods insofar that it shows regular bands of parenchyma, 3 – 5 cells wide, in combination with *Pterospermum*-type tile cells.

Specimen Kw 20291 (*Pentaplaris doroteae*) has the following features (Table 5.2.): growth rings indistinct (Plate 5.8., I); wood diffuse porous (Plate 5.8., 1); vessels in radial multiples of 2 – 4 (Plate 5.8., 2); vessels with an oval outline (Plate 5.8., 3); perforation plates simple (Plate 5.8., 4); intervessel pitting alternate, polygonal and minute (Plate 5.8., 5); vessel – ray pitting similar in shape and size to the intervessel pitting (Plate 5.8., 6); parenchyma strands mainly 8 cells high (Plate 5.8., 7); fibre pits common on both radial and tangential walls; axial parenchyma in regular broad bands, 3 – 5 cells wide (Plate 5.8., 1, 2); conspicuous sheath cells present (Plate 5.8., 8); *Pterospermum*-type tile cells present (Plate 5.8., 9); rays heterocellular, commonly 2– 4-seriate (Plate 5.8., 8); ray density 4 – 13 rays per mm (Plate 5.8., 8); and rhomboidal crystals present in square ray cells and tile cells (Plate 5.8., 9, 10) and in the axial parenchyma cells.

Plate 5.8. *Pentaplaris doroteae* L.O. Williams & Standley, Jodrell Laboratory, Royal Botanic Gardens, Kew, specimen number: Kw 20291.

1. Growth rings indistinct; wood diffuse-porous; regular bands of apotracheal parenchyma 3 – 5 cells wide. TS, scale: 200 µm.
2. Vessels in radial multiples of 2 – 4 and apotracheal banded parenchyma 3 – 5 cells wide. TS, scale: 100 µm.
3. Close up of solitary vessels with oval outline. TS, scale 50 µm.
4. Perforation plate simple (SPP). RLS, scale 100 µm
5. Intervessel pitting alternate, polygonal and minute. TLS, scale: 40 µm.
6. Detail of bordered vessel – ray pits, similar in size and shape to the intervessel pits. RLS, scale: 50 µm.
7. Parenchyma strands mainly 8 cells high. TLS, scale: 25 µm.
8. Rays 2 – 4 (– 5)-seriate, showing conspicuous sheath cells (arrows). Ray density 4 –13 per mm. TLS, scale: 100 µm.
9. *Pterospermum*-type tile cells (TC), some containing rhomboidal crystals (C) interspersed with procumbent ray cells. TLS, scale 100 µm
10. Rhomboidal crystals in square ray cells. RLS scale: 50 µm.

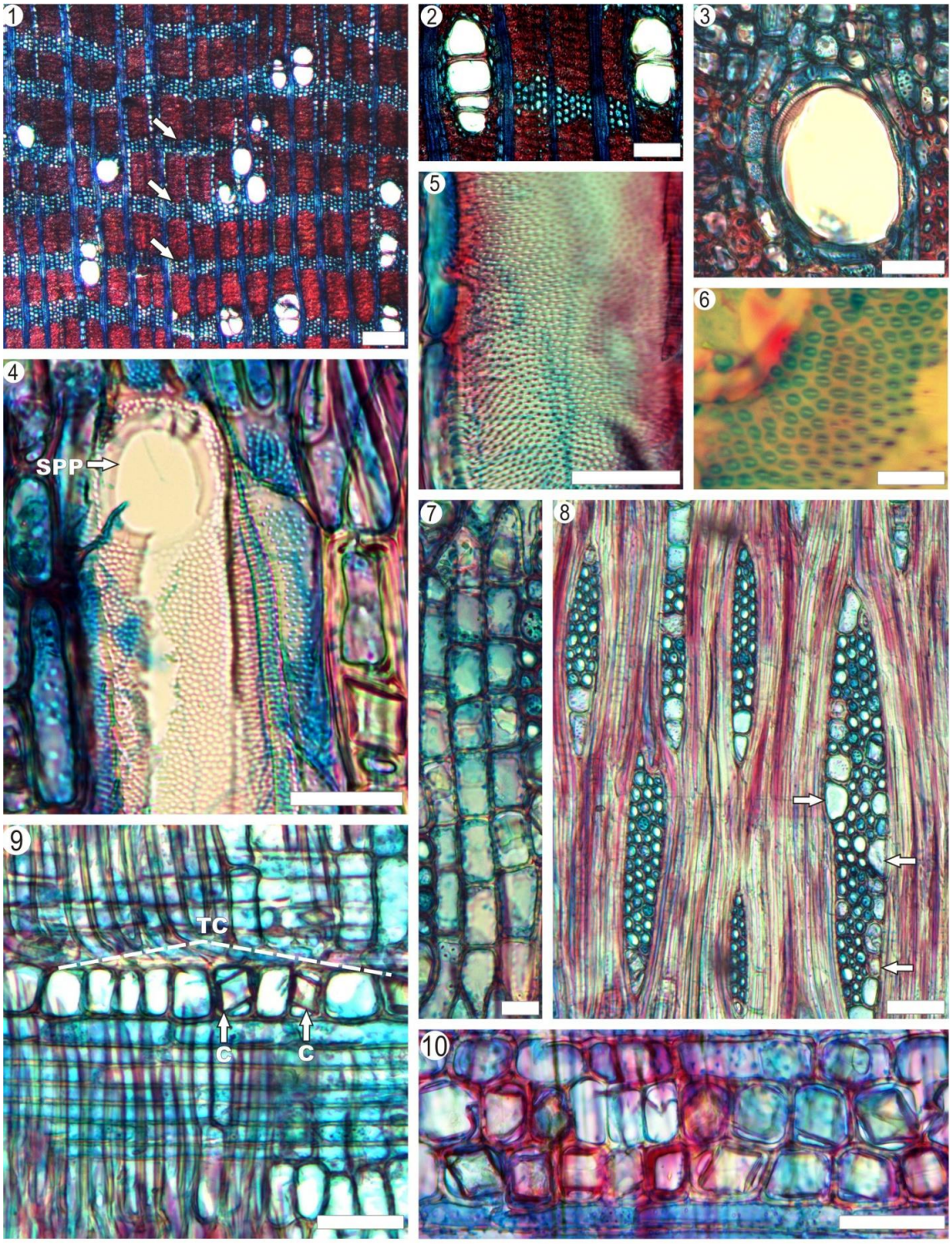

Plate 5.8

The Fossil Wood Type 5 specimens share all of the previously listed features of *Pentaplaris,* except that pits on the tangential fibre walls were not seen in the fossil. However, this may be a taphonomic feature as fibre pits are very difficult to observe in these fossil specimens. Furthermore, some of the juvenile fossil specimens show aggregate rays and locally storied fibres and parenchyma strands, features absent in *Pentaplaris doroteae*, but I did not count with juvenile material of *Pentaplaris* for comparison, and consider that the absence of storeying in the fossil is outweighed by the combination of these features. In addition, no fossil woods with features closely similar to those seen in *Periplanetoxylon panamense* are known. Therefore this survey of malvacean fossil woods supports a view that this fossil type is a novel taxon.

5.8. PCA MORPHOMETRICS

In order to further assess the identity of the malvalean woods presented herein, a Principal Component Analysis (PCA) was conducted for the fossils and comparable taxa revised from Kew and the Inside Wood Database. The tested data matrix consisted of the two fossil types and 259 species of Malvaceae (Table 5.3., Appendix 5.8), using 36 different characters (Table 5.3) that were mainly obtained from the IAWA suggested list of features (1989). I note that some of the features were stated slightly different from the list, in order to assess the most important features and to do not overweight characters that are not important for this family. The total variance obtained from the two first Principal Components (PC) was of 25%. This is a low value for this type of analysis, however considering the amount of variables (features) one could expect the variance is not explained in the first two PC. Additionally, although qualitative data can

be used in PCA, higher values of variance are classically obtained when including numerical data (Hammer and Harper, 2006).

Number	Species	Number	Species
1	*Guazumaoxylon miocenica*	**131**	*Hibiscus grewiaefolius*
2	*Periplanetoxylon panamense*	**132**	*Hibiscus heterophyllus*
3	*Abutilon fruticosum*	**133**	*Hibiscus ludwigi*
4	*Abutilon mollisimum*	**134**	*Hibiscus hastatus*
5	*Actinophora mastersii*	**135**	*Hibiscus macrophyllus*
6	*Adansonia digitata*	**136**	*Hibiscus pleyteri*
7	*Adansonia sp*	**137**	*Hibiscus rosa-sinensis*
8	*Adansonia niveum*	**138**	*Hibiscus similis*
9	*Althaea cannabina*	**139**	*Hibiscus syriacuss*
10	*Apeiba albiflora*	**140**	*Hibiscus schizopetalus*
11	*Apeiba aspera*	**141**	*Hibiscus tiliaceous*
12	*Apeiba tiborbou*	**142**	*Hoheria populnea*
13	*Apeiba petuomo*	**143**	*Hydrogascar trinerve*
14	*Argyrodendron actinophylla*	**144**	*Kleinhovia hospita*
15	*Argyrodendron trifoliolatum*	**145**	*Kostermansia malayana*
16	*Ayenia praeclara*	**146**	*Kydia calicina*
17	*Azanza gardicana*	**147**	*Lagunaria patersoni*
18	*Belotia campbelli*	**148**	*Lavatera alba*
19	*Belotia panamensis*	**149**	*Luehea divaricata*
20	*Belotia mexicana*	**150**	*Lueheopsis rugosa*
21	*Berrya ammonilla*	**151**	*Lueheopsis flavescens*
22	*Berrya cordifolia*	**152**	*Malvaviscus arborescens*
23	*Bombacopsis quinata*	**153**	*Malvaviscus conzattii*
24	*Bombax brevicuspe*	**154**	*Malvaviscus cordata*
25	*Bombaxs aquatica*	**155**	*Mansonia gagei*
26	*Bombax cambodiense*	**156**	*Matisia dowdingii*
27	*Bombax cyathoporum*	**157**	*Matisia bicolor*
28	*Bombax buonopozenze*	**158**	*Melania odorata*
29	*Bombax ceiba*	**159**	*Melochia arborea*
30	*Bombax costatum*	**160**	*Microcos hirsuta*
31	*Bombax ellipticum*	**161**	*Montezuma speciossisima*
32	*Bombax insigne*	**162**	*Muntingia calabura*
33	*Bombax larutense*	**163**	*Neesia synandra*
34	*Bombax mala*	**164**	*Neesia altissima*
35	*Bombax neryosum*	**165**	*Ochroma boliviana*
36	*Bombax surinamensis*	**166**	*Ochroma lagopus*
37	*Boschia griffitisii*	**167**	*Ochroma pyramidale*
38	*Brachychiton acerifolius*	**168**	*Octolobus angustatus*
39	*Brownlonia argentata*	**169**	*Pachira aquatica*
40	*Brownlonia elata*	**170**	*Pachira curtisii*
41	*Byttneria germinifolia*	**171**	*Pachira macrocarpa*
42	*Byttneria maingayi*	**172**	*Paritium tiliaceum*
43	*Camptostemon philippensis*	**173**	*Pavonia fruticosa*
44	*Carpodiptera africana*	**174**	*Pentace burmanica*
45	*Cavanillesia platanifolia*	**175**	*Pentace griffithii*
46	*Ceiba pentandra*	**176**	*Pentace perakensis*
47	*Chorisia crispiflora*	**177**	*Pentace strychnoidea*
48	*Chorisia speciosa*	**178**	*Pentace triptera*
49	*Christiana africana*	**179**	*Pentaplaris doroteae*
50	*Cistanthera papaverifera*	**180**	*Prockia crucis*

51	*Cleirostemom platanoides*	**181**	*Prockia deltoides*
52	*Cola acuminata*	**182**	*Pterocymbium tinctorium*
53	*Cola bracteata*	**183**	*Pterocymbium tubulatum*
54	*Coelostegia griffithii*	**184**	*Pterocymbium splendens*
55	*Colona auriculata*	**185**	*Pterocymbium splendens*
56	*Cola scabra*	**186**	*Pterocymbium semisagittatum*
57	*Columbia annilao*	**187**	*Pterospermum acerifolium*
58	*Commersonia fraseri*	**188**	*Pterospermum diversifolium*
59	*Commersonia platyphilla*	**189**	*Pterospermum blumeanum*
60	*Cullenia excelsa*	**190**	*Pterospermum jackianum*
61	*Dicraspidia donnele-smithli*	**191**	*Pterospermum niveum*
62	*Diplophractum auriculatum*	**192**	*Pterospermum hyneaum*
63	*Diplanthemum veridiflorum*	**193**	*Pterygota bequaertii*
64	*Dombeya runsardensis*	**194**	*Pterygota mildbraedii*
65	*Dombeya mastersii*	**195**	*Pterygota kamerunensis*
66	*Dombeya mukale*	**196**	*Pseudobombax ellipticum*
67	*Duboscia sp.*	**197**	*Pityranthe verrucosa*
68	*Durio axleyianus*	**198**	*Quararibea asterolepis*
69	*Durio carinatus*	**199**	*Quararibea parvifolia*
70	*Durio conicus*	**200**	*Reevesia cavaleirei*
71	*Durio macrophyllum*	**201**	*Reevesia clarkii*
72	*Durio Iwioanus*	**202**	*Reevesia formosana*
73	*Durio lissocarpa*	**203**	*Reevesia pubescens*
74	*Durio liberthinus*	**204**	*Reevesia thyrosidea*
75	*Entelea arborescens*	**205**	*Reevesia wallichii*
76	*Eriobroma klaineana*	**206**	*Scaphium affini*
77	*Eriodendron anfractuosum*	**207**	*Schoutenia ovata*
78	*Eriolena candollei*	**208**	*Sterculia acerifolia*
79	*Eriolena spectabilis*	**209**	*Sterculia alata*
80	*Erinocarpus ninimonii*	**210**	*Sterculia apendiculata*
81	*Firmiana barteri*	**211**	*Sterculia campanulata*
82	*Firmiana colorata*	**212**	*Sterculia caribaea*
83	*Firmiana simplex*	**213**	*Sterculia ceramica*
84	*Firmiana papuana*	**214**	*Sterculia chicha*
85	*Firmiana malayana*	**215**	*Sterculia chicha*
86	*Fremontia californica*	**216**	*Sterculia colombiana*
87	*Glyphaea grewioides*	**217**	*Sterculia elegantiflora*
88	*Glyphaea brevis*	**218**	*Sterculia excelsa*
89	*Grewia asiatica*	**219**	*Sterculia foetida*
90	*Grewia bicolor*	**220**	*Sterculia hugelii*
91	*Grewia crenata*	**221**	*Sterculia linearicarpum*
92	*Grewia globifera*	**222**	*Sterculia murex*
93	*Grewia latifolia*	**223**	*Sterculia multinervia*
94	*Grewia laurifolia*	**224**	*Sterculia murex*
95	*Grewia laevigata*	**225**	*Sterculia oblonga*
96	*Grewia miqueliana*	**226**	*Sterculia ornata*
97	*Grewia microcos*	**227**	*Sterculia pallens*
98	*Grewia oppositifolia*	**228**	*Sterculia populnifolia*
99	*Grewia orientalis*	**229**	*Sterculia pruriens*
100	*Grewiapaniculata*	**230**	*Sterculia quinquefolia*
101	*Grewia populnifolia*	**231**	*Sterculia rhinopetala*
102	*Grewia polygama*	**232**	*Sterculia rubiginosa*
103	*Grewia pubescens*	**233**	*Sterculia scaphisera*
104	*Grewia tiliaefolia*	**234**	*Sterculia setigera*
105	*Grewia tenax*	**235**	*Sterculia subviolacea*
106	*Grewia umbellata*	**236**	*Sterculia tragacantha*
107	*Grewia villosa*	**237**	*Sterculia villosa*
108	*Grewia vestitata*	**238**	*Sterculia versicolor*

109	*Guaribea floribunda*	**239**	*Theobroma bernoullii*
110	*Guazuma tomentosa*	**240**	*Theobroma bicolor*
111	*Guazuma tomentosa*	**241**	*Theobroma cacao*
112	*Guazuma crinita*	**242**	*Thespesia glandiflora*
113	*Guazuma ulmifolia*	**243**	*Thespesia populnea*
114	*Guazuma ulmifolia*	**244**	*Tilia americana*
115	*Hasseltia floribunda*	**245**	*Tilia caucasica*
116	*Hasseltiopsis dioica*	**246**	*Tilia cordata*
117	*Helicteres guazumaefolia*	**247**	*Tilia europaea*
118	*Heliocarpus appendiculatus*	**248**	*Tilia floridana*
119	*Heritiera elata*	**249**	*Tilia glabra*
120	*Heritiera carrioni*	**250**	*Tilia heterophylla*
121	*Heritiera fomes*	**251**	*Tilia japonica*
122	*Heritiera litoralis*	**252**	*Tilia rubra*
123	*Heritiera macrophylla*	**253**	*Tilia maltkei*
124	*Heritiera ornitocephala*	**254**	*Tilia tomentosa*
125	*Heritiera javanica*	**255**	*Tilia vulgaris*
126	*Heritiera utilis*	**256**	*Trachetiopsis melanoxylon*
127	*Hibiscus borneensis*	**257**	*Triplochiton scleroxylon*
128	*Hibiscus columnaris*	**258**	*Trichospermum richii*
129	*Hibiscus elatus*	**259**	*Triumfetta hintonii*
130	*Hibiscus floccosus*		

Table 5.3. Key table of species for the PCA of malvalean woods.

As seen in the scatter (Figure 5.3.), *Guazumaoxylon* is considerably close to a cluster of species including: *Grewia globifera, Bombax ceiba, Bombax cambodiense, Eriobroma klaineana and Byttneria geminifolia.* All these species were ruled out in the previous comparison in this study because several of them have septate fibres and abundant diffuse parenchyma. The species of *Guazuma* are diverse anatomically, even sometimes varying between samples from different environments. This fact together with certain differences with the fossil, previously discussed in this chapter, may explain that these are not clustering with the fossil.

Regarding to the fossil type 5, it could be concluded the results are better contrasted with the fossil Type 4, since *Pentaplaris doroteae* is very close to the fossil as seen in the scatter (Figure 5.3).

Malvaceae is a large family and it has been complicated to unify the anatomy characteristics with its phylogeny, due to the complexity and diversity of its features. Despite the Fossil Type 4 did not match *Guazuma* as expected, the Fossil Type 5 presented more satisfactory results, meaning perhaps that this Type is a closer match to the proposed identity.

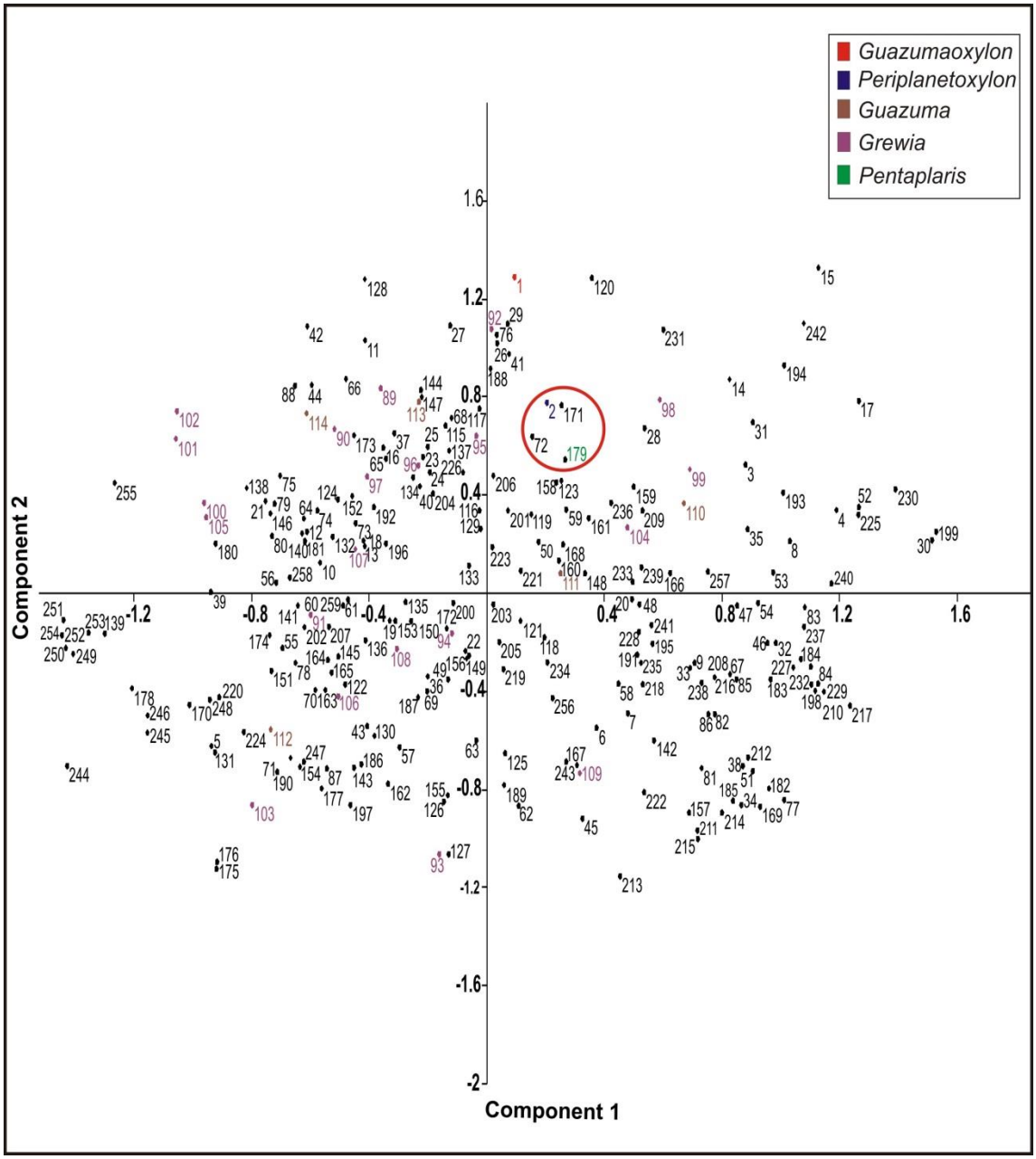

Figure 5.3. Principal component analysis of species of the malvalean wood types from the permineralised assemblage (Hodges Hill) and modern Malvaceae species revised in Kew and Inside Wood.

5.9. COMPARISON WITH FOSSIL WOODS PREVIOUSLY ASSIGNED TO MALVACEAE

In this section, I summarise the previously reported malvacean woods in the fossil record from the Cretaceous to Miocene. I focus on the main aspects, and for each fossil, list how it differs from the two wood types described in this paper.

5.9.1. Cretaceous woods

The oldest known malvalean woods date from the latest Cretaceous (Campanian – Maastrichtian) and include *Javelinoxylon* (Wheeler et al., 1994; Estrada-Ruizet al., 2007), *Bombacoxylon langstonii* (Wheeler and Lehman, 2000) and *Wheeleroxylon atascoense* (Estrada-Ruiz et al., 2010). *Javelinoxylon* woods contain common tyloses and scarce paratracheal and apotracheal parenchyma; *B. langstonii* shows diffuse-in-aggregates parenchyma, rays typically composed of only procumbent cells and no tile cells, whereas *W. atascoense* has tyloses, diffuse axial parenchyma, and rays that are homocellular and storied. Other Cretaceous woods that have been reported as Malvaceae include *Parabombacaceoxylon magniporosum,* from the Upper Cretaceous (Maastrichtian) of Illinois, U.S.A. (Wheeler, et al., 1987), with > 10 bars scalariform perforation plates and axial parenchyma diffuse-in-aggregates; *Hibiscoxylon niloticum* from Lebanon (Beauchamp and Lemoigne, 1973), with tyloses common, axial parenchyma diffuse and occasionally, confluent and banded, rays of two distinct sizes; and woods of uncertain Late Cretaceous or Eocene age from Ethiopia described as *Dombeyoxylon owenii*, showing parenchyma diffuse and all storied rays, and *Hibiscoxylon niloticum* Kräusel, which resembles *Hibiscus*, having tyloses, axial parenchyma diffuse but combined with bands of 1 – 3 and > 3 cells wide, rays of two

distinct sizes, and crystals abundant in ray and axial parenchyma cells (Beauchamp et al., 1973).

5.9.2. Paleocene-Eocene woods

Paleocene-Eocene records of putative malvacean woods are more common. In Paleocene sediments, they include *Camptostemomonoxylon mahurzarii*, *Dryoxylon mahurzarii*, *Dryoxylon intertrappea, Grewioxylon intertrappeaeum, Hibiscoxylon intertrappeum, Sterculioxylon shahpuraensis* (Trivedi, 1971; Trivedi and Ambwani, 1976; Bande and Prakash, 1982; Bande and Prakash, 1980b), *Parabombacaceoxylon* (Wheeler and Michalski, 2003), *Sessaoxylon paleocenicum* (Koeniguer, 1971), *Tarrietioxylon hazzeldinewarrenii* (Crawley, 1989) and *Tilioxylon lueheaformis* (Crawley, 2001). All of these woods lack either dominantly banded or aliform parenchyma, but instead show parenchyma that is diffuse and diffuse-in-aggregates. Additionally, it is common to find two distinct sizes of rays in these taxa.

For the Eocene, the number of reports increases even further (especially in Europe and North America) and some of the woods show more diverse parenchyma types: *Bombacoxylon monodii* Boureau (Gottwald, 1969) has vessels arranged radially or diagonally, tyloses common and parenchyma that is diffuse-in-aggregates; *Chattawaya paliforme* (Wheeler and Manchester, 2002) has distinct growth rings, parenchyma that is diffuse-in-aggregates and rays in two distinct size classes; *Helictoxylon wilcoxianum* (Berry, 1923), as originally described in the Wilcox palaeoflora, resembles a liana with very closely spaced wide rays and abundant diffuse parenchyma; *Sterculioxylon freulonii* of southwest Germany (Guleria, 1982), shows axial parenchyma in concentric confluent bands, with some not confluent aliform parenchyma, axial parenchyma and fibres storied, and a few axial canals; *Sterculioxylon*

deccanensis (Lakhanpal et al., 1976) has narrow paratracheal sheaths and apotracheal parenchyma diffuse to diffuse in aggregates; *Triplochitioxylon oregonensis* (Manchester, 1979; Wheeler and Manchester, 2002) has distinct growth rings, axial parenchyma diffuse-in-aggregates with occasional 1–3 cells wide parenchyma bands and axial parenchyma storied.

5.9.3. Oligocene-Miocene woods

Several more malvacean woods are known in the Oligocene-Miocene. These include diverse *Sterculioxylon* specimens from Oligocene localities in India and Egypt described as *S. giarabubensis* (Kräusel, 1939), *S. foetidense* (Guleria, 1982), and *S. dattai* (Prakash and Tripathi, 1972, Guleria, 1982). In these specimens, parenchyma is dominantly diffuse-in-aggregates except for *S. giarabubensis*, where it is aliform and confluent forming concentric bands. *Pterospermoxylon*, found in the Kachchh Flora (Guleria, 1982) has distinct growth rings, common tyloses and parenchyma scanty paratracheal.

Other reports from the Miocene include *Dryoxylon siamensis* (Prakash, 1977) with distinct growth rings, semi-ring porous wood, common tyloses, axial parenchyma in narrow bands up to 3 cells wide, but without tile or sheath cells. Still other Miocene examples include *Reevesia japonoxyla* (Terada and Suzuki, 1998) with wood distinctly ring-porous, scanty paratracheal and diffuse apotracheal parenchyma with storied and fusiform strands; *Sterculioxylon kalagarhense* (Guleria, 1982), with paratracheal axial parenchyma in narrow to thick sheath around the vessels and some regular bands, rays 1 – 16 seriate and axial canals present; *Sterculioxylon pondicherriense* (Guleria, 1982) shows banded parenchyma 3 – 12 cells wide and rays up to 25-seriate; *Tarrietioxylon sumatrense* (Kraüsel, 1922) shows common tyloses, axial parenchyma diffuse in

aggregates combined with vasicentric and aliform parenchyma and all rays storied. Terada and Suzuki (1998) erected a new genus from Japan, *Wataria*, and reported two species: *W. miocenica* (Terada and Suzuki, 1998) with ring-porous wood, axial parenchyma diffuse in aggregates and rays of two distinct sizes and *W. parvipora* (Terada and Suzuki, 1998) with apotracheal parenchyma 1 – 2 cells wide, rays in two distinct sizes and no crystals.

5.9.3.1. Miocene specimens of *Grewioxylon*

Most similar to the Fossil Wood Type 4 specimen are specimens of *Grewioxylon*, a genus containing woods with similarities to extant *Grewia*, which are rather numerous in Miocene deposits. However, these woods differ from the fossils in having axial parenchyma that is dominantly diffuse and diffuse-in-aggregates (e.g., *G. fontanesii* Srivastava, 2000; *G. neumaieri* Selmeier, 1985; *G. ortenburgense* Selmeier, 1985; *G. microcoides* Agarwal, 1991; *G. intertrappea* Shallom, 1963). Additionally, it is common to see bimodal and storied rays (*G. indicum* Prakash and Dayal, 1964; *G. burmense* Gottwald, 1994; *G. canalisum* Bande and Srivastava, 1994; *G. macroporosum* Gottwald, 1994; *G. intertrappea*) in these specimens. Although some of these *Grewioxylon* with bimodal and storied rays show aliform parenchyma as in *Guazumaoxylon miocenica* (Fossil Wood Type 1) it is conspicuously confluent and combined with narrow or broad apotracheal bands as in *G. fontanesii*, *G. burmense*, and *G. canalisum*.

In constrast, I know of no fossils woods with features closely similar to those seen in *Periplanetoxylon panamense* (Fossil Wood Type 5). Therefore this survey of malvacean fossil woods supports the view that the two fossil types described in this thesis are novel.

5.10. DISCUSSION

Malvaceae *sensu* APG III comprises c. 243 genera containing c. 4225 species, ranging from shrubs to trees, with a few herbaceous members. The family is characterized by leaves that show, typically, palmate secondary venation, inflorescences consisting of cymose units, and fruits comprising a capsule, berry or schizocarp (Stevens, 2001 onwards). Malvaceae *sensu* APG III is mostly tropical in distribution but also contains numerous representatives in the temperate zones (Bayer and Kubitzki, 2003; Carvalho et al., 2011; Judd and Manchester, 1997), with a few examples, such as *Malva pusilla* Sm., reaching up to 65°N in Europe (Hinsley, 2004 onwards). In the tropics, the family can be found in a diverse range of habitats including humid, semi-arid and arid zones (Hinsley, 2004 onwards).

5.10.1. Phylogeny and evolution

Delimitation of groups inside Malvaceae *sensu* APG III, especially within the traditional Malvaceae, has been inconsistent for a long time, and there have been many attempts to establish a degree of order (Rendle, 1925; Edlin, 1935; Brizicky, 1965; Hutchinson, 1967; Cronquist, 1981; Chang and Miau, 1989; Dorr, 1990; Manchester, 1992; Judd et al., 1994; Zomlefer, 1994; Judd and Manchester, 1997). Based primarily on molecular data and morphology, with limited support from the anatomy, nine monophyletic subfamilies are now recognized as follows: Grewiodeae, Byttnerioideae, Sterculioideae, Tilioideae, Dombeyoideae, Brownlowioideae, Helicteroideae, Helicteroideae, Malvoideae and Bombacoideae (APG III, 2009). The fossils include representatives of the subfamilies Byttnerioideae (Fossil Wood Type 1) and Malvoideae (Fossil Wood Type 2).

Most of the diversity of Byttnerioideae is endemic to Central and South America suggesting an origin in this region, consistent with the fossil discoveries reported here. In contrast, the subfamily Malvoideae, which is one of the most basal and diverse clades in the Malvaceae (Angiosperm Phylogeny Group; Hinsley, 2004; Baum et al., 2004), has traditionally been to considered to be of Australasian origin with multiple long-distance migrations invoked to explain the occurrence of the group in the Neotropics (Pfeil et al., 2002; Duarte et al., 2011). However, megafossils found in the Paleocene of Colombia (Carvalho, 2011) offer an alternative explanation suggesting a broader distribution in the past, favoured by warmer conditions, and more likely with a South American origin. Again, this is consistent with our new Miocene data.

5.10.2. Biogeographic significance of fossils

The two fossil woods described herein from the Lower Miocene of Panama comprise material similar to extant *Guazuma* (Byttnerioideae) especially *G. ulmifolia* (Fossil Wood Type 1) and *Pentaplaris* (Malvoideae), especially *P. doroteae* (Fossil Wood Type 2). *G. ulmifolia* is a shrub or tree 3 – 25 m tall and with trunk diameters up to 80 cm, found in lowland deciduous forest and pastures of Central America (Garguillo et al., 2008; USDA, 2013). *Pentaplaris* is a genus of large rainforest trees restricted to the present-day Neotropics of Costa Rica, Bolivia, and Peru (Baum et al., 2004). The presence of South American taxa in the Lower Miocene strata of Panama suggests floral interchange of large tree species through the Isthmus of Panama as early as 18 – 20 Ma. This is consistent with the recently proposed emergence of the Isthmus in the Miocene (Montes et al., 2012) evidenced by studies of plutonic zircons and inferences from mammal biostratigraphy.

CHAPTER 6. CHARCOALIFIED WOODS: TAXONOMY

6.1. INTRODUCTION

This chapter describes nine distinct taxa of charcoalified wood based on 22 specimens of tree stumps and trunks obtained from a fossil forest found in growth position (cf. DiMichele and Falcon-Lang, 2011) exposed near the top of the formation. The geological context of these fossils, which are entombed beneath the deposits of a hot pyroclastic flow (ignimbrite), are described in Chapter 2. The material was obtained from the same correlative geological horizon at two localities, Centenario Bridge and Contractors Hill in the Panama Canal Zone (see Chapter 2; Figure 2.4, 2.5). Although there were also charcoalified trunks and branches at a third site, Hodges Hill, no samples were collected.

In most cases, the quality of preservation of the charcoalified material is much inferior to the permineralised material documented in Chapters 4 and 5. The charcoalified woods from the Cucaracha Formation (as common with most charcoalified material) are difficult to study under the optical light microscope because of the opaque nature of this type of material (Scott, 1989). A few of these samples were studied with SEM, which is a more suitable method to approach the description and identification of charred material (Scott, 2000), although the best results have been obtained for wildfire-produced charcoal, not for tree charcoalified in hot volcanic deposits.

In this current study, the SEM results were not entirely satisfactory although this technique offered some additional aid to the descriptions done with regular thin sections. A further point is that the contraction that occurs during the charring process makes direct comparison between extant (uncharred) and fossil material (charred) challenging

because the application of contraction coefficients requires a degree of educated guesswork. In order to correctly code some quantitative characters in the IWD, a contraction coefficient of 33% was assumed (however, see Falcon-Lang et al., 2012 for a full discussion of the pit-falls in this approach).

In view of these limitations, the charcoalified material described here is merely grouped into morphotypes and a general assessment of affinity is made, where possible. In a few cases, charcoalified material includes examples of, somewhat similar, or identical, morphotypes to those seen in the permineralised assemblage. These are listed first in the descriptive section. However, in general, the charcoalified assemblage differs, rather strikingly, in composition from the permineralised assemblage (as discussed below).

6.2. cf. FOSSIL WOOD TYPE 2

Note: This material is closely similar, or identical to permineralised material described in Chapter 4 as Fossil Wood Type 2. I have described the charcoalified material separately because, as noted, the dimensional changes that occur during the charring process (Falcon-Lang et al., 2012) make direct comparison with the permineralised material problematic. However, the likelihood of identity with the permineralised material is very strong in my opinion.

Order: Fabales Bromhead

Family: Fabaceae Lindley

Subfamily: Caesalpinioideae De Candolle

Tribe: Detarieae De Candolle

Genus: cf. *Prioria* Griseb.

Material: STRI 15368, STRI 15369, STRI 15370, STRI 13625, STRI 14198, STRI 21046, STRI 21047.

Repository: Center for Tropical Paleoecology and Archaeology, Smithsonian Tropical Research Institute, Panama.

Locality: Contractors Hill (Gaillard Cut of Panama Canal) near Paraiso, Panama City, Panama (Latitude 09°02'51.75''N; Longitude 79°39'14.02''W).

Stratigraphic horizon: ~ 20 m below the top of the Cucaracha Formation (Gaillard Group); Lower Miocene (19 Ma)

6.2.1. Description

IAWA features numbers present: 2, 5, 9v, 13, 22, 23, 25, 30, 42, 47, 53, 61, 66, 69, 79, 80, 82, 86, 89, 97, 98v; 109, 107, 115, 127v, 128, 136, 137.

Description: Growth rings indistinct; wood diffuse-porous (Plate 6.1, 1; 6.3, 1); vessels commonly solitary, locally exclusively solitary (79 – 95 %) or in radial multiples of 2 – 3 (Plate 6.1, 2, 8); vessel outline oval to circular (Plate 6.1, 2, 8); perforation plates simple (Plate 6.1., 3; Plate 6.3., 3); intervessel pits alternate, polygonal and small (mean range 4 – 5 μm, n = 50; total range 3 – 7 μm) (Plate 6.1., 4; Plate 6.3, 3); vessel – ray pitting similar to intervessel pits in size and shape (2 , SD 0.83, n = 23; range 1 – 3) (Plate 6.1., 5); mean tangential vessel diameter ranges 108 – 142 μm (n = 150; total range 50 – 210 μm); mean vessel density range 6.6– 13.1 per mm^2 (n = 60; total range 4 – 19 per mm^2); tyloses absent; vascular tracheids not observed.

Plate 6.1. cf. Fossil wood type 2

1. Wood diffuse-porous. STRI 15364, TS, scale: 500 μm
2. Vessels commonly in radial multiples of 2 – 3 with vessel outline oval to circular. STRI 15367, TS, scale: 500 μm.
3. Perforation plates simple (arrow). STRI 21046, RLS, scale: 50 μm.
4. Intervessel pits alternate. STRI 21046, TLS, scale: 25 μm.
5. Vessel–ray pitting similar to intervessel pits. STRI 21046, RLS, scale: 50 μm.
6. Fibre pits minutely bordered pits. STRI 21047, RLS, scale 100 μm.
7. Rays mostly 1 – 3-seriate. STRI 21046, TLS, scale 100 μm.
8. Axial parenchyma vasicentric to winged-aliform. STRI 15364, TS, scale 100 μm.

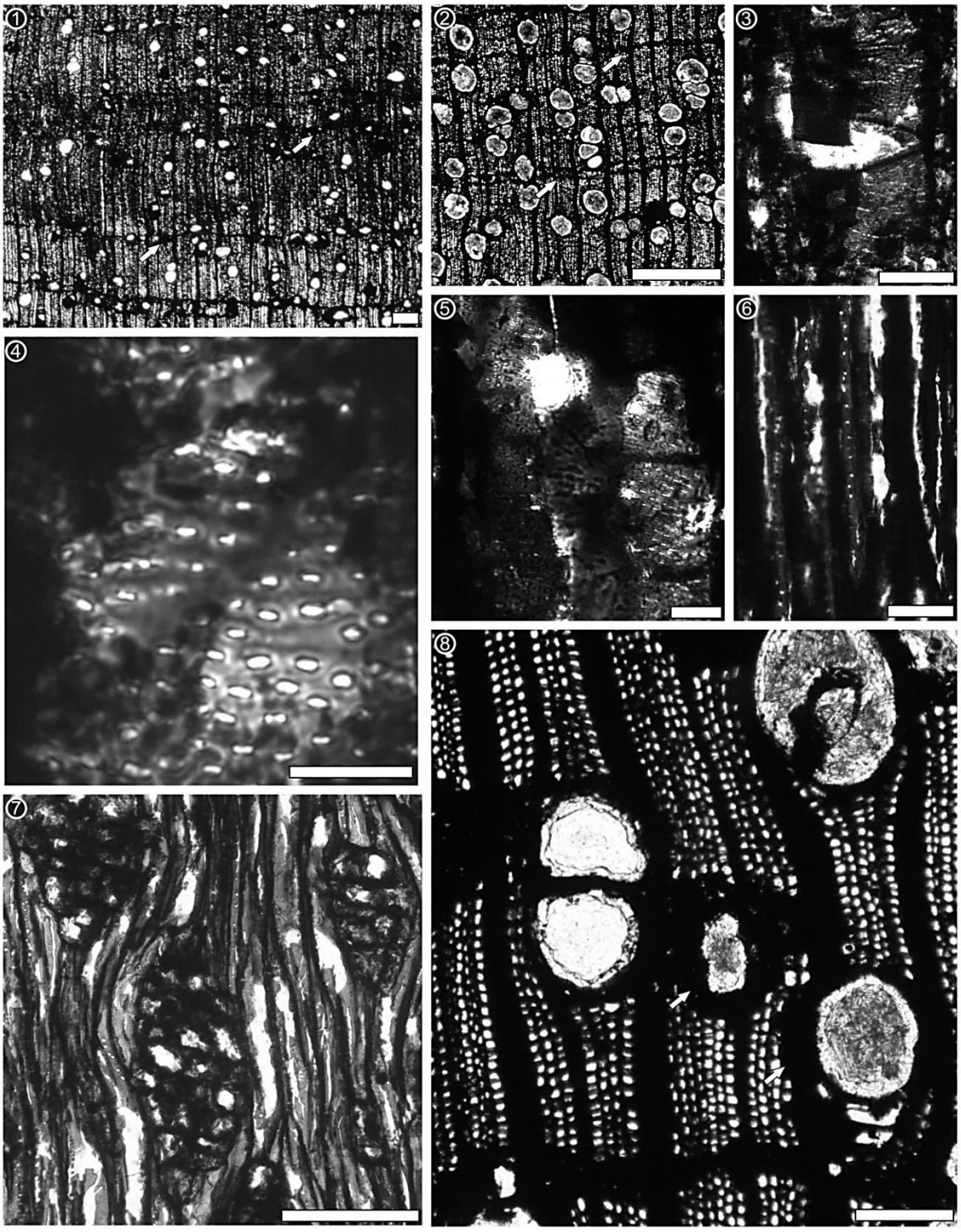

Plate 6.1

Plate 6.2. cf. Fossil wood type 2

1. Axial parenchyma in apotracheal bands 1 – 3 cells wide. STRI 21047, TS, scale: 100 μm.
2. Rays heterocellular 1 – 3 (– 5)-seriate. STRI 21047, TLS, scale: 100 μm.
3. Rays heterocellular 1 – 3 (– 5)-seriate. STRI 21046, TLS, scale: 100 μm.
4. Rays composed of procumbent, square and upright cells mixed throughout the body. STRI 15370, RLS, scale: 100 μm.
5. Axial canals in short tangential lines. STRI 15370, TS, scale 100 μm.
6. Solitary rhomboidal crystals present in square ray cells. STRI 14198, RLS, scale 100 μm.

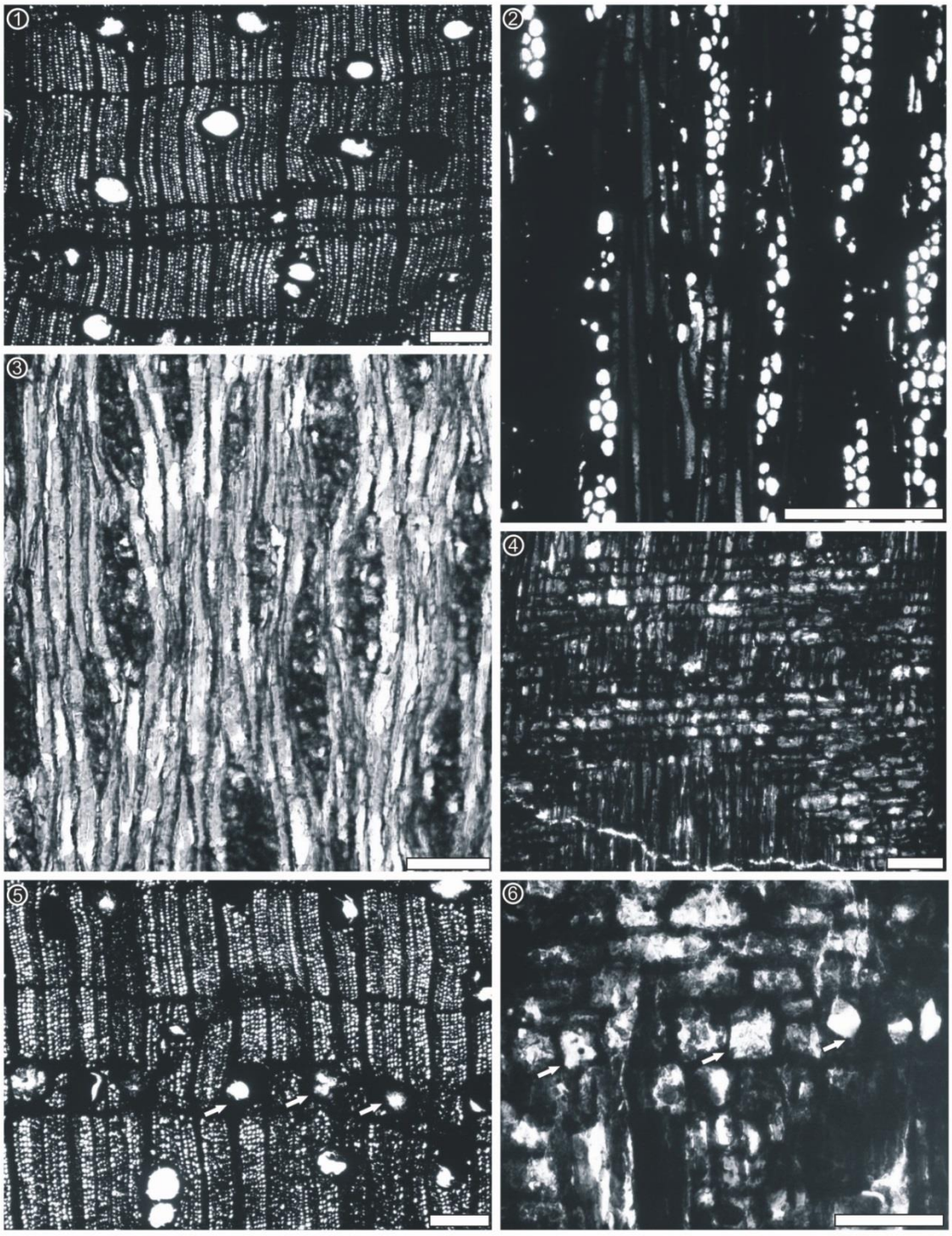

Plate 6.2

Plate 6.3. SEM, cf. Fossil wood type 2

1. Wood diffuse-porous. STRI 14198, TS, 50µm.
2. Axial canals in short tangential lines (arrows). STRI 14198, TS, 100µm.
3. Intervessel pitting alternate (IVP). STRI 14198, TLS, 50µm.
4. Fibre thin-to-thick walled. STRI 14198, TS, 50µm.
5. Axial vasicentric parenchyma (arrows). STRI 14198, TS, 50µm.
6. Apotracheal bands of parenchyma 1 – 3 cells wide. STRI 14198, TS, 50µm.
7. Fibres non-septate. STRI 14198, TS, 50µm.
8. Rays composed of procumbent (PC), square (SC) and upright cells mixed throughout the body. STRI 14198, RLS, scale: 50 µm.

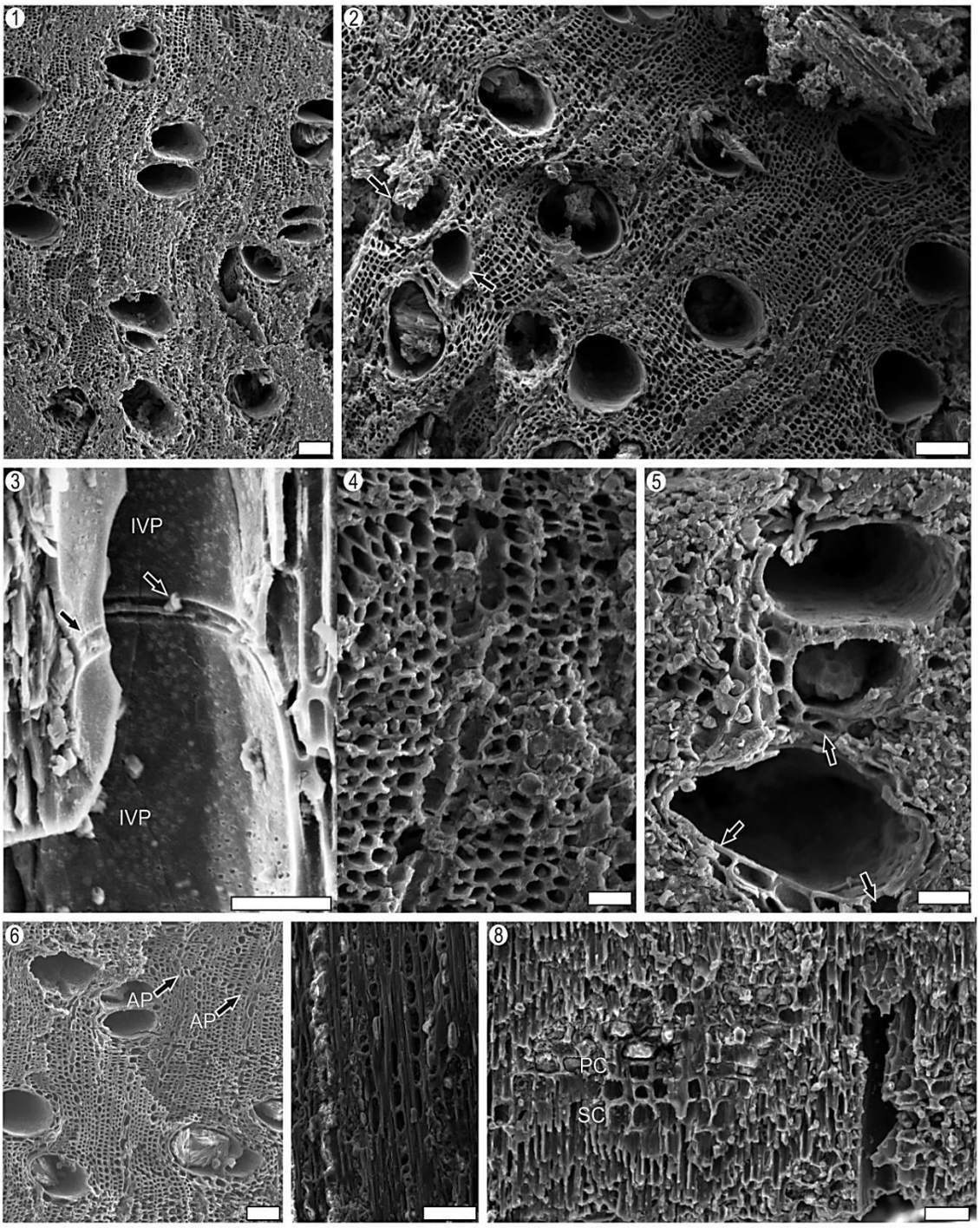

Plate 6.3

Fibres non-septate (Plate 6.3., 7) with pits minutely bordered (Plate 6.1., 6) and common in radial and tangential walls. Fibre walls mostly thin-to thick-walled (Plate 6.1, 8; 6.2, 4).

Axial parenchyma paratracheal vasicentric to winged aliform (Plate 6.1, 8; Plate 6.3, 5) and apotracheal bands 1 – 3 cells wide (Plate 6.2, 1; Plate 6.3, 6; Plate 6.4, 1, 2) with some marginal bands (Plate 6.2, 1, 5); axial parenchyma strands poorly preserved and only partially observed.

Rays heterocellular, 1 – 3 (– 5)-seriate (mean 1.9, SD 0.90, n = 25; range 1 – 5) (Plate 6.2, 2, 3; Plate 6.4, 4; Plate 6.1, 7) and commonly < 1 mm (mean ranges 0.29 – 0.41mm, n = 150; total range 0.2 – 0.8 mm); rays composed of procumbent, square and upright cells mixed throughout the body (Plate 6.2, 4; Plate 6.3, 8; Plate 6.4, 5); mean ray spacing 10.2 ± 1.89 per mm, n = 15; range 7 – 12 per mm) (Plate 6.2, 3).

Solitary rhomboidal crystals present in square ray cells (Plate 6.2, 6). Axial canals present in short tangential lines (Plate 6.2, 5; Plate 6.3, 2; Plate 6.4, 6).

Plate 6.4. cf. Fossil wood type 2

1. Apotracheal bands of parenchyma (AP) 1 – 3 cells wide. STRI 14198, TS, 100µm.
2. Apotracheal bands of parenchyma (AP) 1 – 3 cells wide. STRI 14198, TS, 100µm.
3. Intervessel pitting alternate (IVP). STRI 14198, TLS, 50µm.
4. Rays 1 – 3 (– 5)-seriate. STRI 14198, TLS, scale: 100 µm.
5. Rays composed of procumbent (PC), square (SC) and upright cells mixed throughout the body. STRI 14198, RLS, scale: 50 µm.
6. Axial canals in short tangential lines (arrows). STRI 14198, TS, scale: 100 µm.

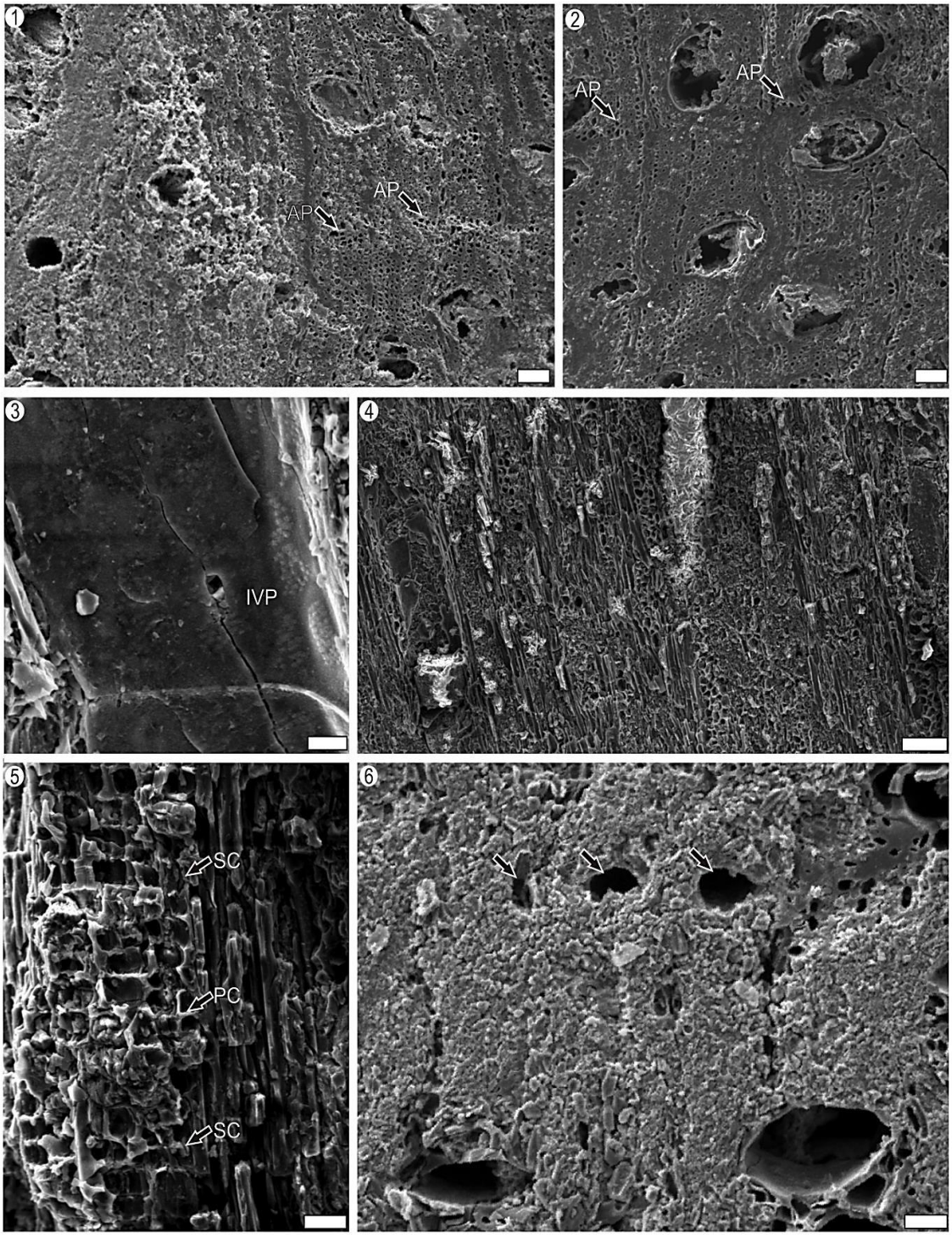

Plate 6.4

6.2.2. Comparison with extant woods

The following combination of characters present in this morphotype are considered diagnostic for the Leguminosae (Gasson, 1994; Gasson et al., 2003; Wheeler and Manchester, 2002; Pujana et al., 2011): wood diffuse-porous (5 p), perforation plates simple (13 p), intervessel pitting alternate (22 p), vessel – ray pitting with distinct borders and similar to intervessel pitting in size and shape (30 p), fibres non-septate (66 p), paratracheal parenchyma vasicentric (79 p) to winged-aliform (82 p), apotracheal parenchyma in marginal bands (89 p), rays 1 – 3-seriate (97 p) and normal axial canals in short tangential lines (128 p). It is complex to differentiate within the Leguminosae because of the size and diversity of the family (Pujana et al., 2011). However, certain features allow sub-groups to be distinguished. The distinctly winged-aliform parenchyma, combined with narrow rays and tangential lines of normal axial canals are very common in some sections of the caesalpinioid subfamily (Baretta-Kuipers, 1994). Specifically, normal axial canals, distributed in diverse patterns, are of exclusive occurrence in the tribe Detarieae (see Chapter 4 for full discussion).

This morphotype, probably, represents the same Leguminosae type collected from the base of the Cucaracha Formation and determined as Fossil Wood Type 2, *Prioria canalensis* sp. nov. (Chapter 4). It has exactly the same suite of characters with certain quantitative differences (e.g., intervessel pitting size mean, mean vessel length), which can be explained by contraction during charcoalification (McParland et al., 2005, 2009; Falcon-Lang et al., 2012). The discovery of this taxon in both major fossil wood assemblages would imply that this species represented a relatively widespread element of the Miocene Panama Canal flora. The close modern species, *Prioria copaifera* occupies habitats adjacent to rivers and estuarine areas (see Chapter 4 for more discussion).

6.3. FOSSIL WOOD TYPE 6

Order: Fabales Bromhead

Family: Fabaceae Lindley

Material: STRI 15405

Repository: Center for Tropical Paleoecology and Archaeology, Smithsonian Tropical Research Institute, Panama.

Locality: Contractors Hill (Gaillard Cut of Panama Canal) near Paraiso, Panama City, Panama (Latitude 09°02’51.75’’N; Longitude 79°39’14.02’’W).

Stratigraphic horizon: ~ 20 m below the top of the Cucaracha Formation (Gaillard Group); Lower Miocene (19 Ma).

6.3.1. Description

IAWA features numbers present: 2, 5,?13, 41, 45, 46, 66, 68, 76v, 86, 97, 115, 128, 131.

Description: Growth rings indistinct; wood diffuse-porous (Plate 6.5, 1); vessels commonly solitary (84 %) or in small clusters of 5 – 7; vessel outline circular (Plate 6.5, 2); perforation plates simple; vessels in two size classes (Plate 6.5, 1, 3); mean tangential diameter of large vessels 182 μm (n= 25; range 127 – 268 μm) and mean tangential diameter of small vessels 59 μm (n = 25; range 35 –96 μm); mean vessel density range 4.2 per mm^2 (n= 10; range 3 – 8 per mm^2); tyloses absent; vascular tracheids not observed.

Fibres with insufficient preservation for observation but they seem to be non septate (Plate 6.5, 5) and very thin walled (Plate 6.5, 4).

Axial parenchyma apotracheal in bands 1 – 3 cells wide (Plate 6.5, 1, 6); axial parenchyma strands poorly preserved and not measured.

Rays heterocellular, 1 – 3-seriate (mean 2.9 ± 0.7, n = 25; range 1 – 4) (Plate 6.5, 5) and significantly < 1 mm (mean 0.2, SD 0.06mm, n = 25; range 0.1– 0.4 mm); mean ray spacing 9.16 ± 1.72 per mm, n = 15; range 7 – 11 per mm).

Axial canals in short lines (Plate 6.5, 3) and probably canals of traumatic origin also present (Plate 6.5, 1, 6).

6.3.2. Similarities to extant woods

The following characters were used in an IWD search: growth rings indistinct (2p), wood diffuse porous; perforation plates simple (13p), vessels of two distinct sizes (45p), rays 1 – 3-seriate (97p), canals in short tangential lines (128p), canals of traumatic origin (131p). The results suggested Leguminosae as the best match with 0 allowed mismatches. If the uncertain presence of traumatic canals (131 p) is excluded from the search, the same results are obtained. Because of the presence of diverse axial canals, this wood may resemble some members of the tribe Detarieae (see Chapter 4 for a discussion). Nevertheless, because of the poor preservation of this specimen, especially in the longitudinal sections, it is not recommended to infer any particular Fabaceae genus or the listed characters are not enough to justify further identifications to subfamily or genus level.

Plate 6.5. Fossil Wood Type 6-Caesalpinioid 2.

1. Growth rings indistinct and wood diffuse-porous and vessels in two distinct size classes. Apotracheal parenchyma in narrow bands 1– 3 cells wide. STRI 15405, TS, scale: 100 μm.
2. Vessel outline circular. STRI 15405, TS, scale: 100 μm.
3. Vessels in two distinct size classes. STRI 15405, TS, scale: 200 μm.
4. Fibres very thin-walled. STRI 15405, TS, scale: 100 μm
5. Rays heterocellular, 1 – 3-seriate. STRI 15405, TLS, scale: 100 μm
6. Canals of traumatic origin (arrows). Apotracheal parenchyma in narrow bands 1– 3 cells wide. STRI 15405, TS, scale: 250 μm.

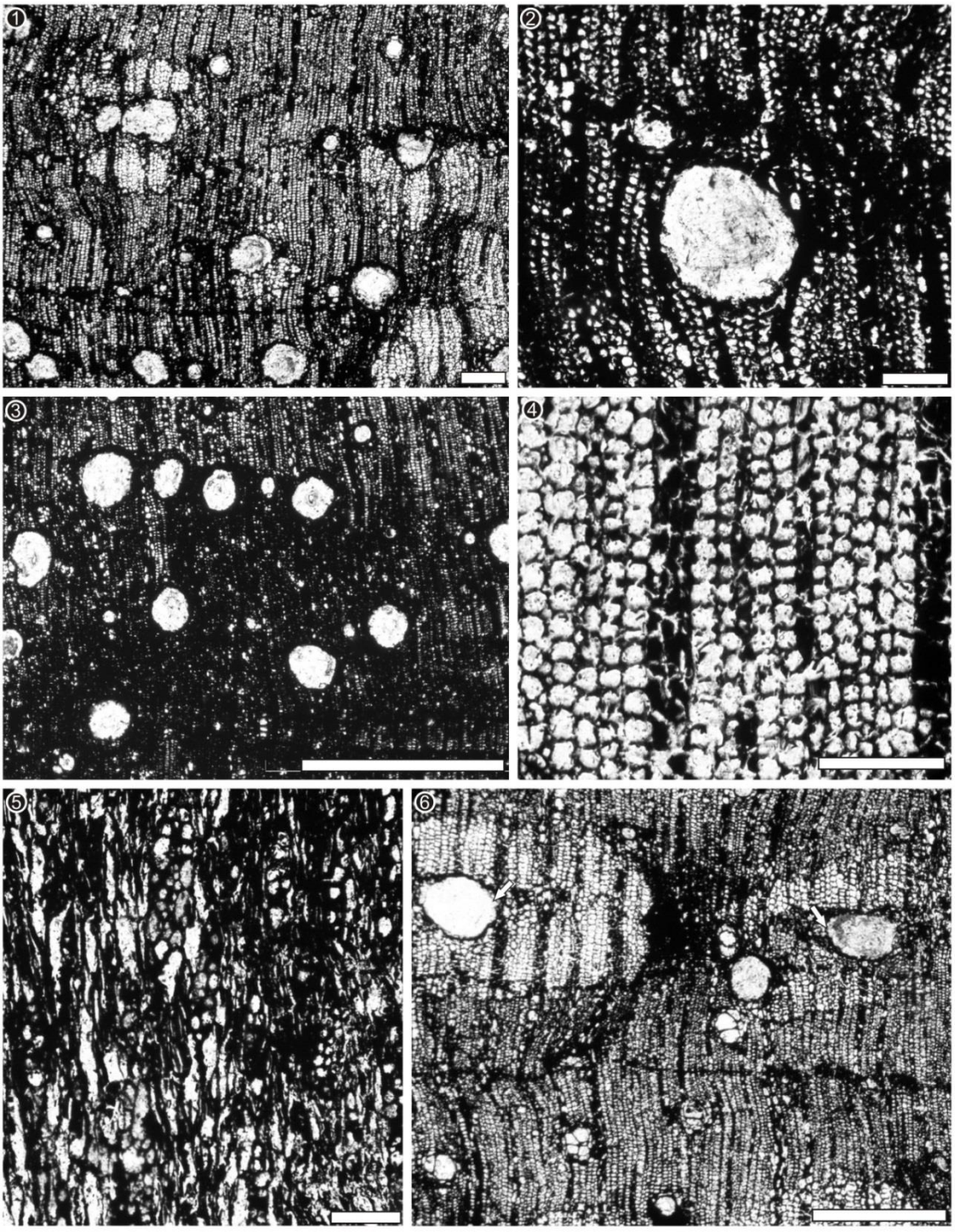

Plate 6.5

6.4. FOSSIL WOOD TYPE 7

Order: Malvales Berchtold & J. Presl.

Family: Malvaceae Jussieu

Material: STRI 15371, STRI 15519, STRI 14193

Repository: Center for Tropical Paleoecology and Archaeology, Smithsonian Tropical Research Institute, Panama.

Locality: Contractors Hill (Gaillard Cut of Panama Canal) near Paraiso, Panama City, Panama (Latitude 09°02’51.75’’N; Longitude 79°39’14.02’’W).

Stratigraphic horizon: ~ 20 m below the top of the Cucaracha Formation (Gaillard Group); Lower Miocene (19 Ma).

6.4.1. Description

IAWA features numbers present: 2, 5, 13, 22, 25, 30, 42, 47, 61, 66, 69, 79, 87, 92, 93, 98, 102, 109, 110, 111, 115, ?144.

Description: Growth rings indistinct; wood diffuse-porous (Plate 6.6, 1); vessels commonly solitary (72 %) or in radial multiples of 2 –3 (Plate 6.6, 2, 3); vessel outline circular (Plate 6.6, 2); perforation plates simple (Plate 6.6, 4); intervessel pits alternate and small (mean 4, SD 1.54 μm, n= 25; range 2 – 8 μm) (Plate 6.6, 5, 6); vessel – ray pitting not well observed due to preservation but probably similar to intervessel pits in size and shape; mean tangential diameter of vessel lumina 115.2 μm ± 37 (n= 25; range 37 – 230); mean vessel density 8.8 per mm^2 (n= 10; range 8 – 10 per mm^2); tyloses absent; vascular tracheids not observed.

Plate 6.6. Fossil Wood Type 7.

1. Growth rings indistinct and wood diffuse-porous. Apotracheal parenchyma reticulate. STRI, 14193 TS, scale: 500 μm.
2. Vessels commonly in radial multiples of 2 – 3. STRI 14193, TS, scale: 500 μm.
3. Vessels commonly in radial multiples of 2 – 3. Vasicentric parenchyma present. STRI 15371, TS, scale: 100 μm.
4. Perforation plates simple. STRI 14193, RLS, 100 μm.
5. Intervessel pitting alternate. STRI 14193, TLS, 100 μm.
6. Close-up of intervessel pitting. STRI 14193, TLS, 100 μm.
7. Fibre pits minutely bordered. STRI 14193, RLS, 100 μm.

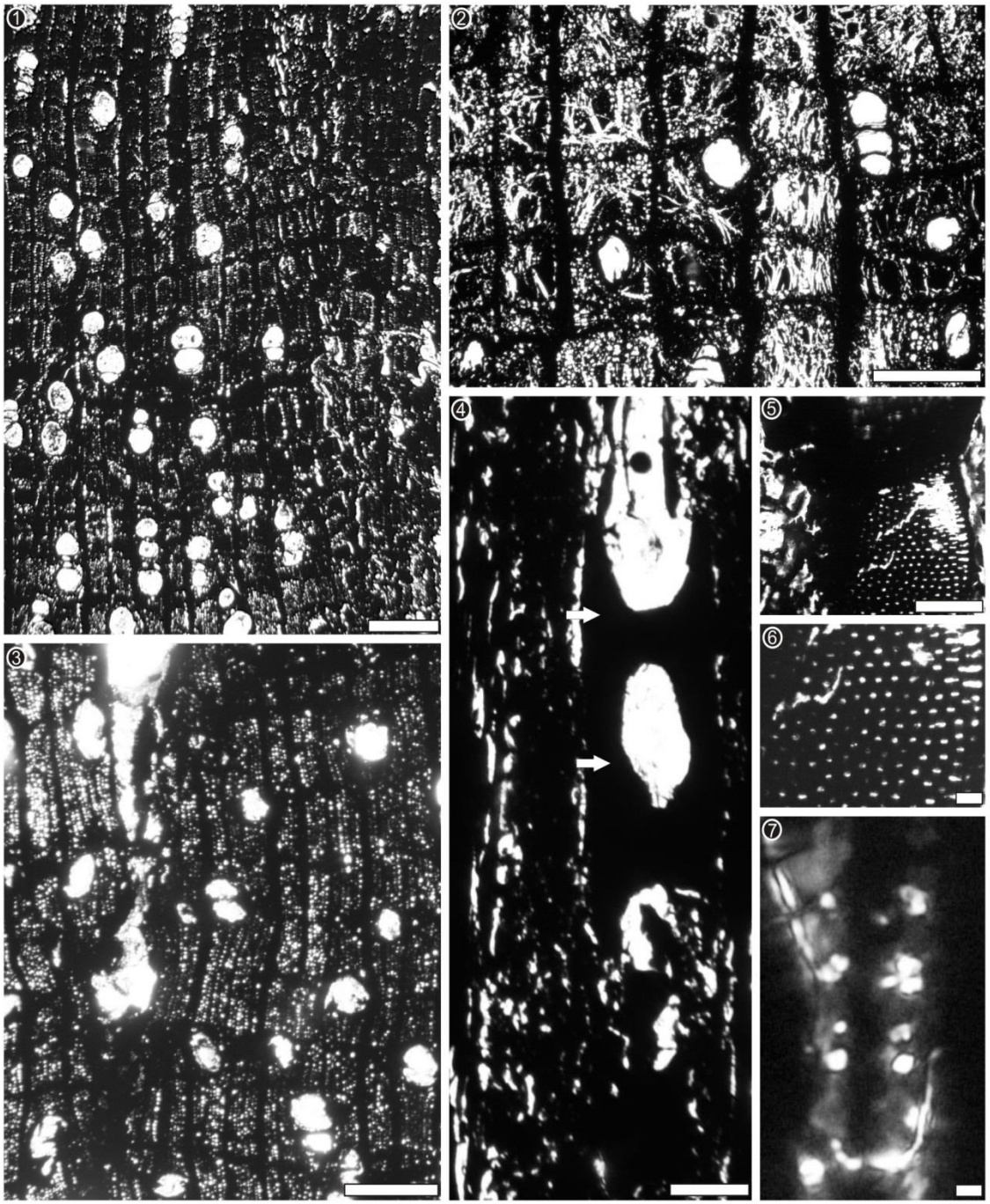

Plate 6.6

Fibres with pits minutely bordered (Plate 6.6, 7), non-septate and thin to thick walled (Plate 6.10, 2, 3).

Axial parenchyma paratracheal vasicentric (Plate 6.6, 3) and apotracheal in a very distinct reticulate pattern (Plate 6.6, 1, 2, 3); a few parenchyma strands can be observed and seem to be 3 – 4 cells in length (Plate 6.7, 1).

Rays heterocellular (Plate 6.7, 2), 4 – 10-seriate (mean 7, SD 3.4, n = 25; range 1 – 15) (Plate 6.7, 3) and commonly > 1 mm (mean 0.7, SD 0.3 mm, n = 25; range 0.2–1.25 mm); rays composed of square, procumbent and upright cells mixed throughout it (Plate 6.7, 2, 4); tile cells of the *Pterospermum* type (Plate 6.7, 2) and prominent sheath cells present (Plate 6.7, 3).

Rhomboidal crystals have not been observed, but druses are probably present (Plate 6.7, 5, 6).

Plate 6.7. Fossil Wood Type 7.

1. Parenchyma strands 3 – 4 cells high. STRI 14193, TLS, 100 μm.
2. Rays composed of square, procumbent and upright cells mixed throughout it. Tile cells of the '*Pterospermum*' type (dotted circles). STRI 14193, RLS, 1mm.
3. Rays heterocellular, 4 – 10-seriate. Sheath cells present (SC). STRI 14193, TLS, 100 μm.
4. Rays composed of square, procumbent and upright cells mixed throughout it. STRI 15519, RLS, 100 μm.
5. Druses in ray cells (arrows). STRI 14193, RLS, 100 μm.
6. Close-up of druses in ray cells (arrows). STRI 14193, RLS, 100 μm.

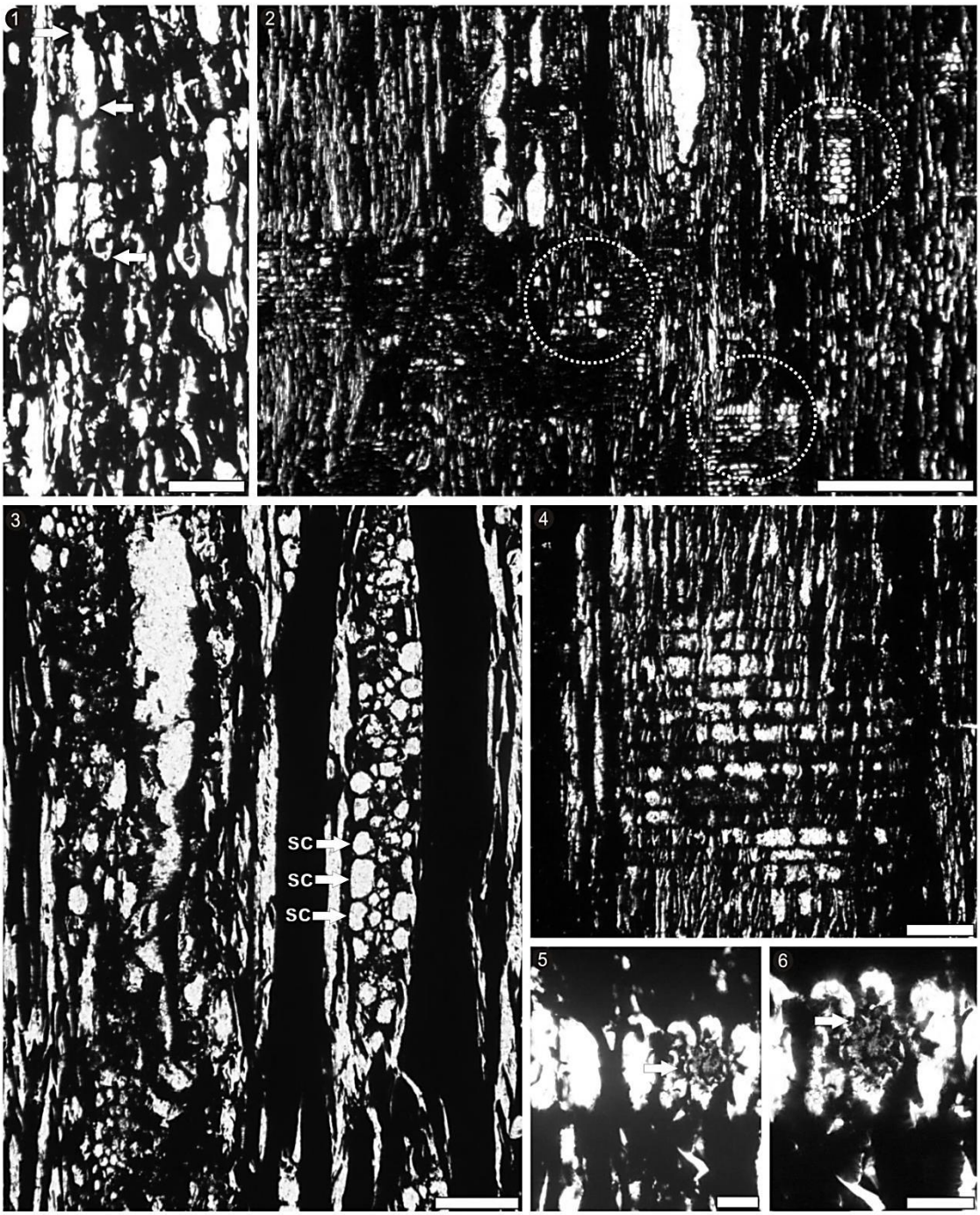

Plate 6.7

6.4.1. Similarities to extant woods

Tile cells are diagnostic for the Malvales order (see Chapter 5 for a full discussion). In that earlier chapter, permineralised woods of Malvaceae were sub-divided into two distinct morphotypes, both with prominent tile cells, but with different patterns of parenchyma distribution: *Guazumaoxylon* showed winged aliform parenchyma and *Periplanetoxylon* showed banded parenchyma. The Malvaceae-type wood in the charcoalified assemblage differs from both of these taxa in showing reticulate parenchyma combined with *Pterospermum*-type tile cells.

Malvaceae with reticulate parenchyma were explored in the IWD and the Kew Gardens collection (see Table 6.1). However, none of the surveyed genera that showed reticulate parenchyma closely resembled the fossil morphotype; hence identification is restricted to a general attribution to the Malvaceae family only. As noted in Chapter 5, only about half of the c. 243 genera of Malvaceae were available for comparison so it is possible that further study (involving analysis of additional collections in North America; Manchester, 2006) might improve this situation.

I note that unpublished palynological studies show that pollen grains related to Malvaceae are particularly abundant in the Cucaracha Formation (Carlos Jaramillo pers. com., 2012).

Species	Subfamily	Source
Bombax lauretense	Bombacoideae	Kew
Ceiba parvifolia	Bombacoideae	IWD
Cistanthera papaverifera	Dombeyoideae	Kew
**Neosogordonia kabingaensis*		
Eriotheca crassa	Bombacoideae	IWD
Heritiera ornitocephala	Sterculioideae	Kew
Huberodendron patinoi	Bombacoideae	Kew
Pachira faroensis	Bombacoideae	IWD
Vasivaea alchorneoides	Grewioideae	IWD

Table 6.1. Malvaceae with reticulate parenchyma and *Pterospermum* type-tile cells studied in the Kew Gardens collection and the Inside Wood Database.

6.5. FOSSIL WOOD TYPE 8

Order: Ericales Dumortier

Family: Sapotaceae Jussieu

Material: STRI 15515

Repository: Center for Tropical Paleoecology and Archaeology, Smithsonian Tropical Research Institute, Panama.

Locality: Centenario Bridge (Gaillard Cut of Panama Canal) near Paraiso, Panama City, Panama (Latitude 09°02’51.75’’N; Longitude 79°39’14.02’’W).

Stratigraphic horizon: ~ 20 m below the top of the Cucaracha Formation (Gaillard Group); Lower Miocene (19 Ma).

6.5.1. Description

IAWA features numbers present: 2, 5, 10, 11, 22, 24, 26, 30, 41, 48, 52, 56, 77, 86, 97.

Description: Growth rings indistinct; wood diffuse-porous (Plate 6.8, 1); vessels grouped in its majority (97%) (Plate 6.8, 1, 4) and with radial multiples until 6 very common (Plate 6.8, 1); perforation plates simple; intervessel pits alternate and minute (mean 3, SD 0.6 μm, n= 25; range 2 – 4 μm) (Plate 6.8, 2, 3); vessel – ray pits rarely observed but presumably similar to intervessel pits in size according to observations; mean tangential diameter of vessel lumina 97 μm (n= 25; range 50 – 160), after correction for shrinkage (Mean = 144 μm; total range= 75 – 239 μm) ; mean vessel density 22.9 per mm^2 (n= 10; range 11 – 35 per mm^2); tyloses abundant (Plate 6.8, 6); vascular tracheids not observed.

Fibres are very difficult to observe in TS and TLS.

Axial parenchyma apotracheal in narrow bands or lines up to three cells wide and some diffuse parenchyma also present (Plate 6.8, 4); parenchyma strands not measured nor clearly observed.

Because of the very poor resolution in the TLS view, rays width and length were estimated assuming the spatial limit of each one. We are well aware these values are

rough estimations, but it also helps giving a broad range for the rays dimensions in the comparison with modern woods. The rays are probably heterocellular and 1 – 3-seriate in its majority (mean 2.2) (Plate 6.8, 5) and commonly < 1 mm (mean 0.24; range 0.2 – 0.2). Mean ray spacing is 5 per mm.

Plate 6.8. Fossil Wood Type 8

1. Growth rings indistinct; wood diffuse-porous. Vessels grouped in a 97% and with radial multiples up to 6 vessels. STRI 15515, TS, scale 500 µm.
2. Intervessel pitting alternate (IVP). STRI 15515, TLS, scale 100 µm.
3. Intervessel pitting alternate (IVP). STRI 15515, TLS, scale 100 µm.
4. Axial parenchyma apotracheal in narrow bands or lines up to three cells wide and some diffuse parenchyma also present. STRI 15515, TS, scale 100 µm.
5. Rays probably heterocellular and 1 – 3-seriate in its majority. STRI 15515, TLS, scale 100 µm.
6. Tyloses abundant (arrows). STRI 15515, TLS, scale 100 µm.

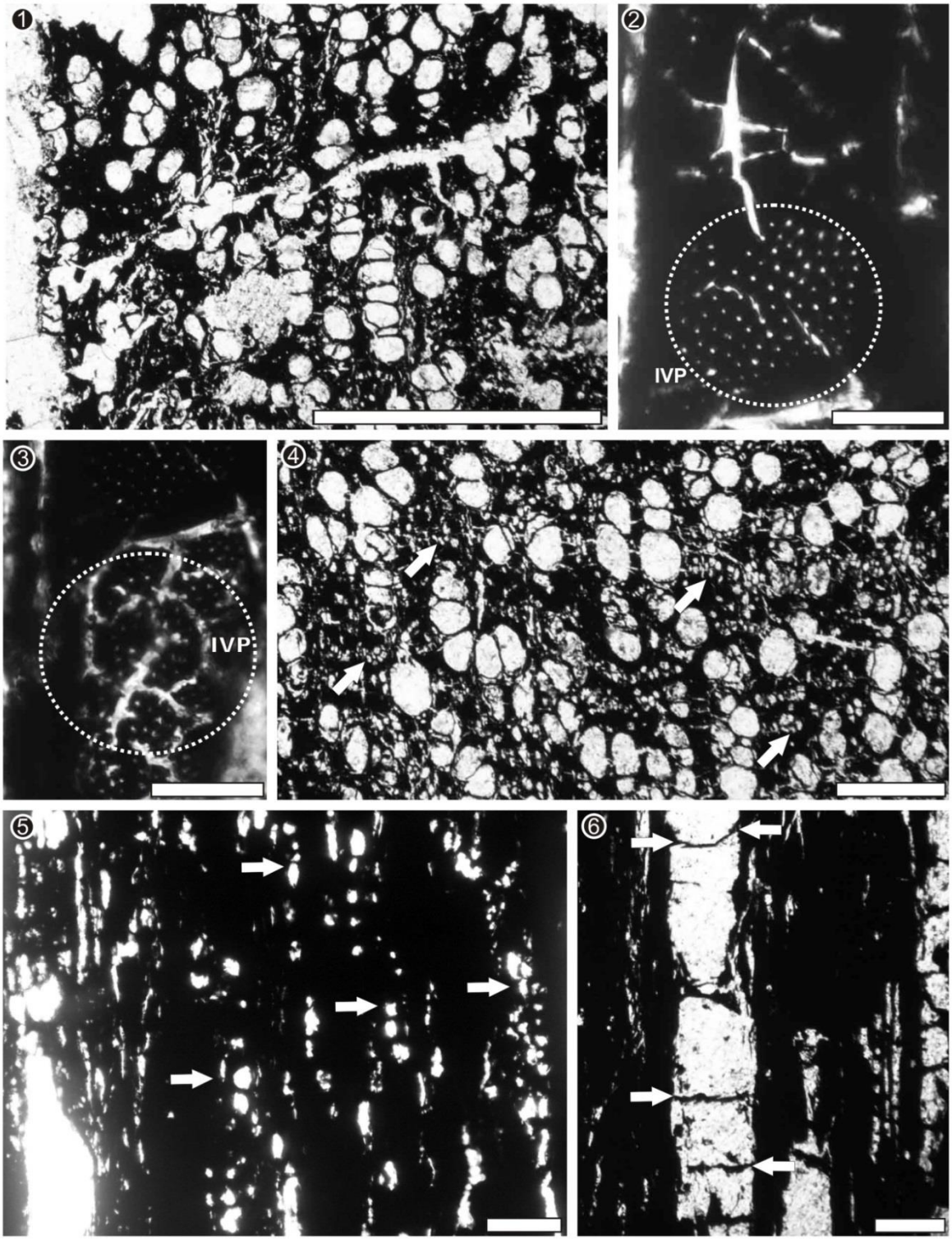

Plate 6.8

6.5.2. Similarities to extant woods

As already noted and shown in images, this morphotype is difficult to observe in the TLS and RLS, which makes its IWD codification challenging. Despite this, it is clear that this specimen is unique in the Panama Canal flora. There is no other fossil wood covered in the present thesis that exhibits such a combination of characters: relatively small vessels, almost all grouped and mostly in radial multiples, with narrow bands of parenchyma and very abundant tyloses that can be readily observed in the TLS. With a few features were certain, I made a search in IWD using the next features: 2p, 5p, 10p 11p, 13p, 56p, 86p. The search produced results almost exclusively for the family Sapotaceae, except for a Lauraceae, *Dehaasia* sp, that was excluded because of the presence of two distinct sizes of vessels and abundant paratracheal parenchyma that does not seem to be present in the fossil. Therefore, the distinctive combination of features in the fossil is characteristic of the Sapotaceae. After a review of this family, with the descriptions and images available in the IWD and the specimens in the Royal Botanic Gardens Kew, the highest frequency of the above features is observed in the species *Manilkara zapota* L., *Manilkara bidentata* (A.D.C.) A. Chev. and *Autranella congolensis* (De Wild.) A. Chev. (Plate 6.9), and in fact, in most of the surveyed Sapotaceae, to some degree. Some features that are common in the Sapotaceae are next listed: growth rings indistinct, diffuse porous wood, vessels arranged in long radial multiples, fibres non septate and with very thick walls, and rays 1 – 3-seriate. Among the surveyed genera, *Manilkara* shows the closest resemblance to the fossil but, because of the limited observation of features in the longitudinal sections, it is not possible to attribute the fossil with certainty to this genus. However, the identification to Sapotaceae is very well supported in general.

Plate 6.9 . Sapotaceae. *Manilkara zapota* (L.) P. Royen (Kew 415); *Autranella congolensis* D. Wild. (Kew 6797); *Manilkara bidentata* A. DC. (AC DECHEN, Trinidad & Tobago)

1. Vessels grouped in a 97% or more. Axial parenchyma apotracheal in narrow bands or lines up to three cells wide (arrows). *M. zapota*, TS, scale: 100 μm.
2. Tyloses common (arrows). *M. zapota*, TS, scale: 200 μm.
3. Intervessel pitting alternate (IVP). *M. zapota*, TLS, scale: 20 μm.
4. Rays composed of procumbent, square and upright cells mixed throughout the body. *M. zapota*, RLS, scale: 100 μm.
5. Vessel groupings common. *A. congolensis*, TS, scale: 100 μm.
6. Rays 1 – 3-seriate. Tyloses common. *A. congolensis*, TS, scale: 200 μm.
7. Vessel groupings common. Parenchyma in narrow bands 1 – 3 cells wide. *M. bidentata*, TS, 200 μm.
8. Rays 1 – 3-seriate. Tyloses common. *M. bidentata*, TLS, 200 μm.

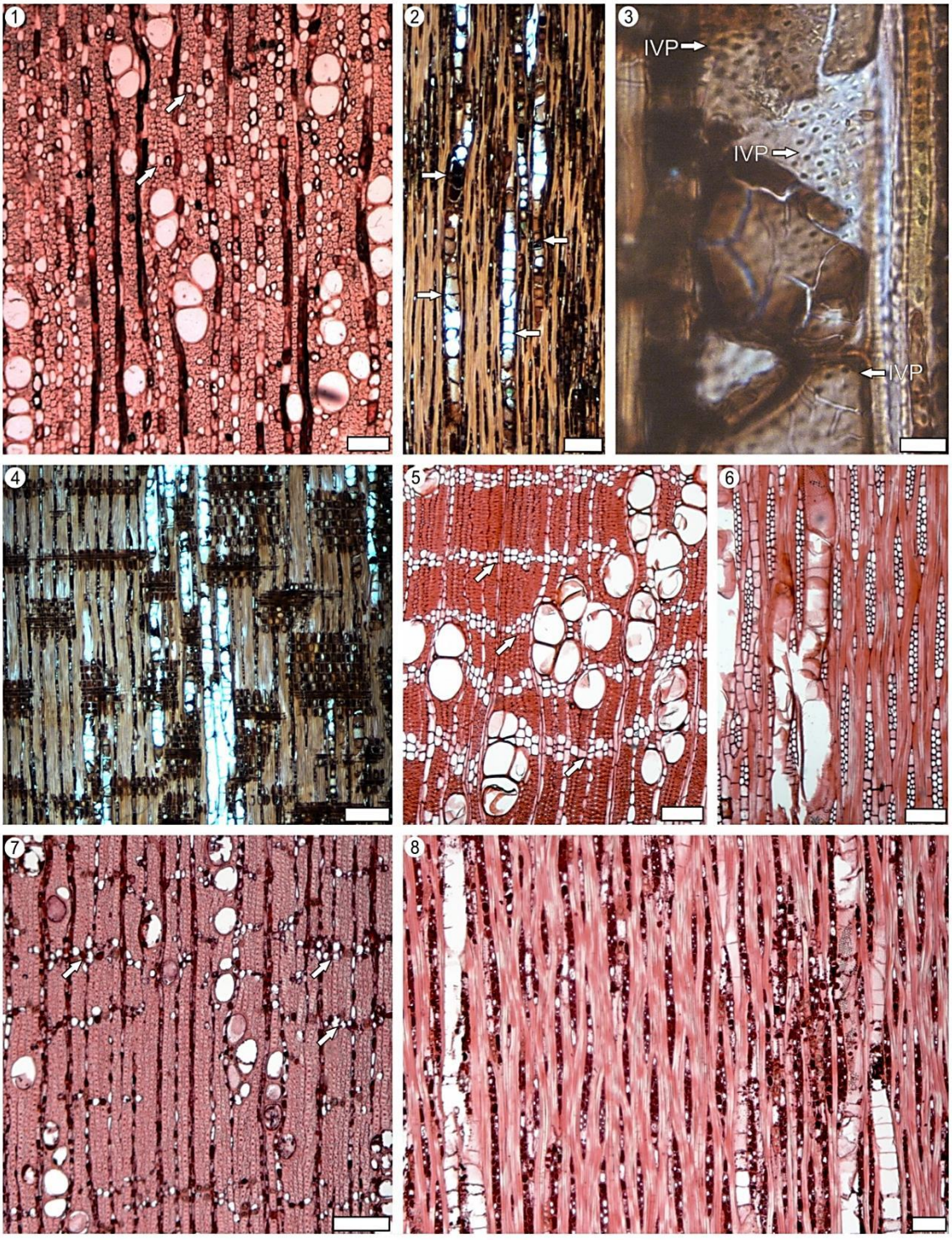

Plate 6.9

Sapotaceae are an important component in rain forests in all tropical regions (Bartish et al., 2010) and *Manilkara* is one of the common elements of the extant flora in rainforests of Central Panama.

6.5.3. Sapotaceae fossil woods

Much of the diversification of the Sapotaceae is considered to be Neogene in age (Bartish et al., 2010; Stevens, 2013). This premise is consistent with an abundant fossil record of woods concentrated in the Miocene and Pliocene all over the world with greater abundance in Europe and Asia. Reports from Europe include *Bassia* (Navale, 1973), *Bumelioxylon holleisii* (Selmeier, 1991; Gottwald, 2004), *Chrysophylloxylon reticulatum* (Awasthi, 1975), *Manilkarioxylon bohemicum* (Petrescu, 1978), and *Palaeosideroxylon densiporosum* (Petrescu, 1978). Reports in Asia include *Chrysophylloxylon pondicherriense* (Awasthi, 1975), *Madhuca palaeolongifolia* (Awasthi and Mehrotra, 1993), *Manilkara cacharense* (Awasthi and Mehrotra, 1993), *Mimusops* (Navale, 1971), *Sapotoxylon prepayena* (Awasthi and Srivastava, 1989). Reports from Africa include *Chrysophyllum zairense* (Bande et al., 1987), *Sapotoxylon aethiopicum* (Lemoigne, Beauchamp and Samuel, 1974), *Sapotoxylon lecomtedoxoides* (Lemoigne, 1978), *Sapotoxylon* sp. (Wheeler et al., 2007).

The reports of Sapotaceae in South America are scarce compared to those in Europe, but this could be due to the lack of studies in certain regions. A key fossil is *Psilatricolporites maculosus*, a pollen species known from the Paleocene/Eocene (c. 55 Ma) in the Maracaibo Basin of Venezuela and from the Early Eocene in Colombia (Lorente, 1986; Jaramillo and Dilcher, 2001) and that represents the oldest reported representative of the Chrysophylloideae in the Neotropics. Only a single report of fossil

Sapotaceae wood has been done from South America, *Manilkaroxylon diluviale* (Hoffman, 1948), but later considered as invalid according to Grambast and Fessard (1968) and no further reports can be found in the literature.

6.6. FOSSIL WOOD TYPE 9

Order: Myrtales Reichenbach

Family: ?Melastomataceae Jussieu

Material: STRI 13691

Repository: Center for Tropical Paleoecology and Archaeology, Smithsonian Tropical Research Institute, Panama.

Locality: Contractors Hill (Gaillard Cut of Panama Canal) near Paraiso, Panama City, Panama (Latitude 09°02’51.75’’N; Longitude 79°39’14.02’’W).

Stratigraphic horizon: ~ 20 m below the top of the Cucaracha Formation (Gaillard Group); Lower Miocene (19 Ma).

6.6.1. Description

IAWA features numbers present: 2, 5, 9, 13, 22, 23, 26, 30, 42, 47, 66, 69, 80, 96, 115.

Description: Growth rings indistinct; wood diffuse-porous (Plate 6.10, 1); vessels commonly solitary (93 %) (Plate 6.10, 1); perforation plates simple (Plate 6.10, 2); intervessel pits alternate, polygonal and small (mean 9, SD 1.5 μm, n= 25; range 3 –

15 μm) (Plate 6.10, 3, 4); vessel – ray similar to intervessel pits in size and shape (mean 4, SD 1.3 μm, n= 25; range 2 – 7 μm) (Plate 6.10, 5); mean tangential diameter of vessel lumina 120 μm (n= 25; range 69 – 179); mean vessel density 4.4 per mm^2 (n= 10; range3 – 7 per mm^2); tyloses absent; vascular tracheids not observed.

Fibres thin to thick walled (Plate 6.10, 6) and not clearly observed in TLS, but probably non septate.

Axial parenchyma paratracheal winged-aliform (Plate 6.10, 6); parenchyma strands not measured or clearly observed.

Rays homocellular and exclusively uniseriate (Plate 6.10, 7) and commonly < 1 mm. Some rays composed by excusively procumbent cells and others by square cells (Plate 6.12, 8).

Plate 6.10. Fossil Wood Type 9.

1. Growth rings indistinct, wood diffuse-porous, vessels exclusively solitary (90% or more). STRI 13691, TS, scale: 100 µm.
2. Perforation plate simple. STRI 13691, RLS, scale: 100 µm.
3. Intervessel pitting alternate. STRI 13691, TLS, scale: 50 µm.
4. Intervessel pits polygonal shaped (circle). STRI 13691, TLS, scale: 50 µm.
5. Vessel– ray pitting (VRP) similar to intervessel pits. STRI 13691, RLS, 50 µm.
6. Fibres thin-to-thick walled. Parenchyma paratracheal winged-aliform. STRI 13691, TS, 100 µm.
7. Rays exclusively uniseriate. STRI 13691, TLS, 100 µm.
8. Rays homocellular (circle). STRI 13691, RLS, 100 µm.

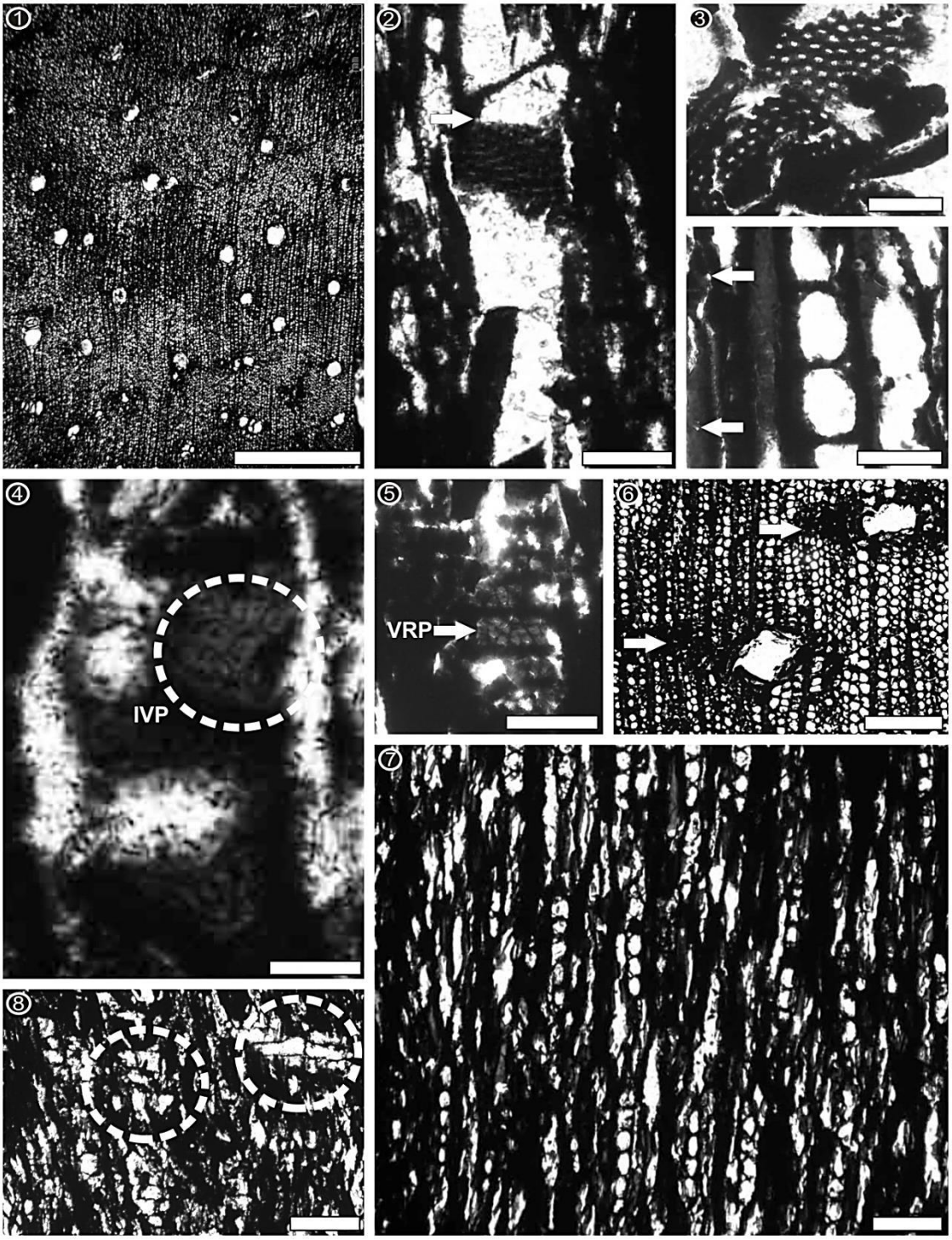

Plate 6.10

6.6.2. Comparison with extant woods

A search was conducted in the IWD with this suite of characters: growth rings indistinct (2p), wood diffuse porous (5p), vessels exclusively solitary (9p), perforation plates simple (13p), intervessel pits alternate (22p) and polygonal (23p), vessel-ray pits similar to intervessel pits (30p), axial parenchyma aliform (80p), rays exclusively uniseriate (96p). The results suggested the following diverse families: Asteropeiaceae (*Asteropeia rhopaloides* Baill.), Celastraceae (*Salacia reticulata*), (Combretaceae (*Combretum collinum* Fressen. ex. DC., *Combretum glutinosum* Perr., *Combretum micranthum* G. Don, *Combretum molle* R. Br. ex G. Don, *Combretum nigricans* Leprieur ex Guill & Perr.), Dipterocarpaceae (*Marquesia excelsa* R.E. Fries), Melastomataceae (*Mouriri huberi* Cogn.), Polygalaceae (*Carpolobia alba* G. Don, *Xanthophyllum* sp.) and Rubiaceae (*Kutchubaea palustris* Ducke). A survey was undertaken with available images and descriptions from the IWD and microscopic slides from the Kew Gadens collection.

Asteropeia woods are unlikely to be related to the morphotype described herein, because of a distinct unilateral paratracheal parenchyma, that is not observed in the fossils (based on examination of images in the IWD). *Combretum* and *Terminalia,* two largely tropical genera, were also surveyed. STRI 13691 differs from species of *Terminalia* in that the latter shows a predominance of vessel grouping. The genus *Combretum* differs from the fossil in its confluent bands of parenchyma, as well as included phloem that, although not present in all the species, occurs in most of them. The remaing results from the initial IWD search include dipterocarps, which usually have axial canals combined with tile cells in some of the genera. Another potential match, *Carpolobia*, has palisade and/or gash-like vessel–ray pits, parenchyma distinctly aliform and diffuse in aggregates and highly heterocellular rays, all features that are

absent in the fossil. *Kutchubaea* has distinct bands of scalariform parenchyma that contrast with the aliform parenchyma in this fossil morphotype.

The best match found from this initial search in the IWD is *Mouriri completens*, a member of Melastomataceae. Unfortunately, there were not microscopic slides available for comparison at Kew, thus a rough comparison was established based on images from the IWD. A few qualitative characters that can be coded from those images are shared with the fossil wood presented here as follows: growth rings indistinct, wood diffuse porous, vessels exclusively solitary (90% or more), simple perforation plates, intervessel pitting alternate, parenchyma predominantly winged-aliform, and rays exclusively uniseriate. However, I highlight that the seven species of *Mouriri* coded in the IWD have included phloem, which is not observed in the fossil.

A general revision of the Melastomataceae samples available in the Kew Botanic Gardens was then undertaken in order to make a more detailed comparison. A few other characters that are shared with the fossils were recognised, such as: vessel–ray pitting similar to intervessel pitting, and short homocellular rays (Plate 6.11). During this survey, other important features commonly observed were septate fibres and vestured pits; however it is not possible to confirm their occurrence in the fossils due to the opaque nature of the charcoalified material. Probably *Mouriri* cannot be confirmed as the genus matching this morphotype; however it is legitimate to propose a strong similarity to some Melastomataceae. Plate 6.11offers examples found in the Jodrell Laboratory collection to illustrate these views.

Plate 6.11. Melastomataceae. *Pachyanthus cubensis* A. Rich (Kew 22061); *Conostegia chiriquensis* Gleason (W-15587); *Miconia darienensis* Pittier (W-76); *Pachyanthus pedicellatus* Urb.; *Tetrazygia ellegans* .

1. Growth rings indistinct, wood diffuse-porous, vessels exclusively solitary (90% or more). *P. cubensis*, TS, scale: 200 µm.
2. Intervessel pitting alternate, polygonal (IVP). *C. chiriquensis*, TLS, scale: 20 µm.
3. Detail of intervessel pits shaped (circle). *C. chiriquensis*, TLS, scale: 40 µm.
4. Vessel– ray pitting similar to intervessel pits. *M. dareniensis*, RLS, scale: 20 µm.
5. Rays exclusively uniseriate. *P. cubensis*, TLS, scale: 100 µm.
6. Rays homocellular. *P. cubensis*, RLS, scale: 100 µm.
7. Growth rings indistinct, wood diffuse-porous. *P. pedicellatus*, TS, scale: 200 µm.
8. Growth rings indistinct, wood diffuse-porous. *T. ellegans*, TS, scale: 100 µm.
9. Rays exclusively uniseriate. *T. ellegans*, TLS, scale: 50 µm.

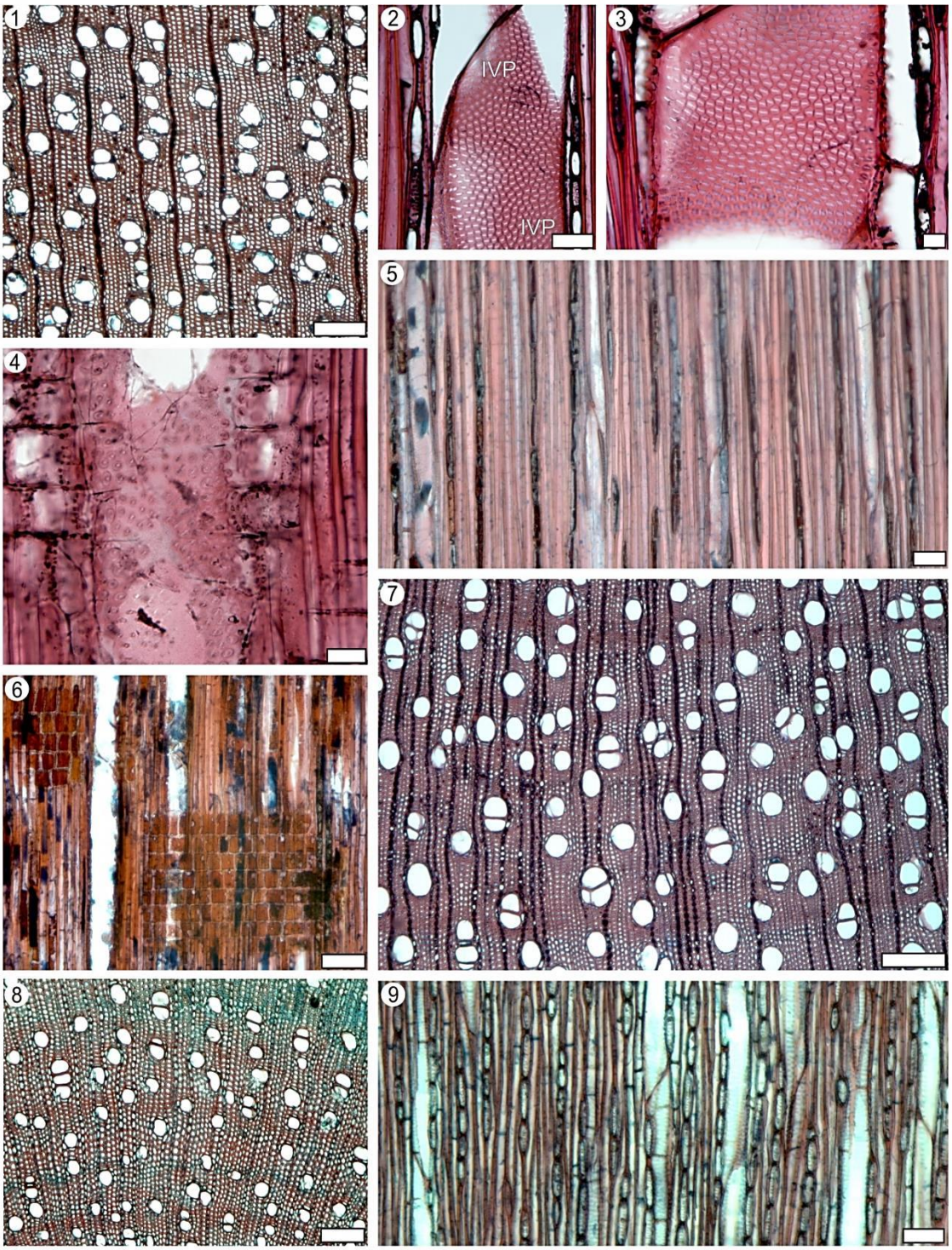

Plate 6.11

6.7. FOSSIL WOOD TYPE 10

Family: Meliaceae Jussieu

Genus: *?Guarea* Kunth

Material: STRI 15364, STRI 15367, STRI 15514.

Repository: Center for Tropical Paleoecology and Archaeology, Smithsonian Tropical Research Institute, Panama.

Locality: Contractors Hill (Gaillard Cut of Panama Canal) near Paraiso, Panama City, Panama (Latitude 09°02’51.75’’N; Longitude 79°39’14.02’’W).

Stratigraphic horizon: ~ 20 m below the top of the Cucaracha Formation (Gaillard Group); Lower Miocene (19 Ma).

6.5.1. Description

IAWA features numbers present: 2, 5, 10, 13, 22, 41, 48, ?61, 66, 69, 85, 86, 97, 109, 115.

Description: Growth rings indistinct; wood diffuse-porous (Plate 6.12, 1); vessels commonly solitary (76 – 78 %) or in radial multiples of 4 (– 6) (Plate 6.12, 1, 2); vessel outline oval (Plate 6.12, 2); perforation plates simple (Plate 6.12, 3; Plate 6.13, 1); intervessel pits alternate (Plate 6.13, 2); vessel – ray pits not clearly observed; mean tangential vessel diameter range 45 – 71 μm (n = 75; total range 23 – 95 μm); mean vessel density range 26 – 39 per mm^2 (n = 30; total range 15 – 50 per mm^2) (Plate 6.12, 1, 2); tyloses absent; vascular tracheids not observed.

Plate 6.12. Fossil Wood Type 10.

1. Growth rings indistinct and wood diffuse-porous. Mean vessel density range 25.9 – 39 per mm^2. STRI 15364, TS, scale: 500 μm
2. Vessels commonly in radial multiples of 4 (– 6). Mean vessel density range 25.9 – 39 per mm^2. STRI 15364, TS, scale: 100 μm
3. Perforation plates simple (arrow). STRI 15367, RLS, scale: 100 μm.
4. Close-up of fibres thin to thick walled. STRI 15367, scale: 100 μm.
5. Axial parenchyma paratracheal in bands 2 – 4 cells wide. STRI 15514, TS, scale: 100 μm.
6. Rays 1 – 3-seriate. STRI 15634, TLS, scale 100 μm.
7. Composition of rays. STRI 15367, RLS, scale: 100 μm.

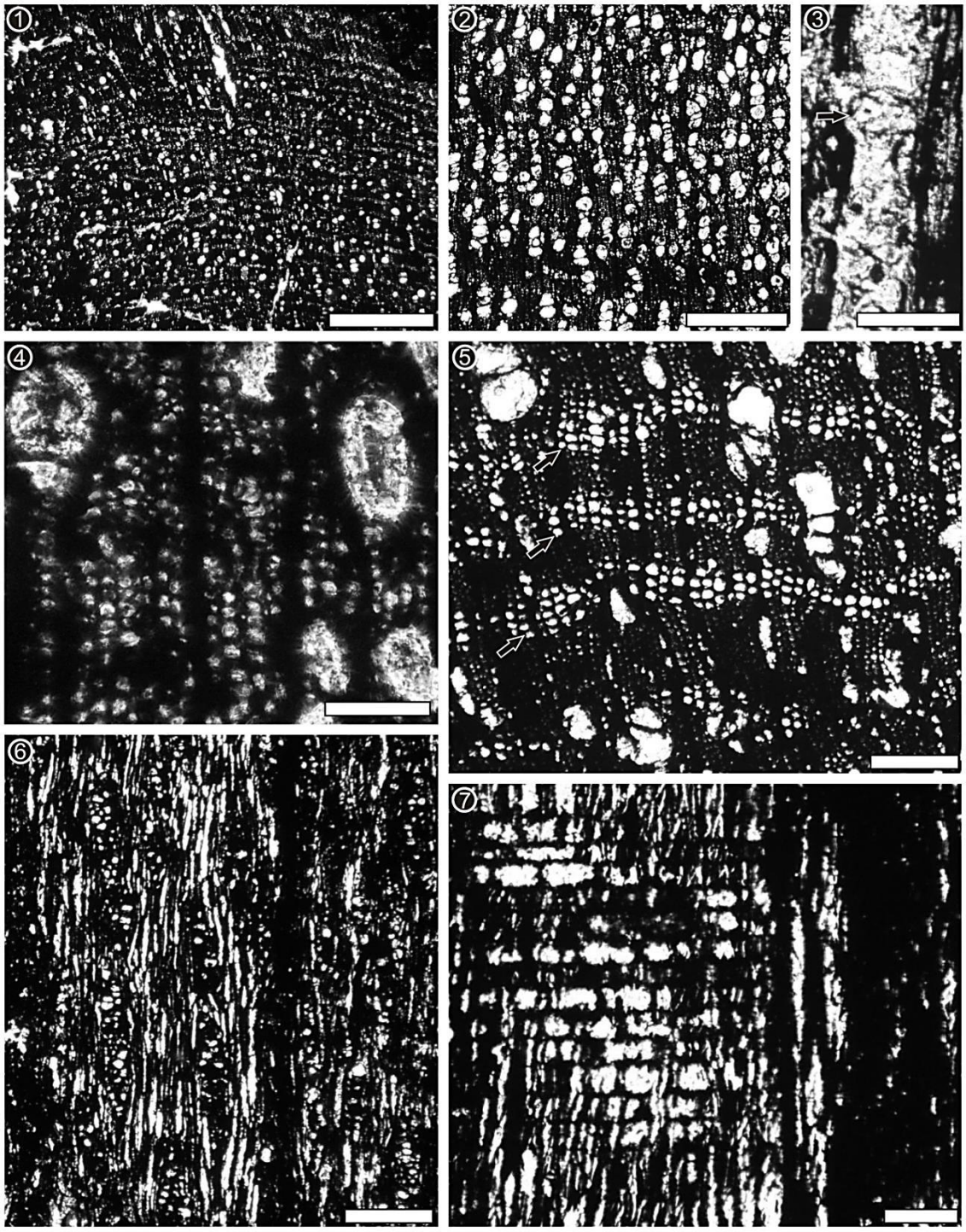

Plate 6.12

Plate 6.13. SEM images of Fossil Wood Type 10.

1. Perforation plates simple (arrows). STRI 15514, TLS, scale: 50 μm
2. Intervessel pitting alternate (IVP). STRI 15514, TLS, scale: 50 μm.
3. Rays composed of procumbent (PC), square (SC) and upright cells (UC) mixed throughout the body. STRI 15514, RLS, scale: 50 μm.

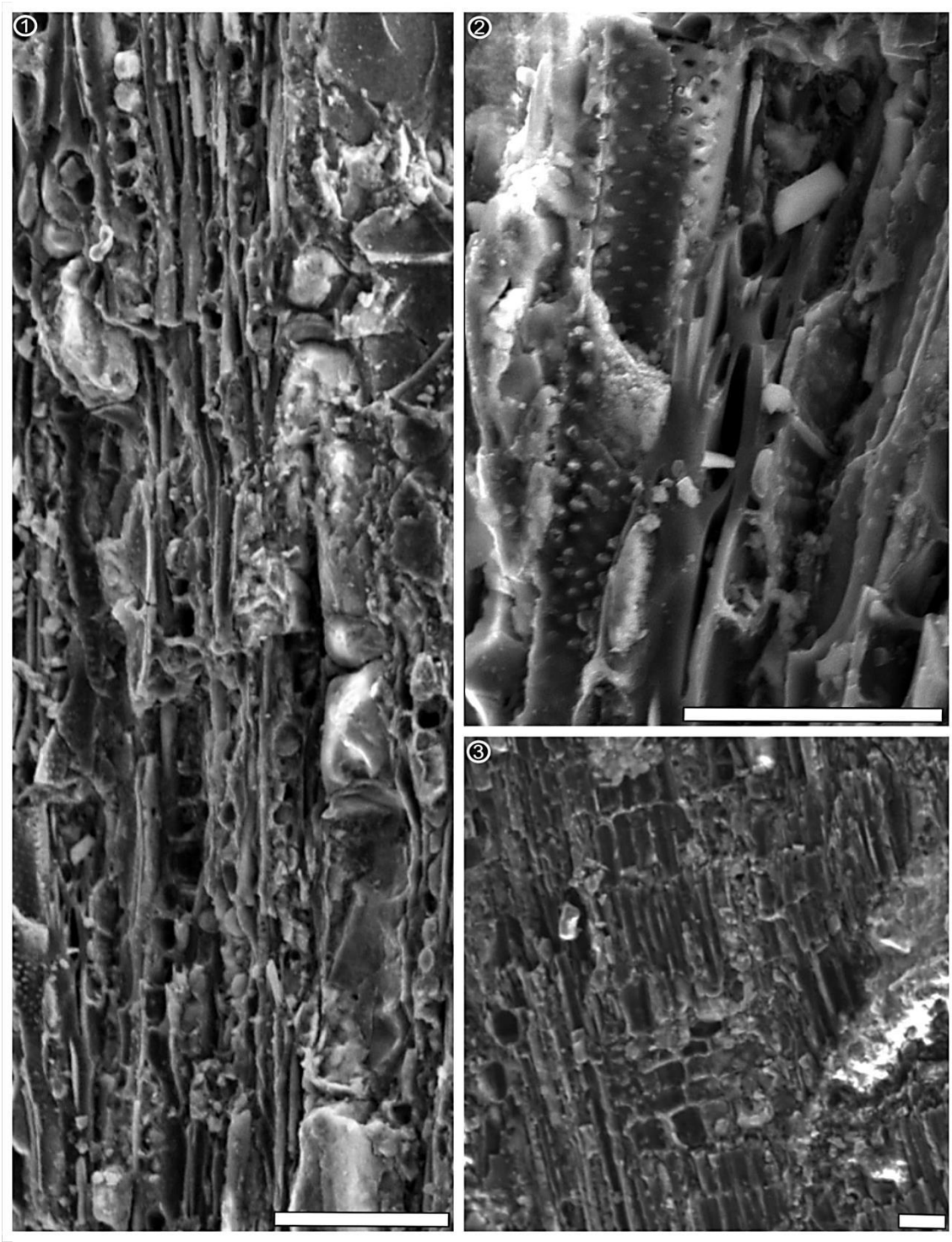

Plate 6.13

Fibres mostly thin- to thick-walled (Plate 6.1, 4). Fibres not clearly observed in tangential view due to preservation, but probably non-septate.

Axial parenchyma in bands 2 – 6 cells wide (Plate 6.12, 5; Plate 6.13, 1); axial parenchyma strands poorly preserved and not measured.

Rays heterocellular, 1 – 3 (– 4)-seriate (mean 2.6 ± 0.6, n = 25) (Plate 6.12, 6; Plate 6.13, 1) and commonly < 1 mm (mean 0.2, SD 0.05 mm, n = 25; range 0.2 – 0.3 mm); rays composed of procumbent, square and upright cells mixed throughout the body (Plate 6.1, 7; Plate 6.2, 3); mean ray spacing 12.8 ± 1.2 per mm, n = 15; range 11 – 15 per mm).

Note: SEM images were not entirely satisfactory but they allowed the observation and confirmation of simple perforation plates and intervessel pitting alternate (Plate 6.13).

6.5.2. Comparison with extant woods

This morphotype contains woods with the smallest vessels and the highest vessel density of all of the studied woods from the Panama Canal, even when a 33% contraction coefficient due to charcoalification is taken into account (Falcon-Lang et al., 2012). After correction for charring, the mean tangential diameter of vessels in the range of 68 – 106 μm (total range= 34 –141 μm). The vessel density was also corrected using 25% in the radial face and 33% in the tangential face, thus the non-charred vessel density of this specimen is presumably 12.95 – 19.5 vessels/mm^2.

A search in the IWD for 2p, 5p, 10p, 13p, 22p, 43a, 49a, 50a, 85p, and 97p gave results in the next listed families: Acanthaceae Jussieu (*Avicennia germinans* L.,

Avicennia marina Forssk.), Apocynaceae (*Alstonia verticillosa* F. Muell, *Cerbera manghas* L.), Lauraceae (*Alseodaphne sp*) Leguminosae (*Bauhinia malabarica* Roxb., *Bauhinia rufescens* Lam., *Philenoptera eriocalyx* (Harms) Schrire), Meliaceae (*Syonum glandulosum* (Sm.) Juss.), Rubiaceae (*Gaertnera paniculata* Benth., *Gaertnera sp, Morinda germinata* DC), Rutaceae (*Casimiroa claderoniae* f. Chiang & Medrano) and Sapotaceae (*Pouteria gardneriana* Raldk) and Solanaceae *Nothocestrum breviflorum* A. Gray). Two quantitative characters were included in this search (vessel density and mean vessel diameter); although not to be recommended this was done due to the lack of certainty in the coding of other qualitative features and because these seem to be important in this morphotype. *A. germinans* and *A. marina* possess included phloem and vessels arranged diagonally, characters absent in this fossil type. The Apocynaceae were excluded because of predominant uniseriate rays, long radial multiples and common laticifers that are absent in the fossils. Both of the Fabaceae from the results of IWD are ruled out, because the species of *Bauhinia* and *Philenoptera* frequently have storied rays. *Casimiroa* woods have helical thickenings and homocellular rays, characters absent in the fossil compared herein. Another suggestion from IWD that can be ruled out is *Gaertnera* has rays in two distinct sizes. *Pouteria gardneriana* has distinct vessels arranged in diagonal pattern, another trait that is absent in these fossils. The only suggestion from the IWD that has enough similar traits to the fossil is the Meliaceae. Therefore, I conducted further revision focused on that family.

On the revision of key literature of woods in the tropics (e.g., Detiénne and Jacquet, 1983), there was one genus with considerable resemblance to these fossil woods, *Guarea* F. Allam ex. L. (Meliaceae). Some of the common features of the woods of this genus observed in the Kew Gardens collection, the available images in IWD and the literature (White and Gasson, 2000; Detiénne and Jacquet, 1983; Metcalfe

and Chalk., 1950): growth rings indistinct, wood diffuse porous , simple perforation plates, intervessel pitting alternate, vessel-ray pitting similar to intervessel pits in shape and size, mean tangential diameter 100 – 200 µm, septate fibres, paratracheal parenchyma vasicentric and winged-aliform, parenchyma bands more than 3 cells wide, rays 1 –3-seriate and prismatic crystals in parenchyma cells. Most of these features are present in the Fossil Wood Type 8, however, characters such as septate fibres and crystals in parenchyma cells are not possible to confirm in the fossils due to preservation issues. Additionally, *Guarea* commonly possesses medium vessels 100 – 200 µm, whereas these fossil woods tend to have small vessels, even considering shrinkage artifacts during fossilization. Although several characters can not be confirmed for this wood, G*uarea* is the most similar wood found within the available comparative material supported on the characters next listed: growth rings absent, wood diffuse porous, vessels in radial multiples of 2–4 (5), simple perforation plates, alternate intervessel pitting, axial apotracheal parenchyma bands >3 cells wide, rays 1–2(3)-seriate (White and Gasson, 2008; Inside Wood, 2011) (Plate 6.14).

Plate 6.14. Meliaceae. *Guarea thompsonii* Sprague and Hutch (Kew 462); *Guarea excelsa* Kunth (Madison 11051); *Guarea macrophylla* Vahl. (CEPECLO 188).

1. Growth rings indistinct, wood diffuse-porous. Parenchyma banded (arrows).*G. excelsa*, TS, scale: 200 µm.
2. Rays 1– 3-seriate. *G. excelsa*, TLS, scale: 100 µm.
3. Parenchyma with bands >3 cells wide. *G. thompsonii*, TS, scale: 100 µm.
4. Rays 1– 3-seriate. *G. thompsonii*, TLS, scale: 100 µm.
5. Ray composition in *G. thompsonii*. TLS, scale: 200 µm.
6. Parenchyma confluent and with bands >3 cells wide. *G. macrophylla*, TS, scale: 200 µm.
7. Rays 1– 3-seriate. *G. macrophylla*, TLS, scale: 100 µm.

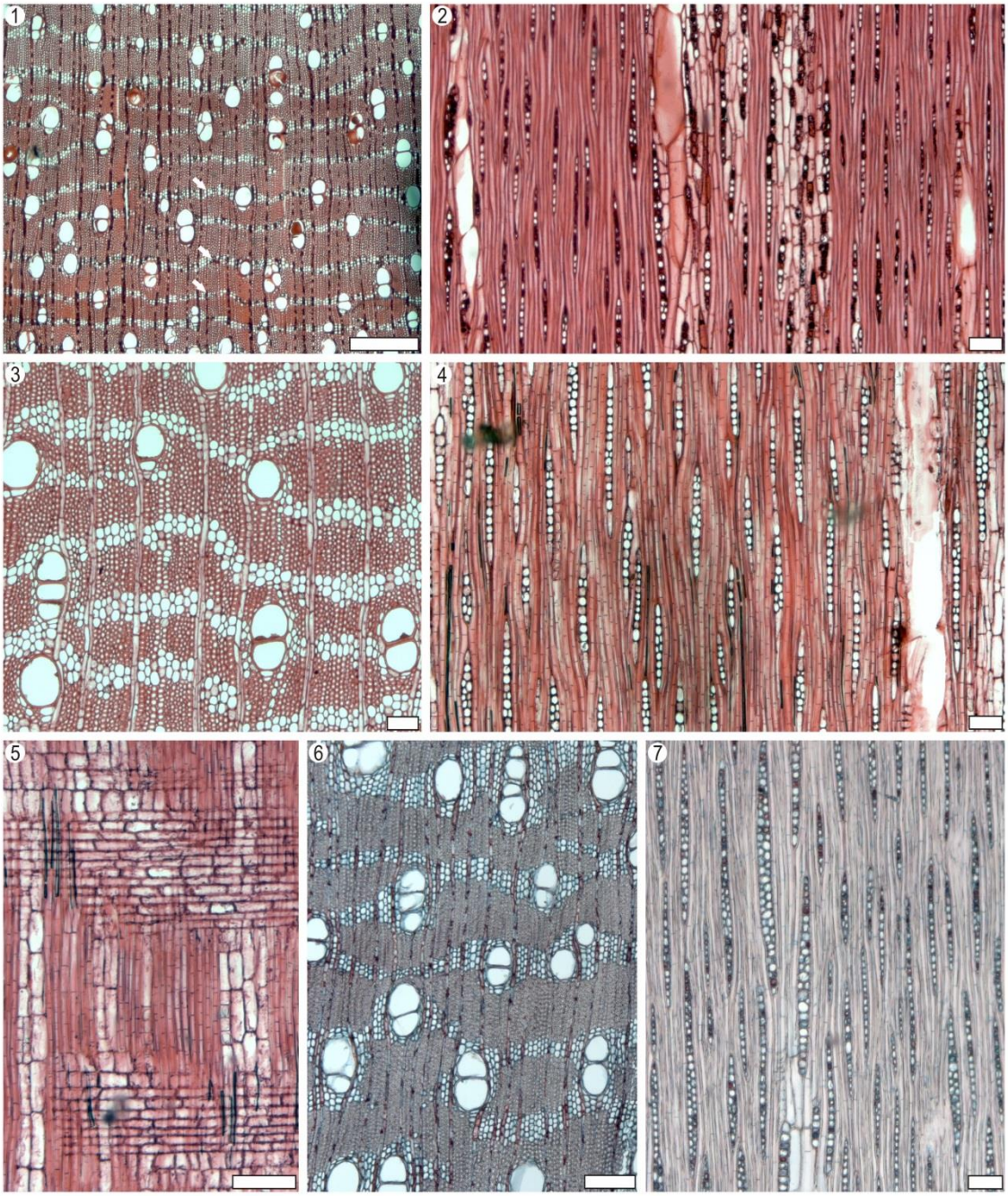

Plate 6.14

6.8. FOSSIL WOOD TYPE 11

Order: Arecales Bromhead

Family: Arecaceae Berchtold et J. Presl

Subfamily: ?Coryphoideae Burnett

Material: STRI 14196**,** STRI 15516, STRI 15517, STRI 15522 . This morphotype comprises four different logs with preserved trunk diameters ranging from 0.12 m to 0.28m. STRI 15516 is the sample with the best preservation, thus the descriptions are mostly based on it.

Repository: Center for Tropical Paleoecology and Archaeology, Smithsonian Tropical Research Institute, Panama.

Locality: Centenario Bridge (Gaillard Cut of Panama Canal) near Paraiso, Panama City, Panama (Latitude 09°02’51.75’’N; Longitude 79°39’14.02’’W).

Stratigraphic horizon: ~ 20 m below the top of the Cucaracha Formation (Gaillard Group); Lower Miocene (19 Ma).

6.8.1. Description

Note: Studies of the stem of palms is in its infancy. The descriptions below were made based on terminology and classification schemes on the Palm-ID website (Thomas, 2011) and other recent key literature (e.g., Thomas and De Franceschi, 2012, 2013).

The central cylinder is delimited from the cortical zone by an increase in the density, and decrease in the diameter, of fibrous vascular bundles. There is no radial

elongation of the fibrous part in the cortical zone. The general stem pattern (Von Mohl classification; Von Mohl, 1845) is *Cocos*-typ, with the density of the fibrous vascular bundles being highly constant (Plate 6.15., 1). The shape of the fibrous part in TS (Stenzel classification; Stenzel, 1904) is reniform with an auricular sinus observable in some of the bundles. There are 2 (3 – 4) vessels per fibre vascular bundle (Plate 6.15., 2, 3, 4). The ground parenchyma is not well preserved, but the cells seem to be spheroid. The fibre vascular bundles have the following mean dimension ranges: H_{max} (total height of fibre vascular bundle) = 0.520– 540 µm, H_{vasc} (height of vascular part)= 110 –140 µm. The mean vessel diameter ranges from 65 – 120 µm. There is one phloem strand in the central zone of the vascular bundles. Vascular bridges are occasionally present and well developed (Plate 6.15., 5).

6.8.2. Similarities to extant plants

The three specimens collected from Centenario Bridge and the one from Contractors Hill present very similar characteristics that would justify including all of them in the same morphotype and, thus, they are interpreted as the same taxon. The preservation of the specimens is relatively poor and there are some features that cannot be described with certainty (e.g., presence/absence of phytoliths, shape of parenchyma).

Plate 6.15. Wood Type 11. Palm trees (Arecaceae)

1. Cocos-Type pattern (vascular bundle density constant from pith to bark. STRI 15516, scale: 1 mm.
2. Close-up of vascular bundles. 2 metaxylem vessels per vascular bundle (arrows). STRI 15516, scale: 500 μm.
3. Close-up of vascular bundles. 2 metaxylem vessels per vascular bundle (arrows). STRI 15522, scale: 500 μm.
4. Fibre vascular bundles with 3 – 4 metaxylem vessels (arrows). STRI 15517, scale: 500 μm.
5. Vascular bridges occasionally present and well developed (arrow). STRI 15522, scale: 500 μm.

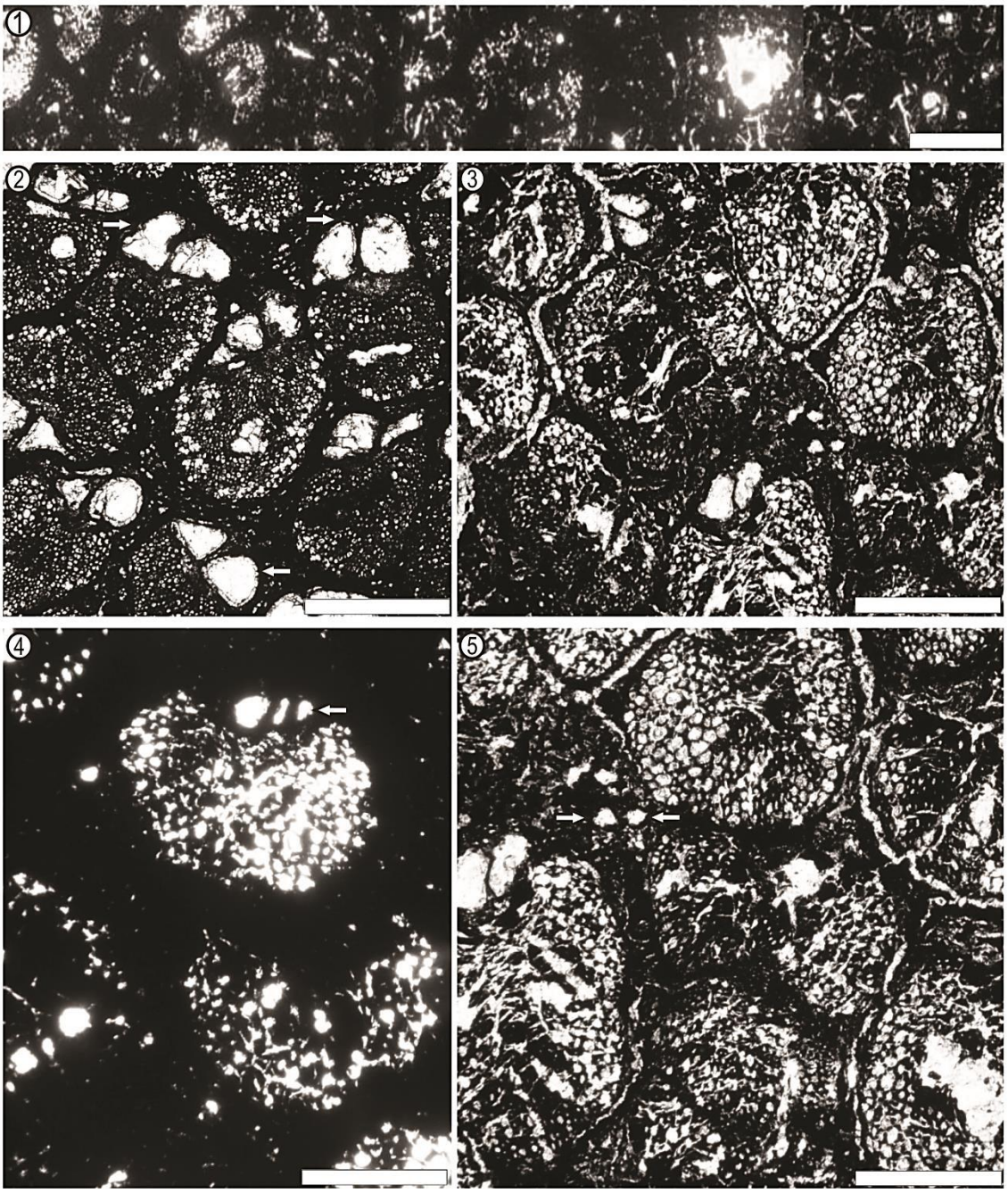

Plate 6.15

The combination of the *Cocos*-type general stem pattern with the lunaria to reniforma fibre vascular bundle with mainly two vessels per bundle is commonly found in the Cryosophileae and some Cocoseae, although the latter tend to have a single vessel element per vascular bundle (Tomlinson, 1961; Tomlinson et al., 2011; Thomas and De Franceschi, 2012). Thomas and De Franceschi (2013) discuss the affinities between one of the numerous *Palmoxylon* species, *Palmoxylon vestitus* and the members of the Cryosophileae tribe (subfamily Coryphoideae) to justify the first evidence of that tribe outside the Americas. Other characters such as spheroidal ground parenchyma, vascular bridges and reniforma-shaped fibre vascular bundles are also common in the newly reported specimens of Cryosophileae (Thomas and De Franceschi, 2012).

I consider there are not enough supporting characters to certainly assign the Panamanian charcoalified palm trees to the Cryosophilae; however, the modern Crysophileae are mainly distributed in Central America and the Antilles with some representatives in South America (e.g., *Tithrinax, Chelyocarpus*). Thus one would expect to find its representatives in the Miocene of Panama and additionally, the characters do suggest affinities with the subfamily Coryphoideae. These palms are adapted to rain forests, but they are mostly found in coastal zones (Thomas and De Franceschi, 2012).

6.8.3. Fossil record of Coryphoideae woods

Fossil palms have been collected at different locations around the world and in rocks as early as in the Cretaceous (Harley, 2006). Accordingly with surveys of the palms fossil record, most of them have been included in the morphotaxon *Palmoxylon*. The record of *Palmoxylon* is quite extensive and the listing of all its putative affinities is

beyond the scope of the present thesis. However, a literature review shows that specimens assigned to Coryphoideae are numerous (for a complete survey of Coryphoid palms see Devore and Pigg, 2010), e.g., *Sabal*-like palms abundantly found in North America (Devore and Pigg, 2010; Wheeler and Manchester, 2002); palm woods related to coryphoid modern taxa such as *Rhapidophyllum* H.Wendl. and Drude, *Brahea* Mart. ex Endl. and *Hyphaene* Gartn are abundant in India, represented by *P. shahpuraensis, P. hyphaenoides, P. licualense* among others.

During the survey of fossil palms, it was noticed that the fossil specimens, reported here from the Panama Canal, have some resemblance to the "Group Reniformia Stenzel" described in El-Saadawi et al. (2004), which includes several woods from the Early Eocene of Egypt and also across Libya, India, Pakistan and United States (El-Saadawi et al., 2004; Nambudiri and Tidwell, 1998; Mahabale and Kulkarni, 1981; Trivedi and Verma, 1972; Tidwell et al., 1973; Sahni, 1964; Stenzel, 1904). The latter woods are considered to be *Corypha*-type (El-Saadawi et al., 2004); thus it gives more support to the assignation of the fossil palms presented herein to the Coryphoideae .

Berry (1918) reported fruits, leaves and wood from several localities in the Panama Canal Zone, including a permineralised palm stem that was retrieved by D.F.MacDonald from the Cucaracha Formation in the Gaillard Cut (presumably from the same localities from where STRI 15685 was collected, but probably from the lower part of the formation). Berry (1918) named it *Palmoxylon palmacites* and described it with this suite of characters: "small, numerous and closely spaced vascular bundles; two metaxylem vessels per vascular bundle ranging 72 – 180 µm in diameter; the phloem portion probably represented by one strand per bundle; and the general stem pattern *Cocos* –type". Berry (1918) only compared his fossils with other specimens of *Palmoxylon* previously identified by Felix in 1883 from different collections from the

Caribbean. Based on Berry (1918)'s descriptions, it is possible that his *Palmoxylon* is the same palm wood type described here; however, the low resolution images provided in Berry's publication hamper comparison and the location of the type material is unknown.

6.9. INDETERMINATE SAMPLE A

Material: STRI 15520

Repository: Center for Tropical Paleoecology and Archaeology, Smithsonian Tropical Research Institute, Panama.

Locality: Centenario Bridge (Gaillard Cut of Panama Canal) near Paraiso, Panama City, Panama (Latitude 09°02'51.75''N; Longitude 79°39'14.02''W).

Stratigraphic horizon: ~ 20 m below the top of the Cucaracha Formation (Gaillard Group); Lower Miocene, (?17 – 15 Ma).

6.9.1. Description

IAWA features numbers present: 2, ?4, 5, 13, 22, 25,? 30, 41, 48, ?66, ?69, 85, 97, 109.

Description: Growth rings indistinct; wood seems to have a tendency to semi-ring porosity (Plate 6.16, 1, 2); vessels solitary (88 %) or in radial multiples of 2 (– 3) (Plate 6.16, 1, 2, 3); no scalariform perforation plates were observed, so probably they are simple; intervessel pitting alternate (Plate 6.16, 4, 5) and small (mean 6, SD 0.5 μm, n =25; range 5 – 6); vessel – ray pitting no observable; mean tangential vessel

diameter 59 μm (n = 50; range 31 – 91 μm), after correction for shrinkage (Mean = 87 μm; range 46 – 135 μm) ; mean vessel density 31 (n = 15; range 25 – 45 per mm^2); tyloses absent; vascular tracheids not observed.

Fibres are difficult to observe and code, but they seem to be very thin-walled to thin- to thick-walled (Plate 6.16, 3).

Axial parenchyma apotracheal with bands up to 3 cells wide, tending to be up 5 cells wide occasionally (Plate 6.16, 1, 2).

Rays heterocellular, 1 – 3-seriate (mean 2.4; range 1 – 3) (Plate 6.16, 6, 7) and commonly < 1 mm (mean 0.13, n = 50; range 0.10 – 0.18 mm) (Plate 6.16, 6, 7); rays composed of procumbent, square and upright cells mixed throughout the body.

Plate 6.16. Indetermined sample A.

1. Growth rings indistinct. Wood with a tendency to semi ring porosity. STRI 15520, TS, scale: 1 mm
2. Vessels in radial multiples of 2 (– 3). Wood with a tendency to semi ring porosity. STRI 15520, TS, scale: 500 μm.
3. Vessels in radial multiples of 2 (– 3). Fibres thin-t -thick. STRI 15520, TS, scale: 100 μm.
4. Intervessel pitting alternate. STRI 15520, TLS, scale: 100 μm.
5. Intervessel pitting alternate (arrows). STRI 15520, TLS, scale: 20 μm.
6. Rays mostly 1 – 3-seriate. STRI 15520, TLS, scale: 100 μm.
7. Rays mostly 1 – 3-seriate. STRI 15520, TLS, scale: 100 μm.

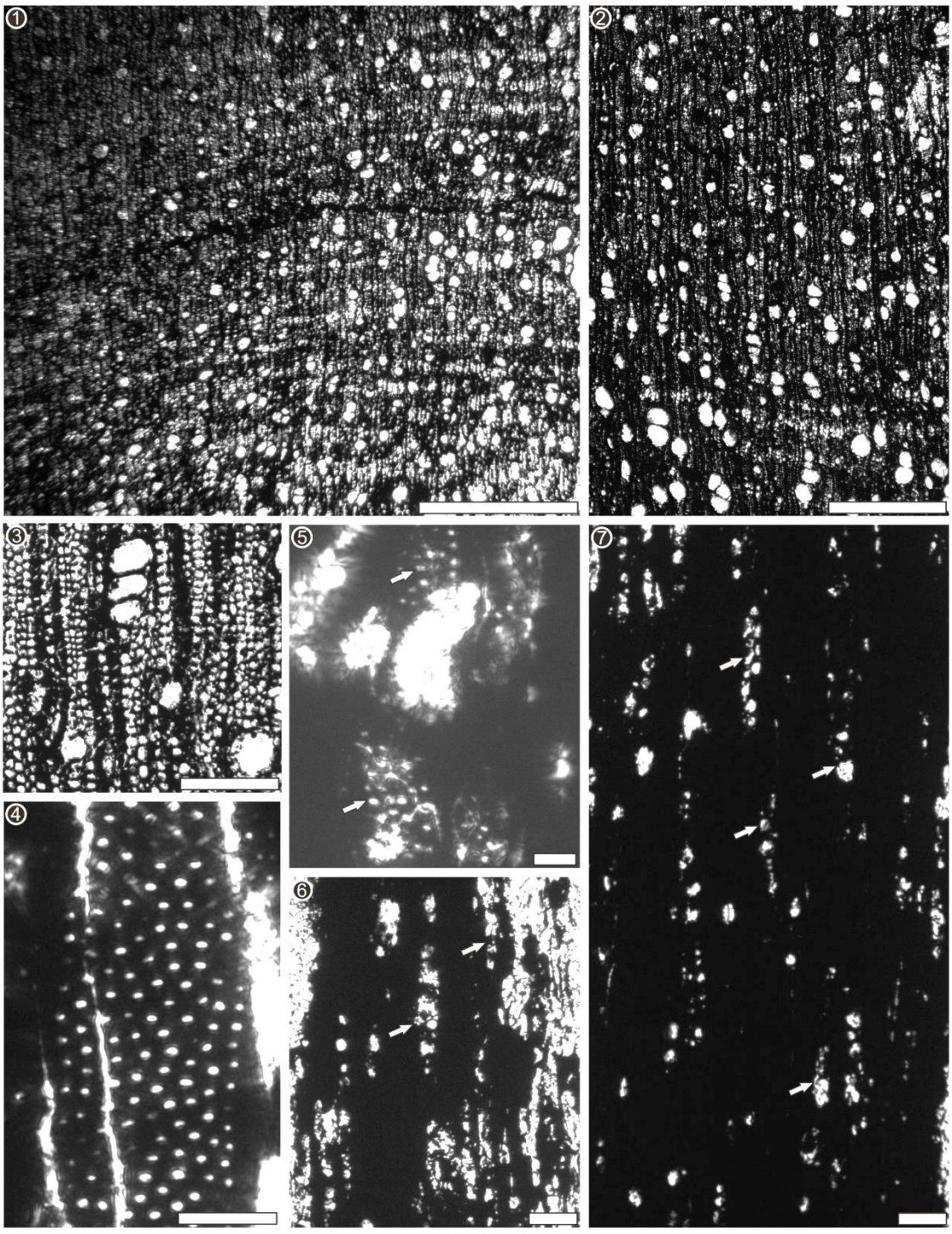

Plate 6.16

6.9.2. Comparison with extant taxa

The description of this wood type is not detailed due to limitations in the coding of many key features. For instance, the very opaque TLS and RLS make it difficult to observe the perforation plate type and the fibres and parenchyma strands. The features observed and coded with more confidence for this morphotype are common to many woods in the IWD; a search conducted using these features (2p, 13p, 22p, 30p, 85p, and 97p) produced a list of over 300 woods. Coding for "semi-ring porous" wood present (4p) gave more restricted results for Bignoniaceae, Fabaceae and Lythraceae. However this latter search is not recommended because there is no certainty in the presence of semi-ring porous wood for this specimen or the presence/absence of other features observed in TLS and RLS. Although it is justified to keep this morphotype as a distinguishable wood from the others in the Cucaracha Formation, it is not recommended to assign any affinity based on the specimens studied herein.

6.10. INDETERMINATE SAMPLE B

Material: STRI 15523

Locality: Centenario Hill (Gaillard Cut of Panama Canal) near Paraiso, Panama City, Panama (Latitude 09°02'51.75''N; Longitude 79°39'14.02''W).

Stratigraphic horizon: ~ 20 m below the top of the Cucaracha Formation (Gaillard Group); Lower Miocene, (19 Ma).

6.10.1. Description

IAWA features numbers present: 2, 5, 13, 22, 24, 40, 47, 66, 68, 79, 80, 82, 86, 97, 109.

Description: Growth rings indistinct; wood diffuse porous (Plate 6.17, 1, 2); vessels solitary (88 %) or in radial multiples of 2 –3 (– 4) (Plate 6.17, 1, 2); simple perforation plates (Plate 6.17, 3); intervessel pitting alternate and minute (mean 3, SD 0.6 μm, n =25; range 2 – 3); vessel – ray pitting no observable; mean tangential vessel diameter 96.1μm (n = 50; range 50.5 – 138 μm), after correction for shrinkage (Mean= 143 μm; range 75 – 206); mean vessel density 9.2 (n = 15; range 6 – 12 per mm^2); tyloses absent; vascular tracheids not observed.

Fibres non septate (seen from RLS) (Plate 6.17, 8) and very thin walled (Plate 6.18, 5, 6).

Axial parenchyma paratracheal vasicentric and winged-aliform (Plate 6.17, 5, 6). Apotracheal parenchyma with bands up to 3 cells wide (Plate 6.17, 6).

Rays heterocellular, 1 – 3-seriate and commonly < 1 mm (mean 0.18 mm, n = 25; range 0.13– 0.23 mm) (Plate 6.17, 7); rays composed of procumbent bodies and 4 or more marginal rows of square cells (Plate 6.17, 8). Ray density 9.2, SD 1.7 (n= 15; range= 7 – 11).

Plate 6.17. Indetermined sample B.

1. Growth rings indistinct and wood diffuse porous. STRI 15523, TS, scale: 100 μm.
2. Vessels in radial multiples of 2 – 3. STRI 15523, TS, scale: 100 μm.
3. Perforation plates simple. STRI 15523, RLS, scale: 500 μm.
4. Intervessel pits alternate. STRI 15523, TLS, scale: 100 μm.
5. Paratracheal parenchyma vasicentric to winged-aliform (arrows). STRI 15523, TS, scale: 100 μm.
6. Parenchyma apotracheal with bands up to 3 cells wide. STRI 15523, TS, 500 μm.
7. Rays mostly 1 – 3-seriate. STRI 15523, TLS, 100 μm.
8. Rays composed of procumbent bodies and 4 or more rows of square cells. STRI 15523, RLS, 100 μm.

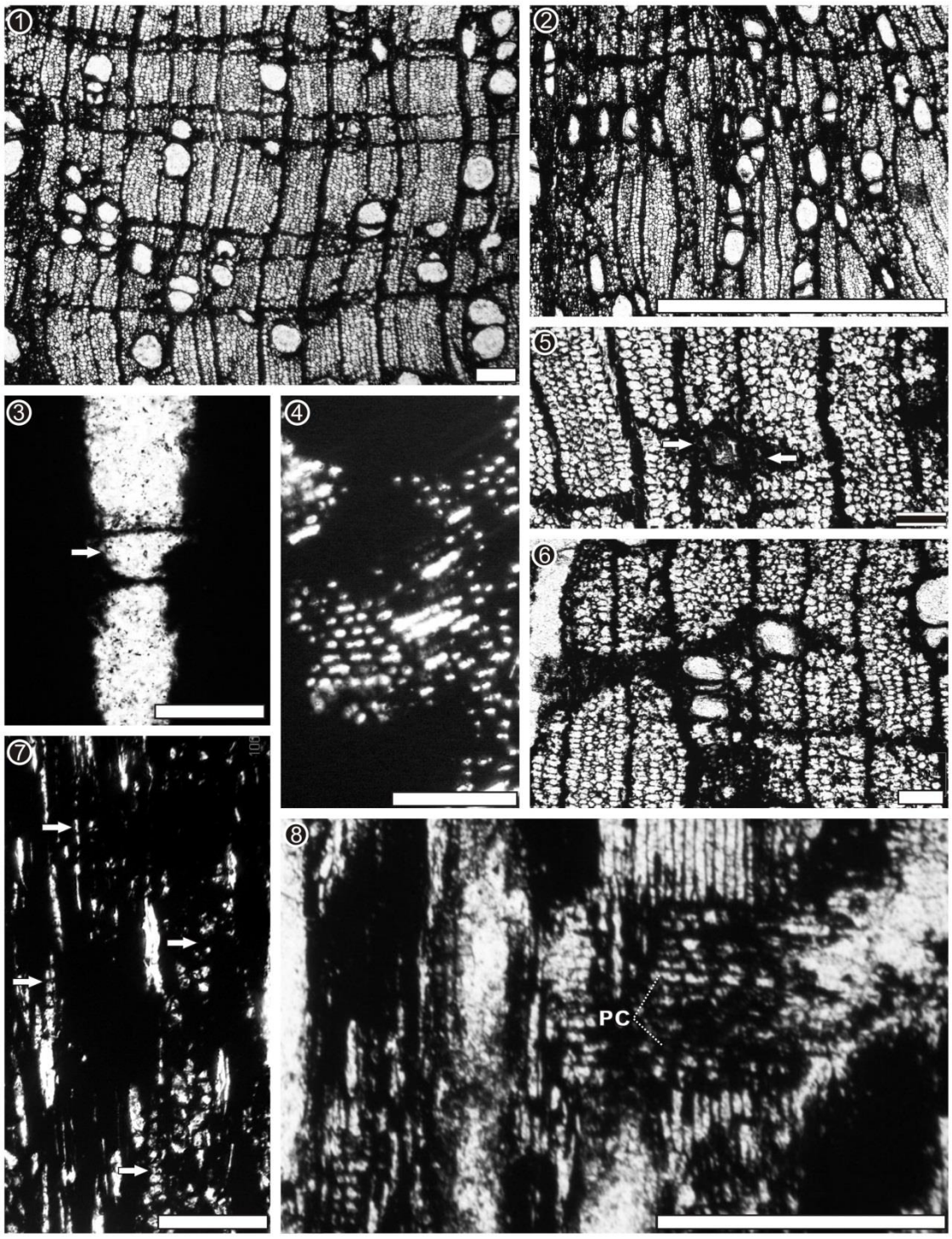

Plate 6.17

6.10.2. Comparison with extant taxa

The description of this specimen has similar issues to that of Indeterminate Sample A, but probably it has a few more distinct features that better constrain the suggestions from the IWD. A search with the following features was used with 0 allowable mismatches: 2p, 5p, 13p, 22p, 79p, 80p, 86p. Although the results listed half of the number of taxa obtained for Undertermined Sample A, the list was still large (more than 150) and given the limitations in coding of certain features, I am therefore reluctant to assign an affinity to this specimen.

6.11. DISCUSSION

The charcoalified fossil forest, buried by an ignimbrite, is interestingly diverse, with most material assignable to families or even lower taxonomic ranks in some cases. From a total of 22 charcoalified samples, at least 9 are distinct morphotypes that represent 6 identified families (? Meliaceae, Fabaceae, Malvaceae, Melastomataceae, Sapotaceae and Arecaceae) and two additional morphotypes that could not be assigned precisely to any taxonomic rank.

Overall, the families identified from the charcoalified woods of Cucaracha are well represented in the wood fossil record of the New World, except for Melastomataceae (Gregory et al., 2009). However, the Melastomataceae are well represented in the New World fossil record in leaves, seeds and pollen (Morley et al., 2003). An interesting note is that the Coryphoid palms, one of the subfamilies assigned here, are considered to be of Laurasian origin (Bjorholm et al., 2006). It seems that the taxa identified from the Panama Canal are mostly related to South American elements, but that will be further detailed in the general discussion of this thesis (Chapter 9).

6.11.1. Comparison with previous records from the Miocene of Panama

Supporting evidence for these taxa in the Miocene of Panama comes from previously reported fossil data (woods, leaves, pollen). For example, the presence and abundance of Malvaceae is confirmed by palynology from the Cucaracha Formation (Jaramillo, 2012 pers. com). Also, I have personally identified Melastomataceae leaves in collections retrieved from the underlying Culebra Formation in the Panama Canal (unpublished research, 2010). *Crysophila*-type palm pollen was reported by Graham (1988), supports the presence of coryphoid palms in the Cucaracha Formation. *Crudia* pollen grains (Graham, 1988) also confirm the presence of Fabaceae (Detarieae) in these localities.

6.11.2. Previously reported fossil woods, not represented here

A fossil wood described as *Taenioxylon multiradiatum* (Berry, 1918) was collected in outcrops corresponding with the upper parts of the Cucaracha Formation, presumably from a site nearby the localities where the charcoalified woods studied here come from; however, this is a wood type not represented in the current larger collection. *Taenioxylon* was a form genus proposed by Felix (1882-1886) as assignable to the Fabaceae. Nonetheless, if the illustrations in both publications are compared (Felix 1882-1886; Berry 1918), an important difference can be noticed, the rays in the Felix illustrations look storied; whereas the rays of the Berry's descriptions are not storied (neither is storeying mentioned in the Berry's description). The presence of storied rays is an important feature in the Leguminosae (Gasson et al., 2003). A few species of *Taenioxylon* were later confirmed as Leguminosae (Gregory et al., 2009), but other

species were later identified as Meliaceae (Madel, 1960). *T. multiradiatum* was eventually revised as *Eudiospiroxylon multiradiatum* (Müller-Stoll and Mädel-Angeliewa, 1984) and compared to the Ebenaceae. I would be therefore inclined to think that the wood described by Berry (1918) is more likely related to the Ebenaceae, in agreement with Müller-Stoll and Mädel-Angeliewa (1984).

6.11.3. Diversity of wood flora: charred and permineralised

All the charcoalified woods are 'dicots' except the four palm trees (three collected at Centenario Bridge and one from Contractors Hill). This accords with a field survey that showed that about 20% of the total wood samples, either as logs or stumps; from the Cucaracha Formation are palms (Chapter 2). This assemblage could be considered as highly diverse, when rarefaction curves are used to infer the original forest diversity, i.e., given that 22 specimens yield 9 taxa, the likelihood is that only a small proportion of the total diversity has been captured, and larger collections would yield greater diversity. This is supported by Berry's (1918) documentation of *T. multiradiatum*, which was not found in the present study.

The charcoalified fossil forest horizon contains a far more diverse assemblage (9 taxa) compared to the permineralised assemblage in tidal channels (5 taxa), with only one taxon in common, *Prioria*, and other members of the general Detarieae tribe. This is despite a similar sample size for both assemblages. These differences cannot be adequately accounted for by variable taphonomy, and may provide further evidence for a highly diverse, patchy rainforest ecosystem; with different sample sites containing different taxa (cf. DiMichele et al., 2007).

Alternatively, the permineralised flora may record ecosystems adapted to tidal mangroves while the charcoal flora inhabited more stable floodplains. The palms and some other taxa (e.g., *Prioria*) may have been adapted to flooded, estuarine and coastal areas and the geological setting of this area is interpreted as a transition from estuarine environment to fully continental areas with the presence of paleosols and river channels (Chapter 2; Kirby and McFadden, 2005; Retallack and Kirby, 2007; Montes et al., 2010; Rodriguez-Reyes et al., 2014).

6.11.3. Size range of studied samples and implications

The preserved dimensions of tree stumps and root wood range from 7 - 42 cm in diameter, suggesting that this charcoalified assemblage is a mix of young and adult trees (see Table 2.7; Chapter 2), although potentially some branches of small dimensions are included in this study. However, attempts were made to positively identify branches; Chapman, 1994). The largest stump found in this charcoalified forest (D= 42 cm) is related to Leguminosae, identified as *Prioria*, and some of the other trunks correspond to younger trees that were downed by the blast and transported in the ignimbrite flow.

CHAPTER 7: REFLECTANCE DATA OF CHARRED WOODS

7.1. INTRODUCTION

The aims of this chapter are: 1) to infer temperatures of charring based on reflectance data of *In situ* dicot stumps and monocot root clusters collected in two localities from the top of the Cucaracha Formation. 2) To see the variation of reflectance values at different positions with regard to the pyroclastic flows. 3) To constrain the temperature of the pyroclastic flow. 4) To compare the results with examples of charred woods from other pyroclastic flows.

Wildfires and volcanic events produce charcoalified trunks and logs, when those are exposed to charring in absence of oxygen and without combustion (Scott and Glasspool, 2005). When plants are charred in a wildfire, they are exposed to rapid high temperature heating that causes breakdown of cellulose in the plant tissues (Pyne et al., 1996); this promotes the liberation of volatiles (e.g., CO2, CO and CH4). These volatiles mix with oxygen and combust (Pyne et al., 1996). Therefore, woods exposed to wildfire may not be completely charcoalified, because the outer layers may combust before any of the inner parts are charred (Scott, 2000). In contrast, plants charred within hot volcanic pyroclastic flows are only subject to charcoalification and not to combustion (Scott, 2010). The conditions of charcoalification vary depending on the temperatures reached during the event. Plants charred in volcanic events are exposed to the heat for much longer than in wildfires, although this length of contact between the plant and the pyroclastic flows vary from a few hours to months in some cases (Scott and Glasspool, 2005).

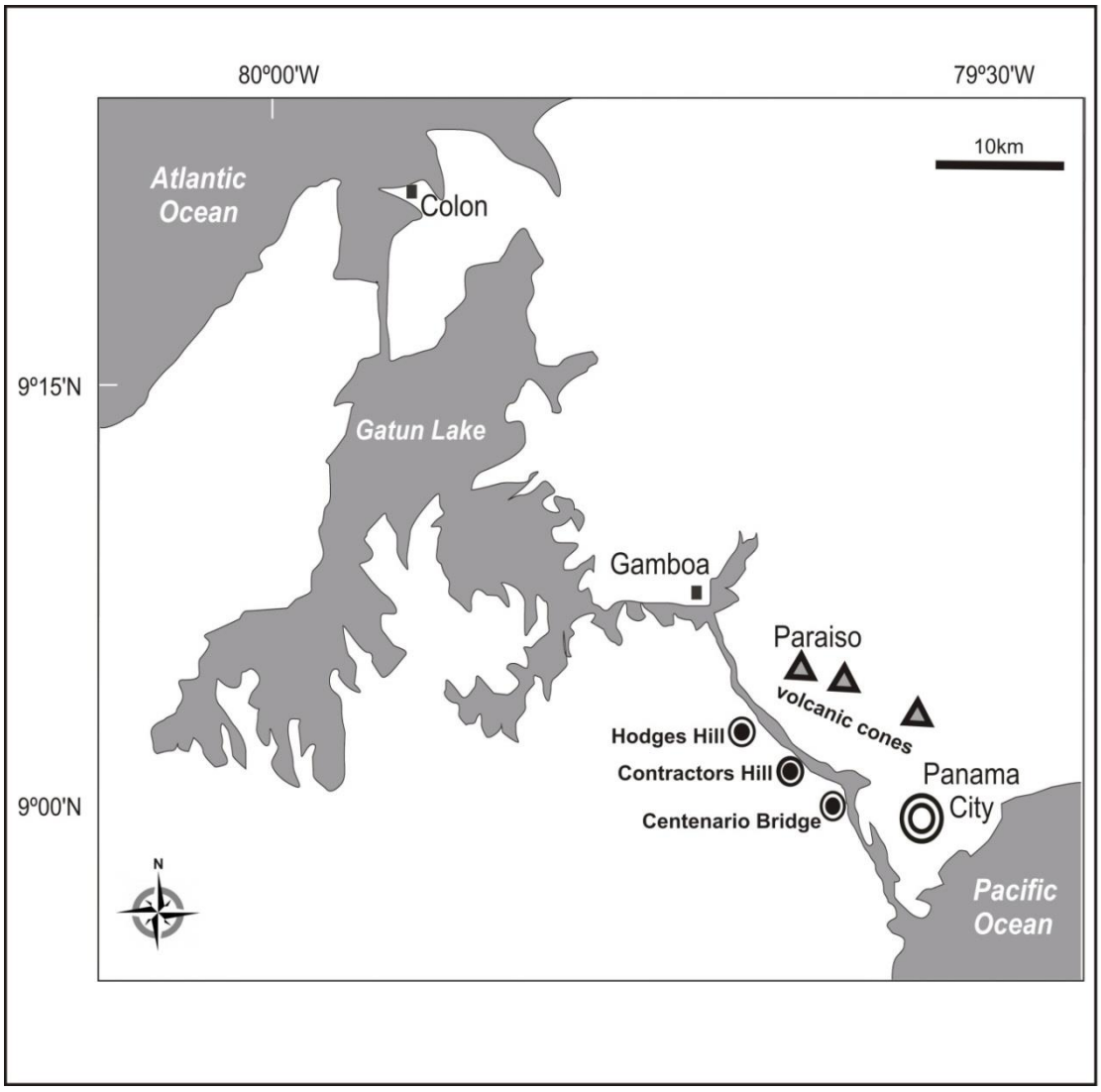

Figure 7.1. Localities with a charcoalified assemblage at the top of the Cucaracha Formation (circles) shown in the Panama Canal Area. The potential sources of pyroclastic flows (volcanic cones) are shown as triangles (based on map on Figure 2.11, Chapter 2).

Mean random reflectance (R_o Mean) is derived from photometric measurement of the fraction of incident light radiation reflected from a sample surface under oil. R_o Mean has shown to have positive relationship with formation temperatures (Jones et al., 1991, Scott and Glasspool, 2005, McParland et al., 2007, McParland et al., 2009b and Scott and Jones, 1991). Reflectance data allow study of both ancient and

freshly-produced charcoal samples (McParland et al., 2007, McParland et al., 2009a, Hudspith et al., 2010).

7.1.2. Experimental charcoalification and calibration curves

A considerable amount of experiments using controlled charcoal production can be found in the literature (see Scott, 2010 for a recent list). Those experiments have documented the relationship between charcoalification temperatures and reflectance values under oil: 1) several types of plants (dicots, conifers, ferns and fungi) show increasing reflectance with increasing temperatures (Jones et al., 1991, Scott and Jones, 1991a, Bustin and Guo, 1999; Scott and Glasspool, 2005, Scott, 2000; McParland et al., 2007, McParland et al., 2009 and Braadbaart and Poole, 2008). 2) Charcoal becomes more resistant to decay with increasing charring temperatures (Bird et al., 1999; Ascough et al., 2010); 3) time plays an important role in the reflectance/charcoalification relationship (Bustin and Guo, 1999); 4) reflectance under oil values stabilize after 24 24 hours (Scott, 2000); Bustin and Guo, 1999).

Two calibration curves are used here to infer temperature of emplacement of the volcanic deposits based on reflectance data (Figure 7.2). The calibration curves were obtained through laboratory experimentation with known temperatures and duration of charring and then plotting the reflectance values. To obtain the Scott and Glasspool (2005) calibration curve, samples of the conifer *Sequoia sempervirens* were charred at temperatures ranging between 200 – 900 ˚C for periods of 0.5 – 168 hours. The results demonstrated rapid increase of reflectance within the first 30 minutes, followed by a gradual increase in values and then stabilizing after 24 hours. McParland et al. (2009) charred samples of hardwoods (*Quercus, Fraxinus, Corylus and Acer*) at a range of

temperatures of 300 – 1100 ˚C within 1 hour and 24 hours, so two calibration curves were produced.

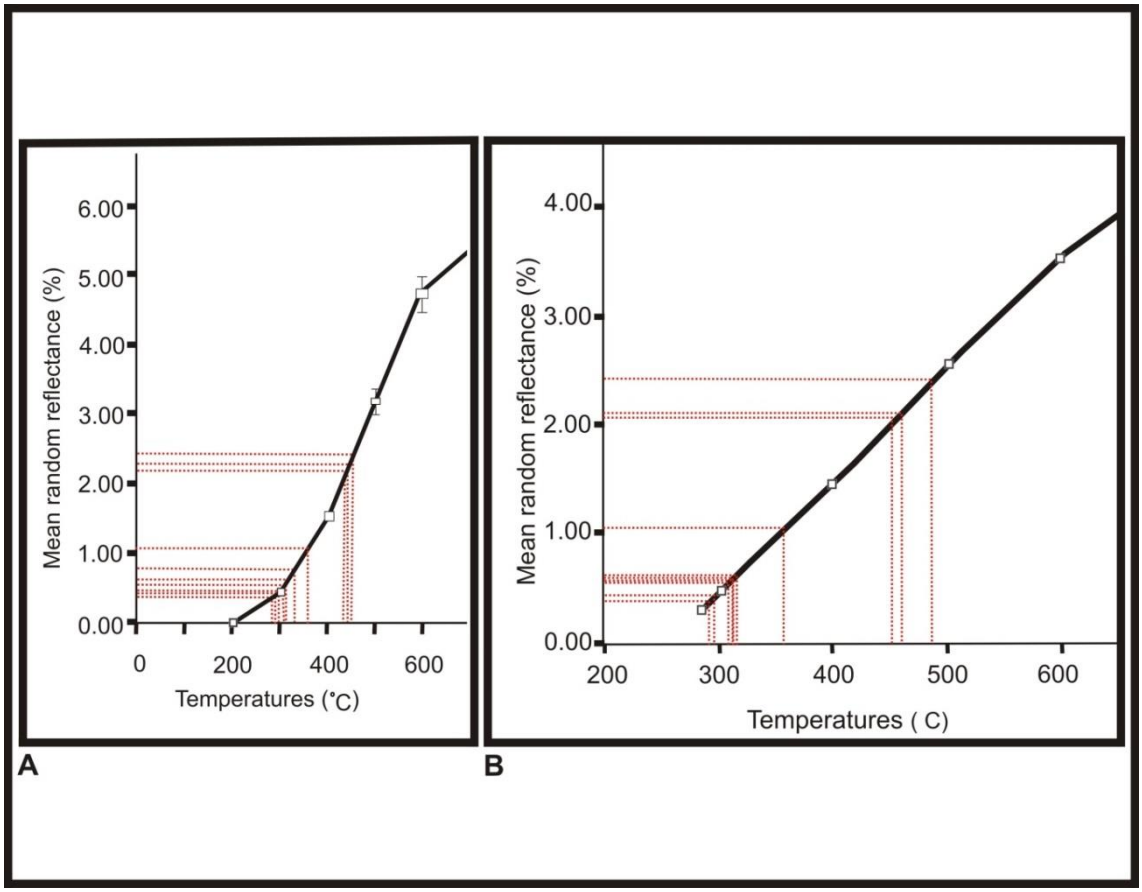

Figure 7.2. 24-h Calibration curves used to infer temperatures from reflectance values. A, Scott and Glaspool (2005; Figure 1. B) and B, McParland et al., (2009; Figure 4). The red dotted lines represent the reflectance values from the Cucaracha Formation samples and extrapolation of temperature values using the R_o Mean.

The McParland study included other experiments that were conducted in the field that produced further data, but only the 24 hour laboratory calibration curve is considered here together with the Scott and Glasspool (2005) 24 hour calibration curve (Figure 7.2). Because reflectance values stabilize after 24 h a 1h-calibration curve would not be ideal to estimate temperatures of final emplacement of volcanic deposits.

Furthermore the woods are entombed by the volcanic deposits for much longer than one hour, indeed permanently.

7.2. METHODS

7.2.1. Sampling for reflectance analysis

Charcoalified *in situ* charcoalified stumps and monocot root clusters are found along two localities of the Cucaracha Formation, Centenario Bridge and Contractors Hill (Figure 7.1). Although the Hodges Hill locality also exposes the charred layer (see Chapter 2; Figure 7.1), no *in situ* stumps were found there; therefore it was not included in the reflectance analysis. The three localities are at approximately the same distance from the potential sources of the pyroclastic flows. (Figure 7.1; see Chapter 2). Four rooted stumps were found in Centenario Bridge, two were dicots and two were root clusters corresponding to monocots, more likely to be related to palm trees (See Chapter 6). Only one rooted stump was found in Contractors Hill that corresponded to a "dicot" that was the largest *in situ* charcoalified stump included in the reflectance analysis (Stump 1, STRI 15650 and STRI 15653; Figure 7.8 A). The local geological setting was complex and it was difficult to determine the exact position of the stumps in relationship to the ignimbrite in most of the cases. Therefore, different sections of the stumps were sampled (Figure 7.3), including portions facing the inferred blast side and the opposite side, as well as samples taken from the top of the charred layer and from roots a few centimeters down (Table 7.1) (Figure 7.3). All samples were assigned a collection number, labelled and sent to Royal Holloway, University of London for their preparation and analysis.

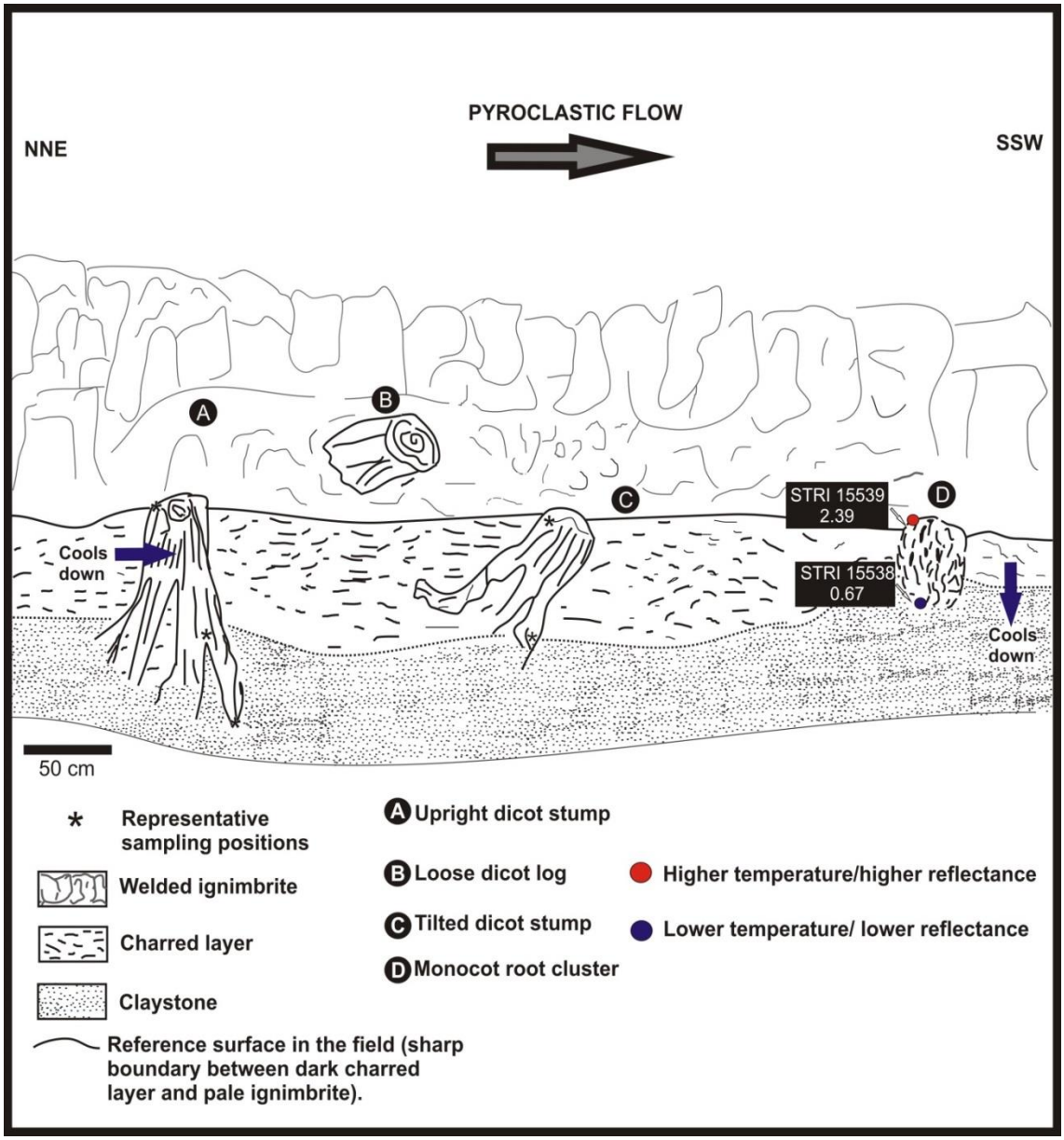

Figure 7.3. Diagram to illustrate local context of charred stumps and logs at the top of the Cucaracha Formation.

7.2.2. Preparation of samples for reflectance analysis

Thirteen wood samples were embedded in polyester resin and polished at the Department of Earth Sciences, RHUL, by Neil Holloway. The samples were chosen to represent different areas of the stumps and root clusters in relationship to the ignimbrite (Figure 7.3). However, only 12 samples (Table 7.1) were used, because one sample was

too poor to allow reflectance measurements under oil. Each polished block contained at least 3 different pieces from the original collected samples. An initial survey was focused on exploring the better areas to measure the reflectance in the polished blocks. Reflectance values and photographs of each sample were obtained using reflected light under oil. All images are produced in identical lighting conditions for visual comparison of reflectance.

Because a PhD project has a constrained time to be completed, no more samples were prepared nor included in this thesis.

7.2.3. Measurements and inferred temperatures using the Scott and Glasspool (2005) and MacParland et al. (2009) curves

All samples were analysed using a Nikon Microphot reflectance microscope under oil of RI 1.514 at 23 °C, using the 40x magnification. Trial measurements were first done to establish the appropriate standards to measure each sample. Reflectance was measured using Leica QWin image analysis software. The light source was a Nikon fibre optic LS-101 with a 546 nm filter. One group of samples (STRI 15524, STRI 15539, STRI15532) was measured relative to low-medium reflectance standards [silica glass (Ro 0.038), spinel (Ro 0.393) and YAG (yttrium aluminum garnet) (R_o 0.929)], a second group of samples (STRI 15538, STRI 15529, STRI 15533, STRI 15535, STRI 15650, STRI 15653, STRI 15531) was measured relative to medium-high reflectance standards [spinel (R_o 0.393) and YAG (Ro 0.929) and GGG (gadolinium gallium garnet) (R_o 1.749)] and a few other samples (STRI 15536, STRI 15537, STRI 15539) were measured relative to high standards [YAG (Ro 0.929), GGG (gadolinium gallium garnet) (R_o 1.749) and CZ (cubic zirconium) (R_o 3.188)]. Typically, 50 measurements

were taken for all the samples. A few samples were problematic, and the reflectance varied along the specimen, therefore several sets of data (50 values each) were taken in different areas in order to take account of the variation.

With the R_o Mean (Mean random reflectance) values, inferred minimum charring temperatures were obtained extrapolating the values from the Scott and Glasspool (2005) and McParland et al. (2009) calibration curves (Figure 7.2). In addition to the Mean reflectance values (R_o Mean), the mean of the three maximum values ($3R_o$ Max) is also considered (Table 7.1) to follow the methodology of Hudspith et al., (2010) and to infer the minimum temperatures of charring.

Sample ID	Field label	Locality	Position of sampling in the stump	Dicot/ Monocot	R_o Mean	R_o Mean SD	R_o Mean temperature (Scott and Glasspool, 2005) 24-h curve (°C)	R_o Mean temperature. 24 h McParland, (2009) curve (°C)	Mean of $3R_o$ Max	$3R_o$ Max temperature (Scott and Glaspoool, 2005) (°C)	$3R_o$ Max temperature Mc Parland (2009, 24-h curve)(°C)	Figures
STRI 15524	stump 1.1	Centenario Bridge	Top of the charred layer	Dicot	0.32	0.11	275	265	0.46	315	305	Figure 6.3; B, C, D
STRI 15529	stump 2.1	Centenario Bridge	Top of the charred layer	Dicot	0.5	0.12	315	305	0.76	355	325	Figure 6.4; B
STRI 15533	stump 2.5	Centenario Bridge	19 cm down from top of the charred layer	Dicot	0.5	0.15	315	305	0.68	335	318	Figure 6.4; C
STRI 15532	stump 2.4	Centenario Bridge	24 cm down from top of the charred layer	Dicot	0.37	0.07	290	280	0.51	315	310	Figure 6.4; D
STRI 15531	stump 2.3	Centenario Bridge	Root 31 cm down from top of the charred layer	Dicot	0.48	0.1	300	305	0.65	340	320	Figure 6.4; E
STRI 15537	root cluster 3.3	Centenario Bridge	Top of the charred layer, facing inferred blast side	Monocot (Arecaceae)	2.47	0.11	455	470	2.67	480	500	Figure 6.5; B
STRI 15536	root cluster 3.2	Centenario Bridge	Top of the charred layer	Monocot (Arecaceae)	2.14	0.08	425	430	2.3	440	480	Figure 6.5; C,D
STRI 15535	root cluster 3.1	Centenario Bridge	10 cm down from the top of the charred layer	Monocot (Arecaceae)	0.54	0.05	325	305	0.62	335	318	Figure 6.5; E
STRI 15539	root cluster 4.2	Centenario Bridge	Top of the charred layer	Monocot (Arecaceae)	2.39	0.2	430	450	2.74	490	505	Figure 6.6; B, C
STRI 15538	root cluster 4.1	Centenario Bridge	9 cm down from the top of the charred layer	Monocot (Arecaceae)	0.67	0.07	335	325	0.75	350	320	Figure 6.6; D
STRI 15653	stump 1.4	Contractors Hill	Top of the charred layer, facing inferred blast side	Dicot	1.03	0.05	360	355	1.11	370	360	Figure 6.7; B
STRI 15650	stump 1.1	Contractors Hill	14 cm down from the charred layer	Dicot	0.75	0.05	350	320	0.84	355	340	Figure 6.7; C

Table 7.1. R_o Mean values and inferred temperatures from the Glasspool and Scott (2005) and McParland (2009) curves. 1, 2, 3, 4= stump number; 1.x, 2.x, 3.x. 4.x= subsample of one stump.

7.2.4. Limitations of the reflectance measurements from the Cucaracha Formation samples.

A diagram of the fossils in their stratigraphic context is given in Figure 7.3. The welded ignimbrite at the top of the Cucaracha Formation is not well exposed in most of the total sampling area and it was difficult to establish the exact position of each sample with regards to the ignimbrite. The three localities were approximately at the same distance from the potential sources of pyroclastic flows; hence differences in temperatures at different proximities to the vent could not be studied. Overall, it was noted that the monocots tended to be better polished compared to the dicots and the thick-walled sclerenchyma cells also allowed more fields to measure the reflectance. For example, the STRI 15533 (Centenario Bridge Dicot Stump 2, 19 cm down from top of charred layer) presented numerous broken and crushed cells in most of the sample, allowing very few fibre walls to be measured (Figure 7.5, B). The Centenario Bridge dicot Stump 1 (STRI 15524, STRI 15527) presented issues in its polishing, to the point of requiring repolishing with limited improvement (Figure 7.4, B, C). There were also multiple scratches in nearly all the samples, probably related to mineral grains plucking during polishing (Margaret Collinson pers. com.). It was difficult to avoid the scratches during the measurements, so the values were obtained from several different areas, also trying to measure where the cell walls were thicker with few scratches (Figures 7.4 – 7.7).

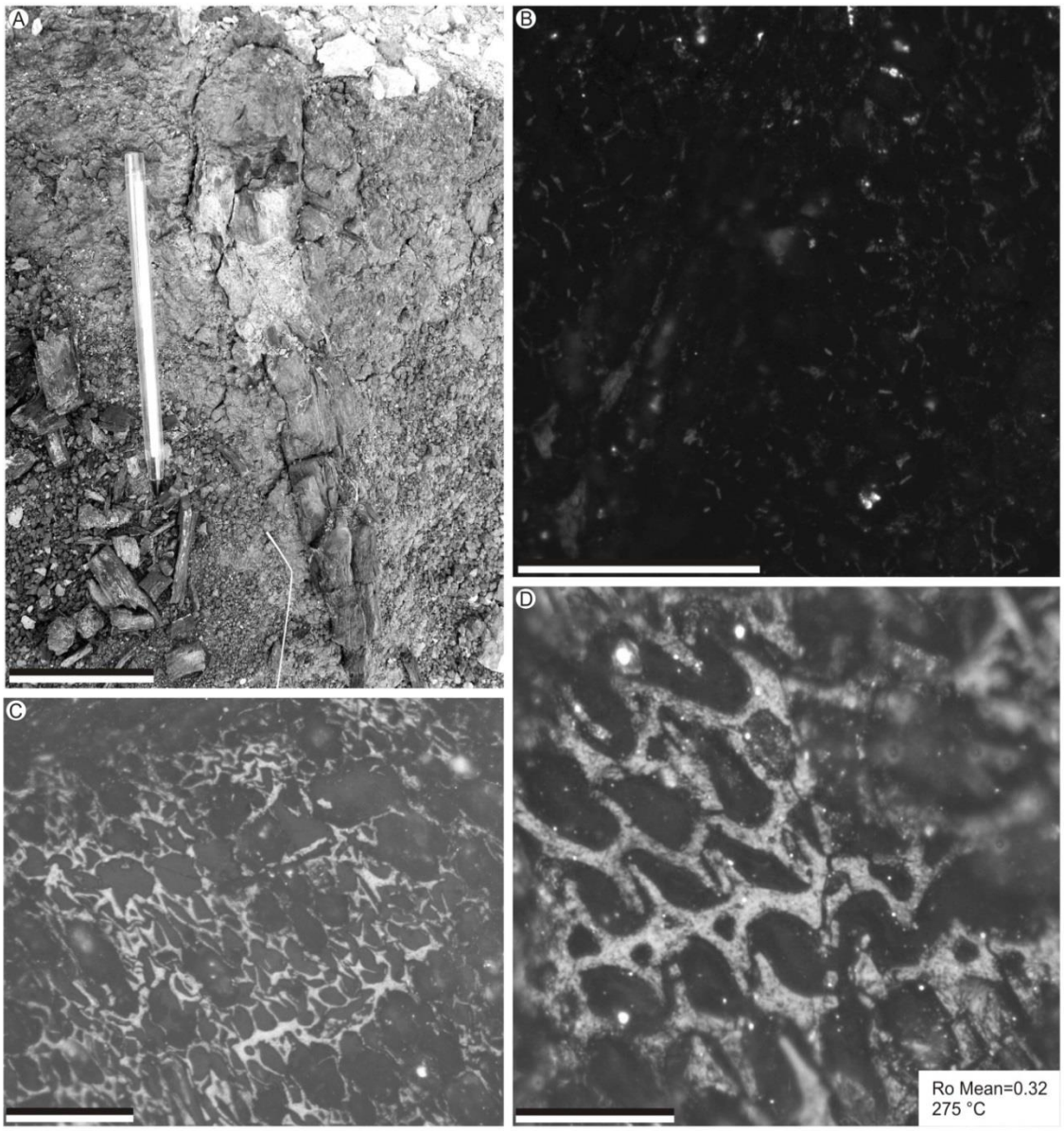

Figure 7.4. Centenario Bridge Dicot stump. A, Stump 1 in the field. B, sample STRI 15524 (stump 1.1) prior to repolishing; C, STRI 15524 sample repolished and measured (top of the stump). D, Close-up of repolished STRI 15524 samples. Scales: A= 5 cm; B, C= 100 µm; D= 40 µm. Temperature values are inferred using the Scott and Glaspool (2005) calibration curve. B, C, D were photographed with reflected light under oil and imaged in identical lighting conditions to allow visual comparison of reflectance.

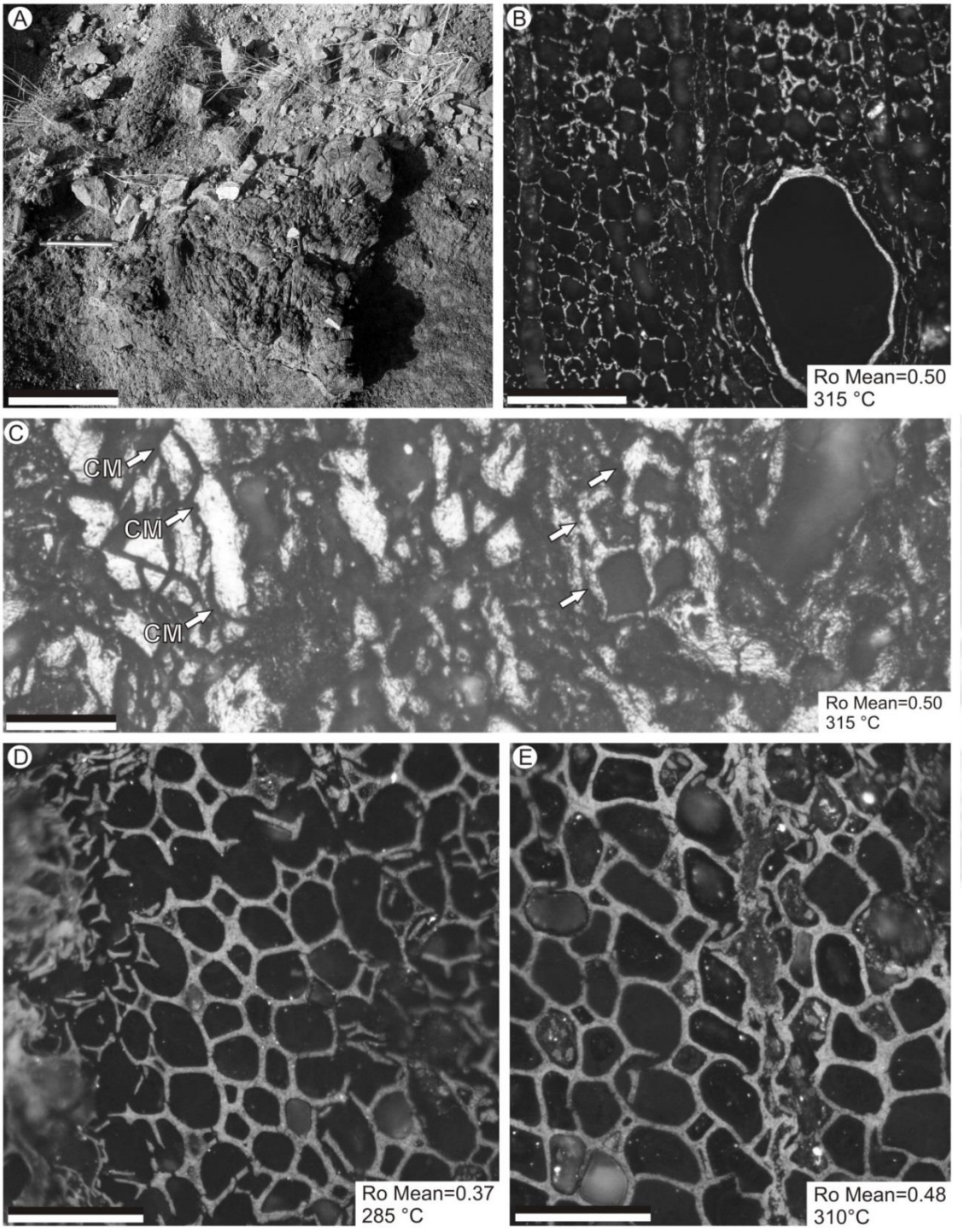

Figure 7.5. Centenario Bridge Dicot stump 2. A, stump 2 as found in the field. B, STRI 15529 (stump 2.1; top of stump, facing inferred blast side); C, STRI 15533 (stump 2.5; 19 cm down from top of stump) with numerous broken cells and polishing issues, arrows show some of the fibres and clastic material (CM) from the surrounding soil; D, STRI 15532 (stump 2.4; 24 cm down from top of stump); E, STRI 15531 (stump 2.3; 31 cm down from top of stump). Scales: A= 20 cm; B, D= 100 µm; C= 50 µm; E= 40 µm. Temperature values are inferred using the Scott and Glaspool (2005) calibration.

7.3. RESULTS AND DISCUSSION: REFLECTANCE DATA

7.3.1. Homogenisation of cell walls and reflectance values

One of the signs of charcoalification is the homogenisation of cell walls at > 290 – 325 º C (Scott, 1989; Scott, 2000; MacParland et al., 2009; Hudspith et al., 2010). Most of the samples from the Panama Canal have inferred temperatures above this range (Tables 7.1 – 7.3). Homogenisation of walls can be observed in several samples analysed here, either under oil with reflectance microscopy or with scanning electron microscopy (Figures 7.4 –7.8) (Table 7.2). Thus, the cell wall features of the samples support the inference from reflectance values that the tree stumps in the Centenario Bridge and Contractor Hill locality were charred at temperatures higher than 290 – 325 º C.

sample	Temperature (range of Scott and Glaspool (2007) and MacParland et al (2009) combined)	homogenisation of walls as seen by reflectance under oil
STRI 15524	265 – 275	granular
STRI 15529	305 – 315	homogenised
STRI 15533	305 – 315	granular
STRI 15532	280 – 290	granular
STRI 15531	300 – 305	granular
STRI 15537	455 – 470	homogenised
STRI 15536	425 – 430	homogenised
STRI 15535	305 – 325	granular
STRI 15539	430 – 450	homogenised
STRI 15538	325 – 335	homogenised
STRI 15653	355 – 360	homogenised
STRI 15650	320 – 350	homogenised

Table 7.2. Comparison of charring temperature vs appearance of cell walls.

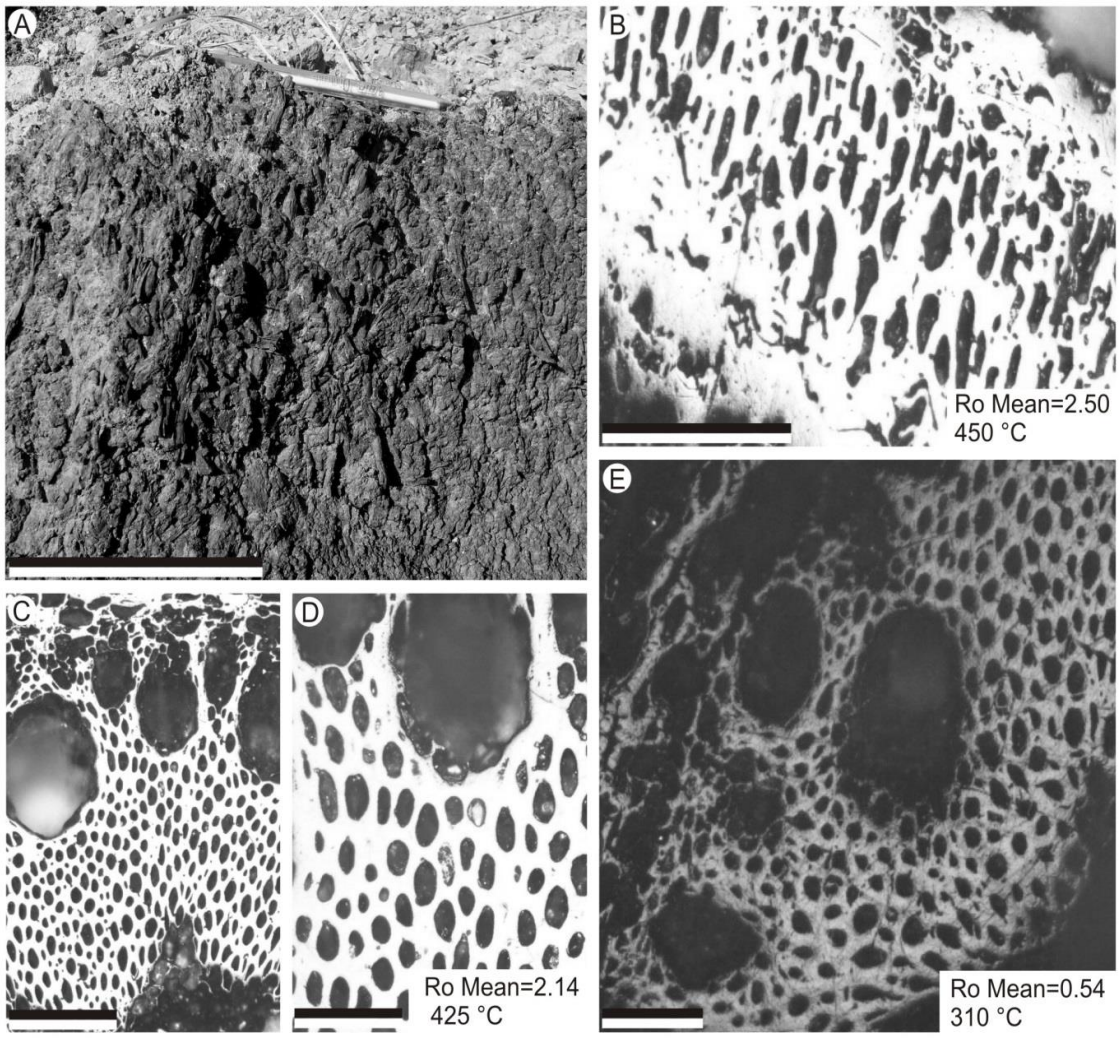

Figure 7.6. Centenario Bridge Monocot stump 3. A, stump in the field; B, STRI 15537 (stump 3.3; top of the stump, facing the blast side); C, 15536 (stump 3.2; top of the stump, opposite to blast side); D, detail of STRI 15536; E, STRI 15535 (stump 3.1; 10 cm down from top of the stump). Scales: A= 15 cm; D= 40 µm; B, 100; C= 50 µm; E= 50 µm. Temperature values are inferred using the Scott and Glaspool (2005) calibration curve. B –E were photographed with reflected light under oil and imaged in identical lighting conditions to allow visual comparison of reflectance.

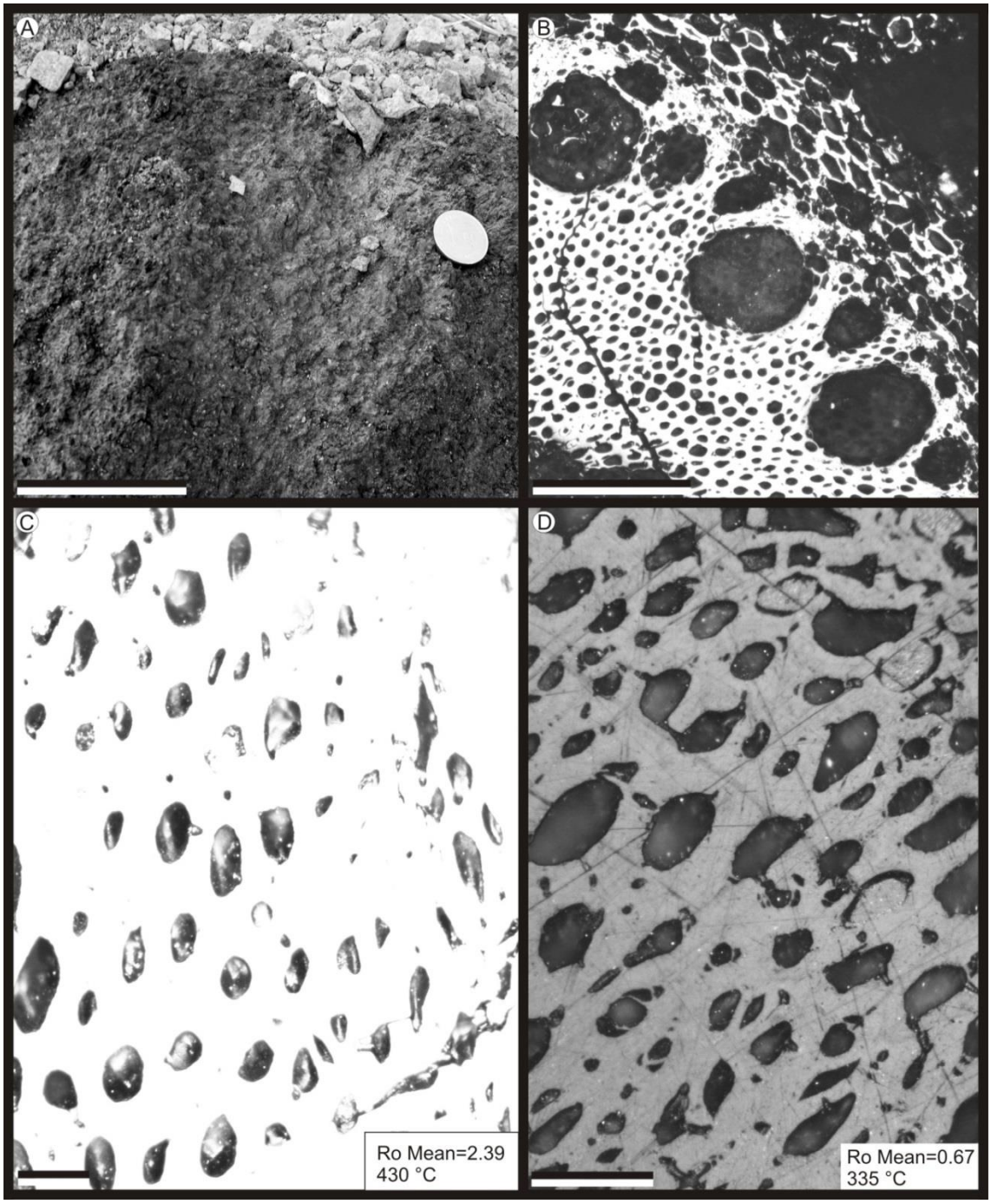

Figure 7.7. Centenario Bridge Monocot Stump 4. A, Stump in the field; B, STRI 15539 (stump 4.2; top of the stump, facing inferred blast side); C, detail of 15539; D, STRI 15538 (stump 4.1; 9 cm down top of stump). Scales: A= 5cm; B,= 100 µm; C, D= 25 µm. Temperature values are inferred using the Scott and Glaspool (2005) calibration curve. B - D were photographed with reflected light under oil and imaged in identical lighting conditions to allow visual comparison of reflectance.

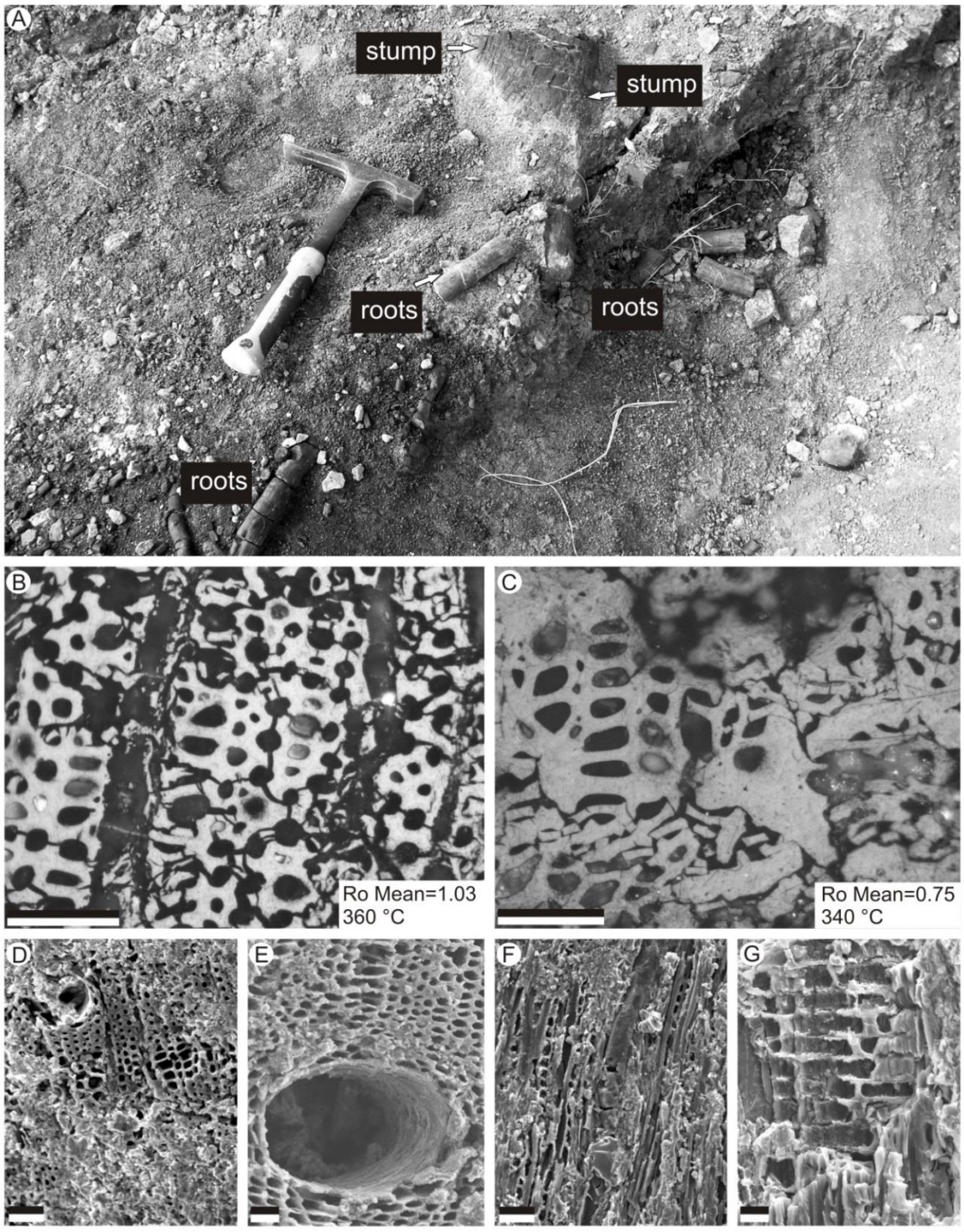

Figure 7.8. Contractors Hill Dicot Stump 1. A, stump in the field; B, STRI 15653 (top of stump, facing inferred blast side); B, 15653 (stump 1.4; top of the stump, facing inferred blast side); C, 15650 (stump 1.1; root 14 cm down from top of stump), arrows show fibres. D –G, SEM images of Stump 1 Contractors Hill. D, TS of STRI 15652 (top of stump, opposite to blast side); E, Detail of fibre walls and solitary vessel; F, TLS of STRI 15652; G, RLS of STRI 15652. Scales: D, E, F, G= 100 µm; B, C= 25 µm. Temperature values are inferred using the Scott and Glaspool (2005) calibration curve.B - C were photographed with reflected light under oil and imaged in identical lighting conditions to allow visual comparison of reflectance.

7.3.2. Maximum inferred temperature of flows at emplacement

The inferred temperatures were similar when using both curves in most of the cases (Table 7.1). The highest temperature has been found in Centenario Bridge, from one of the measured monocot root clusters (STRI 15537, Centenario Stump 3; R_o Mean = 2.47, inferred temperature from R_o Mean= 455 – 470 º C). However because no monocot stumps were sampled and measured in Contractors Hill, monocots cannot be compared between localities. When the dicots R_o Mean per locality are compared (Table 7.3), the R_o Mean values in Contractors Hill (R_o Mean = 0.89) are higher than in Centenario Bridge (R_o Mean = 0.43). It is difficult to interpret if the trees in Contractors Hill (350– 360 ˚C) were charred at higher temperatures than in Centenario Bridge (290 – 300 ˚C), because the differences in the reflectance values might be related to polishing issues and thin walled cells, given that the comparative number of analysed samples is limited. The significantly higher R_o Mean obtained from monocot root clusters in Centenario Bridge could be related to a more direct exposure of tissues to the pyroclastic flows in contrast to dicot woods where the flows probably cooled down as a result of contact with the water contents from the plant tissues. It is not ideal to compare monocots and dicots because the thick walled sclerenchyma fibres in monocots may polish more reliably (Figures 7.6, 7.7) than the thinner fibre walls in dicots especially Figure 7.5 B (Margaret Collinson, pers. com.). From the results of the $3R_o$ Max, the highest inferred temperature was found in another monocot sample from Centenario Bridge (15539, Centenario Stump 4; $3R_o$ Max = 2.74, 490 – 505 ˚C) (Table 7.1). This stump yields very similar values to sample STRI 15537 (Stump 3; $3R_o$ Max= 2.67, 480 – 500 ˚C) (Table 7.1) with the highest R_o Mean values (2.47). The appearance of these samples under the reflectance microscope is consistent with the high reflectance values (Figures 7.6, 7.7).

Based on these results, the minimum temperature of the pyroclastic flows entombing the trees in the Cucaracha Formation probably ranged from 490 – 505 º C.

7.3.3. Positions of sampling in the stumps and inferred temperatures

The charred stumps at Centenario Bridge and Contractors Hill are frequently coated by crystalline pyroclastic material, confirming that these trees were engulfed by hot ashes. It might be expected that samples taken from the top of the charred layer, that were in more direct contact with the pyroclastic flows, would yield higher reflectance values than those obtained below from the top of the charred layer (Figure 7.3). However, the local setting of this charcoalified forest is complex, thus it was difficult to determine the exact positions of the samples with respect to the volcanic entombment and the original soil level. Therefore, each stump was sampled in different positions, such as: from the top of the stump, central part of the stump, part of the root system (Figure 7.3), etc. Some results (Table 7.1) show higher temperatures in the same stump when sampled at the top of the stump in contrast with samples below the ground level (e.g., Figures 7.6 – 7.8), but with inconsistent trends in others (Figure 7.5).

7.3.4. Comparison of the charcoalified assemblage in the Cucaracha Formation with other examples

Just a few similar examples to the Cucaracha Formation event occurring in the modern tropics can be found in the literature. Some of the most recent works in this field include two studies performed on the Chaiten Volcano in Chile (Major et al., 2013 and Swanson et al., 2013). The disturbance of the flanking forests of Chaiten was

analysed based on observations in the field and not with reflectance data. I have only found three published examples of a volcanic event evaluated with reflectance analysis: 1) Donoghue et al., (2009) studied block-ash deposits from the Merapi volcano, Indonesia, where reflectance was applied to determine the internal structure and composition of the woods, but not to constrain temperature of the pyroclastic flows.

2) Scott et al., (2008) studied vegetation charcoalified by ash-surges coming from the eruption of the Soufriére Hills Volcano in Montserrat which occurred in 1997. In this study, reflectance was applied to constrain the minimum temperatures of the pyroclastic flows from three different samples. A range of charcoalified plants from small rootlets to small wood fragments was used. The samples yielded R_o Mean values of 1.16, 0.97 and 0.72, the latter value coming from the locality furthest from the vent. These values are comparable to the data obtained from the Cucaracha Formation, apart than the higher values from the monocot root clusters from the latter. In summary, the Monserrat samples yield R_o Mean values in a range of 0.72– 1.16 with a maximum value of 1.77, thus suggesting flow temperatures of 425 ˚C, which is slightly cooler than for the Cucaracha Formation flow.

3) Hudspith et al. (2010) studied the Taupo ignimbrite in New Zealand using 84 charcoalified wood samples. The latter is perhaps the best available example for comparison with the Cucaracha Formation. The 1800-year old Taupo volcano represents one of most explosive examples of burial and charcoalification of plants by pyroclastic flows (Hudspdith et al., 2010). The Taupo example is not directly comparable because the charcoals and charred wood fragments from Taupo are not *in situ* unlike those in the Cucaracha Formation. Also, whereas the Cucaracha ignimbrite is welded, the Taupo ignimbrite is sheet-like morphology, maybe implying different conditions prior to deposition. However a summarised comparison is provided here

(Table 7.3). The reflectance values of charcoals from the Taupo ignimbrite and the Cucaracha charred forest are very similar, especially for the Contractors Hill locality. In Centenario Bridge, the average value of reflectance per locality is strongly influenced by the monocot values that are higher, as mentioned before. If the monocots are excluded and only dicot reflectance values are used for comparison, then the values from Taupo are similar to those at Centenario Bridge (Table 7.3).

The volcanic cones inferred as sources of the pyroclastic flows that entombed the forest at the top of the Cucaracha Formation are located c. 10 km from both of the studied localities (See Chapter 2). In Taupo, the only locality with a similar distance is the TAP 052, located 13 km from the vent. The 4 samples studied from this locality yield very low reflectance values (R_o Mean: 0.23, range: 0.16 – 0.29) and suggest inferred temperatures of entombment of 223 – 258 ˚C (Table 7.3).

Samples from the Panama Canal yield higher values of reflectance, thus, temperatures are in a total range of 355 – 365 ˚C in Centenario Bridge and 350 – 360 ˚C, in Contractors Hill (Table 7.3). If the $3R_o$ Max is considered, then the range of temperatures in TAP 052 would be 250 – 300 ˚C and 490 – 505 ˚C in Centenario Bridge and 360 – 370 ˚C, in Contractors Hill. Hudspith et al., 2010 found a trend of increasing temperatures away from the vent, with a few exceptions in certain localities that were more likely related to the R_o Mean skewed by a few samples with very low reflectance. This trend was also found by McClelland et al. (2004) using paleomagnetic techniques to infer temperatures of entombment in the Taupo ignimbrite. The cooling rate of pyroclastic flows has been inferred to be slower at greater distances from the vent. McClelland et al. (2004) suggested that temperatures can increase to 400 – 500 ˚C at at distances > 40 km from the vent. Overall, the temperatures inferred from the

localities in the Panama Canal show higher temperatures at much shorter distances than reported in the previous two studies.

Taupo (Huspdih et al., 2010)					**Panama Canal (this work)**				
Taupo locality 052TaTaupo	**R_oMean per locality**	**3R_o Max per Taupo locality**	**Range of temperature using R_oMean (˚ C)**	**Range of temperature using 3R_oMax (˚ C)**	**Panama Canal locality**	**R_oMean per locality**	**Range of temperature per locality using R_oMean (˚ C)**	**3 R_o Max per locality**	**Range of temperature per locality using 3R_oMax (˚ C)**
TAP 052	0.23	0.38	223–258	250 – 300	Centenario Bridge	1.04	355–365	2.74	490 – 505
TAP 022	0.38	0.68	219–335	229 – 351	Contractors Hill	0.89	350 – 360	1.11	360 – 370
TAP 032	0.47	0.76	244 – 337	259 – 359	**Dicotyledonous stumps**				
TAP 019	0.31	1.00	<200 – 364	<200 – 378	Centenario Bridge	0.43	290 – 300	0.71	315 – 340
TAP 020	0.47	0.77	251 – 319	337	Contractors Hill	0.89	350 – 360	1.11	360 – 370
TAP 027	0.54	0.77	310	337	**Monocotyledonous roots/clusters**				
TAP 022	0.33	0.44	259 – 266	269 – 294	Centenario Bridge	1.64	390–410	2.74	490–505
TAP 032	0.64	0.94	250 – 337	259 – 358					
TAP 019	0.87	1.08	343	366					
TAP 026	0.74	1.46	275–375	308 – 407					
TAP 026	0.50	0.65	258 – 321	267 – 340					
TAP 028	1.00	1.50	324 – 375	343 – 414					

Table 7.3. Comparative and synthesis table of R_oMean and 3R_oMax values from the Taupo ignimbrite and the Cucaracha Formation. Taupo temperatures were inferred using the Scott and Glasspool, 2005 and Scott and Glasspool, 2007 calibration curves. Panama Canal temperatures were inferred using the Scott and Glaspool, 2005 and the McParland et al., 2009 24-h calibration curves.

CHAPTER 8: CLIMATIC IMPLICATIONS OF WOOD ANATOMY VARIATION IN MODERN WET AND DRY FORESTS AND MIOCENE FORESTS OF PANAMA

8.1. INTRODUCTION

This chapter aims to provide palaeoclimatological insights into the Miocene of Panama using wood anatomical data from modern woods and fossil woods from the Cucaracha Formation. Two main approaches are used: 1) tree ring analysis to determine the percentage occurrence of ring types and their relationship to climatic conditions (cf. Creber and Chaloner 1984, 1985), and 2) Multivariate analysis to make preliminary estimations of climatic conditions using equations based on wood anatomical characters (Wiemann et al. 1998, 1999). In applying both these techniques, fossil material is compared with a modern dataset comprising wood cores from wet tropical forests (Barro Colorado Island) and subhumid tropical forests (Achotines, Divisa and Coronado towns) in Panama.

8.1.1. Previous palaeoclimatological studies in the Cucaracha Formation

The literature about the Miocene climate is voluminous and I do not address it here (see Chapter 1 for a partial review). In this chapter, I focus on the Miocene climate of Panama only. However, this, in turn, has implications for understanding global climate because the formation of the Panama Isthmus exerted a very significant impact on ocean circulation and inter-regional climate.

There have been numerous studies of Miocene climate based on material from Panama, particularly on the Cucaracha Formation (Panama Canal Basin, in particular). As noted in Chapter 2, this unit is particularly rich in mammal and plant remains that offer an opportunity to understand the climate of the area in the Miocene. However, previous studies of the Cucaracha Formation provide little consensus about Miocene climate. Studies of pollen grains (Graham, 1988) have suggested a wet and warm environment, more likely to resemble the conditions of modern rainforests forests in Panama. Kirby and MacFadden (2005) and Kirby et al. (2008) studied body size of mammals, generally indicating a peninsular connection to North America with drier climate. Retallack and Kirby (2007) reported drier and cooler conditions for the Miocene based on paleosols. In another study about *Cynorca occidentale* , a mostly herbivorous mammal, (McFadden et al., 2010) interpreted this animal to have occupied a variety of environments, ranging from forested to open country habitat mosaics and fed on the diverse array of available plants, all suggesting a drier tropical climate. Herrera et al (2010) reported plant families mainly adapted to warm and humid conditions with a mix of biogeographical elements from North and South America, based on fossil endocarps.

8.2. TECHNIQUES OF ANALYSIS RELATING CLIMATIC VARIABLES AND WOOD ANATOMICAL DATA.

8.2.1. Tree-rings and climate

The first method to study the Miocene climate of Panama involves analysis of tree-rings. In this section, I give some background on the application of tree-rings to past climate before using examples from the fossil woods described in Chapters 4-6 to interpret palaeoclimate.

8.2.1.1. Tree rings and factors causing their formation:

Tree rings are defined as an increment of wood during a single growth period (Esau, 2006; see Chapter 3). They are most commonly formed by fluctuations in temperature; however, in the tropics, rainfall variations may be a more significant factor, and even internal endogeneous rhythms related to flowering may be a factor in their generation (Jacoby 1989). Presence/absence of growth rings are understood as a record of a varying degree of both external and internal conditions (Creber and Chaloner, 1984).

Growth rings are probably the better known approach to relate wood anatomical features to climatic variables (Poole and Van Bergen, 2006). The production of an entire season's
growth of wood is genetically controlled, so it varies among species, but external factors have greater influence on it (Creber and Chaloner, 1984).

Growth rings mark the contrast between active radial growth and dormancy. The most typical external factors influencing growth ring occurrence are: light, temperature, rainfall, available soil water and length of the growing season (Kozlowski and Pallardy, 1997). These factors are also linked to the variation in width of individual rings among years (Esau, 2006).

The “visual distinctness” of the growth rings is the structural difference between the xylem produced in the early and late parts of the growing season. In trees growing in temperate latitudes, the cambial activity ceases during the winter, thus corresponding between the rings and calendar years (Creber and Chaloner, 1984). In temperate woods the early wood has wider cells and proportionally thinner walls compared to more dense late wood with narrower cells and proportionally thicker walls. In most species the early

wood of a given season merges more or less gradually with the latewood of the same season, but then the boundary between the latewood of one season and the early wood of the following season is typically sharp.

8.2.1.2. Variation of width in growth rings:

The width of growth rings may vary from year to year, because it is well correlated with environmental changes in temperature and availability of water and light (Esau, 2006). Therefore, the variation in the growth ring width can be used as an index of the rainfall and temperature in a particular year. Under favorable conditions (adequate and abundant rainfall), the growth ring will be wide and under less favorable conditions, the ring will be narrower (Chaloner, 1990; Esau, 2006). Therefore, growth rings do not only provide information on climates in the past, but they also are informative on the productivity in specific seasons and favorable/non favorable conditions. The ring width can vary with different ontogenic stages in the same species, as well as in different parts of the same specimen (lateral branch vs main stem) (Gasson 1985, 1987a, 1987b; Poole and Van Bergen., 2006). This can be an issue when studying fossil woods, since in many cases it is difficult to recognise if dealing with mature or juvenile specimens.

8.2.1.3. Types of growth rings:

Growth rings are of variable distinctness, depending on the species and the conditions of growth (Schweingruber, 1988). The IAWA (1989) list of features for hardwood identification classifies ring boundaries in two categories: growth ring boundaries **distinct,** that is "a growth ring with an abrupt structural change at the boundaries between them, usually including a change in fibre wall thickness and/or fibre diameter" and the growth ring boundaries **indistinct or absent**, that are "growth

rings vague and marked by more or less gradual structural changes at their poorly defined boundaries or not visible". Among the structural changes that can mark boundaries are: thick-walled and radially narrowed latewood fibres or tracheids; semi-ring porous and ring-porous wood (see Chapter 3); marginal parenchyma (see Chapter 3), decreasing frequency of parenchyma bands towards the latewood resulting in distinct fibre zones, and distended rays among others.

Other conditions such as fire, frost, drought, flooding, defoliation and increased light towards the end of the growth season can produce a gradual decrease and subsequent increase in cell diameter, but that is not continous around the circumference of the tree. These rings are considered "false" or "traumatic" rings and they seem to be very commonly restricted to juvenile trunks and lateral branches (Worbes, 1989; Poole et al., 2006).

8.2.1.4. Growth rings in tropical trees

Although tree rings are easily observed and best studied in temperate trees, tropical trees can also develop growth rings. Growth rings in tropical trees may or may not represent anual increments, e.g., several rings can be formed in one single year due to several wet and dry periods occurring within a year (Duke et al., 1981; Jacoby, 1989; Creber and Chaloner, 1984; Myburg and Sederoff, 2001).

Determination of growth rings in tropical trees has been largely controversial and the parameters to classify them are still not well understood. Probably the main factor inducing formation of growth rings in tropical trees is water availability (Bräuning et al., 2008). Studies report the formation of distinct growth rings in tropical trees with a dry season of at least 2 months with less than 50 mm of rain (Worbes 1999; Dunisch et al. 2003; Fichtler et al. 2003). However, it seems boundaries marked with

parenchyma bands are a more common feature in tropical woods than in temperate woods (Gourlay, 1995). Studies of growth rings of African *Acacia* species suggest a strong relationship between rainfall peaks and production of marginal parenchyma (Gourlay, 1995). Although marginal parenchyma is most commonly seen in the Fabaceae (Banks and Gasson, 2000) and so genetically controlled, marginal parenchyma has a functional significance mainly related to starch storage. Carlquist (1988) found that marginal parenchyma could promote conduction when the growth season (wet season) was renewed and the starch supported rapid flushes of growth, flowering and fruiting.

8.2.1.5. Analysis of growth rings

Several of the methods to analyse growth rings are considered difficult to define consistently and somewhat arbitrary (e.g., amount of early and late wood, X-ray densitometry) (Creber and Chaloner, 1984). One of the problems affecting the utility of these techniques is that in some woods, especially in tropical woods, several rings per year can be produced, so establishing the boundaries of the beginning and end of the growing season is uncertain. Those rings are called non-annual growth rings and their occurrence can be correlated with several factors: fire, drought, disease, floods and defoliation among others (Creber, 1977).

Although growth rings offer a rich record of paleoclimatic data, they have to be used carefully, because fossils can be misinterpreted frequently and ideally an analysis should include at least 20 specimens of fossil wood, and as many taxa as possible to get a range of variability of ring types present in an assemblage. Ring patterns are more useful if derived from known organs seen in relation to the whole trunk diameter (Francis and Poole et al., 2002). In general, a high percentage of woods in a fossil assemblage with distinct rings would be considered indicative of some sort of

seasonality (Wheeler and Manchester, 2002), and as noted above, in a tropical climate, the source of that seasonality would probably be precipitation.

In this chapter, I utilize only the presence/absence of growth rings and I examine the specific changes in cambial products related to the growth ring boundaries.

I also make direct comparison with ring types in modern tropical dry/wet forests from Panama to improve climate interpretation.

8.2.2. Weimann multivariate analysis:

The second palaeoclimate technique used here involves multivariate analysis of wood anatomical properties. Wiemann et al. (1998, 1999) developed equations to predict climatic conditions based on wood anatomical characters. Their studies consisted of a compilation of data from the literature from 37 sites in North, Central and South America, Africa, Malaysia and the Pacific Islands. Thirty three of thirty seven sites were low elevation, and other sites were mountainous. In order to reduce bias, the low elevation sites were chosen to be all less than 500 m of elevation and the mountainous sites were between 500m and 900 m. Additionally, latitudinal range and precipitation were taken into account. The wood types were often genera, with some occasional species types. Each site had at least 25 wood types. Climatic data were obtained from Wernstedt (1972); De la Sota (1972) and NOAA (1985). 50 wood anatomical characters were originally tested with stepwise regression. The climatic variables of interest were MAT (Mean Annual Temperature), MART (Mean Annual Range Temperature), MAP (Mean Annual Precipitation), CMMT (Coldest Month Mean Temperature), DMP (Driest Month Precipitation) and DRY (Length of Dry Season, in months). The

regressors (anatomical variables) with high significant correlation coefficients ($r2 > 0.50$, $p < 0.01$) were selected to produce the equations.

The ten climate-significant characters selected were: multiple perforation plates, spiral thickenings present in vessels, vessel mean tangential diameter less than 100 µm, fibres septate, rays commonly more than 10 cells wide, rays heterocellular with 4 or more rows of upright cells, rays storied, axial parenchyma absent or rare, marginal parenchyma and wood ring-porous. The equations were tested in 13 new "validation sites" or sites where the actual data were known, so the predictions could be evaluated (see Table 5, Wiemann et al., 1998). MAP, unexpectedly, was poorly correlated with wood anatomical characters and the equation for MAP generally overestimated precipitation in the validation sites. This consistent overestimate might be because several of the original used sites to derive the equations had very high rainfall. Also the DRY (dry season duration) gave very inaccurate predictions. The authors explain that it could be due to the way of measuring of the climatic data, so instead of considering dry season as the number of months with less than 50 mm of precipitation, it should be measured in terms of the number of consecutive weeks or days without precipitation.

Since MAT (Mean Annual Temperature) was the climatic variable with the highest correlation to the wood anatomical characters, Wiemann et al. (1999) derived further equations, using 42 new sites in North, Central and South America, England, Africa, Malaysia and the Pacific Islands. The sites were then divided into regression sites and validation sites. 12 wood anatomical characters were used in Wiemann et al. (1999) and equations for calculation of MAT were derived as a function of frequencies of wood anatomical characters using regression procedures on transformed and untransformed data.

The regression equations derived using arcsine transformation were comparable to those obtained from untransformed data, but the equations using transformed data gave more reliable predictions. These equations were then applied to fossil wood assemblages from North America to calculate paleotemperature. The selected fossil wood sites had at least 25 different types of wood.

Wiemann et al. (1989) point out that the equations could be improved with improved datasets, which would be ideally collected from the woods directly and not from databases or literature since the measurement and descriptions might vary if produced by different authors. Nonetheless, they considered that those equations were probably acceptable and the predicted values were comparable with the known values in the validation sites, even considering the limitation of such a development of predictors.

8.3. METHODS

8.3.1. Growth rings percentage of occurrence

All the prepared fossil wood specimens previously thin-sectioned for systematics were observed in order to determine the presence or absence of growth rings. For some morphotypes, e.g., Wood Type 5 (Malvaceae) several specimens were observed.

Interpretation of growth ring distinctiveness varies between authors, e.g., in tropical trees studied in La Selva, Costa Rica, woods of *Guatteria aeruginosa*, *Protium pittieri* were described as having distinct rings (Fichtler et al., 2003). However, they do not appear distinct in the images (see Fichtler et al., 2003; Figure 2). In contrast, descriptions in IWD code *Lannea afzelii* as having variable rings (distinct to indistinct),

however in the images, the rings look rather indistinct. In this thesis the rings were classified according to the IAWA, 1989 terminology (see Figure 8.1).

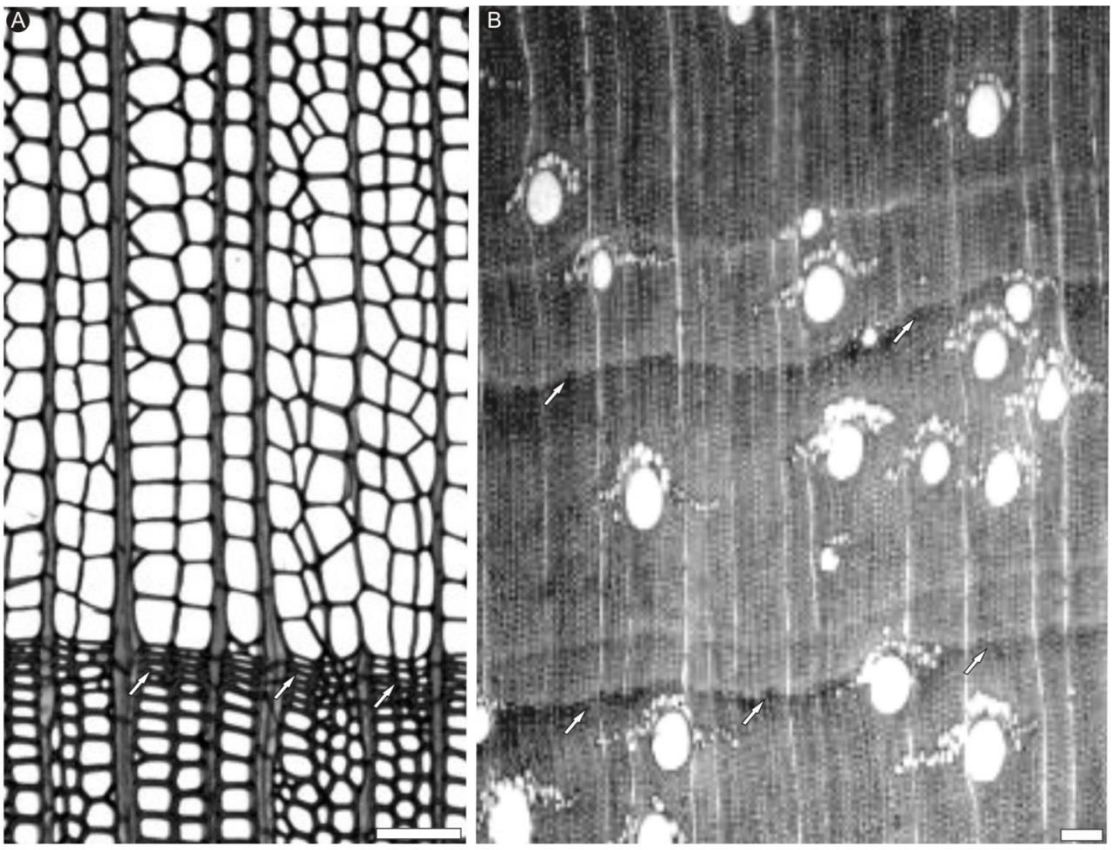

Figure 8.1. A, *Tetracentron sinense* (Trochodendraceae) with typical distinct ring (arrows) marked by radially narrowed fibres; B, *Asteropeia multiflora* (Asteropeiaceae) with indistinct rings (arrows), marked by marginal band of parenchyma. Scale bars: A=100 µm, B=150 µm. Images and information taken from IWD.

Rings are termed **distinct (**1), when the "growth ring has an abrupt structural change at the boundaries between them, usually including a change in fibre wall thickness and/or fibre radial diameter" and **indistinct or absent** (0), when "the growth rings are vague and marked by more or less gradual structural changes at their poorly defined boundaries or not visible, Thus, all the species with indistinct rings or absent rings were considered together in a single category (0). The same criterion was also

applied to modern woods. The difficulties with classifying growth rings in tropical woods are further discussed in Chapter 9.

The change in cambial products that established the boundary from one ring to another is recorded in the Appendix 8.3.1.a, 8.3.1.b., 8.3.1.c Examples of the rings in the fossil woods are provided in Figure 8.2 and in modern species are shown in figure 8.3. It is important to note that the growth ring analysis here only includes classification of distinctness and description of the variation in cambial products. I avoided including measurements of ring width to estimate productivity or density because of some ambiguities and this work is primarily aimed at inferring the seasonal or non-seasonal character of wood assemblages of Panama.

For the fossil woods, the same sections studied in Chapters 4, 5, 6 were used. The modern woods were cores collected from two types of forests in Panama. The wood samples representing wet forests were collected from Barro Colorado Island (BCI; 9° 09’ 00’ N and 79°51’ 00’ W) a 1560 ha island located in Gatun Lake in the Panama Canal, where the Smithsonian Tropical Research Institute has based a primary site for the study of lowland moist tropical forests. BCI has a mean annual precipitation (MAP) of 2600 mm and a mean annual temperature (MAT) of 27 ˚C. The wet season extends typically for at least 9 months. The island is covered by semi-deciduous lowland moist tropical forest. (Dietrich et al., 1982; Grimm et al., 2008; STRI, 2014). For the dry forests, the samples were obtained from three localities where the dry season is typically well marked and lasts 4 to 5 months per year (Lopez, pers. comm.): Coronado (8° 31’ 0’’ N and 79° 53' 0’’W; MAP: 1752 mm), a beach community in the Pacific Coast, where the dry forest area covers approximately 45 ha, with a MAP 1327 mm and 26 ˚C; Achotines (7° 15’ 30’ N and 80° 00’ 15’ W; MAP: 1641mm), a station for the tuna fish breeding and research, with 70 ha of dry forests, MAP 1650 mm and MAT 28˚C

(www.biotapanama); and Divisa (8° 8’ 0’’N and 80° 41’ 0’’), where the dry forest patch covers approximately 5 ha that extends alongside the Santa Maria River, Veraguas. Divisa has a MAP of 1375 mm and a MAT 28 ˚C. Only samples of mature trees were included for all the analysis. All the samples are housed in the Botany Institute, BOKU (University of Natural Resources and Life Sciences, Vienna, Austria).

For the BCI samples, previously prepared stained transverse sections of 289 species were available to record data and 47 transverse sections were prepared for the dry forests.

The terminology and procedure followed to classify rings for the fossil woods, was also used for the modern samples.

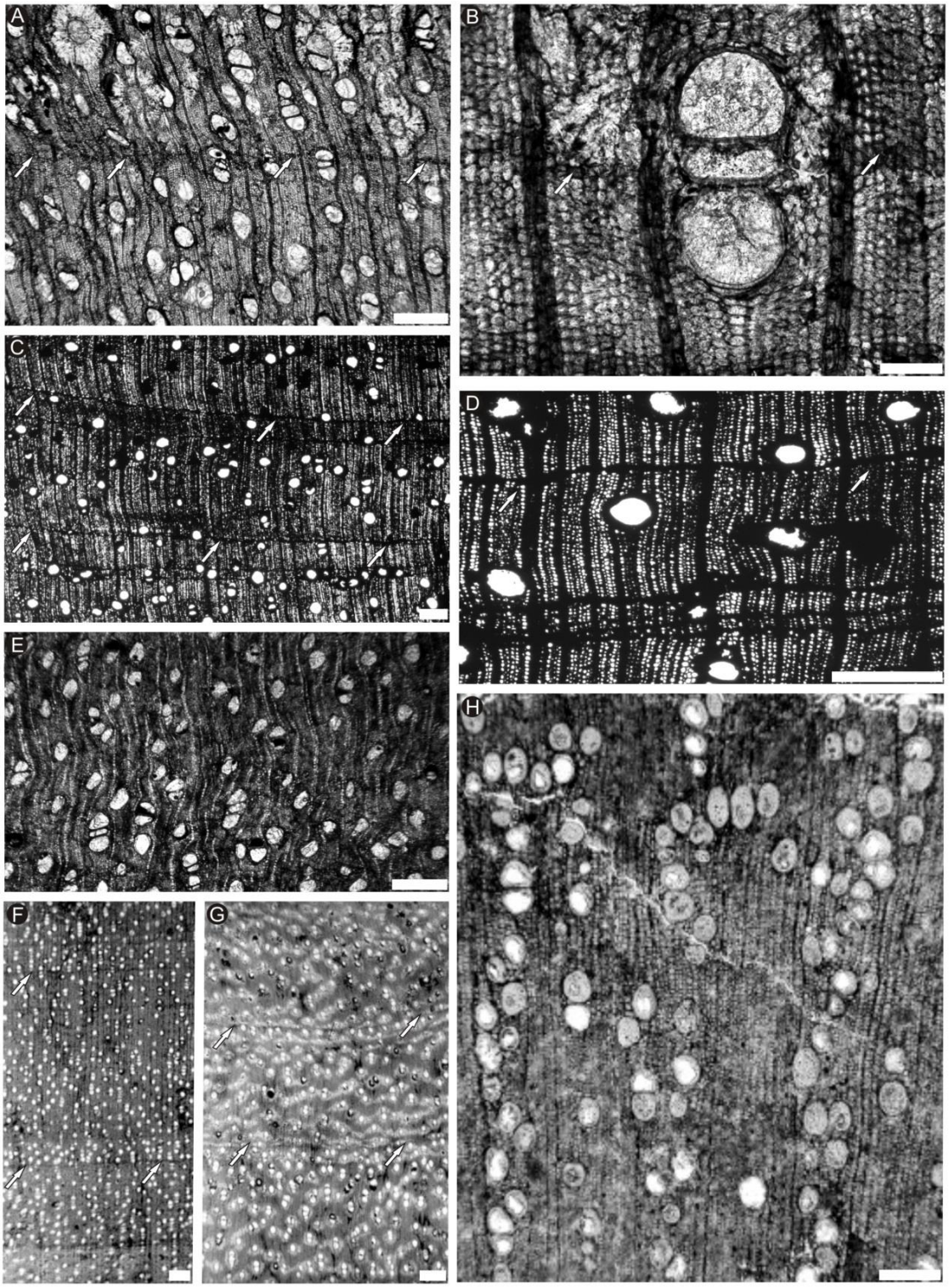

Figure 8.2. A- E, Examples of growth rings in fossil woods from the Cucaracha Formation. The boundaries are marked by arrows. A,B, STRI 36273 (Fabaceae) with indistinct rings, boundary marked by marginal parenchyma. C,D, STRI 21046, with indistinct rings, boundary marked by marginal parenchyma bands. E, STRI 14151 (Malvaceae) with absent growth rings. F, *Cynometroxylon* with boundaries marked by marginal parenchyma bands. G, Fejej Group III-Wood Type 4 with indistinct rings and boundaries marked by marginal parenchyma bands. H, *Carpinoxylon ostryopsoides* with absent rings. Scale bars: B= 100 µm; A, C, D, E= 500 µm; F, G, H= 200 µm. Images F-H taken from Inside Wood.

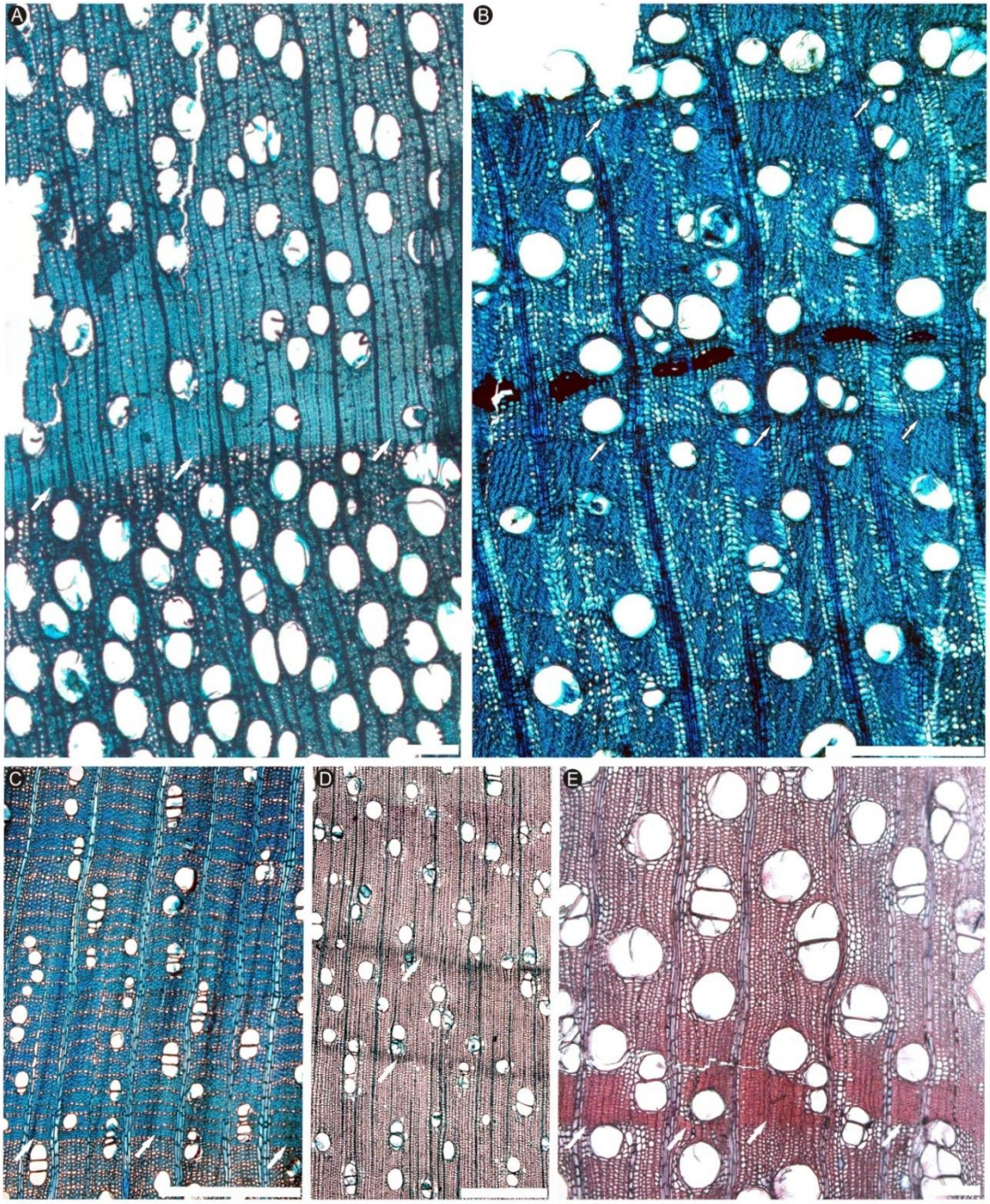

Figure 8.3. Growth rings in modern plants of BCI with boundaries marked by arrows A, *Hyeronima alchoerneoides*(Euphorbiaceae) with distinct rings and boundaries (arrows) marked by thickened fibre walls; B, *Cordia alliodora* (Boraginaceae), distinct rings with boundaries marked by tangential lines of vessels; C, *Duguetia confusa* (Annonaceae), indistinct rings with boundaries marked by thick-walled fibres; D, *Ocotea insularis* (Lauraceae), indistinct rings with boundaries marked by fibres radially narrowed; E, *Nectandra globosa* (Lauraceae), distinct rings with boundaries marked by thick walled fibres. Scale bars: A, B, C= 500 µm; D= 250 µm; E=200 µm.

8.3.2. Wiemann multivariate analysis using wood anatomical characters

To record data such as proportion of rays > 10-seriate, storied rays and septate fibres, 77 tangential longitudinal sections were prepared to record further wood anatomical data from the wet forests. Because of constraints in time, not all the 289 species from BCI were sectioned. Tangential longitudinal sections were also produced for 37 cores from the dry forests. Each sample was sectioned in a Leica microtome calibrated at 25-30 µm. The best sections were stained and mounted onto microscope slides and imaged. Wiemann et al (1998, 1999) equations were applied to fossil and modern wood assemblages. For the fossil assemblages, a datamatrix in Appendix 8.4.a was produced for these characters: presence/absence of tangential vessel arrangement, presence/absence of spiral thickenings, rays >10-seriate, exclusively homocellular rays, presence/absence of storied rays, absent or rare parenchyma, presence/absence of paratracheal parenchyma, presence/absence of marginal parenchyma, mean vessel diameter <100 µm, presence/absence of multiple perforation plates (scalariform perforation plates), presence/absence of septate fibres, presence/absence of ring-porous wood, heterocellular rays with >4 rows of upright cells.

The characters were coded as "1", for present; "0", for absent, "0.5" for variable characters and "?"for uncertain character states, e.g., *Eleaocarpus*- Wood type 3 was coded 0.5 for septate fibres, because it alternates septate and non-septate fibres. The proportion of each character was obtained to be applied in the equations. For the fossil woods, I used the three standard sections (TS, TLS, and RLS), however, for the modern woods, RLS sections were not prepared, because of constraints of time so those were not available to record certain characters (e.g., heterocellular rays >4 rows of upright cells). The datamatrix for the modern woods is provided in Appendix 8.4.b. Firstly, all the equations from Wiemann et al (1998, 1999) were tested in the modern wood dataset.

The predicted values were compared to known values in the nearby forests and those that yielded comparable values were applied to fossil wood assemblages. However, because for the fossil woods, there were RLS available and more data could be recorded directly from the specimens, a few extra equations were included here (See Table 8.5).

Certain characters were difficult to record for some of the fossils. For the rays >10-seriate, the *Periplanetoxylon* type was coded "0" because only mature specimens were included in the analysis, despite the inferred young material having rays exceptionally wide >10-seriate. Marginal parenchyma was coded 0.5 in the *Prioria* wood type because it was occasionally present. Corrections for shrinkage were also applied (33%) for the mean vessel diameter of the charcoalified woods. The character "heterocellular rays >10-seriate was coded as "?" in a few cases, because some morphotypes had unclear RL sections. The equations from Wiemann (1998, 1999) were applied and MAT, CMMT, MART, MAP, DRY were calculated.

8.4. RESULTS

8.4.1. Growth ring percentage occurrence

In the Cucaracha Formation, none of the woods has distinct rings, and rings are only present (but indistinct) in 10 % of observed specimens. Appendix 8.3.1.a. provide growth ring information data of each wood specimen. Most of the rings were marked by marginal parenchyma bands, but these specimens are Fabaceae, related to *Prioria* (see Chapter 4, 6). Marginal parenchyma bands are common in the Fabaceae (Gasson et al., 2003). The percentage of growth rings with distinct boundaries in the Cucaracha Formation out of 30 different observed specimens is 0. Comparatively growth rings were present (but indistinct) in 11% of a total of 289 species from BCI, from which only

2% had distinct growth rings rings. In dry forests indistinct growth rings were observed in a 17% of the species with only 13% showing distinct growth rings. (Appendix 8.3.1.b, 8.3.4.1.c).

Most of the species from BCI with distinct rings showed boundaries marked by changes in the fibre wall thickness (Table 8.3.1.b), especially in the Annonaceae. In the dry forests, the rings were also marked because of changes in the wall thickness, but no particular family was characterised by this feature.

8.4.2. Wiemann analysis

The first two equations applied to both modern and fossil wood assemblages were 12 and 15. Wiemann et al., (1999) obtained the best results using those equations and suggested those as the best to use with fossil wood data.

For the equations 12 and 15 applied to the modern wood dataset herein, the predicted MAT (22.7 ˚C, 21.7 ˚C; Table 8.1) are slightly lower than the modern known parameters in BCI and Buena Vista (towns close to BCI) where MAT ranges from 25-27°C (ETESA, 2014). However, for the Cucaracha Formation woods, the values (16.7 ˚C, 13.2 ˚C; Table 8.4) are much lower in comparison to the nearby modern known forests. Interestingly those values are comparable to those reported in Retallack and Kirby (2007, 15 - 16°C), using equations derived from extensive databases of modern soils. Other equations from the Wiemann methods gave additional similar values with regard to the known in modern nearby vegetation, e.g., 29.3 ˚C with equation 3, 22.8 ˚C with equation 6 (Table 8.5).

Other variables such as MART, CMMT, MAP and DRY were also obtained for the modern woods (Table 8.3) and the Cucaracha Formation assemblage (Table 8.6), using equations of Wiemann et al (1998). MART was erratic (Table 8.6), as expected

because CMMT and MART were also erratic in the Wiemann tests (Wiemann et al., 1998). MAP and DRY calculations were also generally erratic (Table 8.6).

	Equation	Applied equation (BCI+dry)	Predicted MAT (°C)
12	24.78 + 36.57 (stor) – 15.61 (marg) – 16.41 (abs)	24.78 + 36.57 (0.21) - 15.61 (0.27) – 16.41 (0.34)	22.7
15	17.07 +25.23 (stor) – 23.17 (abs) + 13.79 (sept)	17.07 + 25.23 (0.21) – 23.17 (0.34) + 13.79 (0.52)	21.7

Table 8.1. Wiemann et al. (1999) suggested equations as best predictors of MAT. The equations are applied to modern wood Panama assemblages (wet and dry). Stor=storied rays; marg= marginal parenchyma; sept=septate fibres.

Number of equation	Equation	Applied equation BCI+dry)	Predicted MAT (°C)
Equations using no transformed data			
2	21.31 + 0.855 (stor) – 0.258 (marg)	21.31 + 0.855 (4.4) – 0.258 (7)	23.3
4	25.14 + 0.785 (stor) – 0.188 (marg) – 0.500 (abs)	25.14 + 0.785 (4.4) – 0.188 (7) – 0.500 (11.4)	21.5
Equations using Arcsine transformed data			
10	21.70 + 38.23 (stor) – 20.29 (marg)	21.70 + 38.23 0.21) – 20.29 (0.27)	24.2

Table 8.2. Wiemann et al (1999) equations applied to modern woods where the predicted MAT is comparable to known modern climate data for the area. Stor= storied rays; marg=marginal parenchyma; abs= absent parenchyma.

Climatic variable	Equation	Applied equation (BCI+dry)	Predicted climatic variables
MAP (cm)	-6.06 + 6.332 (sept) + 0.7901 (abs)	-6.06 + 6.332 (24.4) + 0.7901 (11.4)	238.5
DRY (months)	6.81 – 0.186 (mult) – 0.122 (sept)	6.81 – 0.186 (6.14) – 0.122 (24.4)	3

Table 8.3. Equations from Wiemann et al. (1998) applied to modern woods from Panama to calculate MAP (Mean Annual Precipitation) and DRY (Duration of dry season) applied to modern wood assemblages of Panama. Sept= septate fibres; abs= absent parenchyma; mult=multiple perforation plates.

Number of equation	Equation	Applied equation (Cucaracha Formation)	Predicted MAT (°C)
12	24.78 + 36.57 (stor) – 15.61 (marg) – 16.41 (abs)	24.78 + 36.57 (0) - 15.61 (0.21) – 16.41 (0.29)	16.7
15	17.07 +25.23 (stor) – 23.17 (abs) + 13.79 (sept)	17.07 + 25.23 (0) – 23.17 (0.29) + 13.79 (0.21)	13.2

Table 8.4. Wiemann et al. (1999) suggested equations as best predictors of MAT. The equations are applied to fossil woods from the Cucaracha Formation.

In general, the MAT obtained from the modern woods using the equations seems to be slightly lower or slightly higher (e.g., 29.3 ˚C with equation 3) than the known climate values of MAT of BCI (25-27◦C) (ETESA, 2014), especially when using the equation 4 (Table 8.2). Non transformed equations seem to be more suitable based on the results of these BCI species. MAP (239.7 cm) and DRY (3 months) obtained values with modern woods were closer to actual parameters of BCI forests in contrast to the values from fossil wood assemblages (Table 8.6).

Number of equation	Equation	Applied equation (Cucaracha Formation)	Predicted MAT (°C)
	Not transformed		
2	21.31 + 0.855 (stor) – 0.258 (marg)	21.31 + 0.855 (0) – 0.258 (4.2)	20.2
*3	37.76 – 0.404 (<100µm) + 0.277 (RP)	37.76 – 0.404 (20.8) + 0.277 (0)	29.3
4	25.14 + 0.785 (stor) – 0.188 (marg) – 0.500 (abs)	25.14 + 0.785 (0) – 0.188 (4.2) – 0.500 (8.3)	20.1
*6	28.91 – 0.230 (homo) + 0.781 (stor) – 0.501 (abs)	28.91 – 0.230 (8.3) + 0.781 (0) – 0.501 (8.3)	22.8
*7	38.17 + 0.266 (mult) – 0.212 (spir) – 0.437 (<100µm) + 0.391 (RP)	38.17 + 0.266 (0) – 0.212 (0) – 0.437 (20.8) + 0.391 (0)	29.1
*8	7.46 + 0.428 (tang) + 0.309 (mult) – 0.277 (spir) – 0.169 (homo) + 0.377 (para)	7.46 + 0.428 (0) + 0.309 (0) – 0.277 (0) – 0.169 (8.3) + 0.377 (41.7)	21.8
	Arcsine transformation		
10	21.70 + 38.23 (stor) – 20.29 (marg)	21.70 + 38.23 (0) – 20.29 (0.21)	17.4

Table 8.5. Equations from Wiemann et al. (1998) applied to woods from the Cucaracha Formation . stor= storied rays; marg=marginal parenchyma; <100= Mean Tangential Vessel Diameter < 100 µm; abs=absent parenchyma; homo= homocellular rays; spir= spiral thickenings; mult= multiple perforation plates; tang= vessels arrange tangentially; para= paratracheal parenchyma.

Climatic variable	Equation	Applied equation (Cucaracha Formation)	Predicted climatic variables
MART (˚C)	4.16 + 0.319 (spir) + 0.135 (<100µm) – 0.373 (>10 ser) – 0.154 (het 4+)	4.16 + 0.319 (0) + 0.135 (20.8) – 0.373 (8.3) – 0.154 (40)	- 2.29
CMMT (˚C)	9.91 – 0.355 (spir) – 0.098 (<100µm) + 0.845 (>10 ser) + 0.368 (het 4+) + 0.528 (stor) – 0.210 (abs)	9.91 – 0.355 (0) – 0.098 (20.8) + 0.845 (8.3) + 0.368 (40) + 0.528 (0) – 0.210 (8.3)	27.9
MAP (mm)	-6.06 + 6.332 (sept) + 0.7901 (abs)	-6.06 + 6.332 (4.2) + 7.901 (8.3)	86.1
DRY (months)	6.81 – 0.186 (mult) – 0.122 (sept)	6.81 – 0.186 (0) – 0.122 (4.2)	6

Table 8.6. Equations from Wiemann et al. (1998) applied to modern woods from Panama to calculate MART (Mean Annual Range Tempreature), CMMT (Coldest Month Mean Temperature), MAP (Mean Annual Precipitation) and DRY (Duration of dry season) applied to fossil wood assemblages of Panama. Sept= septate fibres; abs= absent parenchyma; mult=multiple perforation plates; spir= spiral thickenings; <100= Mean Tangential Vessel Diameter < 100 µm; .10ser= rays.10 seriate; het 4+= rays heterocellular with more than 4 rows of marginal cells.

8.5. DISCUSSION:

8.5.1. Growth ring percentage and type in fossil and modern assemblages

Studies in tropical areas indicate a considerably higher percentage of distinct growth rings in seasonal environments, e.g., a modern forest in Venezuela showed 50% of species with distinct rings in a deciduous forest, 31% in a facultative deciduous forest and 43% in an evergreen forest. This forest is characterised by a dry season of 3 months with less than 50 mm of precipitation (Worbes, 2002), from which it would be expected

to have a well-marked seasonality in several species. In contrast none of the fossil woods from the Cucaracha Formation have distinct growth rings and do not suggest these trees were growing in seasonal conditions, similarly to the wet modern forests (BCI) with 2% of distinct rings. The modern dry forests compared herein had 13% of distinct rings that is higher compared to the modern wet forest analysed herein, but still low in contrast to the seasonal forest in Venezuela (Worbes, 2002). Therefore, neither of the Panamanian wood assemblages (Miocene or Modern) reflects seasonal environments.

The Fabaceae from the Cucaracha Formation include species with indistinct ring boundaries marked by marginal parenchyma. The formation of marginal parenchyma has generally been considered to mark the start of growth periods in tropical trees. In IAWA (1989) marginal parenchyma is defined as parenchyma bands commonly related to growth rings. Carlquist (1988) suggested that the marginal parenchyma is strongly related with promoting conduction when growth was renewed during the wet season because it is related to starch storage to support rapid flushes of growth and fruiting. However in some species, it is difficult to recognise the zones where the growth season starts. In some studies, marginal parenchyma has also been related to flooding periods (Schöngart et al., 2005). According to Gourlay (1995), the marginal parenchyma bands can usually be distinguished from the frequently intra-seasonal banded parenchyma by their fineness, by more regular spacing between broader bands, in contrast to the more irregular, wavy, confluent intra-seasonal bands. However such a classification was not applied here, because measurements of growth ring width were not made, and only data on distinctness and type of cambial changes were recorded.

In the modern wood assemblages, most of the boundaries are marked by changes in fibre wall thickness. An increase in the fibre wall thickness is recognised as an adaptation to compensate for high non-mechanical tissue proportions. Thick walled fibres seem to be common in drought-adapted species, so overall there is a positive correlation between hydraulic safety, wood density and mechanical strength (Hacke et al., 2001, 2006). In the fossil wood assemblages, such changes in fibres were not observed, so it could suggest that the trees from the Cucaracha Formation were developing in similar conditions to a modern tropical wet forest.

8.5.2. Climatic variables predicted by Wiemann equations in fossil and modern assemblages

The applied Wiemann equations to fossil wood assemblages gave MAT values that differ by 3.5°C when using equation 12 in contrast to equation 15 (Table 8.4). Similar values of difference were found in the Post site (late Eocene, Oregon) reported in Wiemann et al. (1999) and are also consistent with previous results from modern validation sites.

From all the tested equations in the Cucaracha Formation, the predictions with closer values to modern known surrounding forests were obtained using the equations 3, 6 and 7 (Table 8.5) in which, proportions of characters such as mean vessel tangential diameter <100 µm, ring-porous woods, exclusively homocellular rays, storied rays, absent or rare parenchyma, spiral thickenings and multiple perforation plates were applied in the equations.

As stated previously in Wiemann et al. (1998, 1999), the more reliable predicted variable is MAT, however the precision on the predictions increase with a larger

number of specimens (25 at least). The low amount of wood types for the Cucaracha Formation included in these tests probably limit reliable predictions. Based on the identified wood types from this thesis, and supported by previous studies on pollen (Graham, 1988) and seed and fruit assemblages (Herrera et al., 2012), the Miocene flora of the Cucaracha Formation had fairly similar ranges of temperature and humidity to the modern nearby Panama forests.

These equations consistently overestimate MAP, because precipitation above 145 cm has no further effect on physiognomy of woods (Wiemann et al., 1998); Similarly, DRY equations probably need improvement according to Wiemann et al. (1998) and calculations tend to be biased (See Section 8.2.6) . The values obtained for MAP (239.7 cm) and DRY (3 months) in the modern assemblages tested here are much more consistent with known modern values than the results from the fossil wood assemblages, where the values in MAT and MAP were lower. Wiemann et al. (1999) pointed out that these equations are reasonably accurate when the number of wood types is sufficiently large, which is confirmed in the predictions obtained from the modern wood assemblage.

The equation to calculate MART generally gives negative values for both the Cucaracha Formation and the modern wood assemblages. However, Wiemann et al. (1998) already noted errors and stated the inaccuracy of that equation. Looking at the equation to predict MART applied to the Cucaracha Formation assemblage , I see that the proportion of heterocellular rays (het 4+) in the Cucaracha Fm is high in comparison to a very low spiral thickening proportion, and then when subtracting from this, the estimation gives a negative value. Another major issue in the results seems to be the CMMT, which gives values higher than the MAT, e.g., CMMT= 27.9 ˚C vs MAT= 22.8

with equation 6. Some of the Wiemann et al. (1998) work gives similar results (see Table 5, Wiemann et al., 1998).

No definitive conclusions can be drawn from the study of the Cucaracha Formation woods, since it only included 13 different wood types (30 different specimens). Additionally, it is not ideally suitable because the wood types come from different levels in the Formation, combining woods of different ages and undergoing different fossilization processes. Wiemann et al. (1999) stated that a minimum number of 25 wood types would be appropriate to obtain more accurate predictions from those equations. Therefore, the data on fossil woods presented herein provides only a first approach to palaeoclimatological inferences with wood anatomical data of woods of Panama.

Few palaeoclimate studies have been performed using wood characters, and the Wiemann equations have not been applied to examples from Central America. Perhaps the most appropriate comparison is with the study by Martinez-Cabrera and Cevallos-Ferriz (2008) where wood anatomical characters were applied to infer forest types from fossil wood assemblages in the Early Miocene El Cien Formation in Baja California. Their results suggested the flora in Baja California was more likely to be mesomorphic in contrast with the modern highly desertic flora. They obtained MAT values of 22.7 - 24.8 ˚C from Wiemann equations with untransformed data. The calculated MAP was lower in Mexico (754 mm) in contrast to the Cucaracha Formation (861 mm). Results from equations suggest that El Cien flora was growing under a tropical climate. Similarly, the obtained MAT in the Cucaracha Formation, together with the nearest living relatives of identified woods (e.g., *Pentaplaris*, *Prioria*, Sapotaceae type), mostly growing in tropical rainforests today, and the low percentage of growth rings, probably indicate a tropical climate.

8.6. SIGNIFICANCE OF APPLIED PALEOCLIMATOLOGICAL ANALYSIS IN PANAMA WOOD ASSEMBLAGES

A low percentage of distinctness in growth rings in both fossil and modern wood assemblages suggests there is no tendency to seasonality. Although the modern dry forests showed a higher percentage of species with distinct growth rings in contrast to the modern wet forest (BCI), the percentage is low for a seasonal forest. Predictions from Wiemann et al (1998, 1999) equations for MAP based on fossil wood assemblages suggest lower rainfall in contrast to known nearby forests in the Panama Canal (e.g., BCI), equally some of the predicted MAT were lower in comparison with modern known values. However, these predictions should be taken cautiously, because the number of tested wood types from the Cucaracha Formation is low, thus the predictions are not accurate from several of the equations.

CHAPTER 9: DISCUSSION

9.1. SUMMARY AND CHAPTER OUTLINE

The following is a brief summary of the findings of this thesis. Forty-three specimens of fossil wood have been sampled and studied at three localities (Centenario Bridge, Contractors Hill and Hodges Hill) in the Cucaracha Formation of Panama. The specimens comprise two different assemblages in different preservation states: (1) a calcified allochtonous assemblage from fluvio-estuarine facies and (2) a charcoalified/silicified autochthonous assemblage buried beneath a silicic ignimbrite (see Chapters 2 and 3). Specimens include eleven wood types within the following families: Cannabaceae (cf. *Celtis*), Fabaceae (cf. *Prioria*), Elaeocarpaceae (cf. *Elaeocarpus*), Malvaceae (*Guazumaoxylon miocenica*, *Periplanetoxylon panamense* and a third taxon not determinate at higher level), Sapotaceae, Melastomataceae, Meliaceae (?*Guarea*) and Arecaceae; two other specimens were not assignable to any family (Chapters 4-6). Charcoal reflectance of thirteen samples buried beneath the silicic ignimbrite comprising dicotyledonous and monocotyledonous woods were measured in order to estimate the minimum charring temperatures of these woods (Chapter 7). Finally, tree-analysis and multivariate anatomical analysis (Wiemann et al., 1998, 1999) were applied to modern and fossil wood assemblages of Panama to infer palaeoclimate (Chapter 8).

This discussion chapter places these new findings in a wider context and covers four main topics:

1- collection and preparation techniques for wood systematics used in this thesis;

2- the use of wood anatomical characters in systematics;

3- the wider distribution of those families recognised from the fossil woods;

4- palaeoclimatological studies based on wood anatomical characters.

9.2. COLLECTION AND PREPARATION TECHNIQUES FOR WOOD SYSTEMATICS

9.2.1. Collection and observations during fieldwork

9.2.1.1. Field observations to estimate forest density

Fossil woods, especially those in growth position, can provide information on forest density (Chaloner and Creber, 1990; Francis and Poole, 2002) which can be estimated using the spacing of in *situ* stumps in the field. To record tree spacing, some studies use the same methods as for modern forests. For example, Cúneo et al. (2003) marked an initial transect, and then recorded the occurrence of tree stumps every 10 m. However, it is difficult to apply this approach to fossil forests due to the variability of stump preservation (Thorn, 2005). In the Cucaracha Formation the overall number of stumps was small. Despite this, calculations of tree-spacing were made along a linear transect, by measuring the distance between stumps, following methods in Falcon-Lang et al. (2011).

15 stumps (13 dicots and 2 monocots) were recorded at the Centenario Bridge locality, because it was the only locality with sufficient exposure to measure them (see Chapter 2; Table 2.5). An even distribution was assumed in order to give a rough estimation (212 trees/ ha) of forest density. In tropical rainforests, studies have shown density of trees >10 cm dbh as follows: 530 trees/ha in Malaysia (Manokaran, 1990); 536 trees/ha in BCI, Panama (Bermingham et al., 2005); 647 trees/ha in Manaus, Brazil

(Gentry, 1990). In tropical dry forests, examples show tree densities (>10 cm dbh) of 155 trees/ha in the Santa Rosa National Park in Costa Rica (Chapman and Chapman, 1990); 437 trees/ha in Concepcion, Bolivia; 519 trees/ha in Nicaragua (Marin et al., 2004); 761 trees/ha at north of Minas Gerais in Brazil (Apgaua et al., 2014). Tree densities exemplified here are higher than the estimated tree density from the Cucaracha Formation, except for the dry forest reported from Costa Rica. However, because the sample size of *in situ* stumps from the Cucaracha Formation is small, this estimate may not be truly representative of the density of these Miocene forests.

9.2.1.2. Field observations necessary to estimate tree height

Niklas (1994) developed equations for "woody species", "non woody" species, and a combination of both, to estimate tree height based on basal tree diameters. In the application of these equations, "woody species" include specimens with secondary xylem or where the xylem represents more than 15% of the total stem volume. Non woody species were then pteridophytes, herbaceous dicots and palm species, which lack secondary xylem or with xylem less than 15 % of the stem volume. The equations are as follows: "woody species" ($\log_{10}H = 1.59 + 0.39 (\log_{10}D) - 0.18 (\log_{10}D)^{2}$" and "non woody species" ($\log_{10}H = 2.51 + 1.4\,l (\log_{10}D) + 0.03 (\log_{10}D)^{2,}$ (H = estimated height and D = measured diameter). The equations are based on measurements of 265 species from a wide range of plant types (e.g., herbaceous, shrubs, palm species, dicot trees). Niklas (1994) acknowledged numerous problems when using allometry to estimate tree height in fossil assemblages, e.g., in the use of the "woody species", there has to be assumptions about whether the wood specimens are from palm trees or dicots, which is occasionally difficult to ascertain in the field. This assumption can result in

overestimations of height (Niklas, 1994) because equations for exclusively "woody plants" in an assemblage differ significantly from the "non woody plants" equations. However, because of the wide range of plants used by Niklas (1994), these equations are extensively used and cited in the literature (e.g., Falcon-Lang and Bashforth, 2004; Parrish and Falcon-Lang, 2007; Artabe et al., 2007; Williams et al., 2008; Gulbarson et al., 2012) and are considered among the most complete and appropriate tools to estimate tree height based on data from the fragmentary fossil record.

It was possible to estimate the original tree height based on charcoalified logs and stumps from the Cucaracha Formation using the above equations for "woody" and "non woody". In order to apply those equations, diameters of logs and uprooted stumps were measured in the field, trying to avoid small logs or probable root samples. However, I note that the *in situ* stump diameters represent more reliable data than the measurements from logs, because the latter can represent parts of the same tree occasionally. For several specimens, it was not possible to establish a rigorous distinction of "woody samples" or "non woody samples" in the field, thus these calculations can provide a tentative idea of tree height in the Cucaracha Formation only. Also, palaeobotanists commonly face the problem of being uncertain whether or not the diameter of a fossil stem faithfully represents the diameter of the original tree, due to changes during fossilization and deposition (Niklas, 1994). The estimates of tree height imply trees up to 38 m (logs total range=6 – 20 m; *in situ* stumps total range= 11 – 38 m). Condit et al. (2006) studied allometry and regeneration requirements of trees from Barro Colorado Island, Panama. They established different categories of trees based on height: <10m, as treelets; 10–20 m, as mid-sized trees; >20m, as tall trees. Surveys from the 50-ha CTFS plot in BCI, Panama report a Mean Canopy Height of 27 – 34m (Wolf et al., 2012). Based on those categories and focusing on the diameter data measured

from stumps, the trees studied from the Cucaracha Formation would be considerably tall, probably being part of the canopy.

9.2.1.3. Field observations on stump orientation

In some assemblages, as in the Cucaracha Formation, where logs and stumps have been entombed by pyroclastic flows, orientation of the stumps and logs is useful to support information on the direction of the flows. The orientations are measured in the field and the data are plotted in rose diagrams to show the major tend. This approach has been used in several studies to infer direction of paleocurrents (e.g., Fritz and Harrison, 1985; see Gastaldo, 2004 and all related literature), direction of lava flows (e.g., Hayward and Hayward, 1995) and location of the vent (Fraggat et al., 1981). The use of fossil woods to determine paleocurrent direction is complex and datasets for this purpose are not very common (Gastaldo, 2004), although those are informative on geomorphology and paleoenvironmental relationships of the area (Gastaldo, 1994), e.g., bimodal orientation is characteristic of logs preserved in alluvial-fan deposits (Evans, 1991). In the Cucaracha Formation most of the stumps are uprooted and tilted towards the SSW (see Chapter 2), suggesting that the pyroclastic flows that entombed the trees came from a vent located to the NNE. An example of similar events where orientation of logs and stumps have been measured is the 1980 Mt St Helens eruption. Logs in St Helens were strongly horizontal and orientated by the flow and by subsequent fluvial processes. In all areas, horizontal logs were oriented parallel to the stream channel and not necessarily radially away from the vent peak as in the blast zone. In this case, wood orientation was used to infer paleocurrent direction. Another two examples of the use of tree orientation, include the: 1) Two Medicine Formation in Montana, USA. Two Medicine Formation contains a petrified forest consisting of >200 aligned, horizontal, silicified trees entombed

within a volcanic tuff and overlying bentonite. It is inferred that the Two Medicine trees were quickly buried by a powerful pyroclastic flow. The mean northeastern azimuthal component of the trees is interpreted to be the transport direction of the ash flow. The azimuthal range measured from the trees was used to confirm the position of the source vent, which revealed powerful pyroclastic flows that travelled long distances from a large caldera located at a northern area to the petrified forest (Roberts and Hendrix, 2000). 2) The lower Permian Chemnitz Petrified Forest, with an outstanding i*n situ* forest that enabled a detailed reconstruction of the original forest (Rößler et al., 2012). In the Chemnitz forest, the tree orientations were used to infer the direction of the eruption of the pyroclastic flows. Those trees were oriented in east-west direction, the top of the trees pointing westward, suggesting the major direction of the pyroclastic flows.

9.2.1.4. Collecting strategy to capture taxonomic diversity

Targeting wood types (e.g. softwood, hardwood, and palm trees) based on field observation of broken sections using a hand lens (Manchester 2006) would not only be useful to determine the appropriate equation to estimate tree height, (see section 2.5.2.4., Chapter 2; section 9.2.1.2., Chapter 9) but also would allow one aspect of diversity to be captured and help to avoid repetition of the same morphotype. Although this would be ideal, it is frequently hard to be certain of the distinction of wood types in the field, also certain conditions during field work (e.g. limitation of time) can also constrain the execution of such a task. Although it is not necessary to collect the whole log for taxonomic determination it is helpful to record the original preserved diameter of the sample (Wheeler and Manchester, 2002) for purposes such as estimating tree height (see section 9.2.1.2.).

The charcoalified assemblage was collected from three different localities (Centenario Bridge, Contractors Hill, Hodges Hill), whereas the permineralised

assemblage was derived from one locality, Hodges Hill. Therefore, more wood types might be expected from the charcoalified assemblage.

Results in Chapter 6 show that more diversity of wood types was found from the charcoalified assemblage than expected. In Contractors Hill and Centenario Bridge, the samples were collected walking along the charred layer, collecting samples that looked big enough (at least bigger than 8 cm in width) to potentially represent adult trees and also avoiding collecting samples that were too close to each other. Charred logs collected in other transects from previous field trips were included in this study, e.g., STRI 13625 and STRI 21046 were retrieved in 2009 by two different collectors whereas STRI 15368 and STRI 15369 were collected during fieldwork for this project in 2011. All those specimens are now identified as the same wood type (cf *Prioria* type) (Chapter 5, Chapter 6).

In Hodges Hill different logs and pieces of wood are all spread over slopes in a small area. In this locality, the collecting strategy was not ideal during the first field trip and logs were sampled very close together, which resulted in repetition of samples, most of them related to Malvaceae. During the second field trip in 2011, the whole area where logs and trunks could be observed in Hodges Hill was covered and wider spacing of samples collected was possible, which enabled the discovery of new specimens of Fabaceae (Wood type 2) and Elaeocarpaceae (Wood type 3). However, more malvacean woods were also obtained, suggesting that, although the first sampling strategy had some limitations, the Malvaceae types were abundant in this assemblage. Traversing the whole area and collecting specimens at different spots would be recommended for such a small area as Hodges Hill in future works.

It is generally recommended to collect mature trunk specimens and try to avoid branches or potential roots because less is known about the anatomy of these organs, and consequently such material is harder to identify and a detailed study to distinguish different ontogenic stages requires excellent preservation of the specimens (Sakala et al., 1999; Falcon-Lang and Cantrill., 2002; Falcon-Lang, 2005; Poole et al., 2006).

Different ontogenic stages might be treated as different morphotypes due to variation in certain traits in juvenile/branch material versus mature material (e.g., wood type 4). Therefore, for this study the collection was focused on specimens with dimensions, greater than 10 cm. Nonetheless, that collection strategy may also miss some woody plants that include woody lianas or shrubby trees (Baas and Schweingruber, 1987; Schweingruber et al., 2006).

Many taxa possess large roots that might be confused with main stems during collecting. One of the fundamental differences between root and stem anatomy is the position of the phloem with regards to the xylem. In stems, the phloem is immediately outside the xylem, whereas in roots, it alternates with the xylem (Taylor et al., 2009). Other studies have reported quantitative and qualitative differences between roots and stem woods, e.g., Machado et al., (1997) found more common occurrence of scalariform perforation plates in the stem wood of *Styrax camporum*, whereas the roots possess simple perforation plates. Also, it has been reported that roots usually have larger tracheids (Cutler et al., 1987) and broader vessel elements (Machado et al., 1997) than stems and growth rings present eccentric patterns towards the pith (Cutler et al., 1987; Chapman, 1994). Also, root samples often have thinner fibre walls than those in stems and in some species the cambium may curve distinctly towards the root centre at each of the wide rays (Cutler et al., 1987). In contrast to main stems, roots do not have not a pith (Taylor et al., 2009).

It is stated in the literature that roots show fewer distinct features that would allow identification in comparison to the main stem (Waisel and Breckel, 1987; Waisel et al., 2002; Pujana et al., 2013), e.g., vessel grouping and axial parenchyma characteristics are among the characters that can help to identification. Additionally, resources to identify main stems using anatomy are much more extensive than in roots (Waisel et al., 2002). For instance, one of the few extensive and classical books for root identification is the work of Cutler et al. (1987), which is used mostly by root identifiers of temperate plants.

In this study, I did not study roots; however, roots could be studied in the future, to compare with previously identified stem material as an additional source of information.

In summary the collection strategies were useful and allowed the recognition of at least 5 different taxa from the permineralised assemblage and 6 different taxa from the charcoalified assemblage, with one wood type occurring in both assemblages. Collecting strategies could be improved, trying to traverse as much of the field area as possible. It is always recommended to obtain as much detailed notes from observations in the field as possible, e.g., total preserved dimensions of trunks in the field, locality, related lithology and a better pre-classification of major wood types in the field could be attempted. If studying *in situ* forests, diameters of stumps are useful to estimate tree height; tree spacing can provide information on forest density and orientation of stumps and logs are useful to know direction of pyroclastic flows.

9.1.2. Different preservation states of woods and recommended preparation techniques:

9.1.2.1. Permineralised woods

Permineralisation of trunks occurs due to the "early infiltration and permeation of tissues by mineral-charged water with intracellular and interstitial precipitation of microcrystalline mineral matter" (Schopf, 1975; Hans and Rowe, 1999; Channing and Edwards, 2004). In woods, the minerals fill the lumina and intercellular spaces, but not completely replacing the cell walls (Taylor et al., 2009).

Permineralisation begins when the plant is immersed in water containing high concentrations of dissolved minerals, permeating cells and tissues, which hardens the tissues and faithfully preserve traits of the original plant (Taylor et al., 2009). The most common modes of permineralisation are **siliceous permineralisation**, when the mineral substitution is mainly composed of microcrystalline quartz, and **calcareous permineralisation,** when the mineral deposition consists of calcite or dolomite (Schopf, 1975). Both types are represented in the Panama material. This type of material can be prepared in petrographic thin sections following the Hans and Rowe (1999) and studied in detail under the microscope (see Chapter 3). For the Cucaracha Formation, standard petrographic sections in TS, TLS RLS were sufficient to allow a detailed study of the specimens and identifications.

9.2.2.2. Charcoalified woods

Charcoal is a product of incomplete combustion, and can be produced by burning in wildfires or as a result of heating due to volcanic events (hot airfall tuffs or flows; Scott and Glasspool, 2005). During wildfire, the plant is subjected to rapid high temperature heating which causes the breakdown of cellulose in the plant tissues (Pyne et al., 1996). This produces volatiles (e.g., CO, CO_2 and $CH_{4)}$ and this mix with atmospheric oxygen and burn (Scott and Jones, 1991; Pyne et al., 1996; Scott, 2009).

Consequently large trunks cannot be completely charcoalified in a wildfire, because the outer parts of the tree would combust before any of the inner parts can be charred (Scott, 2009). In contrast, charring of woods within hot pyroclastic flows implies oxygen exclusion, so there is no combustion, only charcoalification (Scott, 2009).

In the case of the trunks in the Cucaracha Formation, which are mostly large, these were charred by hot pyroclastic flows, which can be confirmed in specimens showing homogenisation of walls typically occurring in charcoalified material (See Chapter 7). Due to the preservation state of these charcoalified woods (partially charcoalified, partially silicified), thin sections could be obtained using similar procedures as used for permineralised woods. However, these samples were hard to study (see Chapter 6) due in some cases to poor preservation, or the difficulty of studying opaque material in thin section (Falcon-Lang et al., 2012). Some of the larger samples could be studied with the regular thin sections under lower magnification, using the light microscope as some of the quantitative traits could easily be observed (e.g., vessel density, mean vessel diameter). In contrast, other samples were more successfully identified using a Scanning Electron Microscope (SEM), e.g., cf Wood Type 2). Eight charcoalified woods from the Cucaracha Formation were studied using the SEM; however, not all of them with satisfactory results (see Chapter 6) as it were not possible to see the structures in several specimens because of debris covering their surface (Figure 9.1). Therefore, for a few specimens, a combination of both techniques was used in the taxonomic identification of these samples. The assignation of genera to these charcoalified and silicified woods was challenging and time-consuming. For some specimens, the observation of certain features under the light microscope such as, intervessel pitting, radial-vessel pitting, perforation plates, and composition of rays was difficult (e.g., intervessel pitting in Wood Type 6; composition of rays in Wood type 8)

(Figure 9.2). Despite these factors, the charcoalified wood types could still be identified to family level in many cases (e.g., Fabaceae, Sapotaceae, Meliaceae).

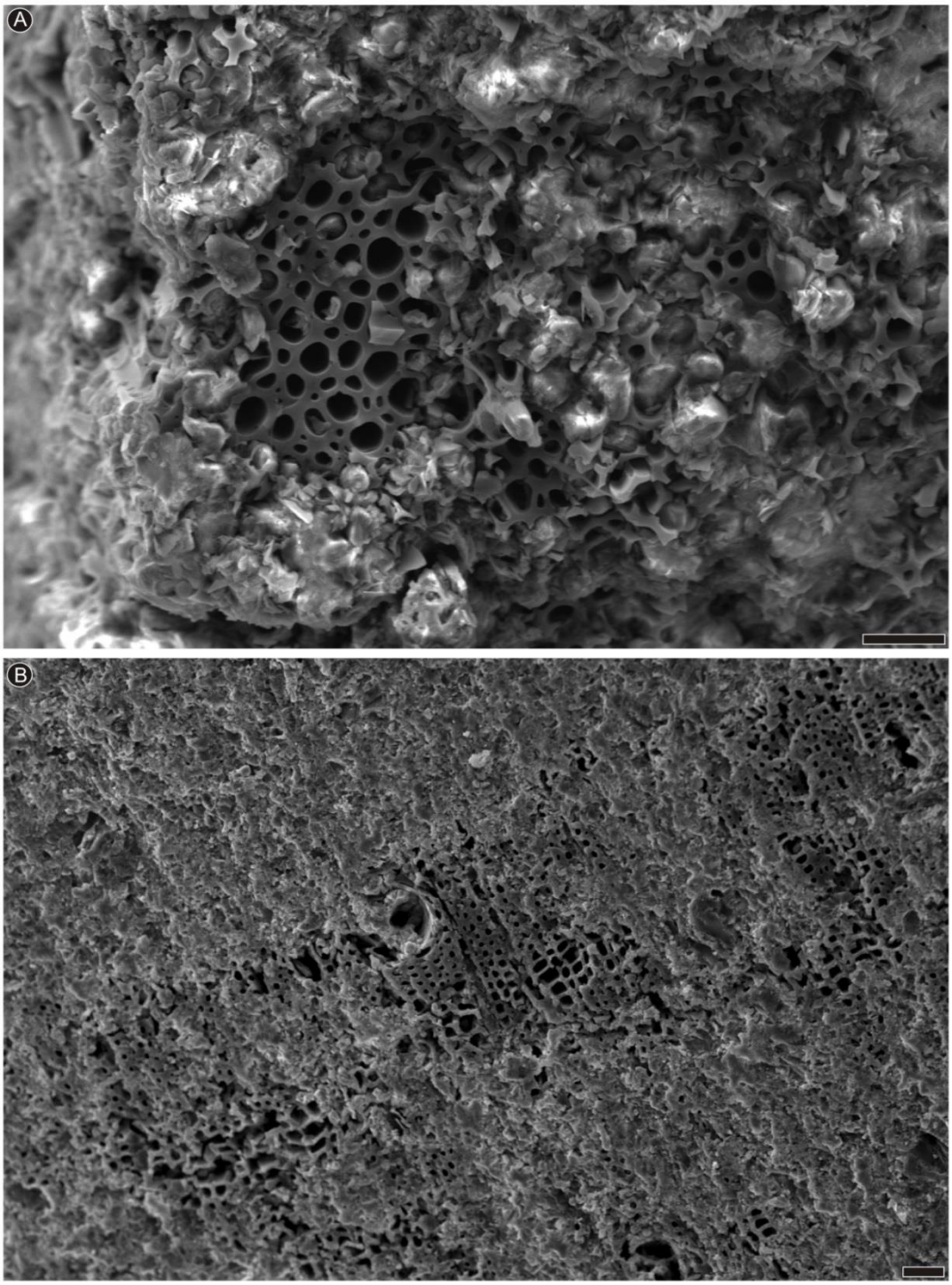

Figure 9.1. SEM TS photographs of charcoalified woods from the Cucaracha Formation showing zones with observable fibres alternating with zones covered with debris. A, STRI 14193, shows a close-up of fibres, surrounded by zones difficult to observe due to debris covering. B, STRI 15652 shows vessels and fibres in areas alternating others covered with debris. Scales: A=30 µm; B= 30 µm.

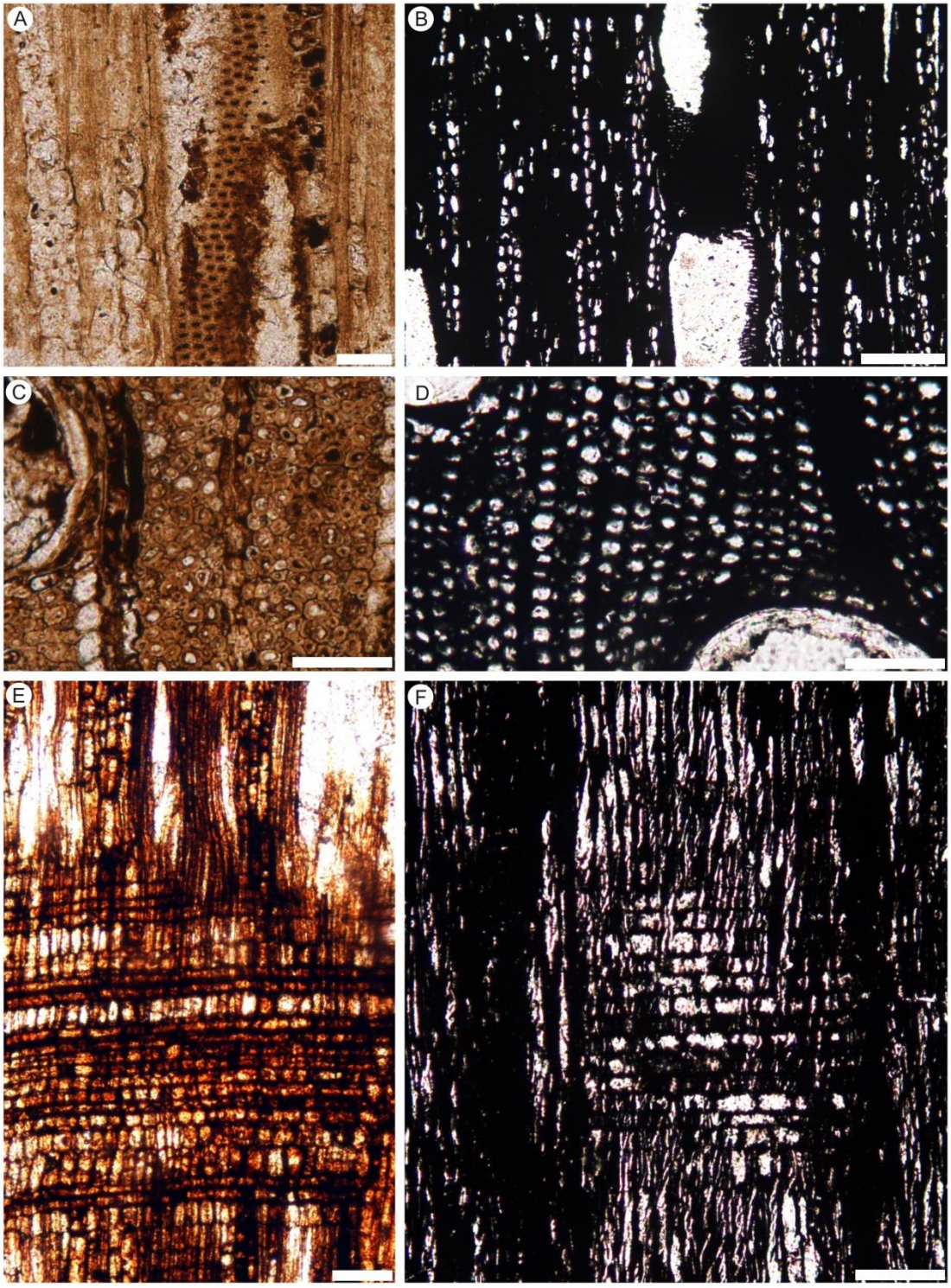

Figure 9.2. Contrast of features in permineralised and charcoalified woods. A, intervessel pitting in STRI 36272; B, intervessel pitting in STRI 14199; C, fibre wall thickness in STRI 36272; D, fibre wall thickness in 14199; E, ray composition in STRI 14160; F, ray composition in STRI 15366. Scales: A=50 µm; B-F=100 µm.

9.3. THE USE OF WOODS IN THE SYSTEMATICS OF FOSSIL PLANTS

9.3.1. Advantages and disadvantages of identifying fossil plants based on wood anatomy

Fossil plant remains are mostly found as disarticulated parts, i.e. stems, leaves, wood, pollen and reproductive structures. The identification of isolated vegetal remains is always challenging. Here I only consider the advantages and disadvantages of identifying taxa based on fossil wood and I do not seek to cover other plant parts in this discussion.

Wood is an abundant and resistant material and is an often-overlooked source of information on past palaeodiversity and palaeoclimatology (Wheeler and Baas, 1991; Wheeler and Baas, 2011; Peralta-Medina and Falcon-Lang, 2012). Nonetheless, wood anatomy has proven diagnostic value at genus level, especially for Miocene and more recent material (Wheeler and Baas, 2011; Baas et al., 2008). Baas et al. (2000) provides a detailed summary of the relation between wood anatomical characters and angiosperm phylogenetic trees (APG II). However, material older than Miocene in age is more difficult to assign to modern taxa (Poole et al., 2000; Falcon-Lang et al., 2012) because material may lie on the phylogenetic stem of multiple families and show a combination of characters not seen in living material (Dilcher et al., 1976; Crane et al., 2004; Wheeler and Baas, 2011). This is especially true for Cretaceous-Eocene material because during this time angiosperms were undergoing a spectacular radiation such that these specimens commonly show a unique combination of traits quite unlike extant forms (Crane et al., 2004; Wheeler et al., 2007; Falcon-Lang et al., 2012). Examples of this phenomenon include woods such as *Javelinoxylon, Gregoryoxylon* and *Paraphyllanthoxylon*, which cannot be certainly assigned to any extant family (e.g.,

Thayn and Tidwell, 1984; Wheeler et al., 1991; Estrada-Ruiz et al., 2007; Estrada-Ruiz and Martinez-Cabrera, 2011; Falcon-Lang et al., 2012) (see Table 9.1)

While there have been advances in wood anatomical studies of particular families (e.g., Fabaceae, Ericaceae, Bignoniaceae; Gasson and Banks, 2000; Pace and Angyalossy, 2013; Lens et al., 2007), there are other families or other areas of the world that are less covered in micromorphology slide collections. For example, South American woods represent a relatively small proportion (15%) of the total of woods in the Royal Botanic Gardens Kew, which is one of the most complete xylotomy collections in the world (Cornish et al., 2014). Studies of modern wood anatomy are crucial for providing comparative material to enable the identification of their fossil wood equivalents (Woodcock and Ignas, 1994; Crane et al., 2004).

Fossil wood anatomical characters are typically analysed qualitatively. This is because quantitative characters such as mean tangential diameter and mean vessel density can be altered during fossilization (Baas et al., 2000) especially during the charcoalification process (Prior and Gasson, 1993; McParland, 2007, 2009; Falcon-Lang et al., 2012) A number of quantitative characters were not measured in several of the charcoalified wood samples from the Cucaracha Formation (e.g., parenchyma strand length in wood type 6 and wood type 8), because of the opacity of the material or in some cases because of poor preservation. Other qualitative features were challenging to observe in charcoalified material, e.g., certainty in presence/absence of septate fibres.

A well-known issue in the recognition of taxa based on fossil wood (or any kind of fossil) assemblage is that it is easy to overlook rare taxa (Henderson and Falcon-Lang, 2011).

Families/characters	Euphorbiaceae	Lauraceae	Phyllanthaceae
Growth rings	indistinct	indistinct	indistinct
Porosity	wood diffuse porous	wood diffuse porous	wood diffuse porous
Pits	Intervessel polygonal, large	Intervessel polygonal, large; vessel-ray pits with much reduced borders	Vessel-ray pits with much reduced borders
Paratracheal parenchyma	rare or absent	rare or absent; occasional scanty paratracheal	rare or absent
Fibres	septate	septate	septate

Table 9.1. Comparative table of common characters of *Paraphyllanthoxylon* with different families.

However it depends on the original diversity of the studied assemblage. If a diverse assemblage is studied, as more individuals are sampled, more species will be recorded (Gotelli and Colwell, 2001) and there is a stronger probabibilty to sample that high diversity.

In addition, detailed quantitative studies of the different ontogenetic states in fossil trunks are also currently lacking (Falcon-Lang, 2005). Indeed, there can be a lot of variation in the wood anatomy of the same tree species if studying a branch in comparison to main stem (Henderson and Falcon-Lang, 2011). Twigs and branches usually show asymmetrical growth with narrow growth rings and tracheids, more

reaction wood, thinner cell walls and high degree of knottiness, among others (Chapman, 1994; Alteyrac et al., 2006). In this study (Chapter 5), the *Periplanetoxylon* wood type (Malvaceae) was described using both mature and juvenile specimens. The juvenile specimens showed variation mainly in the apotracheal parenchyma banding and the width of rays, occasionally showing aggregate rays (Chapter 5).

Phylogenetic studies based on wood anatomical traits should be done cautiously, because in a number of cladistic studies have proven that several wood anatomical variables are homoplastic. "Homoplasies are the result of similar responses to similar selecting pressures that, resulting in similar structure-function relationships in different taxa" (Olson, 2005). Those can be the result of convergence -the presence of a feature in two species that do not share a recent common ancestor (Hall, 2007) and parallelism- the presence of a feature in two species when the feature is not found in their most recent common ancestor but is present in a more distant (basal) ancestor (Hall, 2007). For example, there are many wood anatomical characters that occur in several families that are not closely related or even within the same Order, e.g., woods of some genera of the Combretaceae, Fabaceae, Sapindaceae, Bignoniaceae and Simaroubaceae present similar patterns (Wheeler and Baas, 2011). An example of those overlapping features is the combination of solitary vessels and radial multiples; simple perforation plates; axial parenchyma confluent abundant; uniseriate to biseriate rays; homocellular rays composed exclusively of procumbent cells, and non-septate fibres which is common in the Mimosoideae (Fabaceae; Baretta-Kuipers, 1981) but also occurs in the Bignoniaceae and Sapindaceae (Brea et al., 2010). Although some of those characters are useful in the identification of woods, they do now necessarily reflect phylogenetic relationships (Olson, 2005).

However, in the comparison of wood anatomical variables to the APG classification system, it is revealed that wood anatomy contains a significant phylogenetic signal at the ordinal level (Baas et al., 2000)., e.g., presence of tile cells is unique in the Order Malvales and it is considered synapomorphic (Olson, 2005).

IAWA (1989) provides a list of features used to identify hardwoods. This can be used alongside the Inside Wood Database (IWD) to aid the identification of fossil angiosperm woods (Wheeler, 2011). IWD is an extremely valuable web-resource in the identification of fossil woods; however, there are thousands of species not covered. Additionally, most descriptions are based on a single specimen or just a few specimens that would not reflect the intra-variation of species, as well as some of the species might not be correctly identified (Wheeler, 2011). An important advantage of IWD, however, is that it is not a static resource and it is continuously edited, and new descriptions and images are constantly added by the community (Wheeler, 2011).

Miocene material or younger in age is more certainly linked to modern representatives. For example, woods from the Middle Miocene Vantage Flora, Washington, USA, include taxa confidently assigned to modern genera such as *Liquidambar* L.(Altingiaceae), *Betula* L.(Betulaceae), *Robinia* L. (Fabaceae), *Fagus* L. (Fagaceae), *Quercus* L. (Fagaceae), among others (Wheeler and Dillhoff, 2009). From El Cien Formation in Mexico (early Miocene), woods of *Tapirira* Aubl. (Anacardiaceae) and *Maclura* Nutt. (Moraceae) can be recognised (Martinez-Cabrera et al., 2006). In this thesis, new woods can be related to *Prioria*, or at least to the 'Crudia' Group of the Fabaceae (see Chapter 4, 6).

9.3.2. Diagnostic value of angiosperm wood anatomical characters

Some characters have greater diagnostic value than others. Characters such as vessel density and vessel diameter are highly influenced by ontogeny, habit and climatic and soil conditions. For example, narrow vessels are very common in arid and temperate zones in contrast to humid zones (Lens et al., 2007), and wide vessels (>200 µm) are also more common in woody lianas (IWD) than in trees (Wheeler and Baas, 2011). Due to such environmental influences, it is considered that the identification of fossil woods is conducted mostly using qualitative features with less weight placed on quantitative features.

Also, as noted above, some qualitative features may be altered during fossilization. For instance in charcoalified woods, cells are subject to dimensional changes, mainly by shrinkage (see chapter 3, section 3.4.4.) so quantitative data can be misleading. Nonetheless, there are families where the consideration of these quantitative characters is important; for instance, in Chapter 6, Fossil Wood Type 10 (Meliaceae) relied on quantitative characters to aid identification, such as mean vessel diameter and vessel density. If quantitative characters are used for charcoalified woods then correction indexes are needed in order to determine the likely original dimensions; however, those indexes should be applied cautiously, because dimensional changes to wood anatomical characters differ between species and are affected by many factors. Also, cell types do not respond uniformly to charring (Falcon-Lang et al., 2012; Oakley and Falcon-Lang, 2009).

There are certain characters with a highly diagnostic value at ordinal level. For instance, tile cells are only found in the Malvales (Manchester and Miller, 1978) (see chapter 5) and vestured pits characterise the Fabales, Gentianales and Myrtales (Jansen

et al., 2001; Wheeler and Baas, 2011). Other characters that are important to distinguish families include: (1) Absence of vessels. This is extremely rare and only found in the basal angiosperm families such as Chloranthaceae, Trochodendraceae and Winteraceae (Evert, 1991); (2) Vessels arranged in dendritic patterns are only common in families such as Anacardiaceae, Sapotaceae, and Rhamnaceae (IWD, 2014); (3) Foraminate and reticulate perforation plates are a key character for Ericaceae, Sabiaceae, and Araliaceae (Lens et al., 2007).

For the woods identified in this thesis, some characters and combinations of characters that have been helpful to infer affinities are: (1) presence of axial canals that are solitary, diffuse or in short tangential lines combined with marginal parenchyma are diagnostic of the 'Crudia' group in the Fabaceae (Chapter 4); (2) abundance of sclerotic tyloses and absence of parenchyma is common in the Elaeocarpaceae (Chapter 4); (3) presence of tile cells combined with abundant axial parenchyma (banded and vasicentric) is common in the Malvaceae (Chapter 5).

9.4. WOODS IDENTIFIED FROM THE MIOCENE CUCARACHA FORMATION AND THEIR SIGNIFICANCE

9.4.1. Comparison of woods from the Cucaracha Formation with other Miocene woods from the New World

This section aims to compare the identified taxa in the woods of the Cucaracha Formation and compare them with previous reports of Miocene Woods of the New World.

Reports of Miocene fossil woods are more numerous in North America than in Central America and South America (Gregory et al., 2009). However, it is generally accepted that the Tertiary plant macrofossil record is strongly biased towards the Northern Hemisphere in contrast with less data from the Southern Hemisphere, because of a longer tradition and collection effort in the former areas (e.g., North America, Europe) (Collinson, 1990; Morley and Dick, 2002; Burnham and Johnson, 2004), thus, global conclusions about diversity should not be drawn based literally on the more numerous reports in certain areas.

Most of the fossil woods reported from North America have been identified to families that are typically distributed in temperate zones today, such as: Altingiaceae (e.g., *Liquidambar* cf *styraciflua*) (Prakash and Baghoorn, 1961), Betulaceae (e.g., *Betula scammonii*); Fagaceae (e.g., *Fagus manosii*, *Quercinium album*, , *Quercinium solrederi*, *Quercoxylon anomalum*, *Quercoxylon wardii*, *Quercus leuca*, *Quercus sahnii*, *Quercus virginiana*, *Lithocarpoxylon wardii*) (Boeshore and Jump, 1938; Prakash and Barghoorn, 1961; Privé, 1975; Suzuki and Ohba, 1991; Wheeler and Dillhoff, 2009;); Cyrillaceae (*Cyrilla* sp) (Barghoorn and Spackman, 1950) ; Oleaceae (*Fraxinus washingtoniana*; *Fraxinus macropunctatum*) (Wheeler and Dillhoff, 2009); Platanaceae (*Platanus americana*) (Wheeler and Dillhoff, 2009); Rosaceae (e.g., *Maloidoxylon galbreathii*, *Prunus rodgersae*, *Prunus barneti*) (Wheeler and Matten, 1977; Wheeler and Dillhoff, 2009); Salicaceae (*Salix pawneensis*) (Wheeler and Matten, 1977); Ulmaceae (e.g., *Ulmus baileyana*, *Ulmus miocenica*, *Ulmus pacifica*) (Prakash and Barghoorn, 1961). Some other families of more tropical and subtropical distribution are also reported from the Miocene of U.S.A.(e.g., Moraceae (*Ficoxylon helictoxyloides*) (Platen, 1908), Ebenaceae (e.g., *Diospyros washingtoniana*) (Platen, 1908; Prakash and

Baghoorn, 1961); (e.g.,) (Prakash and Barghoorn, 1961), Hamamelidaceae (*Hamamelidoxylon* ; Wheeler and Dilhoff, 2009); Juglandaceae (e.g., *Carya tertiara, Rhysocaryoxylon tertiarium, Rhysocaryoxylon fryxellii*) (Prakash and Barghoorn, 1961; Wheeler and Dillhoff, 2009), Lauraceae (e.g., *Laurinium brandonianum, Laurinium californicum, Laurinoxylon eberi, Perseoxylon californicum, Perseoxylon eberi, Richteroxylon micropunctatum*) (Platen, 1908; Edwards, 1931; Wheeler and Dillhoff, 2009), Nyssaceae (e.g., *Nyssa eydei*) (Wheeler and Dillhoff, 2009), Sapindaceae (e.g., *Acer beckianum*, *Acer puratanum*, *Acer olearyi* , *Aesculus hankinsii*) (Wheeler and Dillhoff, 2009), Vitaceae (*Vitoxylon opalinum*; Brown, 1942). There are some other reports of widely distributed families such as Araliaceae (e.g., *Araliaceoxylon miocenica*) (Wheeler and Dillhoff, 2009); Fabaceae (e.g., *Albizzia vantagiensis*, *Dichrostachyoxylon latiradiatum, Gleditsia columbiana*, *Gleditsioxylon montanense*, *Leguminoxylon occidentale*, *Robinia zirkelii*, *Robinioxylon breweri*) (Prakash and Barghoorn, 1961; Müller-Stoll and Mädel, 1967; Wheeler, 2001)

By contrast, in South America, most of the families represented by fossil woods are of tropical distribution today: Anacardiaceae (cf *Anacardium*) (Pons and De Franceschi, 2007); Combretaceae (cf *Terminalia*, *Terminalioxylon naranjo, Terminalioxylon portae*, cf *Buchenavia*) (Pons and Franceschi, 2007); Clusiaceae (e.g., *Guttiferoxylon compactum*, cf *Calophyllum*) (Mirioni, 1965); Lauraceae (*Laurinoxylon ruei*; Nishida et al., 1988); Meliaceae (cf *Guarea*; Pons and De Franceschi, 1983, 2007); Humiriaceae (*Humiriastrum* sp; Pons and Franceschi, 2007); Monimiaceae (Unnamed; Schöning and Bandel, 2004); Lecythidaceae (cf *Cariniana*; Pons and Franceschi, 2007); Myrtaceae (*Myrceugenellites maytenoides*); Nishida et al., 1988); Verbenaceae (*Rhaphithamnus*; Franco et al., 2014). A few of the reports are families of temperate distribution (e.g., Fagaceae (unnamed; Schöning and Bandel, 2004) and other reports

are of more widespread families: Fabaceae (*Crudioxylon pinalense*, *Enterrioxylon victoriensis*, cf *Hymenolobium, Mimosoxylon santamariensis,* ***Paraalbizioxylon caccavariae*** (Pons, 1980; Lutz, 1980, 1987; Martinez, 2013; Pons and De Franceschi, 2007); Euphorbiaceae (*Euphorbioxylon bridelioides*; Salard, 1961). There are reports of families exclusively South American today e.g. Aetoxicaceae (*Aetoxicoxylon;* Terada et al., 2006) and Goupiaceae (*Goupioxylon stuetzeri*) (Mirioni, 1965). Other families as Nothofagaceae distributed in South America, New Zealand, New Caledonia (APW, 2014) have also been identified from woods of South America (*Nothofagoxylon aconcaguense*, *Nothofagoxylon antarcticum*, *Nothofagoxylon menendezii*, *Nothofagoxylon scalariforme, Nothofagoxylon boureaui*, *Nothofagoxylon krauseli*, *Nothofagoxylon neuquenense, Nothofagoxylon pseudoobliquum, Nothofagus* sp) (Pons and Vicente, 1985; Ragonese, 1977; Poole, 2002; Nishida et al., 1985; Nishida, 1984).

Fossil woods reported from the Miocene of Mexico include: Anacardiaceae (*Tapirira peninsularis*, Martinez-Cabrera and Cevallos-Ferriz, 2004); Moraceae (*Ficoxylon bajacaliforniense* and *Maclura martinezii;* Martinez-Cabrera and Cevallos-Ferriz); Combretaceae (*Terminalioxylon panotlensis***,** Castañeda-Posadas et al., 2009; Meliaceae (*Cedreloxylon tlaxcaliensis***,** Castañeda-Posadas et al., 2009), Fabaceae (*Mimosoxylon tenax*; Cevallos-Ferriz and Barajas-Morales, 1994) and Lauraceae (*Argapaloxylon richterii***,** Castañeda-Posadas et al., 2009).

The fossil record of plants is very scarce in Central America. A few reports of woods include *Taenioxylon multiradiatum* and *Palmoxylon palmacites* reported from the Cucaracha Formation in the Panama Canal (Berry, 1918). *T. multiradiatum was* initially recognised as a Fabaceae. However, through observation of images and descriptions, it has been determined that *T. multidariatum* is more likely to be an Ebenaceae (Manchester, 2011 pers. com). Very recent unpublished reports,

include a wood similar to *Laurinoxylon* (Lauraceae) from the Miocene Chalatenango Formation (Cevallos-Ferriz et al., 2014).

So far, common families of the Cucaracha Formation found in previous reports in the regional record of woods, include the Fabaceae and the Meliaceae. The occurence of Fabaceae in the Miocene of Panama is not surprising, since Miocene Fabaceae woods reports are extensive around the world (Lavin et al., 2004; Gregory et al., 2009). Fabaceae are understood to have rapidly diversified, probably during early Paleogene (Lavin et al., 2005).

The Miocene fossil record of Fabaceae is quite extensive with particularly abundant reports for the Caesalpinioideae (Gregory et al., 2009). The fossil record of Fabaceae woods with axial canals, as in the fossil found herein, suggests these were more widespread in the past than today (Brea et al., 2012). Elements related to the modern 'Crudia Group'(Fabaceae, Caesalpinioideae, Detarieae) such as *Entrerrioxylon victoriensis* (Paraná Formation, Argentina; Brea et al., 2012) and *Crudioxylon pinalense* (El Descanso Formation, Colombia; Pons, 1983), represent close links to the cf. *Prioria* (Wood Type 2), that is also part of the 'Crudia Group'.

Miocene Meliaceae woods are uncommon in the New World in contrast to the European, African and Asian fossil record (Gregory et al., 2009). The only published examples are from the Middle Miocene Pebas Formation in Iquitos, Peru (cf *Guarea* ; Pons and De Franceschi, 2007) and the Late Miocene in Tlaxcala, Mexico (*Cedreloxylon tlaxcaliensis* ;Castañeda-Posadas et al., 2009). Although, the Wood Type 10 (see Chapter 6) has not been assigned to any specific genus, it has been suggested that *Guarea* is the more similar genus amongst the compared modern taxa.

Other families identified in the woods from the Cucaracha Formation (Malvaceae, Melastomataceae, Sapotaceae and Cannabaceae), are not common in the fossil record of the New World (Gregory et al., 2009). The wood cf. *Elaeocarpus* would represent only the second report of the genus in the Neotropics, after *Elaeocarpoxylon sloanoides* (considered in the Tropical South America area, Gregory et al., 2009; Petriella, 1972) (see Chapter 4). However, the occurence of these families in the regional Miocene fossil record is evident from other plant organs that will be further discussed in the next section.

Based on the occurrence of Fabaceae (mainly *Entrerrioxylon victoriensis* and *Crudioxylon pinalense*), Meliaceae, Elaeocarpaceae in the Cucaracha Formation, this assemblage seems to be more linked to woods reported in Mexico and northern South America.

9.4.2. Records of woods from the Cucaracha Formation compared with those of other organs (seeds, fruits, leaves, pollen) from the Miocene Neotropics

Miocene *Celtis* woods are not common in the New World, however, the genus has a large fossil record of leaves (e.g., numerous specimens of *Celtis obliquifolia* from the Succor Creek Flora, Nebraska, USA) and endocarps, (e.g., *Celtis willistonii* from the Nebraska Great Plains, Ash Hollow and Valentine Formations (Gabel et al., 1998). Additionally, endocarps of *Celtis* have been recorded from the Cucaracha Formation (Herrera et al., 2012), therefore, the discovery of *Celtis* wood in the Cucaracha Formation is consistent with previous reports.

The Miocene fossil record of Fabaceae is quite extensive not only in woods, but also in leaves, pollen and fruits (Herendeen et al., 1992). To cover the numerous reports of Fabaceae is out of the scope of the present discussion. Recommended sources to get

a broad picture of the Miocene fossil record of Fabaceae are provided in the following works (Taylor, 1990; Herendeen et al., 1992; Barreda et al., 1992; Herendeen, 2001; Pujana et al., 2011). The tribe Detarieae is thought to have diversified by Late Oligocene to early Miocene (Bruneau et al., 2008) and specifically most of the Dominican amber is thought to come from *Prioria* trees (Nudds and Selden, 2008; Poinar and Poinar, 1996).

Elaeocarpus fossil wood has previously been reported in temperate South America (Petriella, 1972; See Chapter 4) and in Neogene leaves from Alaska named *Elaeocarpus alaskensis* Hollick, 1936.

The malvacean woods (*Guazumaoxylon miocenica* and *Periplanetoxylon panamense*) described herein and published in Rodriguez-Reyes et al (2014) are the first fossils with affinity to *Pentaplaris* that have been reported to date. On the other hand, *Guazuma* pollen grains have been described from the Lower Miocene Culebra Formation in the Panama Canal, underlying the Cucaracha Formation (Graham, 1988) and from the Miocene of Veracruz, Mexico (Graham, 1976). Fossil pollen grains related to Malvaceae (*Bombacacidites*) have also been reported from mangrove deposits of the Miocene Barreiras Formation of Brazil (Dutra et al. 2001). As mentioned before in this thesis (Chapter 5), pollen grains of Malvaceae are abundant in the Cucaracha Formation (Carlos Jaramillo, 2012 pers. comm.). Malvaceae is a key component of modern tropical forests not only in the Panama Isthmus, but worldwide (APW, 2014).

Sapotaceae woods are uncommon in the fossil record of the New World, although it seems the family was widespread in Miocene times (Bartish et al., 2011). The subfamily Chrysophylloideae is represented in the Paleocene microfossils of South

America and pollen grains of cf *Pouteria* were found in the Lower Miocene Culebra Formation, Panama (Graham, 1988).

The putative pollen fossil record of Melastomataceae is extensive; however one should be cautious considering those taxa because Melastomataceae pollen is difficult to differentiate from Combretaceae pollen (Morley and Dick, 2002). In South America, for example, numerous macrofossil and microfossil studies have yielded melastome fossils approximately in proportion to the present-day diversity of the family (Burnham and Graham, 1999). The? Melastomataceae wood reported herein as well as reports of Melastomataceae pollen grains from the the Miocene Uscari Formation, Costa Rica (Graham, 1987) and Melastomataceae-like leaves (unpublished research, 2010) (Figure 9.3) may confirm the occurrence of Melastomataceae in Panama and Central America during the Miocene.

Meliaceae together with Malvaceae and Melastomataceae pollen have been recorded from the Miocene Pirabas Formation in Brazil (Jaramillo et al., 2010). These are considered some of the most important families present in modern lowland rainforests, especially in the neotropics (Jaramillo et al., 2010). Also *Guarea* (Meliaceae) pollen was found in other Miocene assemblages in Peru (Jaramillo et al., 2010) and flowers (Castañeda-Posadas and Cevallos-Ferriz, 2007) from the Simojovel flora in Mexico.

The biogeographical history of Coryphoideae (Arecaceae) is complex, but the presence of this subfamily in South America is thought to be the product of Boretropical invasions (Bjorholm et al., 2006; Dransfield et al., 2008). Miocene Coryphoideae include flowers entombed in amber from Simojovel, Mexico (Poinar, 2001) and numerous leaves, providing strong evidence for the palaeodistribution of the coryphoid

subfamily, although their assignment to modern genera is less certain (Reid and Chandler, 1933; Dilcher, 1971, 2000; Gregor, 1980; Van der Burgh, 1984; Zona, 1990; Mai, 1995; Poinar, 1999).

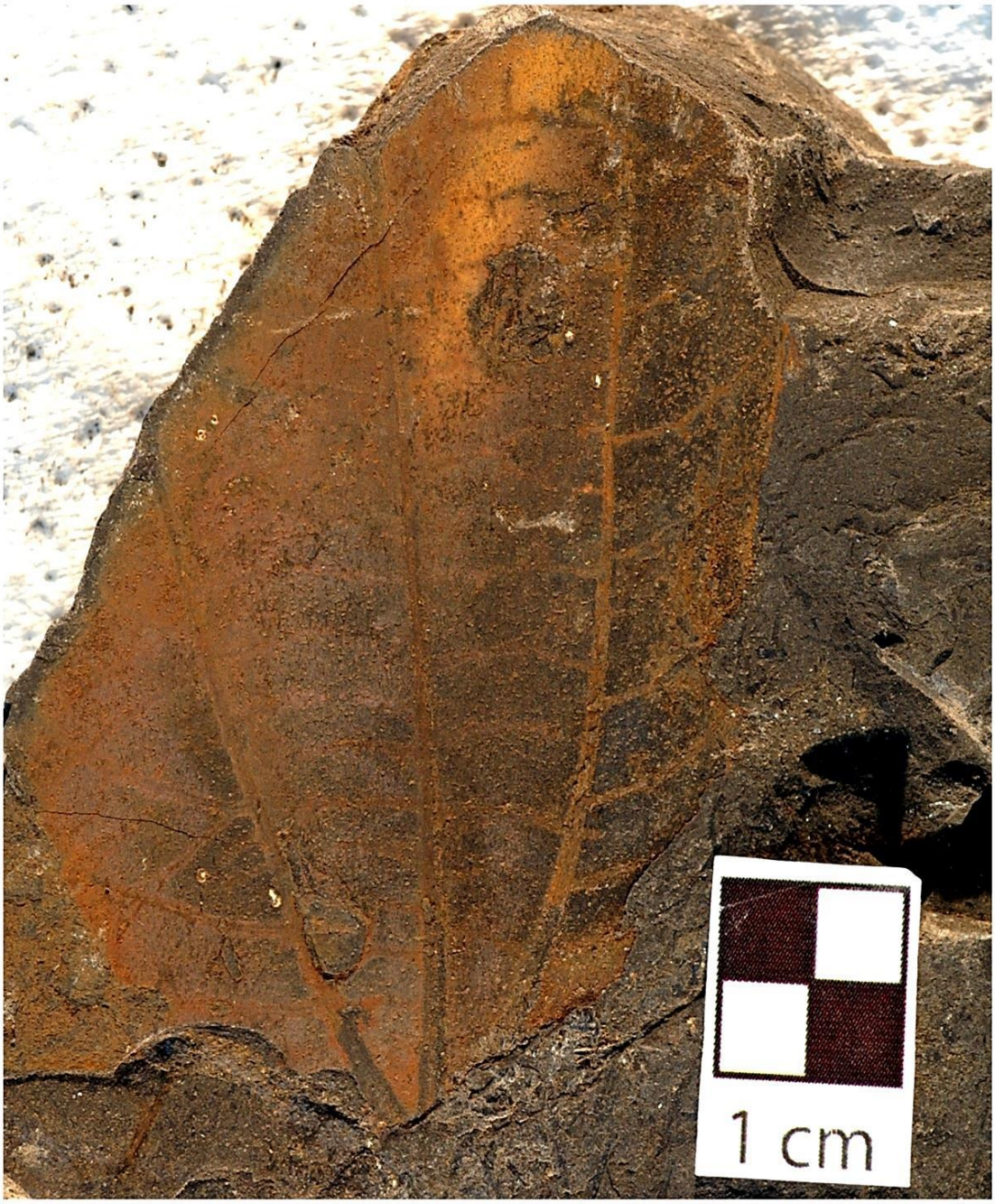

Figure 9.3. Melastomataceae-type fossil leaf retrieved from the Culebra Formation in 2010.

Elements found in the woods of the Middle Miocene Cucaracha Formation such as Malvaceae, Sapotaceae, Melastomataceae, Meliaceae Arecaceae, Fabaceae (Caesalpinioideae) are also represented by other Neogene Amazonian taxa identified from pollen and leaves (see Jaramillo et al., 2010). Cannabaceae (*Celtis*) is reported in pollen grains from Miocene communities in Mexico (Paraje Solo Formation) (Graham, 1987) and from Miocene communities in Patagonia, Argentina (Palazzesi et al., 2014). I have found no reports of Elaeocarpaceae in the literature of Miocene neotropical pollen.

Pollen and trunks are produced in different proportions in a tree, e.g., a single main stem will be produced in one tree throughout its life, but thousands of leaves, flowers and therefore, pollen grains will be produced each year. It means the potentialities of the fossilization of different plant organs vary considerably (Greenwood, 1992). Therefore, different organs in plants respond differently to transportation and deposition processes, so woods are less mobile and less reworked than pollen (Philippe et al., 2004). Also, the presence of non-arboreal pollen or spores provides compensates for the potential absence of megafloral remains (Gastaldo et al., 1998). This could explain that taxa found in fossil pollen can not be always correlated with the taxa found in the fossil woods.

The woods identified from the Cucaracha Formation woods are well confirmed in extensive fossil record in other plant parts (leaves, pollen, fruits, seeds), especially for the Malvaceae, Fabaceae, Meliaceae and Arecaceae. Elaeocarpaceae has a sparse fossil record in the New World. However, the palaeodiversity of *Elaeocarpus* is low in comparison with the extant diversity (360 species) (Dettmann and Clifford, 2001). Despite this, the fossil record suggests that this genus was more widespread in the past (Crayn et al., 2006).

9.4.3. Distribution and ecology of modern taxa related to the Cucaracha Formation woods with emphasis on Central and South American representatives

This section aims to compare the reported taxa from the woods of the Cucaracha Formation and the modern distribution.

Celtis (Cannabaceae) is a widespread genus in tropical and warm temperate zones; however, species are more common in Asia (Mabberley, 2008). *Celtis* are usually medium-size trees, rarely attaining >30 m height (More and White, 2003). *Celtis schippi* is usually found in the understory in Panama and Costa Rica and *Celtis iguananea* has been found usually in coastlines and along rivers (STRI, 2012).

Prioria trees are up to 40 m in height that can form a zone behind the mangrove. These can be in swamps that are underwater during a portion of the year, along rivers or in slopes lying inland form the coastal plain (Lopez and Kursar, 1999; Grauel and Putz, 2003; Sandi and Flores, 2004). *Prioria* is distributed from Nicaragua to Colombia (Lopez and Kursar, 1999). This taxon is one of the main indicators of trees adapted to tidally-influenced estuarine deposits consistent with the environmental setting inferred from the geology of the Formation.

Elaeocarpus is the most species-rich genus of Elaeocarpaceae, but it is rare in the modern Neotropics (APW, 2014). The second largest Elaeocarpaceae genus, *Sloanea*, is distributed throughout the tropics and subtropics, with the exception of Africa (APW, 2014). However, the elaeocarpacean wood found in the Cucaracha Formation shares more anatomical traits with *Elaeocarpus*. *Elaeocarpus* mostly include species of trees that range from 15 up to 40 m in height, related to lowland wet forests (Mabberley, 2002; Kerrigan and Dixon, 2011).

The Malvaceae identified from the Cucaracha Formation are affin to modern trees of *Guazuma*, which include trees up to 30 m high, that are usually in pastures and disturbed forests, sometimes also found along coastal lines (USDA, 2013), whereas trees of *Pentaplaris*, the most similar genus to *Periplanetoxylon panamense*, *is* an inland tree of rainforests in Costa Rica, Panama Bolivia and Peru (Baum et al., 2004). *Pentaplaris* are usually tall and butressed trees (18 -40 m) (Hinsley, 2005 onwards).

Other families, identified in this thesis, such as Sapotaceae, Melastomataceae, Meliaceae and Arecaceae are widespread and considered among the most important components of neotropical rainforests today (Wing et al., 2009; Jaramillo et al., 2010). These have been used as evidence of the presence of similar rainforests since the Paleocene (Wing et al., 2009; Jaramillo et al., 2010).

Based on the trees identified in this thesis with affinities to the generic level, the modern representants are trees (commonly tall) and distributed in the neotropics, especially in Central and South America, except for *Celtis* and *Elaeocarpus* that are more common in the Old World today. The extant related trees are found in coastal areas (e.g., *Celtis*, occasionally *Guazuma*), others in tidally-influence estuarine and swamp environments (e.g., *Prioria*) and in lowland wet forests (e.g., *Pentaplaris*, *Elaeocarpus*).

9.4.4. Comparison between charcoalified and permineralised assemblages from the Cucaracha Formation

Some families and wood types (Chapters 4-6) in the Cucaracha Formation have been found in both assemblages (charcoalified and permineralised). The *Prioria*-type wood was identified from large permineralised trunks in Hodges Hill (base of the

formation) as well as large charcoalified and silicified trunks in Contractors Hill (top of the formation).

Malvaceae were also found in both assemblages in the Cucaracha Formation. However, the Malvaceae from the charcoalified assemblage is a different taxon (potentially a different genus) than the ones recognised in the permineralised flora. The charcoalified Malvacean wood can be distinguished because it possesses reticulate parenchyma, which does not occur in the permineralised woods. Malvaceae specimens not only are represented in both assemblages, but several specimens can be assigned to the family in at least three different taxa (see Chapter 5, Chapter 6) which suggests abundance of the family in this paleoflora.

The rest of the identified woods are not found in both assemblages. *Celtis* and *Elaeocarpus* were only found in the permineralised assemblage in Hodges Hill, whereas Meliaceae, Melastomataceae and Sapotaceae were only found in the charcoalified assemblage, as well as a different Fabaceae (Wood Type, 6; Chapter 6) and a Malvaceae wood (Fossil wood type 7; Chapter 6). However, I consider this could be more related to sampling bias, because the permineralised assemblage was small compared to the area of collection of the charcoalified woods (see Section 9.2.1.4.)

9.5. COLLECTION AND PREPARATION TECHNIQUES FOR REFLECTANCE ANALYSIS

Stump samples from the charcoalified assemblage from Centenario Bridge and Contractors Hill were analysed to interpret the minimum charring temperature of the trees at the top of the Cucaracha Formation (see Chapter 7 for details). Thirteen samples were prepared and analysed. Reflectance values from different samples in the same

stump were obtained in order to document the change in charring temperature with depth into the soil. There was not a straightforward reduction in charring temperature with depth. However, these inconsistencies may be influenced by the quality of the polish (grains plucking during polishing) resulting in non-satisfactory results from several of the samples (e.g., STRI 15524, STRI 15533). It would had been useful to prepare more polished blocks, so some specimens could had been tested and therefore obtained more data and estimations of charring temperature, according to the different sample positions. However, it was not possible because of time constraint of this PhD project.

9.6. WOOD ANATOMICAL DATA AND CLIMATIC VARIABLES

9.6.1. Brief introduction to regional Miocene palaeoclimatological studies using fossil vegetal remains

Miocene palaeoclimatological studies using plant physiognomic characters have rarely used datasets from Central America (Pound et al., 2012). Most of the interpretations come from palynological studies (Graham, 1987-1989). For example, microfloras in the Miocene of Panama and Costa Rica suggest warm and humid conditions (Graham, 1987, 1988). Although other studies based on different approaches such as paleosols suggest cooler and drier conditions in Panama by the Middle Miocene (Retallack and Kirby, 2007).

The determination of palaeoclimates with fossil plants have more commonly used leaf physiognomy than wood characters (Wiemann et al., 1999; Wheeler and Baas, 2011). Some studies using CLAMP have been tested in floras of Chile and Argentina. Those studies predict MAT of 26 ˚C, CMMT of 8.1-8.6 ˚C and MAP of 930 mm

(Hinojosa and Villagran, 2006). Other approaches that have been used regionally with fossil plants include TEVIS (Tertiary Environments Vegetation System) based models applied for the early to middle Miocene indicate Northern North America was dominated by cool temperate forests during the Middle Miocene, whereas Western North America was dominated by warm-temperate broad-leaved mixed forests with a tendency to be drier forests towards the Late Miocene (Pound et al., 2012). The palaeobotanical evidence for Mexico, Central America and the Caribbean was more limited (Pound et al., 2012), however, the model results evidence the development of tropical climates by Middle Miocene with a dominance of evergreen broad leaf forests which seemed to remain towards the Messinian (Pound et al., 2011; Graham, 1998). In northern South America, tropical evergreen broad-leaved forests are inferred for the Serravalian, as suggested by studies in La Venta Formation (Colombia), with a predicted MAP of 1750± 250 mm (Kay and Madden, 1997). Other studies interpret the existence of rainforests in Ecuador based on vegetal macrofossils (Burnham and Graham, 1999).

Results from CLAMP and confirmed by TEVIS models for Tortonian (Late Miocene) suggest an increased MAT and MAP during the Miocene in Western and Eastern USA in comparison to modern known values in the region (See Table 9.1; Pound et al., 2011), whereas in Bolivia (South America) similar analysis yielded considerably higher MAT and lower MAP during the Miocene, consistent with the idea of the expansion of savannas by Late Miocene (Pound et al., 2011). That increase of grasslands has been proposed to be a consequence of a large-scale decrease in the atmospheric carbon dioxide concentration, however, it is debatable and it could be also attributed to tectonically related episodes or changes in seasonal precipitation patterns (Pagani et al., 1999).

9.6.2. Use of wood anatomical characters for palaeoclimatological studies

Although woods are a rich archive of external signals that modify its attributes and therefore has high potential for climatological studies, the use of wood anatomical characters in palaeoclimatology is scarce in contrast to leaf physiognomy traits (Wheeler and Baas, 2011; Wiemann et al., 1998; Wiemann et al., 1999).

There are limitations when studying fossil woods and try to link them to climatic variables, e.g., it may be difficult to determine if a piece of fossilised trunk comes from a root, a branch or the main stem (Wiemann et al., 1999; Falcon-Lang, 2005).

Growth ring analysis can yield information about seasonality and productivity (Creber and Chaloner, 1984). However, growth rings vary radially within the same specimen, in different sections of the same tree (root, branch, main stem) and with ontogenic state (mature or juvenile) (Poole et al., 2006). False rings (see Chapter 8) can be misinterpreted as well, additionally, the formation of growth rings in the tropics is still poorly understood (Jacoby, 1989). All those previously stated facts make it difficult to make conclusive interpretation from growth rings of tropical trees. In this thesis, the analysis of growth rings revealed absence of distinct rings in 30 specimens placed in 13 different morphotypes from the Cucaracha Formation. When present indistinct rings were marked by marginal parenchyma bands, but this seems to be more related to its common occurrence in certain families (e.g., Fabaceae; Herendeen, 2000; Gasson et al., 2003) rather than linked to climatic factors.

Another approach using wood anatomical characters is Wood Specific Gravity (SG) to infer climatic variables (Wiemann and Williamson, 1989; Woodcock, 2000; Wiemann and Williamson, 2002; Woodcock and Shier, 2003; Martinez-Cabrera et al.,

2012). SG can be basically defined as the ratio of a dry-weight of a piece of wood to the weight when the wood is completely fresh (green volume) (IAWA, 1998). SG has been progressively more used to infer climatic variables because it is linked to plant life strategies, physiology and mechanical properties (Hacke and Sperry, 2001) and it is also inversely proportional to wood productivity (Martinez-Cabrera et al., 2012).

Wiemann et al. (1988, 1999) derived equations from large worldwide databases using wood anatomical characters. Some of those equations have been applied in this thesis and further discussed in Chapter 9.

9.6.3. Percentages of growth rings in regional modern forests

A few studies have used growth ring distinctness analysis to infer seasonality in the neotropics. Some of those have shown 60% of species with distinct rings e.g. in El Cerrado (Marcati et al., 2006).

Other growth ring analysis in Brazil has reported 48% of the species with distinct rings in tropical and subtropical forests and 66% in semi-deciduous forests (Lisi et al., 2008). That latter forest was interpreted as strongly seasonal. In contrast, a very low percentage of distinct growth rings is found in Atlantic rainforests of Brazil (Callado et al., 2001). In studies conducted in Venezuela, evergreen forests had 50% of trees with distinct rings (Worbes, 1999).

Dry forests from Panama evaluated in this thesis showed a higher percentage of distinct rings (13%) in comparison with wet forests (0%). Dry forests develop in a long dry season of at least 5 months that promotes the formation of growth rings (Biota Panama, 2014). However, the percentage of distinct rings is still low (much less than 50% of the assemblage), thus, these forests do not record strong seasonality despite the prevailing climatic conditions.

9.7. FUTURE WORK

(1) More specimens from Hodges Hill are needed to confirm whether the fossil woods studied in this thesis represent the true forest diversity. Further identification of the charcoalified palms, to subfamily or generic level, could hopefully be achieved by studying other specimens housed in the STRI collection in Corozal, Panama.

(2) More charcoalified specimens could be analysed using the SEM, since this is the recommended technique for these types of specimens. Charcoalified samples are abundant in the STRI collection, thus further specimens could be analysed to improve the identification of the specimens.

(3) More specimens could be prepared for reflectance analysis in order to explore potential relationships between charring temperature and the position of the wood sample within the pyroclastic flow.

(4) Wiemann equations could be applied to an increased number of wood types from the Cucaracha Formation in order to yield more accurate palaeoclimatological predictions.

(5) Radial longitudinal sections should also be obtained from the modern wood samples, so further characteristics can be coded and used in the Wiemann equations to infer palaeoclimates.

CHAPTER 10: CONCLUSIONS

(1) The widening of the Panama Canal has provided access to Miocene sections containing two assemblages of fossil woods. Assemblage 1 comprises permineralised woods, found in the Hodges Hill locality, within a conglomerate facies near the base of the Cucaracha Formation. Detrital zircon populations with maximal ages of 19 – 20 Ma (early Burdigalian) have been recovered from this part of the Cucaracha Formation (Montes et al., 2012). Assemblage 2 comprises charcoalified woods preserved in growth position directly below a welded silicic tuff near the top of the Formation. The tuff is known as the "Cucaracha Tuff" and has been recently dated with U-Pb analysis, giving a mean age of 18.81± 0.30 Ma (MacFadden et al., 2014). Therefore, both assemblages are of Lower Miocene age.

(2) The permineralised assemblage occurs in units interpreted as tidally-influenced estuaries, based on the extensive *Teredolites* borings observed in the woods. The charred assemblage is found beneath a welded silicic ignimbrite with strong N-S flow elongation of crystals. The tuff layer is interpreted as a hot pyroclastic flow deposit, and associated air fall deposits, which buried and preserved the forest in charred state.

(3) From the well-preserved calcareous-permineralised woods, two distinct new Malvaceae wood types were recognised: *Guazumaoxylon miocenica* Rodríguez-Reyes, Falcon-Lang, Gasson, Collinson, Jaramillo gen. nov. sp. nov. and *Periplanetoxylon panamense* Rodríguez-Reyes, Falcon-Lang, Gasson, Collinson, Jaramillo gen. nov. sp. nov., which are abundant in the Hodges Hill locality (Middle Miocene, Cucaracha Formation, Panama). These Malvaceae have similarities to the modern genera, *Guazuma* and *Pentaplaris*, respectively, but with a few different characters that justified assignation to new fossil wood taxa. The two Malvaceae types

can be distinguished from one another because of the combination of *Guazuma*-type tile cells and winged-aliform paratracheal parenchyma in *Guazumaoxylon*, in contrast to *Pterospermum*-type tile cells and banded apotracheal parenchyma in *Periplanetoxylon.*

(4) Several other wood types were identified in the permineralised assemblage from the Hodges Hill locality, including representatives of the Fabaceae (cf *Prioria*), Cannabaceae (cf *Celtis*) and Elaeocarpaceae (cf *Elaeocarpus*). *Prioria* and *Elaeocarpus* are uncommon in the regional fossil record whereas *Celtis* has an extensive, well-supported fossil wood record as well as contemporaneous occurrences of endocarps and pollen in Panama.

(5) In contrast, the charcoalified wood assemblage comprises representatives of the families Fabaceae, Malvaceae, Sapotaceae, Melastomataceae, Meliaceae and Arecaceae were identified. Approximately 20% of the charcoalified woods are Arecaceae (palm trees) based on field counts. All the aforementioned families are dominants in modern neotropical rainforests.

(6) The *Prioria* wood type was found in both permineralised and charcoalified assemblages. Malvacean woods were also found in both assemblages. However, generally the two assemblages are somewhat different in composition.

(7) Most of the determinate taxa from the Cucaracha Formation have modern relatives in Central and South America. These woods include: cf. *Prioria* (Fabaceae), *Periplanetoxylon panamense* (*Pentaplaris*, Malvaceae), *Guazumaoxylon miocenica* (*Guazuma*, Malvaceae), Sapotaceae, Melastomataceae, ?*Guarea* type (Meliaceae), and ?*Crysophyla* (Arecaceae).

(8) Some of the fossil wood types (e.g., *Prioria, Elaeocarpus, Celtis*) comprise trees that favour saline-influenced gallery forest settings in modern coastal forests, consistent

with the facies interpretation of tidally-influence estuarine setting reported above (Retallack and Kirby, 2007; Kirby et al., 2008).

(9) The charcoalified assemblage from the Cucaracha Formation provides a rare record of a tropical forest assemblage entombed by hot pyroclastic flows. The charred woods show homogenisation of cell walls, which is indicative of charring temperatures >325 ºC (Scott, 2000; MacParland et al., 2009; Hudspith et al., 2010). Reflectance data indicate that the woods were entombed by pyroclastic flows at minimum temperatures that ranged between 490 and 505 º C. The pyroclastic flows came from a vent located to the North as shown by the orientation of *in situ* stumps at Centenario Bridge and Contractors Hill.

(10) None of the fossil wood morphotypes show distinct growth rings; however, a few Fabaceae samples have indistinct rings marked by marginal parenchyma bands. In modern wet forest analogues, only 2% of taxa have distinct growth rings contrasting with modern dry forests that show 13% of the species showing distinct growth rings. This, perhaps, favours interpretation of the Miocene assemblage as a wet forest setting.

(11) Application of Wiemann climate-anatomy regressions (equation 10) to the fossil wood assemblages, yielded a MAT (Mean Annual Temperature) of 17 º C; however, applied to modern floras of Panama, the same technique predicted a MAT (24 ºC) slightly cooler than that actual MAT of 25–27 ºC. In addition, MAP (Mean Annual Precipitation) prediction yielded a low value (860 mm) for fossil assemblages in comparison to the results from modern wet forest assemblages (MAP= 2380 mm). These data imply that Miocene forests were somewhat cooler and drier than extant examples.

(12) In the Miocene Cucaracha Formation assemblage, the applied Wiemann equation that yielded the highest MAT was equation number 7, which used percentage of multiple perforation plates, spiral thickenings in vessels, mean vessel diameter <100 µm ring- porous wood as predictors. The lowest predicted MAT was obtained with the application of equation number 15, which used percentage of storied rays, present septate fibres and absence of parenchyma as predictors.

REFERENCES

Alteyrac, J., Cloutier, A., Zhang, S. Y., 2006. Characterization of juvenile wood to mature wood transition age in black spruce (*Picea mariana* (Mill.) BSP) at different stand densities and sampling heights. Wood science and technology 40 (2), 124–138.

Amos, B., 2005. Birefringence for facetors I: what is birefringence?. The Journal of the UK Facet Cutter's Guild. homepage.ntlworld.com/w.amos2/BR1.pdf (last accessed, 20 August, 2014).

Angeles G., 2001. New techniques for the anatomical study of charcoalified wood. IAWA Journal 22, 245–254.

APG (Angiosperm Phylogeny Group) III, 2009. An update of the Angiosperm Phylogeny Group classification for the orders and families of flowering plants: APG III. Botanical Journal of the Linnean Society 161, 105–121.

Apgaua, D.M.G., Coelho, P. A., Santos, R.M.D., Santos, P.F., Oliveira-Filho, A.T.D., 2014. Tree community structure in a seasonally dry tropical forest remnant, Brazil. Cerne, 20 (2), 173–182.

Agarwal, A., 1991. Fossil wood of *Grewia* from Neyveli lignite deposits, India.Vegetos 4, 1–2, 5–7.

Agarwal, A., 1991b. Occurrence of *Altingia* and *Bauhinia* in the Neyvele lignite deposits, India (Miocene). Journal of Indian Botanical Society 70, 119 –121.

Artabe, A. E., Spalletti, L. A., Brea, M., Iglesias, A., Morel, E. M., Ganuza, D. G., 2007. Structure of a corystosperm fossil forest from the Late Triassic of Argentina. Palaeogeography, Palaeoclimatology, Palaeoecology 243(3), 451–470.

Ascough, P. L., Bird, M. I., Scott, A. C., Collinson, M. E., Cohen-Ofri, I., Snape, C. E., Le Manquais, K., 2010. Charcoal reflectance measurements: implications for structural characterization and assessment of diagenetic alteration. Journal of Archaeological Science. 37(7), 1590–1599.

Autoridad del Turismo de Panama, 2014. Available online at: http://www.atp.gob.pa/ (last accessed 25 August, 2014).

Awasthi, N., 1975. On two new fossil woods resembling *Chrysophyllum* and *Holoptelea* from the Cuddalore series near Pondicherry. Palaeobotanist.

Awasthi, N., 1992. Indian fossil legumes. In: Herendeen, P.S., Dilcher, D.L. (Eds.).

Advances in Legume Systermatics, Part 4. The fossil record. 225–250. Royal Botanic Gardens, Kew, United Kingdom.

Awasthi, N., Mehrotra, R.C., 1993. Further contributions to the Neogene Flora of northeast India and significance occurrence of African element. Geophytology 23, 81-92.

Awasthi, N., Mehrotra, R.C., 1997. Some fossil woods from Tipam sandstone of Assam and Nagaland. Palaeobotanist 38, 277–284.

Awasthi, N, Prakash, U., 1987. Fossil woods of *Kingiodendron* and *Bauhinia* from the Nansang beds of Deomali, Arunachal Pradesh. Palaeobotanist 35, 178–183.

Awasthi, N, Srivastava, R., 1989. Some new carbonized woods from the Neogene of Kerala Coast and their bearing on palaeoclimate. Palaeobotanist 38, 285–292.

Baas, P., 2013. Wood Structure in Plant Biology and Ecology. Koninklijke Brill NV, Leiden, The Netherlands. Pp 341–342.

Baas, P., Schweingruber, F. H., 1987. Ecological trends in the wood anatomy of trees, shrubs and climbers from Europe. IAWA Bulletin 8, 245–274.

Baas, P., Jansen, S., Wheeler, E.A., 2003. Ecological adaptations and deep phylogenetic splits: evidence from the secondary xylem. In: Stuessy, T., Mayer, V, Hörandl, E. (Eds.). Deep morphology in plant systematics. Regnum Vegetabile 141, 221– 239

Baas, P., Wheeler, E.A., Chase, M., 2000. Dicotyledonous wood anatomy and the APG system of angiosperm classification. Botanical Journal of the Linnean Society of London 134–317.

Baas, P., Wheeler, E.A., Chase, M., 2008. Dicotyledonous wood anatomy and the APG system of angiosperm classification. Botanical Journal of the Linnean Society of London 134 (1–2), 3–17.

Bailey, I.W., 1924, The Problem of identifying the wood of Cretaceous and Later Dicotyledons: *Paraphyllanthoxylon arizonense:* Annals of Botany 34, 439–451.

Baker, R. A., DiMichele, W. A., 1997. Biomass allocation in Late Pennsylvanian coal-swamp plants. Palaios 127–132.

Bancroft H., 1935b. The wood anatomy of representative members of the Monotoideae. American Journal of Botany 22, 717–739.

Bande, M.B., Prakash, U., 1980a. Four new fossil dicotyledonous woods from the Deccan Intertrappean beds near Shahpura, Mandla District, M.P. Geophytology 10, 268–271.

Bande, M., Prakash, U., 1980b. Fossil woods from the Tertiary of West Bengal, India.

Geophytology 10, 146–157.

Bande, M.B., Prakash, U., 1982. Fossil dicotyledonous woods from the Deccan Intertrappean beds near Shahpura, Mandla District, Madhya Pradesh. Palaeobotanist 31, 13–29.

Bande, M.B., Srivastava, 1994. *Grewia*–type fossil Woods from the Deccan Intertrappean Beds of India. Geopthytology 24, 131–135.

Bande, M.B., Deschamps, R., Lakhanpal, R.N., Prakash, U., 1987. Some new fossil woods from the Cenozoic of Zaire. Royal Museum for Central Africa Tervuren. Annual Report. 1985-6, 113–140.

Banks, H., Gasson, P., 2000. Pollen morphology and wood anatomy of the Crudia group (Leguminosae, Caesalpinioideae, Detarieae). Botanical Journal of the Linnean Society 134, 19–59.

Baretta-Kuipers, T., 1981. Wood anatomy of Leguminosae: its relevance to taxonomy. In: Polhill, K.M., Raven, P.H (Eds.). Advances in Legume Systematics, Part 2. 677–705.

Barghoorn, E.S., Spackman, W., 1950. Geological and botanical study of the Brandon Lignite and its significance in coal petrology. Economic Geology 45, 344–357.

Barreda, V. D., Caccavari, M., 1992. Mimosoideae (Leguminosae) occurrences in the early Miocene of Patagonia (Argentina). Palaeogeography, Palaeoclimatology, Palaeoecology 94(1), 243–252.

Barry, J.C., Johnson, N.M., Raza, S.M., Jacobs, L.L., 1985. Neogene mammalian faunal change in southern Asia: Correlations with climatic, tectonic, and eustatic events. Geology 13, 637–640.

Barry, J.C., Morgan, M.E., Winkler, A.J., Flynn, L.J., Lindsay, E.H., Jacobs, L.L., Pilbeam, D., 1991. Faunal interchange and Miocene terrestrial vertebrates of southern Asia. Paleobiology, 231–245.

Bartish, I. V., Antonelli, A., Richardson, J. E., Swenson, U., 2011. Vicariance or long-distance dispersal: historical biogeography of the pantropical subfamily Chrysophylloideae (Sapotaceae). Journal of Biogeography 38(1), 177–190.

Baum, D.A., Dewitt -Smith, S., Yen, A., Alverson, W.S., Nyffeler, R., Whitlock, B.A., Oldham, R. L., 2004. Phylogenetic relationships of Malvatheca (Bombacoideae and Malvoideae; Malvaceae *sensu lato*) as inferred from plastid and nuclear DNA

sequences and their bearing on the mallow radiation. American Journal of Botany 91, 1863–1871.

Bayer, C., Kubitzki, K., 2003. Malvaceae. In: Kubitzki, K., Bayer, C. (Eds.). Flowering plants. Dicotyledons: Malvales, Capparales, and non-betalain Caryophyllales. Springer, Berlin, pp. 225–311.

Beauchamp, J., Lemoigne, Y., 1973. Description d' une paleoflora du Crétacé terminal Eocéne dans le massif du Chercher (Province d' Harar, Ethiopie). Documents des Laboratories. Géologie de Lyon 56, 167–179.

Beauchamp, J., Lemoigne, Y., Petrescu, J. 1973. Les paléoflores tertiaries de Debré-Libanos (Ethiopie). Annales de la Societe Geologique de Nord Ille. Six-Horemans, Lille, France. 93, pp. 17–32+ 5 pl.

Bermingham, E., Dick, C. W., Moritz, C., 2005. Tropical rainforests: past, present, and future. University of Chicago Press.

Bernor, R.L., 1984. A zoogeographic theater and biochronologic play: the time-biofacies phenomena of Eurasian and African Miocene mammal provinces. Paléobiologie continentale 14, 121-142.

Bernor, R. L., Tobien, H., Woodburne, M. O., 1989. Patterns of Old World hipparionine evolutionary diversification and biogeographic extension. European Neogene mammal chronology Springer US. Pp. 263–319.

Berry, E.W., 1918. The fossil higher plants from the Canal Zone. Smithsonian Institution, United States National Museum 103, 15–44.

Berry, E.W., 1923. Additions to the flora of the Wilcox Group. Shorter contributions to general geology. United States Geological Survey, Professional Papers 131A, 1–

20. Biota Panama, 2014 onwards. http://biota.wordpress.com/ (last accessed 3 September, 2014).

Bird, M. I., Ayliffe, L. K., Fifield, L. K., Turney, C. M., Cresswell, R.G., Barrows, T. T., David, B., 1999. Radiocarbon dating of old charcoal using a wet oxidation, stepped-combustion procedure. Radiocarbon 41(2), 127–140.

Bjorholm, S., Svenning, J.C., Bake, W.J.r, Skov, F., Baslev, H., 2006. Historical legacies in the geographical diversity patterns of New World palm (Arecaceae) subfamilies.Botanical Journal of the Linnean Society 151, 113–125.

Bliss, L.C., Heal, O., Moore, J.J., 1981. Tundra Ecosystems: A Comparative Analysis, CUP Archive. International Biological Programme 25. 257–284. Cambridge, Cambridge

University Press.

Boeshore, I., Jump, J.A., 1938. A new fossil oak Wood from Idaho. American Journal of Botany 25, 307–311.

Bohlman, S., O'Brien, S., 2006. Allometry, adult stature and regeneration requirement of 65 tree species on Barro Colorado Island, Panama. Journal of Tropical Ecology 22 (02), 123–136.

Boureau, E., 1957. Etude anatomique et dendroclimatologique d' un bois silicifié tertiaire des environs de Laruscade (Gironde), *Leguminoxylon schoelleri*. C.r. 82e Congrés des Sociétés Savantes de Paris. 181–189.

Boureau, E., Louvet, P., 1970. Sur deux espéces ligneuses tertiaries nouvelles de la région de Ouaou en Namous (Libye). Congrés des Sociétés Savantes de Paris 3, 11–42.

Braadbaart, F., Poole, I., 2008. Morphological, chemical and physical changes during charcoalification of wood and its relevance to archaeological contexts. Journal of archaeological science 35(9), 2434–2445.

Brandes, A.F. das N., Barros, C.F., 2007. Wood anatomy of eight liana species of the Leguminosae family from Atlantic rain forest. Acta Botanica Brasilica 22 (2), 465–480.

Bräuning, A., Homeier J, Cueva E., Beck E., Günter S., 2008 a. Growth dynamics of trees in tropical mountain ecosystems. Ecological studies 198. 291–302. Springer, Berlin.

Brea, M., Zucol, A. F., Patterer, N., 2010. Fossil woods from late Pleistocene sediments from El Palmar Formation, Uruguay Basin, Eastern Argentina. Review of Palaeobotany and Palynology 163(1), 35–51.

Brea, M., Franco, M.J., Lutz, A., 2012. Redescription and reassignment of *Entrerrioxylon victoriensis* from the Upper Miocene, Paraná Formation, South America. Review of Palaeobotany and Palynology 185, 13–25.

Brizicky, G.K., 1965. The genera of Tiliaceae and Elaeocarpaceae in the Southeastern United States. Journal of the Arnold Arboretum 46, 286–307.

Brown, R. W., 1942. A Miocene grapevine from the valley of Virgin Creek in northwestern Nevada. Journal of the Washington Academy of Sciences 32, 287-291.

Bruneau, A., Forest, F., Herendeen, P.S., Klitgaard, B.B., 2001. Phylogenetic relationships in Caesalpinioideae (Leguminosae) as inferred from chloroplast trnL intron sequences. Systematic Botany 26, 487–514.

Bruneau, A., Mercure, M., Lewis, G. P., Herendeen, P. S., 2008. Phylogenetic patterns and

diversification in the caesalpinioid legumes This paper is one of a selection of papers published in the Special Issue on Systematics Research. Botany 86(7), 697–718.

Burnham, R., Graham, A., 1999. The history of Neotropical vegetation: new developments and status. Annals of the Missouri Botanical Garden 86, 546–589.

Burnham, R. J., Johnson, K. R., 2004. South American palaeobotany and the origins of neotropical rainforests. Philosophical Transactions of the Royal Society of London. Series B: Biological Sciences 359(1450), 1595–1610.

Bustin, R. M., Guo, Y., 1999. Abrupt changes (jumps) in reflectance values and chemical compositions of artificial charcoals and inertinite in coals.International Journal of Coal Geology 38(3), 237–260.

Cadena, E. A., Schweitzer, M. H., 2012. Variation in osteocytes morphology vs bone type in turtle shell and their exceptional preservation from the Jurassic to the present. Bone 51(3), 614–620.

Callado, C., da Silva Neto, S., Scarano, F., Costa, C., 2001. Periodicity of growth rings in some flood-prone trees of the Atlantic Rain Forest in Rio de Janeiro, Brazil. Trees 15(8), 492–497.

Cane, M.A., Molnar, P., 2001. Closing of the Indonesian seaway as a precursor to east African aridification around 3–4 million years ago. Nature 411, 157–162.

Cantera, J., 2010. Bivalvos preforadores de Madera (Mollusca: Teredinidae, Pholadidae) en la costa Pacifica colombiana. Biologia Marina 34, 277–288.

Carlquist, S. 2001b. Comparative Wood Anatomy: Systematic, Ecological, and Evolutionary Aspects of Dicotyledon Wood. Ed. 2. Springer, Berlin. 457 pp.

Carlton J.T., Ruckelshaus, M.H., 1997. Nonindigenous marine invertebrates and algae. In: Simberloff, D., Schmitz D.C., Brown, T.C. (Eds). Strangers in Paradise. Island Press, Washington, D.C., pp. 187–201.

Carvalho, M.R., Herrera, F., Jaramillo, C., Wing, S., Callejas, R., 2011. Paleocene Malvaceae from Northern South America and their biogeographical implications. American Journal of Botany 98, 1337–1355.

Case, J., Holcombe, T.L., Martin, R.G., 1984. Geologic-tectonic map of the Caribbean region. United States Geological Survey Miscellaneous Investigation Series Map I-1100.

Castañeda-Posadas, C., Calvillo-Canadell, L., Cevallos-Ferriz, S. R.S., 2009. Woods from

Miocene sediments in Panotla, Tlaxcala, Mexico. Review of Palaeobotany and Palynology 156(3), 494–506.

Cerling, T. E., Solomon, D. K., Quade, J., Bowman, J. R. 1991. On the isotopic composition of carbon in soil carbon dioxide. Geochimica et Cosmochimica Acta 55(11), 3403–3405.

Cevallos-Ferriz, S. R. S., Barajas Morales, J., 1994. Fossil woods from the El Cien formation in Baja California Sur: Leguminosae. IAWA Journal 15, 229–245.

Cevallos-Ferriz, S.R.S., Cerén-López, G., Flores-Rocha, L.A., Echeverria, E., 2014. *Laurinoxylon* from the Miocene Chalatenango Formation, El Salvador. Botany, 2014. July 26 - 30 2014 - The Boise Centre - Boise, Idaho, USA.

Chaloner, W. G.,Creber, G. T., 1990. Do fossil plants give a climatic signal?. Journal of the Geological Society 147(2), 343–350.

Chang, H.T., Miau., R.H., 1989. Tiliaceae. Flora of Republic Popular of Singapore 49, 47–125.

Channing, A., Edwards, D., Sturtevant, S., 2004. A geothermally influenced wetland containing unconsolidated geochemical sediments. Canadian Journal of Earth Sciences 41(7), 809–827.

Chapman, C. A., Chapman, L. J., 1990. Density and growth rate of some tropical dry forest trees: comparisons between successional forest types.Bulletin of the Torrey Botanical Club 226–231.

Chapman, J. L., 1994. Distinguishing internal developmental characteristics from external palaeoenvironmental effects in fossil wood. Review of Palaeobotany and Palynology 81(1) 19–32.

Chattaway, M.M., 1933. Tile cells in the rays of the Malvales. New Phytologist 32, 261–273.

Chattaway, M.M., 1937. The wood anatomy of the family Sterculiaceae. Philosophical Transactions of the Royal Society of London, Series B, Biological Sciences 228, 313–365.

Chesters, K.I., 1957. The Miocene flora of Rusinga Island, Lake Victoria, Kenya. Palaeontographica Abteilung 101, 30–71.

Chowdhury, K.A., Ghosh, S.S., 1946. On the anatomy of *Cynometroxylon indicum* gen. et sp. nov. A fossil dicotyledonous wood from Nailalung, Assam. Proceedings of Natural Institute of India 12, 435–447.

Chowdhury, K.A., Ghosh, S., Kazmi, M., 1960. *Pahudioxylon bankurensis* gen. et sp. nov. A fossil wood from the Miocene bed of the Bankura District, West Bengal., India. Proceedings of Natural Institute of India 26B, 22–28.

Christiansen, R. L., Yeats, R. S., Graham, S. A., Niem, W. A., Niem, A. R., 1992. Post-Laramide geology of the US Cordilleran region. The Geology of North America, 3, 261– 406.

Chung, R.C.K., Lim, S.C., 2005. Wood anatomy of *Grewia* and *Microcos* from Peninsular Malasya and Borneo. Journal of Tropical Forest Science 17(2), 175–196.

Coates, A., 1999. Lithostratigraphy of the Neogene strata of the Caribbean coast from Limon, Costa Rica, to Colon, Panama. Bulletin of American Paleontology. 113, 17–37.

Coates, A., Obando, J., 1996. The geological evolution of the Central American Isthmus. In: Jackson, J.B.C., Budd, A.F., Coates, A.G. (Eds.). Evolution and Environment in Tropical America, pp. 21–56.

Coates, A., Collins, L.S., Aubry, M-P., Berggren,W.A., 2004. The Geology of the Darien, Panama, and the late Miocene-Pliocene collision of the Panama arc with northwestern South America. Geological Society of America Bulletin 116, 1327–1344.

Coates A., Aubry, M-P. Berggren, W., Collins, L., Kunk, M., 2003. Early Neogene history of the Central American arc from Bocas del Toro, western Panama. Bulletin of the American Association of Petroleum Geologists 115, 271–287.

Cohen A.N., Carlton, J.T. 1995. Nonindigenous aquatic species in a United States estuary: a case study of the biological invasions of the San Francisco Bay and Delta. A Report for the United States Fish and Wildlife Service, Washington D.C. and the National Sea Grant College Program, Connecticut Sea Grant. Maritime Studies Program Williams College, Connecticut. 285 pp.

Collinson, M.E., 1999. Scanning electronic microscopy of megafossils and mesofossils. In: Jones, T.P. and Rowe, N.P. (Eds.). Fossil plants and spores: modern techniques. Geological Society of London. Pp 57–64.

Cornish, C., Gasson, P., Nesbitt, M., 2014. The wood collection (xylarium) of the Royal Botanic Gardens, Kew. IAWA Journal 35(1), 85–104.

Crane, P. R., Herendeen, P., Friis, E. M., 2004. Fossils and plant phylogeny. American Journal of Botany 91(10), 1683–1699.

Crawley, M., 1988. Palaeocene woods from the Republic of Mali. Bulletin of the British Museum of Natural History (Geology) 44, 3–14.

Crawley, M., 1989. Dicotyledonous wood from the Lower Tertiary of Britain. Palaeontology 32, 597–622.

Crawley, M., 2001. Angiosperm woods from the British Lower Cretaceous and Palaeogene deposits. The Palaeontological Association. Special Papers in Palaeontology 66, 1–100.

Crayn, D. M., Rossetto, M., Maynard, D. J., 2006. Molecular phylogeny and dating reveals an Oligo-Miocene radiation of dry-adapted shrubs (former Tremandraceae) from rainforest tree progenitors (Elaeocarpaceae) in Australia. American Journal of Botany 93(9), 1328–1342.

Creber, G. T., 1977. Tree rings: a natural data-storage system. Biological Reviews 52 (3), 349–381.

Creber, G. T., Chaloner, W. G., 1984. Influence of environmental factors on the wood structure of living and fossil trees. The Botanical Review 50(4), 357–448.

Creber, G. T., Chaloner, W. G., 1985. Three growth in the Mesozoic and Early Tertiary and the reconstruction of palaeoclimates. Palaeogeography, Palaeoclimatology, Palaeoecology 52(1), 35–59.

Crepet, W., Herendeen, P.S., 1992. Papilionoid flowers from the early Eocene of southeastern North America. In: Herendeen, P.S., Dilcher, D.L. (Eds.). Advances in Legume Systematics, Part 4. The fossil record. Royal Botanic Gardens, Kew, United Kingdom. Pp 43–55.

Crepet, W., Taylor, D., 1985. The diversification of the Leguminosae: first fossil evidence of the Mimosoideae and Papilionoideae. Science 228, 1087–1089.

Cronquist, A., 1981. An integrated system of classification of flowering plants. Columbia University Press, New York, 1262 pp.

Cúneo, N. R., Taylor, E. L., Taylor, T. N., Krings, M., 2003. In situ fossil forest from the upper Fremouw Formation (Triassic) of Antarctica: paleoenvironmental setting and paleoclimate analysis. Palaeogeography, Palaeoclimatology, Palaeoecology 197 (3), 239–261.

Cutler, D.F., Rudall, P.J., Gasson, P.E., Gale, R.M.O., 1987. Root identification: Manual of Trees and Shrubs. Chapman and Hall. London, UK. 245 pp.

Cutter, B. E., Cumbie, B. G., McGinnes Jr, E. A., 1980. SEM and shrinkage analyses of

Southern pine wood following pyrolysis. Wood Science and Technology 14(2), 115–130.

Dana, H., 1965. Manual de mineralogia. 2da edicion. Editorial Reverte. 578 pp.

De Francheschi, D., De Plöeg., G., 2003. Origine de l'ambre des facies sparnaciens (Éocene inférieur) du Bassin de Paris: le bois de l´arbre producteur. Geodiversitas. 25, 633–647.

De la Sota, E.R., 1972. Las pteridofitas y el epifitismo en el Departamento del Choco (Colombia). An. Soc. Cien. Argentina 194, 245–278.

Delteil-Desneux, F., 1981. Sur l' association de trois bois fossils dans meme gisement tertiaire du Djebel Nara (Tunisie centrale). Review of Palaeobotany and Palynology 31, 289–310.

Delzon, S., Douthe, C., Sala, A., Cochard, H., 2010. Mechanism of water-stress induced cavitation in conifers: bordered pit structure and function support the hypothesis of seal capillary-seeding. Plant, cell and environment 33(12), 2101–2111.

Demir, F., Dogan, H., Özcan, M., Haciseferoğullari, H. 2001. Nutritional and physical properties of hackberry (*Celtis australis* L.). Journal of Food Engineering 54 (3), 241–247.

Detienne, P., Jacquet, P., 1983. Atlas d'identification des bois de l'Amazone et des regions voisines. Centre Technique Forestier Tropical. 640 pp.

Dettmann, M., Clifford, H. T., 2001. The fossil record of Elaeocarpus L. fruits. Memoirs of the Queensland Museum 46 (2), 461–497.

DeVore, M. L., Pigg, K. B., 2010. Floristic composition and comparison of middle Eocene to late Eocene and Oligocene floras in North America. Bulletin of Geosciences 85(1), 111–134.

Dias-Leme, C.L., Cartwright C., Gasson, P., 2010. Anatomical changes to the wood of *Mimosa ophthalmocentra* and *Mimosa tenuiflora* when charred at different temperatures. IAWA Journal 31, 333–351.

Didziulis, V., 2007. "NOBANIS-invasive alien species fact sheet, *Teredo navalis*" (On-line pdf). [last updated June 01, 2011]. NOBANIS-European network on invasive alien species. http://www.nobanis.org/files/factsheets/Teredo_navalis.pdf (last accessed, 20 June, 2013).

Dietrich W. E., Windsor D. M., Dunn T., 1982. Geology, climate and hydrology of Barro

Colorado Island. In The Ecology of a Tropical Forest: Seasonal rhythms and Long-retm Changes (E. Leigh and Windsor D. (Eds). Smithsonian Institution, Washington, 21–46.

Dilcher, D. L., 2000. Geological history of the vegetation in southeast United States. Sida, Botanical Miscellany 18, 1–21.

Dilcher, D.L., Crepet, W.L., Beeker, C.D., Reynolds, H.C., 1976. Reproductive and vegetative morphology of a Cretaceous angiosperm. Science, 191, 854–856.

DiMichele, W. A., Falcon-Lang, H. J., 2011. Pennsylvanian 'fossil forests' in growth position (T0 assemblages): origin, taphonomic bias and palaeoecological insights. Journal of the Geological Society 168(2), 585–605.

DiMichele, W. A., Falcon-Lang, H. J., Nelson, W. J., Elrick, S. D., Ames, P. R., 2007. Ecological gradients within a Pennsylvanian mire forest. Geology 35(5), 415–418.

Donoghue, E., Troll, V. R., Schwarzkopf, L. M., Clayton, G., Goodhue, R., 2009. Organic block coatings in block-and-ash flow deposits at Merapi Volcano, central Java. Geological Magazine 146(01), 113–120.

Dorr, L.J., 1990. An expansion and revision of the Malagasy genus *Humbertiella* (Malvaceae). Bulletin du Musée National d'Historie Naturelle de Paris, Adansonia 12, 7–27.

Dransfield J., Uhl N. W., Asmussen C. B., Baker W. J., Harley M. M., Lewis C. E., 2008. Genera palmarum: The evolution and classification of palms. Royal Botanic Gardens, Kew, UK.

Du, N., 1988. Fossil wood from the late Tertiary of Burma. Kononklijke Nederlandse Akademie van Wetenschappen 91, 213–236.

Duarte, M.C., Esteves, G.L., Salatino, M.L., Walsh, K., Baum, D., 2011. Phylogenetic Analyses of *Eriotheca* and Related Genera (Bombacoideae, Malvaceae)**.** Systematic Botany 36, 690–701.

Duke, N. C., Birch, W. R.,Williams, W. T., 1981. Growth rings and rainfall correlations in a mangrove tree of the genus Diospyros (Ebenaceae). Australian Journal of Botany 29 (2), 135–142.

Dünisch, O., Montóia, V. R., Bauch, J., 2003. Dendroecological investigations on *Swietenia macrophylla* King and *Cedrela odorata* L. (Meliaceae) in the central Amazon. Trees 17(3), 244-250.

Dutra, T.L., Rossetti, D.F., Stranz, A., 2001. Bombacacceae Kuhnt, 1821 from the Middle

Miocene Barreiras Formation (Depositional Sequence B), in Para State, Brazil. In: 17th Congresso Brasileiro de Paleontologia, Boletim de Resumos 1, 77.

Edlin, H.L., 1935. A critical revision of certain taxonomic groups of the Malvales. New Phytologist 34, 1–20, 122–143.

Edwards, W.N., 1931. Dicotyledones (Ligna). In W. Jogmans (Eds.), Fossilium catalogus II: Plantae, Pars 17. W. Junk, Berlin. 1–95.

eFloras, 2008. Missouri Botanical Garden, St. Louis, MO. Harvard University Herbaria, Cambridge, MA. Available online at: http://www.efloras.org (last accessed February 2012).

Elming, S.A., Layer, P., Ubieta, K., 2001. A paleomagnetic study of Tertiary rocks in Nicaragua, Central America. Geophysics Journal International 147, 294–309.

El-Saadawi, W., Youssef, S. G., Kamal-EL-Din, M. M., 2004. Fossil palm woods of Egypt: II. Seven Tertiary *Palmoxylon* species new to the country. Review of Palaeobotany and Palynology 129(4), 199–211.

Empresa de Transmision Electrica S.A, Panama. http://www.etesa.com.pa/ (last accessed 12 August 2014).

Esau, K., 1977. Plant Anatomy, Meristems, Cells, and Tissues of the Plant Body: their Structure, Function, and Development. John Wiley and Sons, New york, USA.

Escalante, G., 1990. The geology of southern Central America and western Colombia. The Caribbean Region, 201–230.

Estrada-Ruiz, E., Martinez-Cabrera, H.I, Cevallos-Ferriz, S.R.S., 2007. Fossil Woods from the late Campanian-Early Maastrichtian Olmos Formation, Coahuila, Mexico. Review of Palaeobotany and Palynology 145, 123–133.

Estrada-Ruiz, E., Martinez-Cabrera, H.I, Cevallos-Ferriz, S.R.S., 2010. Upper Cretaceous woods from the Olmos Formation (Late Campanian-Early Maastrichtian), Coahuila, Mexico. American Journal of Botany 97, 1179–1194.

Evans, J. E., 1991. Facies relationships, alluvial architecture, and paleohydrology of a Paleogene, humid-tropical alluvial-fan system: Chumstick Formation, Washington State, USA. Journal of Sedimentary Research 61(5).

Evert, R., 2006. Esau's Plant Anatomy, Meristems, Cells, and Tissues of the Plant Body: their Structure, Function, and Development. 3rd edn. RF Evert. New Jersey: John Wiley and Sons, Inc. 601 pp.

Falcon-Lang, H., 2005. Intra-tree variability in wood anatomy, and its implications for fossil wood systematics and palaeoclimatic studies. Palaeontology 48 (1) 171–183.

Falcon-Lang, H. J., Bashforth, A. R., 2004. Pennsylvanian uplands were forested by giant cordaitalean trees. Geology 32 (5), 417–420.

Falcon-Lang, H. J., Cantrill, D. J., 2002. Terrestrial paleoecology of the Cretaceous (early Aptian) Cerro Negro Formation, South Shetlands Islands, Antarctica: a record of polar vegetation in a volcanic arc environment. Palaios,17(5), 491–506.

Falcon-Lang H.J., Judd, N.A., Nelson W.J., DiMichele W.A., Chaney D.S., Lucas S.G., 2011. Pennsylvanian coniferopsid forests in sabkha facies reveal the nature of seasonal tropical biome. Geology 39, 371–374.

Falcon-Lang, H., Wheeler, E.A., Baas, P., Herendeen, P.H., 2012. A diverse charcoalified assemblage of Cretaceous (Santonian) angiosperm woods from Upatoi Creek, Georgia, U.S.A. Part 1. Morphotypes with scalariform perforation Plates. Review of Palaeobotany and Palynology 184, 49–73.

February, E. C., 1994. Rainfall reconstruction using wood charcoal from two archaeological sites in South Africa. Quaternary Research 42(1), 100–107.

Ferrusquia-Villafranca, I., 1978. Distribution of Cenozoic vertebrate faunas in Middle America and problems of migration between North and South America. Conexiones terrestres entre Norte y Sudamérica. 101, 193–321.

Felix, J., 1882. Studien über fossile Hölzer. Diss.. Leipzig. Von Pöschel and Trepte.

Felix, J., 1883. Die fossilen Hölzer Westindiens. T. Fischer, Cassel.

Felix, J., 1886. Untersuchungen über fossile Hölzer. 2. Zeitschrift Deutschen Geologischen Gellesschraft 38, 483–492.

Felix, J., 1887b. Untersuchungen über fossile Hölzer. 2. Zeitschrift Deutschen Geologischen Gellesschraft. 39, 517–528.

Fessler-Vrolant, C., 1977. Sur la presence d’ un nouveau bois fossile de Legumineuse dans l’Oligocéne de la Tunisie septentrionale. Congrés des Sociétés Savantes de Paris 1, 143–160.

Fichtler, E., Clark, D. A., Worbes, M., 2003. Age and Long-term Growth of Trees in an Old-growth Tropical Rain Forest, Based on Analyses of Tree Rings and 14C1. Biotropica 35(3), 306–317.

Figueiral, I., 1999. Lignified and charcoalified wood. In: Jones, T.P. and Rowe, N.P. (Eds.). Fossil plants and spores: modern techniques. Geological Society of London. 92–96.

France-Lanord, C., Derry, L.A., 1997. Organic carbon burial forcing of the carbon cycle from Himalayan erosion. Nature 390, 65–67.

Francis, J. E., Poole, I., 2002. Cretaceous and early Tertiary climates of Antarctica: evidence from fossil wood. Palaeogeography, Palaeoclimatology, Palaeoecology 182(1), 47–64.

Franco, M. J., Brea, M., Zavattieri, A. M., 2014. First record of fossil woods from the Mariño Formation (Miocene), Mendoza, Argentina and their palaeobiogeographical implications. Alcheringa: An Australasian Journal of Palaeontology, (ahead-of-print), 1–16.

Frisch, W., Dunkl, I., Kuhlemann, J., 2000. Post-collisional orogen-parallel large-scale extension in the Eastern Alps. Tectonophysics 327 (2), 239–265.

Fritz, W. J., Harrison, S., 1985. Transported trees from the 1982 Mount St. Helens sediment flows: their use as paleocurrent indicators. Sedimentary geology 42(1), 49–64.

Froggatt, P.C., Wilson, C.J.N., Walker, G.P.L., 1981. Orientation of logs in the Taupo ignimbrite as an indicator of flow direction and vent position. Geology 9, 109–111.

Gabel ML, Backlund, D.C., Haffner, J., 1998. The Miocene macroflora of the northern Ogallala Group, northern Nebraska and southern South Dakota. Journal of Paleontolology 72, 388–397.

Galtier, J., Phillips, T.L., 1999. The acetate peel technique. In: Jones, T.P., Rowe, N.P. (Eds.). Fossil plants and spores: modern techniques. Geological Society of London. Pp 67–70.

Garguillo, M., Magnuson, B., Kimball, L., 2008. A field guide to Plants of Costa Rica. Oxford University Press, New York. 77 pp.

Gasson, P., 1985. Automatic measurement of vessel lumen area and diameter with particular reference to pedunculate oak and common beech. IAWA Bulletin 6, 219–237.

Gasson, P., 1987. Growth rings in the aerial and root xylem of some north temperate hardwoods. In “Applications of Tree Ring Studies: Current Research in Dendrochronology and Related Areas”, ed. R.G. Ward. BAR, International Series 333, Oxford.

Gasson, P., 1987. Some implications of anatomical variations in the wood of pedunculate

oak (*Quercus robur* L.), including comparisons with common beech (Fagus sylvatica L.). IAWA Bulletin 8, 149–166.

Gasson, P., 1994. Wood anatomy of the Sophoreae and related Caesalpinioideae and Papilionoideae. In: Ferguson, I.K., Tucker, S.C. (Eds.). Advances in Legume Systematics, Part 6, Structural Botany. Royal Botanic Gardens, Kew, United Kingdom. Pp 165–203.

Gasson, P., 1994. Wood anatomy of the Elaeocarpaceae. In*:* Donaldson, L.A., Singh, A.P., Butterfield, B.G., Whitehouse, L.H. (Eds.). Recent Advances in Wood Anatomy. New Zealand Forest Research Institute Limited. Pp 47–71.

Gasson, P., Baas, P., Wheeler, E., 2011. Wood anatomy of CITES-listed tree species. IAWA Journal 32 (2), 155–198.

Gasson, P., Trafford, C., Matthews, B., 2003. Wood anatomy of the Caesalpinioideae. In: Klitgaard, B.B., Bruneau, A. (Eds.). Advances in Legume Systematics, Part 10, Higher level Systematics. Royal Botanic Gardens, Kew, United Kingdom. Pp 63–93.

Gastaldo, R. A., 2004. The relationship between bedform and log orientation in a Paleogene fluvial channel, Weißelster Basin, Germany: implications for the use of coarse woody debris for paleocurrent analysis. Palaios 19(6), 587–597.

Gastaldo, R. A., Pfefferkorn, H. W., DiMichele, W. A., 1994. Taphonomic and sedimentologic characterization of roof-shale floras. Geological Society of America Memoirs 185, 341–352.

Gastaldo, R. A., Riegel, W., Püttmann, W., Linnemann, U. G., Zetter, R., 1998. A multidisciplinary approach to reconstruct the Late Oligocene vegetation in central Europe. Review of Palaeobotany and Palynology 101(1), 71–94.

Gentry, A. H., 1990. Four neotropical rainforests. Yale University Press.

Goddéris, Y., François, L., 1996. Balancing the Cenozoic carbon and alkalinity cycles: constraints from isotopic records. Geophysics Research Letters 23, 3743–3746.

Gonçalves, T. A., Marcati, C. R., Scheel-Ybert, R., 2012. The effect of carbonization on wood structure of *Dalbergia violacea*, *Stryphnodendron polyphyllum*, *Tapirira guianensis*, *Vochysia tucanorum*, and *Pouteria torta* from the Brazilian cerrado. IAWA Journal 33(1), 73–90.

Gotelli, N. J., Colwell, R. K., 2001. Quantifying biodiversity: procedures and pitfalls in the measurement and comparison of species richness. Ecology letters 4(4), 379–391.

Gottwald, H., 1969. Zwei Kieselhölzer aus dem Oligozän von Tunis, *Bombacoxylon oweni* und *Pseudolachnostyloxylon weylandii*. Palaeontographica 119B, 112–118.

Gottwald, H., 1994. Tertiäre Hölzer aus dem Chindwinn-Bassin in nordwestlichen Myanmar (Birma). Documentae Naturae, München. 86, 1–90, 1–83+4pl.

Gottwald, H, 2004. Neue taxonomische Untersuchungen and 205 tertiären Hölzern und 2 verkieselten Rindenresten aus der Südlichen Frankenalb unf deren Randgebieten– mit Aussagen über Herkunft und Flora, Klima und Alter. Documentae Naturae 153, 1–93.

Gourlay, I. D., 1995. The definition of seasonal growth zones in some African *Acacia* species-a review. IAWA Journal 16(4), 353–359.

Gradstein, F. M., Ogg, J. G., Smith, A. G., 2004. A geologic time scale. Cambridge University Press. 86 pp.

Graham, A., 1976. Studies in neotropical paleobotany. II. The Miocene communities of Veracruz, Mexico. Annals of the Missouri Botanical Garden, 787–842.

Graham, A., 1987. Tropical American Tertiary floras and paleoenvironments: Mexico, Costa Rica, and Panama. American Journal of Botany. 1519–1531.

Graham, A., 1988. Studies in Neotropical Paleobotany VI. The Lower Miocene Communities of Panama-the Cucaracha Formation. Annals of the Missouri Botanical Garden, 1467–1479.

Graham, S. A., Stanley, R. G., Bent, J. V., Carter, J. B., 1989. Oligocene and Miocene paleogeography of central California and displacement along the San Andreas fault. Geological Society of America Bulletin 101(5), 711–730.

Grambast-Fessard, N., 1968. Contribution a l'etude des flores tertiaires des regions provencales et alpines: IV-Deux structures ligneuses nouvelles de Sapotacees. Naturalia Monspeliensia. Série botanique. 19, 57–74.

Grauel, W., Putz, F.E., 2004. Effects of lianas on growth and regeneration of *Prioria copaifera* in Darien, Panama. Forest Ecology and Management 190 (1), 99–108.

Greenwood, D. R., 1992. Taphonomic constraints on foliar physiognomie interpretations of Late Cretaceous and Tertiary palaeoeclimates. Review of Palaeobotany and Palynology 71(1), 149–190.

Gregor H.J., 1980. Zum vorkommen fossiler Palmenreste im Jungtertiär Europas unter

besonderer Berücksichtigung der Ablagerung der Oberen Süßwasser-Molasse Süd-Deutschlands. Berichte der Bayerischen Botanischen Gesellschaft zur Erforschungder Heimischen Flora 4: 121–147.

Gregory, M., Poole, I., Wheeler, E.A., 2009. Fossil Dicot Wood Names: An Annotated List with Full Bibliography. IAWA Journal, Supplement 6.

Greguss, P, 1943. Bemerkungen zu der Arbeit. Verkieselte Hölzer aus dem Sarmat des Tokaj–Eperjeser Gebirges von E. Hoffman. Földtani Közlöny 73, 582–593 + 36–44.

Greguss, P., 1969. Tertiary angiosperm woods in Hungary. Akademiai Kiado. Budapest, Hungary.

Grimm, R., Behrens, T., Märker, M., Elsenbeer, H., 2008. Soil organic carbon concentrations and stocks on Barro Colorado Island—digital soil mapping using Random Forests analysis. Geoderma 146 (1), 102–113.

Gulbranson, E. L., Isbell, J. L., Taylor, E. L., Ryberg, P. E., Taylor, T. N., Flaig, P. P., 2012. Permian polar forests: deciduousness and environmental variation. Geobiology 10(6), 479-495.

Guleria, J.S., 1982. Some fossil woods from the Tertiary of Kachchh, Western India. Palaeobotanist 31, 35–43.

Guleria, J.S., 1984. Leguminous woods from the Tertiary of District Kachchh, Gujarat, western India. Palaeobotanist. 31, 238–254.

Hacke, U. G., Sperry, J. S., Wheeler, J. K., Castro, L., 2006. Scaling of angiosperm xylem structure with safety and efficiency. Tree Physiology 26(6), 689–701.

Hacke, U. G., Sperry, J. S., Pockman, W. T., Davis, S. D., McCulloh, K. A., 2001. Trends in wood density and structure are linked to prevention of xylem implosion by negative pressure. Oecologia 126(4), 457–461.

Hall, B. K., 2007. Homoplasy and homology: dichotomy or continuum? Journal of Human Evolution 52 (5), 473–479.

Hammer, O., Harper, D., Ryan, P.D., 2001. PAST version 1.39: Paleontological statistical software package for education and data analysis. Paleontology Eletronica 4, 1–9.

Hammer O., Harper, D., 2006. Paleontological Data Analysis. Blackwell Publishing, Oxford, 351 pp.

Harley, M. M., 2006. A summary of fossil records for Arecaceae. Botanical Journal of the Linnean Society 151(1), 39–67.

Hass, H., Rowe, N. P., 1999. Thin sections and wafering. Fossil plants and spores: modern

techniques, 76–81.

Hastings, A. K., Bloch, J. I., Jaramillo, C. A., Rincon, A. F., Macfadden, B. J., 2013. Systematics and biogeography of crocodylians from the Miocene of Panama. Journal of Vertebrate Paleontology. 33(2), 239–263.

Hayward, J. J., Hayward, B. W., 1996. Fossil forests preserved in volcanic ash and lava at Ihumatao and Takapuna, Auckland. Tane 35, 127–142.

Head, J., J., Rincon, A. F., Suarez, C., Montes, C., and Jaramillo, C., 2012. Fossil evidence for earliest Neogene American faunal interchange: Boa (Serpentes, Boinae) from the early Miocene of Panama. Journal of Vertebrate Paleontology 32 (6), 1328-1334.

Henderson, E., Falcon-Lang, H. J., 2011. Diversity and ontogeny of *Pitus* tree-trunks in the early Mississippian rocks of the Isle of Bute, Scotland: The importance of sample size and quantitative analysis for fossil wood systematics. Review of Palaeobotany and Palynology 166 (3), 202–212.

Hendy, A.J.W., 2011. Taphonomic overprints on Phanerozoic trends in biodiversity: Lithification and other secular megabiases. In: Allison, P.A., Bottjer, D.J. (Eds.), Taphonomy: Process and Bias through Time. Topics in Geobiology 32, 19–77.

Henrot, A. J., François, L., Favre, E., Butzin, M., Ouberdous, M., Munhoven, G., 2010. Effects of CO_2, continental distribution, topography and vegetation changes on the climate at the Middle Miocene: A model study. Climate of the Past 6 (5), 675–694.

Herendeen, P.S., 2000. Structural variation in the Caesalpinioideae. *In*: Herendeen, P.S., Bruneau, A. (Eds.). Advances in Legume Systematics, Part 9. Royal Botanic Gardens, Kew, United Kingdom. Pp 45–64.

Herendeen, P. S., 2001. Structural evolution in the Caesalpinioideae (Leguminosae). Advances in legume systematics: part, 9, 45-64.

Herendeen, P. S., W. L. Crepet, D. L. Dilcher. 1992. The fossil history of the Leguminosae: phylogenetic and biogeographic implications. *In* P. S. Herendeen and D. L. Dilcher [eds.], Advances in legume systematics, part 4, The fossil record, Royal Botanic Gardens, Kew, Richmond, Surrey, UK. Pp.303–316.

Herendeen, P.S., Bruneau, A., Lewis, G.P., 2003. Phylogenetic relationships in Caesalpinoid legumes: a preliminary analysis based on morphological and molecular data. In: Klitgaard, Bruneau, B.B. (Eds.) Advances in Legume Systematics, Part 10. Royal Botanic Gardens, Kew, United Kingdom.

Herrera, F., Manchester, S., Vélez-Juarbe, J., Jaramillo, C., 2014. Phytogeograpic History of the Humiriaceae (Part 2). International Journal of Plant Sciences 175. DOI: 0.1086/676818.

Herrera, F., Manchester, S. R., Jaramillo, C., MacFadden, B., Da Silva-Caminha, S. A., 2010. Phytogeographic history and phylogeny of the Humiriaceae. International Journal of Plant Sciences 171(4), 392–408.

Herrera, F., Manchester, S., Carvalho, M., Correa, E., Jaramillo, C., 2012. Permineralized fruits and seeds from the Early Miocene Cucaracha Formation of Panama. Botany 2012. Columbus, Ohio, July 7-11.

Hickey, L., 1980. Paleocene and stratigraphy of the Clark´s Fork Basin. In: Gingerich, P.D. (Eds.). Early Cenozoic paleontology and stratigraphy of the Bighorn Basin, Wyoming. Papers on Paleontology. University of Michigan.

Hickey, M., King, C., 2001. The Cambridge illustrated glossary of botanical terms. Photosynthetica. 39, 3. 402 pp.

Hill, R. T., 1898. The geological history of the Isthmus of Panama and portions of Costa Rica. Bulletin of the Museum of Comparative Zoology 28, 151–285.

Hinojosa, L. F., Armesto, J. J., Villagrán, C., 2006. Are Chilean coastal forests pre-Pleistocene relicts? Evidence from foliar physiognomy, palaeoclimate, and phytogeography. Journal of Biogeography 33(2), 331–341.

Hinsley, S.R., 2004 onwards. Malvaceae Info. [Last updated March, 2009]. Available online at: http://www.malvaceae.info/ (last accessed 30 June, 2013).

Hodel, D. R., 2009. A new species of *Pritchardia* and the rediscovery of *P. lowreyana* on Oahu, Hawaii. Palms 53(4), 173–179.

Hoffman E., 1928. Verkieselte Pflanzenreste aus dem Tertiär von Leoben. Berg-und Hutenmannisches Jb 76 (4), 146–152.

Hofmann, E., 1948. *Manilkaroxylon diluviale* n. sp. Ein fossiles Sapotaceen Holz aus dem Quartar von Sta. Paula in Ekuador. Paläobiologica 8, 280-282.

Hollick, C. A., 1936. The tertiary floras of Alaska. US Government. Pp 181–184.

Horváth, E., 1954. A megyaszói Csordáskút kovásodott fatörzeinek vizsgálata. Untersuchung der verkieselten Baumstämme von Csordaskut bei Megyaszo. Botanikai Közlem 45, 141–150.

Hovenkamp, P. National Herbarium Nederland . http://www.nationaalherbarium.nl/ (last modified 9 december, 2009).

Hsü, K. J., 1983.The Mediterranean was a desert: a voyage of the Glomar Challenger. Princeton, NJ: Princeton University Press.

Hudspith, V. A., Scott, A. C., Wilson, C. J., Collinson, M. E., 2010. Charring of woods by volcanic processes: An example from the Taupo ignimbrite, New Zealand. Palaeogeography, Palaeoclimatology, Palaeoecology 291(1), 40–51.

Hutchinson, L., 1967. The Genera of Flowering Plants. Clarendon Press, Oxford, 117 pp.

IAWA (International Association of Wood Anatomists) Committee, 1964. Multilingual glossary of terms used in wood anatomy. Konkordia, Winterthur.

IAWA Hardwood Committee, 1989. List of microscopic features for hardwood identification. International Association of Wood Anatomists Bulletin 10, 176 – 219.

InsideWood. 2004 onwards. Available online at: http://insidewood.lib.ncsu.edu/search (last accessed 30 June 2013).

International Union of Geological Sciences, 2009 onwards. Avaliable online at http://www.iugs.org/ (last accessed 15 January 2014).

Jacoby, G. C., 1989. Overview of tree-ring analysis in tropical regions. IAWA Bulletin 10, 99–108.

Janis, C.M., 1993. Tertiary mammal evolution in the context of changing climates, vegetation, and tectonic events. Annual Review of Ecological Systematics 24, 467–500.

Janis, C., Damuth, J., 1990. Mammals. In McNamara, K. J. (Eds.). Evolutionary trends. London, Belkna. 301-345 pp.

Jansen, S., Baas, P., Smets, E., 2001. Vestured pits: their occurrence and systematic importance in eudicots. Taxon 135–167.

Jansen, S., Sano, Y., Choat, B., Rabaey, D., Lens, F., Dute, R., 2007. Pit memäanes in tracheary elements of Rosaceae and related families: new records of tori and pseudotori. American Journal of Botany 94 (4), 503–514

Jaramillo, C.A., Dilcher, D.L., 2001. Middle Paleogene palynology of Central Colombia, South America: a study of pollen and spores from tropical latitudes. Palaeontographica Abteilung B, 87–213.

Jaramillo, C., Rueda, M. J., Mora, G., 2006. Cenozoic plant diversity in the Neotropics. Science, 311(5769), 1893–1896.

Jaramillo, C., Hoorn, C., Silva, S., Leite, F., Herrera, F., Quiroz, L., Antonioli, L., 2010.

The origin of the modern Amazon rainforest: implications of the palynological and palaeobotanical record. Amazonia, Landscape and Species Evolution. 317–334.

Judd, W.S., Sanders, R.W., Donoghue, M.J., 1994. Angiosperm family pairs: Preliminary phylogenetic analyses. Harvard Papers Botany 5, 1–51.

Jones, S. M., 1950. Geology of Gatun Lake and Vicinity, Panama. Geological Society of America Bulletin 61(9), 893–922.

Jones, T.P., Chaloner, W.G., 1991. Fossil charcoal, its recognition and palaeoatmospheric significance. Palaeogeography, Palaeoclimatology, Palaeoecology 97, 39–50.

Judd, W.S., Manchester, S., 1997. Circumscription of Malvaceae (Malvales) as determined by a preliminary cladistic analysis of morphological, anatomical, palynological, and chemical characters. Brittonia 49, 384–405.

Kay, R. F., Madden, R. H., 1997. Mammals and rainfall: paleoecology of the middle Miocene at La Venta (Colombia, South America). Journal of Human Evolution 32(2), 161–199.

Kennett, J. P., Keller, G., Srinivasan, M. S., 1985. Miocene planktonic foraminiferal biogeography and paleoceanographic development of the Indo-Pacific region. Geological Society of America Memoirs 163, 197–236.

Kerrigan, R.A., Dixon, D.J., 2011. Elaeocarpaceae. In: Short, P.S., Cowie, I.D. (Eds.). Flora of the Darwin Region Volume 1. National Library of Australia. Northern Territory Government Publisher, Australia. 6 pp.

Kirby, M.X., MacFadden, B.J., 2005. Was southern Central America an archipelago or a peninsula in the middle Miocene? A test using land-mammal body size. Palaeogeography, Palaeoclimatology, Palaeoecology 228, 193– 202.

Kirby, M.X., Jones, D.S., MacFadden, B.J., 2008. Lower Miocene Stratigraphy along the Panama Canal and Its Bearing on the Central American Peninsula. PLoS ONE 3, 3–14.

Klitgärd, B.B., Lewis, G.P., 2010. Neotropical Leguminosae (Caesalpinioideae). In: Milliken, W., Klitgärd, B., Baracat, A. 2009 onwards. Neotropikey - Interactive key and information resources for flowering plants of the Neotropics. .http://www.kew.org/science/tropamerica/neotropikey/families/Leguminosae_(Caesalpinioideae).htm

Koeniguer J.C., 1971. Sur le bois fossils du Paléocene de Sessao (Niger). Review of Palaeobotany and Palynology 12, 303–323.

Koeniguer, J., 1973. Sur deux bois fossils du Quaternaire de l' Angamma (Tchad). Actes 98e. Congrés des Sociétés Savantes de Sint-Etienne 2, 41–46.

Koeniguer, J., 1974. Les bois fossiles de *Tamarix*, d' *Acacia* et de Retama du Plio-Quaternaire saharien. Congrés des Sociétés Savantes de Paris 278, 3069–3072.

Kozlowski, T. T., Pallardy, S. G., 1997. Growth control in woody plants. Elsevier.

Kramer, K., 1974a. Die Tertiären Hölzer südost-Asiens. Palaeontographica 144B, 45–181.

Kraüsel, R., 1922. Ueber einen fossilen Baumstamm von Bolang (Java), ein Beitrag zur Kenntnis der fossilen Flora Niederlandisch-Indiens. Koninklijke Akademie Wetenschappen Amsterdam, Verslagen der Zittingen van de Wis-en Natuurkundige Afdeeling 31, Proc. Sec. Sci, 25, 9–15.

Kräusel, R., 1939. Ergebnisse der Forschungsreisen Prof. E. Stromers in der Wüsten Agyptens. IV. Die fossilen Floren Agyptens. 3. Die fossilen Pflanzen Agyptens. Abhandlungen der Bayerischen Akademie der Wissenschaften. Mathematisch-naturwissenschaftliche Abteilung 47–140.

Krijgsman W., Hilgen F. J., Raffi, I., Sierro, F. J., Wilson, D. S. 1999. Chronology, causes and progression of the Messinian salinity crisis. Nature 400. 652–655.

Kukachka, F., Rees, L.W., 1943. Systematic anatomy of the woods of the Tiliaceae. University of Minnesota Agricultural Experiment Station Technical Bulletin, 78, 70 pp.

Lagabrielle, Y., Goddéris, Y., Donnadieu, Y., Malavieille, J., Suarez, M., 2009. The tectonic history of Drake Passage and its possible impacts on global climate. Earth Planet. Science Letters 279, 197–211.

Lakhanpal, R.N., Prakash, U., 1970. Cenozoic plants from Congo. I. Fossil woods from the Miocene of Lake Albert. Annals of the Royal Museum for Central Africa. Tervuren, Belgium 64, 1–20+13 pl.

Lakhanpal, R.N., Guleria, J.S., Awasthi, N., 1984. The fossil floras of Kachchh III. Tertiary megafossils. Palaeobotanist 33, 228–319.

Lakhanpal, R.N., Prakash, U., Bande, M.B., 1976. Fossil dicotyledonous woods from the Deccan Intertrappean beds of Mandla Distinct in Madhya Pradesh. Palaeobotanist 25, 190–204.

Lane C.E., 1959. Some aspects of the general biology of *Teredo*. In: Ray, D.L. (Ed.) Marine Boring and Fouling Organisms. University of Washington Press, Seattle, WA., pp. 137–144.

Larson, P. R., 1994. The vascular cambium: development and structure. Springer-Verlag.

Lavin, M., Herendeen, P. S.,Wojciechowski, M. F., 2005. Evolutionary rates analysis of Leguminosae implicates a rapid diversification of lineages during the Tertiary. Systematic Biology, 54(4), 575–594.

Lemoigne, Y., 1978. Flores tertiaries de la haute vallée de l'Olmo (Ethiopie).Palaeontographica. 165B, 189–157+12 pl.

Lemoigne, Y., Beauchamp, J., Samuel, E., 1974. Etude paléobotanique des depots volcaniques d´age tertiarie des bordures est et ouest du Systéme de Rifts éthiopiens. Geobios (Lyon) 7, 267–288.

Lens, F., Schönenberger, J., Baas, P., Jansen, S., Smets, E., 2007. The role of wood anatomy in phylogeny reconstruction of Ericales. Cladistics 23(3), 229–294.

Leopold, E., Liu, G., Clay-Poole, S., 1992. Low-biomass vegetation in the Oligocene. Eocene-Oligocene climatic and biotic evolution. In: Prothero, D., Berggren, W.A. (Eds.). Eocene-Oligocene Climatic and Biotic Evolution. Princeton University Press. Pp 399–420.

Lewis, G., Schrire, B., MacKinder, B., Lock, M., 2005. Legumes of the world. Royal Botanic Gardens, Kew, United Kingdom.

Lisi, C. S., Fo, M. T., Botosso, P. C., Roig, F. A., Maria, V. R., Ferreira-Fedele, L., Voigt, A.R., 2008. Tree-ring formation, radial increment periodicity, and phenology of tree species from a seasonal semi-deciduous forest in southeast Brazil. IAWA Journal 29 (2), 189–207.

Lopez, O.R., Kursar, T., 1999. Flood tolerance of four tropical tree species. Tree Physiology 19, 925–932.

Lorch, J., Fahn, A., 1959. A new species of *Leguminoxylon* from the Mio-Pliocene of Israel. Bulletin de Recherche. Council Israel. 7D, 65–70.

Lorente, M., 1986. Palynology and Palynofacies of the Upper Tertiary in Venezuela. Dissertationes Botanicae 99, 1–222.

Louvet, P., 1966. Ser une Légumineuse fossile nouvelle de Tinrhert (Algérie). Congrés des Sociétés Savantes de Paris. 2, 317–322.

Louvet, P., 1975. Sur trois bois fossiles du Tertiaire de Libye. Bulletin de la Société Botanique de France 121, 269–280.

Lutz, A.I., 1980. *Entrerrioxylon victoriensis* nov. gen. et sp. (Leguminosae) del Mioceno

superior (Fm. Parana) de la Provincia de Entre Rios, Argentina, Facena, Corrientes Argentina 4, 21–29.

Lutz, A.I., 1987. Estudio anatomico de maderas terciarias del Valle de Santa Maria (Catamarca-Tucuman), Argentina, Facena, Corrientes Argentina 7, 125–143.

Mabberley, D. J., 2008. A portable dictionary of plants, their classification and uses. Cambridge University Press. MacFadden, B., Higgins, P., 2004. Ancient ecology of 15-million-year-old browsing mammals within C3 plant communities from Panama. Oecologia 140, 169–182.

MacDonald, D. F., 1919. The sedimentary formations of the Panama Canal Zone, with special reference to the stratigraphic relations of the fossiliferous beds. United States National Museum Bulletin 103, 525–545.

MacFadden, B. J., 2000. Cenozoic mammalian herbivores from the Americas: reconstructing ancient diets and terrestrial communities. Annual Review of Ecology and Systematics 33–59.

MacFadden, B.J., 2006. North American Miocene land mammals from Panama. Journal of Vertebrate Paleontology 26, 720–734.

MacFadden, B.J., Higgins, P., 2004. Ancient ecology of 15-million-year-old browsing mammals within C3 plant communities from Panama. Oecologia. 140, 169–182.

MacFadden, B. J., Higgins, P., Clementz, M. T., Jones, D. S., 2009. Diets, habitat preferences, and niche differentiation of Cenozoic sirenians from Florida: evidence from stable isotopes. Paleobiology 30:297–324.

MacFadden, B.J., Kirby, M.X., Rincon, A., Montes, C., Moron, S., Strong, N., Jaramillo, C., 2010. Extinct peccary "*Cynorca*" *occidentale* (Tayassuidae, Tayassuinae) from the Miocene of Panama and correlations to North America. Journal of Paleontology 84 (2), 288–298.

MacFadden, B.J., Bloch, J., Evans, H., Foster, D., Morgan, G., Rincon, A., Wood, A., 2014. Temporal Calibration of the Centenario Fauna, Early Miocene of Panama. The Journal of Geology 122 (2), 113–135.

Machado et al. (1997, IAWA Bulletin 18: 13–25)

Mackinder, B. A., 2006. Two new species of *Berlinia* (Leguminosae- Caesalpinioideae: Detarieae). Kew Bulletin 161–166.

MacMillan et al., 2004

Mädel, E., 1960. Mahagoniholzer der Gattung *Carapoxylon* ng (Meliaceae) aus dem

Europaischen.Tertiar. Senckenbergiana Lethaea 41, 393–421.

Mädel-Angeliewa, E., 1968. Eichen-und Pappelholz aus der pliozänenKolhe im Gebiet von Baccinello (Toskana, Italien). Geol. Jb 86, 433–470.

Mahabale, T. S., Kulkarni, K. M., 1981. A new fossil palm from Kondhali, District Nagpur, Maharashtra. Palaeobotanist 27, 174–81.

Mai, D. H., 1995. Tertiäre Vegetationsgeschichte Europas. Fischer, Jena, Stuttgart, New York.

Major, J.J., Lara, L.E., 2013. Overview of Chaitén Volcano, Chile, and its 2008-2009 eruption. Andean Geology 40, 196–215.

Maki, T., Hase, Y., Kawamuro, K., Shichi, K., Minoura, K., Oda, T., Miyoshi, N., 2003. Vegetation changes in the Baikal region during the Late Miocene based on pollen analysis of the BDP-98-2 coreIn: Anonymous Long Continental Records from Lake Baikal, Springer. Pp. 123–135.

Manchester, S., 1979. *Triplochitioxylon* (Sterculiaceae): a new genus of wood from the Eocene of Oregon and its bearing on xylem evolution of the extant genus

Manchester, S., 1989. Systematics and fossil history of the Ulmaceae. In: Crane, P., Blackmore, S. (Eds.). Evolution, systematic and fossil history of the Hamamelidae 2. Higher Hamamelidae. Systematics Association special volume 40B. Clarendon, Oxford.

Manchester, S., 1992. Flowers, fruits and pollen of *Florissantia*, an extinct malvalean genus from the Eocene and Oligocene of Western North America. American Journal of Botany 79, 996–1008.

Manchester, S., 1994. Fruits and seeds of the middle Eocene Nut Beds flora, Clarno Formation, Oregon. Paleontographica Americana 58, 1–205.

Manchester, S. 1996. Collecting fossil plants in Florida. Florida Paleontology. 8. The Florida Paleontological Society. Florida, U.S.A.

Manchester, S., 1999. Biogeographical relationships of North American Tertiary floras. Annals of the Missouri Botanical Garden 86, 472–522.

Manchester, S., 2002. Leaves and fruits of *Celtis aspera* (newberry) Comb. Nov. (Celtidaceae) from the Paleocene of North America and Eastern Asia. International Journal of Plant Sciences 163 (5), 725–726.

Manchester, S, Miller. R.B., 1978. Tile cells and their occurrence in Malvalean fossil woods. International Association of Wood Anatomists Bulletin 2–3, 23–28.

Triplochiton. American Journal of Botany 66, 699–708.

Manchester, S., Chen, Z., Zhou, Z., 2006. Wood anatomy of *Craigia* (Malvales) from Southeastern Yunnan, China. IAWA Journal 27 (2), 129–136.

Manokaran, N., LaFrankie, J.V., Kochummen, K.M., Quah, E.S., Klahn, J.E., Ashton, P.S., Hubbell, S.P., 1990. Methodology for the fifty hectare research plot at Pasoh Forest Reserve. Res. Pamphlet Forest Res. Institute Malaysia 104, 1–69.

Marcati, C. R., Oliveira, J. S., Machado, S. R., 2006. Growth rings in cerrado woody species: occurrence and anatomical markers. Biota Neotropica, 6 (3).

Marín, G. C., Nygård, R., Rivas, B. G., Oden, P. C., 2005. Stand dynamics and basal area change in a tropical dry forest reserve in Nicaragua. Forest ecology and management 208 (1), 63–75.

Marshall, L.G., Webb, S.D., Sepkoski, J.J., Raup, D.M., 1982. Mammalian evolution and the Great American Interchange. Science 215, 1351–1357.

Martínez, L., 2013. Fossil legume woods from the Late Miocene, Chiquimil Formation (Santa María Basin), Argentina. Review of Palaeobotany and Palynology 201, 1–11.

Martínez-Cabrera, H.I., S.R.S. Cevallos-Ferriz., 2004. A new species of *Tapirira* (Anacardiaceae) from the Early Miocene sediments of the El Cien Formation, Baja California, Mexico. IAWA Journal 25, 103–117.

Martínez-Cabrera, H. I., Cevallos-Ferriz, S. R., 2006. Maclura (Moraceae) wood from the Miocene of the Baja California Peninsula, Mexico: Fossil and biogeographic history of its closer allies. Review of Palaeobotany and Palynology 140(1), 113–122.

Martinez-Cabrera, H.I., Cevallos-Ferriz, S.R.S., 2008. Palaeoecology of the Miocene El Cien Formation (Mexico) as determined from wood anatomical characters. Review of Palaeobotany and Palynology 150, 154–167.

Martínez-Cabrera, H. I., Estrada-Ruiz, E., Castañeda-Posadas, C., Woodcock, D., 2012. Wood specific gravity estimation based on wood anatomical traits: Inference of key ecological characteristics in fossil assemblages. Review of Palaeobotany and Palynology 187, 1–10.

Mauseth, J., 1988. Plant anatomy. Benjamin/Cummings Publishing Company Menlo Park, California. 560 pp.

McClelland, E., Wilson, C.J., Bardot, L., 2004. Palaeotemperature determinations for the 1.8-ka Taupo ignimbrite, New Zealand, and implications for the emplacement history of a high-velocity pyroclastic flow. Bulletin of volcanology 66, 492–513.

McParland, L.C., Collinson, M.E., Scott, A.C., Campbell, G., 2009. The use of reflectance values for the interpretation of natural and anthropogenic charcoal assemblages. Archaeological and Anthropological Sciences 1, 249–261.

McParland, L.C., Collinson, M.E., Scott, A.C., Steart, D.C., Grassineau, N.V., Gibbons, S.J., 2007. Ferns and fires: experimental charring of ferns compared to wood and implications for paleobiology, paleoecology, coal petrology, and isotope geochemistry. Palaios 22, 528–538.

Medeanic, S., 2001. The Sarmatian (Middle-late miocene) paleoflora evolution in the eastern paratethys. Acta Palaeontologica Sinica. 41, 592-600.

Mennega, A.M.W., 1987. Wood anatomy of the Euphorbiaceae, in particular of the subfamily Phyllanthoideae. Botanical Journal of the Linnean Society of London. 94, 111–126.

Metcalfe, C.R., Chalk, L., 1950. Anatomy of the Dicotyledons (2 vols), Second Edition, Clarendon Press, Oxford, 1500 pp.

Metcalfe, C. R., and L. Chalk. 1983. Anatomy of the Dicotyledons. Vol. 2. Clarendon, Oxford.

Miall, A.D., 1977. A review of the braided river depositional environment. Earth Science Review 13, 1–62.

Miall, A.D., 1992. Alluvial deposits. In: Walker, R.G., James, N.P. (Eds). Facies Models: Response to Sea Level Change. Geological Association of Canada, pp. 119–142.

Miller, K. G., Wright, J. D., Fairbanks, R., G., 1991. Unlocking the ice house: Oligocene-Miocene oxygen isotopes, eustasy, and margin erosion. Journal of Geophysical Research: Solid Earth 96(B4), 6829–6848.

Mirioni, 1965. Etude anatomique de quelques bois tertiaires de Colombie. Boletin Geologico de la Universidad Industrial de Santander 20, 27–59.

Montes, C., Cardona, A., McFadden, R.R., Moron, S., Silva, C.A., Restrepo-Moreno, S., Ramirez, D., Hoyos, N., Wilson, J., Farris, D.W., Bayona, G., Jaramillo, C., Valencia, V., Bryan, J., Flores, J.A., 2012. Evidence for middle Eocene and younger emergence in Central Panama: implications for the Ishtmus closure. Geological Society of America Bulletin 39, 1–20.

More, D., White, J., 2003. Cassell's Trees of Britain and Northern Europe. Cassell, London, UK.

Morley, R. J., Dick, C. W., 2003. Missing fossils, molecular clocks, and the

origin of the Melastomataceae. American Journal of Botany 90 (11), 1638– 1644.

Mosbrugger, V., Gee, C. T., Belz, G., Ashraf, A. R., 1994. Three-dimensional reconstruction of an in-situ Miocene peat forest from the Lower Rhine Embayment, northwestern Germany- new methods in palaeovegetation analysis. Palaeogeography, Palaeoclimatology, Palaeoecology 110 (3), 295–317.

Muellner, A. N., Savolainen, V., Samuel, R., Chase, M. W., 2006. The mahogany family "out-of-Africa": Divergence time estimation, global biogeographic patterns inferred from plastid< i> rbcL</i> DNA sequences, extant, and fossil distribution of diversity. Molecular phylogenetics and evolution 40(1), 236–250.

Müller, J., 1968. Palynology of the Pedawan and Plateau Sandstone Formations (Cretaceous–Eocene) in Sarawak. Micropalaeontology 14, 1–37.

Müller, J. 1981. Fossil Pollen Records of Extant Angiosperms. Botanical Review 47 (1), 1–142.

Müller-Stoll, W.R., Mädel., E., 1967. Die fossilen Leguminosen-Hölzer. Eine revision der mit Leguminosen verglichenen fossilen Hölzer und Beschreibungen älterer und neuer Arten. Palaeontographica 119B, 95 –174.

Muller-Stoll, W. R., Madel-Angeliewa, E., 1984. Fossile Holzer mit schmalen apotrachealen Parenchymbandern. II. Arten aus den Gattungen *Ebenoxylon* Felix und *Eudiospyroxylon* gen. nov. Feddes Repertorium.

Myburg, A. A., 2001. Genetic architecture of hybrid fitness and wood quality traits in a wide interspecific cross of *Eucalyptus* tree species. And sederoff?

Nambudiri, E. M. V., Tidwell, W. D. ,1998. *Palmoxylon hebbertii,* from the Lower Oligocene Goldens Ranch Formation of central Utah, USA, with an analysis of some characteristics previously used in the classification of *Palmoxylon*. Canadian Journal of Botany 76(3), 517 –529.

Native Plants of Hawaii, 2009. University of Hawaii. http://nativeplants.hawaii.edu/index/ (last accessed 29 october, 2013).

Navale, G.B.K., 1959. On the occurence of fossil Cynometra from the Sindalore series close to Pondicherry, India. Palaeobotanist 7, 6–11.

Navale, G., 1963. Fossil woods of Leguminosae from Tertiary rocks of the Cuddalore Series near Pondicherry, India. Palaeobotanist. 11, 54 – 65.

Niklas, K.J., 1994. Predicting the height of fossil plant remains: an allometric approach to an old problem. American Journal of Botany 1235–1242.

Nisancioglu, K.H., Raymo, M.E., Stone, P.H., 2003. Reorganization of Miocene deep water circulation in response to the shoaling of the Central American seaway. Paleoceanography 18 (1), PA1006.

Nishida, M., 1984. The anatomy and affinities of the petrified plants from the Tertiary of Chile. I. In: Nishida, M. (Ed.).Contributions to the botany in the Andes, I. Academia Scientific Book Inc. Tokyo, Japan. Pp 81–85+pl. 77–78.

Nishida, M., Nishida, H., Nasa, T., 1986. A synopsis of Nothofagoxylon from South America with special reference to the species from Ultima Esperanza and Tierra del Fuego, Chile. Res. Inst. Evolut. Biol. Sci. Rep. 3, 22–32.

Nishida, M., Nishida, H., Rancusi, M.H., 1988. Notes on the petrified plants from Chile (1). Journal of Japanese Botany 63, 39–48.

NOAA, 1985. Climates of the States. 3rd edition. Gale Research, Detroit, USA.

Nudds, J., Selden, P., 2008. Fossil Ecosystems of North America. Manson Publishing.

Oakley, D., Falcon-Lang, H.J., Gasson, P., 2009. Morphometric analysis of some Cretaceous angiosperm woods and modern structural and phylogenetic analogues: implications for systematics. Review of Paleobotany and Palynology 157, 375–390.

Olson, M. E., 2005. Commentary: typology, homology, and homoplasy in comparative wood anatomy. IAWA Journal 26 (4), 507.

Pace, M., Angyalossy, V., 2013. Wood anatomy and evolution: a case in the Bignoniaceae. International Journal of Plant Sciences 174 (7), 1014–1048.

Pagani, M., Freeman, K. H., Arthur, M. A., 1999. Late Miocene atmospheric CO2 concentrations and the expansion of C4 grasses. Science 285(5429), 876–879.

Palazzesi, L., Barreda, V. D., Cuitiño, J. I., Guler, M. V., Tellería, M. C., Santos, R. V., 2014. Fossil pollen records indicate that Patagonian desertification was not solely a consequence of Andean uplift. Nature communications 5.

Parrish, J. T., Falcon-lang, H. J., 2007. Coniferous trees associated with interdune deposits in the Jurassic Navajo Sandstone Formation, Utah, USA. Palaeontology 50(4), 829–843.

Patton, T. H., Taylor, B. E., 1973. The Protoceratinae (Mammalia, Tylopoda, Protoceratidae) and the systematics of the Protoceratidae. Bulletin of the American Museum of Natural History 150, 347–414.

Peralta-Medina, E., Falcon-Lang, H. J., 2012. Cretaceous forest composition and productivity inferred from a global fossil wood database. Geology 40(3), 219–222.

Petrescu, I., 1978. Studiul lemnelor fosile din Oligocenul din nor-vestul Transilvaniei. Institut de géologie et de géophysique. 27, 113–184+74 pl.

Petriella, B., 1972. Estudio de las maderas petrificadas del Terciario Inferior del área Central de Chubut (Cerro Bororó). Revista del Museo de La Plata. Paleontologia. 6 (41), 158 –254.

Pfeil, B.E., Brubaker C., Craven L., Crisp M., 2002. Phylogeny of *Hibiscus* and the tribe Hibisceae (Malvaceae) using chloroplast DNA sequences of ndhF and the rpl16 intron. Systematic Botany 27, 333–350.

Philippe, M., Bamford, M. , McLoughlin, S. , Alves, L.S.R. , Falcon-Lang, H.J. , Gnaedinger, S. , Ottone, E.G. , Pole, M. , Rajanikanth, A. , Shoemaker, R.E. , Torres, T. , Zamuner, A. , 2004. Biogeographic analysis of Jurassic–Early Cretaceous wood assemblages from Gondwana. Review of Palaeobotany and Palynology 129, 141-173.

Piqué, A., Tricart, Guiraud, P., Laville, R., Bouaziz, E., Amrhar S., Ouali, R. A. 2002. The Mesozoic-Cenozoic Atlas belt (North Africa): an overview.Geodinamica Acta 15(3), 185–208.

Plant Resources of Tropical Africa available online at: www.prota.org (last accessed 28 July 2014).

Platen, P., 1908. Untersuchungen fossiles Hölzer aus der Western der Vereinigten Staaten von Nordamerika. Sber . Naturf. Ges. Leipzig 34, 1–155.

PlantNET - The Plant Information Network System of The Royal Botanic Gardens and Domain Trust, Sydney, Australia. http://plantnet.rbgsyd.nsw.gov.au (last accessed 25 october, 2013).

Plomion, C., Leprovost, G., Stokes, A., 2001. Wood formation in trees. Plant physiology, 127(4), 1513–1523.

Poinar, G., 2001. Fossil palm flowers in Dominican and Mexican amber. Department of Entomology, Oregon State University, Corvallis, OR 97331, USA.

Poinar, G. O., Poinar, R., 1999. The amber forest: a reconstruction of a vanished world. Princeton University Press.

Poinar, H. N., Melzer, R. R., Poinar Jr, G. O., 1996. Ultrastructure of 30–40 million year old leaflets from Dominican amber (*Hymenaea protera*, Fabaceae: Angiospermae). Experientia 52(4), 387–390.

Pons, D., 1980. Les bios fossiles du Tertiaire superieur de la region de Toluviejo-Corozal (Dept. de Sucre, Colombie). CR 105 Congrés des Sociétés Savantes de Paris. I, 163-82.

Pons, J.C., 1985. Découverte d'un bois fossile de fagaceae dans la Formation Farellones (Miocène) des Andes d'Aconcagua (Chili): importance paléobotanique et signification paléo-orographique. 110e Congrès National des Sociétés Savantes.

Poole I. (2002) Systematics of Cretaceous and Tertiary Nothofagoxylon: Implications for Southern Hemisphere biogeography and evolution of the Nothofagaceae. Australian Systematic Botany 15 (2): 247-276.

Pons, D., De Franceschi, D., 2007. Neogene woods from western Peruvian Amazon and palaeoenvironmental interpretation. Bulletin of Geosciences. 82, 343–354.

Poole, I., Van Bergen, P. F., 2006. Physiognomic and chemical characters in wood as palaeoclimate proxies. In Plants and Climate Change. Springer Netherlands.Pp. 175–196.

Poole, I., Richter, H. G., Francis, J. E., 2000. Evidence for Gondwanan origins for *Sassafras* (Lauraceae)? Late Cretaceous fossil wood of Antarctica. IAWA J ournal. 21(4), 463-475.

Potter, P. E., Szatmari, P., 2009. Global Miocene tectonics and the modern world. Earth-Science Reviews, 96 (4), 279–295.

Potts, R., Behrensmeyer, A., 1992. Late Cenozoic terrestrial ecosystems. Terrestrial ecosystems through time: evolutionary paleoecology of terrestrial plants and animals, In: Behrensmeyer, A. K., Damuth, J. D, DiMichele, W.A., Potts, R., Sues, R.D., and Wing, S.L. Terrestrial Ecosystems Through Time. 419-451 pp. University of Chicago..

Pound, M. J., Haywood, A. M., Salzmann, U., Riding, J. B., Lunt, D. J., Hunter, S. J., 2011. A Tortonian (late Miocene, 11.61–7.25 Ma) global vegetation reconstruction. Palaeogeography, Palaeoclimatology, Palaeoecology 300(1), 29–45.

Pound, M. J., Haywood, A. M., Salzmann, U., Riding, J. B., 2012. Global vegetation dynamics and latitudinal temperature gradients during the Mid to Late Miocene (15.97–5.33 Ma). Earth-Science Reviews, 112(1), 1–22.

Prakash, U., 1974. Palaeogene angiosperms woods In: Surange, K.R., Lakhanpal, R.N., Bharadwaj, D.C (Eds.), Aspects and appraisal of Indian palaeobotany. Birbal Sahni Institute of Palaeobotany. Lucknow 306–320.

Prakash, U., 1977. Fossil dicotyledonous woods from the Tertiary of Thailand. Palaeobotanist 26, 50–62.

Prakash, U., 1979. Fossil woods from the Lower Siwalik beds of Himachal. Pradesh, India.

Prakash, U., Awasthi, N., 1971. Fossil woods from the Tertiary of eastern India. II. Palaeobotanist 18, 219–225.

Prakash, U., Baghoorn, E.S., 1961a. Miocene fossil woods from the Columbia Basalts of Central Washington. Journal of Arnold Arboretum 42, 165–203

Prakash, U., Baghoorn, E.S., Scott, R.A., 1962. Fossil wood of *Robinia* and *Gleditsia* from the Tertiary of Montana. American Journal of Botany 49, 692–696.
Palaeobotanist 25, 376–392.

Prakash, U., Dayal, R., 1963. Fossil woods resembling *Elaeocarpus* and *Leea* from the Deccan Intertrappean Bedsof Mahurzari near Nagpur, India. Current Science 32, 315–316.

Prakash, U., Dayal, R., 1964. Fossil wood resembling *Grewia* from the Deccan Intertrappean beds of Mahurzari near Nagpur, India. Current Science 32, 315–316.

Prakash, U., Tripathi, P.P., 1972. Fossil woods from the Tertiary of Assam. Palaeobotanist

Prakash, U., Tripathi, P.P., 1975. Fossil dicotyledonous woods from the Tertiary of eastern India. Palaeobotanist. 22, 51–62.
21, 305–316.

Privé, C., 1975. Etude de quelques bois de chênes tertiaries du Massif Central, France. Palaeontographica 183B, 119–140+pl. 33–35.

Prior, J., Alvin, K. L., 1983. Structural changes on charring woods of *Dichrostachys* and *Salix* from southern Africa. IAWA Bulletin 4 (4), 197–206.

Prior, J., Gasson, P., 1993. Anatomical changes on charring six African hardwoods. IAWA Journal 14, 77–86. Pujana, R., Martínez, L., Brea, M., 2011. El registro de maderas fósiles de Leguminosae de Sudamérica. Revista del Museo Argentino de Ciencias Naturales 13 (2), 183–194.

Pujana, R., Martínez, L., Brea, M., 2011. El registro de maderas fósiles de Leguminosae de Sudamérica. Revista del Museo Argentino de Ciencias Naturales 13 (2), 183–194.

Pujana, R. R., Burrieza, H. P., Silva, M. P., Tourn, G. M., Castro, M. A.,

2013. Comparative wood anatomy of vegetative organs (stem and rhizome) of *Sophora linearifolia* (Sophoreae, Papilionoideae, Leguminosae). Boletín de la Sociedad Argentina de Botánica 48 (3-4), 435–442.

Punt, W., Malotaux, M., 1984. Cannabaceae, Moraceae, and Urticaceae. Review of Palaeobotany and Palynology 42, 23–44.

Purser, B. H., Bosence, D. W., 1998. Sedimentation and Tectonics in Rift Basins Red Sae-Gulf of Aden. Springer.

Pyne, S.J., Andrews, P.L., Laven, R.D., 1996. Introduction to Wildland Fires. John Wiley and Sons, Inc., New York, NY.

Qi, G.-F., Yang, J.-J., Xu, R.-H., Yang, M., 1997. Studies on two fossil woods of Ulmaceae excavated from Wuhan area. Acta Palaeontologica Sinica 36, 373–377.

Ragonese, A.M., 1977. *Nothofagoxylon menendezii*, leño petrificado del Terciario de General Roca, Rio Negro, Argentina. Ameghiniana 14, 75–86.

Ramanujam, C.G.K., 1954. On some silicified woods from near Pondicherry, South India. Palaeobotanist. 3, 40–50+2 pl.

Ramstein, G., Fluteau, F., Besse, J., Joussaume, S., 1997. Effect of orogeny, plate motion and land-sea distribution on Eurasian climate change over the past 30 million years. Nature 386, 788–795.

Record, S. J., Hess, R. W., 1949. Timbers of the new world. Yale University Press.

Reid, E. M., Chandler, M. E. J., 1933. London Clay Flora. British Museum of Natural History.

Rendle, A.B., 1925. The classification of flowering plants. 2. Dicotyledons. Cambridge University Press, Cambridge, 640 pp.

Retallack, G. J., 1994. A pedotype approach to latest Cretaceous and earliest Tertiary paleosols in eastern Montana. Geological Society of America Bulletin. 106(11), 1377–1397.

Retallack, G.J., 2001. Cenozoic expansion of grasslands and climatic cooling. Journal of Geology 109, 407-426.

Retallack, G. J., 2005. Pedogenic carbonate proxies for amount and seasonality of precipitation in paleosols. Geology 33(4), 333-336.

Retallack, G., Kirby M.X., 2007. Middle Miocene global change and paleogeography of Panama. Palaios 22, 667–679.

Rich, P., Rich, T., 1983. The Central American dispersal route: biotic history and

paleogeography. Costa Rican natural history.University of Chicago Press, Chicago, 12–34.

Richter., H.G., Dallwitz, M.J., 2000 onwards. Commercial timbers: descriptions, illustrations and information . Version: 25th June, 2009. http://delta-intkey.com.

Rößler, R., Zierold, T., Feng, Z., Kretzschmar, R., Merbitz, M., Annacker, V., Schneider, J.W., 2012. A snapshot of an early permian ecosystem preserved by explosive volcanism: new results from the Chemnitz Petrified Forest, Germany. PALAIOS 27 (11), 814–834.

Roberts, E. M., Hendrix, M. S., 2000. Taphonomy of a petrified forest in the Two Medicine Formation (Campanian), northwest Montana: Implications for palinspastic restoration of the Boulder batholith and Elkhorn Mountains volcanics. Palaios, 15(5), 476–482.

Rodríguez-Reyes, O., Falcon-Lang, H., Gasson, P., Collinson, M., Jaramillo, C., 2014. Fossil woods (Malvaceae) from the lower Miocene (early to mid-Burdigalian) part of the Cucaracha Formation of Panama (Central America) and their biogeographic implications. Review of Palaeobotany and Palynology 209, 11–34.

Rossetto, M., Kooyman, R., Sherwin, W., Jones, R., 2008. Dispersal limitations, rather than bottlenecks or habitat specificity, can restrict the distribution of rare and endemic rainforest trees. American Journal of Botany 95(3), 321-329.

Rost, T., 1996. Section of Plant Biology. Division of Biological Sciences, University of California. http://www.plb.ucdavis.edu/labs/rost/tomato/stems/secstem3.html (last accessed April., 2014).

Rowley, S., 2005. *Teredo navalis*. Great shipworm. Marine Life Information Network: Biology and Sensitivity Key Information Sub-programme. Plymouth: Marine Biological Association of the United Kingdom. http://www.marlin.ac.uk/reproduction.php?speciesID=4447 (Last accessed 28 June 2013).

Royal Botanic Gardens Kew. http://www.kew.org/science-conservation/research-data/science-directory/teams/leguminosae (last accessed 15 august 2014).

Rozema, J., Aerts, R., Cornelissen, H., 2006**.** Plant Ecology. Springer. 261 pp.

Sahni, B., 1964. Revision of Indian fossil plants: Part III. Monocotyledons .Monography Birbal Sahni Institute of Palaeobotany. 1, 1–89.

Sakala, J., Prive-Guilla, C., 1999. Silicified Angiosperm wood from the Dangu locality (Ypresian of the Gisors region, Eure, France): the problem of root wood. Comptes rendus de l'Académie des sciences - Série IIa - Sciences de la terre et des planètes 328, 553–557.

Salard, M., 1961. Euphorbioxylon brideloides n. sp. Bois fossile du Perou. 86 Congrès des Sociètès savants. Poltiers. Pp 581-591.

Sandi, C., Flores, E.M., 2002. *Prioria copaifera* Griseb. In Vozzo, J.A. (Ed.). Tropical tree seed manual. Agriculture Handbook Number 721. Washington, DC, United States Department of Agriculture, Forest Service. Pp. 654 – 656.

Sattarian, R., 2006. Pollen morphology of African *Celtis* (Celtidaceae). Journal of Botanical Taxonomy and Geobotany. 117, 1–2, 34–40.

Sayadi, S., 1973. Contribution á l'étude de la flore miocéne de la Turquie. Universitat de Paris. VI. 81pp.

Scheihing, M. H., Pfefferkorn, H. W., 1984. The taphonomy of land plants in the Orinoco Delta: a model for the incorporation of plant parts in clastic sediments of Late Carboniferous age of Euramerica. Review of Palaeobotany and Palynology, 41(3), 205 – 240.

Schneider, B., Schmittner, A., 2006. Simulating the impact of the Panamanian seaway closure on ocean circulation, marine productivity and nutrient cycling. Earth and Planetary Sciences Letters 246, 367–380.

Schönfeld, G., 1947. Hölzer aus dem Tertiär von Kolumbien. Abhandlungen der Senckenbergischen Naturforschenden Gesellschaft 475, 1–53 + pl. 1–5.

Schöngart, J., Piedade, M. T. F., Wittmann, F., Junk, W. J.,Worbes, M., 2005. Wood growth patterns of *Macrolobium acaciifolium* (Benth.) Benth (Fabaceae) in Amazonian black-water and white-water floodplain forests.Oecologia. 145(3), 454–461.

Schöning, M., Bandel, K., 2004. A diverse assemblage of fossil hardwood from the Upper Tertiary (Miocene?) of the Arauco Peninsula, Chile. Journal of South American Earth Sciences, 17(1), 59–71.

Schopf, J. M., 1975. Modes of fossil preservation.Review of Palaeobotany and Palynology 20, 27-53.

Schweingruber, F. H., 1988. Tree rings-basics and applications of dendrochronology. D. Reidel Publishing Company.

Schweingruber, F.H., 1990. Anatomy of European woods. Paul Haupt.

Schweingruber, F., 2006. From Anatomical Features to Plant Structures. Atlas of Woody Plant Stems: Evolution, Structure, and Environmental Modifications, 187–202.

Schweingruber, F.H., Börner, A., Schulze, E., 2013. Atlas of stem anatomy in herbs, shrubs and trees. Springer, Berlin, pp. 1–4.

Scott, A.C., 1989. Observations on the nature and origin of fusain. International Journal of Coal Geology 12, 443–475.

Scott, A. C., 2000. The Pre-Quaternary history of fire. Palaeogeography, Palaeoclimatology, Palaeoecology. 164(1), 281–329.

Scott, A. C., 2009. Fire Effects on Soils and Restoration Strategies. In: Cerdà, A., Robichaud, P. (Eds.). New Hampshire: Science Publishers Inc. Pp. 1–37

Scott, A. C., 2010. Charcoal recognition, taphonomy and uses in palaeoenvironmental analysis. Palaeogeography, Palaeoclimatology, Palaeoecology, 291(1), 11–39.

Scott, A.C., Glasspool, I.J., 2005. Charcoal reflectance as a proxy for the emplacement temperature of pyroclastic flow deposits. Geology 33, 589–592.

Scott, A. C., Jones, T. P., 1991. Microscopical observations of recent and fossil charcoal. Microsc. Anal. 13-15.

Scott, A.C., R.S., Sparks J., Bull, I.D., Knicker H., Evershed, R.P., 2008. Temperature proxy data and its significance for the understanding of pyroclastic density currents. Geology 36, 143-146.

Scott, R.A., Barghoorn, E.S., Prakash, U., 1962. Wood of Ginkgo in the Tertiary of Western North America. American Journal of Botany 49 (10), 109 –1101.

Scotese, C. R., 2003. Paleomap project home page. Paleomap Project. http://www.scotese.com/ (last accessed 20 August 2014).

Selmeier, A., 1957. Die Kieselhölzer des bayerischen Miozäns. Jber naturwissenschaftliche 23, 1–74.

Selmeier, A., 1985. Jungtertiäre Kieselhölzern (fam. Bombacaceae, Tiliaceae, Meliaceae) aus dem Ortenburger Schotter von Rauscheröd, Niederbayern. Münchner Geowissenschaftliche. Abh., A, 6. 89–140.

Selmeier, A., 1989. Ein jungtertiäries *Celtis*–Holz (Ulmaceae) aus der Südlichen Frankenalb (Bayern). Archaeopteryx. 7, 35–50.

Selmeier, A., 1991. Ein verkieseltes Sapotaceae-Holz, Bumelioxylon holleisii n. gen., n.

sp., aus jungtertiaren Schichten der Sudlichen Frankenalb (Bayern). Archaeopteryx 9, 55–72.

Selmeier, A., 2000. Structural variation of Tertiary *Grewia* woods (Tiliaceae) from East Bavarian Molasse, Germany. Feddes Repertorium 111 (7-8), 465–480.

Selmeier, A., 2001b. Silicified Miocene woods from the North Boheamian Basin (Czech Republic) and from Kuzuluk, district Adapazari (Turkey). Mitt. Bayer. Staatssamml. Palaeontology and Historical Geology. 41, 111–144

Shallom, L.J., 1963. A fossil dicotyledonous wood with tile cells, from the Deccan Intertrappean beds of Chhindwara district. Journal of the Indian Botanical Society 42, 161–169.

Slaughter, B. H., 1981. A new genus of geomyoid rodent from the Miocene of Texas and Panama. Journal of Vertebrate Paleontology, 1(1), 111–115.

Slocum, D., McGinnes Jr, E., Beall, F., 1978. Charcoal yield, shrinkage, and density changes during carbonization of oak and hickory woods. Wood science 11, 42–47.

Smithsonian Tropical Research Institute Herbarium. http://biogeodb.stri.si.edu/herbarium. (last accessed 28 June 2012).

Sperry, J. S., 2003. Evolution of water transport and xylem structure.International Journal of Plant Sciences 164(S3), S115–S127.

Sprent, J., 2001. Nodulation in legumes. Annals of Botany 89 (6), 797–798.

Srivastava, R., Guleria, J. S., 2000. *Grewinium,* a substitute name for *Grewioxylon.* Shallom non Schuster.

Srivastava, R., Suzuki, M., 2001. More fossil woods from the Palaeogene of Northern Kyushu, Japan. IAWA Journal 22, 85–105.

Stenzel, K. G., 1904. Fossile Palmenhölzer. Beiträge zur Paläontologie und Geologie Österreich–Ungarns und des Orients 16, 10 – 28.

Steppuhn, A., Micheels, A., Bruch, A. A., Uhl, D., Utescher, T., Mosbrugger, V., 2007. The sensitivity of ECHAM4/ML to a double CO2/subscenario for the late Miocene and the comparison to terrestrial proxy data.Global and Planetary Change. 57(3), 189-212.

Stevens, P.F., 2001 onwards. Angiosperm Phylogeny Website. Version 9, June 2008 [last updated 08 June 2011]. http://www.mobot.org/mobot/research/apweb/welcome.htm (last accessed 8 July 2013).

Stewart, R., Stewart, J., Woodring, W.P., 1980. Geologic Map of the Panama Canal and

Vicinity, Republic of Panama. United States Geological Survey.

Stewart, R.H., Stewart, J.L., Woodring, W.P., 1982. Geologic Map of the Panama Canal and vicinity. United States Department of the Interior Geological Survey, Reston, VA.

Stewart, W.N., Rothwell, G.W., 1993. Palaeobotany and the evolution of plants. 2nd edition. Cambridge University Press, Cambridge.

Süs, H., Müller-Stoll, W.R., 1977. Untersuchungen über fossile Platanenhölzer. Beiträge zu einer Monographie der Gattung Platanoxylon Andreánszky. Feddes Repert 88, 1–62+pl. 1–14.

Swanson, F.J., Jones, J.A., Crisafulli, C., Lara, A., 2013. Effects of volcanic and hydrologic processes on forest vegetation, Chaitén Volcano, Chile. Andean Geology 40, 359–391.

Sweitzer, E.M., 1971. Comparative anatomy of Ulmaceae. Journal of the Arnold Arboretum 52, 523–585.

Takhtajan., 1980. Outline of the Classification of Flowering Plants Magnoliophyta. The Botanical Review 46 (3), 225–359.

Taylor, D. W., 1990. Paleobiogeographic relationships of angiosperms from the Cretaceous and early Tertiary of the North American area. The Botanical Review 56 (4), 279–417.

Taylor, E. L., Taylor, T. N.,Krings, M., 2009. Paleobotany: the biology and evolution of fossil plants. Academic Press.

Tedford, R., 1970. Principles and practices of mammalian geochronology in North America. 1, 666-703.

Terada, K., Suzuki, M., 1998. Revision of the so-called *'Reevesia'* fossil woods from The Tertiary in Japan – a proposal of the new genus *Wataria* (Sterculiaceae). Review of Palaeobotany and Palynology 103, 235–251.

Terada, K., Asakawa, T. O., Nishida, H., 2006. Fossil woods from Arroyo Cardenio, Chile Chico Province, Aisen (XI) Region, Chile. Post-Cretaceous floristic changes in Southern Patagonia, Chile, 57–65.

Thayn, G.F., Tidwell, W.D., 1984. A review of the genus *Paraphyllanthoxylon*. Review of Palaeobotany and.Palynology 43, 321–335.

The Angiosperm Phylogeny Group. 2009. An update of the Angiosperm Phylogeny Group classification for the orders and families of flowering plants: APG III. Botanical

Journal of the Linnean Society 161, 105–121.

Thomas, R., 2013. Palm-ID, a database to identify the palm stem anatomy with an expert system (Xper^2). http://lis-upmc.snv.jussieu.fr/Palm-ID/en/presentation.php (last accessed 12/1/2013).

Thomas, R., De Franceschi, D., 2013. Palm stem anatomy and computer-aided identification: The Coryphoideae (Arecaceae). American journal of botany. 100(2), 289–313.

Thomasson, J.R., 1991. Sediment-borne "seeds" from Sand Creek, northwestern Kansas: taphonomic significance and paleoecological and paleoenvironmental implications. Palaeogeography, Palaeoclimatology and Palaeoecoly 85, 213–225.

Thorn, V., 2005. A Middle Jurassic fossil forest from New Zealand. Palaeontology 48 (5), 1021–1039.

Tidwell, W.D, Medlyn, D.A, Thayn, G.F., 1973. Three new species of *Palmoxylon* from the Eocene Green River formation, Wyoming. The Great Basin Naturalist 33 (2) (1973), pp. 61–76.

Tidwell, W. D., Medlyn, D. A., Thayn, G. F., 2010. Three new species of *Palmoxylon* from the Eocene Green River formation, Wyoming. Western North American Naturalist 33(2), 61–76.

Tomlinson, P.B., 1961. Anatomy of the monocotyledons. II. Palmae. Clarendon Press. Oxford University Press.

Tomlinson, P. B., 2006. The uniqueness of palms. Botanical Journal of the Linnean Society. 151(1), 5–14.

Tomlinson P. B., Fisher, J. B., Spangler R. E., Richer, R.A., 2001. Stem vascular architecture in the rattan palm *Calamus* (Arecaceae-Calamoideae-Calaminae). American Journal of Botany 88: 797–809.

Trivedi, T.K., 1971. Fossil dicotyledonous woods from the Deccan Intertrappean beds of Mahurzari. Botanique, Nagpur 7, 111–118.

Trivedi, B.S., Ahuja, M., 1978. *Cynometroxylon siwalicus* n. sp. from the Siwalik range. Current Science 47, 638–639.

Trivedi, B.S., Ambwani, K., 1976. A fossil wood *Hibiscoxylon intertrappeum* sp. nov. from the Deccan Intertrappean series of Mahurzari, near Nagpur (India). Journal of the Indian Botanical Society 51, 23–31.

Trivedi, B.S., Panjwani, M., 1986. Fossil wood of *Bauhinia* from the Siwalik Beds of

Kalagarh. Geophytology. 16, 66 –69.

Trivedi, B. S., Verma, C. L., 1974. Petrified palm stem, *Palmoxylon penchense* sp. nov. from the Deccan Intertrappean beds of Madhya Pradesh, India. Palaeobotanist 21, 28–35.

Tyree, M. T., Zimmermann, M. H., 2002. Xylem structure and the ascent of sap. Springer.

Ueda, K., Kosuge, K., Tobe, H. 1997. A molecular phylogeny of Celtidaceae and Ulmaceae (Urticales) based onrbcL Nucleotide sequences. Journal of Plant Research 110 (2): 171–178.

USDA, NRCS., 2013. The PLANTS Database. National Plant Data Team, Greensboro, NC 27401-4901 USA. Available online at: http://plants.usda.gov. (last accessed, 28 June 2013).

U.S. Geological Survey [last modified, February 27, 2013].http://www.usgs.gov/default.asp (last accessed, 1st November, 2013).

Van den Bold, W. A., 1972. Ostracoda of the La Boca formation, Panama canal zone. Micropaleontology, 410–442.

Van der Burgh, J., 1984. Some palms in the Miocene of the Lower Rhenish Plain. Review of Palaeobotany and Palynology 40(4), 359–374.

Van Vliet, J.C.M., Baas, P., 1984. Wood anatomy and classification of the Myrtales. Annals of the Missouri Botanical Garden 71(3), 783–800.

Velichko, A., Spasskaya, I., 2002. Climatic change and the development of landscapes. The physical geography in northern Eurasia.Oxford University Press, Oxford, 36-69.

Velichko, A.A., Wright, H.E., 2005. Cenozoic Climatic and Environmental Changes in Russia, Geological Society of America. Special paper. 382.

Villegas, Z., Peña-Claros, M., Mostacedo, B., Alarcón, A., Licona, J. C., Leaño, C., Choque, U., 2009. Silvicultural treatments enhance growth rates of future crop trees in a tropical dry forest. Forest Ecology and Management 258(6), 971–977.

Von der Heydt, A.S., Dijkstra, H.A., 2006. Effect of ocean gateways on the global ocean circulation in the late Oligocene and early Miocene. Paleoceanography 21(1), PA1011. doi:10.1029/2005PA001149.

Von Mohl H., 1845. Vermischte Schriften botanischen Inhalts. L.F. Fues,Tübingen, Germany.

Vozenin-Serra, C., Privé-Gill, C., 1989. Bois plio-pleistocénes du gisement de Saropée,

Plateau de Khorat, est de la Thailande. Review of Palaeobotany and Palynology 60, 225–254.

Waisel, Y., Breckle, S. W., 1987. Differences in responses of various radish roots to salinity. Plant and Soil 104 (2), 191–194.

Waisel, Y., Eshel, A., 2002. Plant roots: the hidden half, 3. Marcel Dekker Inc. New York, USA.

Watari, S., 1952. Dycotyledonous woods from the Miocene along the Japan-Sea side of Honsyu. Journal of the Faculty of Sciences of the University of Tokyo. III, Botany. 6, 97–134.

Watson, L., and Dallwitz, M.J. 1992 onwards. The families of flowering plants: descriptions, illustrations, identification, and information retrieval.[last modified 19 October 2013]. http://delta-intkey.com.

Webb, S.D., 1977. A history of savanna vertebrates in the New World. Part I: North America. Annual Review of Ecology and Systematics. 8, 355–380.

Webb, S.D., 1984. Ten million years of mammal extinctions in North America. In: Martin, P.S., Klein, R.G. (Eds.). Quaternary extinctions: A prehistoric Revolution. University of Arizona Press, Tucson.

Webb, S.D., 1991. Ecogeography and the Great American Interchange. Paleobiology 17, 266– 280.

Wegner, W., Wörner, G., Harmon, R.S., Jicha, B.R., 2011. Magmatic history and evolution of the Central American land bridge in Panama since Cretaceous times. Geological Society of America Bulletin 123, 703–724.

Welle, B.J.H. ter, Détienne, P., 1995. Wood and timber. Tiliaceae. Dipterocarpaceae. In: Görts-Van Rijn, A.R.A. (Ed.). Flora of the Guianas. Kloetz Scientific Books, Koenigstein, Germany, pp. 53–67.

Wernstedt, F. L., 1972. World climatic data.complete. Press Lemont. PA.

Westra, L.Y.T., Koek-Noorman, J. K., 2004. Wood Atlas of the Euphorbiaceae. IAWA Journal, Supplement 4, 1–110.

Wheeler, E.A., 2011. Inside Wood-a web resource for hardwood anatomy. IAWA Journal 32, 199–211.

Wheeler, E.A., Baas, P., 1992. Fossil wood of the Leguminosae: a case study in xylem

evolution and ecology anatomy. *In:* Herendeen, P.S., Dilcher, D.L. (Eds.).Advances in Legume Systematics 4. The fossil record. Pp 281 –302. Royal Botanic Gardens, Kew, United Kingdom.

Wheeler, E.A., Baas, P., 1998. Wood identification-a review. IAWA Journal19, 241 – 264.

Wheeler, E., Baas, P., 2001. Wood anatomy and climate change. In: Hodkinson, T., Jones, M., Waldren, S., Parnell, J.KA. Climate change, ecology and systematics. Cambridge Unniversity Press. The Edinburgh Building, UK.

Wheeler, E.A., Baas, P., 2011. Wood anatomy and climates change. In Hodkinson, T. (Ed). Climate change, ecology and systematics. Cambridge University Press.

Wheeler, E.A., Dillhoff, T.A., 2009. The Middle Miocene Wood Flora of Vantage, Washington, USA. IAWA Journal, Supplement 7. Pp 1–101.

Wheeler, E.A., Lehman, T.M., 2000. Late Cretaceous woody dicots from the Aguja and Javelina Formations, Big Bend National Park, Texas, USA. International Association of Wood Anatomists Journal 21, 83–120.

Wheeler, E.A., Manchester, S., 2002. Woods of the Middle Miocene Nut Beds flora, Clarno Formation, Oregon, USA. IAWA Journal. 3, 1–88.

Wheeler, E.A., Matten, L.C., 1977. Fossil Wood from an Upper Miocene locality in Northeastern Colorado. Botanical Gazette. Pp 112-118.

Wheeler, E.A., Michalski, T., 2003. Paleocene and early Eocene woods of the Denver Basin, Colorado. Rocky Mountain Geology 38, 29–43.

Wheeler, E.A, La Pasha, C.A., Miller, R.B., 1989. Wood anatomy of Elm (*Ulmus*) and Hackberry (*Celtis*) species native to the United States. IAWA Bulletin 10 (1), 5 – 26.

Wheeler, E.A., Lee, M., Matten, L.C., 1987. Dicotyledonous woods from the Upper Cretaceous of southern Illinois. Botanical Journal of the Linnean Society of London.

Wheeler, E.A., Lehman, T.M., Gasson, P.E., 1994. *Javelinoxylon*, an Upper Cretaceous Dicotyledonous Tree from Big Bend National Park, Texas, with Presumed Malvalean Affinities. American Journal of Botany 81, 703–710.

95, 77–100.

Wheeler, E.A., Scott, R.A., Barghoorn, E.S., 1978. Fossil dicotyledonous woods from Yellowstone National Park II. Journal of Arnold Arboretum 58, 280–306.

Wheeler, E.A., Wiemann, M., Fleagle, J.G., 2007. Woods from the Bakate Formation, Ethiopia. Anatomical characteristics, estimates of original specific gravity and ecological inferences. Review of Palaeobotany and Palynology 146, 193–207.

White, L., Gasson, P., 2008. Mahogany. Royal Botanic Gardens.

Whitmore, F.C., Jr., Stewart, R.H., 1965. Miocene mammals and Central American seaways. Science 148, 180–185.

Whittaker, R.H., Woodwell, G.M., 1968. Dimension and production relations of trees and shrubs in the Brookhaven Forest, New York.

Wickremasinghe, B.K.L., Herat, T.R., 2006. A comparative wood anatomical study of the genus *Diospyros* L. (Ebenaceae) in Sri Lanka. Ceylon Journal of Sciences (Biological Sciences) 35 (2), 115–136.

Wiegrefe, S., Sytsma, R., Guries, R., 1987. The Ulmaceae: one family or two? Evidence from chloroplast DNA restriction site mapping. Plant Systematics and Evolution. 210, 249–270.

Wiemann, M. C., Williamson, G. B., 1989. Wood specific gravity gradients in tropical dry and montane rain forest trees. American Journal of Botany. 924-928.

Wiemann, M. C., Williamson, G. B., 2002. Geographic variation in wood specific gravity: effects of latitude, temperature, and precipitation. Wood and Fiber Science 34(1), 96–107.

Wiemann, M. C., Manchester, S. R., Wheeler, E. A., 1999. Paleotemperature estimation from dicotyledonous wood anatomical characters. Palaios 14(5), 459–474.

Wiemann, M. C., Wheeler, E. A., Manchester, S. R., Portier, K. M., 1998. Dicotyledonous wood anatomical characters as predictors of climate.Palaeogeography, Palaeoclimatology, Palaeoecology 139(1), 83–100.

Williams, C.J., Mendell, E.K., Murphy, J., Court, W., Johnson, A., Richter, S., 2008. Paleoenvironmental reconstruction of a Middle Miocene forest from the western Canadian Arctic. Palaeogeography, Palaeoclimatology, Palaeoecology 261(1-2), 160–176.

Wing, S.L., Alroy, J., Hickey, L., 1995. Plant and mammal diversity in the Paleocene to Early Eocene of the Bighorn Basin. Palaeogeography, Palaeoclimatology and Palaeoecology 115, 117–155.

Wing, S.L., Herrera, F., Jaramillo, C.A., Gómez-Navarro, C., Wilf, P., Labandeira, C., 2009. Late Paleocene fossils from the Cerrejón Formation, Colombia, are the

earliest record of Neotropical rainforest.

Wolf, J., Fricker, G.A., Meyer, V., Hubbell, S., Gillespie, T.W., Saatchi, S., 2012. Plant Species Richness is Associated with Canopy Height and Topography in a Neotropical Forest. Remote Sensing Communication 4010– 4021.

Woodcock, D., 2000. Wood specific gravity of tres and forest types in the Southern Peruvian Amazon. Acta Amazonica 30, 589–599.

Woodcock, D. W., Ignas, C. M., 1994. Prevalence of wood characters in eastern North America: what characters are most promising for interpreting climates from fossil wood?. American Journal of Botany, 1243–1251.

Woodcock, D. W., Shier, A. D., 2003. Does canopy position affect wood specific gravity in temperate forest trees?. Annals of botany 91(5), 529–537.

Woodring, W. P., 1955. Geologic Map of Canal Zone and Adjoining Parts of Panama Department of the Interior, US Geological Survey.

Woodring, W. P., 1957-1982. Geology and paleontology of Canal Zone and adjoining parts of Panama. United States Geological Survey Professional Paper 306A-F. United States Government Printing Office, Washington, DC.

Woodring, W. P., 1974. The Miocene Caribbean faunal province and its subprovinces. Verhandlungen der naturforschenden Gesellschaft in Basel. 84(1), 209-213.

Woodring, W.P., Thompson, T.F., 1949. Tertiary formations of Panama Canal Zone and adjoining parts of Panama. AAPG Bulletin. 33, 223-247.

Worbes, M., 1989. Growth rings, increment and age of trees in inundation forests, savannas and a mountain forest in the Neotropics. IAWA Bulletin 10, 109–22.

Worbes, M., 1995. How to measure growth dynamics in tropical trees: a review. IAWA Journal. 16(4), 337–351.

Worbes, M., 1999. Annual growth rings, rainfall-dependent growth and long-term growth patterns of tropical trees from the Caparo Forest Reserve in Venezuela. Journal of ecology. 87(3), 391–403.

Worbes, M., 2002. One hundred years of tree-ring research in the tropics–a brief history and an outlook to future challenges. Dendrochronologia, 20(1), 217–231.

Wright, J. D., Miller, K. G., Fairbanks, R. G., 1992. Early and middle Miocene stable isotopes: implications for deepwater circulation and climate. Paleoceanography

7(3), 357–389.

Wrigley, J.W., Fagg, M., 1996. Australian Native Plants. New Holland Publishers. 400 pp.

Wurzinger, W., 1953. Palaeobotanische Untersuchungen an tertiären Pflanzenresten aus Steiermark. Diss. Doktorgrade, Phil. Fak., Univ. Wien, 190 pp.

W3 TROPICOS. Missouri Botanical Garden. http://www.tropicos.org (last accessed 28 Jun 2012).

Yadav, R., 1988. Some more fossil Woods from the Lower Siwalik sediments of Kalagarh, Uttar Pradesh and Nalagarh, Hichamal Pradesh. Palaeobotanist 37, 52–62.

Yadav, R.R., 1989. Some more fossil Woods from the Lower siwalik sediments of Kalagarh, Uttar Pradesh and Nalagarh, Himachal Pradesh. Palaeobotanist. 37, 56–62.

Yang, Kung-Chi, Yu-Shiu Huang Yang. 1987. Minute structure of Taiwanese woods. Hua Shiang Yuan Publishing Col, Taipei, Taiwan. 172 p.

Zachos, J., Pagani, M., Sloan, L., Thomas, E., Billups, K., 2001. Trends, rhythms, and aberrations in global climate 65 Ma to present. Science 292, 686-693. doi: 10.1126/science.1059–412.

Zavada, M., Kim, M., 1996. Phylogenetic analysis of Ulmaceae. Plant Systematics and Evolution. 2000, 1–2: 13–20.

Zomlefer, W.B., 1994. Guide to flowering plant families. University of North Carolina Press, Chapel Hill, 430 pp.

Zona, S., 1990. A monograph of *Sabal* (Arecaceae: Coryphoideae). Aliso 12(4), 583–666.

Species/characters	*STRI14165*	*Aphananthe philippinensis*	*Aphananthe sakalava*	*Celtis adolfi-friderici*	*C. africana*	*C. australis*	*C. bifida*	*C. biondii*	*C. bungeana*	*C. cinnamomea*	*C. durardii*	*C. ehrenbergiana*	*C. glycicarpa*	*C. iguanaea*	*C. jessoensis*	*C. integrifolia*	*C. koraiensis*	*C. laevigata*	*C. latifolia*	*C. luzonica*	*C. milbraedii*	*C. occidentalis*	*C. occidentalis*	*C. pacifica*	*C. paniculata*	*C. philippensis*	*C. schippii*	*C. sellenianа*	*c.sinensis*	*C. zenkeri*	*Humulus*	*Pteroceltis tatarinowii*	*Trema angustifolia*	*Trema cannabina*	*T. guinnensis*	*Trema micrantha*
growth rings distinct	0	1	1	1	1	1	1	1	1	1	0	1	0	0	1	0	1	1	1	0	1	1	1	1	1	1	1	1	1	1	0	1	0	1	1	1
growth rings indistinct	1	1	1	1	0	0	1	0	0	0	1	1	1	1	0	1	0	0	1	1	1	0	0	0	0	1	0	0	0	1	1	0	1	0	1	0
ring porous	0	0	0	0	0	1	0	1	1	0	0	0	0	0	1	0	1	0	0	0	0	0	1	0	0	0	0	0	0	0	0	0	0	0	0	0
semi-ring porosity	0	0	0	0	0	0	0	0	0	0	0	0	0	0	1	0	0	1	0	0	0	0	0	0	0	0	0	0	1	0	1	0	0	0	0	0
diffuse porous wood	1	1	1	1	1	0	1	0	0	1	0	1	0	1	0	1	0	0	1	1	1	1	0	1	1	1	1	0	0	1	0	1	1	1	1	1
vessels tang bands	0	0	0	0	0	1	0	0	1	0	0	0	0	0	1	0	1	1	0	0	0	0	1	0	0	0	0	0	1	0	1	0	0	0	0	0
vessels in diagonal	0	0	0	0	1	1	0	1	1	0	0	0	0	0	1	0	1	1	0	0	0	0	1	0	0	0	0	0	1	0	0	0	0	0	0	0
vessels exclusively solitary	0	0	0	0	0	0	0	0	0	0	0	0	0	0	0	0	0	0	0	0	0	0	0	0	0	0	0	0	0	0	0	0	0	0	0	0
2-4 groups common	1	0	0	0	0	1	0	0	1	0	0	1	0	1	0	0	0	0	0	0	0	1	0	0	1	0	0	0	1	1	0	0	1	0	1	0
vessel clusters common	0	0	0	0	0	1	0	1	1	0	0	0	0	0	1	0	1	1	0	0	0	0	1	0	0	0	0	0	1	0	0	0	0	0	0	0
vessel outline angular	0	0	0	0	0	0	0	0	0	0	0	0	0	0	0	0	0	0	0	0	0	0	0	0	0	0	0	0	0	0	0	0	0	0	0	0
simple perforation plates	1	1	1	1	1	1	1	1	1	1	1	1	1	1	1	0	1	1	1	1	1	1	1	1	0	1	1	1	1	1	1	1	1	1	1	1
scalariform perforation plates	0	0	0	0	0	0	0	0	0	1	0	0	0	0	0	0	0	0	0	0	0	0	0	0	1	0	0	0	0	0	0	0	0	0	0	0
iv pits alternate	1	1	1	1	0	1	1	1	1	1	1	1	1	1	1	1	1	1	1	1	1	1	1	1	1	1	1	1	1	1	1	1	1	1	1	1
shape of Iv pits polygonal	1	1	?		1	0	1	?		1	1	1	0	1	0	1	1	1	1	1	0	1	1	1	1	0	0	1	1	1	0	1	1	1	1	0	1
vessel ray pits distinct border	1	1	1	1	1	1	1	0	1	1	1	0	1	1	0	1	1	1	1	0	1	1	0	1	0	0	1	1	0	1	1	1	1	1	1	1
v-r pits much reduced borders	0	1	1	1	0	0	1	1	1	0	0	1	0	0	1	1	0	0	1	0	1	0	0	1	1	1	0	0	1	1	0	0	1	1	0	1
v-r pits gash like or palisade	0	0	0	0	0	0	0	1	0	0	0	1	0	0	0	0	0	0	0	0	0	0	0	0	1	1	0	0	0	0	0	0	0	0	1	1
v-r pits two distinct sizes	0	0	0	0	0	0	0	0	0	0	0	0	0	0	0	0	0	0	0	0	0	0	0	0	0	0	0	0	0	0	0	0	0	0	0	0
v-r pits restricted to margins	0	0	0	0	0	0	0	0	0	0	0	0	0	0	0	0	0	0	0	0	0	0	0	0	0	0	0	0	0	0	0	0	0	0	0	0
helical thickenings	0	0	0	0	0	0	0	1	1	0	0	0	0	0	1	0	0	0	0	0	0	1	0	0	1	0	0	0	0	0	1	0	0	0	0	1
tyloses common	0	1	0	1	0	0	0	1	1	0	0	1	0	1	0	0	0	0	0	0	1	0	0	0	0	0	0	0	0	0	1	0	0	0	0	0
gums and other deposits	0	0	0	0	0	0	0	0	0	0	0	0	0	0	0	0	0	0	0	0	0	0	0	0	0	0	0	0	0	0	0	1	0	0	0	0
vascular tracheids	0	0	0	0	1	0	1	1	1	0	0	0	0	0	0	1	0	0	0	0	0	0	0	1	0	0	1	0	0	0	0	0	0	0	0	0
fib simple to minut border pits	1	1	1	1	1	1	0	1	1	1	1	1	1	0	1	0	1	1	1	1	1	1	1	0	1	1	0	1	1	1	1	1	1	1	1	1
fibres common in tang/rad	0	0	0	0	0	1	0	0	0	1	0	0	0	0	0	0	0	0	0	0	0	?		0	0	0	0	0	1	0	0	0	0	0	0	0
non septate fibres	1	1	1	1	1	1	0	1	1	1	1	1	0	1	1	1	1	1	1	1	1	1	1	1	1	1	1	1	1	1	1	1	1	1	1	1
fibres very thin walled	0	0	0	0	0	0	0	0	0	0	0	0	0	0	0	0	0	0	0	1	0	0	0	0	0	0	0	0	0	0	0	0	1	0	0	1
fibres thin to thick walled	1	0	1	1	1	1	1	1	1	1	1	1	0	1	1	0	1	1	1	1	1	1	1	1	0	1	1	1	0	1	0	1	0	1	1	1
fibres very thick walled	0	1	0	1	0	0	0	0	0	0	0	1	1	0	0	1	0	0	0	0	0	0	0	0	1	0	0	0	1	0	1	1	0	0	0	0
axial parenchyma diffuse	0	0	0	0	0	0	0	0	0	1	1	0	0	0	0	0	0	0	0	1	0	0	1	0	1	0	0	0	0	0	0	1	0	1	1	
axial parenchyma diff in aggregates	0	0	0	0	0	0	0	0	0	0	1	0	0	0	0	0	0	0	0	0	0	0	0	0	0	0	0	0	0	0	0	0	0	0	0	0
axial parenchyma scanty	0	0	1	0	0	0	0	0	0	0	0	0	0	0	0	0	0	0	0	0	0	0	0	0	0	1	0	0	0	1	0	0	1	1	1	0
parenchyma vasicentric	0	1	0	1	1	1	0	1	1	0	1	0	1	1	1	1	1	1	1	1	1	0	0	0	0	1	1	1	1	1	0	0	1	0	1	0
parenchyma lozenge/winged	0	1	0	1	0	0	0	0	0	0	1	0	1	1	0	1	0	0	1	0	1	0	0	0	0	1	1	1	0	1	0	0	1	0	0	0
confluent	0	1	0	1	1	0	1	1	1	0	1	1	0	1	1	1	0	0	1	0	1	0	0	0	0	1	1	1	0	1	0	0	1	0	0	0
unilateral parenchyma	0	0	0	0	0	0	0	0	0	0	0	0	0	1	0	0	0	0	0	0	0	0	0	0	0	0	0	0	0	0	0	0	0	0	0	0
parenchyma bands ≥3	1	1	1	0	0	0	1	0	0	1	1	1	1	1	0	0	0	0	1	0	0	1	0	0	0	1	1	1	0	1	0	1	0	0	0	0

parenchyma bands up 3	0	0	1	0	0	0	1	0	0	0	0	0	0	0	0	0	0	0	0	0	0	0	0	1	0	1	1	0	0	1	0	0	0	0	0	0
par reticulate	0	0	0	0	0	0	0	0	0	0	0	0	0	0	0	0	0	0	0	0	0	0	0	0	0	0	0	0	0	0	0	0	0	0	0	0
par marginal	0	0	0	1	0	0	1	0	1	0	0	0	0	1	1	0	0	0	0	0	1	0	0	0	0	0	1	0	0	1	0	1	0	0	0	0
parenchyma scarce/absent	0	0	0	0	0	0	0	0	0	0	0	0	0	0	0	0	0	0	0	0	0	0	0	0	0	0	0	0	0	0	0	0	1	1	1	0
2 cells /strand	0	0	0	0	1	0	0	0	0	0	0	0	0	1	0	1	1	0	0	0	0	0	0	0	0	0	0	1	1	1	0	0	0	0	0	0
3-4 cells /strand	1	1	1	1	1	1	1	1	1	1	1	1	1	1	1	1	1	1	1	1	1	1	1	1	1	1	1	1	1	1	0	1	1	1	1	1
5-8 cells /strand	1	1	0	1	1	1	1	0	0	0	0	0	0	0	1	0	0	0	1	0	1	0	0	1	1	1	0	0	1	1	0	1	1	1	1	1
over 8 cells /strand	1	0	0	1	0	0	0	0	0	0	0	0	0	1	0	0	0	0	1	0	0	0	0	0	0	0	0	0	0	0	1	0	0	0	0	1	0
rays uniseriate	0	0	0	0	0	0	0	0	0	0	0	0	0	0	0	0	0	0	0	0	1	0	0	0	0	0	0	0	0	0	0	0	1	0	0	0
rays 1-3 cells wide	1	1	0	0	1	0	1	0	0	0	0	0	0	1	0	1	1	0	1	0	1	0	0	0	1	1	0	1	1	1	0	1	0	1	1	1
rays 4-10 seriate	1	1	1	1	1	1	0	1	1	1	1	1	1	0	1	0	1	1	1	1	0	1	1	1	1	1	1	1	1	1	1	1	0	0	0	0
rays >10 seriate	0	0	0	0	1	1	0	1	0	1	0	0	1	0	0	0	1	1	0	0	0	0	0	0	0	0	0	0	0	0	0	1	0	0	0	0
rays 2 sizes	0	0	0	0	1	0	0	0	0	0	0	0	0	0	0	0	1	0	0	0	0	0	0	0	0	0	0	0	0	1	0	0	0	0	0	0
all rays procumbent	0	0	0	0	0	0	0	0	0	0	0	0	0	0	0	0	0	0	0	0	0	0	0	0	0	0	0	0	0	0	0	0	0	0	0	0
all upright/square	0	0	0	0	0	0	0	0	0	0	0	0	0	0	0	0	0	0	1	0	0	0	0	0	0	0	0	0	0	0	0	0	0	0	0	0
one row upright and or square	0	1	1	1	1	1	1	1	1	0	0	1	0	0	1	1	0	0	1	1	1	0	0	1	0	1	0	1	0	1	0	1	0	0	1	0
2-4 rows of upright	1	1	0	1	1	0	1	1	1	1	1	1	0	0	1	1	1	1	1	1	1	0	1	1	1	1	1	1	1	1	0	1	1	1	0	1
>4 rows of upright	0	0	0	0	0	0	0	1	0	0	0	0	0	0	0	0	0	0	1	0	1	0	0	1	1	1	1	0	1	1	0	0	1	1	0	0
rays with mixed cells	0	0	0	0	0	0	0	0	0	0	0	0	1	1	0	0	0	0	0	0	0	1	0	0	0	0	0	0	0	0	0	1	0	0	0	0
sheath cells	0	0	0	0	1	1	0	1	1	1	0	0	1	0	1	1	1	0	0	0	0	0	0	0	0	0	0	1	0	0	0	0	0	0	0	0
perforated ray cells	0	0	0	0	0	0	0	0	1	0	0	0	0	0	0	0	0	0	0	0	0	0	0	0	0	0	0	0	0	0	0	1	0	0	0	1
all rays storied	0	0	0	0	0	0	0	0	0	0	0	0	0	0	0	0	0	0	0	0	0	0	0	0	0	0	0	0	0	0	0	0	0	0	0	0
Parenchyma/vessels storied	0	0	0	0	0	0	0	0	0	0	0	0	0	0	0	0	0	0	0	0	0	0	0	0	0	0	0	0	0	0	0	0	0	0	0	0
fibres storied	0	0	0	0	0	0	0	0	0	0	0	0	0	0	0	0	0	0	0	0	0	0	0	0	0	0	0	0	0	0	0	0	0	0	0	0
elements irregularly storied	0	0	0	0	0	0	0	0	0	0	0	0	0	0	0	0	0	0	0	0	0	0	0	0	0	0	0	0	0	0	0	0	0	0	0	0
crystals in upright/squared cells	1	1	1	1	1	1	1	1	1	1	1	1	1	1	1	1	1	1	1	1	1	1	0	1	0	1	?	1	0	1	0	1	0	0	0	1
crystals procumbent cells	0	1	1	1	0	0	0	0	1	0	0	1	0	0	1	0	1	1	1	0	1	1	1	0	0	0	?	0	1	1	0	0	0	0	0	1
crystals aligned in procumb ray cells	0	0	0	1	0	0	0	0	0	1	1	0	1	0	0	1	0	0	1	0	0	0	0	0	0	0	?	1	0	0	0	1	0	0	0	0
crystals in chamb upright/squ	0	0	0	0	0	0	0	0	0	1	0	0	0	0	0	0	0	0	0	1	0	0	0	0	0	0	1	?	0	0	1	0	0	0	0	0
crystals in non chamb par cells	1	0	0	0	0	1	1	0	0	0	0	0	0	0	0	0	0	0	1	1	1	0	0	1	0	1	1	0	0	1	0	0	0	0	0	0
crystals in chambered parenchyma cells	0	0	0	0	0	0	0	0	0	0	0	0	0	0	0	1	0	0	1	0	0	0	0	0	0	0	0	0	0	1	0	0	0	0	0	0
druses present	0	0	0	0	0	0	0	0	1	0	0	0	0	0	1	0	0	0	0	1	0	0	0	0	0	0	0	1	0	0	0	0	0	0	0	1

Appendix 4.2.4. Data matrix of species of Cannabaceae used for the Principal Component Analysis (PCA). The data were obtained by direct observation of specimens from the Jodrell Laboratory, Kew Gardens, UK. 1=present; 0=absent.

	Growth rings distinct	Wood diffuse-porous	Vessels exclusively solitary	radial multiseriate 4 common	Simple perforation plates	IV pits alternate	V-r pits similar to iv pits	V-r pits reduced borders	V-r pits gash like	helical thickenings	Fibres minutely bordered	2 distinct sizes of vessels	Septate fibres	Fibres very thin walled	Fibres very thick walled	Vasicentric parenchyma	broad-sheathed par	winged/lozenge aliform par	confluent parenchyma	scanty parenchyma	diffuse/in aggregates	narrow bands par 1-3 cells	par bands more than 3 cells	reticulate parenchyma	scalariform parenchyma	marginal parenchyma	par strands more than 8 cells	sheath cells	rays 1-3 -seriate	rays 4-10 -seriate	rays more 10-seriate	rays 2 distinct sizes	tile cells	storied rays/ fib/ par	rhomb crystals in ray cells	crystals in par cells
Guazumaoxylon miocenica	0	1	0	1	1	1	1	0	0	0	1	0	1	0	0	1	1	1	0	0	0	0	0	0	0	0	1	1	1	1	0	0	1	0	1	0
Periplanetoxylon panamense	0	1	0	1	1	1	1	0	0	0	1	0	0	0	0	0	0	0	0	0	0	0	1	0	0	0	1	1	1	1	0	0	1	0	1	0
Abutilon fruticosum	0	1	0	1	1	1	1	0	0	0	1	0	0	0	0	1	0	0	1	0	0	0	1	0	0	1	0	0	0	1	1	0	1	0	1	0
Abutilon mollisimum	0	1	0	1	1	1	1	0	0	0	1	0	0	0	0	1	0	0	1	0	0	0	1	0	0	0	0	1	0	1	1	0	1	0	0	0
Actinophora mastexsii	0	1	0	1	1	1	1	0	0	0	1	0	0	0	0	0	0	0	0	0	1	0	0	0	0	0	0	0	1	0	0	0	0	0	1	0
Adansonia digitata	0	1	0	1	1	0	0	1	0	0	1	0	1	0	0	0	0	0	0	0	1	0	0	0	0	0	0	0	0	1	1	0	1	0	0	0
Adansonia sp	0	1	1	1	1	0	1	1	1	0	1	0	0	0	0	0	0	0	0	0	1	0	1	0	0	0	0	0	0	1	1	0	1	0	0	0
Adansonia niveum	0	1	0	1	1	0	1	0	0	0	1	0	0	0	0	1	0	0	1	0	0	0	0	0	0	0	0	1	0	1	1	0	1	0	0	0
Althaea cannabina	0	1	0	1	1	1	1	0	0	0	1	0	0	0	0	0	0	0	0	0	0	0	1	0	0	0	0	0	0	1	1	0	1	0	0	0
Apeiba albiflora	1	1	0	1	1	1	1	0	0	0	1	0	1	0	0	0	0	0	0	0	1	0	0	0	0	0	0	1	1	0	0	0	1	0	1	0
A. aspera	1	1	1	1	1	1	1	0	0	0	1	0	0	1	0	1	0	0	0	0	0	0	1	0	0	0	1	0	1	1	0	0	1	0	0	0
A. tiborbou	1	1	0	1	1	1	1	0	0	0	1	0	0	0	0	0	0	0	0	0	1	0	0	0	0	0	0	1	1	1	0	0	1	0	0	0
A. petuoumo	0	1	1	1	1	1	1	0	0	0	1	0	0	1	0	0	0	0	0	0	0	0	0	0	0	0	1	0	1	1	0	0	1	0	0	0
Argyrodendron actinophylla	1	0	0	1	1	1	0	0	0	0	1	1	0	0	0	1	0	1	0	0	0	0	1	0	0	0	0	1	0	1	1	0	0	0	1	0
A. trifoliolata	1	0	0	1	1	1	1	0	0	0	1	1	0	0	1	1	0	0	0	0	0	0	1	0	0	0	0	1	0	1	1	0	1	0	1	1
Ayenia praeclara	1	1	0	1	1	1	1	0	0	0	1	0	0	0	0	1	0	0	0	0	0	0	1	0	0	0	0	0	1	0	0	0	1	0	1	0
Azanza gardicana	0	1	0	1	1	1	1	0	0	0	1	0	0	0	0	1	0	0	0	0	0	0	0	0	1	0	0	1	0	1	1	0	1	0	1	1
Belotia campbelli	0	1	0	1	1	1	1	0	0	0	1	0	0	0	0	0	0	0	0	0	0	0	0	0	0	0	1	0	1	1	0	0	1	0	0	0
B. panamensis	0	1	0	1	1	1	1	0	0	0	1	0	0	0	0	0	0	0	0	0	1	0	0	0	0	0	0	1	1	1	0	0	1	0	0	0
B. elotia mexicana	0	1	0	1	1	1	1	0	0	0	1	0	0	0	0	0	0	0	0	0	0	0	0	0	0	0	0	1	1	1	1	0	1	0	0	0
Berrya ammonilla	1	1	0	1	1	1	1	0	0	0	1	0	1	0	0	0	0	1	0	0	0	0	0	0	0	0	0	0	1	1	0	0	1	0	0	0
B. cordifolia	0	1	0	1	1	1	1	1	1	0	1	0	0	0	0	0	0	0	0	0	1	0	0	0	1	0	0	1	1	1	0	0	1	1	0	0

Bombacopsis quinata	0	1	0	1	1	1	0	0	0	0	1	0	1	0	0	0	0	0	0	0	1	0	0	0	0	0	1	1	1	1	0	0	1	0	0	1
Bombax brevicuspe	0	1	0	1	1	1	1	0	0	0	1	0	0	0	0	0	0	0	0	0	0	0	0	0	0	1	0	1	0	1	1	0	0	1	0	1	0
B. aquatica	1	1	0	0	1	1	0	0	0	0	1	0	1	0	0	1	0	0	0	0	0	0	0	0	0	1	0	0	0	1	1	0	0	1	0	0	0
B. cambodiense	0	1	0	1	1	1	0	0	0	0	1	1	1	0	0	1	0	0	0	0	0	0	0	0	0	1	0	1	0	1	1	0	0	1	0	0	1
B. cyathophorum	1	1	0	1	1	1	0	0	0	0	1	0	0	0	0	1	0	0	0	0	0	1	0	0	0	0	1	1	1	1	0	0	1	0	0	0
B. buonopozense	0	1	1	0	1	1	0	1	0	0	0	0	0	0	0	1	0	0	0	0	0	0	0	0	0	1	0	1	1	1	1	0	0	1	0	0	0
B. ceiba	0	1	1	1	1	1	1	1	1	0	1	1	1	1	0	1	0	0	0	0	0	0	0	0	0	1	0	0	0	1	1	0	1	1	0	1	1
B. costatum	0	1	0	0	1	1	0	0	0	0	1	0	1	0	0	1	0	0	0	0	0	0	0	0	0	1	0	1	1	0	1	1	0	1	1	0	0
B. ellipticum	0	1	0	1	1	1	0	0	0	0	1	0	0	0	0	1	1	0	0	0	1	0	0	0	0	0	0	0	1	0	1	1	0	1	0	1	1
B. insigne	0	1	0	0	1	1	0	1	0	0	1	0	0	0	0	0	0	0	0	0	1	0	0	0	0	0	0	1	0	1	1	0	1	0	1	0	0
B. larutense	0	1	0	1	1	1	0	0	0	0	1	0	0	0	0	0	0	0	0	0	0	0	0	1	0	0	1	0	0	1	1	0	1	1	0	0	0
B. mala	0	1	0	0	1	1	1	0	0	0	1	0	0	0	0	0	0	0	0	0	0	0	0	0	0	1	0	0	1	0	0	0	0	1	1	0	0
B. neryosum	0	1	0	1	1	1	0	0	0	0	1	0	0	0	0	1	0	0	0	0	0	0	0	0	0	1	0	1	0	0	1	1	0	1	0	0	0
B. surinamensis	0	1	0	1	1	0	0	0	0	0	1	0	0	0	0	0	0	0	0	0	0	0	0	0	0	1	0	0	0	1	0	0	0	?	0	0	1
Boschia griffitisii	1	1	0	1	1	1	1	0	0	0	1	0	0	0	0	0	0	0	0	0	0	1	0	0	0	0	1	1	1	1	0	0	1	0	0	0
Brachychiton acerifolius	0	1	0	1	1	1	1	0	0	0	1	0	0	0	0	0	0	0	0	0	0	0	0	0	0	0	0	1	0	0	1	0	1	0	0	0
Brownlonia argentata	1	1	0	1	1	1	0	0	0	0	1	0	0	0	0	0	0	0	0	0	0	0	0	0	0	0	0	0	1	1	0	0	0	0	0	0
B. elata	0	1	0	0	1	1	1	1	1	0	1	0	0	0	0	1	0	1	0	0	0	0	1	0	0	0	1	0	1	1	0	0	0	0	0	0
*Byttneria geminifolia * bad TS*	0	1	0	1	1	1	1	0	0	0	1	0	0	0	0	0	0	0	0	0	0	0	1	0	0	0	0	1	1	1	1	0	0	1	0	1	1
B. maingayi	1	1	0	1	1	1	1	0	0	0	1	0	0	0	0	0	0	0	0	0	0	0	0	1	0	0	1	0	1	1	0	0	1	0	1	1
Camptostemon philippensis	0	1	0	1	1	1	1	0	0	0	1	0	0	0	0	0	0	0	0	0	0	1	0	0	0	0	0	0	0	0	0	0	0	0	1	1
C. africana	1	1	0	1	1	1	1	0	0	0	1	0	0	0	0	1	0	1	1	0	0	1	0	0	0	1	0	0	1	1	0	0	1	0	0	0
Cavanillesia platanifolia	0	1	0	0	1	1	0	1	0	1	1	0	0	1	0	0	0	0	0	0	0	1	0	0	0	0	0	0	0	1	0	0	0	0	1	0	0
Ceiba pentandra	0	1	1	0	1	1	0	1	0	0	1	0	0	1	0	0	0	0	0	0	0	1	0	0	0	0	0	0	0	1	0	1	1	0	1	0	0	1
*Chorisia crispiflora *synonym*	0	1	0	1	1	1	0	0	0	0	1	1	1	0	0	1	0	0	0	0	0	0	0	0	0	1	0	0	1	0	0	0	0	1	0	0	0
Ch. speciosa	0	1	0	1	1	1	0	1	0	0	1	0	1	1	0	1	0	0	0	0	0	0	0	0	0	1	0	1	0	0	0	0	0	1	0	0	0
Christiana africana	0	1	0	1	1	1	1	0	0	0	1	0	0	0	0	0	0	0	0	0	0	1	0	0	0	0	0	1	0	0	0	0	0	1	0	1	0
Cistanthera papaverifera	0	1	0	1	1	1	1	0	0	0	1	0	0	0	0	1	0	0	1	0	0	0	1	0	0	0	0	0	0	1	0	0	0	1	0	1

Cleirostemom platanoides	0	1	0	1	1	1	1	0	0	0	1	0	1	0	0	0	0	0	0	1	0	0	0	1	0	0	0	1	0	0	1	0	1	0	0	0
Cola accuminata	0	1	0	1	1	1	1	0	0	0	1	1	0	0	0	1	0	0	0	0	0	0	1	0	0	0	0	1	0	1	1	0	1	0	0	0
C. bracteata	0	1	0	1	1	1	1	0	0	0	1	0	0	0	0	0	0	0	0	0	0	1	0	0	0	0	0	1	0	1	1	0	1	0	1	0
Coelostegia griffithii	0	1	0	1	1	1	0	0	0	0	1	1	0	0	0	0	0	0	0	0	0	0	0	0	1	0	0	0	0	1	1	1	1	0	0	1
Colona auriculata	1	1	0	1	1	1	1	1	1	0	1	0	1	0	0	0	0	0	0	0	0	0	0	0	0	0	0	0	1	0	0	0	1	0	0	0
C. scabra	1	1	0	1	1	1	1	0	0	0	1	0	1	0	0	0	0	0	0	0	0	0	0	1	0	0	1	0	1	0	0	0	1	0	0	0
Columbia annilao	0	1	0	1	1	1	1	0	0	0	1	0	0	0	0	0	0	0	0	0	1	0	0	0	1	0	1	0	0	0	0	0	0	0	0	1
Commersonia fraseri	0	1	0	1	1	1	1	0	0	0	1	0	0	0	0	0	0	0	0	1	0	0	0	0	0	0	1	1	0	0	0	0	1	0	0	0
C. platyphylla	0	1	0	1	0	1	1	0	0	0	1	0	1	0	0	1	0	0	0	0	0	0	0	0	0	0	0	0	0	0	0	0	1	0	1	1
Cullenia excelsa	1	1	0	1	1	1	0	0	0	0	1	?	0	0	0	0	0	0	0	0	0	0	0	1	0	0	1	0	1	0	0	0	1	0	0	0
Dicraspidia donnele-smithli	0	1	0	0	1	1	1	0	0	0	1	0	0	0	0	0	0	0	0	0	1	0	0	0	0	0	0	0	1	1	0	0	1	0	0	1
Diplophractum auriculatum	1	1	0	1	1	1	1	0	0	0	1	0	0	0	0	0	0	0	0	0	0	0	0	0	1	0	0	0	0	0	1	0	0	0	0	0
Diplanthemum veridiflorum	1	1	0	1	1	1	1	0	0	0	1	0	0	0	0	0	0	0	0	0	0	0	0	0	0	0	1	0	0	0	1	0	0	0	0	0
Dombeya runsardensis	0	1	0	1	1	1	1	0	0	0	1	0	0	0	0	1	0	1	0	0	1	0	0	0	0	0	0	0	1	1	0	0	1	0	0	0
D. mastersii	0	1	0	1	1	1	1	0	0	0	1	0	0	0	0	1	0	1	1	0	0	0	0	0	0	1	0	0	1	1	0	0	1	0	0	0
D. mukale	1	1	0	1	1	1	1	0	0	0	1	0	0	0	0	0	0	0	0	0	0	0	1	0	0	0	1	0	1	1	0	0	1	0	0	1
Duboscia sp	0	1	0	0	1	1	1	0	0	0	1	0	0	0	0	0	0	0	0	0	0	0	0	0	0	0	?		0	0	0	1	0	1	0	1	1
Durio axleyianus	0	1	0	1	1	1	1	0	0	0	1	0	0	0	0	1	0	0	0	0	0	0	0	0	1	0	?		0	1	1	0	0	1	0	0	1
D. carinatus	0	1	0	0	1	1	1	0	0	0	1	0	0	0	0	0	0	0	0	0	0	1	0	0	0	0	1	0	1	0	0	0	1	0	0	0
D. conicus	0	1	0	1	1	1	0	0	0	0	1	0	0	0	0	0	0	0	0	0	1	0	0	0	0	0	0	0	1	0	0	0	1	0	0	1
D. macrophyllum	0	1	0	1	1	1	0	0	0	0	1	0	0	0	0	0	0	0	0	0	1	0	0	0	0	0	0	0	1	0	0	0	1	0	0	0
D. Iwioanus	0	1	0	1	1	1	1	0	0	0	1	0	0	0	0	0	0	0	0	0	0	0	0	1	0	1	1	1	1	0	0	1	0	0	1	0
D. lissocarpa	0	1	0	1	1	1	0	0	0	0	1	1	0	0	0	1	0	0	0	0	1	0	0	0	0	0	0	0	1	1	0	0	1	0	0	0
D. libethinus	0	1	0	1	1	1	0	0	0	0	1	0	0	0	0	0	0	0	0	0	1	0	0	0	0	0	1	0	1	1	0	0	1	0	0	1
Entelea arborescens	1	1	0	1	1	1	1	0	0	0	1	0	0	0	0	0	0	0	0	0	0	0	0	0	0	0	1	0	1	1	0	0	1	0	0	0
Eribroma klaineana	0	1	0	0	1	1	1	0	0	0	1	0	0	0	0	1	1	1	0	0	1	0	0	0	0	1	0	1	1	1	0	0	1	0	1	1
Eriodendron anfractuosum	0	1	0	0	1	1	0	0	0	0	1	0	0	0	0	0	0	0	0	0	1	0	0	0	0	0	0	1	0	0	1	0	1	1	0	1
Eriolena candollei	0	1	0	1	1	1	0	0	0	0	1	0	0	0	0	0	0	0	0	0	0	0	0	0	0	0	0	0	1	1	0	0	0	0	0	0

E. spectabilis	1	1	1	0	1	1	1	0	0	0	1	0	0	0	0	1	0	0	0	0	0	0	0	0	0	1	0	0	1	1	0	0	0	0	0	0
Erinocarpus ninimonii	1	1	0	1	1	1	1	0	0	0	1	0	0	0	0	0	0	0	0	0	0	0	0	0	1	0	0	0	0	1	1	0	0	1	0	0	0
Firmiana barteri	0	1	0	0	1	1	1	0	0	0	1	0	0	0	0	0	0	0	0	1	0	0	0	0	0	0	0	0	1	1	0	1	1	1	1	0	0
F. colorata	0	1	0	1	1	1	1	0	0	0	1	0	0	0	0	0	0	0	0	0	0	0	0	0	1	0	0	1	0	1	1	0	0	0	0	0	0
F. simplex	1	0	0	0	1	1	1	0	0	0	1	0	0	0	0	0	0	0	0	0	0	0	0	1	0	0	0	0	1	0	1	1	0	1	1	0	0
F. papuana	0	0	0	1	1	0	1	0	0	0	1	1	0	0	0	0	0	0	0	0	0	0	0	0	0	0	0	1	0	1	1	0	1	1	0	0	0
F. malayana	0	1	0	1	1	1	1	0	0	0	1	1	0	0	0	0	0	0	0	0	1	0	0	0	1	0	0	1	0	1	1	0	1	0	0	0	0
F. californica	0	1	0	1	1	1	1	0	0	0	1	0	0	0	0	0	0	0	0	0	0	0	1	0	0	0	0	0	0	0	0	1	0	1	0	0	1
Glyphaea grewioides	0	1	0	1	1	1	1	0	0	0	1	0	0	0	0	0	0	0	0	0	1	0	0	0	1	0	0	0	1	0	0	0	1	0	0	0	0
G. brevis	1	1	0	1	1	1	1	0	0	0	1	0	1	0	0	0	0	0	0	0	0	0	0	0	0	0	1	0	1	1	0	0	1	0	1	0	0
G. asiatica	1	1	0	0	1	1	1	0	0	0	1	0	0	0	0	0	0	1	0	0	1	0	0	0	0	0	0	1	1	1	0	0	1	0	1	1	0
G. bicolor	1	1	0	1	1	1	1	0	0	0	1	0	0	0	0	1	0	0	0	0	1	0	0	0	0	0	0	1	1	1	0	0	1	0	0	0	0
G. crenata	0	1	0	1	1	1	1	0	0	0	1	0	0	0	0	0	0	0	0	0	0	1	0	0	0	0	0	0	0	1	0	0	0	1	0	1	1
G. globifera	1	1	0	1	1	1	1	0	0	0	1	0	0	0	1	1	0	0	0	0	0	0	0	0	0	0	0	0	0	1	0	0	1	0	1	1	0
G. latifolia	1	1	0	0	1	1	1	0	0	0	1	0	1	0	0	0	0	0	0	0	0	1	0	0	0	0	0	0	0	0	0	1	0	0	0	0	0
G. laurifolia	0	1	0	1	1	1	1	0	0	0	1	1	1	0	0	0	0	0	0	0	0	0	0	0	0	0	1	0	0	1	0	0	0	0	0	0	0
G. laevigata	1	1	0	1	1	1	1	0	0	0	1	0	0	0	0	0	0	0	0	0	0	1	0	0	0	0	0	0	1	0	1	0	0	1	0	1	1
G. miqueliana	1	1	0	1	1	1	1	0	0	0	1	1	0	0	0	1	0	0	0	0	1	0	0	0	0	0	1	1	0	1	0	0	0	0	0	0	0
G. microcos	1	1	0	1	1	1	1	0	0	0	1	0	0	0	0	0	0	0	0	0	0	1	0	0	0	0	0	0	0	0	0	1	0	0	1	0	1	1
G. oppositifolia	1	1	0	1	1	1	1	0	0	0	1	1	0	0	0	1	0	1	0	0	0	0	1	0	0	0	0	1	1	0	1	1	1	0	1	0	0
G. orientalis	0	1	0	1	1	1	0	0	0	0	1	0	0	0	0	1	0	1	0	0	0	0	0	0	0	0	1	1	0	0	0	0	1	0	1	0	0
G. paniculata	1	1	0	1	1	1	1	0	0	0	1	0	0	0	0	0	0	0	0	0	0	1	0	0	0	0	0	0	0	1	1	0	0	1	0	0	1
G. populnifolia	1	1	0	1	1	1	1	0	0	0	1	0	0	0	0	1	0	0	0	0	1	0	0	0	0	0	1	0	1	0	0	0	0	0	1	1	0
G. polygama	1	1	0	1	1	1	1	0	0	0	1	0	0	0	1	1	0	1	0	0	1	0	0	0	0	0	1	0	1	0	0	0	0	0	1	1	0
G. pubescens	1	1	0	1	1	1	1	0	0	0	1	0	0	0	0	0	0	0	0	0	0	1	0	0	0	0	0	0	0	0	0	0	0	0	0	0	0
G. tiliaefolia	1	1	0	1	1	1	1	0	0	0	1	1	0	0	0	1	0	1	0	0	0	0	0		1	0	0	1	0	0	0	0	1	0	0	0	0
G. tenax	1	1	0	1	1	1	1	0	0	0	1	0	0	0	0	0	0	0	0	0	0	0	0	0	0	0	0	0	0	1	1	0	0	0	0	1	0
G. umbellata	0	1	0	1	1	1	1	0	0	0	1	0	0	0	0	0	0	0	0	0	0	1	0	0	0	0	0	1	0	0	1	0	0	0	0	0	0

G. villosa	1	1	0	1	1	1	1	0	0	0	1	0	0	0	0	0	0	0	0	0	1	0	0	0	0	0	0	0	0	1	0	0	1	0	1	0
G. vestitata	1	1	0	1	1	1	1	0	0	0	1	1	0	0	0	0	0	1	0	0	1	0	0	0	0	0	0	1	0	0	0	0	0	0	1	0
Guaribea floribunda	0	1	0	1	1	1	1	0	0	0	1	0	0	0	0	0	0	0	0	0	1	0	0	0	0		0	0	0	0	1	0	1	0	1	0
Guazuma tomentosa	1	1	0	1	1	1	1	0	0	0	1	0	0	0	0	0	0	0	0	0	0	0	0	0	0	0	0	1	0	1	1	0	1	0	1	0
G. tomentosa?	1	1	0	0	1	1	1	0	0	0	1	0	0	0	0	1	0	0	0	0	0	0	0	0	0	1	0	1	0	0	0	0	0	1	0	0	0
G. crinita	0	1	0	1	1	1	1	0	0	0	1	0	1	0	0	0	0	1	0	0	1	0	0	0	0	0	0	0	0	1	0	0	0	1	0	0	0
G. ulmifolia	0	1	0	1	1	1	1	0	0	0	1	0	0	0	0	0	0	0	0	0	1	1	0	0	0	0	0	1	1	1	1	0	0	1	0	1	1
G. ulmifolia	0	1	0	1	1	1	1	0	0	0	1	0	0	0	0	0	0	1	0	0	1	0	0	0	0	0	1	0	1	1	0	0	1	0	1	1
Hasseltia floribunda	1	1	0	1	1	1	1	0	0	0	1	0	1	0	0	0	0	0	0	0	0	0	0	0	0	0	0	0	0	0	1	0	0	1	0	1	1
Hasseltiopsis dioica	0	1	0	1	1	1	0	0	0	0	1	0	1	0	0	0	0	0	0	0	0	0	0	0	0	0	1	0	0	1	0	0	0	0	1	1
Helicteres guazumaefolia	1	1	0	1	1	1	1	0	0	0	1	0	1	0	0	1	0	0	0	0	1	0	0	0	0	0	1	1	0	1	0	0	1	0	0	0
Heliocarpus appendiculatus	0	1	0	1	1	1	0	1	0	0	1	0	0	0	0	0	0	1	0	0	0	1	0	0	0	0	0	0	0	1	0	0	1	0	0	0
Heritiera elata	0	1	0	1	1	1	1	0	0	0	1	1	0	0	0	1	0	0	0	0	0	0	1	0	0	0	1	0	0	1	0	0	0	0	0	0
H. carrioni	1	1	0	1	1	1	1	0	0	0	1	0	1	0	0	1	0	0	0	0	0	1	0	0	0	0	0	1	0	1	0	0	1	0	1	1
Herietera fomes	1	1	0	1	1	1	0	0	0	0	1	0	0	0	1	0	0	0	0	0	0	0	0	0	1	0	0	0	0	1	0	0	1	1	0	0
H. littoralis	0	1	0	1	1	1	1	0	0	0	1	0	0	0	0	0	0	0	0	0	1	0	0	0	0	0	0	0	0	1	0	0	0	0	0	1
H. macrophylla	0	1	0	1	1	1	1	0	0	0	1	0	1	0	0	0	1	0	0	0	1	0	0	0	0	0	0	1	0	1	0	0	1	0	1	1
H. ornitocephala	1	1	0	1	1	1	1	0	0	0	1	0	0	0	0	0	0	0	0	0	1	0	0	0	0	0	0	1	1	1	0	0	1	1	0	1
H. javanica	0	1	0	1	1	1	1	0	0	0	1	0	1	1	0	0	0	0	0	0	0	1	0	0	0	1	0	0	0	0	0	0	1	0	0	0
H. utilis	0	1	0	1	1	1	0	0	0	0	1	0	1	0	0	0	0	0	0	0	1	0	0	0	0	0	0	0	0	0	0	0	1	0	0	0
Hibiscus borneensis	0	1	0	1	1	1	1	0	0	0	1	0	0	0	0	0	0	0	0	0	1	0	0	0	0	0	0	0	0	0	0	0	1	1	0	0
H. columnaris	1	1	0	1	1	1	1	0	0	0	1	0	0	0	0	1	0	0	0	0	1	0	0	0	0	0	0	1	1	1	0	0	1	0	1	1
H. elatus	0	1	0	0	1	1	1	1	0	0	1	0	0	0	0	1	0	1	0	0	1	0	0	0	0	0	0	1	1	1	0	0	1	0	0	0
H. floccosus	0	1	0	0	1	1	1	0	0	0	1	0	0	0	0	0	0	0	0	0	1	1	0	0	0	0	0	0	1	1	1	0	0	0	1	0	0
H. grewiaefolius	1	1	0	1	1	1	1	0	0	0	1	0	0	0	0	0	0	0	0	0	0	0	0	0	0	0	0	0	0	1	0	0	0	0	1	0	0
H. heterophyllus	1	1	0	1	1	0	0	0	0	0	1	0	0	0	0	0	0	0	0	0	1	0	0	0	0	0	0	1	1	1	0	0	1	0	0	0
H. ludwigi	0	1	0	1	1	1	1	0	0	0	1	0	0	0	0	0	0	0	0	0	0	0	0	0	0	0	0	1	1	1	0	0	1	0	0	0
H. hastatus	0	1	0	1	1	1	1	0	0	0	1	0	0	0	0	1	0	1	0	0	1	0	0	0	0	0	0	1	1	1	0	0	1	0	0	0

H. macrophyllus	0	1	0	1	1	1	1	0	0	0	1	0	1	0	0	0	0	0	0	0	1	0	0	0	0	0	0	1	1	1	0	0	1	0	0	0
H. pleyteri	0	1	0	0	1	1	1	0	0	0	1	0	1	0	0	0	0	0	0	0	0	0	0	0	0	0	0	0	1	1	0	0	0	1	1	0
H. rosa-sinensis	0	0	0	1	1	1	1	0	0	0	1	0	1	0	0	1	0	0	0	0	0	0	1	0	0	0	0	0	1	1	0	0	1	0	0	0
H. similis	1	1	0	1	1	1	1	0	0	0	1	0	0	0	0	1	0	0	0	0	1	0	0	0	0	0	0	1	1	1	0	0	0	0	0	0
H. syriacus	1	1	0	1	1	1	1	0	0	0	1	0	0	0	0	0	0	0	0	0	1	0	0	0	0	0	0	0	1	1	0	0	0	0	0	0
H. schizopetalus	1	1	0	1	1	1	1	0	0	0	1	0	0	0	0	0	0	0	0	0	1	1	0	0	0	0	0	1	1	1	0	0	1	0	0	0
H. tiliaceous	0	1	0	1	1	1	0	0	0	0	1	0	0	1	0	0	0	1	1	0	1	1	0	0	0	0	0	0	1	1	0	0	1	0	0	0
Hoheria populnea	0	1	0	1	1	1	1	0	0	0	1	1	0	0	0	0	0	0	0	0	0	0	0	0	0	1	0	0	1	0	0	0	1	0	1	1	0
Hydrogascar tinerve	1	1	0	1	1	1	1	0	0	0	1	0	1	0	0	0	0	1	0	0	0	1	0	0	0	0	0	0	0	0	0	0	0	1	0	0
Kleinhovia hospita	1	1	0	1	1	1	1	0	0	0	1	0	0	0	0	1	0	0	0	0	1	0	0	0	0	0	0	1	0	1	0	0	0	0	1	1
Kostermansia malayana	0	1	0	1	1	1	1	0	0	0	1	0	0	0	0	0	0	0	0	0	0	0	0	0	1	0	1	0	1	0	0	0	0	0	0	1
Kydia calycina	1	0	1	0	1	1	1	0	0	0	1	0	0	0	0	0	0	0	0	1	1	0	0	0	0	0	0	0	1	1	0	0	1	0	1	0
Lagunaria palersoni	0	1	0	1	1	1	1	0	0	0	1	1	0	0	0	0	0	1	1	0	0	0	0	0	0	1	0	0	1	1	0	1	1	0	1	1
Lavatera alba	0	1	0	0	1	0	1	0	0	0	1	0	0	0	0	0	0	0	0	0	0	0	1	0	0	0	0	1	1	1	0	0	1	0	0	0
Luehea divaricata	0	1	0	1	1	1	1	0	0	0	1	0	0	0	0	0	0	0	0	0	1	1	0	0	0	0	0	0	0	1	0	0	1	1	1	0
Lueheopsis rugosa	0	1	0	1	1	1	1	0	0	0	1	1	0	0	0	0	1	0	0	0	1	1	0	0	0	0	1	0	0	1	0	0	0	1	1	0
L. flavescens	1	1	0	1	1	1	1	0	0	0	1	1	0	0	0	0	0	0	0	0	1	0	0	0	0	0	0	0	0	1	0	0	0	0	0	0
Malvaviscus arborescenses	1	1	0	1	1	1	1	0	0	0	1	0	1	0	0	0	0	0	0	0	1	0	1	0	0	0	0	1	1	1	0	0	1	0	0	0
M. conzattii	0	1	0	1	1	1	1	0	0	0	1	0	0	0	0	1	0	0	0	0	0	0	0	0	0	0	0	0	1	0	0	0	1	0	0	0
M. cordata	0	1	0	1	1	1	0	0	0	0	1	0	0	0	0	0	0	0	0	0	0	0	0	0	0	?		0	1	0	0	0	0	0	0	0
Mansonia gagei	0	1	0	1	1	1	1	0	0	0	1	0	0	0	0	0	0	0	0	0	0	0	0	0	0	0	0	0	0	0	0	0	0	1	1	0
Matisia dowdingii	0	1	0	1	1	1	0	0	0	0	1	0	1	0	0	0	0	0	0	0	0	0	0	0	1	0	0	1	1	0	0	0	0	0	1	0
M. bicolor	0	1	0	1	1	1	1	0	0	0	1	0	?		0	0	0	0	0	0	0	0	0	0	0	1	0	0	0	0	0	1	0	1	0	0	0
Melania odorata	1	1	0	1	1	1	0	0	0	0	1	0	0	0	0	0	0	0	0	0	0	0	0	0	0	0	0	1	1	0	1	0	0	1	0	0	0
Melochia arborea	0	1	0	1	1	1	1	0	0	0	1	0	0	0	0	0	0	0	0	1	0	0	0	0	0	0	1	1	0	1	0	0	1	0	1	0
Microcos hirsuta	0	1	0	1	1	1	1	0	0	0	1	0	1	0	0	0	0	0	0	0	0	0	1	0	0	0	1	0	0	1	0	0	1	0	0	0
Montezuma speciossisima	0	1	0	0	1	1	1	0	0	0	1	0	0	0	0	0	0	0	0	0	0	0	0	0	1	0	0	1	1	1	0	0	1	0	1	0
Muntingia calabura	0	1	0	0	1	1	1	0	0	0	1	0	0	0	0	0	0	0	0	0	1	0	0	0	0	0	0	0	0	1	0	0	0	0	0	0

Neesia synandra	0	1	0	0	1	1	1	0	0	0	1	0	?	0	0	0	0	0	0	0	0	0	0	0	0	0	0	0	1	1	0	0	0	0	0	0
Neesia altissima	0	1	0	0	1	1	1	0	0	0	1	0	1	0	0	0	0	0	0	0	0	1	0	0	0	0	0	0	0	1	1	0	0	1	0	0	0
Ochroma boliviana	0	1	0	0	1	1	1	0	0	0	1	0	0	0	0	0	0	0	0	0	0	1	0	0	0	0	0	0	0	1	1	0	0	1	0	0	0
O. lagopus	0	1	0	1	1	1	0	0	0	0	1	0	1	0	0	0	0	0	0	0	0	0	0	0	0	0	0	1	1	0	0	0	0	1	0	0	1
O. pyramidale	0	1	1	1	1	1	0	1	0	0	1	0	1	0	0	0	0	0	0	0	0	1	0	0	0	0	0	0	1	0	0	0	0	1	0	0	0
Octolobus angustatus	0	1	0	1	1	1	1	0	0	0	1	0	0	0	0	0	0	0	0	0	0	0	1	0	0	0	0	0	0	0	1	0	0	1	1	1	1
Pachira aquatica	0	1	1	1	1	1	0	1	0	0	1	0	0	0	1	0	0	0	0	0	1	0	0	0	1	0	0	1	0	0	1	0	1	0	0	0	
P. curtisiii	0	1	0	1	1	1	1	0	0	0	1	0	0	0	0	0	0	0	0	0	0	1	0	0	0	0	0	0	0	1	1	0	0	0	0	0	0
P. macrocarpa	1	1	0	1	1	1	0	1	0	0	1	0	0	0	0	1	0	0	0	1	1	0	0	0	1	0	0	1	1	1	1	0	1	0	0	1	
Paritium tiliaceum synonym*	0	1	0	0	1	1	1	0	0	0	1	0	0	0	0	0	0	0	0	0	0	1	0	0	0	0	0	0	1	1	1	0	0	1	0	0	0
Pavonia fruticosa	1	1	0	1	1	1	0	0	0	0	1	0	1	0	0	0	0	0	0	0	0	0	1	0	0	0	1	0	1	1	0	0	1	0	0	0	
Pentace burmanica	0	1	0	1	1	1	0	0	0	0	1	0	0	0	0	1	0	0	0	0	1	0	0	0	0	0	0	0	1	1	0	0	0	1	0	0	
P. griffithii	0	1	0	1	1	1	1	0	0	0	1	0	0	0	0	0	0	0	0	0	1	0	0	0	0	0	0	0	1	0	0	0	0	1	0	0	
P. perakensis	0	1	0	1	1	1	1	0	0	0	1	0	0	0	0	0	0	0	0	0	1	0	0	0	0	0	0	0	1	0	0	0	0	1	0	0	
P. strychnoidea	0	1	0	1	1	1	1	0	0	0	1	0	0	0	0	0	0	0	0	0	0	0	0	0	1	0	0	0	1	0	0	0	0	0	0	0	
P. triptera	1	1	0	1	1	1	1	1	1	0	1	0	0	0	0	0	0	0	0	0	1	1	0	0	0	0	0	0	0	1	0	0	0	0	0	1	0
Pentaplaris doroteae	0	1	0	1	1	1	0	0	0	0	1	0	0	0	0	0	0	0	0	0	0	0	0	1	0	0	0	0	1	1	1	0	0	1	0	1	0
Prockia crucis	1	1	0	1	1	1	1	0	0	0	1	0	1	0	0	0	0	0	0	0	0	1	0	0	0	0	0	1	0	1	0	0	0	1	0	1	0
P. deltoides	0	1	0	1	1	1	1	0	0	0	1	0	0	0	0	0	0	0	1	1	0	0	0	0	0	0	0	1	0	1	0	0	0	0	0	1	1
Pterocymbium tinctorium	0	1	0	0	1	1	1	0	0	0	1	1	0	0	0	0	0	0	0	0	0	1	0	0	1	0	0	1	0	0	0	0	1	1	0	0	
P. tubulatum	0	1	0	0	1	1	1	0	0	0	1	1	0	0	0	0	0	1	0	0	0	0	1	0	0	0	1	1	0	0	0	0	1	1	0	0	
P. splendens	0	1	0	0	1	1	1	0	0	0	1	1	0	0	0	0	0	0	0	0	0	1	0	0	0	0	0	0	1	0	1	1	1	1	1	1	0
P. splendens	0	1	0	1	1	1	1	0	0	0	1	0	0	0	0	0	0	0	0	0	0	0	0	1	0	0	0	0	1	0	0	1	1	0	0	0	0
P. semisagittatum	1	1	0	1	1	1	1	0	0	0	1	0	0	0	0	0	0	0	0	0	0	1	0	0	0	0	0	0	1	0	0	0	0	0	0	0	
Pterospermum acerifolium	0	1	0	1	1	1	1	0	0	0	1	0	0	0	0	0	0	0	0	0	0	1	0	0	1	0	0	0	0	0	1	0	0	1	0	0	
P. diversifolium	0	1	0	1	1	1	1	0	0	0	1	0	1	0	0	1	0	0	0	0	1	0	0	0	0	0	1	0	0	1	0	0	1	0	1	1	
P. blumeanum	0	1	0	1	1	1	1	0	0	0	1	0	0	0	0	0	0	0	0	0	1	0	0	0	0	0	0	0	0	0	0	0	1	0	0	0	
P. jackianum	0	1	0	1	1	1	1	0	0	0	1	0	0	0	0	0	0	0	0	0	1	1	0	0	0	0	0	0	0	1	0	0	0	1	0	0	0

P. niveum	0	1	0	1	1	1	1	0	0	0	1	0	0	0	0	0	0	0	0	0	0	0	0	0	0	0	1	0	1	0	0	1	1	0	0
P. heyneanum	1	0	0	1	1	1	1	0	0	0	1	0	0	1	0	1	0	0	0	0	1	0	0	0	0	0	0	0	0	1	0	0	1	0	0	0
Pterygota bequaertii	0	1	0	0	1	1	1	0	0	0	1	0	0	0	0	1	0	0	0	0	0	0	1	0	0	0	1	1	0	1	0	0	1	1	0	0
P. mildbraedii	0	1	0	0	1	1	1	0	0	0	1	0	0	0	0	1	0	0	0	0	0	0	1	0	0	0	0	1	0	1	0	0	1	0	1	1
Petrygota kamerunensis	0	1	0	1	1	1	1	0	0	1	1	0	0	0	0	0	0	0	0	0	0	0	0	1	0	0	0	0	1	0	1	0	0	1	1	0	0
Pseudobombax ellipticum	1	1	0	1	1	1	1	1	0	0	1	0	1	0	0	0	0	0	0	0	0	1	0	1	0	0	0	0	1	1	0	0	0	1	0	1	0
Pityranthe verrucosa	0	1	0	1	1	1	1	0	0	0	1	0	0	0	0	0	0	0	0	0	1	0	0	1	0	0	0	0	0	1	0	0	0	0	1	0	0
Quararibea asterolepis	0	1	0	1	1	1	1	0	0	0	1	0	1	0	0	0	0	0	0	0	0	0	0	0	1	0	0	1	0	0	1	0	1	0	1	0
Q. parvifolia	0	1	0	0	1	1	0	0	0	0	1	0	1	0	0	1	0	0	0	0	0	0	0	0	1	0	0	1	0	0	1	0	1	0	1	1
R. cavaleirei	1	1	0	1	1	1	1	0	0	1	1	0	0	0	0	0	0	0	0	0	0	1	0	0	0	1	0	0	1	0	1	0	0	1	0	0	0
R. clarkii	1	0	0	1	1	1	1	0	0	0	1	0	0	0	0	0	0	0	0	0	1	1	0	0	0	1	0	0	1	0	1	0	0	1	0	0	1
R. formosana	1	0	0	1	1	1	1	0	0	1	1	0	0	0	0	0	0	0	0	0	0	1	0	0	0	0	0	0	0	0	1	0	0	1	0	0	0
R. pubescens	1	0	0	1	1	1	0	0	0	1	1	1	0	0	0	0	0	0	0	0	0	1	0	0	0	0	0	0	1	0	1	0	0	1	1	0	0
R. thyrosidea	1	0	0	1	1	1	1	0	0	1	1	0	1	0	0	0	0	0	0	0	0	1	1	0	0	0	0	0	1	0	1	0	0	1	0	1	0
R. wallichii	0	0	0	1	1	1	1	0	0	1	1	0	1	0	0	0	0	0	0	0	0	1	1	0	0	0	0	0	1	0	1	0	0	1	0	0	0
Scaphium affini	1	1	0	1	1	1	1	0	0	0	1	1	0	1	0	1	0	0	0	0	0	0	0	0	0	1	0	1	0	1	0	0	0	0	0	0	0
Schoutenia ovata	0	1	0	1	1	1	1	0	0	0	1	0	1	0	1	0	0	0	0	0	1	0	0	0	0	0	1	1	1	0	0	0	0	0	1	0	0
Sterculia acerifolia	0	1	0	1	1	1	1	0	0	0	1	0	1	0	0	1	0	1	0	0	1	0	0	0	0	0	0	1	0	0	1	0	1	0	0	0	0
S. alata	0	1	0	0	1	1	1	0	0	0	1	0	0	0	0	0	0	0	0	0	0	0	0	1	0	0	0	0	0	0	1	0	0	1	0	1	1
S. apendiculata	0	1	0	1	1	1	1	1	0	0	1	0	0	0	0	0	0	0	0	0	0	0	0	1	0	0	0	1	1	0	0	1	0	1	0	0	0
S. campanulata	0	1	0	0	1	1	1	0	0	0	1	0	0	0	0	0	0	0	0	0	0	0	0	0	0	1	0	0	0	0	1	0	1	0	0	0	0
S. caribaea	0	1	0	0	1	1	1	0	0	0	1	0	0	0	0	0	0	0	0	0	0	1	1	0	0	0	0	0	1	0	0	1	0	1	0	1	0
S. ceramica	0	1	0	0	1	1	1	0	0	0	1	0	0	0	0	0	0	0	0	0	0	1	1	0	0	0	0	0	0	0	0	1	0	1	0	0	0
S. chicha	0	1	0	0	1	1	1	0	0	0	1	?	0	0	0	0	0	1	0	0	1	0	0	0	0	0	0	1	0	0	1	0	1	0	0	0	0
S. chicha	0	1	0	0	1	1	1	0	0	0	1	0	0	0	0	0	0	0	0	0	0	0	0	0	0	0	0	0	0	0	1	0	1	0	0	0	0
S. colombiana	0	1	0	0	1	1	1	0	0	0	1	0	0	0	0	1	0	0	0	0	1	0	1	0	0	0	0	0	0	0	1	0	1	0	0	1	0
S. elegantiflora	0	1	0	1	1	1	1	0	0	0	1	0	0	0	1	0	0	0	0	0	0	0	1	0	0	0	0	1	0	0	1	0	1	1	0	1	0
S. excelsa	0	1	0	0	1	1	1	0	0	0	1	0	1	0	0	1	0	1	0	0	1	0	0	0	0	0	1	0	0	0	1	0	1	0	0	0	0

S. foetida	0	1	0	1	1	1	1	0	0	0	1	0	0	0	0	1	0	0	0	0	1	0	1	0	0	0	0	0	1	0	1	0	1	0	0	0
S. hugelii	0	1	0	1	1	1	1	0	0	0	1	0	0	0	0	1	0	1	0	0	1	0	0	0	0	0	0	0	1	0	0	0	0	0	0	0
S. linearicarpum	0	1	0	0	1	1	1	0	0	0	1	1	1	0	0	1	0	1	0	0	1	0	0	0	0	0	0	0	0	1	0	0	1	0	0	0
S. murex	0	1	0	0	1	1	1	0	0	0	1	0	0	0	1	0	0	0	0	0	0	0	1	0	0	0	0	1	0	0	0	0	0	0	0	0
S. multinervia	0	1	0	1	1	1	0	0	0	0	1	0	1	0	0	0	0	0	0	0	0	0	0	0	0	0	0	1	1	1	0	0	1	0	0	0
S. murex	0	1	0	0	1	1	1	0	0	0	1	0	0	0	0	0	0	0	0	0	1	0	0	0	0	0	0	0	1	1	0	0	0	0	0	0
S. oblonga	0	1	0	1	1	1	1	0	0	0	1	0	0	0	0	0	0	0	0	0	0	0	1	0	0	0	0	1	0	1	1	0	1	1	1	1
S. ornata	1	1	0	1	1	1	1	0	0	0	1	0	0	0	0	0	0	0	0	1	0	0	0	1	0	0	0	0	1	1	1	0	0	1	0	0	0
S. pallens	0	1	0	0	1	1	0	0	0	0	1	0	0	0	0	0	0	0	1	0	0	1	0	1	0	0	0	0	1	0	1	1	0	1	0	0	0
S. populnifolia	0	1	0	0	1	1	1	0	0	0	1	0	0	0	0	1	0	1	0	0	1	0	0	0	0	0	0	0	0	0	1	1	0	1	0	0	0
S. pruriens	0	1	0	0	1	1	1	0	0	0	1	1	0	0	0	0	0	0	0	0	0	0	1	0	1	0	0	0	0	1	1	0	1	0	0	0	0
S. quinquefolia	0	1	0	0	1	1	1	0	0	0	1	0	0	0	0	1	0	0	0	0	0	0	1	0	0	0	1	1	0	1	1	0	1	0	0	0	0
S. rhinopetala	1	0	0	0	1	1	1	0	0	0	1	0	0	0	1	1	0	0	0	0	1	0	1	0	0	0	1	0	0	1	1	0	1	0	1	1	1
S. rubiginosa	0	1	0	0	1	0	1	0	0	0	1	0	0	0	0	0	0	0	0	0	0	0	0	0	0	0	0	1	0	1	1	0	1	0	0	0	0
S. scaphisera	1	1	0	1	1	1	1	0	0	0	1	1	0	0	0	0	0	0	0	0	0	0	1	0	0	0	0	0	0	1	1	0	1	0	0	0	0
S. setigera	0	1	0	1	1	0	1	0	0	0	1	0	0	0	0	0	0	0	0	0	0	1	0	0	0	1	0	1	0	0	1	1	0	0	0	1	0
S. subviolacea	0	1	0	1	1	1	1	0	0	0	1	0	1	0	0	0	0	0	0	0	0	1	0	0	0	1	0	0	1	0	1	1	0	0	0	1	0
S. tragacantha	1	1	0	1	1	1	1	0	0	0	1	0	1	0	0	1	0	0	0	0	1	0	0	0	0	0	0	1	0	1	1	0	1	0	0	0	0
S. villosa	0	1	0	1	1	1	1	0	0	0	1	0	0	0	0	0	0	0	0	0	0	0	1	0	0	0	0	1	0	1	1	0	1	0	0	0	0
S. versicolor	0	1	0	0	1	1	1	0	0	0	1	0	0	0	0	0	0	0	0	0	0	0	0	0	1	0	1	0	0	1	1	0	0	1	1	0	0
Theobroma bernoullii	1	1	0	0	1	0	1	0	0	0	1	1	1	0	0	0	0	0	0	0	0	0	0	0	0	0	0	1	0	0	1	1	0	1	0	0	0
T. bicolor	0	1	0	1	1	1	0	0	0	0	1	0	0	0	0	0	0	0	0	0	0	0	1	0	0	1	0	1	1	0	1	1	0	1	0	0	0
T. cacao	0	1	0	1	1	1	1	1	0	0	1	0	1	1	0	0	0	0	0	0	0	0	0	0	0	0	0	1	0	0	1	1	0	1	0	0	0
Thespesia grandiflora	1	1	0	1	1	1	1	0	0	0	1	1	0	0	0	1	0	0	0	0	0	0	0	0	0	1	0	1	1	0	1	1	1	1	0	1	0
T. populnea	0	1	0	1	1	1	0	0	0	0	1	1	0	0	0	0	0	0	0	1	1	0	0	0	0	0	0	1	0	0	0	0	1	0	0	0	0
Tilia americana	1	1	0	1	1	1	1	0	0	1	1	0	0	1	0	0	0	0	0	0	1	0	0	0	0	0	0	0	1	0	0	0	0	0	0	0	0
T. caucasica	1	1	0	1	1	1	1	0	0	1	1	0	0	0	0	0	0	0	0	0	0	0	0	0	0	0	0	0	1	0	0	0	0	0	0	0	0
T. cordata	1	1	0	1	1	1	1	0	0	1	1	0	1	0	0	0	0	0	0	0	0	0	0	0	0	0	0	0	1	0	0	0	0	0	0	0	0

T. europaea	0	1	0	1	1	1	1	0	0	1	1	0	1	0	0	0	0	0	0	0	0	1	0	0	0	0	0	0	0	0	1	0	0	0	0	0	0
T. floridana	1	1	0	1	1	1	1	0	0	1	1	0	0	0	0	0	0	0	0	0	0	1	0	0	0	0	0	0	0	0	1	0	0	0	0	0	0
T. glabra	1	1	0	1	1	0	1	0	0	1	1	0	0	0	0	0	0	0	0	0	0	1	0	0	0	0	0	0	0	1	1	0	0	0	0	0	0
T. heterophylla	1	1	0	1	1	1	1	0	0	1	1	0	0	0	0	0	0	0	0	0	0	1	0	0	0	0	0	0	0	1	1	0	0	0	0	0	0
T. japonica	1	1	0	1	1	1	1	0	0	1	1	0	1	0	0	0	0	0	0	0	0	1	0	0	0	0	0	?	0	1	1	0	0	0	0	0	0
T. rubra	1	1	0	1	1	1	1	0	0	1	1	0	0	0	0	0	0	0	0	0	0	1	0	0	0	0	0	0	0	1	1	0	0	0	0	0	0
T. moltkei	1	1	0	1	1	1	1	0	0	1	1	1	0	0	0	0	0	0	0	0	0	1	0	0	0	0	0	0	0	1	1	0	0	0	0	0	0
T. tomentosa	1	1	0	1	1	1	1	0	0	1	1	0	1	0	0	0	0	0	0	0	0	1	0	0	0	0	0	0	0	1	1	0	0	0	0	0	0
T. vulgaris	1	1	0	1	1	1	1	0	0	1	1	1	0	0	0	1	1	1	1	0	1	0	0	0	0	0	0	0	0	1	1	0	0	0	0	0	0
Trachetiopsis melanoxylon	0	1	0	1	1	1	1	0	0	0	1	0	0	0	0	0	0	0	0	0	0	1	0	0	0	0	0	0	1	0	0	0	0	1	0	1	0
Triplochiton scleroxylon	1	1	0	1	1	1	1	0	0	0	1	0	1	0	0	0	0	0	0	0	0	0	0	0	0	1	0	0	1	0	1	1	0	1	0	0	0
Trichospermum richii	0	1	1	1	1	1	0	0	0	1	1	1	0	0	0	0	0	0	0	0	0	1	0	0	0	0	0	1	0	1	1	0	0	1	0	0	0
Triumfetta hintonii	0	1	0	1	1	1	1	0	0	1	1	1	0	0	0	0	0	0	0	0	0	0	0	0	0	0	0	0	0	1	1	0	0	1	0	0	0

Appendix 5.8. Data matrix used in the Principal Component Analysis of malvalean woods. 1, states for present feature and 0, states for absent feature.

Specimen	Distinct/indistinct growth ring	Growth ring code	Type of growth ring boundary	Wood Type	Family	Preservation	Locality
STRI 14165	absent	0		1	Cannabaceae	calcified	Hodges Hill
STRI 36273	indistinct	0	marginal parenchyma	2	Fabaceae	calcified	Hodges Hill
STRI 36272	absent	0		3	Elaeocarpaceae	calcified	Hodges Hill
STRI 14151	indistinct	0	radially narrowed fibres	4	Malvaceae	calcified	Hodges Hill
STRI 36270	absent	0		4	Malvaceae	calcified	Hodges Hill
STRI 14155	absent	0		5	Malvaceae	calcified	Hodges Hill
STRI 14157	absent	0		5	Malvaceae	calcified	Hodges Hill
STRI 14159	absent	0		5	Malvaceae	calcified	Hodges Hill
STRI 14160	absent	0		5	Malvaceae	calcified	Hodges Hill
STRI 14161	absent	0		5	Malvaceae	calcified	Hodges Hill
STRI 14164	absent	0		5	Malvaceae	calcified	Hodges Hill
STRI 36269	absent	0		5	Malvaceae	calcified	Hodges Hill
STRI 15368	absent	0		cf Wood type 2	Fabaceae	charcoalified/silicified	Contractors Hill
STRI 15369	absent	0		cf Wood type 2	Fabaceae	charcoalified/silicified	Contractors Hill
STRI 15370	absent	0		cf Wood type 2	Fabaceae	charcoalified/silicified	Contractors Hill
STRI 13625	absent	0		cf Wood type 2	Fabaceae	charcoalified/silicified	Contractors Hill
STRI 14198	indistinct	0	marginal parenchyma	cf Wood type 2	Fabaceae	charcoalified/silicified	Contractors Hill
STRI 21046	indistinct	0	marginal parenchyma	cf Wood type 2	Fabaceae	charcoalified/silicified	Contractors Hill
STRI 14147	absent	0		cf Wood type 2	Fabaceae	charcoalified/silicified	Contractors Hill
STRI 15405	absent	0		6	Fabaceae	charcoalified/silicified	Contractors Hill
STRI 15371	absent	0		7	Malvaceae	charcoalified/silicified	Contractors Hill
STRI 15519	absent	0		7	Malvaceae	charcoalified/silicified	Centenario Bridge
STRI 14193	absent	0		7	Malvaceae	charcoalified/silicified	Contractors Hill
STRI 15515	absent	0		8	Sapotaceae	charcoalified/silicified	Centenario Bridge
STRI 13691	absent	0		9	Melastomataceae	charcoalified/silicified	Contractors Hill
STRI 15364	absent	0		10	Meliaceae	charcoalified/silicified	Contractors Hill
STRI 15367	indistinct	0		10	Meliaceae	charcoalified/silicified	Contractors Hill
STRI 15514	indistinct	0		10	Meliaceae	charcoalified/silicified	Centenario Bridge
STRI 15520	indistinct	0		Indeterminate A		charcoalified/silicified	Centenario Bridge
STRI 15523	indistinct	0		Inderterminate B		charcoalified/silicified	Centenario Bridge

Appendix 8.3.1.a. Presence/absence of growth rings in Cucaracha Formation specimens. 1= distinct growth ring; 2= indistinct or absent growth ring.

Labels	Species	Family	Growth rings distinct/indistinct	Rings code	Type of boundary
PIT1BA	*Abarema barbouriana*	Fabaceae	absent	0	
ABUTRA	*Abuta racemosa*	Menispermaceae	absent	0	
ADE1TR	*Adelia trilobia*	Euphorbiaceae	absent	0	
AEGIAN	*Aegiphila anomala*	Verbenaceae	absent	0	
AEGIPA	*Aegiphila panamensis*	Verbenaceae	absent	0	
ALBIGU	*Pseudosamanea guachapele*	Fabaceae	absent	0	
ALBINI	*Albizia nipoides*	Fabaceae	absent	0	
ALCHLA	*Alchornea latifolia*	Euphorbiaceae	absent	0	
ALLOGE	*Allophylus gentryi*	Sapindaceae	indistinct	0	marginal parenchyma
ALLOOC	*Allophylus racemosus*	Sapindaceae	indistinct	0	marginal parenchyma
ALLOPS	*Allophylus psilospermus*	Sapindaceae	indistinct	0	thick walled fibres
ALSEBL	*Alseis blackiana*	Rubiaceae	absent	0	
AMAICO	*Amaioua corymbosa*	Rubiaceae	absent	0	
AMANGU	*Amanoa guianensis*	Euphorbiaceae	absent	0	
ANACEX	*Anacardium excelsum*	Anacardiaceae	absent	0	
ANNOPU	*Annona Purpurea*	Annonaceae	absent	0	
ANNOSP	*Annona spraguei*	Annonaceae	absent	0	
ANTITR	*Pittoniotis trichantha*	Rubiaceae	absent	0	
APEIME	*Apeiba membranacea*	Malvaceae	absent	0	
APEITI	*Apeiba tibourbou*	Malvaceae	absent	0	
ASPICR	*Aspidosperma spruceanum*	Apocynaceae	absent	0	
AST2GR	*Astronium graveolens*	Anacardiaceae	absent	0	
BANAGU	*Banara guianensis*	Salicaceae	absent	0	
BAUHGU	*Bauhinia guianensi*	Fabaceae	absent	0	
BEILPE	*Beilschmiedia pendula*	Lauraceae	absent	0	
BROSAL	*Brosimum alicastrum*	Moraceae	absent	0	
BROSCO	*Brosimum costaricanum*	Moraceae	absent	0	
BROSGU	*Brosimum guianense*	Moraceae	absent	0	
BROSLA	*Brosimum lactense*	Moraceae	indistinct	0	thick walled fibres
BROSUT	*Brosimum utile*	Moraceae	absent	0	
BROWMA	*Brownea macrophylla*	Fabaceae	absent	0	
BUCIBU	*Bucida buceras*	Combretaceae	absent	0	
BUNCCO	*Bunchosia nitida*	Malpighiaceae	absent	0	
BURSSI	*Bursera simaruba*	Burseraceae	absent	0	
BYRSCR	*Byrsonima crassifolia*	Malpighiaceae	absent	0	
BYRSSP	*Byrsonima spicata*	Malpighiaceae	absent	0	
CAL2CA	*Calycophyllum candidissimum*	Rubiaceae	absent	0	
CALACO	*Calatola costaricensis*	Icacinaceae	absent	0	
CALLST	*Calliandra laxa*	Fabaceae	absent	0	
CAPPCY	*Capparis cynophallophora*	Brassicaceae	absent	0	
CARYBU	*Caryodaphnopsis, burgeri*	Lauraceae	absent	0	
CASEAC	*Casearia aculeata*	Salicaceae	absent	0	
CASEAR	*Casearia arborea*	Salicaceae	absent	0	
CASECO	*Casearia commersoniana*	Salicaceae	absent	0	
CASEGU	*Casearia guianensis*	Salicaceae	absent	0	
CASESY	*Casearia sylvestris*	Salicaceae	absent	0	
CASSEL	*Cassipourea elliptica*	Rhizophoraceae	absent	0	
CECRPE	*Cecropia peltata*	Urticaceae	absent	0	
CELTSC	*Celtis schippii*	Cannabaceae	absent	0	
CESPMA	*Cespedesia spathulata*	Ochnaceae	absent	0	
CHIMPA	*Chimarrhis parviflora*	Rubiaceae	absent	0	
CHLOMA	*Chloroleucon mangense*	Fabaceae	absent	0	
CHR1EC	*Chrysochlamys eclipes*	Clusiaceae	absent	0	
CHR2AR	*Chrysophyllum argenteum*	Sapotaceae	absent	0	

CHR2CA	*Chrysophyllum cainito*	Sapotaceae	absent	0
CHR2VE	*Chrysophyllum venezuelense*	Sapotaceae	absent	0
PHOECI	*Cinnamomum triplinerve*	Lauraceae	absent	0
CLETLA	*Clethra lanata*	Clethraceae	absent	0
COCCCO	*Coccoloba coronata*	Polygonaceae	absent	0
COCCJO	*Coccoloba johnstonii*	Polygonaceae	absent	0
COCCMA	*Coccoloba manzinellens*	Polygonaceae	absent	0
PIT1RU	*Cojoba rufescens*	Fabaceae	absent	0
COLUGL	*Colubrina glandulosa*	Rhamnaceae	absent	0
COLUHE	*Colubrina heteroneura*	Rhamnaceae	absent	0
COMPCA	*Compsoneura capitellata*	Myristicaceae	absent	0
CONORU	*Conostegia rufescens*	Melastomataceae	absent	0
CONOXA	*Conostegia xalapensis*	Melastomataceae	absent	0
CORDAL	*Cordia alliodora*	Boraginaceae	distinct	1tangential lines vessels, vessel diameter
CORDER	*Cordia eriostigma*	Boraginaceae	indistinct	0fibres narrowed radially
COSMMA	*Cosmibuena macrocarpa*	Rubiaceae	absent	0
COU2CU	*Coussarea curvigemmia*	Rubiaceae	absent	0
COU2LA	*Coussarea latifolia*	Rubiaceae	absent	0
COUTHE	*Coutarea hexandra*	Rubiaceae	absent	0
CRATTA	*Crateva tapia*	Brassicaceae	absent	0
CROTBI	*Croton billbergianu*	Euphorbiaceae	absent	0
CROTDR	*Croton draco*	Euphorbiaceae	absent	0
CRYPAS	*Cryptocaria aschersoniana*	Lauraceae	absent	0
CUPACI	*Cupania cinerea*	Sapindaceae	indistinct	0thick walled fibres
CUPALA	*Cupania latifolia*	Sapindaceae	indistinct	0thick walled fibres
CUPARU	*Cupania rufescens*	Sapindaceae	absent	0
DALBRE	*Dalbergia retusa*	Fabaceae	absent	0
DAPHAM	*Daphnosis americana*	Thymeleaceae	absent	0
DENDAR	*Dendropanax arboreus*	Araliaceae	absent	0
DIO2AR	*Diospyros artanthifolia*	Ebenaceae	absent	0
DIPHRO	*Diphisa americana*	Fabaceae	absent	0
DIPTPA	*Dipteryx oleifera*	Fabaceae	absent	0
DRYPST	*Drypetes standleyi*	Euphorbiaceae	absent	0
DUGUCO	*Duguetia confusa*	Annonaceae	indistinct	0thick walled fibres
DUSSAT	*Dussia atropurpurea*	Fabaceae	absent	0
ELAU1AU	*Elaeagia auriculata*	Rubiaceae	absent	0
ENTECY	*Enterolobium cyclocarpum*	Fabaceae	absent	0
ENTESC	*Enterolobium schomburgkii*	Fabaceae	absent	0
ERBLOD	*Erblichia odorata*	Turneraceae	absent	0
ERY1CO	*Erythrina costaricensi*	Fabaceae	absent	0
ERY2CI	*Erythroxylum citrifolium*	Erythroxylaceae	absent	0
ERY2MA	*Erythroxylum macrophyllum*	Erythroxylaceae	absent	0
ESCHJA	*Eschweilera jacquelyniae*	Lecythidaceae	absent	0
ESCHPI	*Eschweilera pittieri*	Lecythidaceae	absent	0
ESCHSE	*Eschweilera sessilis*	Lecythidaceae	absent	0
EUGECO	*Eugenia coloradoensis*	Myrtaceae	absent	0
EUGEGA	*Eugenia galalonensis*	Myrtaceae	absent	0
EUGENE	*Eugenia nesiotica*	Myrtaceae	absent	0
EUGEOE	*Eugenia oerstediana*	Myrtaceae	absent	0
EUGEPR	*Eugenia principium*	Myrtaceae	absent	0
EXOSME	*Exostema mexicanum*	Rubiaceae	absent	0
FICUIN	*Ficus insipida*	Moraceae	absent	0
FICUMA	*Ficus maxima*	Moraceae	absent	0
FICUPO	*Ficus popenoei*	Moraceae	absent	0

FICUTO	*Ficus tonduzii*	Moraceae	absent	0
FICUYO	*Ficus yoponenis*	Moraceae	indistinct	0thick walled fibres
FISSFE	*Fissicalyx feldleri*	Fabaceae	indistinct	0thick walled fibres
GAR2IN	*Garcinia intermedia*	Clusiaceae	absent	0
GAR2MA	*Garcinia madruno*	Clusiaceae	absent	0
GENIAM	*Genipa americana*	Rubiaceae	absent	0
GUAPST	*Guapira standleyana*	Nyctaginaceae	absent	0
GUARGL	*Guarea glabra*	Meliaceae	absent	0
GUARGR	*Guarea grandifolia*	Meliaceae	absent	0
GUARGU	*Guarea guidonia*	Meliaceae	absent	0
GUARPT	*Guarea pterorhachis*	Meliaceae	absent	0
GUARSP	*Guarea bullata*	Meliaceae	absent	0
GUATAB	*Guatteria aberrans*	Annonaceae	absent	0
GUATDU	*Guatteria dumetorum*	Annonaceae	indistinct	0parenchyma bands frequency
GUAZUL	*Guazuma ulmifolia*	Malvaceae	absent	0
GUETCR	*Guettarda crispiflora*	Rubiaceae	absent	0
GUETFO	*Guettarda foliacea*	Rubiaceae	absent	0
GUSTSU	*Gustavia superba*	Lecythidaceae	absent	0
HAMPAP	*Hampea appendiculata*	Malvaceae	absent	0
HASSFL	*Hasseltia floribunda*	Salicaceae	absent	0
HEDYBO	*Hedyosmum bonplandianu*	Chloranthaceae	absent	0
HEISAC	*Heisteria acuminata*	Olacaceae	absent	0
HEISCO	*Heisteria concinna*	Olacaceae	absent	0
HELIAM	*Heliocarpus americanus*	Malvaceae	absent	0
HENRFA	*Henrietella fascicularis*	Melastomataceae	indistinct	0thick walled fibres
	Henriettea succosa	Melastomataceae	absent	0
HIRTAM	*Hirtella americana*	Chrysobalanaceaae	absent	0
HIRTTR	*Hirtella trianda*	Chrysobalanaceaae	absent	0
HIRTTU	*Hirtella tubiflora*	Chrysobalanaceaae	absent	0
HORTCO	*Hortia colombiana*	Rutaceae	absent	0
HUMIDI	*Humiriastrum diguense*	Humiriaceae	absent	0
HYERAL	*Hyeronima alchorneoides*	Euphorbiaceae	distinct	1thick walled fibres
HYEROB	*Hyeronima oblonga*	Euphorbiaceae	absent	0
HYMECO	*Hymenaea courbaril*	Fabaceae	absent	0
INGACH	*Inga chocoensis*	Fabaceae	distinct	1marginal parenchyma
INGACO	*Inga cocleensis*	Fabaceae	indistinct	0marginal parenchyma
INGAFA	*Inga laurina*	Fabaceae	absent	0
	Inga goldmanii	Fabaceae	absent	0
INGAM1	*Inga mucuna*	Fabaceae	indistinct	0fibres narrowed radially
INGAMA	*Inga marginata*	Fabaceae	absent	0
INGAMI	*Inga oerstediana*	Fabaceae	absent	0
INGAPA	*Inga pauciflora*	Fabaceae	absent	0
INGAPE	*Inga pezizifera*	Fabaceae	absent	0
INGAPU	*Inga punctata*	Fabaceae	absent	0
INGARU	*Inga ruiziana*	Fabaceae	absent	0
INGACU	*Inga acuminata*	Fabaceae	indistinct	0marginal parenchyma
INGASA	*Inga sapindioides*	Fabaceae	absent	0
INGASE	*Inga sertulifera*	Fabaceae	absent	0
INGASP	*Inga spectabilis*	Fabaceae	absent	0
INGATH	*Inga thibaudiana*	Fabaceae	absent	0
INGAUM	*Inga umbellifera*	Fabaceae	absent	0
ISERLA	*Isertia laevis*	Rubiaceae	absent	0
JAC1CO	*Jacaranda copaia*	Bignoniaceae	absent	0
LACIAG	*Lacistema aggregatum*	Salicaceae	absent	0
LACMPA	*Lacmellea panamensis*	Apocynaceae	absent	0
LAETPR	*Laetia procera*	Salicaceae	absent	0
LAETTH	*Laetia thamnia*	Salicaceae	absent	0

LAFOPU	*Lafoensia punicifolia*	Lythraceae	indistinct	0fibres narrowed radially
LAFOSP	*Lafoensia sp*	Salicaceae	absent	0
LENNVI	*Lennea viridiflora*	Fabaceae	absent	0
LICAAF	*Licania affinis*	Chrysobalanaceaae	absent	0
LICAHY	*Licania hypoleuca*	Chrysobalanaceaae	absent	0
LINDLA	*Lindackeria laurina*	Salicaceae	absent	0
LONCAT	*Lonchocarpus atropurpureu*	Fabaceae	absent	0
LONCFE	*Lonchocarpus ferruginea*	Fabaceae	absent	0
LONCLA	*Lonchocarpus heptaphyllus*	Fabaceae	absent	0
LONCMI	*Lonchocarpus minimiflorus*	Fabaceae	absent	0
LOZAPI	*Lozania pittieri*	Lacistemataceae	absent	0
LUEHSE	*Luehea semannii*	Malvaceae	absent	0
LUEHSP	*Luehea speciosa*	Malvaceae	absent	0
MACLTI	*Maclura tinctorea*	Moraceae	absent	0
MACRGL	*Macronemum roseum*	Rubiaceae	absent	0
MALMSP	*Mosannona garwoodii*	Annonaceae	indistinct	0fibres narrowed radially
MANIBI	*Manilkara bidentata*	Sapotaceae	absent	0
MANICH	*Manilkara chicle*	Sapotaceae	absent	0
MAQUCO	*Maquira guianensis*	Sapotaceae	absent	0
MAR1LA	*Marila laxiflora*	Clusiaceae	absent	0
MAR1PL	*Marila pluricostata*	Clusiaceae	absent	0
MARAPA	*Maranthes panamensis*	Chrysobalanaceaae	absent	0
MARGNO	*Margaritaria nobilis*	Euphorbiaceae	absent	0
MATAAP	*Matayba apetala*	Sapindaceae	absent	0
MATASC	*Matayba scrobiculata*	Sapindaceae	absent	0
MAYTSC	*Maytenus schippii*	Celastraceae	absent	0
MIOCAF	*Miconia affinis*	Melastomataceae	absent	0
MICOAR	*Miconia argentea*	Melastomataceae	absent	0
MICOEL	*Miconia elata*	Melastomataceae	absent	0
MICOHO	*Miconia hondurensis*	Melastomataceae	absent	0
MICOPO	*Miconia poeppigii*	Melastomataceae	distinct	1thick walled fibres
MICOPR	*Miconia prasina*	Melastomataceae	absent	0
MICOTR	*Miconia trinervia*	Melastomataceae	absent	0
MORIPA	*Morinda panamensis*	Rubiaceae	absent	0
MORTAN	*Mortoniodendron anysophyllum*	Malvaceae	absent	0
MOSQJA	*Mosquitoxylum jamaicense*	Anacardiaceae	absent	0
MYRCGA	*Myrcia gatunensis*	Myrtaceae	absent	0
MYRSCO	*Myrcine coriacea*	Myrsinaceae	absent	0
NECTCU	*Nectandra cuspidata*	Lauraceae	absent	0
NECTMA	*Nectandra martinicense*	Lauraceae	absent	0
NECTPU	*Nectandra purpurea*	Lauraceae	absent	0
NEEADE	*Neea delicatula*	Nyctaginaceae	absent	0
OCHRPY	*Ochroma pyramidale*	Malvaceae	absent	0
OCOTCER	*Ocotea cernua*	Lauraceae	absent	0
OCOTIR	*Ocotea insularis*	Lauraceae	indistinct	0fibres narrowed radially
OCOTWH	*Ocotea whitei*	Lauraceae	indistinct	0thick walled fibres
TROPCA	*Trophis caucana*	Moraceae	absent	0
ORMOCR	*Ormosia coccinea*	Fabaceae	absent	0
OXANPA	*Oxandra panamensis*	Annonaceae	absent	0
PAR2AM	*Parathesis amplifolia*	Myrsinaceae	absent	0
PARMCE	*Parmentiera cereifera*	Bignoniaceae	indistinct	0narrowed radially
PENTMA	*Pentagonia macrophylla*	Rubiaceae	absent	0
PERAAR	*Pera arborea*	Euphorbiaceae	absent	0
PEREXA	*Perebea xanthochyma*	Moraceae	absent	0
PLA1PI	*Platymiscium pinnatum*	Fabaceae	absent	0
PLA2EL	*Platypodium elegans*	Fabaceae	absent	0
POCHQU	*Pachira aquatica*	Malvaceae	absent	0

POGOSP	*Pogonopus exertus*	Rubiaceae	indistinct	0thick walled fibres
POSOLA	*Posoqueria latifolia*	Rubiaceae	absent	0
POULAR	*Poulsenia armata*	Moraceae	absent	0
POUTF1	*Pouteria foveolata*	Sapotaceae	absent	0
POUTGL	*Pouteria glomerata*	Sapotaceae	indistinct	0thick walled fibres
POUTRE	*Pouteria reticulata*	Sapotaceae	absent	0
PRI2CO	*Prioria copaifera*	Fabaceae	absent	0
PROTCO	*Protium costaricense*	Burseraceae	absent	0
PROTTE	*Protium tenuifolium*	Burseraceae	absent	0
PSE2SP	*Pseudolmedia spuria*	Moraceae	absent	0
PSIDFR	*Psidium friedrichsth*	Myrtaceae	absent	0
PSYCG3	*Psychotria grandis*	Rubiaceae	absent	0
PTEROF	*Pterocarpus officinalis*	Fabaceae	absent	0
PTERRO	*Pterocarpus rohrii*	Fabaceae	absent	0
RANDAR	*Randia armata*	Rubiaceae	absent	0
RANDLA	*Randia lasiantha*	Rubiaceae	absent	0
RAUVLI	*Rauvolfia littoralis*	Apocynaceae	absent	0
RONDBU	*Rondeletia buddleioides*	Rubiaceae	absent	0
ROUPMO	*Roupala montana*	Proteaceae	absent	0
RUDGPI	*Rudgea pittieri*	Rubiaceae	absent	0
SACOTR	*Sacoglottis trichogyna*	Humiriaceae	absent	0
SAP1SA	*Sapindus saponaria*	Sapindaceae	absent	0
SAPIAU	*Sapium glandulosum*	Euphorbiaceae	absent	0
SAPISP	*Sapium "broad leaf"*	Euphorbiaceae	distinct	1thick walled fibres
SCHMO	*Schefflera morototoni*	Araliaceae	absent	0
SCHIPA	*Schizolobium parahyba*	Fabaceae	absent	0
SCIAEX	*Sciadodendron excelsum*	Araliaceae	absent	0
SIDECA	*Sideroxylon capiri*	Sapotaceae	absent	0
SIMAAM	*Simarouba amara*	Simaroubaceae	absent	0
SIPAPA	*Siparuna pauciflora*	Monimiaceae	absent	0
SLOATE	*Sloanea terniflora*	Elaeocarpaceae	absent	0
SOLAHA	*Solanum hayesii*	Solanaceae	absent	0
SWARS1	*Swartzia simplex* var 1	Fabaceae	absent	0
SWARS2	*Swartzia simplex* var 2	Fabaceae	absent	0
SYMPGL	*Symphona globulifera*	Clusiaceae	absent	0
TAB1RO	*Tabebuia rosea*	Bignoniaceae	absent	0
TAB2AR	*Tabernaemontana arborea*	Bignoniaceae	absent	0
TACHVE	*Tachigali versicolor*	Fabaceae	indistinct	0fibres narrowed radially
TALIPR	*Talisia princeps*	Sapindaceae	absent	0
TERNTE	*Ternstroemia tepezapote*	Theaceae	absent	0
THEVAH	*Thevetia ahouai*	Apocynaceae	indistinct	0marginal parenchyma
TOCOPI	*Tocoyena pittieri*	Rubiaceae	absent	0
TOVOLO	*Tovomita longifolia*	Clusiaceae	absent	0
TOVOST	*Tovomita stylosa*	Clusiaceae	absent	0
TOVOWE	*Tovomita weddelliana*	Clusiaceae	absent	0
TREMMI	*Trema micrantha*	Ulmaceae	absent	0
TRI2HI	*Trichilia hirta*	Meliaceae	absent	0
TRI2PA	*Trichilia pallida*	Meliaceae	absent	0
TRI2PL	*Trichilia pleeana*	Meliaceae	absent	0
TRI2TO	*Trichilia martiana*	Meliaceae	absent	0
TURNPA	*Turnera panamensis*	Turneriaceae	absent	0
TURPOC	*Turpinia occidentalis*	Staphyleaceae	absent	0
UNCTO	*Uncaria tomentosa*	Rubiaceae	absent	0
UNONPI	*Unonopsis pittieri*	Annonaceae	absent	0
VANDE	*Vantanea depleta*	Humiriaceae	absent	0
VIROEL	*Virola elongata*	Myristicaceae	absent	0

VIROMA	*Virola macrocarpa*	Myristicaceae	absent	0
VIROSE	*Virola sebifera*	Myristicaceae	indistinct	0thick walled fibres
VISMBA	*Vismia baccifera*	Clusiaceae	absent	0
XYL1FR	*Xylopia frutescens*	Annonaceae	distinct	1thick walled fibres
XYL1MA	*Xylopia macrantha*	Annonaceae	absent	0
XYL1SE	*Xylopia sericea*	Annonaceae	distinct	1thick walled fibres
ZANTP1	*Zanthoxylum panamense*	Rutaceae	absent	0
ZANTPR	*Zanthoxylum acuminatum*	Rutaceae	absent	0
ZANTSE	*Zanthoxylum setulosum*	Rutaceae	absent	0
ZUELGU	*Zuelania guidonia*	Salicaceae	absent	0

Appendix 8.3.1.b. Species from wet forest of Panama (BCI) and classification of growth rings and boundaries. 1= distinct growth ring; 2= indistinct

Labels	Species	Family	Locality	Growth rings	Growth rings distinct/indistinct	Type of boundary
AST2GR-ACH	*Astronium graveolens*	Acanardiaceae	Achotines	0	absent	
BURSSI-ACH	*Bursera simaruba*	Burseraceae	Achotines	0	absent	
CAL2CA-ACH	*Calycophyllum candidissimum*	Rubiaceae	Achotines	0	absent	
CEDROD-ACH						
	Cedrela odorata	Meliaceae	Achotines	1	distinct	fibres narrowed radially
CORPA-ACH	*Cordia panamensis*	Boraginaceae	Achotines	0	absent	
GENAM-ACH	*Genipa americana*	Rubiaceae	Achotines	0	absent	
GUAZUL-ACH	*Guazuma ulmifolia*	Malvaceae	Achotines	0	absent	
HYPATO-ACH	*Hyperbaena tonduzii*	Menispermaceae	Achotines	0	absent	
PLA1PI-ACH	*Platymiscium pinnatum*	Fabaceae	Achotines	0	absent	
POCHQU-ACH	*Pachira quinata*	Malvaceae	Achotines	0	absent	
POUTCAM-ACH	*Pouteria campechiana*	Sapotaceae	Achotines	0	absent	
PTERAC-ACH	*Pterocarpus acuminata*	Fabaceae	Achotines	1	distinct	thick walled fibres
TAB1RO-ACH	*Tabeiuia rosea*	Bignoniaceae	Achotines	0	absent	
PSE1SE-ACH	*Pseudobombax septenatum*	Malvaceae	Achotines	1	distinct	thick walled fibres and lines of vessels
ALLIBEDU-COR	*Alibertia edulis*	Rubiaceae	Coronado	0	absent	
BURSSI-COR	*Bursera simaruba*	Burseraceae	Coronado	0	absent	
BURSTO-COR	*Bursera tomentosa*	Burseraceae	Coronado	0	absent	
BYRSCR-COR	*Byrsonima crassifolia*	Malpighiaceae	Coronado	0	absent	
CORDPA-CO	*Cordia panamensis*	Boraginaceae	Coronado	1	distinct	thick walled fibres
DALBRE-COR	*Dalbergia retusa*	Fabaceae	Coronado	0	absent	
LONGVE-COR	*Lonchocarpus veraguense*	Fabaceae	Coronado	0	absent	
LUEHSE-COR	*Luehea semannii*	Malvaceae	Coronado	0	absent	
PSE1SE-COR	*Pseudobombax septenatum*	Malvaceae	Coronado	1	distinct	thick walled fibres

ROUPMO-COR	*Roupala montana*	Proteaceae	Coronado	0	absent	
	Spondias mombin	Anacardiaceae	Coronado	0	absent	
SCIADEX-COR	*Sciadondendron excelsum*	Araliaceae	Coronado	0	absent	
ANNOPU-DIV	*Annona purpurea*	Annonaceae	Divisa	0	absent	
ANACEX-DIV	*Anacardium excelsum*	Annonaceae	Divisa	0	absent	
CHR2CA-DIV	*Chrysophyllum cainito*	Sapotaceae	Divisa	0	absent	
COCCLA-DIV	*Coccoloba latifolia*	Polygonaceae	Divisa	0	absent	
COCCAR-DIV						
	Coccoloba argentea	Polygonaceae	Divisa	0	indistinct	fibres narrowed radially
CRUDAC-DIV	*Crudia acuminata*	Fabaceae	Divisa	0	absent	
DENDAR-DIV	*Dendropanax arboreus*	Araliaceae	Divisa	0	absent	
ENTECY-DIV						
	Enterolobium cyclocarpum	Fabaceae	Divisa	0	indistinct	marginal parenchyma
FAROCC-DIV	*Faramea acuminata*	Rubiaceae	Divisa	0	absent	
GMELAR-DIV	*Gmelina arborea*	Lamiaceae	Divisa	0	absent	
LICAAF-DIV	*Licania affinis*	Chrysobalanaceae	Divisa	0	absent	
NECTGL-DIV	*Nectandra globosa*	Lauraceae	Divisa	1	distinct	thick walled fibres
POCHQU-DIV	*Pachira quinata*	Malvaceae	Divisa	0	absent	
	Rauvolfia litoralis	Apocynaceae	Divisa	0	absent	
SAMSAM-DIV	*Samanea saman*	Fabaceae	Divisa	0	absent	
SIDEPE-DIV	*Sideroxylon persimile*	Sapotaceae	Divisa	0	absent	
STERAP-DIV	*Sterculia apetala*	Malvaceae	Divisa	0	absent	
TRI2MAR-DIV	*Triplaris melaenodendron*	Polygonaceae	Divisa	0	absent	
	Tropis racemosa	Fabaceae	Divisa	0	absent	
ZANTSE-DIV	*Zanthoxyllum setulosum*	Rutaceae	Divisa	0	absent	

Appendix 8.3.1.c. Species from dry forests of Panama and classification of growth rings and boundaries. 1=distinct growth ring; 0= indistinct or absent growth ring.

	Wood type	Family/affinity	Tang vessel arrangement	Spiral thickenings	Rays >10 -seriate	Homocellular rays	Storied rays	absent parenchyma	paratracheal parenchyma	marginal parenchyma	Tang. Diameter <100 µm	multiple per plates	septate fibres	Ring-porous wood	heterocellular rays >4 rows
1		Cannabaceae	0	0	0	0	0	0	0	0	0	0	0	0	1
2		Fabaceae	0	0	0	0	0	0	1	0.5	0	0	0	0	0
3		Elaeocarpaceae	0	0	0	0	0	1	0	0	0	0	0	0	1
4		*Guazumoxylon*	0	0	0	0	0	0	1	0	0	0	0.5	0	0
5		*Periplanetoxylon*	0	0	0	0	0	0	0	0	0.5	0	0	0	0.5
6		Fabaceae	0	0	0	0	0	0	0	0	0	0	0	0	0
7		Malvaceae	0	0	1	0	0	0	1	0	0	0	0	0	0
8		Sapotaceae	0	0	0	0	0	0	0	0	0	0	0	0	?
9		Melastomataceae	0	0	0	1	0	0	1	0	0	0	0	0	0
10		Meliaceae	0	0	0	0	0	0	0	0	1	0	0	0	0.5
		Indeterminate A	0	0	0	0	0	0	0	0	1	0	0	0	?
		Inderterminate B	0	0	0	0	0	0	1	0	0	0	0	0	1

Appendix 8.4.a Datamatrix of fossil wood types from the Cucaracha Formation used to apply Wiemann et al. (1998, 1999) equations.

Species	Family	Locality	Tangential vessel arrangement	Spiral thickenings	Rays >10-seriate	Exclusively homocellular rays	Storied rays	Absent parenchyma	Paratracheal parenchyma	Marginal parenchyma	Tangential diameter <100 µm	multiple perforation plates	Septate fibres present	Ring -porous
Allophylus psilospermus	Sapindaceae	BCI	**0**	**0**	**0**	1	**0**	0	**0**	0	**1**	0	**1**	0
Apeiba tibourbou	Malvaceae	BCI	**0**	**0**	**0**	0	**0**	0	**0**	0	**0**	0	**1**	0
Banara guianensis	Salicaceae	BCI	**0**	**0**	**0**	0	**0**	0	**0**	1	**1**	0	**0**	0
Bauhinia guianensis	Fabaceae	BCI	**0**	**0**	**0**	1	**0**	0	**1**	0	**1**	0	**0**	0
Beilschmiedia pendula	Lauraceae	BCI	**0**	**0**	**0**	0	**0**	0	**0**	0	**1**	0	**0.5**	0
Brosimum costaricanum	Moraceae	BCI	**0**	**0**	**0**	0	**0**	0	**0**	0	**1**	0	**0**	0
Brownea macrophylla	Fabaceae	BCI	**0**	**0**	**0**	0	**0**	0	**0**	0	**1**	0	**0**	0
Bucida buceras	Combretaceae	BCI	**0**	**0**	**0**	0	**0**	0	**1**	0	**1**	0	**0**	0
Bunchosia nitida	Malpighiaceae	BCI	**0**	**0**	**0**	0	**0**	0	**0**	0	**1**	0	**0**	0
Bursera simaruba	Burseraceae	BCI	**0**	**0**	**0**	0	**0**	0	**1**	0	**1**	0	**0**	0
Byrsonima crassifolia	Malpighiaceae	BCI	**0**	**0**	**0**	0	**0**	0	**1**	0	**0**	0	**1**	0
Byrsonima spicata	Malpighiaceae	BCI	**0**	**0**	**0**	0	**0**	0	**0**	0	**1**	0	**1**	0
Calycophyllum candidissimum	Rubiaceae	BCI	**0**	**0**	**0**	0	**0**	1	**0**	0	**1**	0	**0**	0
Calatola costaricensis	Icacinaceae	BCI	**0**	**0.5**	**0**	0	**0**	0	**0**	0	**1**	0	**0**	0
Calliandra laxa undet.	Fabaceae	BCI	**0**	**0**	**0**	0	**0**	0	**1**	0	**0**	0	**0**	0
Capparis cynophallophora	Brassicaceae	BCI	**0**	**0**	**0**	1	**0**	1	**1**	0	**1**	0	**0**	0
Caryodaphnopsis, burgeri	Lauraceae	BCI	**0**	**0**	**0**	0	**0**	1	**0**	0	**0**	0	**0**	0
Casearia aculeata	Salicaceae	BCI	**0**	**0**	**0**	0	**0**	0	**0**	0	**1**	0	**0**	0
Casearia arborea	Salicaceae	BCI	**0**	**0**	**0**	0	**0**	0	**0**	0	**1**	0	**0**	0
Casearia commersoniana	Salicaceae	BCI	**0**	**0**	**1**	1	**0**	1	**0**	0	**1**	0	**0**	0
Casearia guianensis	Salicaceae	BCI	**0**	**0**	**0**	0	**0**	1	**0**	0	**1**	0	**0**	0
Casearia sylvestris	Salicaceae	BCI	**0**	**0**	**0**	0	**0**	0	**0**	0	**1**	0	**0**	0

Cassipourea elliptica	Rhizophoraceae	BCI	**0**	**0**	**0**	0	**0**	0	**0**	0	**1**	0	**1**	0
Cecropia peltata	Urticaceae	BCI	**0**	**0**	**0**	0	**0**	0	**1**	0	**0**	0	**0**	0
Celtis schippii	Cannabaceae	BCI	**0**	**0**	**0**	0	**0**	0	**1**	0	**1**	0	**0**	0
Cespedesia spathulata	Ochnaceae	BCI	**0**	**0**	**0**	1	**0**	0	**1**	0	**0**	0	**0**	0
Chimarrhis parviflora	Rubiaceae	BCI	**0**	**0**	**0**	0	**0**	0	**1**	0	**0**	0	**0**	0
Chloroleucon mangense	Fabaceae	BCI	**0**	**0**	**0**	1	**0**	0	**1**	0	**1**	0	**1**	0
Chrysochlamys eclipes	Clusiaceae	BCI	**0**	**0**	**0**	1	**0**	0	**0**	0	**1**	0	**0**	0
Chrysophyllum argenteum	Sapotaceae	BCI	**0**	**1**	**0**	1	**0**	0	**0**	0	**1**	0	**0**	0
Chrysophyllum cainito	Sapotaceae	BCI	**0**	**0**	**0**	0	**0**	0	**0**	0	**0**	0	**0**	0
Chrysophyllum venezuelense	Sapotaceae	BCI	**0**	**0**	**0**	0	**0**	0	**0**	0	**1**	0	**0**	0
Clethra lanata	Clethraceae	BCI	**0**	**0**	**0**	0	**0**	0	**1**	0	**1**	1	**0**	0
Coccoloba coronata	Polygonaceae	BCI	**0**	**0**	**0**	1	**0**	0	**0**	0	**1**	0	**0**	0
Coccoloba johnstonii	Polygonaceae	BCI	**0**	**0**	**0**	1	**0**	0	**0**	0	**1**	0	**0**	0
Coccoloba manzinellens	Polygonaceae	BCI	**0**	**0**	**0**	1	**0**	0	**0**	0	**1**	0	**?**	0
Colubrina glandulosa	Rhamnaceae	BCI	**0**	**0**	**0.5**	0	**0**	0	**1**	0	**1**	0	**0**	0
Colubrina heteroneura	Rhamnaceae	BCI	**0**	**0**	**0**	0	**0**	0	**1**	0	**1**	0	**0**	0
Compsoneura capitellata	Myristicaceae	BCI	**0**	**0**	**0**	1	**0**	0	**0**	1	**1**	1	**0**	0
Conostegia rufescens	Melastomataceae	BCI	**0**	**0**	**0**	1	**0**	0	**0**	0	**0**	0	**1**	0
Conostegia xalapensis	Melastomataceae	BCI	**0**	**0**	**0**	1	**0**	0	**1**	0	**1**	0	**1**	0
Cordia alliodora	Boraginaceae	BCI	**0**	**0**	**0**	0	**0**	0	**1**	0	**1**	0	**0**	1
Cordia eriostigma	Boraginaceae	BCI	**0**	**0**	**0**	0	**0**	0	**1**	0	**1**	0	**0**	0
Cosmibuena macrocarpa	Rubiaceae	BCI	**0**	**0**	**0**	0	**0**	0	**0**	0	**1**	0	**0**	0
Coussarea curvigemmia	Rubiaceae	BCI	**0**	**0**	**0**	0	**0**	0	**0**	0	**1**	0	**0**	0
Coussarea latifolia	Rubiaceae	BCI	**0**	**0**	**0**	0	**0**	0	**0**	0	**1**	0	**0**	0
Crateva tapia	Brassicaceae	BCI	**0**	**0**	**0**	0	**0**	0	**1**	0	**0**	0	**0**	0
Croton billbergianu	Euphorbiaceae	BCI	**0**	**0**	**0**	1	**0**	1	**1**	0	**1**	0	**0**	0
Croton draco	Euphorbiaceae	BCI	**0**	**0**	**0**	0	**0**	0	**1**	0	**1**	0	**1**	0

Cryptocaria aschersoniana	Lauraceae	BCI	**0**	**0**	**0**	0	**0**	0	**0**	1	**1**	1	**0**	0
Cupania cinerea	Sapindaceae	BCI	**0**	**0**	**0**	1	**0**	1	**0**	0	**1**	0	**1**	0
Cupania latifolia	Sapindaceae	BCI	**0**	**0**	**0**	1	**0**	1	**0**	0	**1**	0	**0**	0
Cupania rufescens	Sapindaceae	BCI	**0**	**0**	**0**	1	**0**	0	**0**	0	**1**	0	**1**	0
Dalbergia retusa	Fabaceae	BCI	**0**	**0**	**0**	0	**1**	0	**1**	0	**0**	1	**0**	0
Daphnosis americana	Thymeleaceae	BCI	**0**	**0**	**0**	1	**1**	0	**1**	0	**1**	0	**0**	0
Dendropanax arboreus	Araliaceae	BCI	**0**	**0**	**0**	0	**0**	1	**1**	0	**1**	0	**0**	0
Erythroxylum macrophyllum	Erythroxylaceae	BCI	**0**	**0**	**0**	0	**0**	0	**0**	0	**1**	0	**1**	0
Eugenia principium	Myrtaceae	BCI	**0**	**0**	**0**	0	**0**	0	**0**	0	**1**	0	**0**	0
Exostema mexicanum	Rubiaceae	BCI	**0**	**1**	**0**	0	**0**	0	**0**	0	**1**	0	**0**	0
Ficus insipida	Moraceae	BCI	**0**	**0**	**0**	0	**0**	0	**0**	0	**0**	0	**0**	0
Ficus maxima	Moraceae	BCI	**0**	**0**	**0**	0	**0**	0	**0**	0	**0**	0	**0**	0
Ficus popenoei	Moraceae	BCI	**0**	**0**	**0**	0	**0**	0	**0**	0	**0**	0	**0**	0
Ficus tonduzii	Moraceae	BCI	**0**	**0**	**0**	0	**0**	0	**0**	0	**0**	0	**0**	0
Ficus yoponenis	Moraceae	BCI	**0**	**0**	**0**	0	**0**	0	**0**	0	**0**	0	**0**	0
Fissicalyx feldleri	Fabaceae	BCI	**0**	**0**	**0**	1	**0**	0	**1**	0	**1**	0	**0**	0
Garcinia intermedia	Clusiaceae	BCI	**0**	**0**	**0**	0	**0**	0	**1**	0	**1**	0	**0**	0
Garcinia madruno	Clusiaceae	BCI	**0**	**0**	**0**	0	**0**	0	**1**	0	**0**	0	**0**	0
Genipa americana	Rubiaceae	BCI	**0**	**0**	**0**	0	**0**	0	**0**	0	**1**	0	**0**	0
Guapira standleyana	Nyctaginaceae	BCI	**0**	**0**	**0**	1	**0**	1	**0**	0	**1**	0	**0**	0
Guarea glabra	Meliaceae	BCI	**0**	**0**	**0**	1	**0**	0	**1**	0	**1**	0	**0**	0
Guarea grandifolia	Meliaceae	BCI	**0**	**0**	**0**	0	**0**	0	**1**	0	**0**	0	**0**	0
Guarea guidonia	Meliaceae	BCI	**0**	**0**	**0**	0	**0**	0	**1**	0	**0**	0	**0**	0
Guarea pterorhachis	Meliaceae	BCI	**0**	**0**	**0**	1	**0**	0	**1**	0	**1**	0	**1**	0
Guatteria aberrans	Annonaceae	BCI	**0**	**0**	**0**	0	**0**	0	**1**	0	**0**	0	**0.5**	0
Guazuma ulmifolia	Malvaceae	BCI	**0**	**0**	**0**	0	**0**	0	**1**	0	**1**	0	**0.5**	0
Guettarda crispiflora	Rubiaceae	BCI	**0**	**0**	**0**	0	**0**	0	**1**	0	**1**	0	**0.5**	0

Guettarda foliacea	Rubiaceae	BCI	**0**	**0**	**0**	0	**0**	1	**0**	0	**1**	0	**1**	0
Astronium graveolens	Acanardiaceae	Achotines	**0**	**0**	**0**	0	**0**	0	**1**	0	**1**	0	**0**	0
Bursera	Burseraceae	Achotines	**0**	**0**	**0**	0	**0**	0	**0**	0	**1**	0	**1**	0
Calycophyllum	Rubiaceae	Achotines	**0**	**1**	**0**	0	**0**	1	**0**	0	**1**	0	**0**	0
Cedrela odorata	Meliaceae	Achotines	1	**0**	**0**	0	**0**	0	**1**	1	**0**	0	**0**	1
Cordia panamensis	Boraginaceae	Achotines	**1**	**0**	**0**	0	**0**	0	**0**	0	**1**	0	**0**	1
Guazuma ulmifolia	Malvaceae	Achotines	**0**	**0**	**0**	0	**0**	0	**0**	0	**1**	1	**0.5**	0
Hyperbaena	Menispermaceae	Achotines	**0**	**1**	**1**	0	**0**	0	**0**	0	**0**	1	**0**	0
Platymiscium	Fabaceae	Achotines	**0**	**0**	**0**	1	**1**	0	**1**	0	**0**	0	**0**	0
Pouteria campechiana	Sapotaceae	Achotines	**0**	**0**	**0**	1	**0**	0	**0**	0	**1**	0	**0**	0
Tabeiuia rosea	Bignoniaceae	Achotines	**0**	**0**	**0**	1	**0**	0	**1**	1	**0**	0	**0**	0
Alibertia edulis	Rubiaceaee	Coronado	0	**0**	**0**	0	**0**	0	**0**	0	**1**	0	**0**	0
Bursera simaruba	Burseraceae	Coronado	0	**0**	**0**	0	**0**	0	**0**	0	**1**	0	**0**	0
Bursera tomentosa	Burseraceae	Coronado	0	**0**	**0**	0	**0**	0	**0**	0	**1**	0	**0.5**	0
Byrsonima crassifolia	Malpighiaceae	Coronado	0	**0**	**0**	0	**0**	0	**1**	1	**0**	0	**1**	0
Coccoloba	Polygonaceae	Divisa	0	**0**	**0**	1	**0**	0	**0**	1	**1**	0	**1**	0
Cordia	Boraginaceae	Coronado	0	**0**	**0**	0	**0**	0	**1**	0	**1**	0	**1**	0
Dalbergia retusa	Fabaceae	Coronado	0	**0**	**0**	0	**1**	0	**1**	0	**0**	0	**0**	0
Lonchocarpus	Fabaceae	Coronado	0	**0**	**0**	0	**1**	0	**0**	0	**0**	0	**0**	0
Luehea semannii	Malvaceae	Coronado	0	**0**	**0**	0	**0**	0	**0**	0	**1**	0	**0**	0
Roupala montana	Proteaceae	Coronado	1	**0**	**1**	0	**0**	0	**0**	0	**0**	0	**0.1**	0
Annona purpurea	Annonaceae	Divisa	0	**0**	**0**	0	**0**	0	**0**	0	**0**	1	**0**	0
Anacardium excelsum	Annonaceae	Divisa	0	**0**	**0**	1	**0**	0	**0**	0	**0**	0	**1**	0
Chrysophyllum cainito	Sapotaceae	Divisa	0	**0**	**0**	1	**0**	0	**0**	0	**1**	0	**0**	0
Coccoloba latifolia	Polygonaceae	Divisa	0	**0**	**0**	0	**0**	0	**0**	0	**1**	0	**1**	0
Coccoloba argentea	Polygonaceae	Divisa	0	**0**	**0**	1	**0**	0	**0**	0	**1**	0	**0**	0
Crudia acuminata	Fabaceae	Divisa	0	**0**	**0**	0	**0**	0	**0**	0	**0**	0	**0.5**	0

Dendropanax arboreus	Araliaceae	Divisa	0	**0**	**0**	0	**0**	1	**0**	0	**1**	0	**1**	0
Enterolobium cyclocarpum	Fabaceae	Divisa	0	**0**	**0**	0	**0**	0	**1**	1	**0**	0	**0**	0
Faramea acuminata	Rubiaceae	Divisa	0	**0**	**0**	0	**0**	0	**0**	0	**1**	0	**0**	0
Gmelina arborea	Lamiaceae	Divisa	0	**0**	**0**	0	**0**	0	**0**	0	**0**	0	**1**	0
Licania affinis	Chrysobalanaceae	Divisa	0	**0**	**0**	0	**0**	0	**0**	0	**0**	0	**0**	0
Nectandra globosa	Lauraceae	Divisa	0	**0**	**0**	0	**0**	0	**1**	0	**0**	0	**1**	0
Pachira quinata	Malvaceae	Divisa	0	**0**	**0**	0	**0**	0	**0**	0	**0**	0	**0**	0
Samanea saman	Fabaceae	Divisa	0	**0**	**0**	0	**0**	0	**1**	0	**0**	0	**0**	0
Sideroxylon	Sapotaceae	Divisa	0	**0**	**0**	0	**0**	0	**0**	0	**0**	0	**1**	0
Triplaris	Polygonaceae	Divisa	0	**0**	**0**	1	**0**	0	**1**	0	**1**	0	**0**	0
Zanthoxyllum setulosum	Rutaceae	Divisa	0	**1**	**1**	0	**0**	0	**1**	0	**1**	0	**0**	0

Appendix 8.4.b. Datamatrix of modern wood anatomical characters form dry and wet forests of Panama used for the Wiemann et al. (1998, 1999) equations.